AUA 2023 Annual Meeting

Scientific Abstracts

Table of Contents

Airway Management

Airway Management 1 - Intubation Conditions Achieved with Rapid Co-administration of Rocuronium and Propofol versus Classical Induction: A Prospective Randomized and Blind Trial

Lauren Nakazawa[1], Travis Markham[2], Kyle Alyson Chi[3], Carolyn Fan[3], David McClendon[3], Sepideh Saroukhani[3], Yandong Jiang[3]

UT Health Houston[1] University of Texas Health Science Center at Houston[2] McGovern Medical School at UT Health Houston[3]

Introduction: Patients with difficult airways are at increased risk of morbidity and mortality. In a "cannot ventilate and cannot intubate" scenario, significant desaturations or death can occur if effective spontaneous breathing cannot be resumed in a timely fashion. In classic induction (CI), a sedative-hypnotic is given, mask ventilation is attempted, and neuromuscular blocking drugs (NMBD) are administered. If intubation attempts are unsuccessful and reversal of neuromuscular blockade is given to resume spontaneous ventilation, patients may be past the limits of safe apnea time. Modified time principle induction (MTPI) is a variation of "time principle induction," which has been shown in prior studies to provide similar intubating conditions and intubation success rate (1-7). The proposed modification entails administration of rocuronium, immediately followed by propofol, which can potentially shorten apnea time from roughly 8 to about 5 minutes compared to CI if a "cannot intubate and cannot ventilate" scenario is encountered and sugammadex is used (Figure 1). We hypothesize that the intubating conditions will be similar between MTPI and CI groups, without increased incidence of awareness of muscle weakness.

Methods: This is an ongoing randomized prospective blind trial comparing MTPI to CI in patients in the main operating rooms at an academic medical center. A preliminary analysis was performed on 45 of 53 patients. Inclusion criteria are age 18+ years**,** with potential difficult airway **(**BMI >30 kg/M^2 and/or Mallampati class III/IV**)** requiring general anesthesia and endotracheal intubation. Exclusion criteria includes ASA physical status classification > III, emergency surgery, and patients requiring awake intubation.

After obtaining informed consent, patients were randomized to MTPI or CI groups. Premedication was given in the usual manner and the patient brought to the operating room. ASA monitors were applied, the patient was preoxygenated, 1mg/kg lidocaine was given, followed by an opioid such as fentanyl. Patients assigned to MTPI were given 0.6mg/kg rocuronium, followed by 1-2mg/kg IV propofol as a single bolus within 10 seconds. Once apnea occurred, intubation with C-MAC began and the laryngoscopy was continuously recorded and saved. If the intubation was unsuccessful, mask ventilation was attempted, followed by SGA ventilation. If unsuccessful, sugammadex was given. Patients assigned to CI were induced as per routine care. In CI, once apneic, attempted mask ventilation began, 0.6mg/kg rocuronium was administered, and after 3 minutes intubation was performed with C-MAC and recorded. Once the patient recovered in PACU, the study team conducted a post-operative survey to assess for awareness during induction and intubation.

The primary outcome was intubation time (laryngoscope insertion into the mouth to first end tidal CO2 reading). Secondary outcomes were vocal cord view, vocal cord opening grade, and vital signs including blood pressure and heart rate. The distributions of patient characteristics and study outcomes were compared between the two study arms using Mann-Whitney U test for the intubation time, independent sample t-test for continuous variables, and chi-square test for categorical variables. All statistical tests were performed at 0.05 level of significance.

Results: Patient baseline characteristics were not significantly different between the two study groups. Of 53 patients enrolled, four patients from each study arm (n = 8) were excluded because the information on primary outcome could not be captured due to technical failure or other issues. Although marginally significant (P = 0.06), median intubation time in the MTPI group [median interquartile range (IQR): 41.0 sec (35.0, 51.0)] was shorter compared to the CI group [median IQR: 53.0 sec (42.0, 63.0)]. There was no difference in secondary outcomes, including vocal cord view and glottic opening (all $P \geq 0.111$) (Table 1). No patients in either group reported awareness during intubation or intra-operatively.

Conclusions: Although ongoing, current data from our study indicates that MTPI trended towards decreased intubation times compared to CI. Other intubating conditions, such as vocal cord view and vocal cord opening were comparable between both groups, and there was no increase in the incidence of awareness. By shortening apnea time by around 3 minutes, we expect that MTPI has potential to improve difficult airway management if a "cannot intubate and ventilate" scenario occurs.

References: 1. J Clin Anesth, 9(4),317-20,1997
2. Anesth Analg, 86(5),1137-40,1998
3. Can J Anaesth, 41(8),688-93,1994
4. J Anaesthesiol Clin Pharmacol, 26(4),493-7,2010
5. J Clin Anesth, 1(6),422-5,1989
6. Anesthesiology, 73(2),244-8,1990
7. Acad Emerg Med, 26(9),1014-21,2019

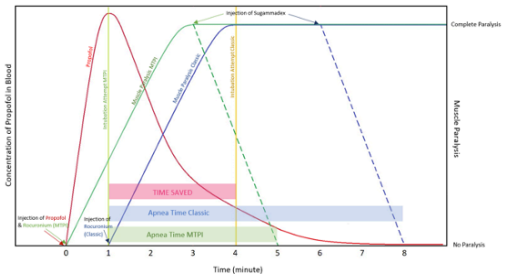

Figure 1. Schematic demonstration of intubating conditions created by Classic Induction vs. Modified Time Principle Induction (MTPI) with propofol and rocuronium. Propofol concentration in plasma in the brain (red line). Rocuronium induced muscle paralysis for classic induction (blue solid line) and Modified Time Principle Induction (green solid line). Muscle paralysis reversal after Sugammadex after MTPI (green dotted line) and classic induction (blue dotted line).

Table 1

Variable	CI (n=23)	MTPI (n=22)	*P*
Baseline characteristics			
Age (Mean ± SD)	46.8 ± 15.3	51.2 ± 15.6	0.345
Sex			0.999
Male	10 (43.5)	9 (42.9)	
Female	13 (56.5)	12 (57.1)	
Height (Mean ± SD)	170.1 ± 11.7	170.8 ± 11.7	0.849
Weight (Mean ± SD)	105.6 ± 25.4	114.1 ± 32.4	0.331
BMI (Mean ± SD)	36.5 ± 8.2	38.7 ± 8.2	0.367
Mallampati class			0.224
1	4 (17.4)	3 (13.6)	
2	6 (29.1)	12 (54.6)	
3	9 (39.1)	6 (27.3)	
4	4 (17.4)	1 (4.5)	
Intubator Skill level			0.368
Attending	4 (17.4)	1 (4.5)	
Anesthesiology Assistant	2 (8.7)	4 (18.2)	
Resident	17 (73.9)	17 (77.3)	
Primary outcome			
Intubation time in seconds [median (IQR)]	53.0 (42.0, 63.0)	41.0 (35.0, 51.0)	0.06
Secondary outcomes			
Vocal cord view			0.273
1	9 (39.1)	12 (54.5)	
2	11 (47.8)	10 (45.4)	
3	3 (13.0)	0 (0)	
Vocal cord opening grade			0.156
A	13 (56.5)	18 (81.8)	
B	6 (26.1)	4 (18.2)	
C	2 (8.7)	0 (0)	
Uncertain	2 (8.7)	0 (0)	
Systolic blood pressure			
Minimum	120.4 ± 25.6	132.8 ± 24.9	0.111
Maximum	147.0 ± 32.5	155.1 ± 15.2	0.299
Diastolic blood pressure			
Minimum	71.3 ± 17.0	79.0 ± 16.6	0.137
Maximum	92.2 ± 17.6	97.4 ±14.6	0.289
Heart Rate			
Minimum	68.8 ± 14.5	70.4 ± 11.3	0.686
Maximum	100.0 ± 21.1	103.6 ± 18.8	0.555

* Data are reported as frequencies (percentages), otherwise as indicated; SD: standard deviation; IQR: Interquartile range; BMI: body mass index.

Airway Management 2 - Anesthetic Management of Tracheal Stenosis: A Retrospective Study

Jamie Sparling[1], Hovig Chilitian, Paul Alfille[1], Carly Eiduson[2], Josephina Lin[2], Xiaodong Bao[3]

Massachusetts General Hospital[1] University of Rochester School of Medicine & Dentistry[2]

Introduction: Anesthetic care for patients with tracheal stenosis carries the risk of airway collapse upon induction, the risk of difficult intubation due to inability to pass an endotracheal tube beyond the stenotic segment, and the risk of anastomotic damage should airway manipulation be required in the immediate post-operative period. For these reasons, inhalational induction has traditionally been recommended. Tracheal resection and reconstruction (TRR) requires specific attention to these risks, as well as careful coordination with the surgeon due to the shared airway. To date, only case series have described the anesthetic experience for TRR.

Methods: A retrospective chart review was conducted for all patients undergoing TRR at a single academic hospital from January 1, 2006 to May 24, 2022 using a standardized abstraction tool. Intra-operative complications were defined as oxygen saturation <90% within 15 minutes of induction, inability to mask ventilate, >2 intubation attempts, or need for rescue with rigid bronchoscopy or another unplanned airway technique. Post-operative complications were defined as mechanical ventilation, reintubation, or non-invasive positive pressure ventilation (NIPPV) on post-operative day 0 or 1 (POD 0 or 1).

Results: A total of 608 patients underwent TRR during the period studied. 310 (51.0%) had a preoperative minimum tracheal diameter 4-7.99mm. Inhalation induction was chosen for 6 patients (1.0%). Ten patients had COVID-associated tracheal stenosis. 57 intraoperative complications occurred in 51 (8.4%) patients, most commonly post-induction hypoxemia. 4 postoperative complications occurred in 3 patients.

Conclusions: The incidence of intra-operative (8.4%) and post-operative (0.5%) complications was low, reflecting the safety of anesthetic care when coupled with meticulous preparation for potential airway complications and close coordination amongst anesthesiologists and surgeons during shared airway procedures.

Figure 1: Patient flow diagram. TRR = tracheal resection and reconstruction; * inclusive of 34 patients for whom anesthesia record was available but BMI was unavailable and 23 for whom pre-operative tracheal dimension was unavailable

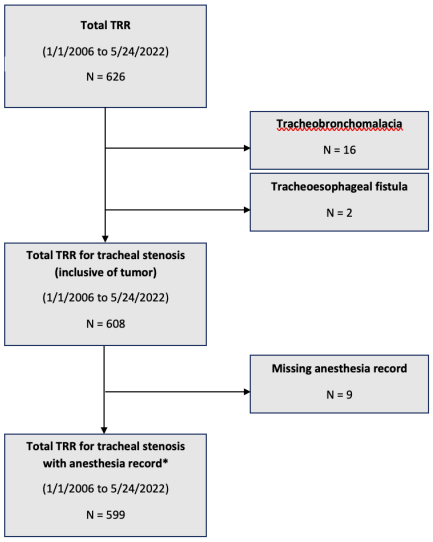

Table 1: Induction choice and event occurrence by minimum pre-operative tracheal diameter

Minimum pre-operative tracheal diameter	Number of cases	Inhalation induction (%)	Intra-operative complication (%)	Post-operative complication (%)
0-3.99mm	67	1 (1.5)	5 (7.5)	0 (0.0)
4-7.99mm	310	4 (1.3)	19 (6.1)	2 (0.6)
8-9.99mm	58	0 (0.0)	5 (8.6)	0 (0.0)
≥10mm	48	0 (0.0)	6 (12.5)	0 (0.0)
Tumor	61	0 (0.0)	4 (6.6)	0 (0.0)
In situ tracheostomy or T-tube	41	1 (2.4)	7 (17.1)	0 (0.0)
Unavailable	23	0 (0.0)	5 (21.7)	1 (4.3)
Total	**608**	**6 (1.0)**	**51 (8.4)**	**3 (0.5)**

Table 2: Intra-operative and post-operative complications by anesthesia induction type

Anesthesia induction type	Number of cases	Intra-operative complication (%)	Post-operative complication (%)
Intravenous (IV)	553	44 (8.0)	3 (0.5)
Inhalation	5	0 (0.0)	0 (0.0)
Secure airway in situ*	41	7 (17.1)	0 (0.0)
Unavailable	9	0 (0.0)	0 (0.0)
Total	**608**	**51 (8.4)**	**3 (0.5)**

* Secure airway defined as presence of tracheostomy or T-tube in situ pre-operatively; 1 patient with a secure airway in situ received in inhalation induction, while 40 received IV inductions

Table 3: Induction choice and event occurrence by presence or absence of COVID-related tracheal stenosis

Presence of COVID-related tracheal stenosis	Number of cases	Inhalation induction (%)	Intra-operative complication (%)	Post-operative complication (%)
Yes	10	0 (0.0)	1 (10.0)	0 (0.0)
No	598	6 (1.0)	50 (8.4)	3 (0.5)
Total	**608**	**6 (1.0)**	**51 (8.4)**	**3 (0.5)**

Table 4: COVID-related tracheal stenosis cases

Case	Demographic	Tracheostomy placed	Duration of intubation prior to tracheostomy	Interval since extubation / decannulation
1	33F	No	9 days	2 months
2	48M	No	21 days	6 months
3	70F	Yes, still present	Unknown	7 months[1]
4	67M	Yes, decannulated but required repeat tracheostomy	45 days	8.5 months[1]
5	43F	No	7 days	2 months
6	60M	Yes, still present	Unknown	8 months[1]
7	35M	Yes, decannulated	12 days	7 weeks
8	24M	Yes, decannulated	14 days	2 months
9	32M	Yes, still present	34 days[2]	5.5 months[1]
10	43M	Yes, decannulated	13 days	11 months

1 In patients with a tracheostomy in situ at the time of resection, interval since initial intubation is reported

2 Inclusive of two failed extubations and re-intubations

Ambulatory Anesthesia 1 - COVID-19 pandemic and patient enrollment in the OSPREy clinical trial

Evan Kharasch[1], Carrie Schlabaugh[1], Emmalee Metzler[1], Alicja Schultz[2]

Duke University School of Medicine[1] Duke University[2]

Introduction: The COVID-19 pandemic has markedly influenced clinical care, clinical trials initiation, processes, conduct, and progress, and patient attitudes towards participation in clinical research. The Outpatient Surgery Pain Relief Enhancement trial (OSPREy) is a single-center, randomized, double-blinded comparative effectiveness trial in adults undergoing moderately painful outpatient (same-day discharge or next-day discharge) surgery. It evaluates intraoperative anesthesia/ PACU analgesia using long-duration compared vs short-duration opioids, in patients who receive post-discharge oral opioids. Outcomes include daily pain, opioid use, and recovery parameters assessed for 30d after surgery. With the exception of intraoperative and PACU opioid assignment, anesthesia and surgery are not changed for study purposes. The trial began enrollment in December 2018 and is ongoing. Our institution suspended all clinical research activities (March 16, 2020 – May 22, 2020) at the height of the COVID-19 pandemic. The purpose of this investigation was to evaluate patient enrollment rates in the OSPREy trial before the pandemic and after resumption of clinical research activity.

Methods: The OSPREy trial received IRB approval, was prospectively registered (NCT03726268), and all participants provided written informed consent. We quantified the number of eligible qualifying patients who were approached for participation in the trial, the number enrolled to participate, and the number declining enrollment, during several periods before (pre-COVID) and after (during COVID) the research suspension period.

Results: In two 2018-2019 epochs before the pandemic, essentially half (50%) of the patients agreed to participate and half actively declined participation (figure). Participation after research resumption following the Spring 2020 research suspension was less (37%) and declined further to a nadir of 30% in the first quarter of 2021. The fraction of patients declining participation increased from 50% to 63% after resumption of research, and increased further to a peak of 70% in the first quarter of 2021. After the first quarter of 2021, research participation has steadily increased, and returned to pre-COVID participation patterns in the latest audit period (May 2022-September 2022).

Conclusions: Patient participation in the OSPREy comparative effectiveness trial substantially decreased beginning coincident with the peak of the COVID pandemic. This occurred despite research process adaptations and all-electronic remote processes (email and telephone communication, e-consent, electronic data collection). Reduced patient enrollment in research, as exemplified in the OSPRey trial, has major implications for accrual, meeting enrollment goals specified in protocol and grant sample-size justifications, statistical power, and ability to adequately test hypotheses and achieve valid conclusions. Although the peak of COVID-19 disease passed, there was continuing COVID-19 effect on clinical research. (Supported by NIH R01-DA042985).

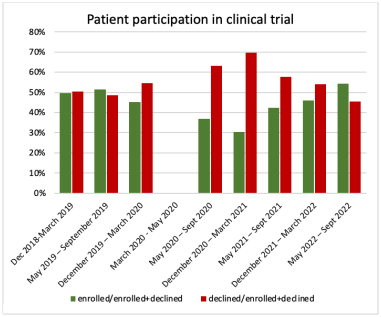

Figure. Fraction of eligible patients approached for research participation in the OSPREy comparative effectiveness trial who affirmatively agreed or declined to enroll.

Ambulatory Anesthesia

Ambulatory Anesthesia 2 - A Retrospective Review of Intraoperative Hypotension in Otolaryngology Surgeries Requiring Cranial Nerve Monitoring and Post-operative Outcomes

Daniel Phan[1], Hyun Seong Seo[2], Landon Cohen[3], Andrea Grote[1], Elizabeth Hong[4], Tamara Chambers[5], Mary Joseph[6]

Keck School of Medicine of USC[1] Keck USC School of Medicine[2] USC, UCLA[3] LAC+USC Medical Center[4] University of Southern California[5] Keck School of Medicine of University of Southern California[6]

Introduction: Intraoperative hypotension (IOH) occurs frequently, with incidence in the current literature varying between 5-99% (1, 2, 3). IOH has been associated with organ ischemia resulting in increased morbidity and mortality (2). The concern for IOH is particularly relevant in otolaryngologic procedures as many require cranial nerve monitoring which prohibits the use of muscle relaxants, thus requiring deeper anesthesia and an increased risk of hypotension. In addition, because many otolaryngologic procedures are short in duration and have minimal estimated blood loss, no Foley catheter is placed and fluid resuscitation is restricted. Finally, controlled hypotension with blood pressures 10-20% below a patient's baseline is often used to minimize bleeding and maintain an adequate surgical field. The combination of these factors creates challenges for the anesthesiologist to maintain optimal blood pressures. The objective of this study was to identify the incidence of IOH in otolaryngologic surgical cases utilizing cranial nerve monitoring, review risk factors contributing to IOH, and review postoperative adverse outcomes secondary to IOH.

Methods: We performed a retrospective chart review of 411 adult patients who underwent otolaryngologic surgery with cranial nerve monitoring at our institution between 1/1/2017-12/31/2019. Data collected included patient characteristics, comorbidities, medications, pre- and post-operative laboratory values, post-operative complications, patient disposition, and 30-day mortality. Intraoperative data collected included cranial nerves monitored, anesthetic technique, intraoperative medications, incidence of hypotension, and pressers used to address IOH. IOH was defined as >5 minutes of systolic <80 mmHg and/or diastolic <50 mmHg. Data was de-identified and analyzed via appropriate statistical analysis.

Results: Our study included 130 male and 281 female patients with and mean age of 48.1 years, and mean BMI of 29.2. ASA physical status was recorded, and our study included ASA-I (48), ASA-II (248), ASA-III (88), and ASA-IV (2) patients. Procedures included middle ear surgery (41%), thyroidectomies (33%), parathyroidectomies (19%), and parotidectomies (7%). The overall incidence rate of IOH in our study was 52%. Of patients taking anti-hypertensive medications prior to surgery, IOH incidence rate was 64.6% compared to 45.3% for patients not on anti-hypertensive medication. Furthermore, among patients taking ACEi/ARB therapy prior to surgery, IOH incidence rate was 71.6%.

Conclusions: The association between IOH and adverse clinical outcomes is well known in the literature. The incidence of IOH reported by Bijker et al. for all surgeries was 41% compared to 52% in our study focused specifically on otolaryngologic cases (3). In our patient population, the greatest risk factor for IOH was pre-existing hypertension, particularly patients on ACEi/ARB therapy. Given the known association between IOH and increased morbidity and mortality, our study supports the importance of considering a patient's antihypertensive regimen when making clinical decisions during induction, emergence, and during the postoperative period. Prospective studies and studies with a larger sample size, and thus more statistical power, may help to evaluate pre- and intraoperative interventions needed to successfully counter IOH and its associated adverse outcomes.

References: Relationship between intraoperative hypotension, defined either reduction from baseline or absolute thresholds, and acute kidney and myocardial injury after noncardiac surgery: A retrospective cohort analysis. Anesthesiology:2017, Vol 126, p 47-65.

Intraoperative Hypotension is Associated With Adverse Clinical Outcomes After Non Cardiac Surgery. Anesthesia and Analgesia, June 2021, Vol 2, p 1654-1665.

Incidence of intraoperative hypotension as a function of the chosen definition: Literature definitions applied to a retrospective cohort using automated data collection. Anesthesiology:2007, Vol 107, p 213-220

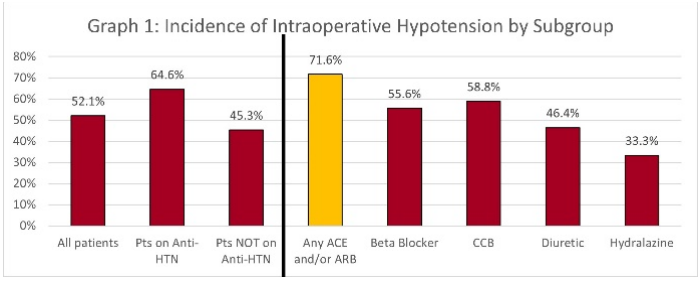

Table 1: Physical Characteristics & Comorbidities		
	Mean	SD
Age (years)	48.10	13.61
BMI	29.20	6.16
	#	%
Male:	130	32%
Female	281	68%
Comorbidities:		
Hypertension	139	34%
Diabetes Mellitus	81	20%
Chronic Kidney Disease	26	6%
Liver Disease	11	3%
Thyroid Disease	152	37%
Parathyroid Disease	73	18%
Head and Neck Malignancy	95	23%
ASA Status:		
ASA 1	48	12%
ASA 2	248	64%
ASA 3	88	23%
ASA 4	2	1%
ASA 5	0	0%

Table 2: Type of Procedure Performed			
Procedure	**CN Monitored**	**#**	**%**
Thyroidectomy	CN X	133	33%
Parathyroidectomy	CN X	75	19%
Parotidectomy	CN VII	29	7%
Middle Ear Surgery	CN VII	165	41%

Table 3: Preoperative Anti-Hypertensive Medications		
Medication	**#**	**%**
ACE Inhibitor	58	40%
ARB	23	16%
Beta Blocker	45	31%
Calcium Channel Blocker	51	35%
Hydralazine	3	2%
Diuretic	28	19%
Other	7	5%

Table 4: Post-operative Complications		
Complications:	**#**	**%**
Myocardial Infarction	1	0.3%
Arrhythmias	2	0.7%
Consult to Cardiology	2	0.7%
Emergence Delirium	1	0.3%
30-day Mortality	0	0%
Disposition		
Discharge Home	215	53%
Admit to Ward	183	45%
Admit to ICU	11	3%

Ambulatory Anesthesia 3 - Perioperative Management of Patients undergoing Endoscopic Retrograde Cholangiopancreatography (ERCP)-A modified Delphi consensus study

Omid Azimaraghi[1], Mohammad Bilal[1], Somchai Amornyotin[2], Mustafa Arain[2], Matthias Behrends[3], Tyler Berzin[3], James Buxbaum[4], Curtis Choice[4], Philipp Fassbender[5], Mandeep Sawhney[5], Eswar Sunder[5], Karuna Wongtangman[1], Kate Leslie[6], Matthias Eikermann[6]

Montefiore Medical Center[1] Faculty of Medicine Siriraj Hospital, Mahidol University[2] UCSF[3] University of Southern California[4] Montefiore Medical Center, Department of Anesthesiology[5] Royal Melbourne Hospital[6]

Introduction: The number of endoscopic retrograde cholangiopancreatography (ERCP) procedures is increasing. Over 600,000 ERCP procedures are performed annually in the United States. (1-3) Monitored anesthesia care (MAC) and general anesthesia are commonly used during ERCP procedures. There are distinct pathophysiological differences in the effects of MAC and general anesthesia that need to be considered depending on the severity of patients' underlying disease, comorbidities, and procedural-related risks.
Our aim was to provide recommendations for the use of general anesthesia with endotracheal intubation versus deep sedation without endotracheal intubation (MAC) using a modified Delphi process. We took into account patient comorbidities, procedural risk factors, and individual preferences of a group of international authors and their institutions.

Methods: To provide guidance on the anesthetic management of patients undergoing ERCP procedures, a modified Delphi approach was used. The modified Delphi approach is a validated and structured group consensus strategy to obtain expert consensus. (4,5) The modified Delphi approach uses multiple iterations to review the expert judgement and reach an agreement. Each iteration modifies the survey to incorporate feedback from the previous round until consensus emerges. It has the advantage of avoiding the influence of dominant individuals or group pressure for conformity.
In this study, a panel of 12 experts was selected to attain expert consensus regarding relevant patient management questions. An expert was defined as an individual (attending/consultant level or equal qualification) with extensive experience as an anesthesiologist or gastroenterologist with expertise in interventional endoscopy. The research question was identified as the choice of general anesthesia with endotracheal intubation versus deep sedation without endotracheal intubation, (MAC) for patients undergoing ERCP.
Survey questions were organized into five main topic domains including pathophysiology, comorbidities, procedural factors, patient management and quality metrics. Questions attributable to the five domains were created by the work groups and sent to all panel members. To add additional topic suggestions open response questions were used. Experts graded each item using a 5-point Likert scale: 'strongly disagree', 'disagree', 'no opinion', 'agree' or 'strongly agree'. We defined consensus agreement a priori as at least 75% of respondents choosing 'agree', 'strongly agree' or 'strongly disagree', 'disagree' responses in the online questionnaire iteration or at the live discussion session. Once consensus was achieved on the questions, experts used literature summaries to generate, debate and refine a list of essential facts to guide the generation of recommendations. Responses to the survey questions were analysed with descriptive statistical methods and presented as percentages.

Results: The same twelve panelists participated in all survey rounds. Panelists were based in North America, Asia and Australia. MAC was the preferred method of anesthesia in patients with high risk of postoperative nausea and vomiting (100%), low ejection fraction (83%), and in patients with low arterial blood pressure (75%). (see figure1)
The panel also agreed that patients undergoing short procedures (91%) and in the presence of experienced anesthesiologists, MAC is the preferred method. For instances where the patients were at high risk of aspiration risk (91%), or respiratory failure (100%) and hypoxia, panelists preferred general anesthesia over MAC.
Procedural factors such as gastrointestinal bleeding risk (75%), prolonged procedures (91%) high perforation risk (91%) and gastric outlet obstruction were also seen as panelists as factors that GA was preferred. Patient age and American Society of Anesthesiologists' physical status were not thought to be determinants of choosing between MAC and general anaesthesia.

Conclusions: The panel concludes that Monitored Anesthesia Care is the favored anesthesia plan for ERCP. However, an individual risk-benefit analysis which takes into account provider and institutional experience levels, comorbidities, and procedural risks is needed. The risk of intraprocedural hypoxia, hypercapnia, and apnea is greater with MAC compared to general anesthesia with endotracheal sedation. Risks of hypotension and decrease in cardiac output are higher during general anesthesia compared to MAC.

References: 1 Unplanned Hospital Encounters After Endoscopic Retrograde Cholangiopancreatography in 3 Large North American States. *Gastroenterology* **156**, 119-129.e3 (2019).

2. Adverse events associated with ERCP. *Gastrointest Endosc* **85**, 32-47 (2017).

3. Prevalence of Anesthetic and Gastrointestinal Complications of Endoscopic Retrograde Cholangiopancreatography. *Anesth Pain Med* **9**, e95796 (2019).

4 The RAND/UCLA Appropriateness Method User's Manual, Santa Monica, Calif. 2001

5 Defining consensus: a systematic review recommends methodologic criteria for reporting of Delphi studies. J Clin Epidemiol 2014; 67: 401-9

AUA 2023 Annual Meeting Scientific Abstracts

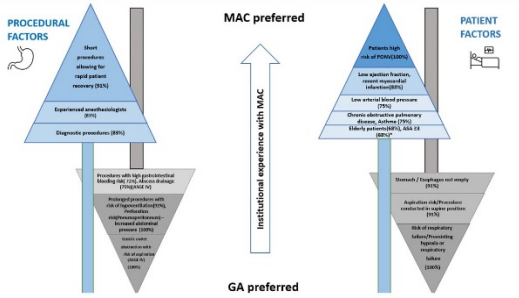

Figure1. Monitored anesthesia care versus general anesthesia in patients undergoing ERCP procedures - decision support criteria. the anesthetist's decision to provide monitored anesthesia care (MAC) versus general anesthesia with endotracheal intubation depends on procedural and patient's characteristics. Percentage values represent the level of agreement of the expert panel. The direction of the arrows indicates the expert panel's final recommendation. A modified Delphi method was used to aggregate opinions from a panel of experts. * No consensus on age of ASA; ASGE: th'American Society for Gastrointestinal Endoscopy level-I procedures e.g Endoscopic ultrasound guided trans-luminal second drainage

Table 1. ERCP consensus guideline timeline.
All the steps taken to prepare the consensus guideline are summarized below.

Activity		Description of activity
Preparation phase	Preliminary input	✓ Prepare a list of possible available panel experts
	Expert selection	✓ Select and invite expert panel members
	Topic selection	✓ State the broad question (choice of general anesthesia with endotracheal intubation versus deep sedation without endotracheal intubation (MAC)) ✓ Proposed taskforces/Pathophysiology, Patient risks, Patient Management, Quality metrics, Procedural factors)
Implementation phase	Identify taskforce members	✓ Identified taskforce members ✓ Discussed topics in each taskforce
	Send topics to panel members and receive input from panel members	✓ Identify highest priority topics in each taskforce.
	Summarize input and refine questions	✓ Based on the identification of high priority topics, questions created, and the expert panel members were asked to comment on the specificity and importance of questions (and whether they should be edited)
Feedback and results analysis phase	Send out questions to all panel members	✓ Expert panel members reviewed questions created and approved under each taskforce and were given the opportunity to agree or disagree and provide comments or suggest edits
	Receive feedback	✓ Final exercise to obtain responses on all the questions.
	Primary conclusion of topic	✓ Send out the answers to questions to all expert panel members to see if anyone has any objection to the answers received
	Discuss and revise results within the panel	✓ Meet with all the expert members and summarize and integrate key results
Consensus and recommendation phase	Summarize Key points	✓ Summarize all key points
	Consensus recommendations #1	✓ Revise and finalize Statement #1
	Consensus recommendations #2	✓ Revise and finalize Statement #2
	Consensus recommendations #3	✓ Revise and finalize Statement #3

Ambulatory Anesthesia 4 - Propofol Based Sedation During Colonoscopy Associated with Increased Serrated Polyp Detection

Aurora Quaye[1], Lynn Butterly[1], Christina Robinson[1], William Hisey[1], Todd Mackenzi[1]e, Dave Warters[1], Joseph Anderson[2]

Maine Medical Center[1] Dartmouth[2]

Introduction: Colorectal cancer (CRC) is the 2nd leading cause of cancer-related death and resection of precancerous polyps using colonoscopy substantially reduces CRC incidence. There are two groups of potential CRC precursor polyps: adenomas and serrated polyps. Serrated polyps are responsible for up to one-third of CRCs and can be difficult to detect since they are flat with indistinct borders, typically located in the proximal colon. Missed serrated lesions may be an important driver of CRC incidence. Given the significant challenges inherent to serrated polyp detection, it is critical to determine strategies to improve their identification during colonoscopy. Patients are usually sedated to mitigate discomfort during colonoscopy by receiving either mild-moderate sedation using benzodiazepines and opioids, or deep sedation using propofol. The purpose of our study was to assess whether there are significant differences in polyp detection in patients undergoing colonoscopy when propofol based sedation is used, compared to cases using mild-moderate sedation. Furthermore, we aimed to investigate the influence of propofol administration on the detection of serrated polyps vs adenomas.

Methods: After obtaining Institutional Review Board Approval, we performed a retrospective cohort study using data from 28 endoscopy practices included in the New Hampshire Colonoscopy Registry. Patients aged 50 or older with screening or surveillance exams between 1/1/2015 and 2/28/2020 were included in our analysis. Diagnostic exams, exams performed with no sedation, missing sedation or histology data, and poor bowel preparation were excluded. Patient covariates included age, sex, risk factors for serrated polyps, smoking status, Body Mass Index, and alcohol use. Data were summarized as mean (SD) or frequency (%), as appropriate. Differences between propofol vs no propofol exams were analyzed using chi square, Kruskal-Wallis test or Fisher's exact test, as appropriate. Our multivariable statistical model used logistic regression to model the occurrence of serrated polyps or adenomas while adjusting for the covariates listed above. Analyses were performed using SPSS Statistical Software version 28 (IBM SPSS Inc., Armonk, NY). A total of 54,063 exams met inclusion criteria - 24,751 exams without propofol and 29,312 exams with propofol.

Results: Aside from the percentage of patients with prior colonoscopy and smoking status, there were no meaningful differences in key characteristics between the groups (Table 1). We found a large difference in serrated polyp incidence between the mild-moderate sedation and propofol exams 24.9%, 95% CI [24.4, 25.5] vs. 34.2, 95% CI [33.7, 34.8] but only a small difference in adenoma incidence 37.3, 95% CI [36.7, 38.0] vs 39.5, 95% CI [38.9, 40.0] (Table 2). This was reflected in our regression results; exams using propofol were 57% more likely to find serrated polyps (OR 1.57 [1.51-1.63]) while only 2% more likely to find adenomas (OR 1.02 [1.01-1.03]). These differences persisted following adjustment for key confounders (Table 3).

Conclusions: In our large dataset, we identified that propofol use was associated with increased serrated polyp detection before and after adjustment for confounders. The difference in adenoma detection was substantially smaller. These findings warrant further investigation regarding the impact of propofol use during colonoscopy, particularly for serrated polyp detection, to maximize CRC prevention. Our next steps will be to determine the impact of propofol on the frequency of missed serrated polyps- an outcome not currently described in the literature. Since the majority of polyps are slow growing, two colonoscopies performed within a short period of time can identify whether polyps were missed during the first colonoscopy examination. Our subsequent study would analyze patients from our dataset with more than one colonoscopy performed within a 5year period to calculate missed colorectal adenomas and serrated polyps, with and without propofol, in patients at average and also increased risk for serrated polyps. We anticipate that this evidence will enhance personalized screening programs for colonoscopy.

References: Global colorectal cancer burden in 2020 and projections to 2040. *Transl Oncol.* 2021;14(10):101174.

Colonoscopic polypectomy and long-term prevention of colorectal-cancer deaths. *N Engl J Med.* 2012;366(8):687-696.

Colorectal Cancer Screening for the Serrated Pathway. *Gastrointest Endosc Clin N Am.* 2020;30(3):457-478.

Sessile Serrated Polyp Detection Rate of 2% or Greater Is Associated with a Lower Risk for Post-Colonoscopy Colorectal Cancer. *Official journal of the American College of Gastroenterology | ACG.* 2021;116:S128.

Propofol sedation in colonoscopy: from satisfied patients to improved quality indicators. *Clin Exp Gastroenterol.* 2019;12:105-110.

Table 1: Patient and exam characteristics, by sedation method

	No propofol (N = 24,751)	Propofol (N = 29,312)	
Patient and exam characteristics	**Mean / %**	**Mean / %**	**p-value**
Age (mean)	62.3	61.2	<0.001*
BMI (mean)	28.3	29.3	<0.001*
Male sex	49.3	48.9	0.328
First degree family history of CRC	24.7	23.5	0.005
Indication for colonoscopy screening	66.8	64.1	<0.001
surveillance	33.3	35.9	
Prior colonoscopy	71.5	67.4	<0.001
History of neoplastic findings	36.5	37.7	0.005
Regular aspirin use	31.8	30.3	<0.001
Regular NSAID use	16.0	15.0	0.006
Blood thinner use	2.2	2.3	0.497
Smoking status: current smoker	6.1	8.7	<0.001
never smoked	56.5	52.7	
Alcohol use: more than 8 drinks/wk	12.1	10.3	<0.001
Self reported health: good or better	95.2	93.4	<0.001**
poor	0.3	0.6	
Bowel preparation: excellent	32.5	27.4	<0.001
good	60.2	63.5	
fair	5.4	6.6	
missing	1.8	2.6	

* Kruskal-Wallis test
** Fisher's exact test

Table 2: Colonoscopy findings, by sedation method

	Sedation method	
	No propofol N = 24,751	Propofol N = 29,312
	% [95% CI]	% (95% CI)
At least one adenoma	37.3 [36.7, 38.0]	39.5 [38.9, 40.0]
At least one serrated polyp	24.9 [24.4,25.5]	34.2 [33.7, 34.8]

Table 3: Unadjusted and adjusted association between sedation type and risk of any neoplastic findings, adenomas, or serrated polyps (no propofol as reference)

Odds ratios for propofol use		
	Adenoma	Serrated polyp
	OR (95% CI)	OR (95% CI)
Unadjusted	1.02 (1.01 - 1.03)	1.57 (1.51 - 1.63)
Adjusted	1.07 (1.02 - 1.12)	1.47 (1.40 - 1.54)

NOTE: regression included the following covariates: Age (years over 50), patient sex, smoking status (never vs former or current), alcohol intake, BMI (centered on 25), prior colonoscopy, prior neoplastic findings, and health status (good or better vs fair or poor)

Anesthetic Pharmacology 1 - Antagonism of Propofol in Zebrafish by Altering the Electronics of Propofol Derivatives

Ceilia Leso[1], Diana Plasencia[1], Roderic Eckenhoff[2], Elizabeth White[1]

University of Pennsylvania[1] University of Pennsylvania Perleman Scho[2]

Introduction: Propofol is a commonly used intravenous anesthetic, but unlike many of the medications in the OR that can cause life-threatening hypoxia, there is no reliable way to reverse its effects except to give it time to be metabolized. The need for a clinically useful antagonist that could rescue patients from a propofol anesthetic would be welcomed by clinicians, but the route to achieving this has been historically fraught with difficulty. Based on previous work, it is thought that hydrogen bonding is a key feature of the anesthetic potency of propofol, and that alterations of this feature may confer antagonistic properties.[1,2] Presented here is a library of propofol-derived molecules that diminish the hydrogen bonding character of propofol, and an analysis of their relative potency as anesthetic antagonists.

Methods: A library of propofol analogues was designed such that it would contain various perturbations in the electronics of propofol that would weaken or enhance the hydrogen-bonding of propofol. The means of altering the electronics were categorized into three groups: hydrogen bond limiting derivatives, electron withdrawing and donating groups, and halogen substitution. Each library member was first tested for toxicity in larval zebrafish, which was determined by administering increasing concentrations of each drug to fish for a 30-minute exposure and observing for lethality immediately and after a 24-hour recovery period. Each analogue was then tested using a behavioral assay that has been previously validated to test general anesthetic potency using larval zebrafish.[3] Each compound was tested first for any innate anesthetic activity or excitatory phenotypes, and then they were co-administered with propofol to assess for additivity/synergy or antagonism. Based on quantified movement, compounds were then categorized for their ability to antagonize the activity of propofol. As an additional assessment, the proposed library was tested for their ability to bind to the 'anesthetic site' of the model protein horse spleen apoferritin (HSAF).[4, 5, 6] This binding will be correlated to anesthetic activity or antagonism in zebrafish.

Results: In vivo, molecules with structures that minimally altered hydrogen bonding electronics produced anesthetic effects in larval zebrafish while those that reduced the hydrogen bonding ability showed varying levels of antagonism. While altering the electron density around the hydrogen bond produced varying results regarding antagonism, those with halogen substitutions consistently demonstrated propofol antagonism. Competition assays to determine affinity to the HSAF 'anesthetic site' are ongoing.

Conclusions: Our results further demonstrate that the hydroxyl group and its hydrogen bond-donation is an important contributor to propofol's anesthetic effect and that abrogating this hydrogen-bonding may produce promising anesthetic antagonists. Results vary depending on the type of electronic alterations of the library molecules, but general trends can be observed such as within the halogen group. Compounds are still being tested to present a more complete analysis of the library in vivo as well as in vitro in the binding assay.

References:

1. Role for the propofol hydroxyl in anesthetic protein target molecular recognition, 6, 927-935, 2015.
2. The role of the hydroxyl group in propofol-protein target recognition: insights from ONIOM studies, 121, 5883-5896, 2017.
3. A vertebrate model to reveal neural substrates underlying the transitions between conscious and unconscious states, 10, 15789, 2020.
4. Identification of a fluorescent general anesthetic, 1-aminoanthracene, 106, 6501-6506, 2009.
5. Structural Basis for High-Affinity Volatile Anesthetic Binding in a Natural 4-Helix Bundle Protein, 19, 567-576, 2005.
6. Synthesis and Characterization of a Diazirine-Based Photolabel of the Nonanesthetic Fropofol, 12, 176-183, 2021.

Anesthetic Pharmacology 2 - Comparing Morphine and Hydromorphone Effects and Side Effects – a Crossover Study in Human Volunteers

Konrad Meissner[1], Albert Dahan[1], Erik Olofsen[1], Jane Blood[2], Johannes Wieditz[2], Evan Kharasch[3]

Universitätsmedizin Göttingen[1] Washington University School of Medicine[2] Duke University School of Medicine[3]

Introduction: Balancing between opioid analgesia and respiratory depression continues to challenge clinicians in perioperative, emergency department and other acute care settings. Morphine and hydromorphone are postoperative analgesic standards. Nevertheless, their comparative effects and side effects and relative timing remain incompletely understood. We tested the hypothesis that IV morphine and hydromorphone differ in onset, magnitude, and duration of analgesic and ventilatory effects.

Methods: We conducted a randomized crossover in healthy volunteers. Forty-two subjects received a 2-hour intravenous infusion of hydromorphone (0.05 mg/kg) and morphine (0.2 mg/kg) 1-2 weeks apart. We measured arterial opioid concentrations, analgesia in response to heat pain (maximally tolerated temperature, and verbal analog pain scores at six discreet preset temperatures to determine half-maximum temperature effect), dark-adapted pupil diameter and miosis, end-expired CO_2, and respiratory rate for 12 hours after dosing.

Results: For morphine and hydromorphone, respectively: maximum miosis was less (3.9 [3.4,4.2] vs 4.6 mm [4.0,5.0], P<0.001; median and 25%-75% quantiles) and occurred later (3.1±0.9 vs. 2.3±0.7 hours after infusion start, P<0.001; mean ± SD); maximum tolerated temperature was less (49±2 vs. 50±2°C, P<0.001); and in contrast verbal pain scores at end-infusion at the most informative stimulus (48.2°C) were greater (82±4 vs. 59±3, P<0.001). Maximum end-expired CO_2 was 47 [45,50] and 48 mmHg [46,51] (P=0.007), and occurred later (5.5±2.8 vs. 3.0±1.5 hours after infusion start, P<0.001); respiratory nadir was 9±1 and 11±2 breaths/min (P<0.001) and occurred at similar times. Area under the temperature tolerance-time curve was less for morphine (1.8 [0.0,4.4]) than hydromorphone (5.4°C-h [1.6,12.1] P<0.001)

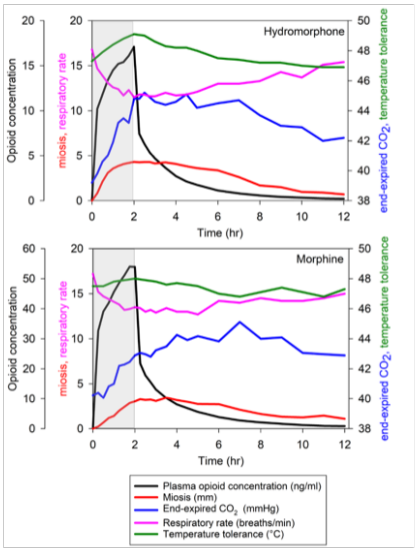

Figure1: Summary of opioid concentrations, effects and side effects. Results are the arithmetic means for 42 subjects receiving 0.05 mg/kg hydromorphone (upper panel) and 0.2 mg/kg morphine (lower panel) as a 2-hour infusion (grey bar)

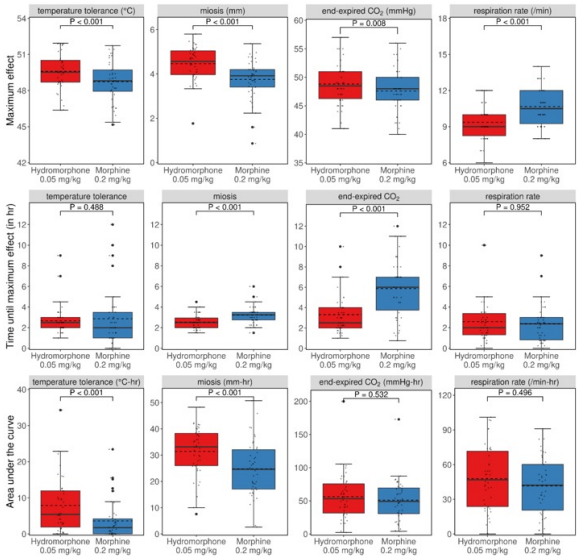

Figure 2: Morphine and hydromorphone clinical effects. (Top row) Maximum drug effect, (middle row) time to maximum drug effect, (bottom row) area under the effect-time curve. Clinical effects are analgesia (maximum tolerated temperature), miosis, end-expired carbon dioxide, and minimum respiratory rate. Dashed lines are the mean, solid lines are median. The lower and upper ends of the box correspond to the 25th and 75th percentiles, defining the interquartile range (IQR). The whiskers extend from 25th and 75th percentiles to the smallest and largest values, but no further than 1.5 * IQR from its origin, with data points lying further out defined as outliers (enlarged dots). Pairwise tests for equality of medians used Wilcoxon signed-rank tests. The corresponding P values are stated at the top in the respective panel.

Conclusions: The magnitude and time course of analgesic, respiratory and miotic effects of morphine differed significantly, as they did for hydromorphone, and differently between the two opioids. For morphine compared to hydromorphone, analgesia and analgesia relative to respiratory depression were less, onset of miosis and respiratory depression was later, and duration of respiratory depression was longer. For each opioid, timing of the various clinical effects was not coincident. These results suggest that hydromorphone may have clinical advantages compared with morphine for treating acute pain in perioperative, emergency department and other acute care settings. Results may enable more rational opioid selection.

References: Postoperative opioid administration characteristics associated with opioid-induced respiratory depression: Results from the PRODIGY trial. J Clin Anesth 2021;70:110167

Frequency and Temporal Distribution of Postoperative Respiratory Depressive Events. Anesth Analg 2021;132: 1206-1214

Opioid-induced respiratory depression increases hospital costs and length of stay in patients recovering on the general care floor. BMC Anesthesiol 2021;21: 88

Comparative clinical effects of hydromorphone and morphine: a meta-analysis. Br J Anaesth 2011;107:319-28

Anesthetic Pharmacology 3 - Discovery of a New Quinone Anesthetic Leads to Identification of a Novel Pharmacological Target in Mice

Richard Levy[1], Keren Griffiths[2], Guang Yang[3], Max Kelz[4], Yash Somnay[5]

NY Presbyterian Hosp - Columbia U[1] Columbia University[2] Columbia University Department of Anesth[3] University of Pennsylvania[4] Columbia University, Department of Anesthesiology[5]

Introduction: The mechanisms by which sedative-hypnotics induce unconsciousness, amnesia, and immobilization are poorly understood.[1] There has been a lack of new anesthetics introduced to field in the last 50 years and it is unknown if all of the pharmacologically relevant targets have been identified. Although ligand-gated ion channels are thought to play a major role in the mechanisms of anesthesia, many believe that a pharmacologically significant target resides within mitochondria. We previously found that propofol interfered with electron transfer at the level of coenzyme Q (CoQ) and induced excessive proton leak within mitochondria. We observed that synthetic CoQ analogs exert similar *in vitro* biological activity. Thus, we hypothesized that quinone analogs would induce propofol-like sedation. We tested our hypothesis using the short-chain CoQ analog, ubiquinone-5 (Ub5). We aimed to characterize the anesthetic phenotype of Ub5 in the mouse and to elucidate the source of Ub5-induced mitochondrial leak.

Methods: Care of mice was in accordance with NIH and IACUC guidelines. 51 young adult male C57/BL6 mice were randomized to a single tail vein injection of either Ub5 or vehicle. A range of Ub5 doses were chosen using a modified up-down approach. Loss of righting reflex (LORR) and latency to return of righting reflex (RORR) were determined. Total distance traveled was quantified using video tracking prior to and after injection. Real-time EEG was recorded during injection. Neuronal activity was determined *in vivo* following Ub5 injection by quantifying calcium transients in the *Thy1.2*-GCaMP6 transgenic mouse living cortex using real-time multiphoton laser imaging. In a subset of animals, Ub5 levels were quantified in forebrain immediately following injection using HPLC. Oxygen consumption and leak respiration were measured polarographically and electron transport chain enzyme complex activities were determined spectrophotometrically in isolated forebrain mitochondria in the presence of relevant concentrations of Ub5 or vehicle. Source of leak was determined in isolated mitochondria using specific inhibitors. LORR was then determined in injected Aralar$^{+/-}$ mice along with wild-type littermate controls. Significance was set at $P < 0.05$ and assessed with ANOVA, post-hoc Tukey's test and regression analysis.

Results: Ub5 immediately induced LORR over a range of doses with an ED50 of 79.5 mg/kg (95% CI 79.93-82.18). Latency to RORR correlated significantly with Ub5 dose and maxed out at 247 seconds. Total distance traveled decreased significantly following Ub5 injection and correlated inversely with dosage. Injection of 200 mg/kg Ub5 induced low-amplitude EEG changes followed by K-complexes, delta waves, spindles and burst suppression. High frequency EEG activity returned 20 minutes post-injection. Ub5 induced a significant decrease in calcium transients in the *Thy1.2*-GCaMP6 transgenic mouse cortex, indicating decreased neuronal activity. During *in vitro* exposure to relevant concentrations of Ub5, forebrain mitochondria demonstrated a dose-dependent increase in oxygen consumption and impaired membrane potential during leak respiration, indicating excessive proton leak. In isolated mitochondria, Ub5 enhanced Complex II+III activity and inhibited Complex I and IV. Inhibition of the mitochondrial aspartate-glutamate carrier, Aralar, blocked the Ub5-mediated effects on leak respiration and membrane potential in isolated mitochondria indicating that Aralar is the major source of Ub5-induced leak. The LORR curve was right-shifted in Aralar$^{+/-}$ mice with a significantly higher ED50 compared to controls.

Conclusions: Ub5 induced unconsciousness and immobilization in a manner consistent with other intravenous anesthetics. The immediate onset and rapid offset suggest a short-acting mechanism. Thus, Ub5 acts as a novel anesthetic agent. As with propofol, Ub5 induced excessive proton leak in isolated forebrain mitochondria, inhibited the ETC, and compromised the mitochondrial membrane potential. We identified Aralar as the source of Ub5-induced leak within mitochondria and Aralar mutants were relatively resistant to Ub5. Thus, excessive proton leak leading to compromise of the mitochondrial membrane potential is a contributory mechanism of anesthesia and Aralar is a novel pharmacological anesthetic target. Future work will focus on further defining the mechanism of action, resolving the safety and efficacy of Ub5, and determining if Aralar is a target of other anesthetic agents.

References: 1. Trends Pharmacol Sci. 2019; 40:464-481.

Anesthetic Pharmacology 4 - Evaluation of Two Thermal Pain Models for Assessing Morphine and Hydromorphone Comparative Analgesia in Human Volunteers

Konrad Meissner[1], Erik Olofsen[1], Albert Dahan[1], Johannes Wieditz[1], Evan Kharasch[2]

Universitätsmedizin Göttingen[1] Duke University School of Medicine[2]

Introduction: Morphine and hydromorphone are postoperative analgesic standards. Nevertheless, their comparative effects, timing, and respective variabilities, remain poorly understood. Experimental evoked human pain models for assessing drug analgesia include thermal (contact heat and cold pressor pain,) mechanical (pressure pain), electrical (transcutaneous or dental stimulation) and chemical (hypertonic saline, capsaicin) stimulation. Measuring pain threshold and/or pain tolerance, and pain models using heat pain tolerance are effective for parenteral opioids, but the optimal pain model remains unknown. We therefore evaluated IV morphine and hydromorphone onset, magnitude, duration and variability of analgesia, comparing two established heat pain assessment models.

Methods: We conducted a randomized crossover in healthy volunteers. Forty-two subjects received a 2-hour IV infusion of hydromorphone (0.05 mg/kg) and morphine (0.2 mg/kg) 1-2 weeks apart. For 12 hours after dosing, two analgesia measurement models were implemented sequentially using a Peltier-type thermode applied to the forearm (Pathway, Medoc Advanced Medical Systems, Ramat Yishay, Israel). The "method of limits" used a continuous increase from 32°C at 0.8°C/sec until a pain tolerance threshold was reached (with a safety level in place), at which point the subject pressed a button and the thermode cooled. The mean of three successive temperature measurements was the result, with the thermode moved between measurements. The "ramp and hold method" was the single application of 6 different specific temperatures (41, 43, 44.8, 46.5, 48.2, and 50°C, each applied once in random order), with the probe moved after each measurement. Subjects rated the pain at each temperature on a 0-100 verbal analogue scale (VAS). In addition, we determined the temperature eliciting half-maximum pain score using a sigmoid Emax model.

Results: Maximum tolerated temperature using the method of limits was less for morphine (49±2°C) than for hydromorphone (50±2°C, P<0.001). Area under the temperature tolerance-time curve was less for morphine (1.8 [0.0,4.4]) than hydromorphone (5.4°C-h [1.6,12.1] P<0.001). In the ramp and hold method, verbal pain scores at end-infusion at the most informative stimulus (48.2°C) were 82±4 and 59±3 (P<0.001). T_{50} at the end of the opioid infusion was 44.7± 0.4 and 46.5 ± 0.5°C for morphine and hydromorphone, respectively.

Fig 1: Maximally tolerated temperature for subjects receiving 0.2 mg/kg morphine (blue) and 0.05 mg/kg hydromorphone (red, marginal mean and 25% and 75% quantiles). Opioids were administered as a 2 h infusion (shaded area). (A) Results for each opioid. (B) Pairwise differences between opioids. Asterisks indicate significant differences between the two opioid treatments after Tukey adjustment in pairwise contrast tests on a linear mixed effect model for the maximal limit temperature.
Fig 2: Self-reported verbal pain scores (0-100) over time at six specific discrete temperatures ("ramp and hold"). (A) Results for each opioid. (B) Pairwise differences between opioids. Asterisks indicate significance between the two opioids after Tukey adjustment in pairwise contrast tests on a linear mixed effect model for VAS.
Fig 3: Relationship between thermal stimulus temperature and verbal pain scores. Lines represent the population NONMEM model fits to a sigmoidal Emax model determined by nonlinear regression. Also shown are the half-maximal temperature (T_{50}, arrow). Results are shown for (A) before (0 h), (B) 3 h after the start (1 h after the end), and 12 h after the start (10 hours after the end) of the opioid infusion.
Fig 4: Half-maximal temperature (T_{50}) over time for all 42 subjects receiving 0.05 mg/kg hydromorphone (red), 0.2 mg/kg morphine (blue), and the difference between the two (black). Results are the marginal mean with corresponding 95% confidence intervals (whiskers).

Conclusions: Results of both thermal testing models appeared equally informative. Hydromorphone, the drug with the highest tolerable temperature, also elicited the largest increase of T_{50}, representing analgesic effect. In the ramp and hold method, the most informative temperature was an intermediate one (48.2°), and higher and lower temperatures were less informative. The ramp and hold method, analyzing six temperatures, was more time consuming. Although the approach afforded a more elegant, model-dependent outcome, the ramp and hold method appeared similarly informative and more efficient.

References: Dexmedetomidine pharmacodynamics: Part II: Crossover comparison of the analgesic effect of dexmedetomidine and remifentanil in healthy volunteers. Anesthesiology 2004;101:1077-83

Analgesic effects of morphine and morphine-6-glucuronide in a transcutaneous electrical pain model in healthy volunteers. Clin Pharmacol Ther 2003;73:107-21

Sex differences in morphine analgesia: an experimental study in healthy volunteers. Anesthesiology 2000;93:1245-54

Dose-dependent effects of morphine on experimentally induced cutaneous pain in healthy volunteers. Pain 2005;116:366-374

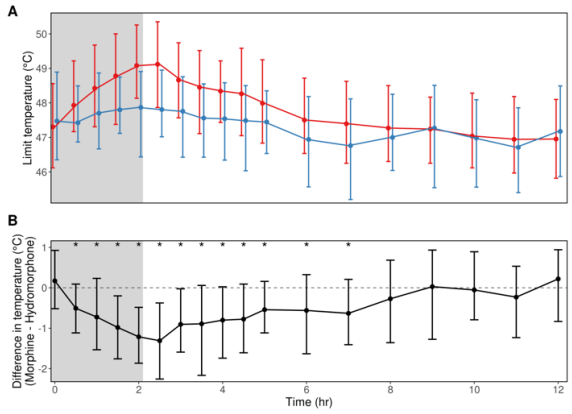
A
Limit temperature (°C)
B
Difference in temperature (°C) (Morphine - Hydromorphone)
Time (hr)

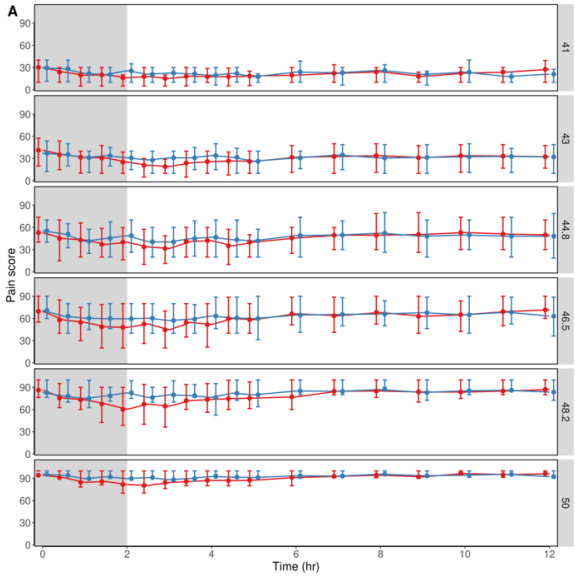
A
Pain score
41
43
44.8
46.5
48.2
50
Time (hr)

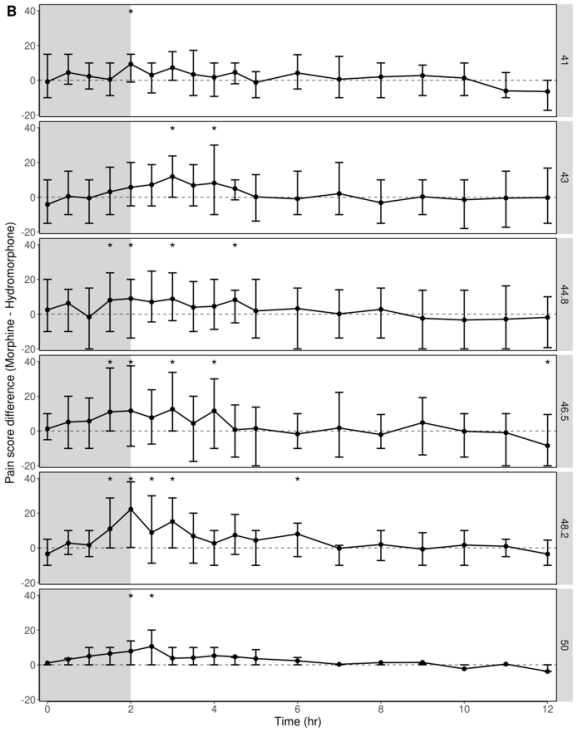
B
Pain score difference (Morphine - Hydromorphone)
41
43
44.8
46.5
48.2
50
Time (hr)

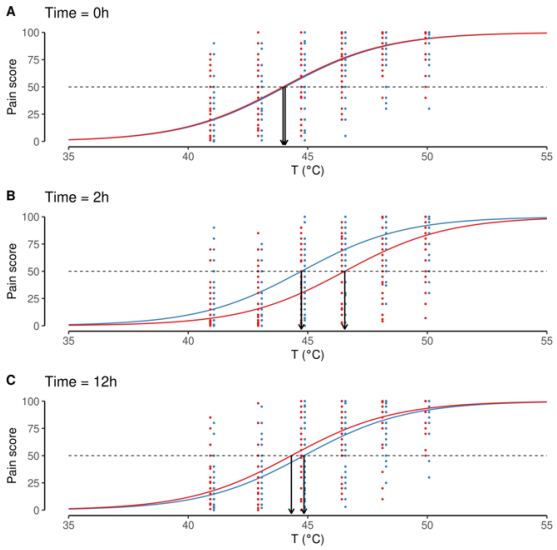
A
Time = 0h
B
Time = 2h
C
Time = 12h
Pain score
T (°C)

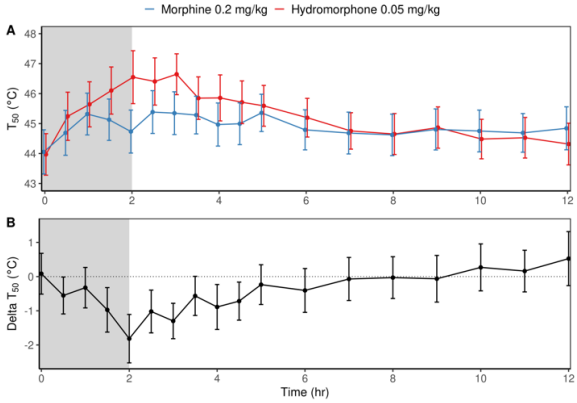
Morphine 0.2 mg/kg
Hydromorphone 0.05 mg/kg
A
T50 (°C)
B
Delta T50 (°C)
Time (hr)

Anesthetic Pharmacology 5 - Genetic background modulates responsiveness to anesthetic preconditioning in a *Drosophila melanogaster* model of traumatic brain injury

Misha Perouansky[1], Dena Johnson-Schlitz[1], David Wassarman[1]

University of Wisconsin-Madison[1]

Introduction: Anesthetic preconditioning (AP) with volatile general anesthetics (VGAs) prior to injury protects a variety of organs from damage caused by ischemia and subsequent reperfusion. We have previously shown that exposure of flies to the VGAs isoflurane (ISO) and sevoflurane (SEVO) prior to traumatic brain injury (TBI) substantially reduces early mortality and extends lifespan in the standard laboratory fly line w^{1118} mimicking AP (Fischer 2018). By contrast, exposure to hyperoxic ISO after TBI was deleterious, increasing mortality. The increase varied among wildtype fly strains (Schiffman 2020). The aim of this project is to test the hypothesis that the efficacy of AP with ISO is determined by genetic background.
Methods: In preliminary experiments we determined that maximal suppression of the MI_{24} was achieved with 15 min of 2% isoflurane immediately prior to injury. This protocol was used for AP in all fly lines. TBI was induced using a High-Impact Trauma (HIT) device (Katzenberger 2013), anesthesia was administered using the Serial Anesthesia Array (SAA) (Olufs 2018). We used flies from the DGRP collection (RAL lines, Drosophila Genetic Reference Panel). Flies were cultured at 25°C on cornmeal-molasses food. Young adult flies (1-7 day old) were subjected to TBI either with or without AP. Mortality at 24 h after TBI (Mi_{24}) was used as read-out.
Results: AP reduced the MI_{24} by >50% in the w^{1118} standard laboratory line but did not suppress mortality in Canton-S flies, another standard laboratory line. In RAL lines with similar mortality from TBI, AP resulted in variable suppression of the MI_{24}. The effect of AP across the tested RAL lines varied from suppression of mortality by over 50% to no effect (Fig 1)

Conclusions: Our findings are significant because they demonstrate that (i) a brief exposure to VGAs effectively suppresses mortality after TBI and (ii) the effectiveness of preconditioning is determined by genetic background. Cellular and molecular responses to damage are likely to be similar across tissues and evolutionarily conserved between flies and mammals. Importantly, exposure to anesthetics is largely disregarded in most animal models of TBI. Therefore, both preconditioning and genetic background are likely to affect outcomes and may further contribute to the difficulty in translating pharmacologic brain protection strategies into clinical practice.

References: Anesthetics Influence Mortality in a Drosophila Model of Blunt Trauma With Traumatic Brain Injury. A&A: 2018 Vol. 126 Issue 6 Pages 1979-1986

Ageing and genetic background influence anaesthetic effects in a D. melanogaster model of blunt trauma with brain injury. Br J Anaesth 2020 Vol. 125 Issue 1 Pages 77-86

A Drosophila model of closed head traumatic brain injury. Proc Natl Acad Sci U S A 2013 Vol. 110 Issue 44 Pages E4152-9

Genetic variability affects absolute and relative potencies and kinetics of the anesthetics isoflurane and sevoflurane in Drosophila melanogaster. Sci Rep 2018 Vol. 8 Issue 1 Pages 2348

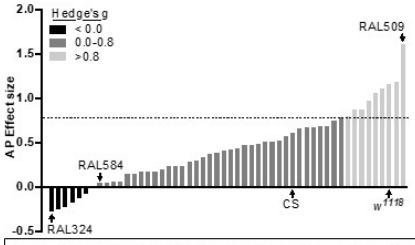

Fig. X . **Genetic background determines efficiency of AP.** Optimal AP affects the MI_{24} in 50 fly lines from the DGRP to highly variable degrees - from a modest increase to a strong .suppression indicating that sensitivity to AP is a quantitative trait.

Anesthetic Pharmacology 6 - Isoflurane alters presynaptic endoplasmic reticulum calcium dynamics in rodent hippocampal neurons

Hugh Hemmings[1], Vanessa Osman[1], Kishan Patel[1], Iris Speigel[1]

Weill Cornell Medical College[1]

Introduction: Despite their widespread clinical use, the cellular and molecular mechanisms of volatile anesthetic action remain unclear. Volatile anesthetics depress synaptic transmission by both presynaptic and postsynaptic actions including inhibition of activity-dependent Ca^{2+} influx into the presynaptic nerve terminal.[1]However, the presynaptic sites of action upstream of extracellular Ca^{2+} entry are unknown. Endoplasmic reticulum (ER) Ca^{2+} release via ryanodine receptor 1 and uptake via SERCA are essential for Ca^{2+} regulation and are possible targets for anesthetic action in neurons.[2] Mutations in skeletal muscle sarcoplasmic reticulum (SR) efflux channels are involved in volatile anesthetic-induced malignant hyperthermia (MH), a potentially fatal pharmacogenetic condition. While we understand MH in skeletal muscle in reasonable detail, the role of ryanodine receptor 1 (RyR1) in neuronal function and the impact of MH mutations on neuronal function are unknown.

Methods: Primary cultures of postnatal rat or mouse hippocampal neurons were used to test isoflurane-induced changes in ER Ca^{2+} concentration. Neurons from wild-type BALB/c mice or mice homozygous for the human MH mutation T4826I in RyR1 in a BALB/c background were transfected with ER-GCaMP6-150, an ER-targeted fluorescent Ca^{2+} sensor. Animal procedures were performed in accordance with Weill Cornell Medicine Institutional Animal Care and Use Committee regulations and conform to National Institutes of Health guidelines.

Results: Isoflurane reduced both baseline and electrical activity-induced increases in ER Ca^{2+} concentration in neurons. This was independent of concurrent activity-induced increases in presynaptic cytoplasmic Ca^{2+}concentration. Isoflurane and sevoflurane, but not propofol, inhibited ER Ca^{2+} concentration transients significantly more in neurons from MH-susceptible mice than in wild-type neurons. This mutation also markedly enhanced isoflurane-induced reductions in presynaptic cytosolic Ca^{2+} and synaptic vesicle exocytosis.

Conclusions: Depression of presynaptic Ca^{2+} entry and synaptic vesicle exocytosis by isoflurane involves effects on ER Ca^{2+} dynamics. An MH-susceptibility mutation in RyR1 markedly enhances volatile anesthetic-induced reductions in electrically-evoked ER Ca^{2+} increases, likely through enhanced efflux from the ER. These implicate anesthetic effects on ER Ca^{2+} handling in their presynaptic effects, with potential pathophysiological implications for the brain of MH mutations.

References: 1. *Proc Natl Acad Sci USA* 2015; 112, 11959-64; 2. *Neuron* 2017; 93, 867-881

Anesthetic Pharmacology 7 - Morphine and Hydromorphone Effects and Side Effects Interindividual Variabilities – a Crossover Study in Human Volunteers

Konrad Meissner[1], Albert Dahan[1], Erik Olofsen[1], Johannes Wieditz[1], Evan Kharasch[2]

Universitätsmedizin Göttingen[1] Duke University School of Medicine[2]

Introduction: Pharmacokinetic and pharmacodynamic investigations of opioids typically focus on and compare population parameters (means and medians), yet interindividual variability in pharmacokinetics, pharmacodynamics and clinical effects (such as analgesia and respiratory depression) may be a major determinant of therapeutic response and safety. We tested the hypothesis that IV morphine and hydromorphone differ in the interindividual variability of analgesic and ventilatory effects.

Methods: We conducted a randomized crossover study in healthy volunteers. Forty-two subjects received a 2-h intravenous infusion of hydromorphone (0.05 mg/kg) and morphine (0.2 mg/kg) 1-2 weeks apart. We measured arterial opioid concentrations, analgesia in response to heat pain (maximally tolerated temperature, and verbal analog pain scores at discreet preset temperatures to determine temperature producing half-maximum effect (T_{50}) and slope (γ) of the sigmoid Emax curve), dark-adapted pupil diameter and miosis, end-expired CO_2, and respiratory rate, for 12 h after dosing. Interindividual variability in opioid effects, based on the coefficients of variation (%CV), were determined for analgesia, miosis, and respiratory depression.

Results: For analgesia, CV was 3% for both opioids based on maximum tolerated temperature, 95% and 145% for hydromorphone and morphine based on the area under the maximum tolerated temperature vs time curves, and was not significantly different between the two drugs based on T_{50} and γ. For miosis, variation in peak effect was 17% and 24%, respectively, for hydromorphone and morphine, and 29% and 43% based on the areas under the curve. For hydromorphone and morphine respiratory depression, variation was 7% and 12% for maximum end-expired CO_2, 63% and 60% for areas under the CO_2 curve, 15% and 14% for minimum respiratory rate, and 58% and 63% based on the areas under the respiratory rate curve.

Fig 1: Morphine and hydromorphone clinical effects. (Top row) Maximum drug effect, (middle row) time to maximum drug effect, (bottom row) area under the effect-time curve. Clinical effects are analgesia (maximum tolerated temperature), miosis, end-expired carbon dioxide, and minimum respiratory rate. Results are for 42 subjects receiving 0.2 mg/kg morphine and 0.05 mg/kg hydromorphone (individual values displayed as small dots). Dashed lines are the mean, solid lines are median. The lower and upper ends of the box correspond to the 25th and 75th percentiles, defining the interquartile range (IQR). The whiskers extend from 25th and 75th percentiles to the smallest and largest values, but no further than 1.5 * IQR from its origin, with data points lying further out defined as outliers (enlarged dots). Pairwise tests for equality of medians used Wilcoxon signed-rank tests. The corresponding P values are stated at the top in the respective panel.

Conclusions: Together, these observations do not support the hypothesis that morphine and hydromorphone differ in interindividual variability of their analgesic and respiratory depressant effects.

References: Prediction of Opioid-Induced Respiratory Depression on Inpatient Wards Using Continuous Capnography and Oximetry: An International Prospective, Observational Trial. Anesth Analg 2020;131:1012-1024

Opioid-Induced Respiratory Depression: Is Hydromorphone Safer Than Morphine? Anesth Analg 2021;132: e60

The side effects of morphine and hydromorphone patient-controlled analgesia. Anesth Analg 2008;107:1384-9

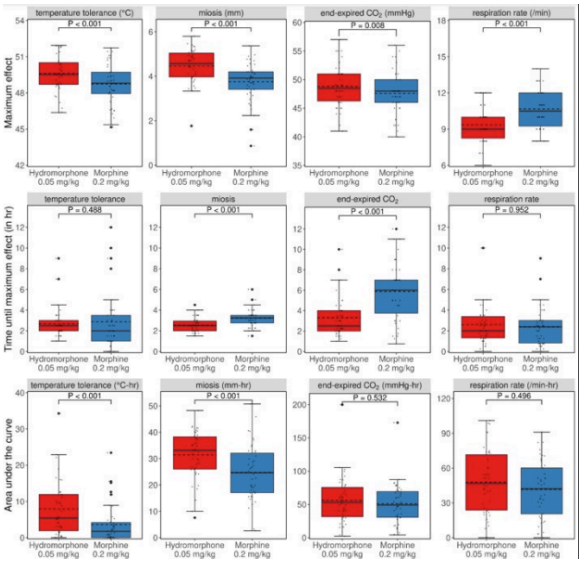

Anesthetic Pharmacology 8 - Raptor Controls Hypoxic Death in *C. elegans* via the Translation Machinery

Mike Crowder[1], Abraham Correa-Medina[2], Omar Itani[2], cong Xu[3], Chun-ling Sun[3], Brock Grill[3], C. Michael Crowder[3]

Department of Anesthesiology and Pain Medicine[1] University of Washington School of Medicine[2] University of Washington[3]

Introduction: Hypoxic cellular injury, in the form of stroke and myocardial infarction, is the leading cause of death and disability in the US. Previous studies suggest that mammalian target of rapamycin (mTOR) inhibitors have neuroprotective properties in experimental stroke models (1). mTOR is a key regulator of anabolic metabolism by promoting protein synthesis, mitochondrial biogenesis, and inhibiting autophagy (2). The mTOR signaling pathway is evolutionarily conserved and includes proteins forming two distinct mTOR complexes, mTORC1 and mTORC2. mTORC1 comprises three core components, mTOR, Raptor, and mLST8. From an unbiased screen for hypoxia resistant *C. elegans* mutants, we report here the discovery of a partial loss-of-function mutation in the *C. elegans* Raptor gene, *daf-15,* that confers hypoxia resistance and the performance of genetic epistasis experiments to define the pathways whereby it controls hypoxic cellular death

Methods: Assays for hypoxic death of *C. elegans* were performed as previously described (3, 4). Mutagenesis screen, genetic mapping, whole genome sequencing, and mutant identification were performed as described (3). Compound mutants were generated as previously described (3). All hypoxic assays were performed with a minimum of three biological replicates (performed independently on different days), each of which was composed of three technical replicates of at least 30 animals/technical replicate. Data are expressed as mean ± SD, and statistical differences were determined by two-tailed unpaired t-tests.

Results: Through an unbiased whole-genome mutagenesis screen in *C. elegans* for mutants resistant to death from severe hypoxia, we isolated the *gc67* mutation. Whole genome sequencing and genetic mapping found that *gc67* carried a temperature sensitive missense mutation in the *daf-15* gene, which encodes the sole *C. elegans* ortholog of Raptor. CRISPR/CAS9 engineering of the gc67 mutation into two independent strains confirmed that *daf-15(gc67)* mutation produced hypoxia resistance (**Fig. 1**). To our knowledge, *daf-15(gc67)* represents the first viable Raptor mutant in any metazoan. Raptor functions as an essential component of the mTORC1 complex, which is a positive regulator of translation, mitochondrial biogenesis, and a negative regulator of autophagy (2). To test whether *daf-15(gc67)* reduces translation rate, we measured incorporation of ^{35}S-methionine and puromycin into nascent proteins *in daf-15(gc67)* and the wild-type strain and found that *daf-15(gc67)* had reduced incorporation of both, indicative of reduced translation rate (**Fig. 2**). We have previously isolated mutations in *C. elegans* that suppress the hypoxia resistance of mutations that similarly reduce global translation rate in *C. elegans* (**Fig. 3**) (3). We tested whether two of these translation machinery suppressors also suppress the hypoxia resistance of *daf-15(gc67)* or the *daf-15*(Crispr). We found that the loss-of-function mutations in *larp-1* and *ncl-1*, which encode negative regulators of translation, strongly suppressed *daf-15(gc67)* hypoxia resistance (**Fig. 4**). However, a gain-of-function mutation in *aatf-1*, which encodes a positive regulator of ribosomal biogenesis, did not suppress the hypoxia resistance of *daf-15*(Crispr) (**Fig. 5**).

Conclusions: To our knowledge, we have isolated the first viable Raptor reduction-of-function mutant in a metazoan. The *daf-15* Raptor(*gc67*) mutation offers the potential to test specific hypotheses with genetic reagents and to screen for and identify novel components of the mTORC1 signaling pathway relevant to hypoxic injury (work in progress). *daf-15*(*gc67*) is hypoxia resistant and has reduced global protein synthesis. Specific negative regulators of the translation machinery are essential for the *daf-15*(*gc67*) hypoxia resistance phenotype. Pharmacological regulators of mTORC1, particularly those regulating translation, should be further evaluated in experimental mammalian models of ischemic injury.

References:

1. J Cereb Blood Flow Metab. 2019;39(1):20-35.
2. Curr Opin Cell Biol. 2017;45:72-82.
3. Current Biology. 2021;31(1):128-37.
4. Science. 2002;296(5577):2388-91.

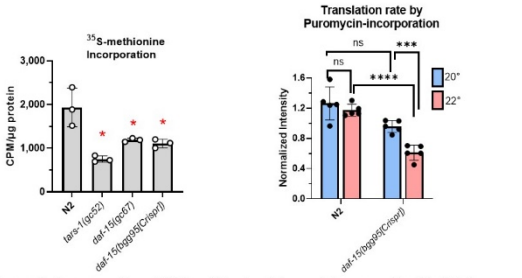

Figure 2. Incorporation of ^{35}S-methionine into protein normalized to total protein in lysate. Worms are fed ^{35}S-methionine labelled bacteria for six hours then lysed and protein purified for scintillation counting and protein quantification. Mean +/- SD of three biologic replicates. * - p < 0.01 vs N2. Quantification of western blots probed with puromycin antibody and normalized to actin of indicated strains treated with puromycin after growth to adults at 20° or 22° . Each dot represents an independent experiment, mean +/- SD. *** p<0.001, **** p<0.0001, ns-not significant @ p<0.01

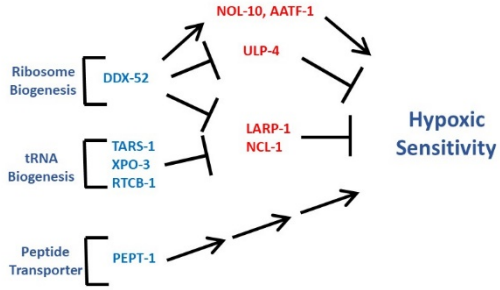

Figure 3. Suppressors of Hypoxia Resistant Mutants are Translation Machinery Regulators. Reduction-of-function hypoxia resistant mutants. Suppressors of hypoxia resistance

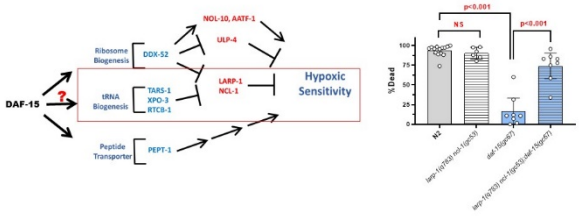

Figure 4. Negative Translation Regulators LARP-1 and/or NCL-1 are Required for *daf-15(gc67)* Hypoxia Resistance. Hypoxic death of strains with indicated genotypes after 20 hr hypoxic incubation. mean +/- SD; Data points are independent biological replicates, minimum 50 animals/replicate.# - p<0.01 vs N2, **** - p<0.0001, ** - p<0.01, 2-tailed unpaired t-test.

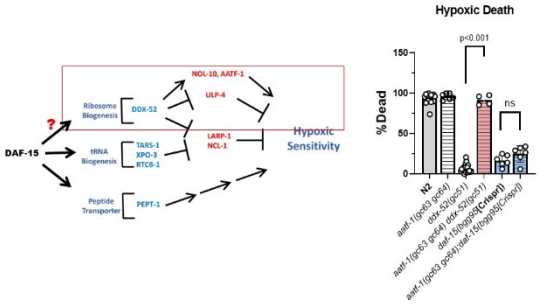

Figure 5. The Ribosomal Biogenesis Positive Regulator AATF-1 is <u>not</u> Required for *daf-15*(rf) Hypoxia Resistance. Hypoxic death of strains with indicated genotypes after 20 hr hypoxic incubation. Data points are independent biological replicates, minimum 50 animals/replicate. mean +/- SD. # - p<0.01 vs N2, **** - p<0.0001, ** - p<0.01, 2-tailed unpaired t-test.

Anesthetic Pharmacology 9- Use of Neuromuscular Blocking and Reversal Agents Across the Spectrum of Renal Impairment Undergoing Major Inpatient Surgery: A Retrospective Observational Cohort Study

Douglas Colquhoun[1], Elizabeth Jewell[1], Graciela Mentz[1], Ruth Bickett-Hickok[2], Sachin Kheterpal[1], Sathish Kumar[3]

University of Michigan[1] UCLA David Geffen School of Medicine[2] Michigan Medicine[3]

Introduction: Since being introduced to the market, sugammadex has been widely adopted for the reversal of neuromuscular blockade. Its use (compared to neostigmine) is associated with lower risks of residual neuromuscular block in PACU and potentially reduced risk of pulmonary complications.[1,2] However, the FDA dose label advises against its use in patients with severe renal impairment (eGFR < 30). Limited data exists regarding it's use in patients with renal impairment.[3,4] We sought to assess how neuromuscular blockade and reversal patterns have changed across the continuum of renal function in the years after introduction of sugammadex, in particular the choice between rocuronium/sugammadex (roc/sug) and cisatracurium/neostigmine (cis/neo). We hypothesized that over time, the odds of receiving cisatracurium-neostigmine for neuromuscular blockade and reversal in patients with severe renal impairment would decrease.

Methods: After obtaining IRB approval (HUM00186906), we queried our institutional research database for cases performed between January 1st, 2017 to December 31st, 2020. We included general anesthetics with an endotracheal tube, extubated in the operating room, with a preoperative creatinine value, for surgeries greater than 2 hours with an associated inpatient admission. Patients must have received a non-depolarizing neuromuscular blocking agent: rocuronium (>10 mg), vecuronium (>4mg) or cisatracurium (t> 4mg) and either sugammadex (total dose between 1.8mg/kg and 4.4mg/kg) or neostigmine (total dose between 27-77 mcg/kg). Cases were excluded if more than one class of non-depolarizing neuromuscular blockade agent or more than one reversal agent were administered, were ASA Physical Status classification 5 or 6 or if the case required Cardiopulmonary bypass or organ transplantation.

We classified the cases into a primary neuromuscular blockade and reversal strategy and calculated the incidence of each strategy over the study period. We compared these groups using standardized differences. Subsequently using generalized estimating equations we modeled the binary outcome of use of cisatracurium/neostigmine vs. rocuronium/sugammadex. The primary exposure was eGFR categorized according to CKD stages. The model included age, co-morbidity burden (as measured by Elixhauser comorbidity index), BMI (WHO classification), ASA Physical Status Classification, anatomical region of surgery and length of surgical procedure.

Results: After application of inclusion and exclusion criteria, a total of 34,856 cases remained. These were classified into primary blockade and reversal strategies: 25,539 received roc/sug and 1,869 received cis/neo. Remaining cases involved other strategies including Rocuronium/Neostigmine (n=5,606). The following analysis included only Roc/Sug and Cis/Neo groups.

The use of cis/neo changed over the study period 18.2% (n=214) of cases in Q1 2017 vs 2.4% (n=48) of cases in Q4 2020, p=<0.001 (Figure 1), decreasing by 12.9 cases per quarter across the study period ($p < 0.001$). The mean eGFR within cases who received cis/neo group was 69.5 ml/min in Q1 2017 and 24.2 ml/min in Q4 2020 p=<0.001 (Figure 2), an decrease of 3.7 ml/min per quarter ($p<0.01$). Full details on these groups are presented in Table 1.

In multivariate models, we calculated the odds of receiving cis/neo across time and across eGFR strata, with a case in 2017 with eGFR > 90 used as a reference. The models included age, sex, number of Elixhuaser comorbidities present, obesity (classified), surgical service and case duration. These results are presented in Figure 3. Adjusted p-values were calculated for differences in odds across time. Statistically significant differences were noted in the CKD 1-3B strata (all $p < 0.001$), but not in CKD 4 ($p = 0.11$) and CKD 5 ($p = 0.98$) strata.

Conclusions: In this single center study, the use of cisatracurium/neostigmine decreased and was predominantly restricted to those with severe renal impairment by the end of study period. The odds of receiving cisatracurium/neostigmine decreased over time within those with CKD 1-3B, but despite large differences in odds ratio over time, did not achieve statistical significance in those with CKD 4/5 due to the small numbers of events. Future work should focus on the impact of institutional and anesthesiologist effects in this practice pattern changes, alongside if differences in patient outcomes are noted in those with severe renal impairment with each blockade and reversal strategy.

References:

1. Cochrane Database Syst Rev. 2017 Aug 14;8(8):CD012763.
2. Anesthesiology. 2020 Jun;132(6):1371-1381.
3. Can J Anaesth. 2020 Dec;67(12):1789-1797
4. Anesth Pain Med (Seoul). 2022 Oct;17(4):371-380

Table 1: Population Characteristics of those in the Rocuronium/Sugammadex and Neostigmine/Cisatracurium Groups

		Rocuronium/ Sugammadex (N=25539)		Neostigmine/ Cisatracurium (N=1869)		Standardized Difference
		N	%	N	%	
Sex	Female	12,697	49.7	931.00	49.8	0.01
	Male	12,840	50.3	938.00	50.2	
	Unknown	2	0	0.00	0	
ASA Physical Status	1	413	1.6	38.00	2	0.48
	2	7,582	29.7	320.00	17.1	
	3	15,970	62.5	1,131.00	60.5	
	4	1,574	6.2	380.00	20.3	
Year Case Performed	2017	3,573	14	889.00	47.6	0.82
	2018	7,151	28	454.00	24.3	
	2019	8,078	31.6	283.00	15.1	
	2020	6,737	26.4	243.00	13	
Surgical Service	ENT	1,077	4.2	35.00	1.9	0.58
	General Surgery/Transplant	4,977	19.5	306.00	16.4	
	Gynecology	2,288	9	321.00	17.2	
	Neurosurgery	3,402	13.3	160.00	8.6	
	NORA	3,580	14	444.00	23.8	
	Orthopedic Surgery	2,849	11.2	80.00	4.3	
	Other Surgical Service	116	0.5	13.00	0.7	
	Plastic Surgery	1,034	4	26.00	1.4	
	Thoracic Surgery	1,924	7.5	49.00	2.6	
	Urology	3,042	11.9	270.00	14.4	
	Vascular Surgery	1,250	4.9	165.00	8.8	
Additional Anesthetic Type	Regional Block	1,208	4.7	54.00	2.9	0.10
	Neuraxial Technique	2,727	10.7	114.00	6.1	0.17
CKD Stage Based on Pre-op eGFR	CKD 1 (eGFR >= 90 ml/min)	12,938	50.7	423.00	22.6	1.46
	CKD 2 (eGFR 60-90 ml/min)	9,825	38.5	258.00	13.8	
	CKD 3a (eGFR 45-60 ml/min)	2,042	8	174.00	9.3	
	CDK 3b (eGFR 30-45 ml/min)	648	2.5	269.00	14.4	
	CKD 4 (eGFR 15-30 ml/min)	75	0.3	316.00	16.9	
	CKD 5 (eGFR <15 ml/min)	8	0	429.00	23	
WHO Obesity Classification	Missing	82	0.3	13.00	0.7	0.13
	Underweight	453	1.8	34.00	1.8	
	Normal Weight	5,630	22	491.00	26.3	
	Pre-Obese	7,890	30.9	577.00	30.9	
	Obese - Class 1	5,632	22.1	384.00	20.5	
	Obese - Class 2	3,176	12.4	217.00	11.6	
	Obese - Class 3	2,676	10.5	153.00	8.2	
		Mean	SD	Mean	SD	Difference
Age In Years		57.4	15.6	57.2	16.9	0.01
Case Duration (Minutes)		235.3	108.4	233.4	108.4	0.02
Cisatracurium Administered (mg)		Not Reported		27.7	16.5	-
Neostigmine Administered (mcg/kg)		Not Reported		41.4	7.6	-
Rocuronium Administered (mg)		123.6	62.0	Not Reported		-
Sugammadex Administered (mg/kg)		2.5	0.7	Not Reported		-

Figure 1: Percentage of Cases Recieving Each Blockade and Reversal Strategy (Dichotimized) By Calendar Quarter

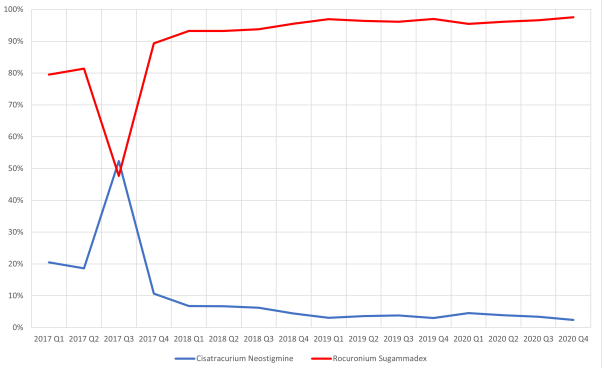

Figure 2: Mean Estimated Glomerular Filtration Rate By Calendar Quarter Within Each Blockade/Reversal Group

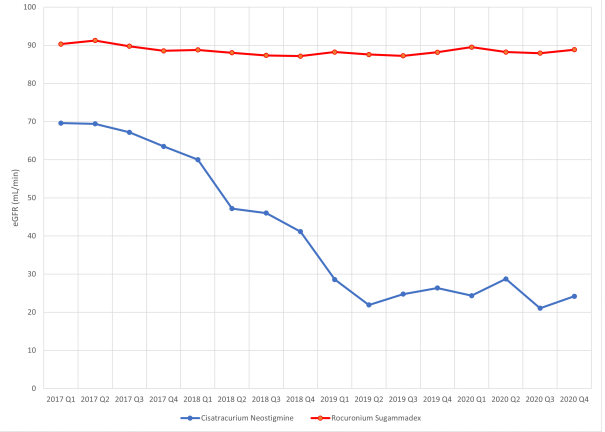

Figure 3: Odds of Receiving Cisatracurium-Neostigmine Across CKD Stage and Time

** Reference Category*

CKD Stage/eGFR	2017	2018	2019	2020
CKD 1 (eGFR >= 90)	1* (95% CI 1-1)	0.15 (95% CI 0.12-0.19)	0.01 (95% CI 0.01-0.03)	0.02 (95% CI 0.01-0.03)
CKD 2 (eGFR 60-90)	1.47 (95% CI 1.18-1.82)	0.17 (95% CI 0.12-0.23)	0.04 (95% CI 0.02-0.07)	0.03 (95% CI 0.01-0.05)
CKD 3A (eGFR 45-60)	6.01 (95% CI 4.44-8.14)	0.81 (95% CI 0.56-1.18)	0.27 (95% CI 0.15-0.47)	0.22 (95% CI 0.11-0.47)
CKD 3B (eGFR 30-45)	27.9 (95% CI 18.6-41.7)	5.63 (95% CI 3.86-8.21)	2.07 (95% CI 1.34-3.19)	2.14 (95% CI 1.33-3.43)
CKD 4 (eGFR 15-30)	173 (95% CI 74-401)	72.5 (95% CI 40.1-130)	53.1 (95% CI 30.3-93.2)	54.9 (95% CI 32.0-94.0)
CKD 5 (eGFR < 15)	998 (95% CI 213-4665)	635 (95% CI 159-2527)	496 (95% CI 157-1565)	664 (95% CI 170-2582)

Year

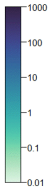

Anesthetic Pharmacology 10 - Altering organelle trafficking in neurons alters response to anesthetics *in vivo*

Victoria Bedell[1], Priya Dubey[1], Michael Pack[1], Max Kelz[2], Roderic Eckenhoff[3]

Hospital of the University of Penn[1] University of Pennsylvania[2] University of Pennsylvania Perleman Scho[3]

Introduction: Worldwide, it is estimated that more than 230 million major surgical procedures are performed under general anesthesia each year. Despite our finesse with general anesthetic medications, we still do not fully understand how these small, structurally diverse compounds induce unconsciousness. A great deal of work has been done to identify the proteins targeted by anesthetics. Previous studies has shown that one of the biochemical targets of propofol and etomidate is the motor domain of kinesin motor proteins[1]. Additionally, it has been shown in cell culture that propofol decreases anterograde vesicular trafficking in neurons[2]. However, it is still unknown if this alteration in trafficking alters anesthetic sensitivity *in vivo*. To explore how kinesin movement affects anesthetic response, we employed the larval zebrafish model and obtained loss of function mutants to two key proteins. Kinesin 5Aa (*kif5Aa*) has been shown to be important in organelle trafficking down the synapse of neurons[3]. Kinesin binding protein (*kbp*) is a key regulator and removes kinesin proteins from microtubules[4]. We used these two mutations to explore how kinesin affects anesthetic response. To alter the energy available for organelle trafficking we added 2-deoxy-D-glucose (2-DG) to decrease glycolysis *in vivo*.

Methods: Using 5 days post fertilization (dpf) zebrafish larvae, we used a previously validated behaviors, spontaneous movement as a surrogate for sedation and the startle response to a tap as a surrogate for general anesthesia, to assess the response to anesthesia over two hours[5,6]. Hill curves were created to obtain the EC50 of propofol and etomidate with and without 2-DG.

Results: We found that, using our sedation phenotype, the *kif5Aa* mutants demonstrated a statistically significant 2-3-fold sensitivity to propofol and etomidate that was consistent over time. Addition of 2-DG did not alter this phenotype. Interestingly, when testing the general anesthetic, tap, phenotype there was no differences early. However, over time the *kif5Aa* became more sensitive to both propofol and etomidate. This phenotype did not change with the addition of 2-DG. When testing the *kbp* mutant, we saw a similar response to propofol in the general anesthetic behavioral phenotype. The mutants demonstrated a significant sensitivity over time. Interestingly, there was no difference when testing etomidate.

Conclusions: Using the 5 dpf larval zebrafish, we found that both *kif5Aa* and *kbp* were sensitive to propofol over time. However, the *kbp* mutant showed no change in response to etomidate. This suggests that delivery of intracellular organelles to the synapse is important for anesthetic sensitivity *in vivo*. Using these mutations, we will be poised to understand how differential organelle trafficking in neurons alters anesthetic sensitivity *in vivo*. Moreover, the transparent nature of the larvae will allow us to fully understand how these genes combined with different anesthetics affect neural signaling pathways.

References:

1. Proc Natl Acad Sci U S A 2017; 114: E4281-E4287
2. Mol Biol Cell 2022; 33: ar119
3. J Neurosci 2014; 34: 14717-32
4. Curr Biol 2016; 26: 849-61
5. Sci Rep 2020; 10: 15789
6. Anesthesiology 2019; 131: 1276-1291

Anesthetic Pharmacology 11 - Effect of Intraoperative Methadone on Postoperative Pain and Opioid Consumption in Oral and Maxillofacial Surgeries

Fei Wu[1], JP Wang[1], Hao Deng[1], Rupeng Li[1], Ariel Mueller[1], Timothy Houle[1]

Massachusetts General Hospital[1]

Introduction: There has been growing evidence that intraoperative methadone helps reduce postoperative pain and opioid consumption in various surgeries. However, it has not yet been studied in oral and maxillofacial (OMF) surgeries.
Methods: Following the Partners Human Research Committee approval, a retrospective cohort study identified 185 patients who had OMF surgeries longer than 4 hours between June 30, 2016 to July 1, 2022. Among them, 17 patients were exposed to intraoperative methadone (5-10mg). 168 patients were identified as the control subjects. The postoperative pain score and opioid consumption in morphine milliequivalent (MME) in PACU, 6 hours after surgery and 12 hours after surgery were compared.

Results: The median (IQR) pain score for methadone group (M group) in PACU, first 6 hours postoperatively and first 12 hours postoperatively were 0.00 [0.00, 5.50], 2.00 [0.00, 4.50], 2.00 [1.50, 4.50]; and those for routine group (R group) were 5.00 [2.00, 7.00], 5.00 [3.00, 6.50], 5.00 [3.00, 6.12] respectively. There were statistically significant differences between the pain scores of M group and R group at all three time points (p=0.045, 0.024 and 0.024). After multivariable analysis, the differences remained statistically significant. The total MME (IQR) for M group in PACU, first 6 hours postoperatively and first 12 hours postoperatively were 4.51 [2.52, 7.70], 4.36 [3.35, 9.86], 6.75 [4.50, 9.86]; those for R group were 5.03 [3.02, 10.03], 5.60 [3.76, 10.48], 8.85 [4.75, 14.00]. There was no statistically significant difference between the two groups at any of the three time points (p=0.527, 0.557, 0.396).

Conclusions: a single dose of intraoperative methadone improves postoperative pain after OMF surgeries but does not reduce postoperative opioid consumption. Future comprehensive large-scale studies are needed to validate the safety and efficacy of methadone use in different surgical populations.

References:

1.J Oral Maxillofac Surg 2018;76:2285-95.
2.Anesth Analg 2019;129:1723-32.

Table 1 Demographic Characteristics for all Participants (N =185)

		Methadone group	Routine Group	SMD
Number		17	168	
Age (mean (SD))		38.0 (14.1)	44.5 (17.1)	0.412
Gender (%)	Female	13 (76.5)	127 (75.6)	0.021
	Male	4 (23.5)	41 (24.4)	
Race (%)	Asian	0 (0.0)	7 (4.2)	0.524
	Other	1 (5.9)	11 (6.5)	
	Black	0 (0.0)	10 (6.0)	
	NA	0 (0.0)	3 (1.8)	
	White	16 (94.1)	137 (81.5)	
Weight kg (mean (SD))		61.2 (12.7)	72.5 (19.7)	0.687
BMI (mean (SD))		22.6(5.0)	26.0 (6.1)	0.603
ASA (%)	1	3 (20.0)	20 (13.2)	0.483
	2	7 (46.7)	97 (63.8)	
	3	4 (26.7)	35 (23.0)	
	4	1 (6.7)	0 (0.0)	
Height cm (mean (SD))		164.7 (9.9)	166.6 (9.2)	0.203
Opiod history (%)	No	4 (23.5)	74 (44.0)	0.444
	Yes	13 (76.5)	94 (56.0)	

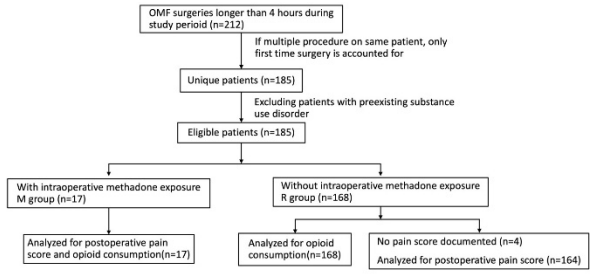

Fig.1 Patient enrollment and allocation to methadone and routine groups

Table 3 Postoperative Opioid Consumption in MME

	Methadone Group (n=17)	Routine Group (n=168)	P Value
In PACU	4.51 [2.52, 7.70]	5.03 [3.02, 10.03]	0.527
6hr postop	4.36 [3.35, 9.86]	5.60 [3.76, 10.48]	0.557
12hr postop	6.75 [4.50, 9.86]	8.85 [4.75, 14.00]	0.396

Table 2 Postoperative Pain Score

	Methadone Group (n=17)	Routine Group (n=164)	P Value
In PACU	0.00 [0.00, 5.50]	5.00 [2.00, 7.00]	0.045*
6hr postop	2.00 [0.00, 4.50]	5.00 [3.00, 6.50]	0.024*
12hr postop	2.00 [1.50, 4.50]	5.00 [3.00, 6.12]	0.024*

Anesthetic Pharmacology 12 - How to Wake Up a Zebrafish: Alkyl-derivatives of Propofluor as Antagonists of Anesthesia

Elizabeth White[1], Diana Plasencia[1], Alexys Knighton[1], Liam Rodgers[1], Roderic Eckenhoff[2]

University of Pennsylvania[1] University of Pennsylvania Perleman Scho[2]

Introduction: The introduction of general anesthesia for "painless" surgery is one of the largest advancements ever made in medicine, yet anesthetics are among the most dangerous drugs in clinical use due to their remarkably narrow therapeutic indices. It is ironic that we have antagonists to nearly every drug commonly administered in the OR, except for the anesthetics themselves.[1] The availability of anesthetic antagonists could have significant benefit to clinical practice and improve the overall safety of anesthetics if achievable. Multiple approaches for anesthetic antagonism have been attempted,[2-4] but one promising development could be a fluorine-substituted propofol-derivative (called propofluor) that has previously been shown to antagonize propofol-induced anesthesia in tadpoles and zebrafish.[5-6] Ways of further exploring this phenomenon are expansive, but our initial focus has been on evaluating the structure-activity-relationship of additional propofol and propofluor analogues to define the chemical elements necessary for this antagonistic effect. Here we present an initial library of propofluor-derived compounds that explores the effect of the alkyl-arrangement of the 'arms' of propofluor and the ability of these derivatives to antagonize propofol-induced anesthesia. This data will expand our still preliminary understanding of this novel class of molecules.

Methods: A 12-member library of molecules purchased from commercial vendors, included custom propofluor derivatives. These compounds consisted of variations in alkyl arm length and position with maintenance of a fluorobezene core in each molecule. In 5 dpf (days post fertilization) larval zebrafish, compounds were first tested for toxicity by measuring lethality at 24 hours after a 30-minute exposure of compounds high enough to calculate an LD_{50}. Each molecule was also tested for anesthetic activity using previously published measures of spontaneous swimming and response to tap stimulus.[7] These same observations were repeated with co-administration of propofol, sevoflurane and isoflurane to test for additivity or antagonism. All experimental procedures with zebrafish were approved by the University of Pennsylvania Institutional Animal Care and Use Committee (IACUC).

Results: All compounds showed far less toxicity than propofol, and when co-administered with propofol there were minimal changes in the LD_{50} compare to propofol alone. Multiple library members showed antagonism of propofol anesthesia, with little to no antagonism of sevoflurane and isoflurane. Interestingly one member (compound 10) showed significantly more antagonism by measures of spontaneous movement compared to the parent compound propofluor. Two different library members (compounds 11 and 13) showed far more antagonism than any other member when measured by response to tap stimulus, but this finding did not hold true for measures of spontaneous movement.

Conclusions: This initial systematic analysis of the alkyl configuration of propofluor analogues has revealed propofluor analogues that were less toxic than propofol and may be more potent anesthetic antagonists than propofluor in this larval zebrafish model. Further testing in other animal models is warranted, and additional analogues exploring electronic modifications, rather than mere allosteric changes, is in progress.

References: 1. *Anesth. Analg.* **2012**, *114* (5), 924–926.

2. *J. Neurophysiol.* **2014**, *111* (6), 1331–1340.

3. *Perioper. Med.* **2012**, *116* (5), 998–1005.

4. *PLOS One* **2015**, *10* (7).

5. *ACS Chem. Neurosci.* **2015**, *6* (6), 927–935.

6. *ACS Chem. Neurosci.* **2021**, *12* (1), 176–183.

7. *Sci. Rep.* **2020**, *10* (1), 1–10.

Anesthetic Pharmacology 13 - Propofol binding sites on ryanodine receptor 1

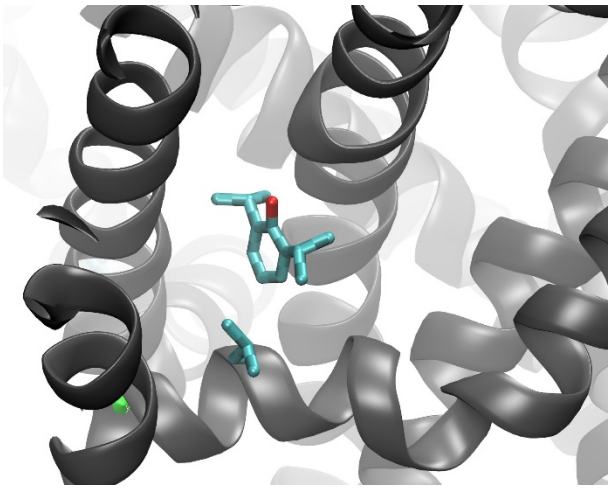

Thomas Joseph[1], Weiming Bu[1], Omid Haji-Ghassemi[1], Kellie Woll[1], Grace Brannigan[1], Filip Van Petegem[2], Roderic Eckenhoff[3]

University of Pennsylvania[1] Univeristy of British Columbi[2] University of Pennsylvania Perleman Scho[3]

Introduction: Ryanodine receptor 1 (RyR1), a calcium channel embedded in skeletal muscle sarcoplasmic reticulum (SR), is biased open during episodes of malignant hyperthermia (MH) [1]. When MH is suspected in an anesthetized patient, any triggering agents must be discontinued in favor of a nontriggering anesthetic. This often includes propofol. However, the binding of propofol with RyR1 has not been described in atomic detail. Here, we identify propofol binding sites on RyR1 and estimate the binding affinity of propofol in one selected site.

Methods: We measured the open probability of RyR1 in planar lipid layers as a function of photoaffinity ligand m-azipropofol (AziPm) and propofol concentrations. We also measured intracellular calcium concentration by Fura-2 imaging [2] in wild-type human skeletal muscle cells, also as a function of propofol concentration. We conducted photoaffinity labeling experiments with AziPm to identify adducted sites, with accompanying protection experiments [3]. Finally, we evaluated one of the identified sites using equilibrium and free energy perturbation (FEP) molecular dynamics (MD) simulations [4].

Results: Propofol was found to decrease the channel opening probability of RyR1 in planar lipid bilayers at 30 uM concentration. In human skeletal muscle cells, the intracellular calcium concentration decreased as the propofol concentration increased. Several binding sites on RyR1 were identified by photoaffinity labeling. A selected site has binding affinity predicted by FEP MD simulations consistent with clinical concentrations of propofol.

Conclusions: Taken together, our data suggests that propofol binds to RyR1 in several sites and inhibits channel opening. At least one of those sites has affinity with propofol compatible with concentrations expected at clinical doses. These results reinforce the idea that beyond simply not aggravating an MH episode, propofol could have a protective effect by inhibiting RyR1 opening.

References: [1] J Biol Chem 1988 Jul 5;263(19):9310-5.

[2] J Pharmacol Toxicol Methods. 1994 Feb;31(1):1-10.

[3] J Med Chem 2010 Aug 12;53(15):5667-75.

[4] J Chem Theory Comput 2018 Dec 11;14(12):6560-6573.

Anesthetic Pharmacology 14 - The Impact of Chronic THC Exposure on Propofol Sensitivity in Pregnant Rhesus Macaques Undergoing Magnetic Resonance Imaging: A Prospective Interventional Controlled Pilot Study

Elizabeth Leimer[1], Brandon Togioka[1], Lauren Martin[2], Jamie Lo[1]

Oregon Health & Science University[1] Oregon National Primate Research Center -ARRS[2]

Introduction: The prevalence of cannabis use in United States adult surgical patients has increased; an estimated 17.9% of Americans used cannabis last year.[1] Studies suggest an association between cannabis use and higher induction and maintenance anesthetic requirement,[2,3] but this relationship remains poorly understood. Human clinical studies have been unable to control for mode of cannabis delivery, composition, and frequency of use, and preclinical rodent models lack the complexity of the human neurologic system. Accordingly, we conducted a study in a translational nonhuman primate (NHP) model to investigate the effect of stable dose delta-9-tetrahydrocannabinol (THC, the main active component of cannabis) ingestion on propofol sensitivity. We hypothesized that propofol MAC-BAR would be higher in THC exposed NHPs compared to naïve control.

Methods: This study was nested within a larger prospective cohort study to determine the impact of chronic THC use on reproductive health in female NHPs. Female Rhesus macaques were divided into a naïve control (n=7) and THC-exposed group (2.5mg/7kg/day edible THC; n=4). All experimental procedures were approved by the Institutional Animal Care and Use Committee. General anesthesia was induced with intramuscular ketamine (10 mg/kg) and maintained with isoflurane 0.4 vol% and propofol infusion to facilitate magnetic resonance imaging at gestational day 110 (G110) and G155 (term is ~168 days, Figure 1). Propofol was titrated to maintain heart rate (HR) and blood pressure (BP) within 10% of baseline during a 5 second hemostat pinch between thumb and index finger. If HR or BP increased > 10% despite 3 dose adjustments, rescue occurred with isoflurane 1-2 vol%. Final propofol dose was considered representative of MAC-BAR. Propofol MAC-BAR was summarized as median, minimum-maximum values. We tested for treatment differences of continuous characteristics using the Mann-Whitney test and categorical characteristics using Fisher's exact test. Hypothesis testing was two-sided, p-value < 0.05 was considered statistically significant.

Results: Propofol MAC-BAR did not differ at G110 [THC-exposed (330, 230-430 mcg/kg/min) vs. control (230, 230-280 mcg/kg/min); p=0.70] or G155 [THC-exposed (330, 280-380 mcg/kg/min) vs. control (280, 230-330 mcg/kg/min; p=0.30; Figure 1]. At G155, isoflurane rescue occurred in 67% (2/3) THC-exposed vs. 0% (0/6) control subjects, p=0.083. The incidence of isoflurane rescue did not differ between groups at G110.

Conclusions: In this pilot study, we observed a trend towards higher propofol MAC-BAR in THC-exposed NHPs. This study is limited by incomplete data collection. Subjects did not undergo toe pinch if general anesthesia was shorter than 60 minutes or if HR or BP increased >10% without a stimulus. Larger studies are needed to clarify the effect of chronic THC exposure on propofol MAC-BAR.

References: 1. "2020 National Survey on Drug Use and Health (NSDUH) Releases." *Substance Abuse and Mental Health Services Administration.* U.S. Department of Health & Human Services. <https://www.samhsa.gov/data/release/2020-national-survey-drug-use-and-health-nsduh-releases>.

2. Cannabis consumption before surgery may be associated with increased tolerance of anesthetic drugs: a case report. Int J Case Rep Images. 2015;6:436-439.

3. Effects of cannabis use on sedation requirements for endoscopic procedures. JOM. 2019;119:307-311.

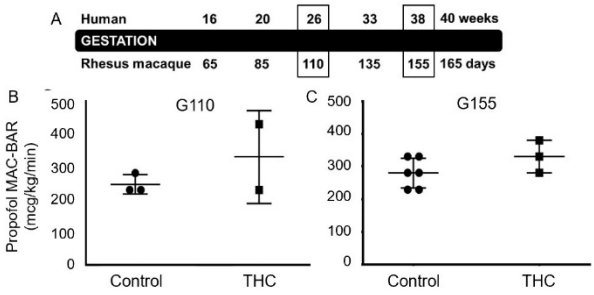

Figure 1. G110 and G155 in NHPs correlates to gestational weeks 26 and 38 in humans (A). Propofol MAC-BAR not differ between groups at either G110 (B) or G155 (C).

Cardiovascular Anesthesiology

Cardiovascular Anesthesiology 1

- Circadian intense light elicited therapies in murine myocardial ischemia and reperfusion injury

Tobias Eckle[1], Lori Walker[1], Yoshimasa Oyama[2]

University of Colorado Anschutz Medical Campus[1] Oita University Faculty of Medicine Anesthesiology[2]

Introduction: Recent studies on light-elicited endothelial PER2-mediated cardioprotection revealed a critical role of PER2/HIF1A-regulated ANGPTL4 for endothelial barrier protection during myocardial ischemia and reperfusion injury.[1-3] Based on these observations; we studied pharmacological approaches to mimic light-elicited cardioprotection.

Methods: All animal and human studies had IACUC approval and followed the APS/ NIH guidelines. To study myocardial ischemia and reperfusion injury, an in-situ mouse model for myocardial ischemia and reperfusion injury was used. To study light-elicited mechanisms during myocardial ischemia and reperfusion injury, endothelial-specific *Per2*-deficient mice were treated with the PER2 enhancer nobiletin, with the HIF1A activator DMOG or with recombinant ANGPTL4. To evaluate if light could improve cardiac function after myocardial ischemia, mice were exposed to intense light (10,000 LUX) for one week during the light period (L:D 14:10h) and compared to room light conditions (200 LUX). Following light therapy, cardiac function was evaluated using echocardiography.

Results: The PER2 enhancer nobiletin or the HIF1A activator DMOG protected from myocardial ischemia and reperfusion injury, which was abolished in endothelial-specific PER2-deficient mice. ANGPTL4 was able to overcome an endothelial *Per2* deficiency and revealed protection during myocardial ischemia and reperfusion injury in endothelial-specific *Per2*-deficient or control mice. Light exposure after myocardial ischemia uncovered a significant improvement in the ejection fraction of wild-type mice.

Conclusions: Our murine studies demonstrate that while the PER2 enhancer nobiletin or the HIF1 activator DMOG is cardioprotective, only the PER2/HIF1A downstream target ANGPTL4 can overcome an endothelial PER2 deficiency. Moreover, we discovered that light exposure after myocardial ischemia significantly improved cardiac function. These studies indicate that light-elicited ANTGPLT4 could represent a promising strategy for myocardial ischemia and reperfusion injury, even in the setting of circadian dysfunction.

References: 1. Oyama, Y.*, et al.* Intense Light-Mediated Circadian Cardioprotection via Transcriptional Reprogramming of the Endothelium. *Cell Rep* **28**, 1471-1484 e1411 (2019).

2. Oyama, Y., Walker, L.A. & Eckle, T. Targeting circadian PER2 as therapy in myocardial ischemia and reperfusion injury. *Chronobiol. Int.* **38**, 1262-1273 (2021).

3. Shuff, S., Oyama, Y., Walker, L. & Eckle, T. Circadian Angiopoietin-Like-4 as a Novel Therapy in Cardiovascular Disease. *Trends Mol. Med.* **27**, 627-629 (2021).

Cardiovascular Anesthesiology 2

- Comparative post-operative outcomes of volatile and intravenous anesthetics: A network meta-analysis

Kiyan Heybati[1], Fangwen Zhou[1], Madison Baltazar[1], Keshav Poudel[1], Domenic Ochal[1], Luqman Ellythy[1], Jiawen Deng[2], Cynthia Chelf[3], Carson Welker[1], Harish Ramakrishna[1]

Mayo Clinic[1] Temerty Faculty of Medicine[2] Mayo Clinic Libraries[3]

Introduction: Volatile and total intravenous anesthesia (TIVA) are commonly used as primary anesthetics and volatile agents have been associated with cardioprotective effects.[1] However, various trials and meta-analyses have demonstrated conflicting findings of no difference or a possible mortality benefit with volatile anesthesia.[2–4] Many trials, though, have administered the anesthetics at different perioperative periods. Therefore, it remains unclear whether patients may experience different outcomes when receiving specific agents as primary anesthetics for maintenance. Additionally, there is limited pooled data on the treatment effects of specific regimens and the potential combination of volatile and intravenous drugs. We conducted a network meta-analysis (NMA) to compare specific regimens used as primary anesthetics in patients undergoing cardiac, thoracic, and vascular surgery.

Methods: This frequentist, random-effects NMA was prospectively registered (CRD42022316328) and conducted according to PRISMA-NMA. Literature searches were conducted from inception to April 1st, 2022, in MEDLINE, EMBASE, CENTRAL, Web of Science, Scopus, and through citations of past reviews. We included randomized controlled trials (RCTs) enrolling adults (≥18) undergoing cardiac, thoracic, and vascular surgery, using the same induction regimens, and comparing volatile and/or TIVA for the maintenance of anesthesia. As most trials focused on cardiac surgery, analyses were restricted to this cohort to ensure sufficient power. Outcomes included ICU length of stay (LOS), myocardial infarction (MI), in-hospital and 30-day mortality, stroke, and delirium. Risk of bias (RoB) and confidence of evidence were assessed by RoB-2 and CINeMA, respectively. Sensitivity analyses were conducted with patients undergoing coronary artery bypass grafting (CABG), and excluding studies with a high RoB.

Results: We included 54 (N=8,362) RCTs, of which 47 (N=6,881) enrolled those undergoing cardiac surgery (**Image 1**). About a quarter of patients were female (2,109, 25.2%) and the average age ranged from 28.85 to 76 years old. Twenty-six (48.1%) were rated as having low RoB, 24 (44.4%) had some concerns, and 4 (7.4%) had a high RoB. No publication bias was detected.
Across 19 trials (N=1,821), studying 9 unique intervention arms, compared with propofol alone, sevoflurane + propofol was associated with decreased ICU LOS (N=100; MD -18.26 hours; 95% CI: -34.78 to -1.73 hours; P=0.03; low confidence) while midazolam + propofol (N=36; MD 17.51 hours; 95% CI: 2.78 to 32.25 hours; P=0.02; low confidence) was associated with a significant increase (**Image 2**). There was substantial heterogeneity (I^2 = 64.5%). Both treatment effects were significant following the exclusion of trials with a high RoB. Among patients undergoing CABG, sevoflurane + propofol was no longer significant and midazolam + propofol was not studied.
Among 27 trials (N=4,080) with 10 unique intervention arms, compared with propofol, midazolam was associated with a significantly greater risk of MI (N=110; RR 1.94; 95% CI: 1.01 to 3.71; P=0.05; low confidence; **Image 3**). There was no heterogeneity (I^2 = 0%). This finding persisted following the exclusion of studies with a high RoB (N=110; RR 1.96; 95% CI: 1.02 to 3.75; P=0.04; I^2 = 0%) and among patients undergoing CABG (N=110; RR 2.06; 95% CI: 1.06 to 4.02; P=0.03; I^2 = 0%).
When compared with propofol, none of the studied regimens were associated with a significant difference in in-hospital (**Image 4**) or 30-day (**Image 5**) mortality, stroke, or delirium. Across 5 trials (N=762) in vascular surgery, none found significant differences, and in-hospital was not studied. Across 2 trials (N=719) in thoracic surgery, neither found significant differences in mortality, nor ICU LOS. Other outcomes of interest were not studied.

Conclusions: Among the studied agents in the cardiac surgical population, sevoflurane + propofol was associated with decreased ICU LOS, when compared with propofol alone. Midazolam + propofol was associated with longer ICU LOS versus propofol, however, this should be interpreted with caution given the limited sample sizes. Midazolam was associated with an increased risk of MI, however, given its limited use as a primary agent for maintenance, further investigation is required. When compared with propofol, none of the treatment arms had a significant impact on in-hospital or 30-day mortality. Larger, randomized trials, particularly in the thoracic and vascular surgical populations, are required.

References: 1. 2017 EACTS Guidelines on perioperative medication in adult cardiac surgery. *Eur J Cardiothorac Surg* 2018; **53**(1): 5-33

2. Contradictory Findings of Two Recent Meta-Analyses: What Are We Supposed to Believe About Anesthetic Technique in Patients Undergoing Cardiac Surgery? *J. Cardiothorac. Vasc. Anesth*. 2021. **35**(12): 3841–3843

3. Volatile Anesthetics versus Propofol for Cardiac Surgery with Cardiopulmonary Bypass: Meta-analysis of Randomized Trials. *Anesthesiology* 2020; **132**(6): 1429–1446

4. A Comparison of Volatile Anesthesia and Total Intravenous Anesthesia (TIVA) Effects on Outcome From Cardiac Surgery: A Systematic Review and Meta-Analysis. *J Cardiothorac Vasc Anesth* 2021; **35**(4): 1096–1105

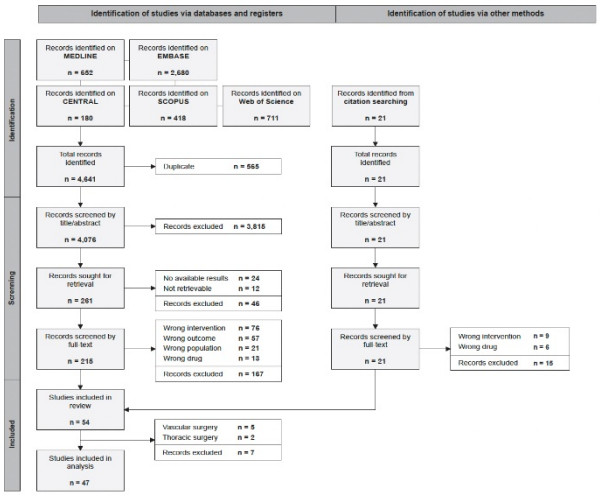
Identification of studies via databases and registers
Identification of studies via other methods
Identification
Screening
Included
Records identified on MEDLINE n = 652
Records identified on EMBASE n = 2,680
Records identified on CENTRAL n = 180
Records identified on SCOPUS n = 418
Records identified on Web of Science n = 711
Records identified from citation searching n = 21
Total records identified n = 4,641
Duplicate n = 565
Total records identified n = 21
Records screened by title/abstract n = 4,076
Records excluded n = 3,816
Records screened by title/abstract n = 21
Records sought for retrieval n = 261
No available results n = 24
Not retrievable n = 12
Records excluded n = 46
Records sought for retrieval n = 21
Records screened by full text n = 215
Wrong intervention n = 76
Wrong outcome n = 67
Wrong population n = 21
Wrong drug n = 13
Records excluded n = 167
Records screened by full text n = 21
Wrong intervention n = 9
Wrong drug n = 6
Records excluded n = 15
Studies included in review n = 54
Vascular surgery n = 5
Thoracic surgery n = 2
Records excluded n = 7
Studies included in analysis n = 47

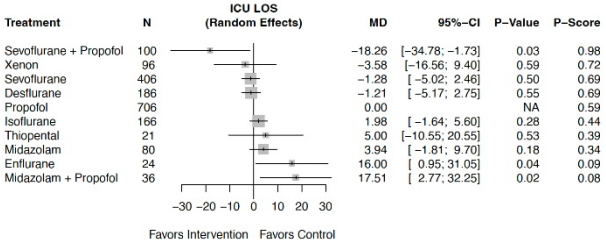
ICU LOS
(Random Effects)
Treatment N MD 95%−CI P−Value P−Score
Sevoflurane + Propofol 100 −18.26 [−34.78; −1.73] 0.03 0.98
Xenon 96 −3.58 [−16.56; 9.40] 0.59 0.72
Sevoflurane 406 −1.28 [−5.02; 2.46] 0.50 0.69
Desflurane 186 −1.21 [−5.17; 2.75] 0.55 0.69
Propofol 706 0.00 NA 0.59
Isoflurane 166 1.98 [−1.64; 5.60] 0.28 0.44
Thiopental 21 5.00 [−10.55; 20.55] 0.53 0.39
Midazolam 80 3.94 [−1.81; 9.70] 0.18 0.34
Enflurane 24 16.00 [0.95; 31.05] 0.04 0.09
Midazolam + Propofol 36 17.51 [2.77; 32.25] 0.02 0.08
−30 −20 −10 0 10 20 30
Favors Intervention Favors Control

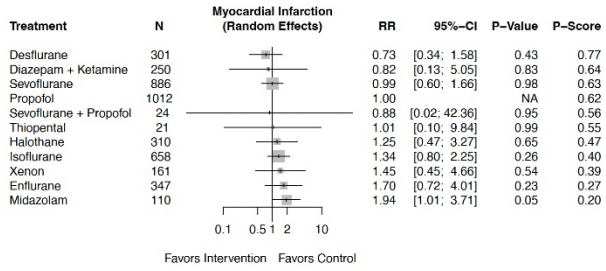
Myocardial Infarction
(Random Effects)
Treatment N RR 95%−CI P−Value P−Score
Desflurane 301 0.73 [0.34; 1.58] 0.43 0.77
Diazepam + Ketamine 250 0.82 [0.13; 5.05] 0.83 0.64
Sevoflurane 886 0.99 [0.60; 1.66] 0.98 0.63
Propofol 1012 1.00 NA 0.62
Sevoflurane + Propofol 24 0.88 [0.02; 42.36] 0.95 0.56
Thiopental 21 1.01 [0.10; 9.84] 0.99 0.55
Halothane 310 1.25 [0.47; 3.27] 0.65 0.47
Isoflurane 658 1.34 [0.80; 2.25] 0.26 0.40
Xenon 161 1.45 [0.45; 4.66] 0.54 0.39
Enflurane 347 1.70 [0.72; 4.01] 0.23 0.27
Midazolam 110 1.94 [1.01; 3.71] 0.05 0.20
0.1 0.5 1 2 10
Favors Intervention Favors Control

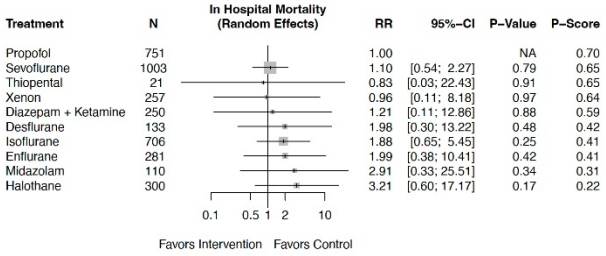
In Hospital Mortality
(Random Effects)
Treatment N RR 95%−CI P−Value P−Score
Propofol 751 1.00 NA 0.70
Sevoflurane 1003 1.10 [0.54; 2.27] 0.79 0.65
Thiopental 21 0.83 [0.03; 22.43] 0.91 0.65
Xenon 257 0.96 [0.11; 8.18] 0.97 0.64
Diazepam + Ketamine 250 1.21 [0.11; 12.86] 0.88 0.59
Desflurane 133 1.98 [0.30; 13.22] 0.48 0.42
Isoflurane 706 1.88 [0.65; 5.45] 0.25 0.41
Enflurane 281 1.99 [0.38; 10.41] 0.42 0.41
Midazolam 110 2.91 [0.33; 25.51] 0.34 0.31
Halothane 300 3.21 [0.60; 17.17] 0.17 0.22
0.1 0.5 1 2 10
Favors Intervention Favors Control

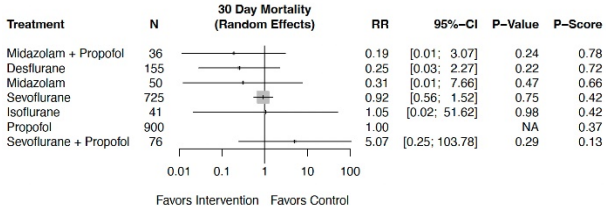
30 Day Mortality
(Random Effects)
Treatment N RR 95%−CI P−Value P−Score
Midazolam + Propofol 36 0.19 [0.01; 3.07] 0.24 0.78
Desflurane 155 0.25 [0.03; 2.27] 0.22 0.72
Midazolam 50 0.31 [0.01; 7.66] 0.47 0.66
Sevoflurane 725 0.92 [0.56; 1.52] 0.75 0.42
Isoflurane 41 1.05 [0.02; 51.62] 0.98 0.42
Propofol 900 1.00 NA 0.37
Sevoflurane + Propofol 76 5.07 [0.25; 103.78] 0.29 0.13
0.01 0.1 1 10 100
Favors Intervention Favors Control

Cardiovascular Anesthesiology 3

- Comparison of NT-proBNP concentrations from right- vs. left heart sampling sites

Peter Nagele[1], Nisha Jain[1], Eslam Samaha[1], Mohammed Helwani[1]

University of Chicago[1]

Introduction: NT-proBNP is an inactive prohormone of brain natriuretic peptide (BNP) secreted by cardiomyocytes in response to ventricular stretch and used clinically as a cardiac biomarker in the diagnosis of heart failure. The discrimination between left-sided and right-sided heart failure is clinically very difficult and we wondered whether comparing plasma NT-proBNP values simultaneously obtained from right heart sampling sites via pulmonary catheter with left heart NT-proBNP values from an arterial line may help distinguishing left- from right-heart failure and strain.

Methods: In this prospective cohort study, we enrolled adult patients scheduled for cardiac surgery with planned placement of a pulmonary artery catheter (or in situ). Our goal was to enroll 10 patients each with the following conditions: (1) severe aortic stenosis; (2) lung transplant surgery; (3) heart failure; (4) LVAD in situ; (5) severe mitral valve regurgitation; (6) control patients (had central venous and arterial line only). Blood samples were collected after induction of general anesthesia and successful placement of a pulmonary artery catheter in chilled 5 ml vacutainers within 2-3 minutes from the following sampling sites: (a) superior vena cava; (b) right atrium; (c) right ventricle; (d) pulmonary artery; (e) radial artery and immediately processed and spun down; serum was stored at -80°C until analyzed. NT-proBNP plasma concentrations were analyzed in one batch on a Roche Elecsys platform.

Results: 61 patients were enrolled in the study (5 aortic stenosis, 9 lung transplantation, 11 heart failure, 11 LVAD; 15 MVR, 10 controls). Right-sided NT-proBNP concentrations were significantly higher compared to left-sided in patients with severe aortic stenosis (+32.7%), heart failure (+11.4%), and with an implanted LVAD (+20.2%; Table 1) but not in lung transplantation or MVR (Figure 1). In control patients, NT-proBNP concentrations differed on average only by 15 pg/mL or 3% between right-sided and left-sided sampling sites. Among all non-control patients, in 84% (43/51) patients, the maximum right-sided NT-proBNP concentration was higher than the NT-proBNP concentration from the radial arterial site.

Conclusions: This pilot study demonstrates that NT-proBNP plasma concentrations can be significantly higher in right-heart sampling sites compared to left-heart sites thereby potentially allowing the clinical diagnosis of dominant left vs. right-heart failure, especially in patients with mechanical support devices.

	Aortic Stenosis		Lung Transplantation		Heart Failure		LVAD		MVR		Control	
	Right Heart Max	Radial Artery	Right Heart Max	Radial Artery	Right Heart Max	Radial Artery	Right Heart Max	Radial Artery	Right Heart Max	Radial Artery	Right Heart Max	Radial Artery
Number of values	5	5	9	9	11	11	11	11	15	15	10	10
Minimum	100	87.0	31.0	26.0	524	410	259	280	124	121	20.0	20.0
25% Percentile	180	116	75.0	47.0	1121	1028	1781	1544	283	233	32.8	35.0
Median (pg/mL)	**391**	**231**	**148**	**126**	**1962**	**1812**	**4150**	**3767**	**899**	**824**	**98.5**	**92.5**
75% Percentile	2586	2144	1014	865	7745	7534	7564	4860	2672	2741	184	182
Maximum	4348	4031	3584	3780	9236	9030	18240	9777	5029	5084	656	519
Range	4248	3944	3553	3754	8712	8620	17981	9497	4905	4963	636	499
Abs Difference (pg/mL)	235		24		356		1849		175		15	
Relative Difference (%)	32.7%		15.6%		11.4%		20.2%		9.4%		2.9%	
P-value	0.063		0.098		0.003		0.03		0.1688		0.09	

Wilcoxon matched pairs signed rank test

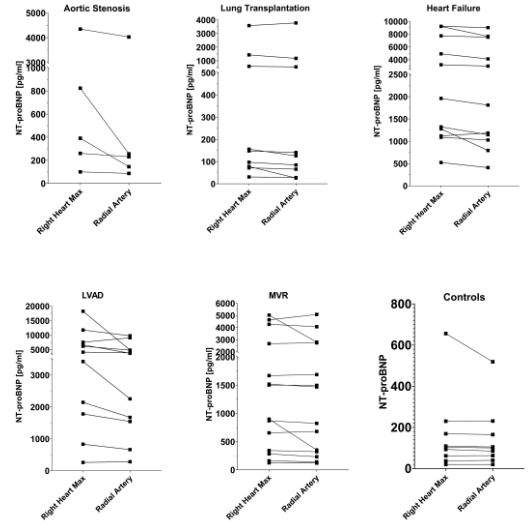

Cardiovascular Anesthesiology 4

- Erythropoietin With and Without Iron Therapy for Perioperative Anemia in Cardiac Surgery: a Systematic Review and Network Meta-analysis

Flora Wen Xin Xu[1], Alex Jia Yang Cheong[1], Khi Yung Fong[2], Christopher Yong En Chia[2], Sneha Rajiv Jain[3], Chong Yao Ho[3], Ka Ting Ng[3], Ming Ann Sim[3], Juanita Jaslin James[3], Sophia Tsong Huey Chew[3], Lian Kah Ti[4]

National University of Singapore[1] Yong Loo Lin School of Medicine, National University of Sing[2] Yong Loo Lin School of Medicine[3] National University Health System[4]

Introduction: Preoperative anemia affects 25-40% of cardiac surgical patients,[1,2] and is associated with greater transfusion requirements, morbidity and mortality.[3–5] Therapeutic options include Erythropoietin (EPO) and Iron. While intravenous iron is recommended as a first line agent,[6] its benefits are debatable.[7,8] EPO has been widely used in mixed surgical cohorts, but remains non-FDA approved for use in cardiac surgery due to prior concerns of thromboembolic complications and mortality.[9] In recent times, EPO has been used in Enhanced Recovery After Cardiac Surgery (ERACS) programmes, but has yet **to** be formally inducted into guidelines.[10] Our systematic review and network meta-analysis aims to evaluate the safety and efficacy of perioperative EPO and Iron use in cardiac surgery.

Methods: A systematic review and meta-analysis was undertaken following PRISMA guidelines. A comprehensive search of PubMed, Embase and Cochrane was conducted up to 1 May 2022. We included all randomised controlled trials (RCTs) and cohort studies meeting our inclusion criteria: (1) involved adult patients undergoing cardiac surgery; (2) administered EPO perioperatively, with or without iron; (3) reported outcome data on blood transfusion requirements, incidence of postoperative complications like cardiac surgery associated acute kidney injury (CSA-AKI), stroke and myocardial infarction, length of hospitalisation and all-cause mortality. Study quality was assessed using the Cochrane Risk of Bias 2.0 tool for randomised studies and the Newcastle–Ottawa Scale for cohort studies.

Results: Of 743 citations, 34 randomised controlled trials and cohort studies totalling 4474 subjects were included, comparing EPO, EPO with Iron, Iron and placebo. Our network analysis showed reduced transfusion risk with EPO-Iron use, compared to Iron alone (OR 0.59; 95%CI 0.41 to 0.85; I2=85%). EPO use correlated with reduced volume blood transfusion compared to placebo (OR -0.65; 95%CI -0.91 to -0.39, I2=17%). Preoperative EPO administration was associated with reduced CSA-AKI incidence (OR 0.59; 95%CI 0.35 to 0.99; I2=62%). Regarding its safety profile, EPO use did not increase risk of thromboembolic events including myocardial infarction and stroke, length of hospitalisation or mortality.

Conclusions: While cardiac surgical guidelines have yet to include EPO in preoperative anemia treatment, our findings suggest that its benefits are multifold. EPO is efficacious in lowering blood transfusion requirements and CSA-AKI occurrence. Moreover, combining EPO with Iron has synergistic effects in reducing transfusion risk compared to Iron alone. Despite prior concerns of thromboembolic complications or mortality, our study suggests no significant risk increment with EPO use. The optimal EPO dosage, length of therapy, and post-treatment hemoglobin targets would be best answered by future RCTs.

References: 1. WHO Global Database of Anaemia (2008).
2. J Hematol 9, 97–108 (2020).
3. Anaesthesia 71, 627–635 (2016).
4. Circulation 117, 478–484 (2008).
5. The Annals of thoracic surgery vol. 110 749–750 (2020).
6. Iron supplementation | Blood transfusion | Quality standards | NICE.
7. Lancet 396, 1353–1361 (2020).
8. Interact. Cardiovasc. Thorac. Surg. 15, 1013–1018 (2012).
9. Food and Drug Administration (2020).
10. Eur. J. Cardiothorac. Surg. 54, 491–497 (2018).

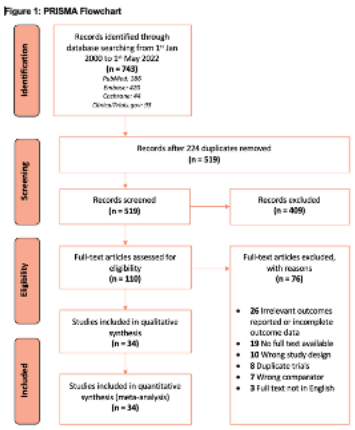

Figure 2: Network analysis of transfusion risk

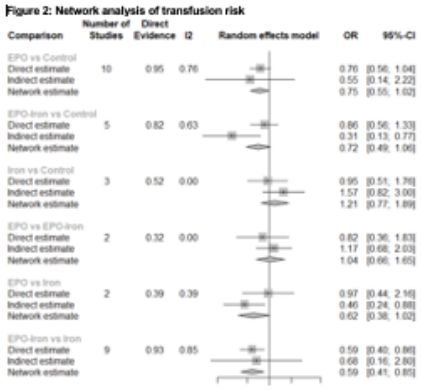

Figure 3: Transfusion volume

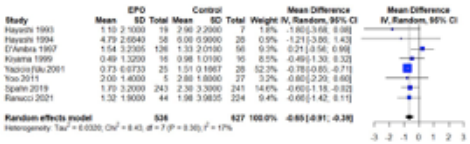

Figure 4: Subgrouped analysis of CSA-AKI risk

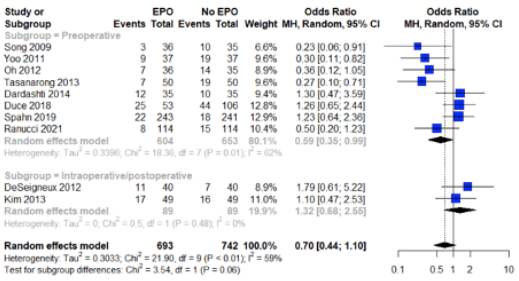

Cardiovascular Anesthesiology 5 - Initial Determination of Inter-rater Agreement in a Retrospective Cohort Study on Dobutamine versus Milrinone Use in Cardiac Surgery

Nicole Maldari[1], Joseph Colao[2], Ramya Baddigam[3], Michelle Chen[4], Emily Fung[1], Japna Kalra[5], Koji Takeda[5], Teresa Mulaikal[6], Aaron Mittel[5]

Columbia University Irving Medical Center[1] New York Presbyterian - Columbia University[2] Columbia University Department of Anesthesiology[3] New York Presbyterian Hospital-Columbia Irving Medical Cente[4] Columbia University Medical Center[5] Columbia University[6]

Introduction: Inotropic support is often utilized in the perioperative setting of cardiopulmonary bypass (CPB) surgeries, where patients have reduced cardiac output. Low cardiac output states can have significant morbidity and mortality. Dobutamine and milrinone are both frequently used for prevention and management of perioperative low cardiac output syndrome (LCOS)[1]. Despite the familiarity with their use, there is little evidence to guide the selection of one agent versus another [2]. Here we study 30-day outcomes related to dobutamine or milrinone use when started during cardiac surgery at our institution. In order to ensure reliable data collection for this study, we reviewed preliminary data and inter-rater agreement among a multi-person team of data abstractors performing manual chart reviews.

Methods: This is a single center retrospective cohort analysis at a New York Metropolitan area hospital. Current preliminary data looks at a three-patient test sample who received isolated coronary artery bypass graft (CABG) surgery. Focus was taken on CABG with moderately reduced (LVEF 30–40%) or severely reduced (LVEF < 30%) ventricular function who are at risk of LCOS in the immediate postoperative period. Patient charts were reviewed for procedural subtype and baseline LVEF, assessed on baseline intraoperative transesophageal echocardiogram. Patients were grouped based on receiving milrinone, dobutamine, or no inotrope started in the operating room or intensive care unit. Investigators performed manual chart review to abstract both primary and secondary outcomes. Primary outcomes, adapted from the DoReMi trial, included: in-hospital death from any cause, resuscitated cardiac arrest, use of mechanical circulatory support, non-fatal MI diagnosed by a cardiologist, TIA/stroke diagnosed by a neurologist, and initiation of renal replacement therapy [3]. Secondary outcomes included: total time of inotropic support, ICU length of stay, total number of days requiring non-invasive mechanical ventilation, presence of AKI defined by KDIGO criteria, normalization of serum lactate (<1.5), and arrhythmia requiring medical treatment defined as new amiodarone therapy or electrical cardioversion documentation. All data points collected were cross referenced between six investigators. Calculation of inter-rater agreement in this analysis was performed with Fleiss kappa testing (Fleiss kappa allows estimation of agreement among > 2 raters). Analyses were performed in RStudio 2022.07.1+554.

Results: Our results showed perfect inter-rater agreement among the six investigators for the outcomes that did not occur in our three-patient sample: in-hospital death, resuscitated cardiac arrest, cardiac transplant, and non-fatal MI. There was inter-rater agreement for the use of MCS (Fleiss kappa 0.723, $p = 0.003$), initiation of renal-replacement therapy (Fleiss kappa 1.0, $p < 0.001$), and occurrence of TIA/stroke (Fleiss kappa 1.0, $p < 0.001$). Visual assessment of acute kidney injury and lactate normalization also indicated high inter-rater agreement (Figures 1 and 2). The remaining outcomes of length of ICU length of stay, duration of inotropic therapy, and days requiring mechanical ventilation demonstrated variability among raters (Table 1).

Conclusions: Determination of inter-rater agreement is an important initial part of a multi-reviewer chart review study. Our three-patient test sample identified high inter-rater agreement on several clinical outcomes. Although serious complications of CABG (in-hospital death, cardiac transplant, resuscitated cardiac arrest, and non-fatal MI) are rare, and it is possible that this high inter-rater agreement occurred by chance, high inter-rater agreement in the more common postoperative complications (MCS, TIA/stroke, and initiation of renal-replacement therapy) suggest that portions of our chart review process are effective. More work is necessary to improve our abstraction process for all outcomes to definitively confirm correlation values. Future work will include further analysis on areas with lower inter-rater agreement and making changes to the current abstraction protocol to improve inter-rater agreement. With an updated abstraction protocol, we will continue the chart review process with the remaining patients in our sample to determine any significant findings in clinical outcomes. This study can then be expanded to include a larger sample size from the database of patients collated in collaboration with our cardiothoracic surgical colleagues

References: [1] Intraoperative milrinone versus dobutamine in cardiac surgery patients: a retrospective cohort study on mortality. Crit Care. 2018 Feb 26;22(1):51.

[2] Comparative Effectiveness and Safety Between Milrinone or Dobutamine as Initial Inotrope Therapy in Cardiogenic Shock. Journal of Cardiovascular Pharmacology and Therapeutics. 2019;24(2):130-138.

[3] Milrinone as Compared with Dobutamine in the Treatment of Cardiogenic Shock. New England Journal of Medicine, vol. 385, no. 6, 2021, pp. 516–525.

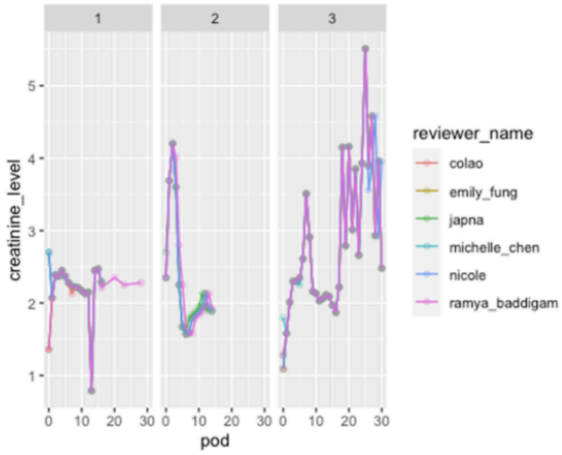

Figure 1

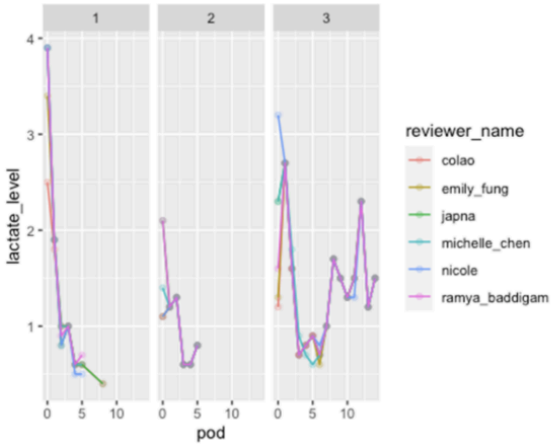

Figure 2

		Reviewer 1	Reviewer 2	Reviewer 3	Reviewer 4	Reviewer 5	R
Subject 1	ICU Length of Stay (days)	6	6	6	6	6	
	Final Postop Day of Dobutamine Use	5	5	5	5	5	
	Final Postop Day of Postop Milrinone Use	11	9	11	9	11	
	Total Days Requiring Non-Invasive Mechanical Ventilation	NA	NA	NA	4	NA	
Subject 2	ICU Length of Stay (days)	6	5	5	6	9	
	Final Postop Day of Dobutamine Use	5	NA	5	5	5	
	Total Days Requiring Non-Invasive Mechanical Ventilation	1	1	1	NA	1	
Subject 3	ICU Length of Stay (days)	17	17	17	NA	17	
	Final Postop Day of Dobutamine Use	16	16	16	16	16	
	Total Days Requiring Non-Invasive Mechanical Ventilation	NA	13	NA	NA	NA	

Table 1

Cardiovascular Anesthesiology 6

- Ischemic Post-Conditioning Increases Rate of Return of Spontaneous Circulation after Cardiac Arrest in Diabetic Rats

Matthew Barajas[1], Takuro Oyama[1], Masakazu Shiota[1], Maximilian Zaum[2], Zhu Li[2], Matthias Riess[1]

Vanderbilt University Medical Center[1] Universität Greifswald[2]

Introduction: Type 2 Diabetes (DM) is an increasing epidemic with multi-organ sequelae including increased risk of coronary artery disease, resultant increased risk of cardiac arrest (CA) and decreased rates of survival after CA.[1] Classic post-arrest therapies such as targeted temperature management are less effective in abrogating injury in diabetics.[2] While cardiopulmonary resuscitation (CPR) guidelines emphasize high-quality compressions with minimal interruptions, abrupt restoration of blood flow after prolonged ischemic insult may result in molecular and metabolic changes more injurious than the ischemia itself.[3,4] Ischemic post-conditioning (IPoC) alters cardiopulmonary resuscitation (CPR) protocol to slow reperfusion and thus limit cellular and mitochondrial reperfusion injury. In IPoC, a limited number of brief pauses in compressions are purposefully implemented shortly after the initiation of CPR. IPoC has been shown to improve neurologic and cardiac outcomes in young healthy swine after prolonged fibrillatory arrest but has never been confirmed in other models.[5] As a wide-spread, high morbidity disease with increased susceptibility to ischemia reperfusion injury, DMs are a critical target of future implementation of this novel, non-invasive, technique. We hypothesized that IPoC would be beneficial for survival of both non-DM and DM rats after asphyxial CA.

Methods: Institutional IACUC approval was obtained for this protocol. Male Wistar rats (539 ± 77g) were utilized, 18 of 34 underwent induction of type II diabetic phenotype with an injection of low dose streptozotocin (30mg/kg) IP and feeding of high-fat high-sugar western diet for 12 weeks. The phenotype was ensured with random blood glucose >200 mg dL^{-1}. On the day of experiment, rats were intubated, mechanically ventilated, and anesthetized with isoflurane. A non-invasive flow probe was placed on the carotid artery. The right internal jugular vein and femoral artery and vein were cannulated for pressure monitoring and drug delivery. Electrocardiogram, transthoracic echocardiogram (TTE), and arterial blood gases (ABG) were analyzed. Asphyxial CA was induced by rocuronium and cessation of mechanical ventilation and allowed to proceed for 7 min. CPR was initiated utilizing an automated chest compressor at a rate of 200 min^{-1} with a controlled depth. Animals were randomly assigned to standard CPR (S-CPR) or IPoC. IPoC was initiated after 40 seconds of CPR and consisted of a 20-second pause followed by 20 seconds of compressions per round, repeated for 4 rounds. Defibrillation and epinephrine were given, in a standardized fashion as necessary. If ROSC was achieved, epinephrine drip was titrated to maintain a mean arterial pressure (MAP) of 70 mmHg. TTE and ABG data were collected at 15 min, 1 hour and 2 hours after return of spontaneous circulation (ROSC). Data were analyzed using ANOVA with pairwise comparisons. Significance set at $p < .05$, two-tailed.

Results: There were no significant differences in cardiac output (CO), pH, MAP, or carotid blood flow at baseline between all groups. Non-DM rats displayed high rates of ROSC in both S-CPR, and IPoC groups, 100% (9 of 9) and 85% (6 of 7) respectively. Only DM rats required defibrillations and DM rats had a significantly longer time to ROSC. DM S-CPR rats had a significantly reduced ROSC rate at 40% (4 of 10) compared to non-DM animals which was rescued by IPoC to 88% (7 of 8). There were no significant hemodynamic differences between DM S-CPR and IPoC groups during CPR to account for this difference. Furthermore, DM S-CPR animals had a significantly elevated epinephrine requirement compared to DM IPoC, p= 0.004, mean 566ml vs. 108ml. There was no difference in any hemodynamic markers between non-DM S-CPR and non-DM IPoC groups after ROSC.

Conclusions: DM subjects experienced an increased injury as compared to non-DM animals. IPoC was safe in non-DMs, consistent with previous studies, and exerted a strong protective effect in DM rats with higher ROSC and thus survival. Furthermore, significantly less inotropic support was required to maintain vital signs in DMs after IPoC. The use of stabilizing epinephrine likely affected the lack of hemodynamic differences between groups. This is a novel demonstration of IPoC utility in a historically conditioning-resistant group.

References: 1. More evidence that out-of-hospital cardiac arrest is preventable. Resuscitation 2019

2. Interaction effects between hypothermia and diabetes mellitus on survival outcomes after out-of-hospital cardiac arrest. Resuscitation 2015; 90: 35-41

3. Cardiopulmonary resuscitation for cardiac arrest: the importance of uninterrupted chest compressions in cardiac arrest resuscitation. The American Journal of Emergency Medicine 2012; 30: 1630-1638

4. Cell Death Pathways in Acute Ischemia/Reperfusion Injury. Journal of Cardiovascular Pharmacology and Therapeutics 2011; 16: 233-238

5. Ischemic postconditioning at the initiation of cardiopulmonary resuscitation facilitates functional cardiac and cerebral recovery after prolonged untreated ventricular fibrillation. Resuscitation 2012; 83: 1397-1403

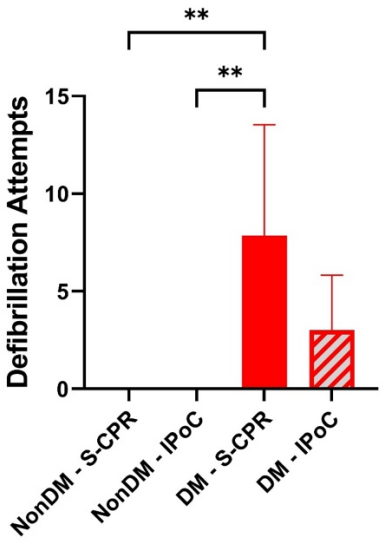
**
**
Defibrillation Attempts
15
10
5
0
NonDM - S-CPR
NonDM - IPoC
DM - S-CPR
DM - IPoC

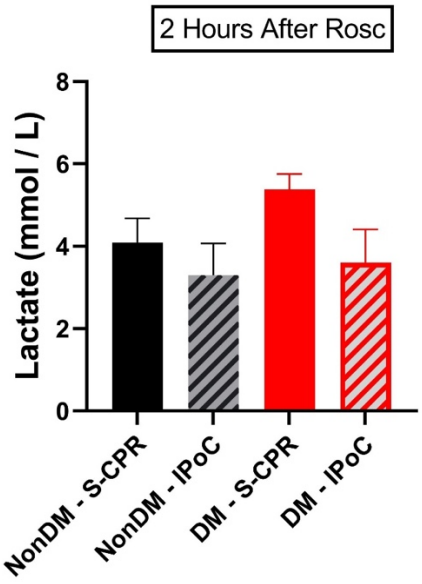
2 Hours After Rosc
Lactate (mmol / L)
8
6
4
2
0
NonDM - S-CPR
NonDM - IPoC
DM - S-CPR
DM - IPoC

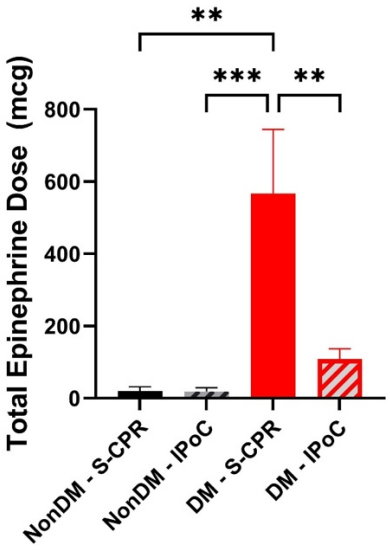
**
***
**
Total Epinephrine Dose (mcg)
800
600
400
200
0
NonDM - S-CPR
NonDM - IPoC
DM - S-CPR
DM - IPoC

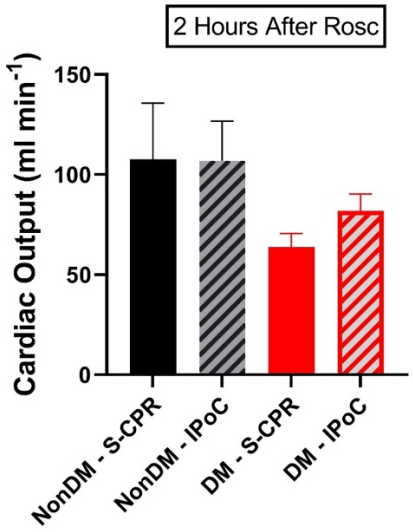
2 Hours After Rosc
Cardiac Output (ml min-1)
150
100
50
0
NonDM - S-CPR
NonDM - IPoC
DM - S-CPR
DM - IPoC

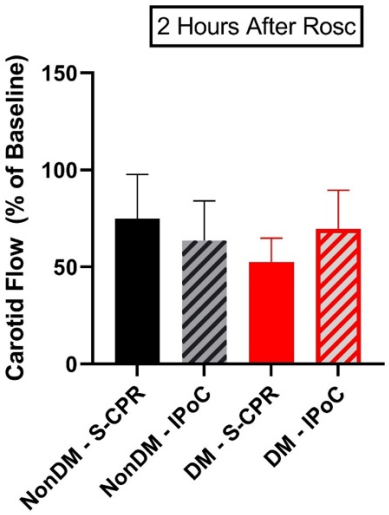
2 Hours After Rosc
Carotid Flow (% of Baseline)
150
100
50
0
NonDM - S-CPR
NonDM - IPoC
DM - S-CPR
DM - IPoC

Cardiovascular Anesthesiology 7

- Norepinephrine versus phenylephrine for treating hypotension during general anesthesia in adult patients undergoing major non-cardiac surgery: multicenter, open-label, cluster-randomized trial (VEGA-1 trial)

Matthieu Legrand[1], Rishi Kothari[2], Nicholas Fong[2], Nandini Palaniappa[1], David Boldt[3], Lee-Lynn Chen[4], Philip Kurien[1], Eilon Gabel[1], Jillene Sturgess-Daprato[1], Michael Harhay[1], Romain Pirracchio[5], Michael Bokoch[6]

UCSF[1] Thomas Jefferson University Hospital[2] UCLA Medical Center[3] University of California San Francisco[4] UCSF Departmnent of Anesthesia[5] University of California, San Francisco[6]

Introduction: Treatment of intraoperative hypotension prevents postoperative complications. The use of vasopressors is often required to correct anesthesia-induced hypotension. The best first-line vasopressor has not been established. The goal of this study was to to evaluate the feasibility of a cluster-randomized trial to compare phenylephrine vs norepinephrine as the first-line vasopressor and the impact of drug choice on outcomes.

Methods: Multicenter, open-label, cluster-randomized trial in Five hospitals in California. Amng patients undergoing major non-cardiac surgery under general anesthesia we randomized centers to use continuous intravenous phenylephrine (PE) vs norepinephrine (NE) infusion as the first-line vasopressor. First-line vasopressor alternated monthly at each hospital for 6 months.
Primary endpoint was first-line vasopressor administration compliance. Secondary endpoints were acute kidney injury (AKI), 30-day mortality, myocardial injury after non-cardiac surgery (MINS), adverse cardio-renal events, hospital length of stay, and rehospitalization via the emergency department within 30 days.

Results: 3626 patients were enrolled over 6 months at each site; 1809 patients were randomized in the NE group, 1817 in the PE group. All randomized patients were analyzed. 88.2% received the assigned first-line vasopressor. Doses of vasopressors received significantly differed between groups (Figure 1). No drug infiltrations requiring treatment were reported in either group. Patients were median 63 years old, 50% female, 58% white. Median duration of surgery was 230 minutes. Blood pressure was not different between groups (Figure 2). AKI occurred in 9.4% in the NE vs 8.9% in the PE group (p=0.6), 30-day mortality was 1.1% in the NE vs 1.2% in the PE group (p=0.868), MINS 2.4% in the NE vs 2.1% in the PE group (p=0.312), emergent rehospitalization occurred in 3.1% in the NE vs 3.6% in the PE group (p=0.257). Hospital length of stay was 4.06 (Q1-Q3 2.10-7.03) days in the NE vs 4.10 (2.08-7.46) days in the PE group (p=0.257). In a generalized, linear, mixed-effects model, randomization in the NE group vs PE group was not significantly associated with post operative outcomes. Adjusted odds of AKI 0.91 (0.27, 3.02; p=0.873), 30-day mortality 0.89 (0.21, 3.73; p=0.869), MINS 1.18 (0.36, 3.85; p=0.782), adverse cardio-renal events 1.44 (0.35, 5.94; p=0.615), readmission via the ED within 30 days in the NE group compared to the PE group was 0.25 (95% CI 0.05, 1.23; p=0.087, Figure 3). No subgroups were associated with significantly increased odds of developing AKI when randomized to the NE versus the PE group.

Conclusions: In this multicenter pragmatic trial, we successfully randomized patients undergoing major surgery under general anesthesia to receive norepinephrine or phenylephrine infusion as the first-line vasopressors. We did not observe statistically significant differences in postoperative outcomes, but the trial was not powered for these outcomes.

References: Trial Registration: ClinicalTrials.gov NCT04789330

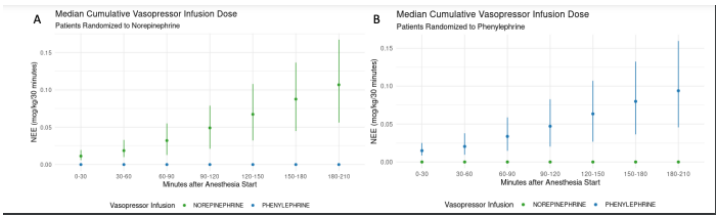

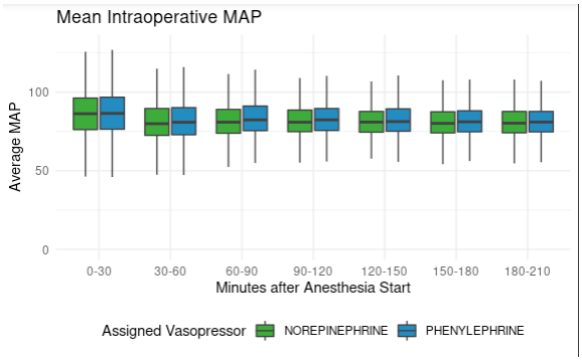

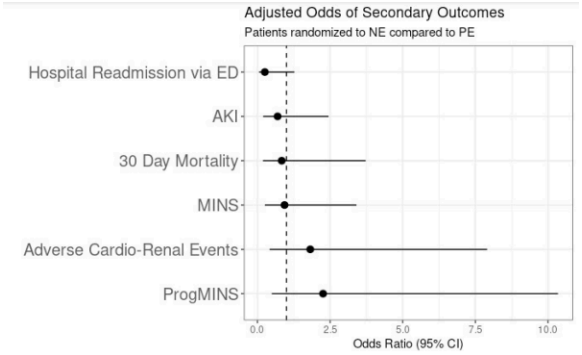

Cardiovascular Anesthesiology 8 - Anesthetic choice and perioperative outcomes in elderly TAVR patients in the United States

Isaac Freedman[1], Andre Dempsey[1], Benjamin Stone[2], Jakob Wollborn[2], Jochen Muehlschlegel[3]

Massachusetts General Hospital, Harvard Medical School[1] Brigham and Women's Hospital[2] BWH[3]

Introduction: Intraoperative anesthetic management of transfemoral transcatheter aortic valve replacement (TAVR) has evolved in recent years. Increasingly clinicians are opting for minimalist anesthetic approaches, such as monitored anesthesia care (MAC), while others continue to use general anesthesia (GA). Observational data suggests that MAC and PDS are associated with similar 30-day mortality rates and shorter hospital stays compared to GA.
The aim of this study was to describe patient-level factors that influence the choice of anesthetic management—GA vs. MAC—in elderly cardiac surgical patients undergoing TAVR in a large nationwide sample.

Methods: The American College of Surgeons National Surgical Quality Improvement Program (NSQIP) dataset from 2016-2020 was used to identify 580 patients over the age of 60 undergoing TAVR. Patient demographics and comorbidities were compared between patients undergoing MAC/IV sedation and those undergoing GA using Wilcoxon-signed rank tests. Multivariate logistic regression was used to identify patient factors that influence the choice of MAC/IV sedation compared to GA as well as factors influencing extended length of stay (eLOS) defined as greater than the 75th percentile of length of stay in the cohort.

Results: Patients undergoing MAC were more likely to have dyspnea on exertion (DOE) and be ASA Class IV compared to those undergoing General Anesthesia (DOE 68.70% versus 57.90%, p = 0.011, ASA Class Class IV 94% versus 77.7%, p < .001). Patients undergoing MAC were less likely to have congestive heart failure (CHF) or metastatic cancer compared to GA (CHF 17.7% versus 25.0%, p = .040, Metastatic Cancer 0.3% versus 2.9%, p = 0.034). Patients undergoing MAC on average spent 1.85 fewer days in the hospital (2.9 days versus 3.7 days, p = 0.016). There was no difference in the rates of surgical adverse events between the groups including surgical site infection (1.4% versus 0.3%, p = 0.329). There were more medical adverse events in the GA group (10.4% versus 5.3%, p = 0.035) which was driven by an increased risk of cardiac arrest (2.1% versus 0.0%, p = 0.033). Factors that were predictive of choice of MAC versus GA included smoking status (OR = 0.48, p = .050), DOE (OR = 1.58, p = 0.014), and CHF (OR = 0.56, p < 0.01). MAC/IV-sedation versus GA (OR = 0.33, p = 0.001) and Male sex (OR = 0.42, p = 0.008) were predictive of eLOS.

Conclusions: MAC is an increasingly popular choice for anesthetic management during TAVR. Patient's undergoing MAC tended to be sicker, as evidenced by higher ASA class and the presence of dyspnea on exertion. Certain populations such as those with clinical congestive heart failure or disseminated cancer were more likely to be chosen for GA. Patients undergoing MAC had significantly shorter length of stay and experienced fewer medical adverse events.

Table 1: Patient Demographics

Variables	General (n = 280)	MAC/IV Sedation (n = 300)	P-value
Age (Years)			
Mean ± SD	78.8 ± 6.8	79.1 ± 7.0	0.65
Median [IQR]	79 [74 - 84]	80 [75 - 85]	0.58
Male (%)	61.40	56.70	0.28
Race (%)			0.89
American Indian or Alaska Native	0.5	0.8	
Asian	0.5	0.3	
Black or African American	4.2	2.8	
White	94.9	93.6	
BMI (kg/m^2)			
Mean ± SD	29.7 ± 7.2	29.0 ± 7.7	0.25

Table 2: Preoperative comorbidities.

Variables	General (n = 280)	MAC/IV Sedation (n = 300)	P-value
Diabetes (%)	36.1	30.0	0.14
Smoking (%)	7.9	4.0	0.072
Dyspnea (%)			**0.011***
No	35.0	28.0	
With Moderate Exertion	57.9	68.7	
At Rest	7.1	3.3	
Dependent Functional Status (%)	6.1	3.3	0.19
COPD (%)	15.4	16.0	0.92
Ascites (%)	0.0	0.3	1.00
CHF (%)	25.0	17.7	**0.040***
HTN (%)	81.1	83.3	0.55
Renal Failure (%)	0.4	0.0	0.97
Dialysis (%)	2.5	2.7	1.00
Metastatic Cancer (%)	2.9	0.3	**0.034***
Wound Infection (%)	1.1	2.3	0.40
Steroids (%)	5.0	3.7	0.56
Malnourished (%)	1.1	1.0	1.00
Bleeding Disorder (%)	20.7	21.0	1.00
Recent Blood Transfusion (%)	0.7	1.0	1.00
Modified Frailty Index (%)			0.080
0	10.4	8.7	
1	35.7	44.7	
2	36.8	36.3	
3	14.3	8.3	
4	2.9	2.0	
ASA Class (%)			**<0.001***
3	22.3	6.0	
4	77.7	94.0	

Table 3: Perioperative outcomes for GA vs. MACI in elderly patients undergoing TAVR.

Variables	General (n = 280)	MAC/IV Sedation (n = 300)	P-value
Length of Stay (Days)			
Mean ± SD	3.7 ± 5.0	2.9 ± 3.4	**0.016***
Median [IQR]	2.0 [1.3-4.0]	2.0 [1.0-3.0]	**<0.001***
Surgical Adverse Events (%)	1.4	0.3	0.33
Superficial SSI	1.1	0.0	0.22
Deep SSI	0.0	0.3	1.00
Organ space SSI	0.4	0.0	0.97
Wound dehiscence	0.4	0.3	1.00
Medical Adverse Events (%)	10.4	5.3	**0.035***
PNA	2.5	1.0	0.29
Intubation/Reintubation	1.8	0.7	0.39
PE	0.4	0.3	1.00
Renal Insufficiency	0.4	0.3	1.00
UTI	2.5	1.3	0.44
Stroke	2.5	3.3	0.73
Cardiac Arrest	2.1	0.0	**0.033***
MI	0.7	0.3	0.95
DVT	0.4	0.0	0.97
C. diff colitis	0.0	0.3	1.00
Systemic sepsis	0.7	0.3	0.95
Number of AEs (%)			**0.027***
0 AE	88.9	94.3	
1 or more AE	11.1	5.7	
AE severity (%)			
Minor AE	6.1	2.7	0.070
Severe AE	6.8	4.7	0.36
Operation Time (hours)			**<0.001***
0 - 1	19.6	33.0	
1 - 2	58.2	57.7	
2 - 3	12.9	8.7	
>3	9.3	0.7	
Reoperation (%)	5.4	5.3	1.00
Readmission (%)			
Unplanned readmission	8.6	9.0	0.97
Related to principal procedure	66.7	63.0	1.00

Table 4: Multivariate logistic regression of factors predictive of MAC (vs. GA).

Variables	OR	95% CI	P-value
Age	1.02	(0.99 - 1.04)	**0.128***
Male Sex	0.94	(0.68 - 1.31)	0.73
Smoking	0.48	(0.23 - 1)	0.050
Dyspnea on exertion	1.56	(1.09 - 2.22)	**0.014***
Congestive Heart Failure	0.56	(0.26 - 1.38)	**<0.01***

Table 5: Multivariate Logistic Model for prediction of eLOS.

Variables	OR	95% CI	P-value
MAC/IV Sedation	0.33	(0.17 - 43.4)	**0.001**
Age	1.04	(0.99 - 2.87)	0.10
Male Sex	0.42	(0.22 - 30.06)	**0.008**
Dyspnea, any	2.35	(0.98 - 10.89)	0.055

Cardiovascular Anesthesiology 9 - Multihospital retrospective study on association between elevated neutrophil to lymphocyte ratio and increased in-hospital mortality in perioperative cardiac surgery patients

Elijah Christensen[1], Nathan Clendenen[1]

University of Colorado - Anschutz[1]

Introduction: In the critical care and perioperative setting significant resources are deployed to closely monitor and then intervene on patients who may rapidly decompensate. With finite resources, intensivists and anesthesiologists are tasked with deciding when a patient is appropriate for lower acuity care. Elevated neutrophil to lymphocyte ratio (NLR) has gained recent attention in several fields of medicine [1] as a biomarker of proinflammatory physiology [2]. While it has been used to stratify preoperative patients in specific surgical subspecialties [3] no large studies have evaluated NLR in cardiac surgery patients where NLR could be used to identify patients at risk of acute decompensation. The response properties of NLR also make it attractive as an early marker of physiologic stress as it rapidly increases in response to acute insult (<6 hours) [2]. We endeavored to evaluate if elevated NLR in cardiac surgery patients is associated with increased post-operative in-hospital mortality.

Methods: This is a retrospective study of hospitalized patients in the UCHealth system comprised of multiple hospitals throughout Colorado. Data was provided by Health Data Compass (HDC), a multi-institutional data warehouse which anonymizes and deidentifies electronic medical record (EMR) data from participating hospitals across Colorado. This study protocol was approved by the University of Colorado Institutional Review Board (COMIRB). We included adult cardiac surgery patients who underwent surgery for either valve replacement/repair and/or coronary artery bypass graft from any UCHealth hospital between 9/3/2011 to 4/17/2022. Neutrophil to lymphocyte ratio (NLR) was calculated for each patient using lymphocyte and neutrophil percentages from every blood cell count with differentials. To standardize timing and comparisons, patients with multiple LNR values were averaged over a 24hr window. The primary outcome was in-hospital mortality. Secondary outcomes included postop myocardial infarction, cerebral infarction, and dialysis dependence in the first 60 days postop as indicated in EMR records. Patients were aligned such that day 0 corresponded to date of surgery. Confidence intervals with confidence level of 95% were estimated at each timepoint using bootstrap resampling (n=1000). We considered $p < 0.05$ statistically significant.

Results: Patient encounters containing a procedure order code for any cardiac valve replacement/repair and/or any coronary artery bypass graft were included for analysis. 2385 patient encounters met inclusion criteria of which 72 patients had in hospital mortality (3.12%). We restricted analysis to data available 48hours prior to surgery out to 60 days after surgery. Both survivors and non-survivors had similar baseline characteristics with no statistically significant differences in gender, race, and facility location. Both groups had similar NLR before, during, and immediately after surgery. Both groups had nearly identical mean NLR on POD1 (12.5) but by POD2 survivors compared to non-survivors had lower NLR (9 vs 12.5) reaching statistical significance. By POD5 survivors compared to non-survivors had NLR values at or near pre-op levels (5 vs 13).

Conclusions: Our multihospital retrospective analysis shows NLR trajectories in cardiac surgery patients, when trended over the perioperative period, can stratify and segregate patients at risk for in-hospital mortality. To our knowledge, this is the first retrospective study of its size on NLR in perioperative cardiac surgery patients which demonstrates its utility as a continuous predictor of perioperative mortality. This may have important implications for the post-operative setting when a patient's clinical trajectory is nonobvious. While preoperative NLR between both groups were similar, they separate very early after surgery, with statistically significant differences apparent 36 hours post-op. Our results indicate NLR has utility as an early warning that a patient may be clinically less well than otherwise suggested by their clinical status.

References:

[1] Varım C, et al. Association between the neutrophil-to-lymphocyte ratio, a new marker of systemic inflammation, and restless legs syndrome. *Singapore Med J*. 2016;57(9):514-516

[2] Zahorec R. Ratio of neutrophil to lymphocyte counts–rapid and simple parameter of systemic inflammation and stress in critically ill. *Bratisl Lek Listy*. 2001;102(1):5-14.

[3] Hajibandeh S, Hajibandeh S, Hobbs N, Mansour M. Neutrophil-to-lymphocyte ratio predicts acute appendicitis and distinguishes between complicated and uncomplicated appendicitis: A systematic review and meta-analysis. *Am J Surg*. April 2019

		Grouped by death_during_encounter			
		Overall	False	True	P-Value
n		2385	2313	72	
age, mean (SD)		62.0 (13.0)	61.9 (13.0)	65.9 (11.7)	0.005
gender, n (%)	Female	717 (30.1)	693 (30.0)	24 (33.3)	0.628
	Male	1668 (69.9)	1620 (70.0)	48 (66.7)	
preop_OSA, n (%)	True	265 (11.1)	260 (11.2)	5 (6.9)	0.341
	False	2120 (88.9)	2053 (88.8)	67 (93.1)	
preop_HF, n (%)	True	1061 (44.5)	1009 (43.6)	52 (72.2)	<0.001
	False	1324 (55.5)	1304 (56.4)	20 (27.8)	
preop_DM, n (%)	True	631 (26.5)	608 (26.3)	23 (31.9)	0.349
	False	1754 (73.5)	1705 (73.7)	49 (68.1)	
postop_CVA, n (%)	True	5 (0.2)	4 (0.2)	1 (1.4)	0.142
	False	2380 (99.8)	2309 (99.8)	71 (98.6)	
postop_RRT, n (%)	True	18 (0.8)	18 (0.8)		1.000
	False	2367 (99.2)	2295 (99.2)	72 (100.0)	
postop_MI, n (%)	True	24 (1.0)	23 (1.0)	1 (1.4)	0.523
	False	2361 (99.0)	2290 (99.0)	71 (98.6)	
facility_location, n (%)	MHC HOSPITAL	644 (27.0)	627 (27.1)	17 (23.6)	0.792
	UCH HOSPITAL	1740 (73.0)	1685 (72.8)	55 (76.4)	
	UCH OUTPATIENT SERVICES	1 (0.0)	1 (0.0)		

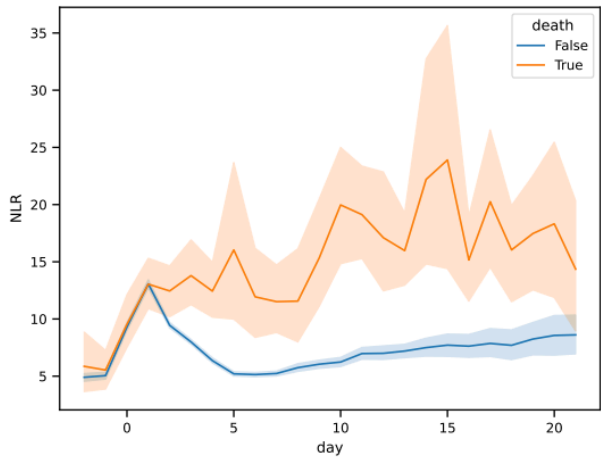
death
False
True
NLR
day
35
30
25
20
15
10
5
0
5
10
15
20

Cardiovascular Anesthesiology 10 - Regulation of Vascular Endothelial Hypoxic-Adenosinergic Signaling by Estrogen: *Implications for microvascular injury and diastolic heart failure in Yentl Syndrome*

Jessica Cassavaugh[1], Nada Qureshi[1], Eva Csizmadia[1], Maria Serena Longhi[1], Robina Matyal[1], Simon Robson[2]

Beth Israel Deaconess Medical Center[1] BIDMC: Beth Israel Deaconess Medical Center[2]

Introduction: Premenopausal women are shielded from vascular disease, at least in part, through the protective effect of estrogen. Loss of estrogen, as occurs with normal aging, can be linked to increased inflammation, pathologic angiogenesis, decreased endothelial cell integrity and impaired mitochondrial functions[1]. Estrogen receptor (ER), a steroid receptor, exerts its effects through transcriptional regulation of target genes. Following ligand binding, ER translocates to the nucleus where it functions either directly as a transcription factor and binds to a target gene, or indirectly through binding to and stabilizing other transcription factors[2]. The influence of estrogen on protective, anti-inflammatory pathways are largely unknown, especially under conditions of hypoxia. However, these effects may be secondary to alterations in extracellular adenosine levels, generated at high levels by CD39 and CD73 ectonucleotidases. We have therefore investigated how estrogen modulates hypoxic-adenosinergic vascular signaling responses and angiogenesis to further define those mechanisms necessary for vascular protection.

Methods: Human umbilical venous endothelial cells (HUVECs) were exposed to hypoxia (1% oxygen for 24 hours) or Cobalt Chloride (100uM for 24 hours). HUVEC treatments include estradiol (E2), fulvestrant (estrogen receptor inhibitor), dipyridamole (adenosine transport inhibitor), caffeine (adenosine receptor antagonist), or gene silencing via siRNA. Expression of CD39, CD73, adenosine transporters (ENT1), ERK1/2 and estrogen receptors (ER) were measured using western blotting and immunofluorescence. Adenosine, adenosine deaminase (ADA) and ATP were measured using fluorescence and luminescence, respectively. Standard tube formation and wound healing assays were performed to assess *in vitro* angiogenesis. To determine impacts on purinergic responses *in vivo,* C57BL/6 mice underwent ovariectomy at 12 weeks, and at 26 weeks, cardiac tissue was evaluated for changes in protein expression.

Results: Expression levels of CD39 and estrogen receptor alpha (ERa) were markedly increased in hypoxia and with estradiol (E2) treatment. Suppression of ESR1 or SP1, a transcription factor known to associate with ERa, via siRNA resulted in decreased CD39 expression[3]. In addition, expression of ENT1, an adenosine transport protein, was decreased in a manner dependent on ER-mediated signaling. Additionally, extracellular ATP and ADA activity levels decreased following E2 exposure, while levels of adenosine increased. Phosphorylation of ERK, a downstream adenosine receptor signaling target, increased following E2 treatment. These effects were attenuated by blocking adenosine receptor and ER activity. Likewise, estradiol boosted angiogenesis *in vitro* while inhibition of ER or adenosine receptors decreased this. Lastly, expression of CD39 and phospho-ERK decreased in cardiac tissue from ovariectomized mice as compared to control animals, while ENT1 expression increased. Similarly, plasma adenosine was also decreased in ovariectomized animals.

Conclusions: E2 treatment and/or hypoxia increases CD39 and ERa levels and decreases the expression of ENT1. These hormonal changes substantially increase adenosine availability and signaling while also augmenting vascular protective signaling responses. Control of CD39 expression by ERa may be via transcriptional regulation, possibly through interactions with SP1. Boosting hypoxic-adenosinergic signaling may ameliorate cardiovascular changes seen in estrogen lack and linked to Yentl syndrome. Our data indicate novel therapeutic avenues to ameliorate post-menopausal cardiovascular disease by modulation of adenosinergic mechanisms.

References: 1. *Frontiers in Endocrinology* 2019;1:442.

2. *Nucleic Acids Res*. 2001;29(14):2905-2919.

3. *Endocrinology*. 2001;142(4):1546-1553.

Cardiovascular Anesthesiology 11 - Sulfide Quinone Oxidoreductase: A New Regulator of The Permeability Transition Pore In Murine Cardiac Mitochondria

Keren Griffiths[1], Richard Levy[2], Christopher Porras Lopez[1], Aili Wang[1]

Columbia University[1] NY Presbyterian Hosp - Columbia U[2]

Introduction: The mitochondrial permeability transition pore (mPTP) is a prime therapeutic target given that its dysfunction plays a role in the pathogenesis of diseases ranging from diabetes to ischemia-reperfusion injury (1,2). Though the precise proteinaceous identity is still debated, it is well accepted that the mPTP is voltage-gated, such that depolarization of the inner mitochondrial membrane (IMM) leads to pore opening (3). There is a major gap in our knowledge, however, because the voltage sensor is unknown. Prior work has demonstrated that the redox status of vicinal thiol groups tunes the putative voltage sensor of the mPTP such that oxidation opens the pore at relatively higher $\Delta\Psi$s and thiol group reduction results in closed mPTP probability (4). In previous work, we identified a pathologically open mPTP within the forebrain of Fragile X syndrome (FXS) mice due to coenzyme Q (CoQ) deficiency and a relatively closed mPTP within the cardiomyocytes of FXS mice due to CoQ excess (5,6). In addition, CoQ replete FXS cardiomyocyte mitochondria appear to have altered voltage gating of their mPTP (7). Thus, it is clear that CoQ regulates the mPTP and may also contribute to its voltage gating. Interestingly, sulfide quinone oxidoreductase (SQOR), a mitochondrial enzyme that catalyzes the first step of catabolism of hydrogen sulfide (H_2S), is a ubiquitously expressed IMM-associated protein, harbors redox-sensitive vicinal thiol groups, and binds CoQ as a requisite electron acceptor. These characteristics render SQOR an attractive candidate to be the voltage gate of the mPTP. Here were we present evidence that SQOR represents a novel regulator of the mPTP.

Methods: The care of mice was in accordance with NIH and CUMC IACUC guidelines. We evaluated cardiac mitochondria harvested from male Fmr1 KO mice (FXS) along with their FVB controls on P10 and 6-8 wks, as well as *Sqor* KO mice along with their C57BL6J controls at 4-6 wks. Oxygen consumption and mitochondrial membrane potential were measured simultaneously using polarography and a tetraphenylphosphonium ion selective electrode (7). Complex II-dependent proton leak respiration was assessed using succinate, rotenone and oligomycin. In separate experiments, CsA was added at a range of membrane potentials in order to determine open or closed mPTP probability based on CsA sensitivity (7). We determined the expression of the SQOR in cardiac mitochondria using Western blot. We evaluated the effect of the SQOR inhibitor, antimycin A, on voltage gating as described above except complex IV-dependent proton leak respiration was measured using N,N,N,N-tetramethyl-p-phenylenediamine/ascorbate, rotenone, malonate and oligomycin. Calcium loading capacity was determined using a calcium selective electrode (5). In situ mPTP open probability was determined by conducting the calcein-cobalt quenching assay in isolated-perfused hearts using real time confocal imaging (8). For quantitative analyses at least 3 animals were used per group. Significance was assessed via Student's test or one-way ANOVA where appropriate with set $p < 0.05$.

Results: Mitochondria from newborn *Fmr1* KOs demonstrated a left shift in voltage threshold for opening based on cyclosporin sensitivity, i.e. the mPTP required lower membrane potential for opening. *Fmr1* KO cardiac mitochondria had increased SQOR expression and activity. Inhibition of SQOR with antimycin A led to opening of the mPTP at higher membrane potential where it would normally be closed and also decreased the calcium loading capacity for mPTP opening. *Sqor* KO mice showed decreased calcium loading capacity for mPTP opening in isolated cardiac mitochondria and showed increased cobalt quenching of calcein in situ in isolated perfused cardiac tissue, suggesting increased mPTP open probability.

Conclusions: We show that *Fmr1* KO mice exhibit lower gating potential of the mPTP that is associate with increased expression and activity of SQOR. We also show that inhibition of SQOR disrupts normal voltage gating of the mPTP and decreases the threshold for calcium induced opening of the mPTP. Sqor KO mice that lack SQOR also exhibit a decreased threshold for calcium-induced opening of the pore both in vitro and in situ. This work identifies SQOR as novel regulator of mPTP and suggests a role in voltage gating of the mPTP.

References:

1. Apoptosis 12:815-33, 2007
2. Cell Cycle 9:3442-8, 2010
3. J. Biol Chem. 267:8834-39, 1992
4. J. Biol Chem. 269:16638-42, 1994
5. FASEB J. 34: 7404-7426, 2020
6. Peds. Res. 89:456-463, 2021
7. J. Vis. Exp. 184: 1-12, 2022
8. Phy. Rep. 10: e15402, 2022

Cardiovascular Anesthesiology 12 - The impact of postoperative atrial fibrillation on mortality after cardiac surgery: 20-year follow-up of a multi-institutional retrospective cohort study.

Sergey Karamnov[1], Natalia Sarkisian[1], Simon Body[1], Jochen Muehlschlegel[2]

Brigham and Women's Hospital[1] BWH[2]

Introduction: Postoperative atrial fibrillation (poAF, AF) is the most common complication after cardiac surgery. Up to 50% of patients who present in normal sinus rhythm prior to surgery will develop poAF. In contrast to the long-held belief that poAF is a benign, transient, self-limiting phenomenon, emerging evidence suggests that poAF may impact postoperative mortality[1][JM1] . However, the magnitude of the impact of poAF remains to be determined as it is unclear how poAF affects patient long-term survival. Furthermore, the effect of poAF in high-risk cardiac surgery groups, such as female patients[2], is of particular concern, as the effect of sex and poAF on mortality may be confounded. To better understand the role poAF plays in postoperative survival of male and female patients, we designed this retrospective cohort study. We hypothesized that female patients with poAF will experience lower survival compared to male poAF patients and that the effect of poAF on mortality is greater than the effect of female sex.

Methods: Study design. This is a retrospective cohort study of adult (> 20 years old) patients who underwent coronary artery bypass graft surgery (CABG), open aortic valve replacement or repair (AVR), open mitral valve replacement or repair (MVR), or combined procedures with cardiopulmonary bypass (CPB) at two tertiary care centers.
Patient Population. We obtained data from two hospital cohorts using identical methodology from an institutional data registry[3]. We included patients with a history of paroxysmal AF but excluded those in chronic AF or those not in normal sinus rhythm at the time of surgery.
Measurement of outcome. Censoring dates were defined as date of death or date of last medical record indicating patient being alive. Patients with missing information beyond their index surgery, or those without available records of death were excluded from the analysis.
Key predictors. PoAF was defined as any new-onset AF that developed during the primary hospitalization on EKG. Additional data were extracted from Society of Thoracic Surgeons (STS) Adult Cardiac Surgery Database (ACSD) database.
Covariates. Covariates included patient demographics, patient-related risk, surgery-related risk factors, laboratory values, as well as medications (Table 1).
Statistics. Descriptive statistics for covariates were calculated separately for those with and without poAF as mean values with standard deviations or as frequencies and percentages of patients. Pearson's chi-square tests for discrete variables and Student t-tests for continuous variables were used. Unadjusted Kaplan Meier (KM) curves separated by sex and poAF were constructed with 95% confidence intervals (CI). A Cox proportional hazard model was estimated, including sex, poAF, sex by poAF interaction, and all the covariates. Adjusted KM curves for the four groups were constructed based on this model, and HR was also calculated for three groups defined by the combination of sex and poAF, as compared to males without poAF. Stata 16.0 was used for all analyses.
Ethics. Institutional review board approval was obtained with waiver of consent as patient data was de-identified.

Results: A total of 20,238 patients who underwent cardiac surgery January 2002-March 2016 were eligible for the analysis (Figure 1). The 20-year follow-up was 98%. Baseline patient characteristics and poAF risk factors are summarized in Table 1. PoAF was diagnosed in 35.8% of the population. PoAF was associated with decreased long-term survival in both male (HR 1.2, 95% CI 1.12 to 1.28) and female (HR 1.44, 95% CI 1.33 to 1.56) patients as compared to males without poAF. Female sex was an independent predictor of mortality (HR 1.08, 95% CI 1.01 to 1.17), however the effect of poAF on mortality was greater than the effect of sex (Figure 2). In addition, the effect of poAF on mortality was greater among females (HR 1.33, 95% CI 1.22 to 1.45) than among males (HR 1.2, 95% CI 1.12 to 1.28).
Conclusions: PoAF increases risk of long-term mortality in male and female patients undergoing open-heart surgery. Female patients who develop poAF after cardiac surgery demonstrate decreased survival compared to male patients. The effect of poAF on mortality is higher than the effect of sex.

References: 1. Postoperative atrial fibrillation significantly increases mortality, hospital readmission, and hospital costs. Ann Thorac Surg. 2014 Aug;98(2):527-33

2. Sex Differences in Long-Term Survival After Major Cardiac Surgery: A Population-Based Cohort Study. J Am Heart Assoc. 2019 Sep 3;8(17).

3. A security architecture for query tools used to access large biomedical databases. Proc AMIA Symp. Published online 2002:552-556.

Table 1. Baseline patient characteristics stratified by poAF

Variable	No poAF		poAF		p value
	N or Mean	% or SD	N or Mean	% or SD	
Females	3874	30	2286	32	0.014
Age	63.9	12.6	70.7	10.8	<0.001
BMI (kg/m2)	28.6	5.6	28.5	5.8	0.29
PVD	1701	13	1117	15	<0.001
History of AF	330	3	416	6	<0.001
History of COPD	259	2	242	3	<0.001
Procedure type					<0.001
CABG	6994	53.9	3048	42.0	
AVR	2965	22.8	1727	23.8	
MVR	1152	8.9	731	10.1	
CABG+AVR	1395	10.8	1222	16.8	
CABG+MVR	476	3.7	528	7.3	
Diabetes	3645	28	1982	27	0.246
Hypertension	9290	72	5705	79	<0.001
Emergent surgery	316	2	241	3	<0.001
Creatinine (mg/dl)	1.13	0.73	1.18	0.71	<0.001
CHF	3035	23	2257	31	<0.001
History of MI					0.411
None	9175	71	5064	70	
Past	1773	14	1026	14	
Recent	2034	16	1166	16	
Race					
Asian	236	2	76	1	<0.001
Black	283	2	84	1	
Caucasian	11966	92	6903	95	
Hispanic	313	2	100	1	
Other	184	1	93	1	
Hyperlipidemia	9875	76	5589	77	0.123
ACE Inhibitors or ARB within 48 hours preceding surgery	1844	14	1014	14	0.653
Beta blockers within 24 hours preceding surgery	7852	60	4484	62	0.066

Values are mean (SD) or n (%); p-values correspond to t tests or chi-square tests. BMI, body-mass index; PVD, peripheral vascular disease; CHF, congestive heart failure; MI, myocardial infarction; poAF, postoperative atrial fibrillation; COPD, chronic obstructive pulmonary disease; AVR aortic valve replacement; MVR, mitral valve replacement; CABG, coronary artery bypass graft surgery.

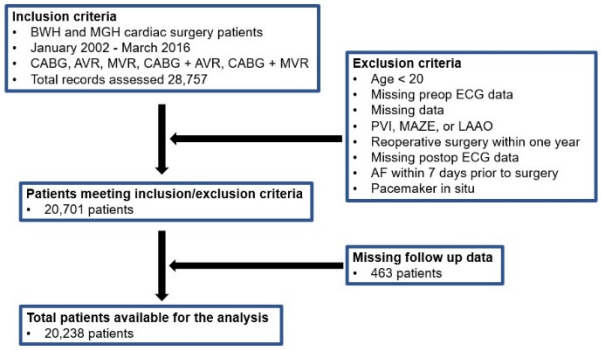

Figure 1. CONSORT diagram of the study demonstrating inclusion and exclusion criteria. CABG, coronary artery bypass surgery; AVR, aortic valve replacement; MVR, mitral valve replacement or repair; ECG, electrocardiogram; AF, atrial fibrillation; PVI, pulmonary vein isolation; LAAO, left atrial appendage occlusion.

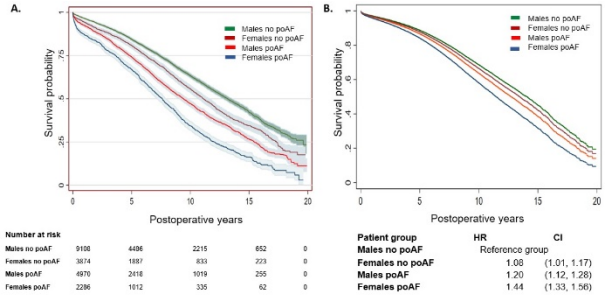

Figure 2. Risk-adjusted survival in all patients. A. Unadjusted Kaplan Meier (KM) curves with 95% confidence intervals (CI). B. Adjusted KM curves and hazard ratios for the four patient groups. PoAF, postoperative atrial fibrillation.

Cardiovascular Anesthesiology 13 - Vasopressor Usage as a Predictor for Mortality in COVID-19 Patients Receiving Venovenous Extracorporeal Membrane Oxygenation

Flora Park[1], Karen Katrivesis[2], Phat Dang[2], Sonali Rao[2], Joseph Rinehart[2], Aalap Shah[3], Kei Togashi[2]

University of California, Irvine School of Medicine[1] University of California Irvine[2] UCI Health[3]

Introduction: Septic shock is a devastating complication among patients already suffering from COVID-19 infection [1]. The use of vasoactive-inotropic scores (VIS) to determine outcomes has still not been widely validated for adult patients who develop septic shock [2, 3]. Our study describes vasopressor usage in COVID-19 patients requiring Venovenous Extracorporeal Membrane Oxygenation (VV-ECMO) and seeks to determine if VIS can be predictive of post-treatment outcomes in this cohort of patients who subsequently developed septic shock.

Methods: A retrospective observational study was performed on 28 adult (18-years-old and older) patients with COVID-19 who required VV-ECMO and developed septic shock between January 2019 and December 2022. The primary outcome was mortality. VIS was calculated based on vasopressor dosage (norepinephrine, phenylephrine, vasopressin, milrinone, epinephrine, dopamine, and dobutamine) for each patient. VIS and vasopressor dosage were then analyzed using receiver operating characteristics (ROC) to assess predictors of mortality.

Results: Out of the 28 COVID-19 VV-ECMO patients studied, seven patients (25%) survived to their dates of transfer or discharge. Overall, a higher VIS was a strong predictor of mortality (AUC=0.88) (**Figure 1**). A higher cumulative norepinephrine administration was found to be a strong predictor of mortality (AUC=0.83) (**Figure 2**). With the exception of phenylephrine (AUC=0.49) (**Figure 3**), any administration of additional pressors was associated with 100% mortality.

Conclusions: VIS is a reliable predictor of mortality in patients with COVID-19 requiring VV-ECMO who subsequently developed septic shock. Additionally, the type of vasoactive/inotropic agent required for hemodynamic stability may further delineate patient demise.

References:

1. Septic shock 3.0 criteria application in severe COVID-19 patients: An unattended sepsis population with high mortality risk. *World J Crit Care Med*. 2022;11(4):246-254.
2. Association between vasoactive-inotropic score and mortality in pediatric septic shock. *Indian Pediatr*. 2015;52(4):311-313.
3. Vasoactive Inotropic Score as a Predictor of Mortality in Adult Patients With Cardiogenic Shock: Medical Therapy Versus ECMO. *Rev Esp Cardiol (Engl Ed)*. 2019;72(1):40-47.

Figure 1. ROC curve determining high predictive accuracy of VIS for mortality.

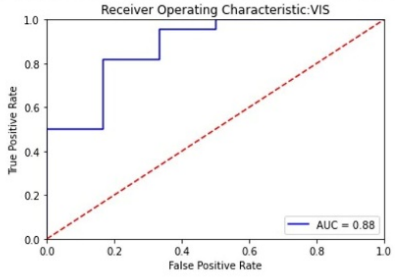

Figure 2. ROC curve determining high predictive accuracy of higher cumulative norepinephrine dose for mortality.

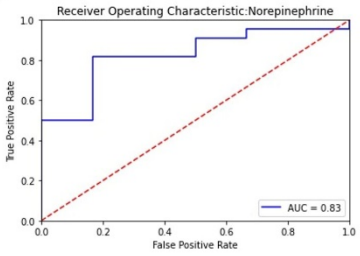

Figure 3. ROC curve determining no association between phenylephrine dosage and mortality.

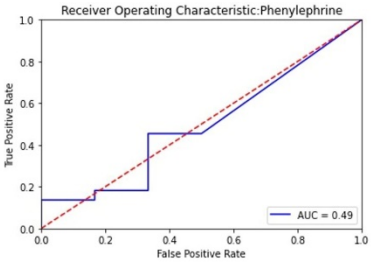

Critical Care

Critical Care 1- $A\beta_{42}$ and Tau in Lavage Fluid of Pneumonia Patients are Associated with End-Organ Dysfunction

Brant Wagener[1], Jean-Francois Pittet[2], Phoibe Renema[3], Angela Brandon[1], Sixto Leal, Jr[1], Steven Gu[1], Grace Promer[1], Andrew Hackney[4], Phillip Braswell[5], Andrew Pickering[4], Grace Rafield[4], Sarah Voth[6], Ron Balczon[6], Mike Lin[6], Kyle Morrow[6], Jonathon Audi[6], Diego Alvarez[6], Troy Stevens[6]

University of Alabama at Birmingham[1] Univ of Alabama at Birmingham[2] University of South Alabama[3] University of Alabama Birmingham School[4] Cone Health[5] Edward Via College of Osteopathic Medicine[6]

Introduction: Bacterial pneumonia and sepsis are both common causes of end-organ dysfunction, especially in immunocompromised and critically ill patients[1,2]. Pre-clinical data demonstrate that bacterial pneumonia and sepsis elicit the production of cytotoxic tau and amyloids from pulmonary endothelial cells, which cause lung and brain injury in naïve animal subjects, independent of the primary infection[3,4]. The contribution of infection-elicited cytotoxic tau and amyloids to end-organ dysfunction has not been examined in the clinical setting. Therefore, we determined whether cytotoxic tau and amyloids are present in the bronchoalveolar lavage fluid of critically ill patients with and without bacterial pneumonia, and assess whether they are associated with end-organ dysfunction.

Methods: We performed a prospective, observational clinical study in the ICU setting from June 2016 to March 2019. Forty-nine bacterial culture-positive and fifty culture-negative mechanically ventilated patients were recruited based upon collected lavage fluid samples having >100,000 CFU of bacteria (positive) or "no growth" (negative). Levels of tau, boiled tau, and $A\beta_{42}$ in, and cytotoxicity of, the bronchoalveolar lavage fluid was measured. Cytotoxic tau and amyloid concentrations were examined in comparison with patient clinical characteristics, including measures of end-organ dysfunction such as acute kidney injury, coagulopathy, and cadiovascular instability. All demographic and clinical variables with continuous measures were expressed as mean ± SD and categorical variables were expressed as proportions. Tau, boiled tau, $A\beta_{42}$, and cytotoxicity are expressed as mean ± SEM. For normally distributed data, we used a student's t-test to compare 2 groups. Statistical analyses were done with Prizm GraphPad 9.0. A p value of ≤ 0.05 was considered statistically significant.

Results: All mechanically ventilated patients with a bronchoalveolar lavage fluid containing >100,000 colony-forming units (CFU) of bacteria or "no growth" were considered. Exclusion criteria included age <18 years, any *prior* positive culture from any source (in either the positive or negative groups), incarceration, pregnancy, patients enrolled in an ongoing, interventional clinical trial, or consent refusal. $A\beta_{42}$ (23.19 ± 4.28 vs 8.76 ± 1.66), tau (2.08 ± 0.16 vs 1.50 ± 0.06), and boiled tau (1.46 ± 0.08 vs 1.15 ± 0.03) were significantly increased in the culture-positive (CP) group compared to the culture-negative (CN) group. $A\beta_{42}$ was higher in CP males compared to CN males (28.80 ± 5.08 vs 8.48 ± 1.28), whereas there were no differences in $A\beta_{42}$ between CP and CN females. Finally, $A\beta_{42}$ was higher in CP compared to CN patients regarding acute kidney injury (26.93 ± 7.99; n=21 vs 9.25 ± 2.05; n=30), coagulopathy (25.84 ± 5.76; n=33 vs 6.23 ± 2.42; 13), and need for vasopressors (18.23 ± 3.49; n=25 vs 7.94 ± 2.55; n=17). There were no differences in $A\beta_{42}$, tau, or boiled tau levels when groups were broken down into specific bacterial species or Gram-stain classification.

Conclusions: In conclusion, we have performed a prospective, controlled, observational clinical study demonstrating that $A\beta_{42}$ and tau levels are elevated in critically ill patients with bacterial pneumonia, and further, that the increase in these cytotoxins is associated with end-organ dysfunction. Future investigations are needed to assess: 1) other organs or body fluids that may contain $A\beta_{42}$ and tau after bacterial infection; 2) the longitudinal dissemination and excretion/decay of the $A\beta_{42}$ and tau; 3) whether other infections cause release of $A\beta_{42}$ and tau; and, 4) whether $A\beta_{42}$ and tau can be used as a prognostic biomarker and/or be a target for prevention and/or treatment of chronic critical illness.

References: 1. Frailty and Subsequent Disability and Mortality among Patients with Critical Illness. 196: 64-72, 2017.

2. Delirium in the ICU and subsequent long-term disability among survivors of mechanical ventilation. 42: 369-377, 2014.

3. Pseudomonas aeruginosa infection liberates transmissible, cytotoxic prion amyloids. 31: 2785-2796, 2017.

4. Nosocomial Pneumonia Elicits an Endothelial Proteinopathy: Evidence for a Source of Neurotoxic Amyloids in Critically Ill Patients. 198:1575-1578, 2018.

Critical Care 2 - An Interaction Profiler to Assess Treatments in Hospitalized Patients for COVID-19

Daniel Raza[1], William Long[2], Shaun Rockelson[3], John-Paul Sara[3], Adrian Alexis Ruiz[4], Tiffany Otero[4], Bobby Nossaman[4]

Tulane University School of Medicine - - New Orleans, LA[1] Ochsner Clinical School[2] Ochsner Medical Center[3] Ochsner Health[4]

Introduction: Although most patients infected with the COVID-19 infection are asymptomatic or have mild upper respiratory tract symptoms, older patients and patients with comorbidities are prone to severe health manifestations, such as pneumonia, that can result in hospitalization.[1,2] We examined the interactions of CDC-recommended therapies and hospital mortality rates using an interaction profiler model in patients hospitalized with the COVID-19 disease during the delta wave of the COVID-19 epidemic.

Methods: Our observational cohort study analyzed 483 patients hospitalized for COVID-19 infection at a large academic center in an urban setting. Patients were selected based on two criteria: a COVID (SARS-CoV-2) diagnosis with the real-time polymerase chain reaction and treatment with CDC-recommended therapies. Our outcome of interest was hospital mortality. Patient characteristics and comorbidities were assessed with measures of effect size.[3] We developed an interaction profile model to investigate the interplay of these therapies in preventing hospital mortality.[4] The statistical program JMP 16.2 (SAS Institute, Cary, NC) was utilized for this study.

Results: Following Institutional Review Board approval, all adult patients over 18 years or older hospitalized for COVID-19 infection from 27th July 2020 to 19th September 2021 who received CDC-recommended therapies during the delta wave of the COVID-19 epidemic were evaluated. We only excluded patients initially treated with the CDC-recommended therapies at an outside hospital before presenting to our academic hospital. Hospital mortality was 28.8% (CI 24.9-33%), with no significant rate decrease during this period (Figure 1). Age and diabetes were associated with higher hospital mortality (Table 1). The use of enoxaparin decreased the incidence of hospital mortality when used in combination with the other therapies (Figure 2).

Conclusions:
The incidence of hospital mortality in patients with COVID-19 continues to be high and did not significantly decrease during the study period. Two risk factors increased mortality: age and diabetes. Enoxaparin use resulted in the lowest hospital mortality rate when combined with the other CDC-recommended treatments in patients with COVID-19. Interaction profiler statistics can help clinicians determine best management practices in complex hospital settings to better patient health outcomes.

References: 1. Clinical predictors of mortality due to COVID-19 based on an analysis of data of 150 patients from Wuhan, China. 46, pages 846–848, 2020.

2. Clinical course and outcomes of critically ill patients with SARS-CoV-2 pneumonia in Wuhan, China: a single-centered, retrospective, observational study. 8(5):475-481, 2020.

3. Using Effect Size-or Why the P Value Is Not Enough. 4(3):279-82, 201.

4. Designing Clinical Research. Third edition, 2007.

5. Multivariable Analysis: A Practical Guide for Clinicians and Public Health Researchers. Third edition, 2011.

Figure 1. Hospital Mortality Rates in patients hospitalized with delta-COVID-19 infection from 27th July 2020 to 19th September 2021.

Table 1. Risk Differences in Hospital Mortality in Patients Admitted for the delta-COVID-19 infection.
CI: 95% confidence intervals; n (%): number and percentage of patients; COPD: Chronic obstructive pulmonary disease.

Variables	Hospital Mortality Yes	No	Risk Differences CI (%)	
Patient Characteristics n (%)				
Age≥60 y	91 (32)	190 (68)	0.08	0.006 to 0.167
Gender, m	77 (28)	194 (72)	0.008	-0.07 to 0.09
BMI≥30 kg/m²	76 (30)	176 (70)	0.07	-0.008 to 0.16
Patient Comorbidities n (%)				
Essential Hypertension	88 (28)	223 (72)	5.1	-3.8 to 14
Diabetes	54 (34)	106 (66)	10.8	2.0 to 19.7
Coronary Artery Disease	23 (32)	50 (68)	5.8	-5.8 to 17.4
Congestive Heart Failure	10 (17)	49 (83)	-11.4	-22.0 to -0.08
Tobacco Abuse	56 (28)	144 (72)	3.3	-5.1 to 11.7
COPD	14 (22)	49 (78)	-5.2	-16.4 to 6.0
Reversible Airway Disease	7 (20)	28 (80)	-7.3	-21 to 6.7
Chronic Kidney Disease	20 (29)	49 (71)	2.6	-9.1 to 14.2
Stroke	15 (37)	26 (63)	11.0	-4.4 to 26
Cirrhosis	5 (36)	9 (64)	9.2	-16.3 to 34.6
Malignancy	21 (31)	46 (67)	5.5	-6.5 to 17.4
Organ Transplantation	3 (13)	21 (87)	-15.0	-28.9 to -1.1

CI: 95% confidence intervals; n (%): number and percentage of patients; COPD: Chronic obstructive pulmonary disease.

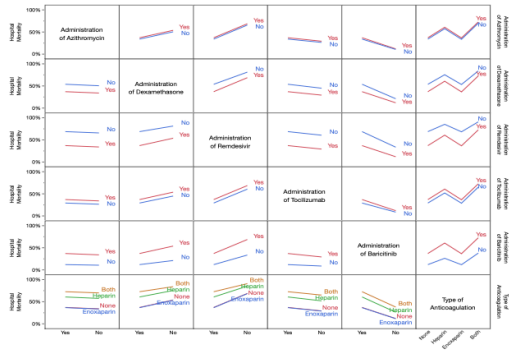

Figure 2. Incidence of hospital mortality with the administration of the medications used to treat the COVID-19 infection.

Critical Care 3 - Comparing Omicron and Delta variant phenotypes of severe COVID-19

Gebhard Wagener[1], Erika Mitsui[2]

Columbia University Irving Medical Center[1] Columbia University Vagelos College of Physicians & Surgeons[2]

Introduction: COVID-19 can result in critical illness. Separate waves of the pandemic are caused by variants of the SARS-CoV-2 virus with differing pathogenicity. The Delta variant was dominant in New York City until the end of December 2021 when the Omicron variant became responsible for almost all cases of COVID-19 [1]. The Omicron variant was thought to be more infectious but milder in symptoms [2]. Although more patients were infected during the Omicron wave, hospital resources were less strained compared to previous waves. We hypothesized that critically ill patients with Omicron COVID-19 requiring mechanical ventilation presented with a different phenotype compared to patients infected with the Delta variant. Specifically, we hypothesized that unlike Delta, Omicron was associated with milder pulmonary symptoms.

Methods: *Confirmed genotype cohorts*
We included 42 patients requiring intubation from November 1, 2021 to February 21, 2022**.** GW and EKM reviewed the phenotype based on P/F ratios and Chest X-ray appearance (bilateral, peripheral multifocal ground glass opacities and consolidations) after intubation while blinded to the genotype.

Assumed genotype cohorts
We identified 23 patients intubated from August 3, 2021, to October 19, 2021, when almost all COVID-19 cases in New York City were caused by the Delta variant and 28 patients intubated from January 7, 2022 to February 8, 2022 when COVID-19 was caused almost exclusively by the Omicron variant.

Results: *Confirmed genotype cohorts*
We identified 17 patients as Delta phenotype and 25 as Omicron phenotype. Of these only 10 patients had genotype information available. Seven of eight (87.5%) patients assigned with the Omicron phenotype were infected by a confirmed Omicron genotype. Of the two patients assigned with the Delta phenotype, one had a confirmed Delta genotype and the other had a confirmed Omicron genotype.

Assumed genotype cohorts
No difference in baseline demographics existed between the groups. While total SOFA scores at the time of intubation were similar between the two groups, patients with assumed Omicron infection had worse coagulation sub-scores and lower platelet counts. Most impressively patients with assumed Delta infections had significantly lower P/F ratios at the time of intubation than patients with assumed Omicron infections (172.9 +/- 112.8 versus 110.3 +/- 67.1, $p < 0.05$). There was no difference between the groups with regard to renal complications (Acute kidney injury and continuous renal-replacement therapy) and outcomes such as lengths of stay. Mortality was high but not different between the groups. (see Table).

Conclusions: Our small study demonstrates that patients with critical COVID-19 requiring mechanical ventilation infected with the Delta variant have worse respiratory function compared to patients with Omicron variant. Not surprisingly, both groups are equally sick as assessed with SOFA scores as they both required mechanical ventilation. However, while Delta COVID-19 critical illness presented with ARDS like features, critically ill patients with Omicron infections may be sick for reasons other than a concomitant COVID-19. This raises the question if critically ill patients with Omicron infections are sick and die “with” COVID-19 and not “because of” COVID-19? Our data supports this hypothesis, but only larger, epidemiological studies will provide conclusive answers. If at this point only few patients die of (not with) COVID-19 the threat of COVID-19 to society is substantially altered and may require a change in response.

References: [1] COVID-19 Variant Data Monitoring the Prevalence of SARS-CoV-2 Variants. New York State, https://coronavirus.health.ny.gov/covid-19-variant-data; 2022. [accessed 13 April 2022].

[2] Menni C, Valdes AM, Polidori L, et al. Symptom prevalence, duration, and risk of hospital admission in individuals infected with SARS-CoV-2 during periods of omicron and delta variant dominance: a prospective observational study from the ZOE COVID Study. Lancet. 2022;399(10335):1618-1624. doi:10.1016/S0140-6736(22)00327-0

Table: Sequential Organ Failure Assessment (SOFA) scores, laboratory and respiratory data at the time of intubation and outcomes

		Omicron n = 28	Delta n = 23	p-value
SOFA score		10.67 +/- 2.56	9.39 +/- 3.06	0.120
SOFA sub scores	**Coagulation**	0.70 +/- 0.87	0.13 +/- 0.46	0.005
	Respiration	2.58 +/- 1.35	3.23 +/- 0.87	0.059
	Cardiovascular	2.67 +/- 1.59	2.09 +/- 1.76	0.231
	Central Nervous System	3.62 +/- 0.98	3.14 +/- 1.55	0.219
	Renal	1.22 +/- 1.22	1.00 +/- 1.04	0.491
	Liver	0.29 +/- 0.72	0.130 +/- 0.46	0.331
Platelet count (10^9/L)		171.7 +/- 80.2	242.2 +/- 85.0	0.004
Bilirubin (mg/dL)		1.08 +/- 1.99	0.78 +/- 0.52	0.458
Creatinine (mg/dL)		2.09 +/- 1.73	1.92 +/- 1.69	0.715
Mean arterial pressure (mmHg)		76.4 +/- 30.7	69.8 +/- 14.5	0.329
P/F ratio (mmHg)		172.9 +/- 112.8	110.3 +/- 67.1	0.027
Outcomes	**30-day ICU free days**	2.79 ± 7.77	1.261 ± 3.19	0.350
	90 day ICU free days	17.11 ± 30.03	18.43 ± 26.71	0.868
	90-day mortality, n (%)	20 (39.2%)	14 (27.5%)	0.553
	Acute kidney injury, n (%)	9 (17.7%)	14 (27.5%)	0.051
	Continuous renal-replacement therapy, n (%)	4 (7.8 %)	10 (19.6%)	0.029
	Tracheostomy, n (%)	8 (15.7%)	6 (11.8%)	1

Figure 1 Variant Distribution in New York City Based on Time of Year
(https://coronavirus.health.ny.gov/covid-19-variant-data, accessed on April 13, 2022)

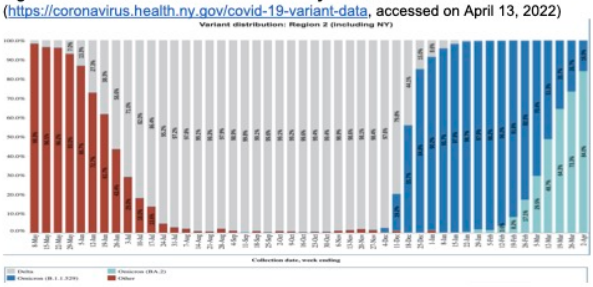

Critical Care 4 - Determinants of Professional Fulfillment and Burnout Among Intensivists: A National Survey by the Society of Critical Care Anesthesiologists in 2022

Shahla Siddiqui[1], Matthew Warner[2], David Douin[3], Shahzad Shaefi[4], Domagoj Mladinov[4], Erika Monteith[1], Avery Tung[5], Robert Sladen[6]

Beth Israel Deaconess Medical Center[1] Mayo Clinic[2] University of Colorado[3] Beth Israel Deaconess Med Center[4] University of Chicago[5] Columbia University Irvine Medical Center[6]

Introduction: Increased burnout and decreased professional fulfillment among intensive care physicians is partly due to ICU workload. Although the COVID-19 pandemic increased ICU workload, it also may have increased feelings of personal fulfillment due to positive public perceptions of physicians caring for COVID patients. We surveyed critical care anesthesiologists to identify the effect of provider demographics, ICU workload, and COVID-19 related workload, on professional fulfillment and burnout.

Methods: We performed an exploratory survey of 606 members of the Society of Critical Care Anesthesiologists in January and February 2022. We used the Stanford Professional Fulfilment Index (PFI) to grade levels of professional fulfillment and markers of burnout (i.e., work exhaustion and disengagement). Univariable and multivariable models were used to identify associations between provider demographics and practice characteristics and professional fulfillment and work exhaustion.

Results: 175 intensivists (29%) responded. 65% were male and 49% were between 36-45 years old. The overall median PFI score (0 (none) to 24 (most professional fulfilment)) was 17 (IQR 1-24), with a wide distribution of responses. In multivariable analysis, factors associated with higher professional fulfillment included age >45 years (p=0.004), ≤15 weeks full-time ICU coverage in 2020 (p=0.02), role as Medical Director (p=0.01), and nighttime home call with supervision of in-house ICU fellows (p=0.01).

Conclusions: Several factors including age ≤45 years, >15 weeks of annual ICU responsibility, and in-house call models were associated with greater work exhaustion and lower professional fulfillment. Importantly, COVID-19 related workload was not associated with increased work exhaustion. The wide range of responses suggests that wellness initiatives may need to be individualized.

References: Maslach C, Leiter MP. Understanding the burnout experience: recent research and its implications for psychiatry. World Psychiatry. 2016 Jun;15(2):103-11. doi: 10.1002/wps.20311. PMID: 27265691; PMCID: PMC4911781.

[1] Azoulay E, De Waele J, Ferrer R,et al.; ESICM. Symptoms of burnout in intensive care unit specialists facing the COVID-19 outbreak. Ann Intensive Care. 2020 Aug 8;10(1):110. doi: 10.1186/s13613-020-00722-3. PMID: 32770449

Figure 1: Distribution of Professional Fulfilment Scores

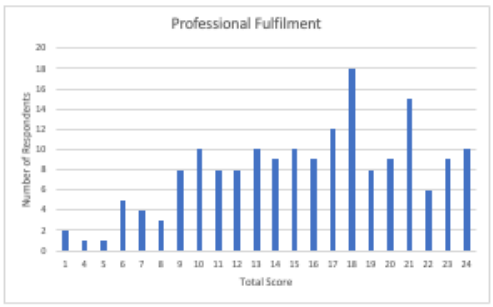

Figure 2: Distribution of Work Exhaustion Scores

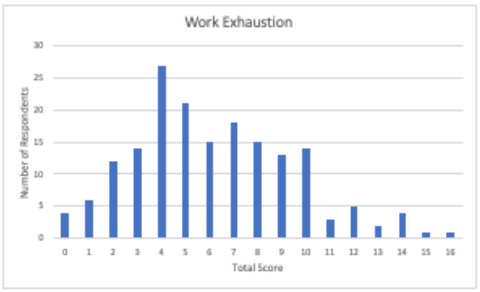

Figure 3: Distribution of Interpersonal Disengagement

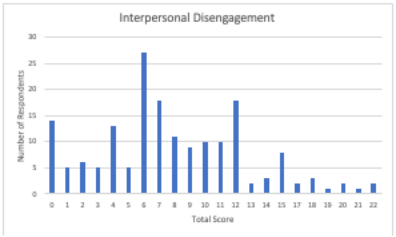

Critical Care 5 - Discharge disposition and loss of independence at discharge among survivors of COVID-19 admitted to intensive care: Results from the SCCM Discovery Viral Infection and Respiratory Illness Universal Study (VIRUS)

Shahla Siddiqui[1], Maximilian Schaefer[2], Valerie Banner Goodspeed[2]

Beth Israel Deaconess Medical Center[1] Beth Israel Deaconess Medical Center

Introduction: To describe loss of previous independent living through non-home discharge, or discharge home with health assistance in survivors of intensive care unit (ICU) admission for Coronavirus Disease 2019 (COVID-19).
DESIGN: Multicenter study including patients admitted to the ICU from January 2020 till June 30, 2021.
HYPOTHESIS: We hypothesized that there is a high risk of non-home discharge in patients surviving Intensive Care Unit (ICU) admission due to COVID-19.

Methods: Data were included from 306 hospitals in 28 countries participating in the SCCM Discovery VIRUS COVID-19 registry. For secondary analyses, data from the Premier Healthcare Database within the United States were included.
PATIENTS: Previously independently living adult ICU survivors of COVID-19.
INTERVENTIONS: None

Results: The primary outcome was non-home discharge. Secondary outcomes were the requirement of health assistance among patients who were discharged home and change in non-home discharge over time. Out of 10,820 included patients, 7101 (66%) were discharged alive. 53% of survivors lost their previous independent living status, either through non-home discharge (29%), or discharge home requiring health assistance (24%). Patients experiencing non-home discharge were older, more prevalent in the Americas, were more likely to be admitted between April-June 2020, and were more often non-Hispanic, and White (p<0.0001). They also had a greater severity of illness as denoted by a longer duration of mechanical ventilation (median IQR 15 (7, 26) vs 8 (4,14) (p<0.0001), a higher median SOFA scores (median IQR 6 (4,9) vs 4 (2,6) (p<0.0001), and a lower median PaO2/ FiO2 (P/F) ratio (median IQR 187 (127, 265) vs 211 (140, 293) (p=0.0009). Factors that predicted non-home discharge were patient age ≥ 65 years [adjusted odds ratio, aOR 2.78 (95% CI 2.47-3.14), p<0.0001)], mechanical ventilation [aOR 4.17 (95% CI 3.69-4.71), p<0.0001)], prone positioning [aOR 1.19 (95% CI 1.03-1.38), p=0.02], and extracorporeal membrane oxygenation (ECMO) [aOR 2.28 (95% CI 1.55-3.34), p<0.0001]. In secondary analyses of a control group admitted for acute respiratory failure, no difference was found in non-home discharge between ICU survivors with and without COVID-19 [aOR 0.99 (95% CI 0.97,1.01) p=0.28)].

Conclusions: More than half of ICU survivors hospitalized for COVID-19 are unable to return to independent living status, even if temporary, reflecting incidences in contemporaneous non-COVID patients with respiratory failure. These findings highlight the significant public health impact of the COVID-19 pandemic.

References:

1. Nandasena HMRKG, Pathirathna ML, Atapattu AMMP, et al. Quality of life of COVID 19 patients after discharge: Systematic review. PLoS One. 2022 Feb 16;17(2):e0263941. doi: 10.1371/journal.pone.0263941. PMID: 35171956; PMCID: PMC8849513.
2. Domecq JP, Lal A, Sheldrick CR, et al, Outcomes of Patients With Coronavirus Disease 2019 Receiving Organ Support Therapies: The International Viral Infection and Respiratory Illness Universal Study Registry. Crit Care Med. 2021 Mar 1;49(3):437-448. doi: 10.1097/CCM.0000000000004879. Erratum in: Crit Care Med. 2021 May 1;49(5):e562. PMID: 33555777.

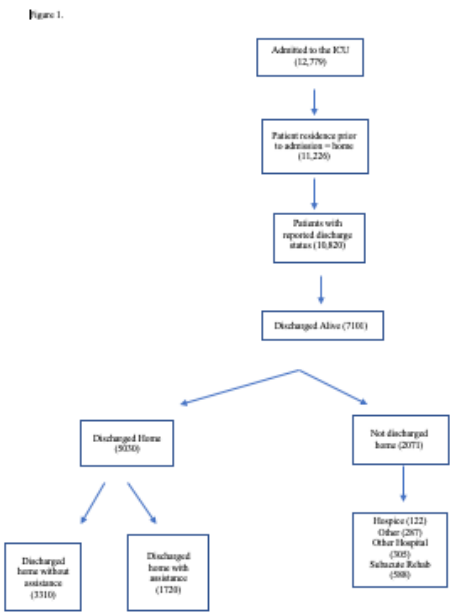

Figure 2.

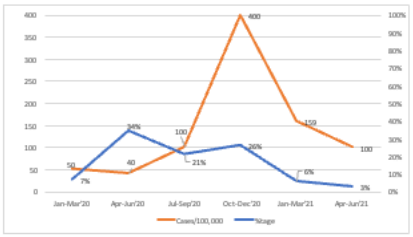

Supplemental Table 1. Descriptive statistics comparing patients who were discharged home and not discharged home.
(*Column percentages)

Characteristic	Discharged Home (n=5030)	Not discharged home (n=2071)	P-Value
	(n=5026)*		<0.0001
Age, Mean (SD)	54.8 (16)	64.1 (15)	
Median (IQR)	56 (44, 66)	65 (55, 75)	
Age Group, No. (%)	(n=5026)		<0.0001
<65	3557 (70.8)	996 (48.1)	
>=65	1469 (29.2)	1075 (51.9)	
Region, No. (%)			<0.0001
European Region (EUR)	375 (7.5)	68 (3.3)	
Region of the Americas (AMR)	3553 (70.6)	1890 (91.3)	
Other	1102 (21.9)	113 (5.5)	
Quarter of Admission, (No.%)	(n=2746)	(n=1010)	<0.0001
Jan-March 2020	186 (6.8)	73 (7.2)	
Apr-June 2020	676 (24.6)	345 (34.2)	
Jul-Sept 2020	991 (36.1)	220 (21.8)	
Oct-Dec 2020	689 (25.1)	271 (26.8)	
Jan-March 2021	149 (5.4)	66 (6.5)	
Apr-June 2021	55 (2)	35 (3.5)	
Admission Source, No. (%)			<0.0001
Home	1308 (26)	466 (22.5)	
Hospital ED	2921 (58.1)	1040 (50.2)	
Outside ED	160 (3.2)	99 (4.8)	
Transfer from other Facility	449 (8.9)	333 (16.1)	
Other	192 (3.8)	133 (6.4)	
Sex, No. (%)			0.26
Male	3084 (61.3)	1253 (60.5)	
Female	1946 (38.7)	817 (39.5)	
Intersex	0 (0)	1 (0.1)	
Ethnicity, No. (%)	(n=5019)	(n=2066)	<0.0001
Unknown	397 (7.9)	111 (5.4)	
Hispanic	1004 (20)	394 (19.1)	
Non-Hispanic	3093 (61.6)	1454 (70.4)	
Not Applicable	525 (10.5)	107 (5.2)	
Race, No (%)	(n=5026)	(n=2069)	<0.0001
African American	893 (17.8)	484 (23.4)	
Asian	1208 (24)	172 (8.3)	
White	2254 (44.9)	1158 (56)	
Mixed	148 (2.9)	53 (2.6)	
Other	473 (9.4)	176 (8.5)	
Unknown	50 (1)	26 (1.3)	
Smoking status, No. (%)			<0.0001
Current	164 (3.3)	90 (4.4)	
Former	641 (12.7)	440 (21.3)	
Non-Smoker	4225 (84)	1541 (74.4)	
Alcohol Use Disorder, No. (%)			0.007
Yes	156 (3.1)	91 (4.4)	
No	4874 (96.9)	1980 (95.6)	
Substance Use Disorder, No. (%)			<0.0001
Yes	134 (2.7)	99 (4.8)	
No	4896 (97.3)	1972 (95.2)	
Mechanical Ventilation, No. (%)			<0.0001
Yes	1310 (26)	1242 (60)	
No	3720 (74)	829 (40)	
Non-Invasive Ventilation, No. (%)			0.57
Yes	765 (15.2)	326 (15.7)	
No	4265 (84.8)	1745 (84.3)	
HFNC, No. (%)			0.11
Yes	1458 (29)	639 (30.9)	
No	3572 (71)	1432 (69.2)	
Prone No. (%)			<0.0001
Yes	836 (16.6)	495 (23.9)	
No	4194 (83.4)	1576 (76.1)	
ECMO, No. (%)			<0.0001
Yes	56 (1.1)	76 (3.7)	
No	4974 (98.9)	1995 (96.3)	
Deep Sedation during ICU stay, No. (%)	(n=664)	(n=242)	<0.0001
Yes (RASS < -3)	174 (26.2)	132 (54.5)	
No (RASS >= -3)	490 (73.8)	110 (45.5)	
Max Number of sedatives or narcotics per day during ICU stay, No. (%)	(n=3623)	(n=1451)	<0.0001
0	3046 (84.1)	991 (68.3)	
1	129 (3.6)	47 (3.2)	
2	165 (4.6)	128 (8.8)	
3	175 (4.8)	173 (11.9)	
4	83 (2.3)	84 (5.8)	
>=5	25 (0.7)	28 (1.9)	
Patient ever received an NMBA, No. (%)	(n=803)	(n=491)	<0.0001
Yes	302 (37.5)	260 (53)	
No	505 (62.5)	231 (47.1)	
Mechanical Ventilation Time, Median (IQR)	(n=1215) 8 (4, 14)	(n=1149) 14.9 (7, 26.2)	<0.0001
Maximum SOFA Scores, Median (IQR)	(n=2571) 4 (2, 6)	(n=1115) 6 (4, 9)	<0.0001
Maximum p/f ratio, Median (IQR)	(n=861) 211.1 (140, 293.3)	(n=499) 186.7 (126.7, 265)	0.0009

*If the number of patients with data for each characteristic is not equal to the total 5030 discharged home and 2071 not discharged home, then the number available for that particular variable is displayed

Supplemental Table 2a: Premier Healthcare Database patients with acute respiratory failure (ARF), admitted to an ICU in 2020 (n=290,394)

Characteristic	Non-COVID-19 (n=247,653)	COVID-19 (n=42,741)
Age, Mean (SD)	63 (17)	62 (15)
Female sex, No. (%)	114352 (46.2)	17977 (42.1)
Elixhauser comorbidity score, Mean (SD)	5.5 (2.4)	4.2 (2.3)
Acute organ dysfunctions, No. (%)		
Cardiovascular	95751 (38.7)	13335 (31.2)
Neurologic	29272 (11.8)	3998 (9.4)
Hematologic	40056 (16.2)	6132 (14.3)
Hepatic	9493 (3.8)	731 (1.7)
Renal	109864 (44.4)	17508 (41.0)

Supplemental Table 2b: Premier Healthcare Database: Outcomes among patients with ARF, admitted to an ICU in 2020

	Outcomes among patients discharged (n=393,224)		Outcomes among patients discharged alive (n=290,394)	
Characteristic	Non-COVID-19 (n=319,322)	COVID-19 (n=73,902)	Non-COVID-19 (n=247,653)	COVID-19 (n=42,741)
Home, No. (%)	124400 (39.0)	22983 (31.1)	124400 (50.2)	22983 (53.8)
SNF/ICF/LTAC, No. (%)	74724 (23.4)	12797 (17.3)	74724 (30.2)	12797 (29.9)
Hospice, No. (%)	25670 (8.0)	3073 (4.2)	25670 (10.4)	3073 (7.2)
Hospital death, No. (%)	71669 (22.4)	31161 (42.2)		
Another hospital, No. (%)	13867 (4.3)	2584 (3.4)	13867 (5.6)	2584 (6.0)
Other, No. (%)	8992 (2.8)	1304 (1.8)	8992 (3.6)	1304 (3.1)

SNF-short term nursing facility, ICF-Intermediate care facility, LTAC- long term acute care facility.

Supplemental Table 3. Multivariable logistic regression model with quarter of admission for all regions vs. in the Americas only

	Adjusted OR's* n=3755 All Regions		Adjusted OR's** n=2442 America's Only	
Characteristic	OR (95% CI)	p-value	OR (95% CI)	p-value
Quarter of Admission				
Jan-March 2020	Ref.		Ref.	
Apr-June 2020	1.63 (1.15 – 2.29)	0.006	1.99 (1.37 – 2.9)	0.003
Jul-Sept 2020	1.15 (0.8 – 1.63)	0.452	1.35 (0.92 – 2.0)	0.12
Oct-Dec 2020	1.65 (1.16 – 2.34)	0.004	1.89 (1.28 – 2.78)	0.001
Jan-March 2021	1.46 (0.92 – 2.3)	0.106	2.09 (1.26 – 3.46)	0.004
Apr-June 2021	1.47 (0.82 – 2.63)	0.199	1.91 (1.04 – 3.49)	0.03

*Adjusted for Hospital admission source, region, age group, sex, race, smoking status, alcohol use disorder, substance use disorder, mechanical ventilation, prone, ECMO
**Adjusted for Hospital admission source, age group, sex, race, smoking status, alcohol use disorder, substance use disorder, mechanical ventilation, prone, ECMO

Supplemental Figure 1. Pattern of missingness for missing variables.

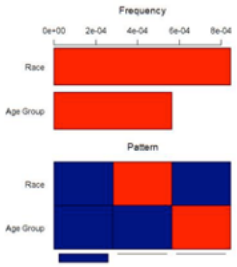

Two variables had missing data among the included patient cases in the Multivariable logistic regression analysis: age group and race. The panel on the above shows the proportion (of 1.0) of missing data (5.6e-04 for age and 8.5e-04 for race). The panel below shows the patterns of missingness (cells in red denote missing data, while cells in blue denote complete data for the respective variable): From the most frequent pattern of missingness on the bottom row (no missing data in either of the 2 variables), to the least frequent on the top row (missing data for age). The histogram below the panel depicts the corresponding frequency of each pattern of missingness. There was no case where data for both variables were missing.

Critical Care 6- Drivers and Drainers of Compassion In Intensive Care Medicine: An Empirical Study Using Video Vignettes

Shahla Siddiqui[1]

Beth Israel Deaconess Medical Center[1]

Introduction: The aim was to determine what factors drive and enhance compassionate care behaviors in the ICU setting and which factors drain and negate such caring attitudes and behaviors.

Methods: This was an observational, qualitative study using video case vignettes and focus group discussions. The Standards for reporting qualitative reports guidelines were used. Participants were invited via email of 2 international critical societies. Informed consent was obtained via email prior to the focus group discussions. Two scripted video vignettes were shown to 3 groups of participants of virtual focus group discussions. These video scenarios were 5 minutes each and were developed using real life scenarios occurring in the ICU. 20 participants agreed to be part of 3 separate focus groups facilitated by the authors.

Results: Thematic analysis revealed emphasis on behavior and nonverbal cues, clinical decision making, communication and sensitivity, and building humane relations. The results show that physicians feel driven by the humanity and sensitivity felt in ICU work, however, there exists structural incompetence, as well as the stress and personal -systemic imbalances of ICU work, which leads to burnout and erosion of such motivations, draining compassion

Conclusions: It seems that physicians working in extremely stressful conditions share a moral imperative and are inspired by the humanism and compassion that fueled their initial motivation to join physically and mentally demanding healthcare work. However, these sentiments are eroded by the pressures of capacity strain, lack of staff, lack of compassionate skills training, dreariness and perfunctory electronic health record maintenance, and other non-humanistic rituals in healthcare, as these take up the precious time and energy rather spent in forming compassionate connections with patients and their families at times when these actions are most required.
Regulatory and scheduling practices must be examined to foster the growth of compassionate behaviors and attitudes in healthcare, and these should be treated as essential patient centered metrics.

References: [1] Kmietowicz Z. Care in hospitals often lacks compassion, says report. BMJ. 2008 Dec 2;337:a2821. doi: 10.1136/bmj.a2821. PMID: 19050330.

[1] https://knowledge.wharton.upenn.edu/article/making-the-case-for-compassion-in-health-care

[1] Sinclair S, Norris JM, McConnell SJ, et al. Compassion: a scoping review of the healthcare literature. *BMC Palliat Care*.

2016;15:6. Published 2016 Jan 19. doi:10.1186/s12904-016-0080-0

Critical Care 7 - Examining the role of race in end-of-life care in the intensive care unit: a single-center observational study

Shahla Siddiqui[1]

Beth Israel Deaconess Medical Center[1]

Introduction: Prior studies have shown variation in the intensity of end-of-life care in intensive care units (ICUs) among patients of different races.
Objective We sought to identify variation in levels of care at the end-of-life in the ICU and to assess for any association with race and ethnicity.

Methods: An observational, retrospective cohort study**.**
Settings A tertiary care center in Boston.
Participants All critically ill patients admitted to medical and surgical ICUs between June 2019 and December 2020.
Exposure Self-identified race and ethnicity.
Main Outcome and measure The primary outcome was death. Secondary outcomes included "code status," markers of intensity of care, markers of communication and the presence of a Palliative care or Ethics consults.

Results A total of 9083 ICU patient encounters were analyzed. 1259 patients (14%) died in the ICU, the mean age was 64 years (SD 16.8), and 44% of patients were women. A large number of decedents (22.7%) did not have their race identified. These patients had a high rate of interventions at death. Code status varied by race, with more White patients designated as "Comfort Measures Only" (CMO) (74%) while more Black patients designated as "Do Not Resuscitate/Do Not Intubate (DNR/DNI) and DNR/ok to intubate" (12.1% and 15.7%) at the end-of-life. Use of dialysis at the end-of-life varied by self-identified race. Specifically, Black and Unknown patients were more likely to receive renal replacement therapy (24% and 20%, P = 0.003).

Conclusions: Our data describe a gap in identification of race and ethnicity, as well as differences at the end-of-life in the ICU, especially with respect to code status and certain markers of intensity of care. Questions arise about how we identify and assign racial groups in healthcare. Opportunities continue to exist to further explore the underlying causes of the differences seen in end-of-life care, including qualitative patient centered inquiry as well as engagement with stakeholder groups.

References:

1. Field M, Cassell C. *(IOM Report)* Washington DC: National Academy Press; 1997. Approaching death: improving care at the end of life
2. Asch D A, Hansen-Flaschen J, Lanken P N. Decisions to limit or continue life-sustaining treatment by critical care physicians in the United States: conflicts between physicians' practices and patients' wishes. *Am J Respir Crit Care Med.* 1995 Feb;151(2 Pt 1):288–92.
3. Institute of Medicine (US) Committee on Care at the End of Life. Approaching Death: Improving Care at the End of Life. Field MJ, Cassel CK, editors. Washington (DC): National Academies Press (US); 1997. PMID: 25121204.

Figure 1 Discharge disposition and code status at death

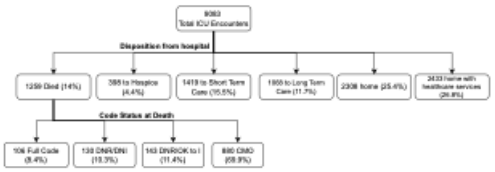

Figure 2. Boxplot of Time from DNR decision until demise by race

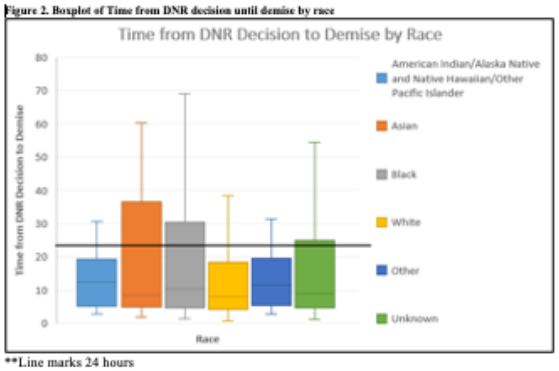

**Line marks 24 hours

Critical Care 8 - Lung entropic hysteresis: The concept of retained energy in mechanically ventilated ARDS patients

Aiman Suleiman[1], Simone Redaelli[1], Dario von Wedel[1], Ricardo Munoz-Acuna[1], Abeer Santarisi[1], Boris Jung[2], Jeremy Beitler[3], Valerie Banner-Goodspeed[4], Daniel Talmor[4], Eduardo Costa[4], Elias Baedorf Kassis[4], Maximilian Schaefer[5]

Beth Israel Deaconess Medical Center, Harvard Medical school[1] Harvard med faculty physicians[2] Columbia University[3] Beth Israel Deaconess Medical Center[4] Beth Israel Deaconess Medical Center & Hospital[5]

Introduction: Mechanical ventilation can be a life-saving therapy for patients with acute respiratory distress syndrome (ARDS), but it is an invasive procedure that can potentially lead to ventilator-induced lung injury (VILI) [1]. Novel ventilation strategies estimate the delivered energy to the lung and respiratory system [2,3]. However, these are unable to differentiate between dissipated and retained energy, the latter of which will be responsible for lung damage. This might be solved with application of the concept of entropy: introduction of positive pressure to the elastic naturally ordered lung tissue during mechanical ventilation will generate entropy in the form of disorder [4]. This can result in elastic fatigue and destruction of (inter-) cellular structures (*Figure 1*). Based on the assumption that the lung adopts a thermodynamic model of entropic rubber, entropy production correlates with the area of hysteresis enclosed in the Pressure–Volume (PV) curve of the lung [5]. In this study, we compared the development of lung entropy, measured from hysteresis over time between mechanically ventilated ARDS patients who died or stayed alive within 28 days of mechanical ventilation.

Methods: We analyzed data collected from the previous EPVent-2 trial, which included mechanically ventilated, adult ARDS patients, in the period between October, 2012, and September, 2017, from 14 centers in North America [6]. Patients with waveforms compromised by artefacts or evidence of multiple spontaneous breaths were excluded. Data were analyzed by trained research fellows blinded to mortality status using the PV loop feature of ADInstruments LabChart 7 application. The exposure of interest was entropic hysteresis in Joules (assuming negligible change in temperature per breathing cycle), defined as the area enclosed in the PV loop (*Figure 2*) [5]. After data analysis, patients were stratified per outcome into alive or dead at 28 days. Two-sample Wilcoxon rank-sum (Mann-Whitney) test was used to compare overall median distributions of entropic hysteresis between patients with and without 28-day mortality. Two-way mixed measures ANOVA was used to compare medians of groups cross-classified by 2 factor variables: between-subject mortality factor, and within-subject time factor. Repetitive measurements up to 7 days from the start of mechanical ventilation (day 0-6) were included. We tested for normality of distribution and homogeneity of variances using Shapiro-Wilk's test of normality and Levene's test ($p > 0.05$), respectively. Mixed effect linear regression model was run to appreciate the effect of at each level of interaction on entropic hysteresis.

Results: Out of 80 randomly selected patients, 76 patients were included, of whom 21 (27.6%) died within 28 days (*Table 1)*. The median (IQR) entropic hysteresis of the respiratory system was 0.44 (0.38-0.63) J in patients who died within 28 days, versus 0.37 (0.26-0.49) J in patients who stayed alive ($p<0.001$). There was a significant two-way interaction between mortality status and time of mechanical ventilation on entropic hysteresis, $F(6, 243) = 3.36$, $p=0.003$. The difference in mortality was associated with differences in entropic hysteresis at days 3, 4 and 6 ($p=0.004$, 0.003, and 0.003, respectively). Pairwise comparisons in within-subject time factor show that the median entropy was significantly different between days 6 ($p=0.002$), 5 ($p=0.03$), 4 ($p=0.04$) and 3 ($p=0.03$) in patients who stayed alive, and 5 ($p=0.04$) and 3 ($p = 0.04$) in patients who died (*Figure 3*). Results from the mixed effect linear regression model were consistent (*Figure 4*). Results also remained consistent in the elastic-after-effect following normalizing entropy for driving pressure as a measure reflecting the inspiratory limb. Neither respiratory rate ($p=0.34$), tidal volume ($p=0.79$), plateau pressure ($p=0.39$) or positive end expiratory pressure ($p=0.61$) differed between patients who died and patients who stayed alive at 28 days.

Conclusions: Entropic hysteresis reflects energy retained in the lung during mechanical ventilation. Despite having similar entropy at the beginning of mechanical ventilation, increased entropy over time identified patients who died within 28 days, while survivors demonstrated decreased entropy. Larger sample size with data collected over longer periods of time will further increase our understanding of the clinical relevance of this concept.

References: [1] Ventilator-induced lung injury. N Engl J Med. 2013;369(22):2126-36

[2] Mechanical Power: A New Concept in Mechanical Ventilation. Am J Med Sci. 2021;362(6):537-545

[3] Lung-protective ventilation strategies in acute lung injury. Crit Care Med. 2003;31(4):312-6

[4] Entropy Stress and Scaling of Vital Organs over Life Span Based on Allometric Laws. Entropy. 2012;14(12):2550-2577

[5] Entropy Production and the Pressure–Volume Curve of the Lung. Front Physiol. 2016;1(7):73

[6] Effect of Titrating PEEP With an Esophageal Pressure-Guided Strategy vs an Empirical High PEEP-Fio2 Strategy on Death and Days Free From Mechanical Ventilation Among Patients With ARDS: A Randomized Clinical Trial. JAMA. 2019;321(9):846-857

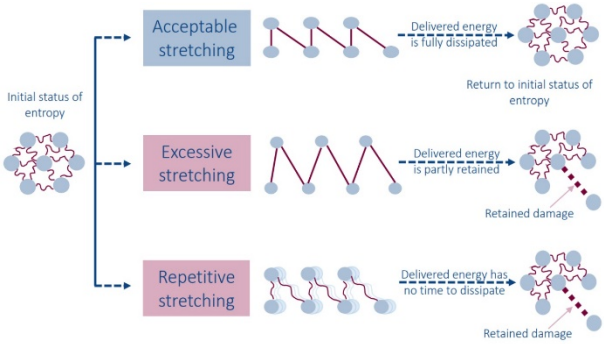

Figure 1. Pathways an entropic rubber material can take following the introduction of energy to the system.

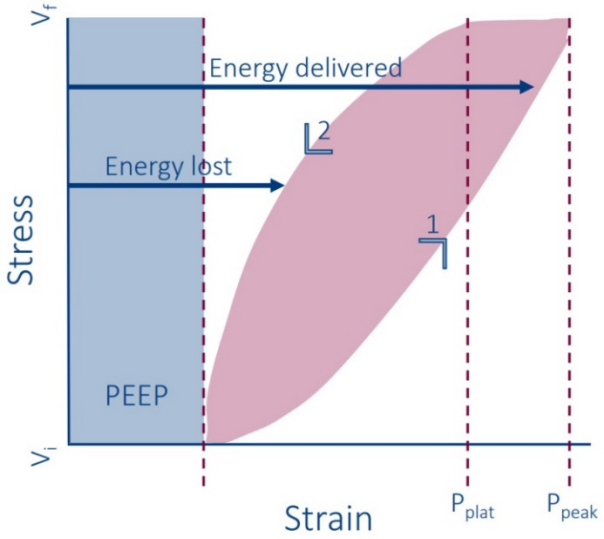

Figure 2. Pressure-Volume loop and area enclosed in red (the entropic hysteresis). 1: Inspiration curve. 2: Expiration curve, which is a reflection of elastic after effect.

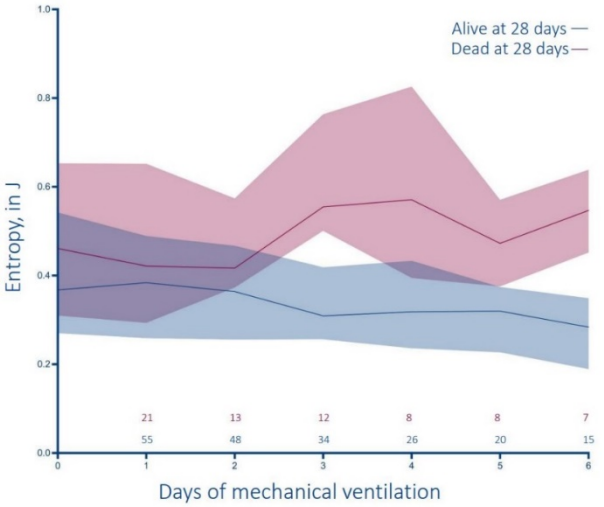

Figure 3. Trends of medians (IQR) of entropic hysteresis per mortality in 28 days over the course of the first 7 days of mechanical ventilation. The number of patients per day is included above the x-axis.

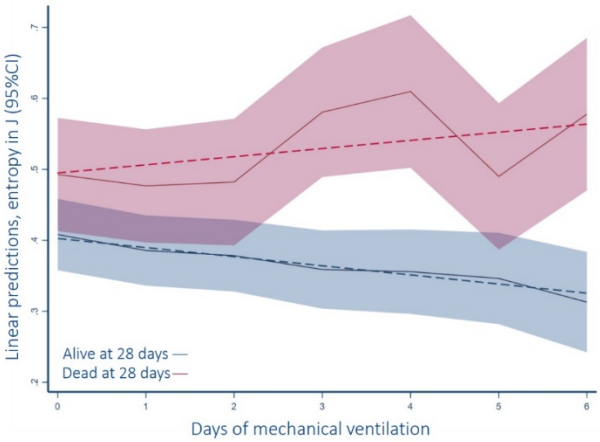

Figure 4. Mixed effect linear regression model with predictive margins of entropy over the 7 days of mechanical ventilation. Dashed lines: fitting a straight line on data points that achieve lowest residuals.

Table 1. Patient characteristics and distribution of variables

	Alive at 28 days N=55	Dead at 28 days N=21
Age	52.0 (38.0 - 67.0)	66.0 (53.0 - 76.0)
Sex		
Female	26 (47%)	9 (43%)
Predicted body weight, kg	60.9 (54.6 - 73.2)	65.9 (56.4 - 70.5)
Actual body weight, kg	84.1 (72.0 - 113.0)	77.1 (68.2 - 111.0)
SOFA score	5.0 (3.0 - 9.0)	5.0 (4.0 - 8.0)
ARDS risk factors		
Pneumonia (non-PJP)	39 (71%)	16 (76%)
PJP Pneumonia	3 (5%)	1 (5%)
Gastric aspiration	10 (18%)	3 (14%)
Multiple transfusions	4 (7%)	1 (5%)
Prolonged shock	9 (16%)	3 (14%)
Sepsis	35 (64%)	11 (52%)
Acute pancreatitis	1 (2%)	1 (5%)
Trauma	3 (5%)	0 (0%)
Drug overdose	5 (9%)	0 (0%)
Other	2 (4%)	0 (0%)
Respiratory characteristics		
pH	7.3 (7.3 - 7.4)	7.3 (7.3 - 7.4)
$PaCO_2$	45.8 (38.8 - 52.0)	43.0 (33.0 - 59.5)
PaO_2	93.0 (76.0 - 110.0)	86.0 (77.0 - 102.0)
FiO_2	0.6 (0.5 - 0.8)	0.6 (0.5 - 0.9)
PaO_2/ FiO_2	103.3 (77.0 - 131.7)	91.5 (73.4 - 135.3)
Tidal volume, mL	400.0 (350.0 - 450.0)	401.0 (350.0 - 450.0)
Plateau Pressure, cmH_2O	27.0 (25.0 - 30.0)	26.0 (24.0 - 31.0)
PEEP, cmH_2O	14.0 (10.0 - 16.0)	12.0 (10.0 - 16.0)
Respiratory rate, breaths per min	24.0 (20.0 - 30.0)	24.0 (18.0 - 26.0)
Minute ventilation, L	10.3 (8.5 - 12.1)	9.3 (8.5 - 10.0)
Pes at the end of inspiration, cmH_2O	18.5 (15.6 - 20.7)	17.2 (15.9 - 23.1)
Pes at the end of expiration, cmH_2O	15.0 (12.3 - 18.5)	13.9 (12.8 - 19.4)
Respiratory system driving pressure, cmH_2O	13.0 (11.0 - 16.0)	13.0 (11.0 - 16.0)
Transpulmonary driving pressure, cmH_2O	8.4 (6.7 - 10.4)	8.3 (6.4 - 11.3)
Respiratory system compliance, mL/cmH_2O	30.0 (24.6 - 37.5)	30.8 (23.4 - 38.5)
Lung compliance, mL/cmH_2O	49.1 (35.3 - 59.5)	45.9 (30.8 - 68.0)
Neuromuscular blockade	24 (44%)	7 (35%)

Patient characteristics and distribution of variables. Data are presented as median (IQR) for continuous measures, and n (%) for categorical measures. SOFA, Sequential Organ Failure Assessment; ARDS, Acute Respiratory Distress Syndrome; PJP, Pneumocystis jiroveci pneumonia; PaCO2 , partial arterial pressure of carbon dioxide; PaO2 , partial arterial pressure of oxygen; FiO2 , fraction of inspired oxygen; PEEP, positive end expiratory pressure.

Critical Care 9 - Plasma Extracellular Vesicles from Septic Mice Induce Brain Inflammation Via Mirna Cargo

Chanhee Park[1], Yun Li[2], Zhoufan Le2[1], Junyun He[2], Fengqian Che2[1], Hui Li[1], Kavitha Brunner[3], Steve Jay[5], Wei Chao[4], Junfang Wu[5], Lin Zou[5]

University of Maryland[1] University of Maryland, School of Medicine[2] University of Maryland, Baltimore School of Medicine[3] The University of Maryland School of Med[4] University of Maryland School of Medicine[5]

Introduction: Sepsis-associated encephalopathy (SAE) occurs in sepsis survivors, where neuronal inflammation plays a critical role in its pathogenesis. Our recent studies demonstrated that plasma extracellular (ex) miRNAs, including miR-146a, miR-122, miR-34a, miR-145, increased in sepsis. These ex-miRNAs cause neuronal inflammation both in microglial cultures and in the intact brain[1]. Extracellular vehicles (EVs) have been proposed as a vehicle for ex-miRNA-mediated intercellular communication. However, the biological function of plasma EVs and their miRNA cargo in neuronal inflammation is unclear. In the current study, we hypothesize that septic plasma EV-miRNAs contribute to neuroinflammation.

Methods: EVs from HEK293 cell cultures (293EVs) were labeled with fluorescent dye PKH26 and used to test EV internalization. Plasma EVs were isolated using ultracentrifugation and quantified by Viewsizer 3000 (Horiba). Microglia and RAW cells were treated with PKH26-labeld 293EVs (293EVs-PKH26) for overnight. The uptake of 293EVs-PKH26 by the cells was observed under a confocal microscope (Nikon). Sepsis was created by cecal ligation and puncture (CLP) in mice. Sham mice had laparotomy only. Brain immune cells and cytokine gene expression were measure by flow cytometry and qRT-PCR. Microglia were isolated from neonatal mouse brain. The function of EV-associated miRNAs was tested by preincubating EVs with control oligos or anti-miRNAs combo prior to the cell treatment. The mouse neuronal cells were treated with the septic EVs or microglial conditioned media (CM), which were collected from the microglial cultures treated with septic or sham EVs. Neuronal apoptotic death was measured by cleaved caspase-3 in Western blot.

Results: Microglia and RAW cells internalized 293EVs-PKH26 after 24 hours of incubation as evidenced by confocal fluorescent images. ICV delivery of CLP-EVs, but not Sham-EVs, led to a marked brain infiltration of immune cells, e.g., neutrophils and monocytes. Brain cytokine/chemokine gene expressions, such as CXCL2, TNFα, IL-6, IL-1 β, were also significantly upregulated in the cerebral cortex following ICV injection of septic EVs. In microglial cultures, CLP-EVs induced a cytokine production including CXCL2 and IL-6 in a dose-dependent manner, while Sham-EVs did not. Pretreatment of EVs with anti-miRNAs combo (anti-miR-146a, -122, -34a, -145) led to a 49.3% inhibition in CLP-EV-mediated CXCL2 production as compared to that of control oligos. Importantly, neuronal cells exhibited an increase in cleaved caspase-3, an active enzyme for cell apoptosis, 24 h after microglial CM treatment, but not by direct CLP-EV treatment.

Conclusions: Plasma EVs of septic mice cause brain inflammation both in the intact animal and in the microglial cultures. Media from activated microglia treated with the septic EVs induce neuronal apoptosis. The proinflammatory property of the EVs in part attributes to their cargo miRNAs.

References: 1. Brain Behav Immun. 2022 (100) 10-24

Critical Care 10 - Predictors of end recruitment maneuver transpulmonary pressure in mechanically ventilated ARDS patients: Re-analysis of a multicenter international randomized clinical trial

Abeer Santarisi[1], Aiman Suleiman, Simone Redaelli[1], Dario von Wedel[1], Jeremy Beitler[2], Daniel Talmor[3], Valerie Banner-Goodspeed[3], Boris Jung[4], Maximilian Schaefer[5], Elias Baedorf Kassis[5]

Beth Israel Deaconess Medical Center, Harvard Medical School[1] Columbia University[2] Beth Israel Deaconess Medical Center[3] harvard med faculty physicians[4] Beth Israel Deaconess Medical Center & Hospital[5]

Introduction: Adult respiratory distress syndrome (ARDS) results in severe lung injury and hypoxemia secondary to loss of aerated lung [1]. Lung recruitment maneuvers (RM), where high airway pressures are applied from 10-30 seconds, may open up collapsed alveoli and enhance alveolar oxygenation and ventilation, and are commonly used in patients with ARDS [2]. Despite these possible benefits, there are widely variable chest wall mechanics between patients, which may impact the relative benefit and outcome from these maneuvers [3]. Successful recruitment will result in decreased lung elastance after the RM due to the gain in volume from the maneuver, an outcome that may be predicted through the resultant end-recruitment transpulmonary pressure (P_L). In contrast, a non-individualized recruitment maneuver could lead to either very high P_L, resulting in potentially harmful overdistension of the lung (with a resulting increase in elastance), or low P_L, resulting in insufficient volume gain from the maneuver [4]. In our study, we aim to improve the individualization of recruitment maneuvers through investigating the association between the resultant P_L and patients' baseline characteristics, and determining which characteristics dominate the prediction of P_L.

Methods: We reanalyzed data from the multicenter international EPVent-2 trial [5]. Adult ARDS patients who received a RM during their first or second day of mechanical ventilation in the intensive care unit and had their flow, pressure and volume waveforms recorded before, during, and after the recruitment maneuver, in the period between October 31, 2012, and September 14, 2017, at 14 hospitals in North America, were included. We excluded patients with poor quality waveforms due to channel drifting, artifact, and evidence of multiple spontaneous breaths interfering with the plateauing needed in pressure waveforms during RM. We investigated height, weight, both APACHE III and SOFA score, tidal volume, positive end expiratory pressure (PEEP), plateau pressure, fraction of inspired oxygen (FiO_2), partial arterial oxygen pressure-to-fraction of inspired oxygen ratio (PaO_2/ FiO_2 Ratio), Berlin ARDS severity, and baseline lung elastance (prior to RM) as potential predictors of P_L through a multivariable linear regression model. Furthermore, we investigated the relative importance of each significant predictor of P_L using dominance analysis of predictors.

Results: 123 patients were included in our reanalysis. The median (IQR) of P_L was 14.55 (11.49-17.10) cmH_2O. *Table 1* summarizes the baseline characteristics and distribution of variables per median P_L. P_L measurements varied from 2.9 to 25.5 cmH2O, for almost the same amount of airway pressure delivered (*Figure 1*). In a multivariable linear regression model, weight, PEEP, SOFA score, PaO2/FiO2 Ratio and baseline lung elastance were significantly correlated with P_L with coefficients of -0.04, -0.23, -0.32, -0.04, and 0.09 (p=0.002, 0.049, 0.049, 0.02, 0.02), respectively. Dominance analyses of the predictors of P_L showed that weight had the strongest dominance of negative predictors (ranking 1, R^2= 0.08), where thin body habitus predicts high P_L, hence overdistension. Other predictors were less dominant with R^2 values ranging between 0.005 and 0.05 (*Figure 2*). Baseline lung elastance was the only positive predictor, where an increase in baseline elastance results in a significant increase of P_L.

Conclusions: Patient's weight was the best predictor of end recruitment P_L. Identifying the dominant predictors of P_L could help clinicians modify the RM, to avoid overdistension and optimize recruitment volume.

References: [1] Ventilator-induced lung injury. N Engl J Med. 2013 Nov 28;369(22):2126-36.

[2] Lung Recruitment Maneuvers for Adult Patients with Acute Respiratory Distress Syndrome. A Systematic Review and Meta-Analysis. Ann Am Thorac Soc. 2017 Oct;14(4):304-S311.

[3] Recruitment Maneuvers and PEEP Titration. Respir Care. 2015 Nov;60(11):1688-704.

[4] Recruitment maneuvers: using transpulmonary pressure to help Goldilocks. Intensive Care Med (2017) 43:1162–1163.

[5] Effect of Titrating Positive End-Expiratory Pressure (PEEP) With an Esophageal Pressure-Guided Strategy vs an Empirical High PEEP-Fio2 Strategy on Death and Days Free From Mechanical Ventilation Among Patients With Acute Respiratory Distress Syndrome: A Randomized Clinical Trial. JAMA. 2019 Mar 5;321(9):846-857.

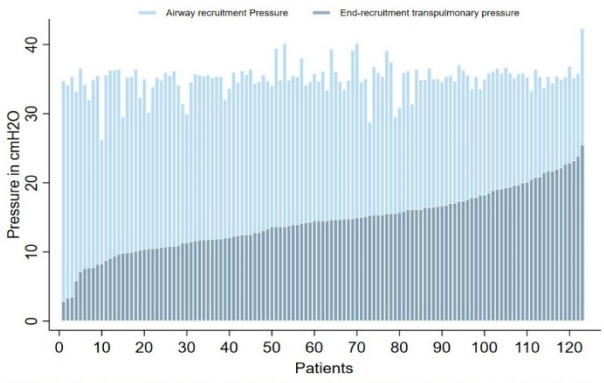

Figure 1. The distribution of 123 patients with esophageal balloon illustrating airway and end-recruitment transpulmonary pressures for each during a standard recruitment maneuver. Transpulmonary pressure was calculated as the airway pressure minus the esophageal pressure.

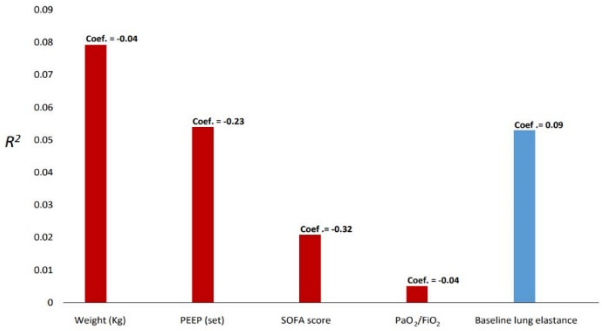

Figure 2. Dominance analysis depicting the individual contribution of predictors of end recruitment transpulmonary pressure (P_L). Overall fitness R^2=0.32. Weight had the strongest dominance, ranking 1 (R^2=0.08). Other predictors were positive end expiratory pressure (PEEP), baseline lung elastance, SOFA score, and PaO_2/FiO_2 ratio. Coefficients derived from the linear regression model are shown in the figure, where predictors with negative coefficients are plotted in red and positive in blue.

Table 1. Patients' characteristics and distribution of variables per median end-recruitment transpulmonary pressure.

	Low end-recruitment transpulmonary pressure N=63	**High end-recruitment transpulmonary pressure N=60**	**p**
Age	58.0 (46.0 - 67.0)	57.0 (43.5 - 66.5)	0.97
Sex			0.92
Female	30 (48%)	28 (47%)	
Race			0.68
White	49 (78%)	45 (75%)	
Black	6 (10%)	9 (15%)	
Asian/Middle Eastern/Indian	1 (2%)	2 (3%)	
Native American/ First Nation	5 (8%)	2 (3%)	
Pacific Island	2 (3%)	2 (3%)	
Height (cm)	170.0 (160.0 - 178.0)	166.0 (158.0 - 175.0)	0.33
Actual body weight (kg)	90.6 (74.7 - 110.3)	77.0 (65.3 - 93.3)	0.006
Predicted body weight (kg)	60.9 (51.9 - 73.2)	59.6 (50.1 - 70.5)	0.44
BMI (kg/m^2)	31.1 (26.4 - 39.1)	27.2 (24.2 - 32.9)	0.005
Clinical characteristics			
Acute physiology and Chronic Health Evaluation III (APACHE) Score	25.5 (21.5 - 32.5)	27.5 (21.5 - 31.5)	0.79
Primary cause of lung injury			0.49
Pulmonary	18 (29%)	18 (30%)	
Abdominal	2 (3%)	0 (0%)	
Trauma	0 (0%)	1 (2%)	
Sepsis	22 (35%)	24 (40%)	
Other	21 (33%)	17 (28%)	
Sequential Organ Failure Assessment (SOFA) Score	9.0 (5.0 - 11.0)	7.0 (4.0 - 9.0)	0.011
Respiratory Characteristics			
Tidal volume (mL)	400.0 (328.0 - 450.0)	400.0 (330.0 - 427.5)	0.21
Tidal volume (mL/kg predicted body weight)	6.1 (5.9 - 6.8)	6.3 (6.0 - 6.7)	0.45
Positive end-expiratory pressure	15.0 (12.0 - 18.0)	12.0 (10.0 - 14.5)	0.001
FiO_2	0.6 (0.5 - 0.8)	0.6 (0.5 - 0.8)	0.43
PaO_2/FiO_2	90.8 (69.0 - 129.0)	103.3 (75.0 - 123.5)	0.55
Berlin acute respiratory distress syndrome severity			0.090
Moderate (100< $PaO_2/FiO_2 \leq$ 200) (%)	24 (38%)	32 (53%)	
Severe ($PaO_2/FiO_2 \leq$ 100) (%)	39 (62%)	28 (47%)	
Plateau pressure (cm H_2O)	28.0 (25.0 - 31.0)	25.5 (22.0 - 29.0)	0.005
Driving pressure (cm H_2O)	11.0 (10.0 - 14.0)	12.0 (10.0 - 14.0)	0.63
Volume of Recruitment Maneuver (mL)	766.7 (537.1 - 1037.8)	801.5 (595.6 - 1071.3)	0.33
Recruitment Maneuver Transpulmonary Elastance (H_2O/mL)	19.0 (13.7 - 24.3)	20.6 (15.9 - 31.8)	0.034
Pre-Recruitment Maneuver Transpulmonary Elastance (H_2O/mL)	19.1 (14.4 - 25.9)	23.5 (18.4 - 32.2)	0.010

Critical Care 11 - Risk Stratification Utilizing Perioperative Echocardiogram for Hip Fractures

Nyla Azam[1], Aria Lucchesi[1], Nibras Bughrara[2], Jeannette Mullins[2], Mahtab Sheikh[2], Ernest Chisena[2]

Albany Medical Center[1] Albany Medical College[2]

Introduction: Hip fractures are associated with increased morbidity and mortality amongst older adults.[1] A review of 300 hip fracture patients showed a thirty-day mortality of 13.3% and total perioperative mortality of 15.6%. Cause of death was reviewed in each case, and mortality was categorized as definitely unavoidable in 28%, but probably unavoidable in 15% or potentially avoidable in 57% of patients.[2] As hip fractures are age related, affected patients are likely to have a multitude of medical comorbidities that put them at risk for perioperative complications. Few interventions have been done to reduce perioperative morbidity and mortality for this patient group.[3] While not routine, hip fracture patients can receive a preoperative transthoracic echocardiogram (TTE) for risk stratification. Several studies, however, have shown the use of preoperative TTE to increase time to surgery, which in turn can increase the risk of complications related to the acute hip fracture.[4,5] The subcostal view, currently used at the bedside for evaluating hypotension, may be a more efficient way to risk stratify surgical hip fracture patients. This is a descriptive study of the hip fracture population at our institution, to lay the groundwork for the goal of evaluating whether the subcostal echocardiographic view alone might be an effective screening tool for the preoperative risk stratification of hip fracture patients.

Methods: This is a retrospective, single-center study of adult patients, older than age 18, with hip fractures who underwent surgical repair between 2015-2020, with a total of 298 patients. We present a cohort of 62, of which 31 received pre-operative TTE. TTEs were classified into one of eight cardiac phenotypes based on the subcostal view.[6] Primary outcome measured is intraoperative hypotension, defined as systolic pressures <90 mmHg or MAP <65, or use of multiple pressors. Preliminary statistical analysis performed was not powered, and so this is a descriptive analysis with additional patients currently being added.

Results: Demographic characteristics are shown in the table below. Hypotension prior to incision was present in approximately half (51.61%) of the patient population. Preliminary analysis reveals that the majority of patients with perioperative hypotension belonged to phenotype 2. Only one patient had intraoperative hypotension requiring multiple pressors, and were in phenotype 7. There was one intraoperative mortality; this patient had cardiac phenotype 2.

Conclusions: The majority of patients receiving surgical treatment for acute hip fracture at our institution are adults over the age of 70. Perioperative hypotension occurred in over half of all patients. According to preliminary analysis there may be an association between certain cardiac phenotypes and perioperative hypotension and mortality. We will continue to expand our study by increasing the time period for data collection. Pre-operative transthoracic echocardiography by an anesthesiologist with a focus on the subcostal view may be an effective and efficient way to risk stratify surgical hip fracture patients. Long term goals include evaluating whether the subcostal view done at the bedside provides adequate information for perioperative management and risk stratification of the surgical hip fracture patient without delaying time to surgery.

References:

Hip Fracture-Related Mortality among Older Adults in the United States: Analysis of the CDC WONDER Multiple Cause of Death Data, 1999–2013. 2016; (2016) 1-5.

Mortality Analysis in hip fracture patients: implications for design of future outcome trials. 2005; (94): 24-29

Preoperative echocardiography for patients with hip fractures undergoing surgery: a retrospective cohort study using a nationwide database. 2019; (128): 213-220

Preoperative Noninvasive Cardiac Testing in Older Adults with Hip Fracture: A Multi-Site Study. 2020; (68):1690-1697.

Preoperative Echo: Overused or Undervalued? 2020; (68):1688-1689

The value of subcostal echocardiographic assessment and directions for future research. 2022; (69):678-679.

	Echo	Control - Non Echo
Count of Subjects	31	31
Male/Female	M= 8, F= 23	M= 12, F= 19
Percent Male	25.8	38.7
Percent Female	74.2	61.3
Average Age	82	75.09
Mode Age Group	81-90	81-100
Average ASA score	3.32	3.13
Mode ASA score	3	3
Race: White %	90.3	93.54
Race: Black or African American %	0	3.2
Race: Asian %	3.2	0
Race: Other %	6.5	3.2
Ethnic Group: Non Hispanic or Latino Origin %	96.8	96.8
Ethnic Group: Hispanic or Latino Origin %	3.2	0
Ethnic Group: Unknown %	0	3.2
CAD %	45.2	25.8
CKD %	29	6.45
COPD %	16.1	25.8
Diabetes %	16.1	45.2
Heart Failure %	19.4	9.7
Obstructive Sleep Apnea %	0	32.2
Peripheral Vascular Disease %	3.2	3.2
Thromboembolic %	0	3.2
Hypotension before incision %	54.8	38.7
Aortic Stenosis %	3.2	3.2
Valve Disease %	3	3.2
In-Hospital Mortality	12.9	0
Anesthesia: General %	77.4	77.4
Anesthesia: Regional %	12.90	16.1
Anesthesia: Both %	9.6	6.45
Origin: Nonhealthcare Facility Point of Origin %	64.5	64.5
Origin: Clinical Referral %	0	3.2
Origin: Transfer from a Hospital %	29	25.8

Origin: Transfer from Another Health Agency %	6.4	6.4
Avg Days from Admission to Surgery	3.10 (SD = 3.78)	2 (SD = 2.32)
Avg Days from Admission to 1st Echo	2.65 (SD = 4.73)	N/A
Avg Days from Admission to Discharge	9.51 (SD = 4.92)	9.10 (SD = 6.49)
Discharge to: SNF %	61.3	54.8
Discharge to: Rehab Facility %	19.4	22.6
Discharge to: Home Health Services %	0	19.35
Discharge to: Home/ Self care %	3.2	3.2
Discharge to: Federal health Care %	3.2	0

Subject ID	Hypotension before incision	IntraOP Hypotension after incision	Hypotension required multiple pressors in PACU	Cardiac Phenotype	Cluster	Quality	IVC	Notes
191	Yes	Yes	No	2	1	1	3	RVH w. Normal function no significant dilation
192	Yes	Yes	No	3	1	1	2	
194	Yes	Yes	No	2	1	2	2	
197	Yes	Yes	No	4	2	4	2	
199	Yes	No	No	3	1	1	1	
200	No	No	No	2	1	2	2	
206	Yes	No	No	2	1	2	2	
207	Yes	Yes	No	3	1	2	2	Apical 3C
208	Yes	Yes	No	2	1	2	2	
211	No	Yes	No	2	1	2	2	
214	Yes	Yes	No	2	1	2	2	
219	No	No	No	3	1	2	1	
222	Yes	Yes	No	3	1	2	1	
229	No	Yes	No	4	2	2	IVC not visible	
232	No	Yes	No	7	3	2	2	
240	No	No	No	2	1	2	2	
242	No	No	No	3	1	2	2	BAE
249	Yes	No	No	3	1	3	3	
251	Yes	No	No	2	1	2	2	
255	No	No	No	3	1	2	3	
259	Yes	Yes	No	2	1	2	2	
261	Yes	Yes	No	5	2	3	3	
265	No	No	No	7	3	2	3	BAE
266	No	Yes	No	2	1	2	2	
271	No	Yes	No	3	1	2	2	
273	Yes	No	No	4	2	1	2	
280	No	No	No	7	3	2	2	
283	No	Yes	No	3	1	2	2	
287	No	No	No	4	2	2	3	BAE
289	Yes	Yes	Yes	7	3	1	1	
298	Yes	Yes	No	2	1	1	2	

Table 2: Cardiac phenotyping for TTE group (n=31)

Critical Care 12 - A comparison of hospital costs among critically ill patients with COVID-19 who did versus did not receive extracorporeal membrane oxygenation in the United States

Raquel Bartz[1], Julien Corbert[1], Matthew Fullller[2], Galen Royce-Nagel[2], Tetsu Ohnuma[2], Vijay Krishnamoorthy[2], Karthik Raghunathan[3]

Harvard Medical School[1] Duke University[2] Duke University Medical Center[3]

Introduction: Use of extracorporeal membrane oxygenation (ECMO) for the treatment of acute respiratory distress syndrome (ARDS) increased significantly during the pandemic. ECMO is an expensive modality to both patients and hospitals to treat severe ARDS.[1] The EuroECMO-COVID study, including 133 centers in 21 countries, reported a hospital case-fatality rate of ~50%, which is consistent with data from North America (ELSO).[2] However, there is no data at scale on hospital costs of caring for patients who receive ECMO. We study hospital costs among ECMO recipients with COVID-19 ARDS in a large sample of US hospitals using the nations' largest national hospital cost-accounting database, the Premier Healthcare Database (PHD).

Methods: This is a retrospective cohort study using data extracted from the Premier Healthcare database which contains day-level billing logs for goods and services.

We restricted this study to Adults discharged between January 2020 to July 2021 with a diagnosis of COVID-19 (ICD-10 code U07.1), receipt of invasive mechanical ventilation within 5 days of admission and for at least 2 days (not necessarily consecutive). We excluded pregnant patients, those who received ketamine (focus of a separate study). Among Patients who met these criteria (based on ICD-10 procedure codes and hospital charge codes), we identified recipients of ECMO (ICD-10 procedure codes and hospital charge codes).

Hospitals calculate costs using either a procedural or a cost-to-charge ratio method, and we report these as they were entered into the PHD. We also describe demographics, comorbidities, and other treatments (using diagnosis and procedure codes contained in reimbursement claims).

Results: Among 195,202 patients discharged with a diagnosis with COVID-19 from 610 hospitals, 39% (76,167) received mechanical ventilation. Among 41,531 patients who met all inclusion and exclusion criteria, 1.15% (477 patients) received ECMO. The median age of those receiving ECMO was 48 years old (IQR 25-75%: 39 – 55). For patients who received ECMO, the median hospital length of stay (LOS) was 29 (IQR 25 – 75%: 18, 46) compared to 14 (IQR 25 – 75%: 8-24) days for those who did not receive ECMO. ICU LOS was 25 (IQR 25 – 75%: 15 – 39) in those receiving ECMO compared to 10 (IQR 25 – 75%: 5 – 17) days. In-hospital mortality was 49% of patients receiving ECMO died compared to 50.6% in those not receiving ECMO. The patient charges for patients receiving ECMO was $931,082 (IQR 25 – 75%: $513,882-$1,513,615) compared to $204,751 (IQR 25 – 75%: $114,227 - $369958) for patients who did not receive ECMO. Total hospital costs were $224,892 (IQR 25 – 75%: $122,554 - $344,325) for those receiving ECMO compared to $52,317 (IQR 25 – 75: $29,828-$90,754).

Conclusions: Overall resource use for patients who receive ECMO is significant for both patients and hospitals. Understanding costs to insurers and hospitals for the use of ECMO and how it has expaned to treat patients with ARDS will allow for improved budgeting of this modality of care.

References: 1. R.P. Barbaro et. al. Extracorporeal membrane oxygenation for COVID-19: evolving outcomes from the international Extracorporeal Life Support Organization Registry. VOLUME 398, P1230-1238, 2021

2. R Lorusso et. al. In-hospital and 6-month outcomes in patients with COVID-19 supported with extracorporeal membrane oxygenation (EuroECMO-COVID): a multicentre, prospective observational study. Volme 22, SS2213-2600

Critical Care 13 - Association of Early Dexmedetomidine Utilization with Clinical and Functional Outcomes following Moderate-Severe Traumatic Brain Injury: A TRACK-TBI Study

Sunny Yang Liu[1], Margot Kelly-Hendrick[1], Nancy Temkin[1], Jordan Komisarow[2], Jordan Hatfield[2], Tetsu Ohnuma[2], Miriam Treggiari[2], Katharine Colton[2], Daniel Laskowitz[2], Joseph Mathew[2], Adrian Hernandez[2], Michael James[2], Karthik Raghunathan[3], Ben Goldstein[3], Vijay Krishnamoorthy[2], Maximilian Hoffman[4]

Duke University School of Medicine/Medical Student[1] Duke University[2] Duke University Medical Center[3] Duke University Hospital[4]

Introduction: Traumatic brain injury (TBI) is a substantial global health problem[1], and the majority of mechanically ventilated TBI patients require sedation[2]. Dexmedetomidine has emerged as a promising choice for early sedation following TBI due to the favorable sedation profile and potential modulation of autonomic dysfunction[3]. However, effects of dexmedetomidine sedation on patient outcomes after msTBI is unclear. In our study, we examined the association of dexmedetomidine exposure with clinical and functional outcomes among mechanically ventilated patients with moderate-severe TBI (msTBI).

Methods: We conducted a retrospective cohort study using prospectively collected data from the Transforming Clinical Research and Knowledge in TBI (TRACK-TBI) study[4]. Critically ill, adult patients (≥ 17 years) with msTBI (defined by Glasgow Coma Scale (GCS) <13[5]) who required mechanical ventilation within 48 hours of intensive care unit (ICU) admission were included. Using propensity-weighted models, we examined the association of early dexmedetomidine exposure (defined as continuous infusion within 48 hours of ICU admission) with the primary outcome of 6-month Glasgow Outcomes Scale Extended (GOS-E) and the following secondary outcomes: length of hospital stay, hospital mortality, 6-month Disability Rating Scale (DRS), and 6-month mortality.

Results: The 349 subjects who met inclusion criteria had a mean (SD) age of 39.8 (16.6) years, and the majority of patients were male (78%), white (81%), and non-Hispanic (81%). The mean GCS on arrival in the emergency department was 5.5 (SD=3.0), with most (n=276/349, 79%) categorized as severe TBI based on presentation GCS, and nearly all (n=301/349, 92%) had an initial CT positive for intracranial bleeding. Compared to no dexmedetomidine, early dexmedetomidine exposure was not associated with better 6-month GOS-E (weighted OR = 1.17; 95% CI, 0.77-1.77) or the proportion of patients with a favorable GOSE score (OR 0.94; 95% CI, 0.69-1.57). Relative to no dexmedetomidine exposure, the hazard for length of hospital stay (HR = 1.03; 95% CI, 0.79-1.34), length of ICU stay (HR = 0.93; 95% CI, 0.70-1.24), and the odds of being discharged alive (OR = 1.27; 95% CI, 0.60-2.72) were not higher in patients receiving dexmedetomidine. Additionally, both groups had a similar 6-month DRS (adjusted mean difference, -1.47; 95% CI, -4.31-1.36) and 6-month mortality rate (HR 0.63, 95% CI 0.33 - 1.23), with Kaplan Meier curve shown in Figure 2.

Conclusions: Early dexmedetomidine exposure was not associated with significantly different 6-month functional outcomes than those not exposed to early dexmedetomidine in our study. Our data suggests that further research is necessary to identify the ideal early sedative to inform TBI guidelines.

References: 1. J Neurosurg 2018:1-18.

2. Crit Care Med 2018;46(9):e825-e873

3. Semin Neurol 2008;28(5):611-30

4. J Neurotrauma 2014;31(17):1457-77

5. Report to Congress on traumatic brain injury in the United States: Epidemiology and rehabilitation

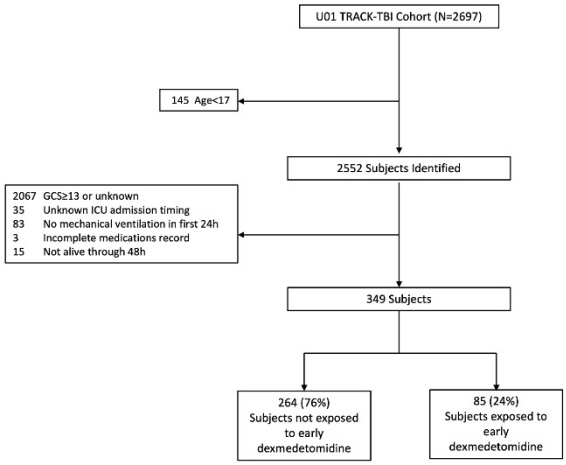

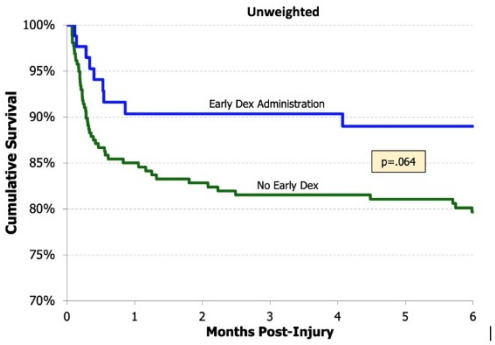
Unweighted
100%
95%
90%
85%
80%
75%
70%
Cumulative Survival
Early Dex Administration
p=.064
No Early Dex
0
1
2
3
4
5
6
Months Post-Injury

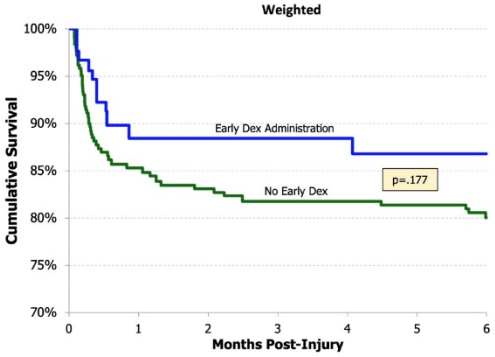
Weighted
100%
95%
90%
85%
80%
75%
70%
Cumulative Survival
Early Dex Administration
p=.177
No Early Dex
0
1
2
3
4
5
6
Months Post-Injury

Critical Care 14 - Beta-blockers exposure and functional outcomes in the acute management of patients with moderate to severe traumatic brain injury: A TRACK-TBI Observational study

Margot Kelly-Hedrick[1], Sunny Liu[1], Tetsu Ohnuma[2], Katharine Colton[2], Miriam Treggiari[2], Vijay Krishnamoorthy[2], Jordan Komisarow[2]

Duke University School of Medicine[1] Duke University[2]

Introduction: Acute management of moderate-severe traumatic brain injury (TBI) is aimed at preventing secondary injury that occurs after the primary insult.[1] Multiple prospective and retrospective studies have found beta-blocker exposure during the acute care of patients with moderate to severe TBI to be associated with lower in-hospital mortality than those not exposed.[2] The mechanism of benefit is unproven but may be related to dampening of sympathetic surge post-TBI.[3] Little has been published on how beta-blockers are used at the granular detail of timing, dose, type, and frequency in the intensive care unit (ICU), as well as long-term functional outcomes associated with its use.

Methods: This study is a retrospective secondary analysis of the Transforming Clinical Research and Knowledge in TBI (TRACK-TBI) study, a prospective cohort study of patients presenting to one of 18 participating level I trauma centers following a blunt TBI. We included patients ≥17 years with moderate-severe TBI (Glasgow Coma Scale (GCS) of <13) admitted to the ICU. We aimed to (1) describe patterns of beta-blocker use, and (2) examine association of beta-blocker exposure with clinical and functional outcomes, with a primary outcome of Glasgow Outcome Scale-Extended (GOSE) at 6 month follow up.

Results: Of the 450 eligible participants, 57 (13%) received beta blockers during the 7-day period in the ICU (BB^+ group). The total sample was on average 40 years old (SD=17 years), 22% female, 16% had a history of hypertension, and 76% had a severe GCS score on presentation. The BB^+ group was on average older (p=0.001), more likely to be on a pre-injury beta-blocker (n=9/57, 16% versus n=11/393, 3% BB^- group, p<0.001), and were more likely to have a history of hypertension (n=18/57, 32% versus n=48/393, 12% BB^- group, p<0.001), but had no significant difference in injury cause, GCS scores, injury severity, or blood pressure measurements on presentation (p>.05). In the BB^+ group, 34 (60%) received metoprolol only, 19 (33) received propranolol only, 3 (5%) received both, and 1 (2%) received atenolol only. The median total dose for metoprolol was 25 mg, and 30 mg for propranolol, with the first day of administration ranging from 0 to 7 days of ICU stay. There was no association between GOSE score at 6 months and BB group (OR=0.86, 95% CI=0.48,1.53), after adjusting for pre-injury beta blocker use, age, and history of hypertension.

Conclusions: About one-sixth of subjects in our study received beta-blockers, and within this group, dose, and timing of beta-blocker administration varied. No significant differences in GOSE score at 6 months were demonstrated; our ability to draw conclusion is in part limited by overall low total doses compared to past randomized trials. This is one of the first studies to look at long-term functional outcomes following beta-blocker use in acute TBI care.

References: 1. Carney N, Totten AM, O'Reilly C, et al. Guidelines for the Management of Severe Traumatic Brain Injury, Fourth Edition. *Neurosurgery*. 2017;80(1):6-15. doi:10.1227/NEU.0000000000001432

2. Ding H, Liao L, Zheng X, et al. β-Blockers for traumatic brain injury: A systematic review and meta-analysis. *J Trauma Acute Care Surg*. 2021;90(6):1077-1085. doi:10.1097/TA.0000000000003094

3. Khalili H, Ahl R, Paydar S, et al. Beta-Blocker Therapy in Severe Traumatic Brain Injury: A Prospective Randomized Controlled Trial. *World J Surg*. 2020;44(6):1844-1853. doi:10.1007/s00268-020-05391-8

Critical Care 15- Characteristics and Short-Term Donation Outcomes of Deceased Organ Donors Supported by Extracorporeal Membrane Oxygenation during Organ Recovery Procedures

Louis Anzalone[1], Audrey Spelde[1], Salim Olia[1], Asad Usman[1], Christian Bermudez[1], Marisa Cevasco[1], Michael Ibrahim[1], Emily Vail[2]

Hospital of the University of Pennsylvania[1] University of Pennsylvania[2]

Introduction: Most organs transplanted in the United States are donated by deceased donors after brain death (DBD) or circulatory death (DCD). Patients supported by extracorporeal membrane support oxygenation (ECMO) who sustain complications, fail to recover, or lose eligibility for transplantation may become eligible for deceased organ donation. This study aimed to compare patients who died on ECMO and donated organs to those who did not, and to compare outcomes of ECMO-supported donors with other deceased donors.

Methods: A retrospective analysis of clinical data in an ECMO dataset and donation outcomes data provided by the local organ procurement organization was performed. All patients who died on ECMO support, including those that donated organs, in 2 US hospitals, from January 2014 to June 2022 were included. The primary outcome was recovery of at least one organ intended for transplant. Secondary outcomes included donation type (DCD or DBD), the number of organs transplanted, and individual organs transplanted. We examined patient demographics and clinical characteristics, including indications for ECMO and type and duration of ECMO support, then compared characteristics and outcomes of organ donors who received and did not receive ECMO support, stratified by donation type. Comparisons were unadjusted.

Results: Over the study period, 521 patients died on ECMO support; 25 (4.8%) became donors. Among decedents on ECMO, donors were younger than other patients (median 32.5 years, interquartile range (IQR 26-44.5) vs. 46 years (IQR 29.5, 58)). Respiratory failure was the most common indication for ECMO among cohort donors (12, 48%), though ECMO-supported donors received both venoarterial (VA) (13, 52%) and venovenous (VV) support (12, 48%). Median duration of ECMO support was 8 days (range 1 - 103). A majority of ECMO-supported donors were DCD (17, 68%).

Donors supported by ECMO successfully donated kidneys, livers, and hearts. DCD donors who were on ECMO donated similar median numbers of organs transplanted (median 2 (range 0-3) vs. 2 (range 0-5) for DCD donors without ECMO; Table 1, Fig. 1). Among DCD donors, rates of liver and kidney transplantation were similar between donors with and without ECMO support. Among DBD donors, those supported by ECMO had fewer median numbers of organs transplanted (2 (range 0-4) vs. 3 for donors without ECMO (0-9), Fig 2.). Rates of individual organ transplantation were lower among DBD donors with ECMO support than those without.

Conclusions: Successful donation from patients supported by VA or VV ECMO is rare but feasible, with similar rates of liver and kidney transplantation among DCD donors. The present study is limited by the small number of donors supported by ECMO and retrospective design. Reported donation outcomes may be influenced by selection bias among organ procurement organization staff and accepting transplant programs, who may be less willing to list or accept organs from donors supported by ECMO than other donor populations as donors' indications for ECMO, or ECMO support itself, may negatively impact graft function and recipient outcomes. Future work is needed to determine whether processes of care (for example, later organ procurement organization notification) may contribute to low donation rates from ECMO, to identify modifiable factors that may increase donation opportunities, and to determine whether long-term donation outcomes differ between donors with and without ECMO support.

Table 1. Comparison of organ donation outcomes among cohort patients

	Donation after circulatory death		Donation after brain death	
	Supported by ECMO at time of death	No ECMO support	Supported by ECMO at time of death	No ECMO support
Total donors (% of cohort)	158 (30.3)		363 (69.7)	
Donors (% of group)	17 (10.8)	141 (89.2)	8 (2.2)	355 (97.8)
Number of organs recovered for transplant per donor, median (range)	2 (2-3)	2 (1-5)	3 (2-4)	3 (1-8)
Number of organs transplanted per donor, median (range)	2 (0-3)	2 (0-5)	2 (0-4)	3 (0-8)
Types of organs transplanted, n donors (% of donors in each group who donated type of organ)				
Kidney	15 (88.2)	119 (84.4)	4 (50.0)	260 (73.2)
Liver	2 (11.8)	16 (11.4)	4 (50.0)	291 (82.0)
Heart	0 (0)	0 (0)	2 (25.0)	112 (31.6)
Lung	0 (0)	5 (3.6)	0 (0)	97 (27.3)
Pancreas	0 (0)	1 (0.7)	0 (0)	35 (9.9)
Intestine	0 (0)	0 (0)	0 (0)	2 (0.6)

[a]At least one organ transplanted from each donor. [b]Whole, split, or partial liver donation.

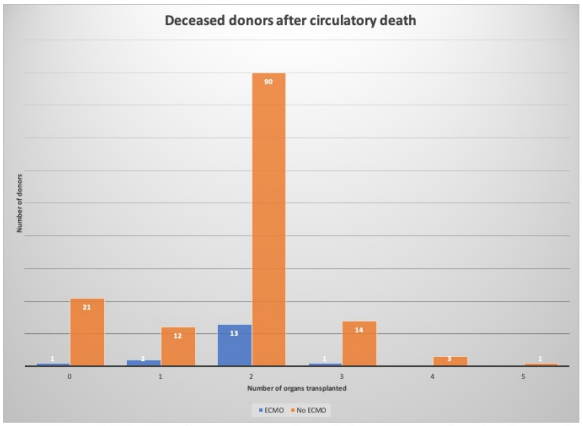

Figure 1. Number of organs transplanted from donors after circulatory death

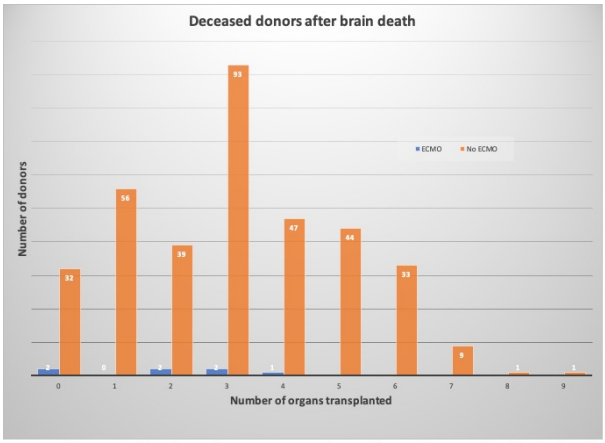

Figure 2. Number of organs transplanted from donors after brain death

Critical Care 16- Characterization of Vital Landmarks Pertaining to Central Line Placement in the Femoral Vein: A Cadaveric Study

Tamara Stojilkovic[1], Kelsey Staudinger[2], Celeste Murtha[1], Anthony Olinger[1]

Kansas City University[1] HCA/Swedish Medical Center[2]

Introduction: Central venous catheters (CVCs) are frequently needed in traumatic and critically ill patients to provide fluid, medication, etc. In the emergent trauma setting, a femoral CVC may be the preferred access site due to the presence of injuries in areas where CVCs are more commonly placed. Although ultrasound can be a helpful adjunct when placing CVCs, a thorough understanding of anatomy remains crucial when using traditional landmarks to locate the femoral vein[1]. Because adipose tissue can alter the relationship between anatomic structures, utilizing traditional landmarks, the anterior superior iliac spine (ASIS) and pubic tubercle, to estimate the location of the femoral vein in overweight patients may be difficult or unreliable. This study seeks to understand if increased BMI alters the anatomic relationship of these classic landmarks, which could weaken the reliability of using traditional landmarks in overweight patients.

Methods: 30 formaldehyde-preserved human cadavers (18 male, 12 female) were obtained through a medical school cadaver lab and permission to dissect for research purposes was granted. BMI was calculated in each cadaver: 19 cadavers had a BMI less than 25 and 11 cadavers had a BMI over 25. A careful dissection of the bilateral femoral triangle was performed to expose the inguinal ligament, femoral artery, and femoral vein. The ASIS and pubic tubercle were also dissected and used as key landmarks for taking measurements. A pin was placed at the most prominent part of the ASIS and pubic tubercle. An additional pin was placed between the femoral artery and the femoral vein. The following measurements were then taken with a digital caliper: (1) the pin at the most prominent part of the ASIS to the pin between the femoral artery and the femoral vein, and (2) the pin between the femoral artery and femoral vein to the pin at the most prominent part of the pubic tubercle. Pearson correlation was utilized in the analyses.

Results: A non-significant weak correlation was found between BMI and the bilateral distance from the ASIS to the lateral side of the femoral vein (left side r=0.058; p=0.760, right side r=0.203; p=0.281) and the lateral side of the femoral vein to the pubic tubercle (left side r=0.041; p=0.831, right side r=-0.161; p=0.397).

Conclusions: An increase in BMI shows no significant difference in the distance between the ASIS and the femoral vein, and the femoral vein and the pubic tubercle. Therefore, when placing a femoral CVC, traditional landmarks can continue to be used with consistency to guide placement if ultrasound is not readily available.

References: 1. Ultrasound-guided central venous catheter placement: a structured review and recommendations for clinical practice. 2017;21(1):225

Critical Care 17 - Critical Anesthesia Outcomes in Underserved Communities: An Epidemiological Study between 2010 through 2022

Faisal Elali[1]

SUNY Downstate Health Sciences University[1]

Introduction: This epidemiological study seeks to examine the usage of critical anesthesia outcomes in patients living in underserved communities from 2010 to 2022. Anesthesia is a critical component of medical care, and its usage in underserved communities is a key indicator of health equity. Anesthesia can be used to reduce pain and discomfort during medical procedures, as well as to reduce the risk of complications and improve outcomes. This study will use a database to analyze the usage of critical anesthesia outcomes in underserved communities over a 12-year period.

Methods: Data for this study was collected from the National Anesthesia Outcomes Database (NAOD), a database of anesthesia outcomes in underserved communities from 2010 to 2022. The database included information on the type of anesthesia used, the patient's age, gender, and other demographic factors, as well as the outcomes of the anesthesia. The data was analyzed using descriptive statistics, including frequency distributions, means, and standard deviations, to examine the usage of critical anesthesia outcomes in underserved communities over the 12-year period. The data was also analyzed to examine any trends in the usage of critical anesthesia outcomes over time.

Results: The results of the analysis showed that the usage of critical anesthesia outcomes in underserved communities increased from 2010 to 2022. The most commonly used anesthesia was general anesthesia, followed by regional anesthesia and sedation. The majority of patients were between the ages of 18 and 64 (mean age = 37.2, SD = 12.3), and the majority of patients were male (62.3%). The most common critical anesthesia outcomes were successful intubation (87.4%), successful ventilation (93.2%), and successful extubation (96.6%). The data also showed that the usage of critical anesthesia outcomes in underserved communities increased over the 12-year period, with a significant increase in the usage of general anesthesia ($p < 0.001$) and regional anesthesia ($p < 0.001$). The data also showed that the success rate for intubation, ventilation, and extubation increased over the 12-year period, with a significant increase in the success rate for intubation ($p < 0.001$) and ventilation ($p < 0.001$).

Conclusions: This study found that the usage of critical anesthesia outcomes in underserved communities increased from 2010 to 2022. The most commonly used anesthesia was general anesthesia, and the most common critical anesthesia outcomes were successful intubation, successful ventilation, and successful extubation. These findings suggest that access to critical anesthesia outcomes in underserved communities is improving, which is a positive step towards health equity. This study highlights the importance of providing access to quality anesthesia care in underserved communities, and further research is needed to understand the factors that contribute to the increased usage of critical anesthesia outcomes in these communities. Additionally, further research is needed to examine the long-term effects of anesthesia on patient outcomes and to identify any potential disparities in access to anesthesia care in underserved communities.

Critical Care 18 - Exploratory genome-wide association study of postoperative pulmonary complications following elective cardiac surgery

Aaron Mittel[1], Casey Drubin[1], Marcos Vidal Melo[1], May Hua[1], Kathleen Yu[2], Itzel Velazquez Sanchez[2], Gebhard Wagener[2]

Columbia University Medical Center[1] Columbia University Irving Medical Center[2]

Introduction: Postoperative pulmonary complications (PPCs) occur in more than 75% of cardiac surgical patients and are associated with poor outcomes.[1,2] PPCs are often attributed to the insults of cardiopulmonary bypass (CPB) and other features inherent in cardiac surgery.[1,2] Plausibly, some patients may have genetic predisposition to PPCs, as has been seen with other perioperative complications.[3,4] Combined with intraoperative events, such as CPB-induced physiologic stress, subclinical genetic variants may exhibit phenotypic effects and permit detection of meaningful relationships between genotype and PPCs despite a small sample size. Thus, we conducted an exploratory genome-wide association study (GWAS) among elective cardiac surgical patients to identify genetic polymorphisms associated with PPCs following cardiac surgery.

Methods: Patients undergoing elective cardiac surgery requiring CPB who provided consent were eligible for this IRB-approved GWAS. Blood samples were obtained following induction of anesthesia, before CPB. We combined data from the Society of Thoracic Surgeons (STS) National Database, local CompuRecord Perioperative Anesthesiology Information System (Philips Healthcare, Andover MA), and medical records to identify pulmonary outcomes within 7 postoperative days. Whole-exome sequencing was performed and genotypes were associated with phenotypic outcomes. The primary outcome was PPC severity, graded from 3 (moderate) – 5 (death) analogous to a scale used in a prior trial (Table 1).[1] PPC grades 1 – 2 were not tabulated. The secondary outcome was final P_aO_2/F_iO_2 ratio (P/F) before patients left the operating room and was explored in a subset of patients from the primary analysis who had complete P/F data. Analyses were adjusted for population stratification and duration of CPB as CPB time can be a marker of baseline cardiac disease severity and also directly contribute to lung injury independent of genetic predisposition; $p < 5e\text{-}8$ was considered significant. Analyses were conducted using PLINK v1.07.[5]

Results: 204 patients were enrolled from 2016 – 2018 and were included in the primary analysis. The overall cohort was older (mean age 66 years), predominantly male (72.1%), and had a mean CPB duration of 111.2 minutes. In total, 50 patients (24.5%) experienced grade 3 or worse PPCs in the primary cohort (Table 2). One allele located within gene SFMBT2 (chr10: 7328467 G, rs139461139) was significantly associated with PPCs ($p = 2.569e\text{-}08$; Figure 1). A 142-patient subset of this group was included in the secondary analysis (58 patients were missing P/F data). The mean final P/F was 327.2 (IQR 232.5 – 423.8) in this group. There were no statistically significant associations between genotype and final P/F though one allele located within gene CEP83 (chr12:94818770 T) approached significance ($p = 9.428e\text{-}07$; Figure 2).

Conclusions: In this exploratory GWAS, we identified a significant association between SFMBT2 gene polymorphism and at least moderate PPCs following elective cardiac surgery requiring CPB. SFMBT2 is expressed in cells throughout the body and is a negative regulator of gene expression. It has been implicated in pathophysiology of vascular disease, cancer, and other illnesses [6,7] though has not previously been associated with perioperative pulmonary disease. We also identified one possible association between CEP83 gene polymorphism and postoperative lung injury. CEP83 encodes for a protein involved in primary ciliary assembly and is expressed in lung and other tissues.[8] Hypothetically, disruptions in lung ciliary function may contribute to an increased risk of pulmonary complications following surgery. This study is limited by its small sample size. However, the significant association between genotype and PPCs suggests the need for further work to better clarify genetic predisposition to perioperative lung injury. Future analysis, inclusive of more patients and predictor covariables beyond CPB duration and population stratification may yield more meaningful results.

References:

1. JAMA. 2017 Apr 11;317(14):1422-1432.
2. Can J Anaesth. 2022 Dec;69(12):1493-1506.
3. Circulation. 2006 Jul 4;114(1 Suppl):I275-81.
4. J Thorac Cardiovasc Surg. 2003 Oct;126(4):1107-12.
5. Am J Hum Genet. 2007 Sep;81(3):559-75.
6. Life Sci. 2021 Jan 1;264:118691.
7. J Cell Mol Med. 2018 Nov;22(11):5753-5758.
8. J Cell Biol. 2019 Oct 7;218(10):3489-3505.

Table 1. Grading of postoperative pulmonary complication severity. (C = Celsius, CXR = chest x-ray, POD = postoperative day, HFNC = high-flow nasal cannula, BiPAP = bilevel positive airway pressure, STS = Society of Thoracic Surgeons, EMR = electronic medical record).

Grade	Definition	Comments
1 – Limited	Dry cough, [illegible] dyspnea not due to other cause	*Not distinctly measured in this study*
2 – Mild	Fever (temp > 37.5 C) and atelectasis (determined via attending radiologist read of CXR on same POD as fever) in first 7 postoperative days	*Not distinctly measured in this study*
3 – Moderate	*One or more of the following:* ▪ Pleural effusion requiring thoracentesis ▪ Pneumonia ▪ Non-invasive ventilation, HFNC or BiPAP ▪ Intubation 24 – 48 hours postoperatively	Pleural effusion, pneumonia, and intubation duration data obtained from STS National Database. Use of non-invasive ventilation determined via retrospective review of patients' EMR. Presence of pneumothorax was scored as grade 3 in prior authors' work[1] but was omitted in this study.
4 – Severe	Intubation > 48 hours or reintubation within 7 days	Intubation duration data obtained from STS National Database.
5 – Death	In-hospital death	Data obtained from STS National Database; death in-hospital at any postoperative time point was scored as grade 5.

Table 2. Demographics of each sample (n = number, cm = centimeter, IQR = interquartile range, kg = kilogram, CPB = cardiopulmonary bypass, PPC = postoperative pulmonary complication, P/F = P_aO_2/FiO_2 ratio).

	Primary Cohort *n = 204*	**Secondary Cohort** *n = 142*
Age, years, median (IQR)	66 (59 – 73)	67 (59 – 73)
Male, n (%)	147 (72.1)	102 (71.8)
Height, cm, mean (IQR)	171.6 (165.0 – 178.0)	171.5 (165.0 – 178.0)
Weight, kg, mean (IQR)	85.4 (74.1 – 94.1)	87.0 (75.2 – 97.0)
CPB duration, min, mean (IQR)	111.2 (81.0 – 129.5)	94.5 (80.3 – 132.5)
Sleep apnea diagnosis, n (%)	7 (3.4)	5 (3.5)
Current smoking habit, n (%)	24 (11.8)	16 (11.3)
PPC grade		
1 – 2, n	154	104
3, n	41	33
4, n	8	4
5, n	1	1
Final P/F, mean (IQR)	324.0 (230.2 – 423.0)	327.2 (232.5 – 423.8)

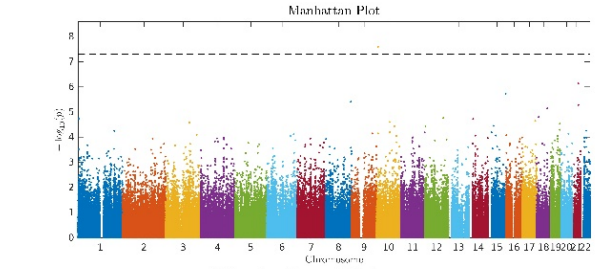

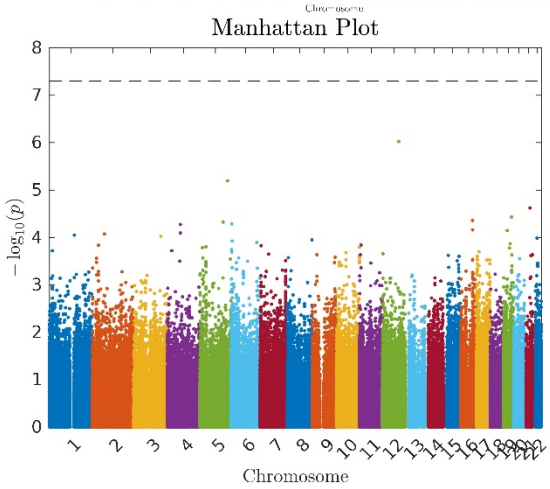

Critical Care 19 - Feasibility of a prospective longitudinal bedside ultrasound protocol to examine muscle health in critical illness

Caroline Ruminski[1], Kimberly Rengel[1]

Vanderbilt University Medical Center[1]

Introduction: A large prospective study described that at one year post-discharge, 27% of surviving critically ill patients developed at least partial ADL disability[1]and 47% of previously employed patients were unable to return to work.[2] Sarcopenia, a progressive and generalized skeletal muscle disorder, may contribute to functional disability after critical illness. While muscle deterioration is often a part of the trajectory of critical illness, risk factors for such deterioration have not been clearly defined.[3]
The Muscle UltraSound in Critical Illness to Understand Long-Term ImpAirment and Recovery (MUSCULAR) study is an ongoing prospective cohort study assessing changes in muscle health throughout critical illness. We plan to define trajectories of muscle health in critical illness and examine their relationship with long-term functional outcomes. This study seeks to clarify the potential influence of muscle health on acquired disability after critical illness. MUSCULAR uses a pragmatic bedside ultrasound examination to quantify muscle mass and quality. In anticipation of completing follow up of this study cohort, we aim to describe the cohort and reflect on our experience thus far regarding feasibility of using a bedside ultrasound protocol to examine muscle mass and quality in the critically ill.

Methods: MUSCULAR is a single-center prospective cohort study, nested within two ongoing NIH-supported prospective cohorts collecting data during subjects' hospital courses and evaluating physical outcomes at 3- and 12-months post-discharge. Enrollment is offered to all patients participating in these parent studies, which include adult trauma, medical, and surgical patients requiring ICU admission for shock, respiratory failure, or neurologic failure. Since November 2020, 139 patients have been enrolled. We have obtained ultrasound images of the bilateral masseter, deltoid, and rectus femoris muscles for each patient on the day of enrollment and every 7 days thereafter, through day 28 of hospital admission or discharge from the hospital. If a patient had injuries, dressings, or discomfort at one of these sites, the images were not obtained.
To characterize the population, in-hospital data recorded in REDCap[4-6] was exported for patients enrolled in MUSCULAR. We report here on descriptive data, including age, sex, admission ICU, surgery prior to enrollment, respiratory failure at enrollment, shock at enrollment, days alive in ICU and hospital, and study withdrawal. Median and interquartile ranges were used to describe continuous variables. Percentages were used to describe categorical variables.
To examine the feasibility of the MUSCULAR ultrasound protocol within this diverse population, we also present the portion of patients for whom we were unable to capture all images.

Results: In-hospital data was complete for 135 of 139 patients enrolled in MUSCULAR at the time of this analysis. The median age of the cohort was 53.5 years (IQR 30.6-67.3). 98 (71%) were admitted to the Trauma ICU. 90 (67%) were male. 70 (52%) had surgery prior to enrollment. 80 (59%) had shock and 92 (68%) had respiratory failure on admission. The median days spent alive in the ICU and hospital was 6.1 days (IQR 2.6-11.7) and 14.7 (IQR 8.6-30.7) days, respectively.
Of the 139 patients enrolled, 90 completed the study protocol and 19 patients died or transitioned to comfort care. 14 patients were discharged prior to the discharge ultrasound exam being completed, and 2 refused further ultrasound exams. 10 had admissions shorter than 5 days and only underwent an Enrollment exam. 4 patients had portions of their exam protocol missed by the investigators.
To date, we have completed analysis of ultrasound images for 65 patients. Of those, 24 had portions of their exam excluded due to an injury, dressing, or discomfort during the exam. Of these 24 patients, 16 patients were missing only one of the six protocol images.

Conclusions: Measuring muscle size and quality over time throughout the duration of critical illness with a bedside ultrasound protocol is feasible in a population with a diverse range of pathology. The ultrasound protocol was completed for three quarters of patients who survived until protocol completion. Most exams that excluded images due to patient injury were only missing one of six images, allowing for analysis of the remaining five muscles over time. Furthermore, this cohort spans a broad range of age and pathology and, in turn, will produce generalizable results.

References:

1. *Lancet Respir Med* 2014; 2: 369-79
2. *Crit Care Med* 2016; 44: 2003-9

3. *JAMA* 2013; 310: 1591-600
4. *J Biomed Inform.* 2009; Apr;42(2):377-81
5. *J Biomed Inform.* 2019; May 9 [doi: 10.1016/j.jbi.2019.103208]
6. *J Biomed Inform.* 2021; Sep;121:103871

Table 1. MUSCULAR Cohort Descriptive Data	
Age, median (IQR), y	*53.5 (30.6-67.3)*
Sex, No. (%)	
Female	*45 (33.3%)*
Male	*90 (66.7%)*
Admission ICU, No. (%)	
Surgical ICU	*11 (7.9%)*
Trauma ICU	*98 (70.5%)*
Cardiac Medical ICU	*3 (2.2%)*
Medical ICU	*27 (19.4%)*
Surgery Prior to Enrollment, No. (%)	*70 (51.8%)*
Respiratory Failure at Enrollment, No. (%)	*92 (68.1%)*
Shock at Enrollment, No. (%)	*80 (59.3%)*
Days Alive in ICU, median (IQR)	*6.1 (2.6-11.7)*
Days Alive in Hospital, median (IQR)	*14.7 (8.6-30.1)*
Study Withdrawal, No. (%)	*9 (6.7%)*

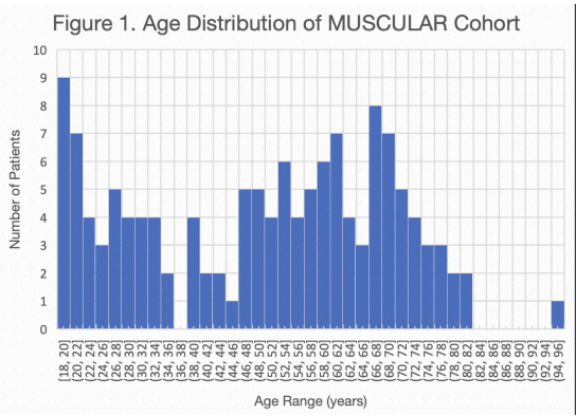

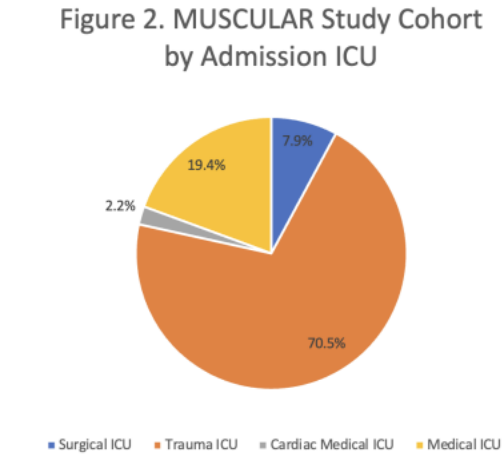

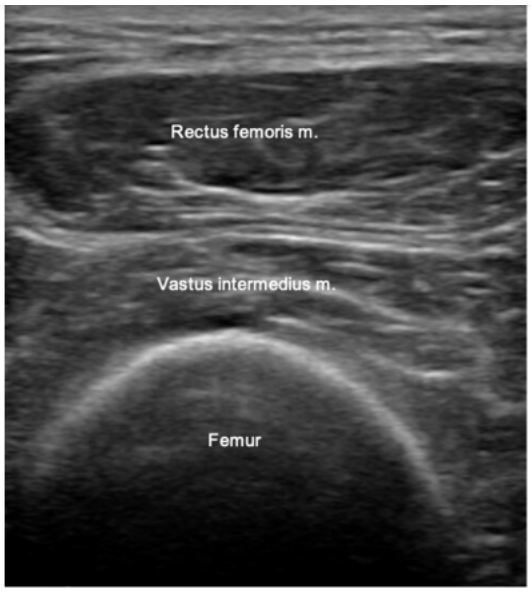

Figure 3. Ultrasound image of right rectus femoris muscle, vastus intermedius muscle, and femur in an enrollment ultrasound exam. "Med" designates the medial side of the image. The vertical width and cross-sectional area of the rectus femoris will be measured using ImageJ.

Critical Care 20- Femoral Vein Pulsatility Doppler Assessment for Evaluation of Venous Congestion

Vimal Bhardwaj[1], Nithish Mukunthan[1], Arjun Alva[1], Kumar Belani[1]

University of Minnesota[1]

Introduction: Bedside ultrasound assessment of the femoral vein is a simple non-invasive tool for the evaluation of the presence of pulsatility and pulsatility with reversed flow as markers of venous congestion and heart failure (Reference 1). In this study, we examined the femoral vein for ultrasound evidence of pulsatility and pulsatility with reversed flow with other markers of venous congestion and heart failure

Methods: After IRB approval we conducted a cohort review of 107 adults, 73% males, with a mean± SD age of 55.7 ± 13 years following cardiac surgery in our tertiary care intensive care unit. All patients had a central venous catheter and in addition to monitoring of hemodynamics and clinical examination they underwent routine ultrasound examination of the hepatic, portal, and right femoral veins in the supine position using a 1.5 MHz ultrasound probe. For central venous pressure measurements, the head was elevated at 30 degrees. The ultrasound findings over the femoral vein were evaluated for correlation with the hepatic and portal vein doppler findings and clinical and hemodynamic measurements at the same time. Venous congestion was graded as mild (femoral vein pulsatile), moderate (femoral vein showing a retrograde flow of > 10 cm/s and severe when the retrograde flow was present along with a velocity amplitude of 1/3rd more than the antegrade flow velocity (see figure). The results of the femoral vein ultrasound findings were compared to the Venous Excess Ultrasound Score (VExUS) findings from the other ultrasound measurements (Reference 2). We used standard statistics to evaluate our results using the SPSS statistics program. We excluded pregnant patients, those with an inadequate window for ultrasound evaluation, presence of respiratory distress (Respiratory rate >35/min, accessory muscles of respiration in use), liver cirrhosis, and deep vein thrombosis of the lower extremity.

Results: There was a significant correlation between femoral venous doppler findings, VExUs grade, and central venous pressure (P value <0.001). A large number (86.4%) of patients who had a VExUs grade between 1-3 had abnormal pulsation in the femoral venous doppler. Similarly, 77.8% of patients who had VExUs grade 0 had normal femoral venous doppler waves.
When analyzed for correlation between edema and femoral venous doppler findings, 32.7% of patients with abnormal femoral vein doppler had edema and only 1.8% of patients with normal femoral vein doppler had edema (P value < 0.001).

Conclusions: The bedside assessment of femoral vein pulsatility provides valuable information for the evaluation of venous congestion and heart failure in cardiac surgical patients during the postoperative period. Bedside clinical findings of heart failure correlate well with the femoral vein doppler findings. Using the femoral vein ultrasound findings is simpler to perform as compared to the VExUS score. Further studies are needed to evaluate the utility of this diagnostic ability during the care of patients with sepsis and shock either in the emergency room or in an intensive care unit.

References: 1. Crit Care Explor. 28;2(10):e0209, 2020 Sep

2. Indian J Crit Care Med. 2020 Sep;24(9):783-789.

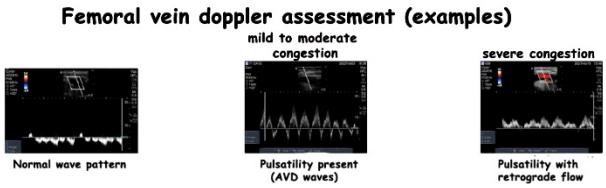

Critical Care 21 - Integrated Mass Cytometry Accurately Predicts Hemorrhagic Transformation Following Acute Ischaemic Stroke

Amy Tsai[1], Julien Hedou[1], Jakob Einhaus[1], Dorien Feyaerts[1], Franck Verdonk[1], Benjamin Choisy[1], Jean Phillipe Desilles[1], Benoit Ho-Tin-Noe[1], Jean Marc Olivot[1], Mikael Mazighi[1], Brice Gaudilliere[1]

Stanford University[1]

Introduction: Acute ischemic stroke (AIS) is one of the leading cause of morbidity and mortality worldwide. Despite the 90% recanalisation rate after endovascular treatment (EVT), over 50% of patients with AIS suffer hemorrhagic transformation (HT), the major modifiable predictor of poor functional recovery(1, 2). However, existing predictive scores of HT after AIS perform poorly. A better understanding of the pathophysiological mechanisms leading to HT after AIS is critical to identify predictive, actionable biomarkers of HT. Emerging preclinical evidence suggests that dysfunctional inflammatory processes resulting in persistent microcirculation thrombosis and blood brain barrier leakage are critical to the pathogenesis of HT(3). Here, we employ a high-dimensional mass cytometry immunoassay to characterize the dynamic changes of over 300 single-cell immune responses in patients with and without HT after an EV treatment for AIS.

Methods: Twenty patients admitted to the hospital for EVT after an AIS were enrolled in a single-center prospective study. The primary outcome of the study was the development of HT within 3 days after EVT. Arterial and venous whole blood samples were collected before EVT then 1h, and 24h after EVT. For each sample the frequency and intracellular signaling responses of 25 major innate and adaptive immune cell subsets and 2 platelet populations were quantified using a custom 47-parameter mass cytometry. Additionally, the thrombus removed during EVT was submitted for imaging mass cytometry (IMC) analysis using a novel 22-parameter assay. Multivariate predictive modeling of the primary outcome was performed using a novel sparse machine learning algorithm (STABL) and predictive performance evaluated with cross-validation (Figure 1).

Results: A multivariate model integrating single-cell data collected pre-EVT accurately classified patients who developed HT from patients with (n=10) and without (n=10) HT with an AUC of 0.92 and pval 0.0017. IMC additionally identified regions of interest comprised of immune cell clusters at RBC and platelet-rich region borders.

Conclusions: The single-cell analysis of immune signaling responses before EVT revealed a systemic immune signature predictive of HT after EVT. While further studies in larger and more diverse patient populations are needed to test the generalizability of the findings, the results provide a promising approach to identify predictive biomarkers of HT after EVT and biologically plausible targets for innovative immunomodulatory treatments.

References: 1. Safety and efficacy of intensive blood pressure lowering after successful endovascular therapy in acute ischaemic stroke (bp- target): A multicentre, open-label, randomised controlled trial. Lancet neurology. 2021;20:265-274

2. What predicts poor outcome after successful thrombectomy in early time window? J Neurointerv Surg. 2021

3. Clinical recovery from surgery correlates with single-cell immune signatures. Science translational medicine. 2014;6:255ra131

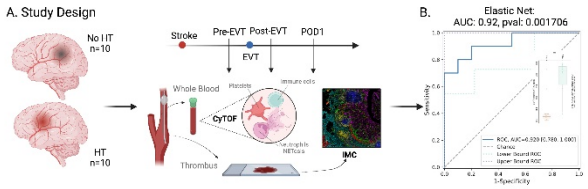

Critical Care 22 - IntraCranial pressure prediction AlgoRithm using machinE learning (I-CARE) - Training and Validation Study -

Romain Pirracchio[1], Nick Fong[1]

UCSF Departmnent of Anesthesia[1]

Introduction: Elevated intracranial pressure (ICP) is a potentially devastating complication of neurologic injury. Successful management of patients with elevated ICP requires early recognition, the judicious use of invasive monitoring, and therapy directed at both reducing ICP and reversing its underlying cause [1]. Predicting the evolution of ICP could help the clinician adjust treatments and potentially prevent elevated ICP episodes.

Methods: Data from the eICU Collaborative Research Database, a multi-center ICU database with high granularity data was used to train an ensemble machine learning model to predict the ICP 30 minutes in the future. Covariates included for the model included baseline demographics (age, assigned sex), labs (ABG, sodium, creatinine, hematocrit, hemoglobin, platelets, glucose, fibrinogen, INR), medications and infusions (sedatives, vasopressors, hypertonic solutions, benzodiazepines, neuromuscular blockers, opioids), input/output, reason for ICU admission, and timeseries vitals (heart rate, ICP, MAP, respiratory rate, Glasgow Coma Scale components, temperature). Vital signs were originally collected at 1-minute intervals, with 5-minute medians archived in the dataset. Each patient ICU stay was divided into successive 95-minute time blocks: 75% of the time blocks were randomized to the training set, and 25% to the test set. For each time block, the model was trained on non-time-varying covariates as well as on 12 observations of time-varying covariates at five-minute intervals, and asked to predict the five-minute median ICP 30 minutes after the last observed ICP value. Our model called I-CARE was trained using the SuperLearner methodology, which is a method for selecting, via cross-validation, the optimal weighted combination of a set of candidate algorithms.

Results: Nine hundred and thirty one patients from the eICU dataset met our inclusion criteria, for a total of 21,729 time blocks: 16,296 timeblocks were included in the training set, 5433 timeblocks were included in the test set. 6835 time blocks from 127 patients from the MIMIC-III dataset were used for external validation. The median ICP (in mmHg) during the observation phase was 9 [6, 14], 10 [6,14] and 9 [6, 12] in the training set, the test set and the external validation set, respectively. During the prediction phase, the observed median median ICP (in mmHg) during the observation phase was 9 [6, 14], 10 [6, 14], and 9 [6, 12] in the training set, the test set and the external validation set, respectively. Model calibration is illustrated in Figure 1. The root mean squared error (RMSE) in the test set was 4.83 mmHg. As illustrated in the Bland and Altman plots (Figure 2), systematic bias in the test set was 0.02 mmHg with limits of agreements of -8.68 mmHg and 8.73 mmHg. When the model was evaluated on 6835 time blocks from an external dataset from other intensive care units, the RMSE was 3.48 mmHg, the systematic bias was 0.20 mmHg with limits of agreements of -6.86 and 7.27. A subset of the test set where the actual ICP value during the prediction window increased by at least 20% of the mean ICP from the observation window was additionally examined. In this subset of time periods, the RMSE was 3.51 mmHg. When a subset of the validation set where the actual ICP value during the prediction window increased by at least 20% of the mean ICP from the observation window, the RMSE was 5.90 mmHg. I-CARE's performance to detect an episode of intracranial hypertension as defined by a median ICP greater than 15, 20 and 22 mmHg during the prediction window is provided in Table 1. We also evaluated the performance of I-CARE to detect an ICP increase in the next 30 minutes of more than 5, 10 and 15 mmHg (Table 1).

Conclusions: I-CARE is the first intracranial prediction algorithm allowing to accurately predict the ICP value 30-minute in the future using advanced machine learning, trained on a large sample of neurocritical care patients and externally validated. More work is still needed to prospectively validate the use of I-CARE in practice and the impact of treatment strategies to prevent the occurence of intracranial pressure in patients with severe brain injury.

References: [1] J.Neurosurgery. 2017 Jan 1;80(1):6-15.

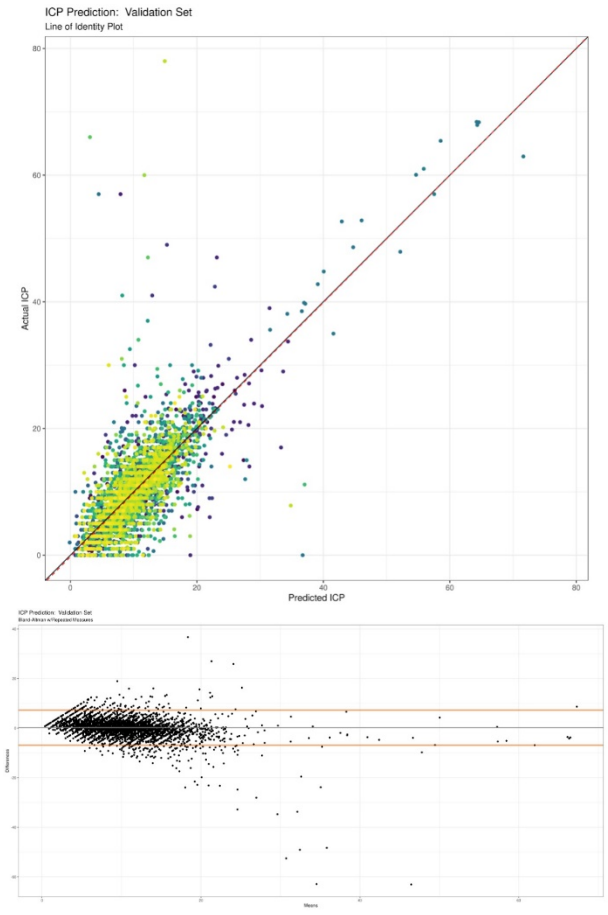

	10% Increase from Baseline	20% Increase from Baseline	30% Increase from Baseline	15 mmHg Hypertension	20 mmHg Hypertension	22 mmHg Hypertension
Accuracy	0.71	0.80	0.86	0.92	0.97	0.98
95% CI	(0.70, 0.72)	(0.79, 0.81)	(0.85, 0.87)	(0.91, 0.92)	(0.97, 0.98)	(0.98, 0.99)
Sensitivity	0.52	0.49	0.51	0.77	0.71	0.67
Specificity	0.77	0.84	0.89	0.93	0.98	0.99
Pos Pred Value	0.42	0.32	0.26	0.53	0.41	0.34
Neg Pred Value	0.83	0.92	0.96	0.98	0.99	0.99
Prevalence	0.25	0.13	0.07	0.09	0.02	0.02
Positive Likelihood Ratio	2.24	3.12	4.52	11.34	34.62	45.99
Negative Likelihood Ratio	0.63	0.61	0.55	0.25	0.29	0.34

Critical Care 23 - Long term outcomes of patients requiring extracorporeal membrane oxygenation (ECMO) for COVID-19: A prospective study

Brendan Mackey[1], Asad Usman[1], Michael Ibrahim[1], Wilson Szeto[1], Marisa Cevasc[1]o, Christian Bermudez[1], Salim Olia[1], Joseph Savino[1], William Vernick[1], Jacob Gutsche[1], Audrey Spelde[1]

University of Pennsylvania[1]

Introduction: Extracorporeal membrane oxygenation (ECMO) is an invasive form of life support associated with long-term physical and psychological impairments[1]. Patients receiving ECMO for COVID-19 have higher incidence of discharge to other care facilities and longer cannulation times than patients requiring ECMO for other indications[2,5]. These findings have been limited to patients receiving veno-venous (VV) ECMO for respiratory failure[2,3,4]. No studies have assessed long-term outcomes for patients with COVID-19 who underwent veno-arterial (VA) ECMO or other support measures such as veno-pulmonary (VP) ECMO.

In this study, we assessed the long-term outcomes of COVID-19 survivors requiring ECMO under various cannulation conditions. Primary objectives include an assessment of functional and cognitive outcomes, burden of anxiety, depression, and post-traumatic stress disorder. Secondary objectives include an examination of outcomes related to cannulation strategies.

Methods: Data was captured from 2 academic medical centers in the same health system. 118 COVID-19 cases were identified with ECMO cannulation dates 3/21/20 to 6/17/22. Overall mortality for patients with COVID-19 treated with ECMO was 39% with increasing survival over the course of the pandemic. Inclusion criteria was met by 64 survivors, of whom 38 (31 male; mean age 45.2 years) were interviewed a mean 373.7 days (range 35-817) post-decannulation.

Standardized instruments administered via telephone included Montreal Cognitive Assessment-Blind (MoCA-Blind), Hospital Anxiety and Depression Scale (HADS), Katz Activities of Daily Living Assessment (Katz ADL) and Lawton Instrumental Activities of Daily Living (Lawton IADL). To assess outcomes by cannulation method, patients were classified as VA ECMO or VP ECMO if they required such at any point during their hospitalization and VV ECMO if they received femoral (fem) -internal jugular (IJ), fem-fem or dual-lumen VV ECMO with no need for VP or VA ECMO.

Results: Patient demographics are listed in Table 1. Study participants received ECMO on average 46.3 days (range 3-168) with 55.3% (21/38) requiring revisions to their cannulation (Fig 1). A 2nd ECMO run was needed in 39.5% (15/38) following decannulation. Nine participants (23.7%) received lung transplantation; 8 participants experienced cardiac arrest (21.1%).

Patients had high incidence of discharge to other care facilities (Table 2). At discharge, 36.8% (14/38) required supplemental oxygen, compared to 15.8% (6/38) at time of interview (all being only as needed). Breathlessness was often described in association with activities (Table 3). Due to their health, 78.9% (30/38) cut back on work with 73.3% (22/30) representing current unemployment (Table 2).

MoCA-Blind assessments revealed normal cognitive function in 68.4% (26/38). Katz ADL assessment found 78.9% (30/38) to be independent in all tasks; Lawton IADL assessment found 52.6% (20/38) to be independent (Table 2). Persistent anxiety was endorsed by 23.7% (9/38) and 21.2% (8/38) indicated significant depressive symptoms (Table 2).

Conclusions: We assessed long-term outcomes of COVID-19 ECMO survivors. Outcomes varied with significant proportion endorsing cognitive or physical impairment impacting ability to work. The majority demonstrated complete independence in most IADLs. Similar outcomes were noted despite cannulation method with exception of improved cognitive function and independence but increased supplemental oxygen use among patients on VP ECMO. Future directions include further investigation of these differences in larger patient populations.

Compared to an assessment of non-COVID VV ECMO survivors published in 2019, we found lower rates of anxiety among COVID ECMO survivors (23.7% (9/38) vs 47.6% (20/42))[1]. Limitations of our study include a small sample size from a single health system. Furthermore, response bias from those who chose or were able to participate in the interview may influence our findings. Application of ECMO for severe COVID offers promise that a significant percentage of patients not only survive but return to an active life. The effect of ECMO on long term physical and cognitive function and its economic impact will guide continued application. Further research is needed to better understand challenges faced by patients receiving ECMO for COVID-19, interventions to improve long term outcomes, and potential benefits and disadvantages of particular cannulation strategies.

References: 1. Long-term outcomes after extracorporeal life support for acute respiratory failure. J Cardiothorac Vasc Anesth. 2019; 33: 72-79.

2. Posthospitalization outcomes after extracorporeal membrane oxygenation (ECMO) for COVID-19. Surgery. 2022.

3. One-year functional, cognitive, and psychological outcomes following the use of extracorporeal membrane oxygenation in coronavirus disease 2019: a prospective study. Crit Care Explor. 2021; 3(9): e0537.

4. Intermediate-term survival and functional outcomes of COVID-19 extracorporeal membrane oxygenation patients. J Card Surg. 2022.

5. ECMO in COVID-19 Patients: A systematic review and meta-analysis. J Cardiothorac Vasc Anesth. 2021.

Table 1. Patient demographics and ECMO cannulation details.

Variable	Non-Survivors (n=44)	Survived to Discharge (n=73)*	Interviewed (n=38)
Age (years) at time of ECMO, mean (range)	47.4 (20-68)	44.5 (19-64)	45.2 (29-64)
Gender			
Male, n (%)	35 (79.5%)	55 (75.3%)	31 (81.6%)
BMI, mean (range)	32.4 (25.6-46.4)	31.9 (20.3-56.8)	31.4 (23.8-56.8)
Mortality status as of June 2022, n (%)	44 (100%)	2 (2.7%)	-
Comorbidities			
Asthma, n (%)	7 (15.9%)	18 (24.7%)	9 (23.7%)
Diabetes, n (%)	8 (18.1%)	12 (16.4%)	6 (15.7%)
Hyperlipidemia, n (%)	9 (20.5%)	15 (20.5%)	10 (26.3%)
Hypertension, n (%)	14 (31.8%)	21 (28.7%)	13 (34.2%)
Sleep apnea, n (%)	5 (11.4%)	6 (8.2%)	4 (10.5%)
Race			
Asian, n (%)	6 (13.6%)	7 (9.6%)	5 (13.2%)
Black or African American, n (%)	6 (13.6%)	12 (16.4%)	4 (10.5%)
Native Hawaiian/Pacific Islander, n (%)	-	1 (1.4%)	1 (2.6%)
White, n (%)	15 (34.1%)	20 (27.4%)	14 (36.8%)
Unknown/Not Reported, n (%)	17 (38.6%)	33 (45.2%)	14 (36.8%)
Ethnicity			
Hispanic or Latino, n (%)	6 (13.6%)	7 (9.6%)	1 (2.6%)
Not Hispanic or Latino, n (%)	32 (72.7%)	56 (76.7%)	32 (84.2%)
Unknown/Not Reported, n (%)	6 (13.6%)	10 (13.7%)	5 (13.2%)
Avg length of hospitalization, days (range)	70.9 (3-218)	95.4 (21-279)	100.6 (24-279)
Avg length of ECMO, days (range)	54.7 (1-201)	40.5 (1-168)	46.3 (3-168)
Initial cannulation method			
VA ECMO, n (%)	6 (13.6%)	9 (12.3%)	5 (13.2%)
VV ECMO (Fem-IJ), n (%)	34 (77.3%)	58 (79.5%)	30 (78.9%)
VV ECMO (Fem-Fem), n (%)	2 (4.5%)	1 (1.4%)	1 (2.6%)
VV ECMO (Dual-lumen)**, n (%)	1 (2.3%)	5 (6.8%)	2 (5.2%)
VP ECMO, n (%)	1 (2.3%)	-	-
Patients requiring reconfiguration, n (%)	28 (63.6%)	36 (49.3%)	21 (55.3%)
Patients requiring ≥ 2 ECMO runs, n (%)	2 (4.5%)	22 (30.1%)	15 (39.5%)
Experienced cardiac arrest, n (%)	11 (25%)	11 (15.1%)	8 (21.1%)
Received lung transplant, n (%)	3 (6.8%)	15 (20.5%)	9 (23.7%)

*1 patient still hospitalized at time of interviews (not included in this analysis).
** Dual-lumen VV ECMO refers to use of a dual-lumen, bicaval cannula.

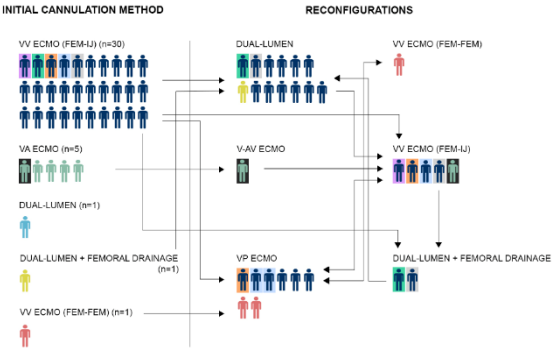

Figure 1: Initial cannulation methods and reconfigurations. Revisions to cannulation strategy were made in 21 of 38 (55.3%) interviewed patients. These patients were revised to dual-lumen bicaval (13/21, 61.9%), VV ECMO (fem-IJ) (5/21, 23.8%), VP ECMO (6/21, 28.6%), dual-lumen bicaval with femoral drainage (2/21, 9.5%), VV ECMO (femoral-femoral) (1/21, 4.8%) and V-AV ECMO (1/21, 4.8%).

Table 2. Summarization of outcome metrics stratified by cannulation strategy.

Variable	VA ECMO (n=5)	VV ECMO (n=27)	VP ECMO (n=6)	Total (n=38)
Normal cognitive function (MoCA-Blind), n (%)	2 (40%)	18 (66.7%)	6 (100%)	26 (68.4%)
Full independence (Katz scale), n (%)	3 (60%)	21 (77.8%)	6 (100%)	30 (78.9%)
Full independence (Lawton scale), n (%)	2 (40%)	13 (48.1%)	5 (83.3%)	20 (52.6%)
Anxiety of clinical significance, n (%)	3 (60%)	5 (18.5%)	1 (16.6%)	9 (23.7%)
Depression of clinical significance, n (%)	3 (60%)	5 (18.5%)	-	8 (21.2%)
Supplemental O2 at time of discharge, n (%)	-	9 (33.3%)	5 (83.3%)	14 (36.8%)
Supplemental O2 at time of interview, n (%)	-	4 (14.8%)	2 (33.3%)	6 (15.8%)
Disposition post-discharge				
Acute rehabilitation center, n (%)	3 (60%)	20 (74.1%)	3 (50%)	26 (68.4%)
Long-term acute care hospital, n (%)	1 (20%)	4 (14.8%)	2 (33.3%)	7 (18.4%)
Home, n (%)	1 (20%)	2 (7.4%)	1 (16.7%)	4 (10.5%)
Skilled nursing facility, n (%)	-	1 (3.7%)	-	1 (2.6%)
Rehospitalized, n (%)	1 (20%)	10 (37%)	1 (16.7%)	12 (31.6%)
Employment status				
Unemployed, n (%)	2 (40%)	16 (59.3%)	4 (66.7%)	22 (57.9%)
Employed full time, n (%)	1 (20%)	8 (29.6%)	2 (33.3%)	11 (28.9%)
Employed part time, n (%)	2 (40%)	3 (11.1%)	-	5 (13.1%)
If employed, switched job due to health, n (%)	3 (100%)	5 (45.5%)	-	8 (50%)

Table 3. Survey responses related to NYHA functional classification and MRC assessments of breathlessness.

Patient Responses	VA ECMO (n=5)	VV ECMO (n=27)	VP ECMO (n=6)	Total (n=38)
NYHA Functional Classification				
I can perform all physical activities without getting short of breath, tired, or having palpitations, n (%)	-	3 (11.1%)	-	3 (7.9%)
I get short of breath or tired, or have palpitations when performing more strenuous activities. For example, walking on steep inclines or walking up several flights of steps, n (%)	2 (40%)	19 (70.4%)	5 (83.3%)	26 (68.4%)
I get short of breath or tired, or have palpitations when performing day to day activities. For example, walking on flat ground, n (%)	-	5 (18.5%)	1 (16.7%)	6 (15.8%)
I feel breathless at rest, and am mostly housebound. I am unable to carry out any physical activity without getting short of breath or tired, or having palpitations, n (%)	3 (60%)	-	-	3 (7.9%)
MRC Breathlessness Scale				
I don't have any trouble with breathlessness, n (%)	-	1 (3.7%)	-	1 (2.6%)
I don't have trouble with breathlessness except on strenuous exercise, n (%)	2 (40%)	11 (40.7%)	4 (66.7%)	17 (44.7%)
I get short of breath when I hurry on flat ground or when I walk up a slight hill, n (%)	-	9 (33.3%)	-	9 (23.7%)
I walk more slowly than most people on flat ground, and I have trouble walking more than a mile or for more than 15 minutes at a time, n (%)	2 (40%)	5 (18.5%)	1 (16.7%)	8 (21.2%)
I have to stop for breath after walking about 100 yards (the length of a football field) or after walking for a few minutes on flat ground, n (%)	-	1 (3.7%)	1 (16.7%)	2 (5.3%)
I get breathless when I dress or undress, or I am often too breathless to leave the house, n (%)	1 (20%)	-	-	1 (2.6%)

Critical Care 24 - Outcomes in ARDS in Patients Hospitalized with CAP

Yousef Ahmed[1], Akash Patel[2], George Kasotakis[1], Charles Trujillo[1], Vijay Krishnamoorthy[3], Karthik Raghunathan[4], Tetsu Ohnuma[3]

Duke University Hospital[1] Duke University School of Medicine[2] Duke University[3] Duke University Medical Center[4]

Introduction: Acute respiratory distress syndrome (ARDS) can occur in critically ill patients with severe community acquired pneumonia (CAP). However, there is little evidence regarding outcomes in ARDS among patients with CAP. Therefore, the objective of this study is to identify outcomes in ARDS in patients with CAP. Understanding outcomes in patients with severe CAP complicated by ARDS can potentially improve the prognosis in patients with CAP.

Methods: Using the Premier Healthcare Database (PHD), we retrieved patients admitted between January 2016 and March 2020 who had a principal diagnosis of pneumonia or a secondary diagnosis of pneumonia paired with a principal diagnosis of respiratory failure or sepsis. Inclusion criteria included age ³18, presence of chest imaging, and mechanical ventilation and antimicrobial treatment within two days of admission. ICD-10-CM diagnosis codes were utilized to identify patients who developed ARDS. The primary outcome was in-hospital mortality, comparing cohort patients who did and did not develop ARDS. Secondary outcomes included length of stay, mechanical ventilation days, and days in the ICU.

Results: Hospitalized patients with CAP who developed ARDS (n=1924, 2.7%) had higher mortality rates (n=648, 33.7%) than those that did not (n=13253, 18.9%; OR, 2.40; 95% CI, 2.16-2.66; *p*<.0001). The Kaplan–Meier statistic showed that the survival probability at 30 day of hospitalization was higher for patients without ARDS compared to those with ARDS (logrank test: p-value <0.0001). Patients with ARDS also had longer mean ± SD length of stay (15.8 ± 13.1), mechanical ventilation days (11.1 ± 10.3), and days in the ICU (11.5 ± 9.6) than patients who did not have ARDS (12.4 ± 12.7, 7.0 ± 9.1, 7.2 ± 7.1, respectively).

Conclusions: When compared to hospitalized patients with CAP and without ARDS, those with ARDS had higher mortality rates, longer hospitalizations, more days in the ICU, and more days on mechanical ventilation.

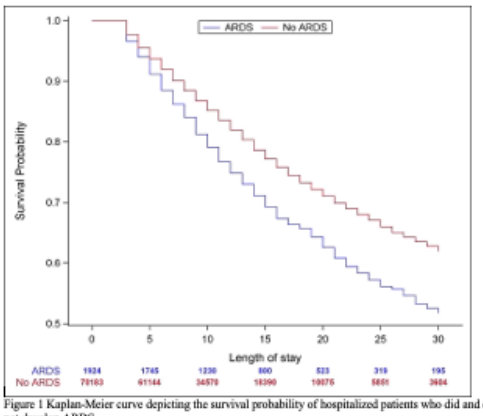

Figure 1 Kaplan-Meier curve depicting the survival probability of hospitalized patients who did and did not develop ARDS.

Critical Care 25- Risk Factors for ARDS in Patients Hospitalized with CAP

Akash Patel[1], George Kasotakis[1], Yousef Ahmed[2], Charles Trujillo[1], Vijay Krishnamoorthy[3], Karthik Raghunathan[4], Tetsu Ohnuma[3]

Duke University School of Medicine[1] Duke University Hospital[2] Duke University[3] Duke University Medical Center[4]

Introduction: Acute respiratory distress syndrome (ARDS) can occur in critically ill patients with severe community acquired pneumonia (CAP). Understanding risk factors for the development of ARDS can help us address them, potentially reducing the incidence of ARDS in patients with CAP. However, there is little evidence regarding ARDS risk factors among patients with CAP. Therefore, the objective of this study is to identify these predictors of ARDS in patients with CAP.

Methods: Using the Premier Healthcare Database (PHD), we retrieved patients admitted between January 2016 and March 2020 who had a principal diagnosis of pneumonia or a secondary diagnosis of pneumonia paired with a principal diagnosis of respiratory failure or sepsis. Inclusion criteria included age ³18, presence of chest imaging, and mechanical ventilation and antimicrobial treatment within two days of admission. ICD-10-CM diagnosis codes were utilized to identify patients who developed ARDS. Using a multilevel logistic regression model, we estimated the odd ratios for developing ARDS given various risk factors (demographics, baseline comorbidities, hospital characteristics, and management).

Results: Of the 72107 patients who met inclusion criteria, 70183 (97.3%) patients (male = 36448, 51.9%; White = 51397, 73.2%; mean ± SD age = 65.1 ± 14.4; Medicare = 46851, 66.8%) did not have ARDS and 1924 (2.7%) patients (male = 961, 49.9%; White = 1416, 73.6%; mean ± SD age = 57.3 ± 15.3; Medicare = 927, 48.2%) did have ARDS. Several factors were associated with a lower incidence of ARDS. These included age 50-59 (OR, 0.60; 95% CI, 0.52-0.70; p<0.0001), age 60-69 (OR, 0.46; 95% CI, 0.39-0.53; p<0.0001), age 70-79 (OR, 0.33; 95% CI, 0.28-0.40; p<0.0001), age ³ 80 (OR, 0.21; 95% CI, 0.17-0.26; p<0.0001), male sex (OR, 0.88; 95% CI, 0.70-0.93; p=0.010), Black race (OR, 0.81; 95% CI, 0.70-0.93; p=0.003), congestive heart failure (OR, 0.84; 95% CI, 0.75-0.95; p=0.005), paralysis (OR, 0.42; 95% CI, 0.32-0.56; p<0.0001), other neurological disorders (OR, 0.69; 95% CI, 0.59-0.81; p<0.0001), chronic pulmonary disease (OR, 0.60; 95% CI, 0.54-0.67; p<0.0001), and renal failure (OR, 0.73; 95% CI, 0.63-0.85; p<0.0001). Several factors were associated with a higher incidence of ARDS. These included arthritis (OR, 1.33; 95% CI, 1.06-1.67; p=0.014), coagulopathy (OR, 1.27; 95% CI, 1.11-1.45; p=0.001), fluid and electrolyte disorders (OR, 1.12; 95% CI, 1.01-1.25; p=0.035), and vasopressor use within two days of admission (OR, 1.58; 95% CI, 1.43-1.74; p<0.0001).

Conclusions: Old age, male sex, Black race, congestive heart failure, paralysis, other neurological factors, chronic pulmonary disease, and renal failure were associated with lower ARDS development in mechanically ventilated patients with pneumonia. However, arthritis, coagulopathies, fluid and electrolyte disorders, and early vasopressor utilization were associated with higher likelihood of ARDS development in these patients.

Critical Care 26- The Effect of Incentive Spirometry Use on Reducing Postoperative Pulmonary Complications in Intensive Care Unit Patients

Blair Costin[1], Stephanie Lumpkin[1], Seth Dever[1], Tasce Bongiovanni[2], Samantha Kaplan[1], Tetsu Ohnuma[1], Vijay Krishnamoorthy[1], Karthik Raghunathan[3], Jennifer Freeman[3], Krista Haines[3]

Duke University[1] UCSF[2] Duke University Medical Center[3]

Introduction: Following surgery, patients are at risk of experiencing adverse events known as postoperative pulmonary complications (PPCs) [1, 2]. These PPCs are broadly defined as respiratory tract infections, atelectasis and pneumonia (defined by chest x-ray), need for bronchoscopy, aspiration pneumonitis, and respiratory failure requiring invasive or non-invasive mechanical ventilation [2]. Such PPCs are a leading cause of mortality following high-risk surgeries [3]. Currently, incentive spirometry (IS), which targets (maximal) inspiratory lung volumes through the recording and visual feedback of successful breathing maneuvers, is used in the Duke University Surgical and Cardiac Intensive Care Units (SICU and CTICU) to aid in preventing PPCs [4]. Despite IS use, the overall effectiveness of IS in preventing PPCs remains unclear. Additionally, a defined protocol does not exist for IS use in the Duke SICU and CTICU. To determine the effectiveness of IS usage following high-risk surgery and the best protocol for IS usage, we will perform a meta-analysis utilizing the Grading of Recommendations, Assessment, Development and Evaluation protocol (GRADE). The overall objective of this study was to determine whether IS for adult patients undergoing high-risk surgery significantly reduces PPCs when compared to other rehabilitation strategies.

Methods: The literature was searched using MEDLINE via PubMed, Embase via Elsevier, CINAHL via Ebsco, and Scopus via Elsevier. For studies to be included, patients had to have abdominal, thoracic, urgent, head and neck, neurosurgery or cardiac surgery requiring ICU level of care, the surgery must be >2 hours, blood loss > 500 ml and the patient extubated within 24 hours after surgery. Patients were excluded if they underwent bariatric, urologic, extremity, gynecologic surgery; surgery lasting < 2 hours, if they were ASA 1s; received neuroaxial or regional anesthesia; or patients were engaged in pulmonary rehab exercises prior to therapy.

Results: Twenty-seven studies involving adults undergoing cardiac, thoracic, neurosurgery or abdominal surgery were originally included. For critically ill patients, 88% of studies were done in the cardiac surgical population, 4% in thoracic surgery patients, 4% in patients undergoing abdominal surgery, and 4% undergoing neurosurgery. The decision was made to focus on the cardiac surgery population and twenty-four RCTs were ultimately included. Of those studies included, 42% of studies showed IS improved patient recovery and prevented PPCs following cardiac surgery. 25% of studies showed non inferior effect of IS when compared to other methods on patient recovery following cardiac surgery. 33% of studies suggest IS may be inferior to other methods of pulmonary toilet following cardiac surgery. The IS protocols used in each study type were evaluated. In half of the studies showing IS improved patient recovery following cardiac surgery, IS was used hourly while the patient was awake. The most consistently documented IS use protocol in the studies showing IS was effective recommended IS use 3x every waking hour. Each time the patient took 5 breaths. In the additional studies, the protocol for IS use varied from every 2 to 3 waking hours verses 1x per day. In the studies indicating IS may be inferior to other methods, only 2 studies indicated that IS was used hourly in patients.

Conclusions: Very few studies on incentive spirometry are done in critically ill adults. The majority of studies completed on critically ill adults have been in patients following cardiac surgery. The majority of studies show that IS either improved patient recovery following cardiac surgery or showed a non-inferior effect when compared to other methods. The use of the IS and evaluation of its use must be expanded to trauma and acute care surgery populations. Based on these findings I would recommend the use of IS hourly with 3 sets of 5 repetitions in critically ill patients.

References: 1. High versus low positive end-expiratory pressure during general anesthesia for open abdominal surgery (PROVHILO trial): a multicenter randomized controlled trial. Lancet. 2014;384:495–503.

2. Postoperative pulmonary complications. Br J Anesthesia. 2017;118: 317–34.

3. Volume rather than flow incentive spirometry is effective in improving chest wall expansion and abdominal displacement using optoelectronic plethysmography. Respir Care. 2013;58(8): 1360–6. 5 Patel 3. RL, Townsend ER, Fountain SW. Elective pneumonectomy: factors associated with morbidity and operative mortality. Ann Thoracic Surg. 1992;54:84–8.

4. Respiratory maneuvers to prevent postoperative pulmonary complications: a critical review. JAMA. 1973;224:1017–21.

Critical Care 27- Tissue-Protective and Immunomodulatory Functions Of Mature B Cells In A Murine Model Of Hyperoxic Lung Injury

Dusan Hanidziar[1], Simon Robson[2], Liam Dwyer[2], Eva Csizmadia[2], Sylvia Ranjeva[2], Saumya Maheshwari[2], Nina Farhat[3], Leo Otterbei[3], Ruxandra Sirbulescu[3], Mark Poznansky[3]

Massachusetts General Hospital[1] BIDMC: Beth Israel Deaconess Medical Center[2] Middlebury College[3]

Introduction: There is a continued need to develop treatments for acute respiratory distress syndrome (ARDS). Novel cellular immune therapies represent one potential strategy. Recent studies have identified B cells as powerful regulators of inflammation, tissue injury, and repair (1-4). We hypothesized that these functions of B cells could be harnessed therapeutically and have explored the effects of systemic B cell therapy in a mouse model of hyperoxic acute lung injury.

Methods: Acute lung injury was modelled in adult (9–12-week-old) C57BL/6 male mice through continuous exposure to hyperoxia (FiO_2 >92%), as we have described previously (5). Mature naive CD45R+/CD19+ B cells for intravenous administration were isolated from spleens of C57BL/6 mice using negative immunomagnetic selection as we have reported previously (1). B cell suspensions (10 x 10^6 B cells in phosphate-buffered saline), or saline alone, were administered intravenously at 24 hours of hyperoxia. Hyperoxic exposure then continued until day 4, when experiments were terminated. The effects of B cells on lung tissue were examined using hematoxylin and eosin staining and immunohistochemistry. Lung injury scores ranging from 0 (normal lung) to 4 (most severe injury) were assigned to each of the 3 evaluated lung lobes and an average score for each mouse was determined. Physiologic variables (heart rate, respiratory rate, SpO_2) were recorded daily for 5 minutes in room air using MouseOx Plus system (STARR Life Sciences, Oakmont, PA). Immune cell composition of the lungs and blood was analyzed with flow cytometry using antibody staining for 28 cell surface and intracellular markers. Exogenous B cells were distinguished by their expression of CD45.1. For normal, parametrically distributed data, differences among experimental groups were analyzed using unpaired Student's t test (for single comparisons) or one-way ANOVA followed by Tukey's test for multiple comparisons. Data that were not normally distributed (e.g., pathology scores) were assessed using nonparametric tests, including the Mann Whitney U for group differences or Spearman's rank correlation. All reported descriptive statistics are estimated marginal means ± standard error of the mean (SEM). P values < 0.05 were considered statistically significant. All experiments received approval from the Institutional Animal Care and Use Committee (IACUC).

Results: Hyperoxic exposure of control mice (n=16) resulted in severe lung injury by day 4, characterized by diffuse alveolar damage, cellular infiltration, and vascular congestion. Lung injury scores and cellular infiltration were significantly reduced in B cell recipients (n=18) (Fig 1). The analysis of oxygenation (SpO_2) recordings revealed that hypoxemic events (SpO_2 <88%) by day 3 were less severe in B cell treated mice, characterized by shorter duration of oxygen desaturations and higher SpO_2 values (Fig 2). We found that hyperoxic injury led to profound depletion of pulmonary B220+ B cells in control mice, while B cell numbers were partially restored in B cell recipients (Fig 3). Mechanistically, B cell therapy attenuated an array of inflammatory responses when analyzed on day 3 of hyperoxic exposure. B cells significantly decreased neutrophil accumulation in the lungs (Fig 4A) and also significantly suppressed production of pro-inflammatory IL-17 in alveolar macrophages (Fig 4B), classical monocytes, and neutrophils. Furthermore, B cell therapy mitigated against the depletion of pulmonary B cells (Fig 4C) and NK cells (Fig 4D) that occured in control mice. While B cell therapy had significant impact on host immune responses, exogenous B cells represented less than 1.5% of B cells in the lungs and in the blood on day 3 of hyperoxic injury (i.e., 48 hours after B cell administration).

Conclusions: Our data indicate that exogenously applied mature B cells ameliorate specific elements of tissue damage and limit acute inflammatory responses during hyperoxic lung injury. B cell therapy promoted immune homeostasis in the lungs by suppressing neutrophil increments, while also mitigating against B cell and NK cell depletion. Further mechanistic studies are required to support the use of novel B cell- based therapies in ARDS.

References: 1. FASEB J 2021;35(8):e21744.

2. FASEB J 2021;35(12):e22019.

3. Elife 2022;11:e78291.

4. J Exp Med 2021;218(9):e20210409.

5. Sci Rep 2020;10(1):4677.

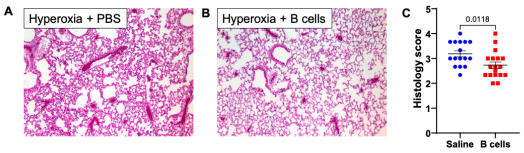

Figure 1. Effect of B cell therapy on hyperoxic lung injury. **A)** Hyperoxic lung injury in control mice, day 4 of hyperoxia exposure, representative image, H&E staining **B)** Hyperoxic lung injury in B cell treated mice, day 4 of hyperoxia exposure, representative image **C)** Lung injury score is significantly reduced in B cell recipients. Injury scores lower than 3 were present in 61.1% (11/18) B cell recipients as compared to 25% (4/16) PBS-treated mice.

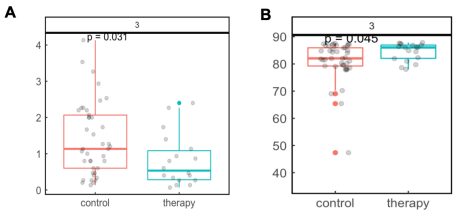

Figure 2. Effect of B cell therapy on oxygenation (SpO_2) in mice with acute lung injury. A) Duration of desaturation events on day 3 of hyperoxic injury for PBS treated (control) mice and B cell treated mice (p =0.031) **B)** Depth of desaturations on day 3 of hyperoxic injury for PBS treated (control) mice and B cell treated mice (p=0.045)

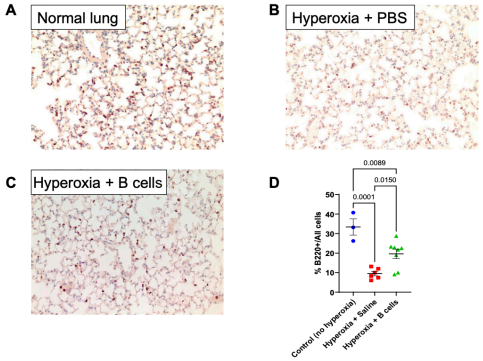

Figure 3. B cell population in the lungs. A) Normal lung parenchyma (B220 immunohistochemistry) **B)** Hyperoxic lung injury in control mice, day 4 of hyperoxia exposure, representative image **C)** Hyperoxic lung injury in B cell treated mice, day 4 of hyperoxia exposure, representative image **D)** Comparison of B cell proportions in the lungs

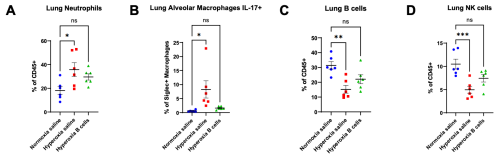

Figure 4. Effect of B cell therapy on host inflammatory responses. Flow cytometry analysis of immune cell populations in the lungs from three conditions: normoxia (n=6), hyperoxia (n=6), and hyperoxia + B cell therapy (n=6). **A)** Proportion of neutrophils among all CD45+ immune cells in three tested conditions **B)** IL-17 production by alveolar macrophages in three tested conditions **C)** Proportion of B cells among all CD45+ immune cells in three tested conditions **D)** Proportion of NK cells among all CD45+ immune cells in three tested conditions

Critical Care 28- Ultrasound during cardiac arrest – the cause for pause

Akiva Leibowitz[1], Ameeka Pannu[1], Achikam Oren-Grinberg[1], Somnath Bose[1], Ariel Mueller[2], Eric Tesoriero[3], Michael Donnino[3], Todd Sarge[4]

Beth Israel Deaconess Medical Center, Harvard Medical School[1] Massachusetts General Hospital[2] St Luke's University Health Network[3] Beth Israel Deaconess Med Ctr[4]

Introduction: There has been an increasing interest in the use of point-of-care ultrasound (POCUS) and echocardiography as a diagnostic aid during cardiac arrest with, different protocols, suggesting the incorporation of ultrasound into the ACLS protocol[1]. POCUS, specifically echo appears to be a feasible and intuitive option in assisting in early and rapid diagnosis of reversible causes of pulseless electric activity (PEA) arrests. However, concerns remain that the use of ultrasound during cardiac arrest may interfere with high-quality chest compressions, that are correlated with outcome[2,3] ; thus, ultrasound has remained excluded from the American Heart Association ACLS guidelines[4]. In this study – we aimed to assess and quantify the effect of incorporating focused ultrasound into the CPR algorithm, specifically the effect on the number and duration of pauses, and to evaluate the compliance with AHA guidelines for cardiac arrest. We hypothesized that incorporation of echocardiography into the ACLS algorithm by ultrasound trained critical care anesthesiologists would not affect the duration of pauses during CPR.

Methods: This is a prospective observational cohort study of 40 inpatients who experienced cardiac arrest between January 2016 and April 2018 in a tertiary academic medical center. We included all instances of CPR in inpatients, during weekday daytime shifts, with non-shockable rhythm at any time during cardiac arrest. Data was analyzed by interrogating the software on the Lifepack defibrillator (Stryker, Kalamazoo MI). Data including timestamps, rhythm and presence or absence of ultrasound was further corroborated by an independent observer. The cohort was separated into 2 groups:

1. Focused Cardiac Ultrasound incorporated into ACLS algorithm.

2. No Focused Cardiac Ultrasound throughout the resuscitation period

Primary outcome was the average duration of pauses in CPR during the "code" event. Descriptive statistics of the data are presented as median (interquartile range) or proportions and frequencies depending on variable type and distribution. Normality of continuous variables was assessed with the Shapiro Wilk test. In order to assess whether ultrasound changed the length of CPR interruptions, each interruption was coded as using ultrasound or not. We then assessed differences between interruptions with and without ultrasound using a non-parametric test. SAS 9.4 (SAS Institute Inc., Cary NC) was used for all analyses with two-sided p-values < 0.05 considered statistically significant.

Results: 40 patients were included in the study. Average age was 73 years (60.5, 82.0); 18 of the patients (45%) were female. Locations of the cardiac arrest were: Hospital Floor – 18 (45%), ICU – 18 (45%) and Procedural area - 4 (10%). Initial rhythm identified was: Asystole – 6 (15%), PEA – 25 (62%), V-fib – 5 (12.5%), V-tach – 4 (10%), Unknown – 2 (5%). Average code length was 20.5 (10.0, 28.0) minutes. Mortality was 53%. Throughout the study – a total of 364 interruptions in CPR were captured. We excluded 109 pauses with a duration of less than 4 seconds, which were due to either switching compressors or artifact, and 16 pauses of greater than 60 seconds. In 22 (55%) of the codes – ultrasound was used. The number of pauses greater than 10 seconds was 111 (45.7%). The number of interruptions in the ultrasound group was significantly smaller than the no-ultrasound group (30 vs. 81, $p<0.001$). The interruption length was significantly longer in the ultrasound group – 18 seconds (10.5, 26.5) vs. 9 seconds (6.0, 14.0) , $P<0.001$).

Conclusions: In our study, we find that the duration of pauses during PEA arrests, when ultrasound is incorporated by clinicians with expertise in critical care ultrasound – exceeds that of recommended duration by AHA. This is the first study to quantitatively assess the effect of ultrasound on the quality of CPR outside of the ED. These findings are consistent with results recently described in the ED[2,3]. With the widespread acceptance of ultrasound in the management of critically ill patients, it is imperative to adhere to clinically accepted guidelines. While incorporation of ultrasound into the ACLS algorithm harbors the potential benefit of identifying reversible causes of PEA arrest, clinicians must avoid offsetting those gains with violation of validated protocols. We find that ultrasound may be a useful tool during CPR, but clinicians must be trained on its proper application, within the allocated 10s pauses suggested by AHA.

References:

1. Focused echocardiographic evaluation in life support and peri-resuscitation of emergency patients: a prospective trial." Resuscitation vol. 81,11 (2010): 1527-33.

2. Ultrasound use during cardiopulmonary resuscitation is associated with delays in chest compressions." Resuscitation vol. 119 (2017): 95-98.
3. Association of ultrasound-related interruption during cardiopulmonary resuscitation with adult cardiac arrest outcomes: A video-reviewed retrospective study." Resuscitation vol. 149 (2020): 74-80.
4. Adult Advanced Life Support: 2020 International Consensus on Cardiopulmonary Resuscitation and Emergency Cardiovascular Care Science With Treatment Recommendations." Circulation vol. 142,16_suppl_1 (2020).

Table 1. Baseline and Patient Characteristics

	Unique Patients *N = 40*
Demographics	
Female gender	18 (45.00)
Age, *years*	73.0 (60.5, 82.0)
Weight, *kg*	85.5 (63.5, 98.9)
Height, *cm*	169.5 (162.6, 176.5)
Body Mass Index	28.4 (22.1, 33.2)
Location of Arrest	
Hospital Floor / Ward	18 (45.00)
Hospital ICU	18 (45.00)
Procedural Area (ex. IR/WPC)	4 (10.00)
Initial rhythm	
Asysole	6 (15.00)
PEA	25 (62.50)
Vfib	5 (12.50)
Vtach	4 (10.00)
Unknown	2 (5.00)
Patient Outcome	
Died at end of code	21 (52.50)
In Hospital Mortality	

Data is presented as n (%) or median (quartile 1, quartile 3) depending on type.

Table 2. Code Characteristics

	Unique Patients *N = 40*
Code Length, *minutes*	20.5 (10.0, 28.0)
Code Length Recorded, *minutes*	16.0 (7.0, 23.0)
Ultrasound use at code	22 (55.00)
Ultrasound performed by trained sonographer	13 (59.09)
Number of Interruptions	8.0 (5.0, 13.0)
CPR Ratio (%)	28.0 (21.0, 37.0)
Compressions Ratio (%)	69.5 (33.5, 84.0)
Compression Rate	132.0 (129.0, 135.5)
Compressions Per Minute	39.0 (29.0, 49.0)

Data is presented as n (%) or median (quartile 1, quartile 3) depending on type.

Table 3. CPR Interruption Characteristics

	CPR Interruptions *N = 243*	**P- Value**
Interruption Reason		
Pulse Check	178 (73.25)	---
Ultrasound	40 (16.46)	---
Compressor Change	112 (46.09)	---
Intubation	4 (1.65)	---
Defibrillation	37 (15.23)	---
Other Reason	8 (3.29)	---
Interruptions Greater than Ten Seconds	111 (45.68)	---
No Ultrasound	81 (39.90)	<0.0001
Ultrasound	30 (75.00)	
Interruption Length	10.0 (6.0, 17.0)	---
No Ultrasound *(N = 203)*	9.0 (6.0, 14.0)	<0.0001
Ultrasound	18.0 (10.5, 26.5)	
Ultrasound Only *(N = 13)*	17.0 (9.0, 21.0)	0.27
Ultrasound Performed Simultaneously With An Additional Procedure* *(N = 27)*	18.0 (11.0, 28.0)	

Data is presented as n (%) or median (quartile 1, quartile 3) depending on type.

**Additional procedures includes compressor changes, defibrillation, intubation or pauses for other reasons.*

Economics, Education and Policy

Economics, Education and Policy 1

- Costs and independent predictors of intraoperative opioids product waste: a hospital registry study

Simone Redaelli[1], Aiman Suleiman[1], Sarah Ashrafian[2], Dario von Wedel[1], Ricardo Munoz-Acuna[2], Mitra Khany[3], Catriona Stewart[3], Nikolai Ratajczak[4], John Hertig[5], Guanqing Chen[5], Sarah Nabel[5], Maximilian Schaefer[6], Satya Krishna[6] Ramachandran[7]

Beth Israel Deaconess Medical Center, Harvard Medical School[1] Beth Israel Deaconess Medical Center[2] BIDMC[3] Beth Israel Deaconess Medical Centre[4] Butler University[5] Beth Israel Deaconess Medical Center & Hospital[6] Harvard Medical School[7]

Introduction: Adequate disposal of controlled substances is associated with substantial costs, related to both the waste of pharmaceutical products and the time of skilled labor needed to report the waste [1]. Optimizing product size and identifying factors contributing to product waste can reduce the associated financial burden on patients and healthcare-systems. In this study, we aimed to estimate costs and identify the predictors of intraoperative opioids waste.

Methods: This retrospective study included 170,607 adult patients who underwent general anesthesia at an academic tertiary healthcare center in Massachusetts, USA, between 2010 and 2020 and received intraoperative fentanyl, hydromorphone or morphine. Patients who had an American Society of Anesthesiology physical status >4, underwent cardiac procedures or were kept intubated after surgery were excluded. For each patient, we predicted the hypothetical product waste that would have occurred with ready-to-be-administered (RTA) syringes of 50 and 100 mcg for fentanyl; 0.2, 0.5, 1, and 2 mg for hydromorphone; and 2 and 4 mg for morphine, based on the actual administered amount of opioids. We further calculated costs associated with product waste, defined as the sum of the cost of the wasted syringe and the cost of skilled labor needed to discard the product. Provider time needed to document and dispose of the remaining product was estimated to be 76.22 seconds [1], while cost of provider time was calculated using median hourly wage for nurse anesthetists [2]. Average wholesale prices in the USA were used for the RTA syringes [3]. To identify the predictors of product waste, we defined occurrence of product waste as discrepancy between the actual dose administered and an aliquot (or the combination of multiple available aliquots) of 50 mcg for fentanyl, 1 mg of hydromorphone and 4 mg for morphine. Dominance analysis was performed to determine the relative importance of the factors shown to independently predict product waste.

Results: Out of 170,607 included patients, 148,806 (87.2%) patients received at least one dose of intraoperative fentanyl, while 81,786 (47.9%) and 10,693 (6.3%) patients received at least one dose of hydromorphone or morphine, respectively. The lowest amount of product waste, as well as the lowest costs associated with product waste were observed for the minimum RTA syringe sizes for each opioid (**Table 1**). Estimated waste-associated cost per year (based on median 17,076 annual cases) ranged between $ 513 (morphine RTA 2mg) and $ 52,997 (hydromorphone RTA 2mg). The waste of a 100 mcg RTA fentanyl syringe leads to an estimated increase of 5.3 times in waste-associated costs, when compared to 50 mcg syringes. Similarly, waste of hydromorphone syringes sized 0.5 mg, 1 mg, 2 mg, would cause additional, estimated costs of 5.8, 6.5, and 9.4 times, respectively, when compared to hydromorphone 0.2 mg. For morphine, waste-associated costs were estimated to be 1.6 times higher with RTA syringes of 4 mg compared to morphine 2 mg (**Table 1**). In the prediction model of intraoperative opioid waste using the complete-case method (N=139,374), opioid waste occurred in 90,155 (64.7%) cases. Among the potential predictors tested, age, clinical referral, intraoperative administration of esmolol, remifentanil, vasopressors, use of analgesic adjuvants as ketamine, lidocaine and dexmedetomidine, total fluids administered, and use of more than one opioids during anesthesia were associated with an increased risk of waste (**Figure 1**). Dominance analysis of individual predictors showed that administration of more than one different opioid intraoperatively had the strongest dominance, as determined by its contribution to waste prediction (aOR 7.64 [7.40-7.89], p-value <0.001; ranking 1, pseudo-R2=0.0654; **Figure 1**).

Conclusions: Smallest RTA syringe sizes are associated with the lowest cost associated with product waste, and larger sizes were associated with an estimated increase of waste-associated costs by up to 9-fold. Opioid waste is further minimized when choosing only one single intraoperative opioid.

References:

1. A Continuous Observation Workflow Time Study to Assess Intravenous Push Waste. Hosp Pharm. 2021 Oct;56(5):584-591.
2. U.S. Bureau of Labor Statistics. https://www.bls.gov/oes/current/oes_nat.htm, Accessed Dec 7, 2022
3. Lexicomp Online. Lexi-Drugs Online. UpToDate Inc. Accessed Dec 7, 2022

	Fentanyl RTA Syringe Sizes		Hydromorphone RTA Syringe Sizes				Morphine RTA Syringe Sizes	
	50 mcg	100 mcg	0.2 mg	0.5 mg	1 mg	2 mg	2 mg	4 mg
Cases with product waste, n (% of total cases)	13,868 (9.3)	68,668 (46.1)	8,688 (11)	47,346 (58)	52,052 (63.6)	71,742 (87.7)	3,038 (28.4)	7,782 (72.8)
Product waste amount, median (IQR)*	25 (25-25)	50 (50-50)	0.1 (0.1-0.15)	0.2 (0.1-0.4)	0.5 (0.4-0.6)	1.2 (1-1.5)	1 (1-1)	2 (2-2)
Number of used syringes per case, median (IQR)	2 (2-4)	1 (1-2)	5 (3-6)	2 (2-3)	1 (1-2)	1 (1-1)	3 (2-4)	2 (1-2)
Total number of used syringes during the study period	446,476	254,718	403,571	181,539	105,538	81,916	33,210	19,814
Loss of provider time per year**, median (IQR), min	1,393 (924-2,495)	8,764 (5,770-11,627)	891 (439-1,081)	5,524 (4,374-8,191)	6,638 (4,485-8,633)	9,658 (8,236-11,358)	120 (45-751)	403 (118-1,836)
Product waste associated cost (cases with waste), $	4.64	5.89	5.59	6.97	6.97	6.97	5.43	5.43
Product waste associated cost per case (cases with and without waste), $	0.43	2.72	0.59	4.04	4.44	6.11	1.54	3.93
Total product waste associated cost per year**, median (IQR), $	5,091 (3,375-9,116)	40,645 (26,760-55,311)	3,919 (1,930-4,758)	30,314 (24,005-44,849)	36,427 (24,611-47,372)	52,997 (34,223-62,328)	513 (194-3,210)	1,722 (505-6,281)

Table 1. Hypothetical estimates of product waste, loss of provider time and related costs of different ready-to-be-administered (RTA) syringe sizes of fentanyl, hydromorphone and morphine. Product waste associated cost is defined as the sum of the cost of the RTA syringe wasted and of the provider time spent to accomplish the product waste report. Loss of provider time to accomplish waste report is equivalent to 76.22 seconds for each waste event [1]. Cost of RTA syringes are based on average wholesale prices in the USA [3]. Cost of provider time to accomplish waste report is calculated using median hourly wage for nurse anesthetists [2].

* Unit of measurement is mcg for fentanyl, and mg for hydromorphone and morphine

** Based on a yearly caseload of 14,477 (13,854-15,154) for fentanyl, 8,805 (5,767-10,187) for hydromorphone and 831 (122-1,946) for morphine

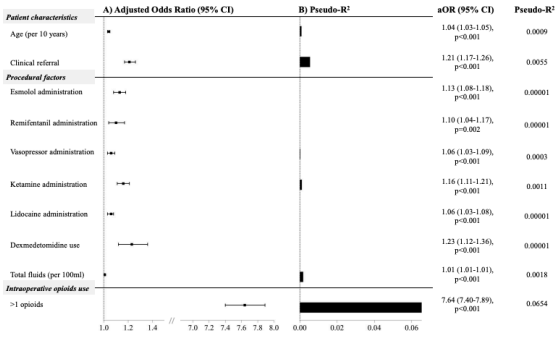

Figure 1. Independent predictors of intraoperative opioid waste. aOR, adjusted odds ratio. A) Adjusted odds ratios of the independent variables predicting the intraoperative opioid waste. B) Dominance analysis depicting the individual contribution to prediction of waste among the independent predictors of opioids waste. Administration of more than one opioids intraoperatively had the strongest dominance, as determined by its contribution to waste prediction (ranking 1, pseudo-R2=0.0654).

Economics, Education and Policy 2 - The Impact of Hindsight Bias on the Diagnosis of Perioperative Events by Anesthesia Providers: A Multicenter, Randomized Crossover Study

Katherine Forkin[1], Patrick Millan[2], Jane Gui[2], Allison Bechtel[2], Amanda Kleiman[2], Lauren Dunn[3], Jeffrey Friedman[1], Stephen Collins[2], Julie Huffmyer[3], Priyanka Dwivedi[4], Jed Wolpaw[5], Edward Nemergut[6], Siny Tsang[3], Katherine Forkin[1]

University of Virginia Health System[1] University of Florida Department of Anesthesiology[2] University of Virginia[3] Icahn School of Medicine, Mount Sinai Urology at New York[4] Johns Hopkins Department of Anesthesiology[5] West Virginia University[6]

Introduction: Hindsight bias has been demonstrated to impact interpretation of past events in many facets of medical care,[1-3] yet its implications in the field of anesthesiology remains unclear. We hypothesized that hindsight bias influences the interpretation of past perioperative clinical scenarios.

Methods: Anesthesiologists (faculty, fellows, and residents) and certified nurse anesthetists (CRNAs) at two academic medical centers were recruited to participate in this randomized crossover study. Participants were asked to review two clinical scenarios in random order. One of the clinical scenarios (Case 1) involved an episode of hypotension and the other clinical scenario (Case 2) involved an episode of hypoxia. After reviewing the first clinical scenario (Foresight case), participants were instructed to assign a probability to each of 3 potential diagnoses based on the information provided (with the 3 assigned probabilities adding up to 100%). Participants then reviewed a second clinical scenario and were instructed to assign a probability to each of 3 potential diagnoses based on the information provided; however, this case (Hindsight case) included one leading sentence stating the diagnosis that was ultimately made (e.g., "This is a case of pulmonary edema."). Participants were randomized both to (1) which case they received as their Foresight case and which as the Hindsight case and (2), for the Hindsight case, which of the 3 potential diagnoses was selected for the leading statement as the supposed ultimate diagnosis. As participants' responses to each case consisted of proportions that sum to 100%, the responses were considered as compositional responses such that the relative values (i.e., proportions) convey information of interest, not their absolute values. We utilized compositional data analysis (CoDA) to examine the differences in responses between the two experimental conditions (Foresight versus Hindsight).

Results: 113 participants completed the study. For the Foresight cases, participants randomized to view Case 2 as the Foresight case were 7.65 times (P<0.001) more likely to place greater weight on Diagnosis C, compared to participants randomized to view Case 1 as the Foresight case [Fig 1]. The relative dominance of Diagnoses A and B were 69.62% and 56.97%, respectively, lower (both Ps<0.001) for Case 2 than Case 1 [Fig 1]. Compared against participants who read Case 1 as the Foresight case, participants who read Case 1 as a Hindsight case with Diagnosis A written in as the ultimate diagnosis demonstrated no significant difference in their relative response to Diagnosis A if (% change =1.03; 95% CI, 0.54 to 1.97; P=0.926). However, participants who read the same Hindsight case with Diagnosis B and C as the ultimate diagnosis were more likely to assign higher value to the corresponding Diagnosis B (% change = 2.82; 95% CI, 1.35 to 5.90; P=0.006) and C (% change = 2.00; 95% CI, 1.12 to 3.58; P=0.02), respectively, compared with participants' responses to Case 1 as a Foresight case [Fig. 2]. Participants randomized to Case 2 as a Hindsight case were more likely to assign higher value to Diagnosis A if randomized to Diagnosis A as the ultimate diagnosis (% change = 1.78; 95% CI, 1.00 to 3.14; P=0.048) and to Diagnosis B if randomized to Diagnosis B as the ultimate diagnosis (% change = 3.72; 95% CI, 1.88 to 7.35; P<0.001), but demonstrated no significant difference in response to Diagnosis C if randomized to Diagnosis C as the ultimate diagnosis (% change = 1.11; 95% CI, 0.56 to 2.21; P=0.757) compared with respective participants' responses to Case 2 as a Foresight case [Fig. 3].

Conclusions: Hindsight bias affects the clinical diagnosis weighting of anesthesia providers in some experimental scenarios. Clinicians should be educated on the presence of hindsight bias in perioperative medicine and consider its impact when interpreting clinical outcomes.

References:

1. Arkes HR, Wortmann RL, Saville PD, Harkness AR. Hindsight bias among physicians weighing the likelihood of diagnoses. J Appl Psychol. 1981;66(2):252-4.
2. Chen J, Littlefair S, Bourne R, Reed WM. The effect of visual hindsight bias on radiologist perception. Acad Radiol. 2020;27(7):977-84.
3. Banham-Hall E, Stevens S. Hindsight bias critically impacts on clinicians' assessment of care quality in retrospective case note review. Clin Med (Lond). 2019;19(1).16-21.

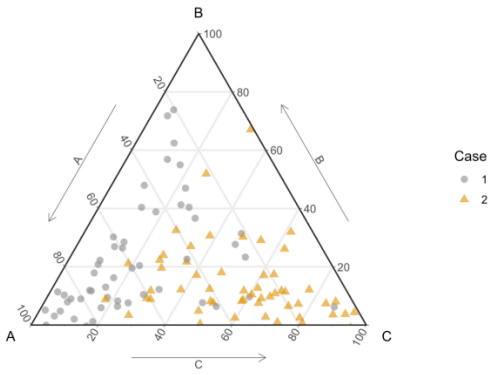

Fig 1. Ternary plot of response compositions for Diagnoses A, B, and C for Case 1 (grey circle) and Case 2 (gold triangle).

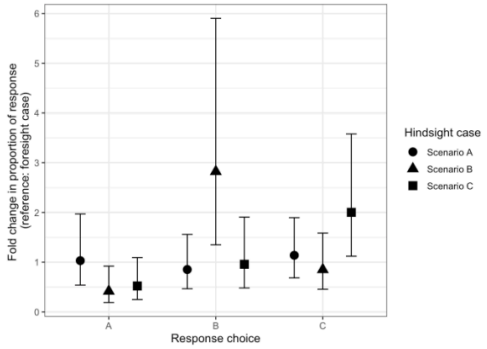

Figure 2. Relative responses of participants to review Case 1 as a Hindsight case (compared to responses from participants randomized to review Case 1 as a Foresight case). The solid circles represent Hindsight responses for participants randomized to read Diagnosis A as the ultimate diagnosis, solid triangles for participants randomized to read Diagnosis B as the ultimate diagnosis, and solid squares for participants randomized to read Diagnosis C as the ultimate diagnosis.

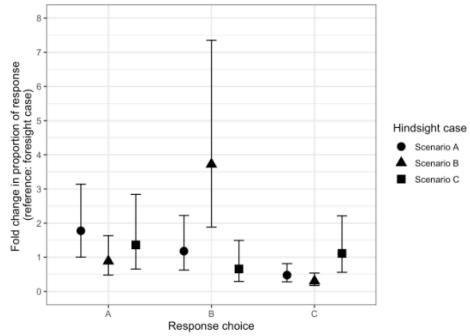

Figure 3. Relative responses of participants to review Case 2 as a Hindsight case (compared to responses from participants randomized to review Case 2 as a Foresight case). The solid circles represent Hindsight responses for participants randomized to read Diagnosis A as the ultimate diagnosis, solid triangles for participants randomized to read Diagnosis B as the ultimate diagnosis, and solid squares for participants randomized to read Diagnosis C as the ultimate diagnosis.

Economics, Education and Policy 3- Assessing Medical Student Understanding and Interest in Anesthesia Before and After a Two-Week Elective Rotation

Bridgett Nelson[1], Emily Peterson[1], Charles Youngblood[1]

Creighton University School of Medicine[1]

Introduction: Anesthesiology has become increasingly popular as a specialty choice. Since 2003, there has been a steady rise in the number of applicants, available positions and filled positions for anesthesiology residencies[1]. In the past decade, the percent of residents matching into anesthesia has increased compared to other specialties, with 4.2% of PGY1 residents matching into anesthesia in 2022 compared to 3.8% in 2012 [2, 3].

Early exposure to a specialty is a key factor in the pursuit of residency training in that area. Our medical school offers early learning opportunities for students including a two-week anesthesiology elective rotation during the M3 or M4 year. It is unknown whether this elective spark interest in the practice of anesthesia.

This study aims to assess how a two-week elective rotation influences medical student understanding of and interest in the practice of anesthesia. It also aims to gather feedback to improve the rotation. This study will benefit not only medical students who enroll in the elective, but also faculty at other medical schools who aim to introduce or restructure their own elective rotations.

Methods: This is a retrospective multivariate analysis of anonymous responses by third- and fourth-year medical students before and after a two-week anesthesiology elective rotation. Responses are recorded using Google Forms. Participants are asked to complete the survey on the first and last days of the rotation. Responses will be collected for a total of 10 rotation groups, each of which consists of approximately 6 students.

The surveys use 4- point Likert scales to rank responses to a series of questions. The post-rotation survey also contains short-answer questions to assess overall experience and obtain feedback.

Results are expressed as frequencies and percentages. Unpaired t-tests are used to compare mean pre and post survey rankings. Patients with missing data have been excluded. All analyses are conducted with SAS version 9.4 and version 26 of SPSS, using a statistical threshold of $p < 0.05$.

Results: Survey data from two elective rotation groups (with a total of 12 students) has been collected and analyzed. Data is still in being collected for ongoing rotation groups. Preliminary analysis shows that students developed an enhanced understanding of various topics related to anesthesiology (intubating, pre-op evaluations, general anesthetics, pain management, ventilator settings) following the rotation. Students became more comfortable with various skills including intubation and mask ventilation. Knowledge of advanced skills such as placing an arterial line or IV remained low following the rotation.

In general, student interest in pursuing anesthesiology increased following the rotation, with 32% interested in pursuing anesthesia prior to the rotation, compared to 45% of students after. The top two reasons for selecting the elective were the opportunity to intubate (selected by 83%) and spend time in the OR (selected by 75%). Two thirds of students felt that this should be a required elective.

Students rated their overall experience of the elective as an average of 3 out of a possible 4. Nearly all students would recommend the elective to their colleagues. A majority of students (75%) felt that their role and expectations during the rotation were unclear, pointing to an area of major improvement in the future. Positive aspects of the rotation included exposure to the field of anesthesiology and the opportunity to learn topics not well covered elsewhere in medical school curriculum. Areas of improvement included incorporating more structure (formal lectures, assigned student-faculty pairs) and increasing learning opportunities (decreasing number of CRNA students, adding academically inclined faculty).

Conclusions: Students developed an enhanced understanding of the practice of anesthesiology and increased interest in pursuing the specialty following the elective rotation. Students selected the rotation primarily to learn to intubate and spend time in the OR. Many students who enrolled in the elective were interested in anesthesia and surgery prior to the rotation.

The rotation was a positive experience for most students. The faculty did adequate job of welcoming and introducing students to the department at the beginning of the rotation. Elective directors must focus on setting clear expectations for students during the rotation in the future. Other suggestions for improvement will also be considered for future rotation groups.

References:

1. Jennifer A. Rock-Klotz, Thomas R. Miller; 2022 Anesthesiology Residency Matches Hit Another Record. *ASA Monitor* 2022; 86:30–31

2. National Resident Matching Program, Results and Data: 2022 Main Residency Match®. National Resident Matching Program, Washington, DC. 2022.

3. National Resident Matching Program, Results and Data: 2012 Main Residency Match℠. National Resident Matching Program, Washington, DC. 2012.

Economics, Education and Policy 4 - Assessment Tool for Peripheral Intravenous Catheter Placement

Ashwini Joshi[1], Jeremy Richards[2]

Massachusetts General Hospital[1] Mount Auburn Hospital[2]

Introduction: Both graduating medical students and residents are not comfortable with performing many basic procedures independently.[1] Reports describing interventions to improve procedural education often measure low-level outcomes such as self-reported confidence and/or self-perceived competence as indicators of proficiency. As such, there is a need for robust assessment tools that can help trainees assess their competence, separately from confidence, in performing procedures. In this context, we created a validated assessment tool for peripheral intravenous catheter (PIV) insertion, a skill that medical students may not gain experience in during medical school[1] but can be expected to perform as interns and residents.

Methods: A PIV insertion assessment tool was created by performing a literature review and combining the assessment tools identified through this search, which were either not created for physician trainees or not validated,[2-4] into a novel checklist. This checklist was then validated using the Lawshe method for content validity, which relies on expert consensus.[2,5] Nine Anesthesia and Internal Medicine Critical Care faculty were recruited via convenience sampling to anonymously rate items on the initial checklist as 'essential', 'useful but not essential', or 'not necessary'. Items rated as 'essential' by 8/9 or 9/9 faculty were included in the final checklist.[5] Further validity evidence, including the checklist's usability, fidelity, feasibility, and response process[6] in formative assessment, was determined in a pilot simulation session in which students placed a PIV in a procedural trainer board. Two faculty observers completed the checklist according to the student's technique, and these data were used to assess internal structure validity through interrater reliability.[6] Students also received feedback from faculty based on the checklist results and answered a post-session survey.

Results: The final checklist included 8 steps (Table 1). Twenty students participated in the pilot simulation session. Fourteen (70%) were first-year medical students and 16 (80%) had never placed a PIV in either simulation or in a patient. All 20 (100%) students agreed or strongly agreed that they would use the checklist in clinical settings and that the checklist was a useful tool in evaluating readiness to independently place PIVs (Table 2). Seventeen (85%) students were able to identify one step in the procedure that needed improvement. Interrater reliability was 90% or higher for 7/8 items on the checklist (Table 1).
Conclusions: This study describes a validation process for creating a tool for procedural formative assessment in early clinical learners. Further work with a more varied group with different levels of training will help to determine whether the tool can accurately discriminate trainee competence. Additionally, this checklist should be piloted in a clinical setting for further validation.[6]

References: 1. Procedural Skills of the Entrustable Professional Activities: Are Graduating US Medical Students Prepared to Perform Procedures in Residency? *J Surg Educ*. 2017;74(4):589-595.

2. Psychometric testing of a checklist for procedural training of peripheral intravenous insertion. *Adv Sim*. 2019;4(1):5.

3. A Clinical Procedures Course for Medical Students. *MedEdPORTAL*. 2016;12(1):mep_2374-8265.10524.

4. Measuring Intravenous Cannulation Skills of Practical Nursing Students Using Rubber Mannequin Intravenous Training Arms. *Mil Med*. 2014;179(11):1361-1367.

5. Critical Values for Lawshe's Content Validity Ratio: Revisiting the Original Methods of Calculation. *Meas Eval Couns Dev*. 2014;47(1):79-86.

6. Validation of educational assessments: a primer for simulation and beyond. *Adv Sim*. 2016;1(1):31.

Table 1. Peripheral Intravenous Catheter Insertion Checklist Steps with Interrater Agreement.

Procedural step in checklist	Interrater agreement (%)
Demonstrates appropriate use of personal protective equipment (wash hands, wear gloves)	100
Maintains sterility of needles prior to venipuncture	95
Inspects/palpates for distal veins	75
Cleans skin with alcohol wipe	90
Advances needle with bevel up	95
Retracts needle	95
Flushes IV catheter with saline	90
Did the student communicate effectively with the patient?	100

Table 2. Medical Student Perception of PIV Assessment Tool in Simulation.

Statement	Number of students who agree or strongly agree, n(%)
Please rate your satisfaction with this SIM* session overall.[a]	20 (100)
This session helped me learn how to place peripheral IVs.	20 (100)
My observed placement was similar to a real-life patient encounter.	12 (60)
I would recommend this session to a classmate.	20 (100)
Please rate your confidence in your peripheral IV placement skills PRIOR to this simulation session.[b]	1 (5)
Please rate your confidence in your peripheral IV placement skills AFTER this simulation session.[b]	15 (75)
This checklist was easy to use.	20 (100)
This checklist accurately assessed my ability in placing peripheral IVs.	20 (100)
I would use this checklist when placing a peripheral IV in a clinical setting.	20 (100)
This checklist is a useful tool in evaluating my readiness to perform peripheral IV placement independently.	20 (100)

*SIM: simulation
[a]Likert scale responses corresponding to agree/strongly agree for this question are satisfied/very satisfied
[b]Likert scale responses corresponding to agree/strongly agree for this question are confident/very confident

Economics, Education and Policy 5 - Comparison of EHR-derived anesthesiology workload and reimbursement: a retrospective observational study

Sunny Lou[1], Laura Baratta[1], Daphne Lew[2], Derek Harford[2], Michael Avidan[1], Thomas Kanammpallil[1]

Washington University in St Louis[1] Washington University School of Medicine[2]

Introduction: Measurement of anesthesiology workload is important to understand the cognitive capabilities and task performance of anesthesiology clinicians during routine and nonroutine clinical care.(*1*) Previous methods to assess anesthesiology workload have relied on direct observation, standardized survey instruments, and physiologic measurements;(*2*) however, such methods are limited by their subjective nature, poor inter-individual reliability, and lack of scalability. Here we describe a novel, objective, and scalable method to measure anesthesiology workload using electronic health record (EHR) audit logs. We compare our EHR-derived workload metric to billing-derived measures of anesthesiology workload and identify discrepancies between apparent clinical workload and the current US reimbursement scheme.

Methods: EHR audit logs are automated trails of clinician activities within the EHR. Originally designed for security access monitoring as mandated by the Health Insurance Portability and Accountability Act, audit logs capture all click actions within the EHR resulting in display or modification of patient data. Because the majority of clinician work occurs within the EHR, audit logs have previously been used to measure clinical workload in many settings.(*3*)
Unlike most specialties, anesthetic care does not require the EHR; however, most clinical care is eventually documented in the EHR, and previous studies have shown that anesthesiologists spend approximately 25% of their time using the EHR.(*4*) Therefore, our metric for EHR-derived workload was the total count of audit log activities performed by all clinicians caring for a patient across the entire perioperative period (i.e., preoperative, intraoperative, and postoperative). All phases of care were included to best capture the intellectual work of preparing for the case (preoperative) as well as direct intraoperative and recovery unit anesthetic care. EHR-derived anesthesia workload was measured for all surgical encounters occurring within a large health system 8/26/2019 – 2/9/2020. For each case, anesthesia billed units were also captured, including procedural base units, time units, and ASA physical status score modifier. This study was performed with a waiver of informed consent (IRB: 202009032). A single mixed-effects linear regression model was used to assess the differential contribution of base units, time units, and ASA modifier to EHR-derived workload versus total billed units; both workload measures were standardized to zero mean and unit variance to facilitate comparison.

Results: This study included 31,730 surgical encounters performed across 11 hospitals (2 academic, 7 community, 2 outpatient surgical centers) (Table 1). 458 anesthesiology clinicians (160 anesthesiologists, 184 CRNAs, 42 resident physicians, 72 other) were included. For each surgical encounter, a median of 258 (IQR 186 - 370) EHR-based actions were performed (Figure 1a). In the intraoperative period, EHR-derived workload was highest around induction and emergence, consistent with prior observational data (Figure 1b).(*1*)
To investigate how EHR-derived workload differed from total billed units as measures of workload, we modeled both as a function of ASA modifier (patient complexity), procedural base units (case complexity), and time units (Table 2). For each independent variable, the difference in coefficient between the billed units outcome and the EHR activity outcome reflected the relative difference in contribution of that variable to each outcome. The contribution of ASA modifier towards EHR activity-based workload (beta = 0.247, 95% CI 0.237-0.256) was nearly 2.5-fold greater than its contribution towards billed units (beta = 0.106, 95% CI 0.097-0.116, $p < 0.001$). The contribution of procedural base units towards EHR activity-based workload (beta = 0.045, 95% CI 0.043-0.048) was approximately half of its contribution towards the billed unit measure of workload (0.106, 95% CI 0.104-0.108, $p < 0.001$).

Conclusions: We developed a novel metric for anesthesiology workload using EHR audit log data that demonstrated face validity and consistency with prior observational results. Comparison of EHR-derived workload to total billed units revealed that the current US reimbursement system may undercompensate for patient complexity while overcompensating for procedural complexity, suggesting that revisions to anesthesia billing may be necessary to appropriately reward clinicians for the challenges of caring for sick patients.

References: 1. *Anesthesia & Analgesia*. **98**, 1419–1425 (2004).

2. *BMJ Simul Technol Enhanc Learn*. **4**, 112–116 (2018).

3. *Journal of the American Medical Informatics Association*, ocac177 (2022).

4. *British Journal of Anaesthesia*. **0** (2021), 126 (3), 633-641

Table 1

Provider Type	**# Users**	**# Cases**
Anesthesiologist	160 (34.9%)	31708 (99.9%)
Nurse Anesthetist	184 (40.2%)	25380 (80.0%)
Resident	42 (9.2%)	9704 (30.6%)
Total	458	31730
ASA Score	**Total Cases**	**Percentage**
1	3822	12.0
2	14789	46.6
3	11579	36.5
4	1502	4.7
5	35	0.1
Disposition	**Number of Cases**	**Percentage**
Outpatient	20042	63.2
Inpatient	9356	29.5
Missing	2332	7.3
Case Urgency		
Elective	26968	85.0
Urgent/Emergent	2378	7.5
Missing	2384	7.5
Location		
Academic	22307	70.3
Community	6176	19.5
Surgical	3246	10.2
Missing	1	0.0
Service		
General Surgery	3737	11.8
Ophthalmology	3221	10.2
Ob/Gyn	2266	7.1
Orthopedics	7586	23.9
Head and Neck	3164	10.0
Urology	2411	7.6
Plastic Surgery	1386	4.4
Cardiovascular	2015	6.4
Neurosurgery	1264	4.0
Other	2348	7.4
Missing	2332	7.3
Pediatrics	6685	21
Adult	25045	79

Figure 1

a.

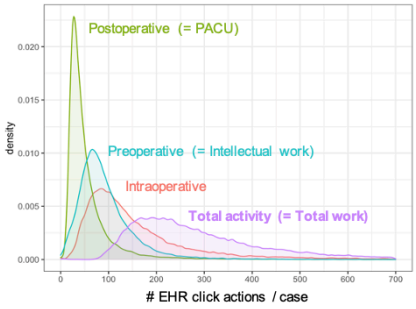

b.

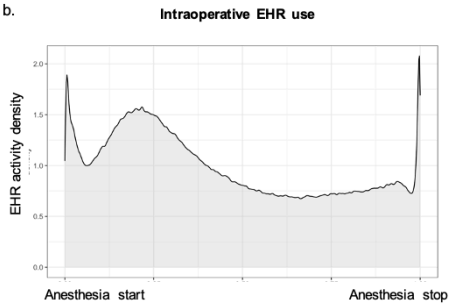

Table 2

Variable	**Effect on Billed Units (95% CI)**	**Effect on EHR-Based Work (95% CI)**
Time units (Case duration)	0.106 (0.105, 0.107)	0.084 (0.083, 0.085)
ASA modifier (Patient complexity)	0.106 (0.097, 0.116)	0.247 (0.237, 0.256)
Procedure base units (Case complexity)	0.106 (0.104, 0.108)	0.045 (0.043, 0.048)

Economics, Education and Policy 6 - Critical Care Obstetrics: A Quarterly Multidisciplinary Educational Conference

Tichaendepi Mundangepfupfu[1], Amol Malshe[1]

University of Rochester[1]

Introduction: The care of the parturient who is critically ill requires a multidisciplinary team including maternal fetal medicine, critical care and other subspecialties as required based on the particular parturient's presenting complaint. While fellows training in maternal fetal medicine and in critical care take care of critically ill parturients as part of their training at our institution there was no formal educational curriculum focused on the multidisciplinary aspects of the care of the critically ill parturient. Following a discussion between the two co-authors we identified a need for a case based Educational conference.

Methods: *Curriculum Development:* We contacted key stakeholders. During development we determined the conference should be based on a single case and follow one parturient's hospital course. The case should be presented by a maternal fetal medicine and a critical care fellow to their faculty moderators. We decided each conference should be 90 mins in duration and that the presentation should highlight key teaching points related to the clinical problem in addition the clinical case. We began the first conference in 2020. Early in the process we also decided to include presentations from other subspecialists as relevant to each particular parturient's case. When we began the conference, it had a blended format where the presenters were in the same room and rest of the conference attendees joined by videoconference. One year later we transitioned to a full videoconference without in-person component. We received CME accreditation for the conference and ABA MOCA credits. The audience for the conference now includes international attendees. Faculty moderators have had specialty expertise in Obstetrics and Gynecology, Maternal Fetal Medicine, Anesthesiology, Obstetric Anesthesiology, Cardiac Anesthesiology, Critical Care, Neurocritical Care, Neurology, Nephrology and Neonatology. The presenters meet multiple times with faculty moderators to discuss their presentation and to discuss their chosen teaching points for the conference. We send an electronic feedback form to attendees which includes questions regarding relevance of the presentation to practice, if the presentation was evidence based, if the presentation would cause changes to the attendees' practice, two things the attendee learnt that would be helpful to their practice. We have also developed an on-demand component to the conference for attendees at our institution as they are able to watch recordings of prior conference sessions through a commercial software service.

Results: Since beginning the conference, the topics for the conference have been: COVID-19, Hyponatremia, Stroke, Pulmonary Edema, HELLP, Eclampsia, ARDS, Aortic Stenosis, Post-Partum Hemorrhage.
The audience for the conference has Included attendees from multiple disciplines Including but not limited to Obstetrics and Gynecology, Anesthesiology and Critical Care. These attendees have been Residents, Fellows, Faculty, Certified Registered Nurse Anesthetists, Nurse Practitioners, Nurses and Midwives. For the current academic year attendance has been approximately 30-40 people per conference and about 1/3 of attendees to each conference filled out the evaluation survey. Using data from the evaluation surveys from the two conferences that have been held this academic year: On a five-point Likert scale 68% strongly agreed and 32% agreed that the conferences were relevant to their practice. On a yes/no scale 100% felt the conferences were evidence based. On a yes/no/no change scale 90% felt the conference increased their knowledge. We asked for attendees to list two things that they learned during our conferences and 55% listed two things they learned.

Conclusions: By early engagement of the key stakeholders and active involvement of the co-directors of the educational program we were able to go from identifying a learning need to implementation within a few months. Through adjustments made to the conference based on input from key stakeholders we were able to get accredited for CME and ABA MOCA credits and have continued to grow the conference and we now have international attendees. Moving forward we would like to explore partnering with other institutions that have an interest in also presenting cases by increasing the number of yearly conference sessions and beyond that looking to partner with societies to further grow the audience for our conference and to engage other educators with similar interests.

Economics, Education and Policy 7- Electroencephalographic Signature of Distress During Procedural Learning in Medical Trainees

F Louis Kirk[1], F Louis Kirk[1], Melissa Davidson[2], Bridget Marroquin[3], Emmett Whitaker[1], Gregory Holmes[3]

University of Vermont[1] Larner College of Medicine at the Univ of Vermont[2] Larner College of Medicine at the University of Vermont[3]

Introduction: The procedural learning environment is inherently stressful, and the success of the trainee depends largely on the ability of training programs to promote learning in the ***zone of proximal development (ZPD)***. The ZPD is the educational space between what the learner has mastered and what they need to master next.[4] Learning in this space requires the leaner to leave their comfort zone and is therefore stress-provoking. Though moderate levels of stress enhance memory formation and play a role in medical education, excess stress (e.g., distress) impedes learning.[1–3] Currently, no study has investigated how distress during training leads to impaired learning and/or performance. The goal of this study was to characterize the neurophysiology of distress in medical trainees using electroencephalography (EEG). We aimed to demonstrate a quantitative endpoint that may allow us to differentiate stress from distress and create novel educational interventions or curricula that leverage this knowledge.

Methods: We assessed the effects of distress on cardiovascular and neurophysiology during a procedural task in 10 medical students. Following Institutional Review Board approval and informed consent, participants were fitted with a 22-channel EEG hat (**Fig 1A**) and a smart shirt capable of continuous electrocardiogram monitoring to allow for assessment of heart rate variability (HRV, **Fig 1B**). EEG baseline recordings (eyes open, eyes closed) were obtained for each participant prior to the experiment. Thereafter, each participant watched a 10-minute video on endotracheal intubation. Each participant was then given a short clinical vignette and asked to enter the high-fidelity simulated operating room. The first scripted scenario was a "calm scenario" during which the participant was asked to perform an endotracheal intubation in an ideal environment. Then, the participant performed the same procedure in a in a distressful environment.

Results: This pilot study established feasibility and proof-of-concept for real-time studies of the EEG and physiologic effects of distress in medical trainees. Analysis of HRV, an established marker of autonomic function, revealed a robust physiologic response to distress when compared to the calm scenario. This response was characterized by an increase in heart rate and a decrease in HRV, reflecting an imbalance in autonomic nervous system activity favoring sympathetic activation (**Figure 2**). Continuous EEG data were analyzed in four states **(Figure 3)**. EEGs were analyzed for power (absolute and relative), coherence, and phase locking value (PLV). In our preliminary EEG analysis, significant differences in power and functional connectivity measures (coherence and PLV) were seen during the four states **(Figures 3 and 4).** During the stressful scenario there was increased power across all frequency bands **(Figure 4, p<0.05).** Voltage changes across frequencies were variable and chaotic **(Figure 3).** Both coherence and PLV were decreased in the the stressful scenario compared to the calm scenario, suggesting impaired cognition **(Figure 3)**. These data indicate that EEG may be a robust measure of acute stress in a procedural setting. The changes in power and functional connectivity measures during the stressful scenario indicate that acute stress can impair brain connectivity, and by extension learning.

Conclusions: This study demonstrated a clear neurophysiologic effect of procedural task training (decreased EEG power and impaired FC) that is significantly exacerbated by stress. These findings represent a previously unidentified biosignature of stress that can be used as a "therapeutic target" for focused educational tools. The long-term goal is to develop a tool that can suppress this biosignature, and hopefully lead to improve retention, performance, and learner satisfaction in procedural trainees.

References: 1. Npj Sci Learn 1, 16011 (2016).

2. Neurobiol Learn Mem 93, 183–8 (2009).

3. Acad Med 84, S25–S33 (2009).

4. Acad Med 95, 1098–1105 (2019).

Figure 1. Example of microEEG device (A) and Hexoskin device(B).

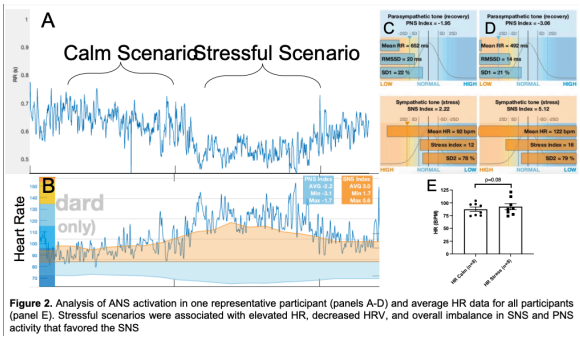

Figure 2. Analysis of ANS activation in one representative participant (panels A-D) and average HR data for all participants (panel E). Stressful scenarios were associated with elevated HR, decreased HRV, and overall imbalance in SNS and PNS activity that favored the SNS

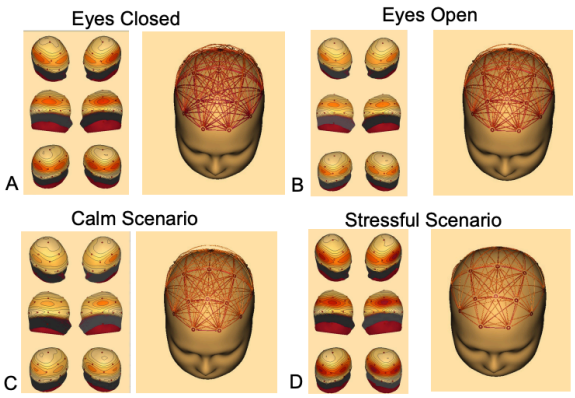

Figure 3. Comparison of voltage maps (left) and phase locking values (right) across four conditions: A. eyes closed; B. eyes open; C. calm scenario; D. stressful scenario. The voltage map shows distribution of power (1-50 Hz) with brighter colors representing higher voltages. The phase locking value between electrode pairs are delineated by red lines with the thickness of the line reflective of signal strength. Phase locking value, a measure of functional connectivity, is decreased during the stressful test compared to the calm test.

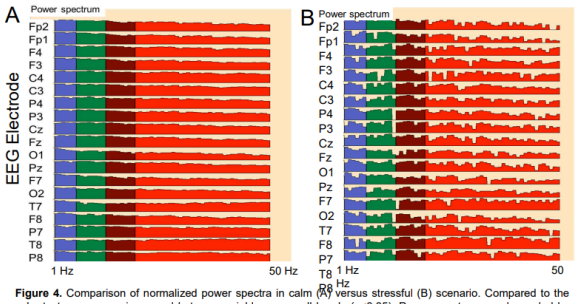

Figure 4. Comparison of normalized power spectra in calm (A) versus stressful (B) scenario. Compared to the calm test, power was increased but was variable across all bands ($p<0.05$). Power spectra are color coded by frequency with purple = delta, green = theta, crimson = alpha and red = beta.

Economics, Education and Policy 8- Entrustable Professional Activities as a Foundation for a Feedback Tool in a Critical Care Medicine Training Program: Using Delphi Surveys to Generate Internal Consensus for a Pilot Program

Albert Yen[1], Kristina Sullivan[1], Bernadette Martin[1], Anne Donovan[2], Christy Boscardin[2], Kevin Thornton[3]

University of California, San Francisco[1] UCSF[2] University of California San Francisco[3]

Introduction: As medical training has evolved; a natural by-product has been the parallel evolution of evaluation and assessment. Translating medical knowledge into practical ability in caring for patients is a challenging and heterogenous process, and the ability to critically evaluate each trainee individually as they progress is incredibly important, not only as a function of gaining independence, but also to guide the trainee's learning in a targeted fashion. This assessment of competence in Critical Care Medicine (CCM) is based upon milestones mandated by the Accreditation Council for Graduate Medical Education (ACGME). While this framework provides a broad outline in which to base assessment of CCM fellowship trainees, these milestones are not granular enough to provide meaningful and actionable feedback that guides trainees towards independent practice, especially in such an integrative field as CCM. Entrustable Professional Activities (EPAs) have arisen as a means of addressing this gap in other specialties. EPAs describe the sub-competencies required to perform specific patient care tasks, thus combining separate competencies into integrated tasks that are performed in a patient care setting. EPAs for CCM that have been developed internationally are a useful starting point, but these are not directly applicable for US institutions given lack of alignment with ACGME milestones. We describe a serial and integrative process used to develop EPAs specific to CCM training in the United States.

Methods: A review of the literature for EPAs in Adult CCM resulted in two sets of existing EPAs, one created in The Netherlands, and one from the Royal College of Physicians of Canada. After further review, we used the EPA set published by van Bockel, et al from The Netherlands' as a launching point. A cross section of education experts from the CCM divisions of Anesthesiology, Pulmonary Medicine, Neurology, and Surgery at our institution created a list of nine potential EPAs for CCM graduates. Each EPA was further broken down into a set of granular sub-competencies (e.g., pathophysiology, technical skill, practical aspects of treatment, medical knowledge, application of judgement, interactions with the multi-disciplinary team), that when taken as a whole, would comprise mastery. These sub-competencies represented under each of the nine EPAs provides a way to characterize the various knowledge, skills, and attitudes necessary to execute these activities. These EPAs were then mapped back to the ACGME competencies to ensure complete alignment. After generation of this initial list, we conducted a two round, modified Delphi survey to achieve consensus on the final set of EPAs and appropriate sub-competencies. All faculty in CCM were invited to participate in the Delphi surveys.

Results: 8 CCM faculty experts participated in two rounds of modified Delphi study. Round 1 achieved consensus (80% agreement) on 91 of 122 total sub-competencies as essential for executing the 9 EPAs. Five additional sub-competencies identified by respondents during Round 1 were included for consensus voting in Round 2. An additional 17 out of 31 sub-competencies reached consensus as essential for inclusion in the final list of sub-competencies after Round 2. All five additional sub-competencies identified during Round 1 reached consensus as essential in Round 2.

Conclusions: Using a modified Delphi process, our group was able to iteratively, and collaboratively create a set of Entrustable Professional Activities suited for a Critical Care Medicine Training program. Remarkably, internal consensus among our group was achieved in an efficient and expeditious fashion, amongst a very diverse group of CCM faculty. This process has informed development of a web-based tool that will be piloted to drive formative feedback from faculty to fellows. Further work will be done to evaluate the impact of these EPAs on fellow development, from pre and post implementation surveys to collect feedback from the fellows and attendings who utilize this tool. Future iterations of the EPAs developed here will again utilize Delphi surveys to rapidly reach consensus, and hopefully similarly accelerate trainee growth.

References: 1. Journal of Critical Care, Volume 54, Pages 261-267, 2019

2. Critical Care Specialty Committee. Adult Critical Care Medicine EPA Guide. Ottawa: Royal College of Physicians and Surgeons of Canada; 2018.

3. Pediatric Critical Care Medicine, Volume 23, Pages 54-59, 2022

4. Medical Teacher, Volume 39, Pages 802-807, 2017

Economics, Education and Policy 9- Introducing Interactive Web-Based Modules to Create More Flexibility and Opportunities for Resident Learning

Benjamin Fiorillo[1], Susan Smith[1], McKenzie Hollon[1], Olabisi Lane[2]

Emory University Department of Anesthesiology[1] Emory Healthcare[2]

Introduction: Anesthesiology residency is a time-demanding field where residents have limited time for learning outside of the operating rooms. This, in combination with time constraints on academic faculty, have led to inefficient learning opportunities for residents.[1,2] As a result, traditional instructor-centered teaching has been shifting to a learner-centered model that puts learners in control of their learning.[1] Over recent decades, e-learning has grown to optimize educational opportunities for learners.[1,3,4] One component of e-learning is the use of interactive infographics to engage learners. An infographic is defined as "a visualization of data or ideas that tries to convey complex information to an audience in a manner that can be quickly consumed and easily understood."[5] This project introduces web-based modules utilizing interactive infographics to provide opportunities for structured, engaging, and flexible learning for anesthesiology residents. The overall objective is to improve resident engagement with the learning material resulting in increased retention.

Methods: A needs assessment survey was sent out to all CA1-CA3 residents at the end of the 2021-2022 academic year asking for feedback to improve the education experience for the 2022-2023 academic year. For this project, regional anesthesiology was chosen as the field of interest with focus on local anesthetics and local anesthetic systemic toxicity. Given that senior residents were very familiar with these topics, participants included only PGY1s and PGY2s.

Following feedback from the needs assessment, two interactive infographics were developed utilizing Genially[6] (Figure 1). Pre and post-test surveys were created utilizing Google Forms.[7] The first question asked for identification of class year. The next five questions were based on material presented in the two infographics (Table 1). The final question asked for participants' confidence in the answers chosen on a scale from 1 (not confident at all) to 5 (completely confident). The post-test survey had one additional question asking for feedback or future directions. Analysis was completed using Excel Data Analysis.[8] A two sample t-test was utilized to determine if there was a statistically significant difference between the pre and post-test surveys as a result of the intervention.

Results: *Needs Assessment:*
The needs assessment survey had 19 total participants. When asked if residents would prefer online learning modules in place of lectures, 9 out 19 participants answered yes, 5 out of 19 answered maybe, and 5 out of 19 answered no.

Pre and Post-test Survey Results:
Fourteen participants completed the pre-test with nine of those fourteen completing the post-test. A higher percentage of post-test survey participants answered the questions correctly when compared to the pre-test survey participants (Table 2). Participants' confidence in the answers varied between the pre and post-test. The mean confidence answering questions prior to seeing the infographics was 1.77 (n=14). The mean confidence answering questions after seeing the infographics was 3.63 (n=9). The F-test had a p value of 0.107 (> 0.05). The paired T-test assuming equal variances had a two-tailed p value of 1.94×10^{-5} (< 0.05).

Additional Feedback:
All post-test survey participants supported integrating these infographics and other similar interactive materials into subspecialty rotations for self-directed learning.

Conclusions: In this project, a needs assessment was completed with residents commenting on inefficiency of lectures and supporting the development of interactive material for self-directed learning. This led to the development of two web-based modules consisting of interactive infographics. The results show that residents were more confident in answering local anesthetics-related questions following the modules ($p < 0.05$) with a larger percentage of individuals answering the questions correctly (Table 2). Residents favored integrating interactive modules in future educational curriculum.

Future directions include the development of more web-based modules focused on regional anesthesiology and acute pain medicine topics, and combination of these web-based modules with a syllabus and procedures videos to be published on a course website. Additionally, if successful, other anesthesiology sub-specialties including Cardiothoracic, Critical Care, Obstetrics, and Pediatrics can adopt this project with material specific to their rotations.

References: 1. The impact of E-learning in medical education. Acad Med. 2006 Mar;81(3):207-12.

2. Undergraduate medical education: thoughts on future challenges. BMC Med Educ. 2002 Jul 30;2:8.

3. Web-Based Radiology Learning Module Design: The Author Perspective. Acad Radiol. 2022 Apr;29(4):584-590.

4. AMEE Guide 32: e-Learning in medical education Part 1: Learning, teaching and assessment. Med Teach. 2008 Jun;30(5):455-73.

5. Role of Infographics in Healthcare. Chin Med J (Engl). 2018 Oct 20;131(20):2514-2517.

6. Genially. 2022. Available at https://genial.ly.

7. Google. 2022. Google Forms, available at https://www.google.com/forms/about/.

8. Microsoft Corporation. 2022. Microsoft Excel, available at https://office.microsoft.com/excel.

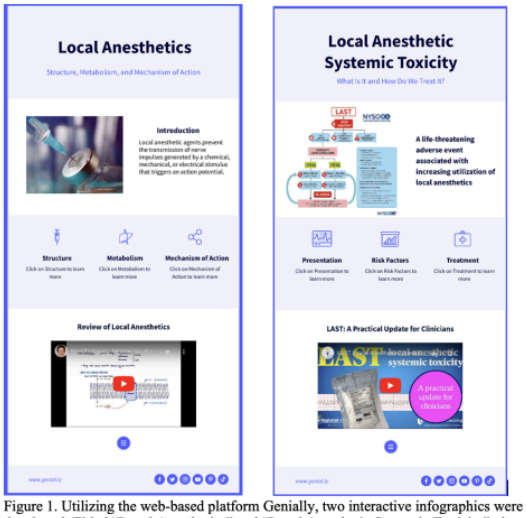

Figure 1. Utilizing the web-based platform Genially, two interactive infographics were developed. Titled "Local Anesthetics" and "Local Anesthetic Systemic Toxicity", the two infographics incorporate figures, text, and videos to create interactive and engaging content for learners.

Table 1: Five local anesthetic-related multiple choice questions covering material introduced in the infographics were chosen for the pre and post-test surveys. Each question is labeled with a number to easily correlate with Table 2 shown in the results section.

1	Which of the following local anesthetics is metabolized through N-dealkylation and hydroxylation via P-450 enzymes in the liver?
2	What is the maximum dose of lidocaine (with epinephrine) in a 70kg male?
3	Following a supraclavicular nerve block with a mixture of lidocaine and bupivacaine, a 65-kg (lean body weight) patient begins developing dizziness and confusion before beginning to have seizures. How much volume of 20% lipid emulsion should be bolused in the first 2-3 minutes before starting an infusion?
4	What local anesthetic is para-aminobenzoic acid a metabolite of?
5	Which of the following Na+ channel states are local anesthetics most likely to bind to?

Table 2: The percentage correct answer for each question prior to and after the educational intervention.

1	64.29%	100.00%
2	50.00%	88.89%
3	14.29%	55.56%
4	57.14%	100.00%
5	57.14%	100.00%

Economics, Education and Policy 10 - Leadership Self-efficacy Is Not What's Holding Women Back.

Jin Min Han[1], Teresa Mulaikal[2], Maya Hastie[3]

Columbia University Medical Center[1] Columbia University[2] Columbia University Vagelos College of Physicians and Surgeo[3]

Introduction: Despite progress made over the past decade, women's careers in medicine still lag behind those of men [1]. This lag appears to start early in career as evidenced by disparity in the rate of promotion between men and women faculty from assistant to associate professor [2]. Based on this finding, it is not surprising that the percentage of women representation decreases further in more senior academic ranks. For example, in the U.S., women represent close to half of medical school graduates, 40% of full-time faculty members, and only 18% of department chairs or deans [1].

One of the hypotheses for this "leaky pipeline" of women in academic medicine is that internal psychological barriers from women's perceived low self-efficacy and self-limiting beliefs hinder women's career progression. The purpose of the study was to determine if there is a difference in perceived self-efficacy between women who are not in positions of leadership and women who are currently or were previously in positions of leadership.

Methods: After institutional board review exemption, a previously validated survey instrument [3] was used to compare the perceived self-efficacy toward leadership between women who are not in positions of leadership and women who are currently or were previously in positions of leadership. Eligible participants were identified by a review of the publicly available clinical departmental listings and followed a non-random, purposive sampling. Faculty members with leadership positions were identified within their respective departments at the program (program directors), departmental (division chiefs, vice chair, chair), institutional (director of clinical centers or hospital units), or decanal (assistant dean, associate dean) levels. Other participants without identified leadership roles were similarly selected from the departmental faculty lists. Clinical affiliations were grouped into three categories: surgical, medical and hospital-based. Gender of the participants was inferred from the used pronouns on their organizational profile page.

The survey consisted of 22 questions that were categorized into three components: Leader action self-efficacy (7 questions), Leader self-regulation efficacy (8 questions), and Leader means efficacy (7 questions). First two components pertained to participant's self-perceived capacity to perform leadership responsibilities and the third component pertained to participant's perception on accessibility of support from the environment, peers, and senior leadership. Each question could be answered on a scale of 0 to 100 with 0 indicating 'not at all confident' and 100 indicating 'totally confident.' The mean scores between the groups for each component were compared using two-tailed student's *t*-test, and statistical significance was considered at $p < 0.05$.

Results: Out of the 42 eligible faculty members who were invited via email to participate in the survey, 30 completed the online survey between January and May 2018, with a response rate of 71%. 13 participants were not in positions of leadership and 17 participants were currently or previously in positions of leadership. Two groups were similar in age, years in practice and specialty affiliation (Table 1). Findings showed that there is no statistically significant difference in mean scores between the two groups for all three components (Table 2): Leader action self-efficacy (mean difference, 1.89; 95% confidence interval [CI], -82.33 to 86.11), Leader self-regulation efficacy (mean difference -55.88; 95% CI, -126.12 to 14.37), and Leader means efficacy (mean difference -46.39; 95% CI, -137.72 to 44.93).

Conclusions: The result showed that there is no difference in perceived self-efficacy between women who are not in positions of leadership and women who are currently or were previously in positions of leadership. Further research with a larger sample is warranted to compare perceptions of self-efficacy toward leadership between men and women or between women in different specialties with varying women representations. Although limited by a small sample size, the result of this study suggests that self-efficacy is not sufficient to explain the gender gap in leadership positions in medicine or gender disparity in promotion rate. Organizational efforts to increase women's representation in leadership would benefit from a shift of focus from individual development toward elucidation of environmental, situational, and structural issues that hinder career advancement.

References: 1. Lautenberger DM, Dandar VM. The State of Women in Academic Medicine 2018-2019: Exploring Pathways to Equity. 2020.

2. Clark L, Wick JA, Erica C, et al. Women physicians and promotion in academic medicine. N Engl J Med. 2020;383(22):2148-2157.

3. Hannah ST, Avolio BJ, Walumbwa FO, Chan A. Leader self and means efficacy: A multi-component approach. Organ Behav Hum Dec. 2012;118(2):143-61.

Table 2. Survey results

	Not in Leadership [a] (n=13)	In Leadership [a] (n=17)	Mean difference [b] (95% CI)	p-value [c]
Leader Action Self-efficacy (7 items)	482.42 (115.97)	480.53 (103.70)	1.89 (-82.33 to 86.11)	0.96
Leader Self-regulation Efficacy (8 items)	578.77 (103.79)	634.65 (84.15)	-55.88 (-126.12 to 14.37)	0.11
Leader Means Efficacy (7 items)	385.92 (111.84)	432.31 (119.54)	-46.39 (-137.72 to 44.93)	0.31

[a]: Results as mean scores (standard deviation).
[b]: difference in means with 95% confidence interval (CI).
[c]: Student's *t*-test with statistical significance at p-value <0.05.

Table 1. Demographics

	Not in Leadership (n=13)	In Leadership (n=17)
Age[a]	42 (8.9)	47 (8.5)
Years in practice		
0-5	8	4
6-10	1	4
11-15	1	4
16-20	2	1
>21	1	4
Specialty[b]		
Surgery	6	6
Hospital-based	5	6
Medicine	2	5

[a]: Mean age (standard deviation).
[b]: Specialties were categorized into surgery (all surgical specialties and subspecialties), medicine (medical specialties including pediatrics and pain medicine), and hospital-based (anesthesiology, radiology, pathology, and emergency medicine).

Economics, Education and Policy 11- Projected cost-savings of replacing desflurane with sevoflurane and adopting low fresh gas flow rates

Matthew Lam[1], Saad Khan[1], Harshaan Dhaliwal[1], Mark Reisbig[2], Cassandra Hays[1]

Creighton University School of Medicine[1] CHI Creighton University Medical Center[2]

Introduction: The increasing cost of healthcare in the United States places a growing burden on individuals and taxpayer-funded institutions. Healthcare spending is projected to increase by an average of 5.4% annually over the next decade, outpacing expected national gross domestic product (GDP) growth [1]. Medicare spending is also anticipated to increase by approximately 7.6% annually in the same time frame, which may overwhelm allotted funds. Operating room costs represent 30-40% of hospital expenditures and roughly half of Medicare spending, offering a potential target for cost reduction [2, 3]. Among these costs are volatile anesthetics, a staple of the anesthetic formulary. The most used are the halogenated agents isoflurane, sevoflurane, and desflurane. Recent studies involving desflurane, the most expensive medication, have demonstrated minimal clinical benefit over its counterparts [4]. Reduced use of desflurane should reduce costs to hospitals, taxpayers, and patients. This study sought to quantify the financial benefits of minimizing desflurane use at one institution and project additional cost savings by lowering fresh gas flow (FGF) rates.

Methods: Detailed purchasing data for desflurane, sevoflurane, and isoflurane were obtained from the pharmacy of a 400-bed academic medical center in the Midwest over a 6-year period. This facility does not perform elective surgeries, therefore surgical case numbers were not restricted during the COVID-19 pandemic. Cost per MAC-hour was calculated using drug costs at our institution, assumed 100% O_2 vehicle, and published national average FGF rates due to rates specific to our institution being inaccessible [5-7]. Calculations and data analysis (linear regression and mixed-model analyses of variance (ANOVA)) and visualization were performed in GraphPad Prism.

Results: During the study period, the prices of isoflurane and desflurane remained unchanged. Available data from early 2022 suggested an increase in the cost of desflurane but are not complete. Surprisingly, the unit cost of sevoflurane decreased between 2018 and 2020 ($p < 0.0001$). The unit cost of desflurane is higher than sevoflurane and isoflurane ($p < 0.0001$). The cost difference normalized by MAC-hour is amplified by the high MAC of desflurane (Figure 1). Desflurane use declined ($p < 0.0001$) with reciprocal increase in sevoflurane ($p < 0.001$) to accommodate for a stable case count (Figure 2). Purchasing of isoflurane was consistently low. Monthly spending on desflurane was reduced 33% from $4210 ± 960 in 2017 to $1125 ± 732 in 2022 ($p = 0.01$). Desflurane reduction in 2019 drove a $26,191.17 decrease in total spending over that time.
Assuming an average sevoflurane FGF of 2.34 L/min, reduction to 1 L/min in line with FDA recommendations would equate to a 57% decrease in drug usage and therefore purchasing. Applied to the volume of sevoflurane purchased in 2021, the combination of desflurane cessation and low flow anesthesia would result in savings of an additional $37,326 per year. Data from 2022 are incomplete at this time and therefore not used as an end.

Conclusions: While surgery volume was stable, desflurane purchasing reduction and compensatory increase in sevoflurane purchasing resulted in meaningful financial savings due to the higher volume cost of desflurane. Given the minimal clinical benefits compared to sevoflurane and potential risk for negative outcomes, the increased price is difficult to justify.
Like others, we show that further savings could be made by adopting low FGF rates. In an era in which healthcare costs are the subject of nationwide controversy and prohibitive to many, these strategies should be considered to rein in costs and pass savings to patients.

References: [1] *Ann Surg*. 2020;271(1):23-28.

[2] *Anesthesiology* 1995; 83:1138–1144.

[3] *AMIA Annu Symp Proc*. 2012;2012:154-163.

[4] *Br J Anaesth*. 2020;125(6):852-856.

[5] *Can J Anaesth*. 1993;40(5 Pt 1):472-474.

[6] *Anesthesiology*. 2013 Apr;118(4):874-84.

[7] *Int J Anesth.* 2018;5(1):064.

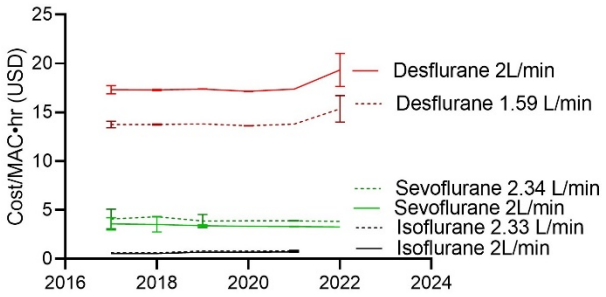

Figure 1. Cost per MAC-hour of inhaled aneshetics at our institution throughout the study period. Solid lines represent equal flow rates of 2 L/min. Dashed lines represent national average flow rates of each agent.

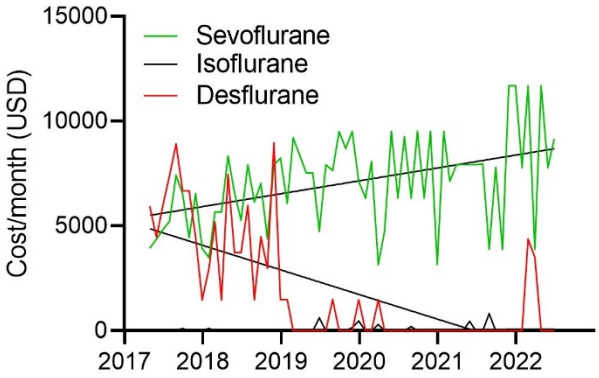

Figure 2. Monthly expenditures on inhaled anesthetics at our institution throughout the study period.

Economics, Education and Policy 12- Reported Industry Payments to Anesthesiologists and Critical Care Physicians in the United States: A 5-Year Analysis of the Open-Payments Database

Isaac Freedman[1], Andre Dempsey[1], Mark Hocevar[2], Oluwaseun Akeju[2], Timothy Gaulton[2]

Massachusetts General Hospital, Harvard Medical School[1] Warren Alpert Medical School of Brown University[2]

Introduction: Most physicians report industry ties in all disciplines of science and medicine. The Patient Protection and Affordable Care Act and the Physician Patient Sunshine Acts encouraged stricter compliance with conflict-of-interest guidelines and mandated that all payments >$10 from group purchasing organizations and drug or device manufacturers be reported to the Centers for Medicare and Medicaid Services. The aim of this study was to characterize outside medical and biomedical industry payments to anesthesiologists and critical care (CC) physicians from 2017 through 2021.

Methods: A retrospective study was performed from 1 January 2017 through 31 December 2021 of the Open Payments Database. Collected data included total number, type, and value of each industry payment to anesthesiologist and to physicians in comparison groups, including internal medicine (IM)-trained pulmonology and CC physicians, general surgeons, and orthopedic and vascular surgeons over the 5-year period. Payments to anesthesiologists were further stratified by practice setting into operating room (OR), critical care, and pain medicine.

Results: A total of 602,191 unique payments to 36,117 anesthesiologists (16.7 payments per physician) were identified during 2017-2021. Over the study period, between $18.4 (2017) and $29.9M (2019) was reported paid to anesthesiologists, totaling more than $102M, compared to more than $2.3B for payments to orthopedic surgery over the same period. The mean payment per provider was $155 and the mean provider was paid $2,835 annually. Less than 0.1% of payments were >$100,000 in size, but these large payments accounted for 13.6% of all payments by value. Food and Beverage payments accounted for the largest number of payments, though consulting Fees and Services other than consulting accounted for the largest portion of payments by dollar value. Industry payments to anesthesiologists increased in number and value of payments over the study period, with an average year-over-year (YOY) increase of 1.26% and a compound annual growth rate (CAGR) of 1.67%. Among anesthesiologists, CC and OR anesthesiologists both received on average <$3,000 per year, while pain medicine anesthesiologists received on average more than $5,600 in industry payments per year. Critical care anesthesiologists received far fewer total payments than did IM-trained CC physicians, but more per provider (anesthesia CC: $2,990 vs IM CC: $2,549). Overall, anesthesiologists made $2,835 per provider, far less than general surgeons ($6,510), vascular surgeons ($19,179), or orthopedic surgeons ($71,455).

Conclusions: Our study shows that over the most recent 5-year period (2017-2021) of the Centers for Medicare and Medicaid Services Open Payments Database, the value of industry payments to anesthesiologists grew by a CAGR of 1.67%. Pain medicine anesthesiologists were reimbursed more by outside industry than were their OR and CC anesthesiology colleagues. Compared to IM-trained CC physicians, CC anesthesiologists were paid more per physician.

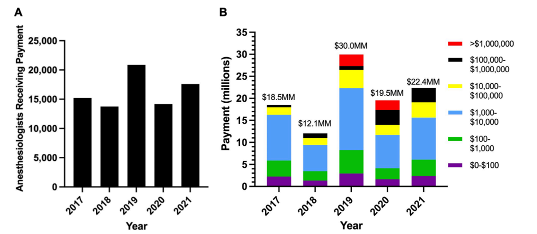

Figure 1. (A) Number of anesthesiologists receiving payments and (B) value of payments to anesthesiologists, 2017-2021.

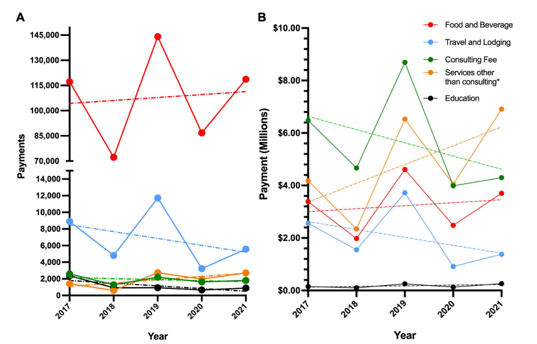

Figure 2. (A) Number of payments and (B) value of payments to anesthesiologists in the 5 top payment categories from 2017 through 2021. and (B) value of payments to anesthesiologists, 2017-2021. All trends not significant with P > 0.05.

Table 1. Distribution of Types of Industry Payments to Anesthesiologists by Number and Monetary Value, 2017-2021

Type of Payment	Number of Payments (% of Total)						Value of Payments (% of Total)						Average Dollars per Payment					
	2017	2018	2019	2020	2021	Total	2017	2018	2019	2020	2021	Total	2017	2018	2019	2020	2021	Average
Food and Beverage	117,233 (88.2%)	72,249 (90%)	144,059 (88.3%)	86,765 (91.1%)	118,710 (90.8%)	539,016 (89.5%)	$3,381,395 (18.3%)	$1,978,191 (16.4%)	$4,611,422 (15.4%)	$2,476,187 (12.7%)	$3,696,881 (16.5%)	$16,144,076 (15.8%)	$29	$27	$32	$29	$31	$30
Travel and Lodging	8,914 (6.7%)	4,802 (6%)	11,728 (7.2%)	3,233 (3.4%)	5,576 (4.3%)	34,253 (5.7%)	$2,560,775 (13.9%)	$1,548,272 (12.8%)	$3,716,906 (12.4%)	$910,877 (4.7%)	$1,378,920 (6.2%)	$10,115,750 (9.9%)	$287	$322	$317	$282	$247	$291
Consulting Fee	2,596 (2%)	1,284 (1.6%)	2,198 (1.3%)	1,633 (1.7%)	1,800 (1.4%)	9,511 (1.6%)	$6,478,901 (35.1%)	$4,670,294 (38.7%)	$8,685,658 (29%)	$3,987,672 (20.4%)	$4,295,696 (19.2%)	$28,118,221 (27.5%)	$2,496	$3,637	$3,952	$2,442	$2,386	$2,983
Services other than consulting*	1,413 (1.1%)	609 (0.8%)	2,735 (1.7%)	1,976 (2.1%)	2,706 (2.1%)	9,439 (1.6%)	$4,180,952 (22.6%)	$2,340,221 (19.4%)	$6,528,043 (21.8%)	$4,043,086 (20.7%)	$6,912,405 (30.9%)	$24,004,707 (23.4%)	$2,959	$3,843	$2,387	$2,046	$2,554	$2,758
Education	2,367 (1.8%)	923 (1.2%)	931 (0.6%)	659 (0.7%)	894 (0.7%)	5,774 (1%)	$153,193 (0.8%)	$96,806 (0.8%)	$249,361 (0.8%)	$134,645 (0.7%)	$264,704 (1.2%)	$898,709 (0.9%)	$65	$105	$268	$204	$296	$188
Honoraria	163 (0.1%)	74 (0.1%)	647 (0.4%)	346 (0.4%)	542 (0.4%)	1,772 (0.3%)	$395,955 (2.1%)	$167,063 (1.4%)	$1,696,884 (5.7%)	$676,819 (3.5%)	$1,392,548 (6.2%)	$4,329,269 (4.2%)	$2,429	$2,258	$2,623	$1,956	$2,569	$2,367
Nonaccredited CEP faculty/speakership	160 (0.1%)	143 (0.2%)	322 (0.2%)	272 (0.3%)	0 (0%)	897 (0.1%)	$580,581 (3.1%)	$603,002 (5%)	$972,673 (3.2%)	$423,054 (2.2%)	$0 (0%)	$2,579,310 (2.5%)	$3,629	$4,217	$3,021	$1,555	$0	$2,484
Grant	48 (0%)	46 (0.1%)	58 (0%)	96 (0.1%)	55 (0%)	303 (0.1%)	$290,194 (1.6%)	$252,283 (2.1%)	$399,558 (1.3%)	$295,525 (1.5%)	$383,166 (1.7%)	$1,620,726 (1.6%)	$6,046	$5,484	$6,889	$3,078	$6,967	$5,693
Royalty or License	0 (0%)	0 (0%)	0 (0%)	0 (0%)	277 (0.2%)	277 (0%)	$0 (0%)	$0 (0%)	$0 (0%)	$0 (0%)	$466,825 (2.1%)	$466,825 (0.5%)	$0	$0	$0	$0	$1,685	$337
Gift	6 (0%)	47 (0.1%)	177 (0.1%)	21 (0%)	9 (0%)	260 (0%)	$449 (0%)	$10,360 (0.1%)	$51,069 (0.2%)	$7,933 (0%)	$270 (0%)	$70,081 (0.1%)	$75	$220	$289	$378	$30	$198
Current or prospective ownership or investment interest	24 (0%)	25 (0%)	92 (0.1%)	45 (0%)	29 (0%)	215 (0%)	$14,780 (0.1%)	$13,254 (0.1%)	$294,410 (1%)	$217,178 (1.1%)	$20,168 (0.1%)	$559,790 (0.5%)	$616	$530	$3,200	$4,826	$695	$1,973
Entertainment	23 (0%)	31 (0%)	40 (0%)	42 (0%)	39 (0%)	175 (0%)	$412,920 (2.2%)	$316,403 (2.6%)	$1,794,877 (6%)	$5,177,207 (26.5%)	$338,299 (1.5%)	$8,039,706 (7.9%)	$17,953	$10,207	$44,872	$123,267	$8,674	$40,995
MEP† faculty/speakership	9 (0%)	2 (0%)	51 (0%)	48 (0.1%)	31 (0%)	141 (0%)	$19,926 (0.1%)	$4,550 (0%)	$654,752 (2.2%)	$929,888 (4.8%)	$735,790 (3.3%)	$2,344,906 (2.3%)	$2,214	$2,275	$12,838	$19,373	$23,735	$12,087
Accredited CEP faculty/speakership	2 (0%)	0 (0%)	27 (0%)	78 (0.1%)	0 (0%)	107 (0%)	$3,600 (0%)	$0 (0%)	$268,935 (0.9%)	$256,764 (1.3%)	$0 (0%)	$529,299 (0.5%)	$1,800	$0	$9,961	$3,292	$0	$3,011
Acquisitions	0 (0%)	0 (0%)	0 (0%)	0 (0%)	28 (0%)	28 (0%)	$0 (0%)	$0 (0%)	$0 (0%)	$0 (0%)	$2,463,247 (11%)	$2,463,247 (2.4%)	$0	$0	$0	$0	$87,973	$17,595
Charitable Contribution	5 (0%)	7 (0%)	4 (0%)	0 (0%)	0 (0%)	17 (0%)	$510 (0%)	$57,360 (0.5%)	$35,250 (0.1%)	$5,640 (0%)	$0 (0%)	$98,760 (0.1%)	$102	$8,194	$8,813	$5,640	$0	$4,550
Long term medical supply or device loan	0 (0%)	0 (0%)	0 (0%)	0 (0%)	3 (0%)	3 (0%)	$0 (0%)	$0 (0%)	$0 (0%)	$0 (0%)	$107 (0%)	$107 (0%)	$0	$0	$0	$0	$36	$7
Debt forgiveness	0 (0%)	0 (0%)	0 (0%)	0 (0%)	3 (0%)	3 (0%)	$0 (0%)	$0 (0%)	$0 (0%)	$0 (0%)	$2,823 (0%)	$2,823 (0%)	$0	$0	$0	$0	$941	$188
Total	$132,963	$80,242	$163,069	$95,215	$130,702	$602,191	$18,474,131	$12,058,059	$29,959,798	$19,542,475	$22,351,849	$102,386,312						

*Services other than consulting includes serving as faculty or as a speaker at a venue other than a continuing education program (CEP).

†Medical Education Program

Table 2. Distribution of Individual Industry Financial Relationships with Anesthesiologists in the Open Payments Database by Monetary Value, 2017-2021

Dollar Value of Payment	Number of Payments						Value of Payments					
	2017	2018	2019	2020	2021	Total	2017	2018	2019	2020	2021	Total
$0-$100	112,955 (85%)	68,889 (85.9%)	135,261 (82.9%)	82,792 (87%)	110,899 (84.8%)	510,796 (84.8%)	$2,236,860 (12.1%)	$1,333,034 (11.1%)	$2,943,348 (9.8%)	$1,644,097 (8.4%)	$2,378,053 (10.6%)	$10,535,392 (10.3%)
$100-$1,000	16,415 (12.3%)	9,510 (11.9%)	23,209 (14.3%)	9,703 (10.2%)	16,291 (12.5%)	75,208 (12.5%)	$3,627,214 (19.6%)	$2,124,408 (17.6%)	$5,303,459 (17.7%)	$2,477,234 (12.7%)	$3,700,371 (16.6%)	$17,232,686 (16.8%)
$1,000-$10,000	3,505 (2.6%)	1,755 (2.2%)	4,315 (2.6%)	2,608 (2.7%)	3,339 (2.6%)	15,522 (2.6%)	$10,401,669 (56.3%)	$5,947,458 (49.3%)	$14,061,190 (46.9%)	$7,372,801 (38.8%)	$9,932,536 (42.7%)	$47,105,574 (46.4%)
$10,000-$100,000	85 (0.1%)	86 (0.1%)	197 (0.1%)	101 (0.1%)	159 (0.1%)	628 (0.1%)	$1,789,018 (9.2%)	$1,507,989 (13%)	$4,143,968 (13.8%)	$2,294,410 (11.7%)	$3,480,260 (15.8%)	$13,186,645 (12.9%)
$100,000-$1,000,000	3 (0%)	2 (0%)	5 (0%)	10 (0%)	14 (0%)	34 (0%)	$508,427 (2.8%)	$1,085,191 (9%)	$856,299 (2.9%)	$3,379,159 (17.3%)	$3,240,629 (14.5%)	$9,069,705 (8.9%)
>$1,000,000	0 (0%)	0 (0%)	2 (0%)	0 (0%)	0 (0%)	3 (0%)	0 (0%)	0 (0%)	$2,651,534 (8.9%)	$2,154,776 (11.1%)	0 (0%)	$4,838,310 (4.7%)
Total	132,963	80,242	163,069	95,215	130,702	602,191	$18,474,128	$12,058,860	$29,959,798	$19,542,477	$22,351,849	$102,386,312

Table 3. Physician Industry Financial Relationships by Specialty, 2017-2021

Specialty	Years	Unique Physicians	New Physicians Receiving Payment	Physicians No Longer Receiving payment	Total Payments	Total Paid	Mean payment per provider	SD of Mean payment per provider	Mean Total payment per provider	SD of Mean Total payment per provider	Maximum total payment
All Physicians	2017	62,465	-	-	625,155	$480,348,664.11	$450.50	$8,394.03	$7,689.88	$125,175.88	$22,969,249.26
	2018	59,232	15,321	18,554	552,221	$444,207,555.57	$478.85	$7,922.26	$7,499.45	$137,659.46	$25,902,328.31
	2019	72,856	25,897	11,495	804,969	$775,858,758.47	$485.94	$8,923.17	$10,624.97	$293,440.56	$50,021,801.62
	2020	57,069	10,817	26,502	453,782	$547,283,706.94	$972.86	$24,830.28	$9,589.86	$155,562.96	$18,220,059.42
	2021	65,223	22,312	14,158	644,783	$602,058,838.29	$880.04	$35,680.96	$9,230.77	$148,794.54	$22,271,490.20
	Total	111,484	-	-	3,142,010	$2,847,757,000.00	$500.22	$21,564.94	$25,544.09	$401,525.50	$76,037,330.00
Anesthesia, only	2017	15,222	-	-	132,963	$18,474,128.92	$116.03	$1,978.46	$1,213.65	$9,214.52	$438,250.55
	2018	13,754	5,635	7,103	80,242	$12,058,060.52	$106.36	$1,565.41	$876.69	$10,747.07	$963,578.99
	2019	20,864	11,260	4,150	163,069	$29,958,798.66	$151.57	$3,839.12	$1,435.96	$16,920.44	$1,598,602.13
	2020	14,167	4,169	10,866	95,215	$19,543,477.08	$247.85	$9,938.00	$1,379.64	$27,584.14	$2,301,858.31
	2021	17,590	8,738	5,315	130,702	$22,351,844.96	$218.66	$5,997.03	$1,270.71	$13,270.65	$797,211.21
	Total	36,117	-	-	602,191	$102,386,308.08	$154.69	$3,101.05	$2,834.85	$32,883.38	$2,582,026.00
All other physicians	2017	47,312	-	-	492,192	$461,874,535.19	$557.69	$9,577.11	$9,762.31	$143,672.30	$22,969,249.26
	2018	45,531	9,755	11,534	451,979	$432,149,494.85	$589.92	$8,991.92	$9,491.32	$156,845.77	$25,902,328.31
	2019	52,153	14,047	7,425	723,080	$743,898,951.81	$618.31	$10,258.68	$14,203.78	$346,545.21	$50,021,801.62
	2020	43,042	6,755	15,886	358,567	$527,741,228.96	$1,208.85	$28,013.23	$12,261.08	$155,204.50	$18,220,059.42
	2021	47,959	13,900	9,003	514,981	$579,706,971.33	$1,117.89	$64,044.41	$12,092.68	$163,932.31	$22,271,490.20
	Total	76,237	-	-	2,539,819	$2,745,371,000.00	$699.52	$25,980.91	$36,011.01	$501,352.00	$76,037,330.00
Anesthesia Critical Care	**All**	1,317	-	-	9,225	$3,938,846.61	$221.51	$1,768.15	$2,990.77	$26,985.16	$587,024.00
Inf-Critical Care	**All**	5,557	-	-	87,260	$14,162,050.00	$189.02	$437.32	$2,548.51	$21,321.86	$950,646.40
Anesthesia Pain Medicine	**All**	5,827	-	-	294,384	$32,857,610.00	$111.21	$1,731.45	$5,638.86	$38,644.33	$1,663,133.00
General Surgery	**All**	30,942	-	-	598,686	$281,430,300.00	$254.15	$3,762.04	$6,589.93	$70,275.32	$8,437,016.00
Orthopedic Surgery	**All**	32,733	-	-	1,372,870	$2,338,940,000.00	$1,210.29	$39,452.85	$71,455.38	$858,920.10	$76,037,330.00
Vascular Surgery	**All**	9,950	-	-	409,085	$190,830,800.00	$364.81	$5,718.79	$15,178.90	$431,120.00	$42,118,160.00

Economics, Education and Policy 13- Visual analysis of provider and patient diversity, equity, and inclusivity in anesthesiology textbooks

David Sender[1], Caitlin Grant[2], Kimberley Nichols[3], Stuart Grant[3]

University of North Carolina[1] Duke University School of Medicine[2] UNC School of Medicine - Department of Anesthesiology[3]

Introduction: The United States population is much more diverse compared to the race and gender profiles of physicians treating them. To combat structural racism we need to examine our historical prejudices that still exist, and begin to deliver our educational resources in a more inclusive and equitable manner. Images of both patients and the physicians treating them are a significant component in medical literature. The "other race effect" is the psychological observation of humans to have difficulty identifying faces of people from other races(1). Psychologists have published on this as a reversible cause of racial bias(2). Representation of individuals as a part of your group leads to increased empathy and improves intergroup attitudes. Visual imaging of role modelling and mentorship is vital for women in underrepresented minorities as they potentially lose the most at the intersection of race and sex(3). We hypothesize the images of patients and physicians in influential anesthesiology textbooks will not represent the demographic diversity of the residency match or US population.

Methods: The project was not human research and did not require IRB approval. The Google Scholar database was then accessed to find all anesthesiology textbooks from January 01, 2005 to June 01, 2022. The full search strategy outcomes are seen in Figure 1(Fig 1. PRISMA flow-chart.). Images of healthcare providers and patients in the 12 most used anesthesiology textbooks were accessed (Table 1. Textbook bibliometric data). All images were batch segregated by a K-means algorithm into 5 clusters based on the Red, Green, Blue (RGB) color-channel histogram(4). Each image was cropped to contain either the face or entire human body. The 2 most dominant colors were extracted from a skin mask of each image by a K-mean clustering algorithm, and presented as a colorbar with RGB valves in Figure 2(Fig 2. Example skin colorbar.) (5). RGB valves for the 6 Fitzpatrick Scale skin tones which range from 1 to 6 , lightest to darkest, and the dominant skin colors were compared using a Delta-E value. The lowest Delta-E value represented the most similar skin tone (Table 2. Delta-E value system.)(Table 3. Example Delta-E values based on Figure 2.)(6). We created 3 classes of skin tones based on the Fitzpatrick Scale they were light as 1-3, olive as 4, and dark as 5-6. Sex classification was defined as female, male, sex unknown.
The dataset was compared to the Association of American Medical Colleges and United States Census Bureau demographic datasets.

Statistical Analysis:
Descriptive statistics was performed with Microsoft Excel. Additional quantitative statistical analysis was performed with GraphPad Prism (Dotmatics, Massachusetts, USA). A Chi square goodness of fit analysis without correction was performed to quantify the significance of the interaction between skin color type and sex in images and AAMC diversity and United States Census Bureau data. For all statistical measurements, a P-value of <0.01 was considered statistically significant.

Results: The textbook images of healthcare providers images showed 106/111 (95.5%) were light skin toned, significantly higher than the percentage of white ACGME anesthesiology residents in 2021 (53.5%, $p < 0.0001$). 5/111 (4.5%) were of dark skin tones which is not significantly different than the percentage of black ACGME anesthesiology residents (5.7%, $p = 0.8349$). In the 26 images where both sex and skin tone were identifiable, no dark skin toned female providers and only 1 dark skin toned male provider image was present. Of the patient images, 653/684(95.5%) were light skin toned, and 23/684 (3.4%) were dark skin toned. Skin tone and sex were both identifiable in 303 patient images, and only 2/303 (0.7%) images of dark skin toned female patients and 4/303 (1.3%) images of dark skin toned male patients were found.

Conclusions: Our study demonstrates the continued underrepresentation of females and darker skin tones in medical textbook imagery. Dark skin female providers were not represented. While textbooks are widely used, journal articles and internet resources have become primary sources. An expansion of this study in the future would assess additional academic resources. Our aim was by highlighting this disparity, we hope to spur actionable change by publishers and authors of educational materials.

References: 1. Culture shapes how we look at faces. PLoS One 2008; 3:e3022

2. A meta-analysis of procedures to change implicit measures. J. Pers. Soc. Psychol. 2019; 117:522–59

3. Women physicians and promotion in academic medicine. N. Engl. J. Med. 2020; 383:2148–57

4. Image Segmentation Using K -means Clustering Algorithm and Subtractive Clustering Algorithm. Procedia Computer Science 2015; 54:764–71

5. Human Skin Detection Using RGB, HSV and YCbCr Color Models, Advances in Intelligent Systems Research, 1st edition. Netherlands, Atlantic-Press, 2016, pp 324–32

6. Skin color match in head and neck reconstructive surgery. Laryngoscope 2022; 132:1753–9

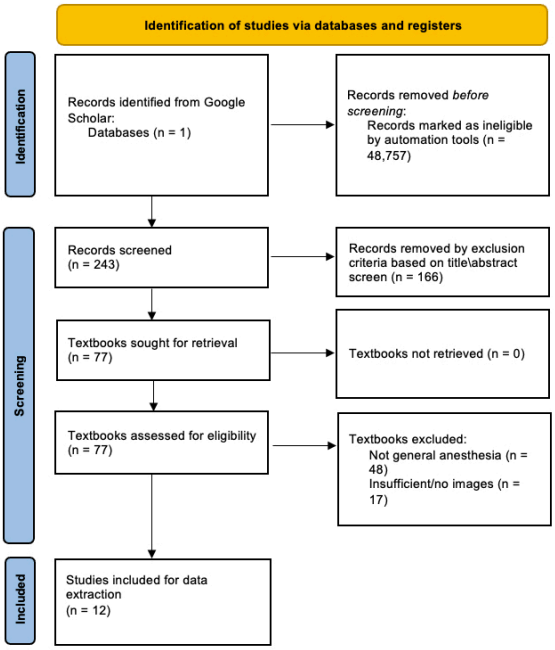

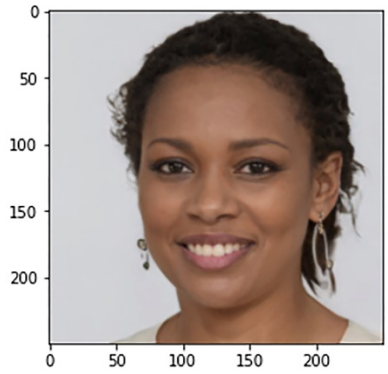

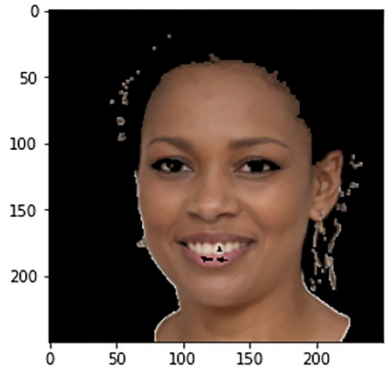

Table 3: Delta E values for the dominant color (120, 82, 64) seen in Figure 1, compared with each of the RGB values for the 6 Fitzpatrick scale groups.

Fitzpatrick Skin Scale Group	Delta E
1	66.5818945
2	80.9554033
3	79.3741475
4	61.4591533
5	33.2823368
6	19.7682399

Table 2: Delta E scale from 0 to 100.

delta E	Perception
≤1	Not perceptible by human eyes
1 – 2	Perceptible by close observation by a trained observer
2 – 3.5	Perceptible to an untrained observer
3.5 – 5	A clear difference
6 – 10	A very obvious difference
10 – 49	Colors are more similar than opposite
50 – 99	Colors are more opposite than similar
100	Colors are exact opposite

Table 1: Anesthesiology textbook bibliometric demographics

Title	Editors	Year	Edition	Language	Citations	Page count	Country of publication	Publisher	ISBN
Clinical Anesthesia	Paul G. Barash, Bruce F. Cullen, Robert K. Stoelting, Michael K. Cahalan, M. Christine Stock, Rafael Ortega, Sam R. Sharar, Natalie F. Holt.	2017	8th	English	1887	1808	USA	Wolters Kluwer	9781496337016, 1496337018
Miller's Anesthesia	Michael A. Gropper, Ronald D. Miller, Lars I. Eriksson, Lee A Fleisher, Jeanine P. Wiener-Kronish, Neal H Cohen, Kate Leslie.	2019	9th	English	1751	3112	USA	Elsevier	9780323612647, 0323812644
Stoelting's Pharmacology & Physiology in Anesthetic Practice	James P. Rathmell, Pamela Flood, Richard D. Urman.	2021	6th	English	1561	984	USA	Wolters Kluwer	9781975126896, 1975126890
Morgan and Mikhail's Clinical Anesthesiology	David C. Mackey, John D. Warnick, John F. Butterworth.	2022	7th	English	661	1456	USA	McGraw-Hill Education	9781260473797, 1260473791
Basics of Anaesthesia	Manuel Pardo, Ronald D. Miller	2017	7th	English	574	936	USA	Elsevier	9780323401159, 0323401155
Smith and Aitkenhead's Textbook of Anaesthesia	Iain Moppett, Jonathan Thompson, Matthew Wiles.	2019	7th	English	436	1084	UK	Elsevier	9780702075346, 0702075345
Anesthesia and Uncommon Diseases	Lee A. Fleisher.	2012	6th	English	209	641	USA	Elsevier Saunders	9781437727876, 1437727875
Anesthesiologist's Manual of Surgical Procedures	Brenda Golianu, Clifford Schmiesing, Richard A. Jaffe.	2014	5th	English	117	1952	USA	Wolters Kluwer	9781496371270, 1496371275
Stoelting's Anesthesia and Co-existing Disease	Roberta L. Hines, Katherine E. Marschall	2017	7th	English	149	736	USA	Elsevier	9780323718608, 0323718604
Pharmacology and Physiology for Anesthesia Foundation and Clinical Application	Hugh C. Hemmings, Talmage D. Egan.	2018	2nd	English	88	784	USA	Elsevier	9780323568869, 0323568866
Yao & Artusio's Anesthesiology: Problem-oriented Patient Management	Fun-Sun F. Yao, Hugh C. Hemmings (Jr.), Jill Fong, Vinod Malhotra.	2021	9th	English	79	1288	USA	Wolters Kluwer	9781975120016, 1975120019
Clinical Anaesthesia	Carl L. Gwinnutt, Matthew Gwinnutt.	2016	5th	English	70	192	UK	Wiley-Blackwell	9781119119852, 1119119855

Geriatric Anesthesia

Geriatric Anesthesia 1- Gut microbiota is associated with postoperative delirium in patients

Yiying (Laura) Zhang[1], Kathryn Baldyga[1], Yuanlin Dong[1], Wenyu Song[1], Edward Marcantonio[2], Zhongcong Xie[3]

Massachusetts General Hospital/Harvard Medical School[1] Beth Israel Deaconess Medical Center[2] Massachusetts General Hospital and Harvard Medical School[3]

Introduction: Postoperative delirium, one of the most common postoperative complications in older patients, is associated with adverse outcomes and $32.9 billion in healthcare costs per year in the United States [1]. However, postoperative delirium's pathogenesis and biomarker(s) remain largely undetermined. It has been well-known that gut microbiota can regulate brain function[2]. Therefore, we set out to test a hypothesis that patients with postoperative delirium have a specific gut microbiota profile. The study outcomes would answer why some patients are more vulnerable to developing postoperative delirium and whether we can target gut microbiota to prevent or treat postoperative delirium in patients, leading to better surgical care.

Methods: This prospective observational cohort study was performed at Massachusetts General Hospital, Boston, MA, between 2016 and 2020 in patients 65 years old or older undergoing laminectomy, knee, or hip replacement under general or spinal anesthesia. The Mass General Brigham Institutional Review Board approved the study protocol. All patients gave written informed consent. Participants were excluded if they had (1) past medical history of neurological and psychiatric diseases, including Alzheimer's disease, other forms of dementia, stroke, or psychosis; (2) severe visual or hearing impairment; (3) current smoking; or (4) taking antibiotics within one week of the day of surgery. The Confusion Assessment Method (CAM) and Memorial Delirium Assessment Scale (MDAS) were performed by trained clinical research coordinators to determine the incidence and severity of postoperative delirium on postoperative day 1 and/or 2 (once per day between 8:00 am and 12:00 noon) as described before[3]. Fecal swabs were collected from participants at the completion of surgery. The 16S rRNA gene sequencing was performed by BGI America (Cambridge, MA) as described before[4].
We developed a novel method that infused current research knowledge into the data-driven methodology, filtering through several hundred variables in a small data set to identify relevant gut bacteria. Finally, we performed logistic regression to determine the association between gut microbiota and postoperative delirium. Results are presented as highly associated bacteria composed of the most significant principal component, in the form of odds ratio per standard deviation increase in the bacteria (i.e., z-score) and their associated 95% confidence intervals.

Results: We screened 491 patients and included 86 participants in the final data analysis. Ten (12%) of 86 participants (73±4.4 years old, 50% female) developed postoperative delirium. There were no significant differences in characteristics between the participants with and without postoperative delirium except for the postoperative MMSE score (Table 1). A total of 740 microbes were identified and used for PCA analysis. The participants with and without postoperative delirium had a different index of principal component 8 from 12 principal component groups (Table 1). Postoperative gut bacteria Parabacteroides distasonis [Odds ratio (OR): 3.13, 95% Confidence intervals (CI): 1.28-7.65, P=0.012], Prevotella (OR: 0.37, 95%CI: 0.14-0.95, P=0.040) and Collinsella (OR: 0.37, 95%CI: 0.14-0.96, P=0.042) were associated with postoperative delirium incidence after adjusting age, sex, preoperative mini-mental state examination, and anesthesia type. The participants who developed postoperative delirium had a higher and lower abundance of postoperative gut bacteria Parabacteroides distasonis and Prevotella, respectively.

Conclusions: In conclusion, we demonstrated that patients who developed postoperative delirium had a higher abundance of postoperative gut bacteria Parabacteroides distasonis and a lower abundance of postoperative gut bacteria Prevotella than those who did not. The abundance of postoperative gut bacteria Parabacteroides distasonis, Prevotella, and Collinsella were associated with the incidence of postoperative delirium in patients. These findings will help physicians and patients understand that anesthesia and surgery are not the only factors associated with postoperative delirium. Instead, patients' gut microbiota dysbiosis significantly contributes to postoperative delirium. Finally, these findings will promote more research to prevent or treat postoperative delirium by restoring gut microbiota dysbiosis.

References: 1. One-Year Medicare Costs Associated With Delirium in Older Patients Undergoing Major Elective Surgery. 2021;156(5):430-442.

2. Mind-altering microorganisms: the impact of the gut microbiota on brain and behaviour. 2012;13(10):701-12.

3. Preoperative Plasma Tau-PT217 and Tau-PT181 Are Associated With Postoperative Delirium. 2022

4. Anesthesia and surgery induce age-dependent changes in behaviors and microbiota. 2020;12(2):1965-1986.

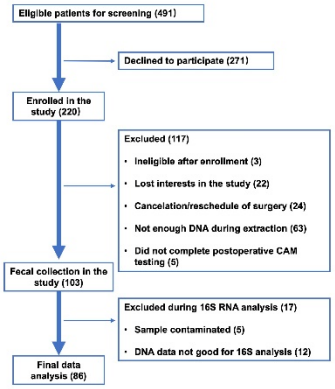

Table 1. Demographic characteristics of the participants

	Delirium N = 10	No Delirium N = 76	P-value
Age, mean ± SD	73 +/- 4.45	72 +/- 5.56	0.217
Female, n (%)	5 (50)	49 (64)	0.521
Non-white or Hispanic, n (%)	1 (8)	3 (3)	0.289
Education years, mean ± SD	15.7 +/- 1.34	16.35 +/- 2.66	0.267
Surgery type, n (%)			
Knee replacement	5 (50)	48 (63)	0.332
Hip replacement	3 (30)	23 (30)	
Spinal stenosis	2 (20)	5 (7)	
Anesthesia type, n (%)			
General	6 (60)	40 (53)	0.661
Spinal	4 (40)	36 (47)	
MMSE			
Pre-surgery score	29.08 +/- 0.95	29.01 +/- 1.07	0.256
Post-surgery score (average)	27.38 +/- 1.96	29.01 +/- 1.16	0.001

MMSE, mini-mental status examination; S.D., standard deviation

Table 2. Parabacteroides distasonis significant predictors of postoperative delirium presence *

	Presence of Postoperative Delirium **			
	Unadjusted		Adjusted for age, sex, preoperative MMSE, and anesthesia type	
	Odds Ratio (95% CI)	P-Value	Odds Ratio (95% CI)	P-Value
Parabacteroides distasonis	2.46 (1.15 to 5.28)	0.021	3.13 (1.28 to 7.65)	0.012
Prevotella	0.43 (0.18 to 1.03)	0.059	0.37 (0.14 to 0.95)	0.040
Collinsella	0.46 (0.19 to 1.11)	0.086	0.37 (0.14 to 0.96)	0.042

*** Models were created to adjust the associations between the bacteria and outcomes for age, education, and preoperative MMSE based on previous studies as deemed clinically relevant.**

**** Results are presented as odds ratio (OR) per one unit change in Parabacteroides distasonis value and its associated 95% confidence intervals (CI) with the null hypothesis of 1.**

Geriatric Anesthesia 2- Long-term cognitive decline after elective total joint arthroplasty: a population-based approach

Angelina Tang[1], L. Grisell Diaz-Ramirez[2], W. John Boscardin[2], Alexander Smith[1], Derek Ward[1], Elizabeth Whitlock[1]

University of California, San Francisco[1] UCSF[2]

Introduction: Twenty percent of older adults undergoing elective total joint arthroplasty (TJA) meet criteria for postoperative neurocognitive disorder (NCD) at twelve months after surgery. (1) However, the population-level clinical significance of this is unknown. Because TJA results in pain relief and improved mobility and sleep, which may be cognitively beneficial, the average long-term cognitive outcome from TJA is important to measure. As older adults continue to be among the highest utilizers of TJA (2), understanding long-term cognitive outcomes after TJA compared to other common surgeries and compared to nonsurgical matched controls will help us contextualize the measured rate of NCD.

Methods: We linked Health and Retirement Study (HRS) data to Medicare claims and identified adults who underwent elective TJA between 1998 and 2018 at age 65 or older. Surgical controls were adults 65 or older who underwent elective surgery not expected to result in functional benefits (e.g., cholecystectomy; hysterectomy). TJA recipients were also compared to age- and sex-matched older adults who did not undergo TJA and either did, or did not, report being often troubled by moderate-severe pain at the HRS interview prior to a randomly-selected date used for modeling purposes ("pain" and "no pain" controls). The primary outcome was change in memory score, a z-score-based summary measure of biennial HRS immediate and delayed word recall scores and proxy cognition reports,(3) from the time of surgery to three years after surgery in the TJA versus the surgical control group. We modeled memory score using linear mixed effects regression adjusted for health and demographic factors, flexibly modeled with restricted cubic splines (knots at -4, 0, 8 years; discontinuity at surgery) and including survey weights to recapitulate the United States population of older adults. Secondarily, we compared this amount of memory decline in TJA recipients to that observed in pain and no-pain controls who did not undergo TJA.

Results: There were 1,947 TJA recipients (average age 74; 63% female, 11% of a race/ethnicity other than white), 1,631 surgical controls (average age 76, 38% female, 15% nonwhite), and 3,894 age- and sex-matched nonsurgical controls. TJA recipients' average memory score declined by 0.17 [0.15-0.19] units from the time of surgery to 3 years postoperatively, while surgical controls' average memory score declined by 0.21 [0.19-0.23] units (difference: 0.04 [0.01-0.07] units; p=0.009). Controls with pain declined 0.03 [0.003-0.05] units more than TJA recipients, and controls without pain were statistically indistinguishable (difference: 0.02 [-0.01 to 0.04] units). (Figure)

Conclusions: The population-average amount of memory decline in the three years after TJA in older adults is smaller than for other surgical procedures or age- and sex-matched older adults with pain, and is indistinguishable from pain-free, age- and sex-matched controls who did not undergo surgery. Despite a measurable rate of NCD after TJA, on average, older TJA recipients experience a favorable long-term cognitive outcome.

References: (1) Anesth Analg 2020; 131:1582-1588

(2) J Bone Joint Surg 2018; 100:1455-1460

(3) Alzheimer Dis Assoc Disord 2013; 27:207-212

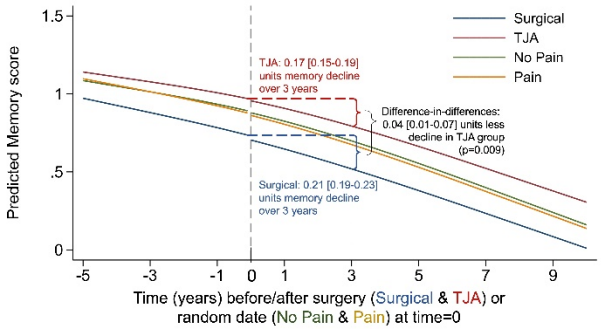

Geriatric Anesthesia 3- Qualitative analysis of lay descriptions of postoperative cognitive dysfunction

Laura Li[1], Adam Staffaroni[1], Daniel Dohan[1], Alexander Smith[2], Elizabeth Whitlock[2]

Chicago Medical School[1] University of California, San Francisco[2]

Introduction: Postoperative cognitive dysfunction (POCD) disproportionately affects older adults after surgery and anesthesia. It is infeasible to conduct neuropsychiatric testing on all older adults after surgery, so patients' reports of POCD symptoms are clinically important. These experiences of symptoms have not been well described.

Methods: We performed inductive qualitative analysis on website user comments anonymously submitted in response to "*The hidden long-term risks of surgery: 'It gives people's brains a hard time'"* published by United Kingdom-based news source The Guardian in April 2022. The analytic team was a preclinical medical student, a clinical anesthesiologist, and a neuropsychologist. We analyzed patient and caregiver-reported symptoms and their alignment with neuropsychiatric domains, particularly those most associated with POCD (memory and executive function).

Results: We analyzed 39 anecdotes from 38 unique users. Nine anecdotes denied cognitive symptoms. Of those with cognitive complaints, memory problems ("used to have a partially photographic memory"), psychological or personality changes ("a strange sort of depression"), and difficulty concentrating ("concentration was woeful") were common. Memory complaints sometimes overlapped with executive function deficits, e.g., difficulty holding complex information in mind (working memory). New reading difficulty appeared to be consistent with a working memory deficit in 3 anecdotes. 6 anecdotes cited brain fog ("I was a foggy mess"), which localizes poorly to traditional neuropsychiatric cognitive domains. Notably absent from the anecdotes were descriptions of visuospatial deficits. See Table for representative quotes.

Conclusions: Patients and caregivers describe deficits in memory and executive function (particularly working memory), psychological symptoms (commonly depression), and brain fog after surgery. These reported symptoms align with and extend beyond neuropsychiatric domain-based deficits seen in POCD. Understanding common subjective symptoms of POCD may support earlier identification and referral for testing and therapy for patients experiencing POCD.

TABLE 1: Representative quotes, by domains and sub-domains.

Memory		
	Isolated memory	"He lost his ability to make new memories overnight and has slowly declined since."
		"My memory, never particularly brilliant, is now distinctly poorer."
	Memory/executive function overlap	"I figured once they find the reason for the memory loss we could try medication to boost the brain back to normal levels… I used to have a partially photographic memory and it's now gone and its hard for me to read like I used too *[sic]*."
		"Until the operation I had a 360° memory, which could retain the multi-layered information & awareness [professionals] require…I can retain the primary info well enough, but I find I lack the circuitry to process the secondary or contradictory without effort…In all other regards my career continues, but I have to make conscious mental notes instead of being able to recall them effortlessly."
Psychological Changes		
	Depression	"I was like a different person when I came out, I had a strange sort of depression and I cried for hours every day, for nearly six weeks."
		"It was like everything was painted in a darker color, as if I had a weaker shell than I usually had and therefore was threatened in a way I usually was not."
		"He had depression afterwards, which was only treated after about 2 years and he was back to normal
	Personality	"He became violent. His violent outbursts culminated in a difficult encounter with police (they did a great job, were amazing, actually)."
		"The vivacious person that went into the operation disappeared replaced with someone who was quieter and not firing on all cylinders."
Executive Function		
	Concentration	"Couldn't work, concentration was woeful, even reading was a struggle."
		"My brain wasn't the same, suffering brain fog, no concentration and a short fuse"
	Working memory	"I found I could no longer read…three years on I am still only managing to read a few pages at a time. ….I have trouble building up an overview of the argument being presented. My mind seems to miss key pieces of information as I go, making the whole more and more incomprehensible."
	Other executive	"I really cannot multi-task anymore."
Brain Fog		
		"I was a foggy mess for a couple of days afterwards."
		"Still have brain fog, lethargy, and other minor niggles."

Geriatric Anesthesia 4- 3D-CAM severity scores correlate with the DRS and with biomarkers of delirium

Richard Lennertz[1], Cameron Rivera[1], David Kunkel[1], Maggie Parker[1], Cameron Casey[2], Robert Pearce[1], Robert Sanders[1]

University of Wisconsin-Madison[1] University of Wisconsin - Madison[2]

Introduction: Numerous methods are used to assess delirium. The advantages of different methods, and whether the methods yield comparable results, are unclear. Here, we focus on two common assessment methods: the 3-Minute Confusion Assessment Method delirium (3D-CAM) and the Delirium Rating Scale – Revised – 98 (DRS). Our primary objective was to compare delirium severity scores derived from the two assessment methods in a postoperative patient population. Secondary objectives were to assess the relationship of severity scores derived from the 3D-CAM with electrophysiologic features and biological markers of delirium. Further, we compare peak severity scores with delirium length and area-under-the-curve (AUC) quantifications of delirium severity.

Methods: Data were collected as part of an ongoing observational cohort study of perioperative delirium. The study was registered with ClinicalTrials.gov and approved by the Institutional Review Board. Patients over the age of 65 undergoing major elective surgery with an anticipated hospital stay of at least 2 days were recruited. Patients were excluded if they had a documented history of dementia, resided in a nursing home, or could not complete neurocognitive testing. Participants completed a preoperative baseline assessment, and postoperative assessments twice daily for up to 4 days (PODs) or until delirium resolved. Blood samples were collected before surgery and on each postoperative day. High density electroencephalogram recordings were performed before surgery and at least once after surgery.

Results: Of 226 subjects enrolled, 204 underwent surgery and completed paired 3D-CAM and DRS assessments after surgery. 27.5% (56/204) of subjects were delirious during their postoperative recovery according to 3D-CAM or CAM-ICU assessments. There was a strong, direct correlation between peak 3D-CAM and DRS severity scores ($\rho = 0.74$, $p < 0.001$, $n = 204$). This correlation was stronger for delirious subjects than for non-delirious subjects (estimated $\rho_{delirious} - \rho_{non\text{-}delirious} = 0.30$, 95% CI [0.15, 0.44]; $p < 0.001$). Higher 3D-CAM severity scores correlated with worse performance on the postoperative Trail Making Test B, a measure of cognitive function and attention ($\rho = 0.40$, $p < 0.001$, $n = 177$). 3D-CAM severity scores directly correlated with slow-wave (0.5-6Hz) EEG power ($\rho = 0.30$, $p = 0.001$, $n = 73$), and the plasma biomarkers neurofilament light ($\rho = 0.37$, $p < 0.05$, $n = 61$) and total tau ($\rho = 0.41$, $p < 0.001$, $n = 63$). Comparing different quantifications of delirium severity, peak 3D-CAM severity scores directly correlated with length of delirium ($\rho = 0.74$, $p < 0.001$, $n = 204$). AUC directly correlated with peak severity scores for both the 3D-CAM ($\rho = 0.90$, $p < 0.001$, $n=182$) and DRS ($\rho = 0.84$, $p < 0.001$, $n=182$).

Conclusions: There was a strong correlation between 3D-CAM and DRS severity scores in postoperative patients. Interestingly, this correlation was stronger for delirious patients than for non-delirious patients. 3D-CAM severity scores correlated with electrophysiologic features and biomarkers of delirium, all of which have previously demonstrated correlations with DRS severity scores. Peak severity scores, length, and AUC quantifications of delirium were strongly correlated with each other. In summary, we observed strong agreement between results using either the 3D-CAM or the DRS assessment method.

Geriatric Anesthesia 5- Chronic pain-induced methylation in the prefrontal cortex targets a microglia gene network associated with human cognition and Alzheimer's disease: an integrative network analysis of multiomic data

Joseph Scarpa[1], Joshua Mincer[2]

New York Presbyterian Hospital - Weill C[1] Memorial Sloan Kettering Cancer Center[2]

Introduction: Significant deficits in memory and executive function have been noted in patients with chronic pain[1], and longitudinal studies show that patients with persistent pain have accelerated memory decline and increased probability of dementia[2]. In this study, we explore the hypothesis that chronic pain and cognition share common molecular mechanisms by examining if the functional epigenetic changes induced by chronic pain target gene networks relevant to cognitive function and Alzheimer's disease (AD).

Methods: This study is a retrospective analysis that integrates large-scale publicly-available epigenomic, genomic, transcriptomic, and pathological data collected for various prospective experiments across multiple species. Two Alzheimer's disease cohorts were used - the Harvard Brain Bank (HBB, Ncases=376, Ncontrols=173)[3] and the Mount Sinai Brain Bank (MSBB, N=125)[4]. Microarray platforms were used to estimate gene expression for each cohort and neuropathologic disease features were estimated by each institution's respective pathology department.

To study molecular pathways in the frontal cortex underlying human cognitive ability, gene expression data in 102 postmortem human brains was used from the UK Brain Expression Consortium[5]. Gene expression was measured on the Affymetrix Human Exon 1.0 ST Array.

To study molecular effects of chronic opioid use, RNA-sequencing gene expression data was used from the dorsolateral prefrontal cortex of people diagnosed with opioid use disorder (n = 20) and unaffected comparison subjects (n = 20)[6].

To study molecular signatures of chronic pain, DNA methylation profiles were used from the prefrontal cortex of Sprague-Dawley rats nine months after spared nerve injury (Ninjury=8, Nsham=8)[7]. DNA methylation and expression were previously validated with gene-specific real-time PCR.

Pain and cognition causal gene signatures were derived from The Mouse Genome Database (MGD), which catalogues phenotypes for gene knockout experiments across several mouse lines.

Weighted gene coexpression analysis (WGCNA) was used to determine how genes are organized into gene networks[8]. Hierarchical clustering defined gene modules were assigned arbitrary labels (names or colors). To associate modules with clinical or neuropathologic phenotypes, the first principal component was correlated with the relevant phenotypic measurement. Fisher's exact test was used to estimate statistical overrepresentation between various gene network, gene expression, and epigenomic gene signatures. The Bonferroni method was used to correct p-values for multiple testing, when appropriate.

Results: We identified 8,176 human homologs for genes previously identified as differentially methylated nine months after spared nerve injury in a rat model. This chronic pain-associated epigenomic landscape (CPAEL) is overrepresented with known causal pain genes (P=2.9x10-8, Odds Ratio=3.2(2.1-4.9)) and causal regulators of abnormal learning, memory, and conditioning phenotypes in experimental mouse models (p=3.6x10-32, OR=2.5(2.2-2.9)) (Fig1).

In human cohorts, CPAEL is enriched with two previously identified cortical networks ("M1" and "M3") associated with human cognition (Fig 2). CPAEL targets 41% of "M1" (P=3.1x10-20, OR=1.8[1.6-2.1]) – a gene network associated with crystalized cognitive ability and delayed recall – and 42% of "M3" (P=0.003, OR=1.7[1.2-2.4]) – a gene network associated with delayed recall and general fluid cognitive flexibility.

Analyses of gene expression and neuropathologic data in an AD cohort (N=549, HBB) revealed that the CPAEL signature also is enriched for several AD-relevant gene networks, including the "Yellow" prefrontal cortex gene network (P=2.7x10-92, OR=4.4[3.9-4.9]), which is associated with microglia and immune pathways, gains connectivity in AD, and correlates with seventeen neuropathologic traits including atrophy of the frontal, temporal, and parietal cortices. This finding was validated in an independent human cohort (N=125, MSBB).

Lastly, we found that chronic opioid use selectively modulates this microglia gene network ($p < 0.05$, OR=6.6[5.1-8.5]), but no other cortical AD networks (Fig 3).

Conclusions: Methylation in response to chronic pain targets a microglia gene network in the prefrontal cortex associated with mouse learning and memory models, human cognitive ability, and human Alzheimer's disease. Chronic opioid use selectively modulates this microglia gene network, but not other cortical networks linking AD and pain.

References: 1. *J Am Geriatr Soc* 2015; 63: 1503 1511

2. *Jama Intern Med* 2017; 177: 1146 1153

3. *Cell* 2013; 153: 707 720

4. *Genome Med* 2016; 8: 104

5. *Nat Neurosci* 2016; 19: 223 232

6. *Biol Psychiat* 2021; 90: 550–62

7. *Sci Rep* 2016; 6: 19615

8. *Stat Appl Genet Mol* 2005; 4: Article17

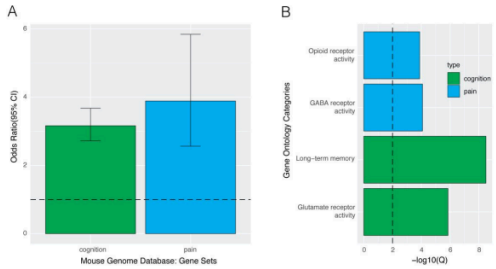

Figure 1. (A) CPAEL is overrepresented for cognition (green) and pain (blue) causal gene signatures from the Mouse Genome Database. Odds Ratio with 95% CI is depicted on the y axis. (B) The cognition (green) and pain (blue) gene signatures are overrepresented for relevant gene ontology categories. -Log10 of adjusted p-values are labeled on the x axis.

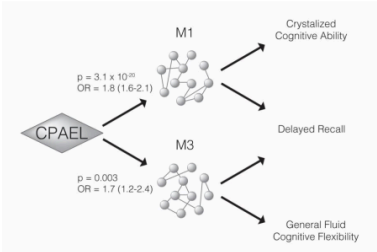

Figure 2. CPAEL is overrepresented for M1 and M3 gene networks associated with human cognitive traits (far right). Fisher exact test p values and odds ratio with 95% CI are labeled for the respective networks.

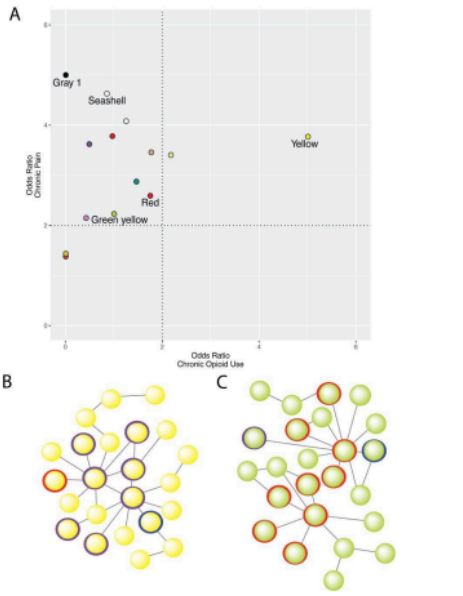

Figure 3. (A) Cortical gene networks in an Alzheimer's cohort are pictured, with the color of each dot corresponding to its module color name. For each AD network, Fisher exact test odds ratio for CPAEL (y-axis) and chronic opioid use gene signatures (x-axis) are plotted. Vertical and horizontal lines each mark a threshold of 2. The five gene networks most strongly associated with AD in previous analyses are labeled. The dots in the top right corner are networks enriched for both chronic pain and chronic opioid use. (B, C) Pictorial representation of "Yellow" network and "Green yellow" network. Red outlines mark nodes modulated by chronic pain, blue nodes are those modulated by opioid use, and purple nodes are those modulated by both conditions.

Geriatric Anesthesia 6- Kidney function and opioid dosing in the older surgical population

Frederick Sieber[1], Naeyuh Wang[1]

Johns Hopkins University - Bayview Medic[1]

Introduction: Previous studies in hip fracture patients demonstrate that during the intraoperative period interaction exists between preoperative kidney function and opioid dosing such that the elevated odds of postoperative delirium (POD) associated with the same amount of increase in opioid dosing are more pronounced with poorer kidney function (1). This effect was not found with opioid dosing in the PACU or during postoperative day1. This finding is important for pain management of older frail surgical patients because changing the manner in which intraoperative opioid dosing is currently done may represent a possible intervention to prevent delirium. The aim of this study was to determine the range of potential effect size for the interaction between poor baseline kidney function and intraoperative opioid dose for increasing odds of POD in the older surgical population. Because some narcotics have metabolites which are primarily renally excreted, it was also determined whether the range of potential effect size for the interaction between poor baseline kidney function and intraoperative opioid dose for increasing odds of POD in the older surgical population is altered by the type of opioid administered.

Methods: Following IRB approval EMR downloads for all surgical patients at our institution ≥ 65 years from 3/2018 – 2/29/2020 were obtained. These downloads include all laboratory values, physiologic values, drugs administered, co-morbidities (e.g., elixir comorbidity index), and pain scores. Also included is preoperative frailty scoring (Edmonton frailty score) as well as postoperative delirium testing (4AT) in the PACU and on the wards.

Inclusion criteria: ≥65 years of age, frailty score performed within six months prior to date of surgery, at least one 4AT score performed within the first two postoperative days, elective surgery with at least 1 night spent in hospital. Only the first case was analyzed if index hospitalization included 2 or more surgeries.

Adjusted odds ratio for risk of having postoperative 4AT score ≥4 was computed, accounting for relevant patient characteristics. Confidence interval was derived to inform the range of potential effect size. All statistical tests were 2-tailed, and $P < .05$ was considered to indicate statistical significance.

Results: Pre and perioperative demographics and variables are seen in tables 1 and 2 where patients are grouped by baseline glomerular filtration rate (GFR). Interaction was observed between perioperative kidney function and intraoperative fentanyl dosing such that the elevated odds of POD associated with the same amount of increase in fentanyl dosing are more pronounced with poorer kidney function (Fig). Significant interaction was not found with any other type of opioid administered either intra or postoperatively.

Conclusions: Intraoperative fentanyl dosing appears to impose greater risk for POD when kidney function is lower. Further study is warranted to determine optimal dosing regimens of fentanyl in older patients with impaired kidney function.

References: 1. J Am Geriatr Soc 69:191-196, 2021.

Table 1: Preoperative demographics

Variable	GFR<60 (n=125)	GFR≥60 (n=212)
Age, Mean (SD)	74.5 (6.5)	72.9 (5.9)
Female, n (%)	52 (41.6)	80 (37.7)
Caucasian, n (%)	88 (70.4)	157 (74.1)
ASA status, n (%)		
II	16 (12.8)	68 (32.1)
III	95 (76.0)	131 (61.8)
IV	14 (11.2)	13 (6.1)
Frailty, n (%)	44 (35.2)	46 (21.7)
Coronary artery disease, n (%)	8 (6.4)	9 (4.3)
Peripheral Vascular disease, n (%)	31 (24.8)	44 (20.8)
Congestive heart failure, n (%)	31 (24.8)	19 (9.0)
Dementia, n (%)	6 (4.8)	6 (2.8)

Table 2: Perioperative Variables

variable		CKD GFR<60	CKD GFR≥60
Type of Surgical procedure, n (%)	General	45 (36.0)	106 (50.0)
	Vascular	42 (33.6)	50 (23.6)
	Neurosurgery	5 (4.0)	17 (8.0)
	Urology	14 (11.2)	15 (7.1)
Postoperative delirium, n (%)		8 (6.4)	10 (4.7)
Postop average pain score	Day of Surgery	4.1 (2.5)	3.6 (2.2)
	Day 1 after Surgery	4.0 (2.3)	3.7 (2.0)
Cumulative opioid dose:	IntraOp	39.2 (28.9)	42.0 (26.7)
(all in oral morphine equivalent, in mg)	PostOp Day of Surgery	17.0 (23.7)	14.0 (20.8)
	PostOp Day 1	21.4 (41.1)	13.8 (21.7)
Length of stay		3.8 (2.9)	4.3 (4.9)
Discharge home, n (%)		73 (58.4)	129 (60.8)
Discharge to Rehab or nursing facility, n (%)		22 (17.6)	43 (20.3)

Figure. Odds ratios of postoperative delirium associated with opioid dose by kidney function level. Odds ratio adjusted for age, American Society of Anesthesiologists status, and dementia status.

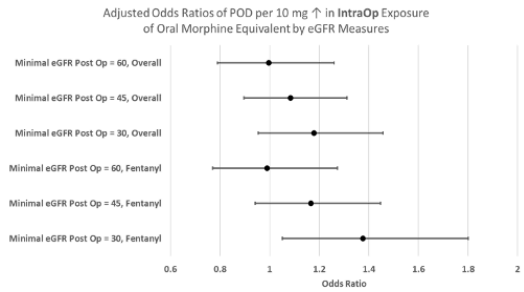

Global Health

Global Health 1- Anesthesiologist Burn-Out During the COVID-19 Pandemic

Faisal Elali[1]

SUNY Downstate Health Sciences University[1]

Introduction: The purpose of this epidemiological study is to investigate the effects of the COVID-19 pandemic on anesthesiologist burnout from 2019 through 2022. Burnout is a psychological phenomenon that is characterized by emotional exhaustion, depersonalization, and a sense of reduced personal accomplishment. Anesthesiologists are particularly vulnerable to burnout due to the high-pressure environment of their profession. The COVID-19 pandemic has had a profound effect on the healthcare system, and it is likely that anesthesiologists have been affected by the increased workload and stress associated with the pandemic. This study will examine the prevalence of burnout among anesthesiologists during the pandemic and investigate potential factors that may be associated with increased burnout.

Methods: Data for this study was collected from the National Practitioner Data Bank (NPDB). The NPDB is a comprehensive database of healthcare practitioners in the United States that includes information on demographic characteristics, professional qualifications, and malpractice claims. It also includes demographic information, such as age, gender, and years of experience, as well as information on burnout, such as the Maslach Burnout Inventory (MBI) scores, once re-coded. The MBI is a widely used measure of burnout that assesses three dimensions of burnout: emotional exhaustion, depersonalization, and personal accomplishment. The data was collected from 2019 through 2022.

The data was analyzed using descriptive statistics and logistic regression. Descriptive statistics were used to examine the prevalence of burnout among anesthesiologists during the pandemic. Logistic regression was used to investigate potential factors associated with increased burnout, such as age, gender, and years of experience.

Results: The results of the study showed that the prevalence of burnout among anesthesiologists during the pandemic was significantly higher than the pre-pandemic levels. The average MBI scores for emotional exhaustion, depersonalization, and personal accomplishment were all significantly higher during the pandemic than before the pandemic (emotional exhaustion: pre-pandemic mean = 2.3, pandemic mean = 3.2; depersonalization: pre-pandemic mean = 1.7, pandemic mean = 2.5; personal accomplishment: pre-pandemic mean = 4.2, pandemic mean = 3.7). The logistic regression analysis revealed that age, gender, and years of experience were all significantly associated with increased burnout (age: odds ratio = 1.2, 95% CI = 1.1-1.3; gender: odds ratio = 1.3, 95% CI = 1.1-1.5; years of experience: odds ratio = 1.1, 95% CI = 1.05-1.2).

Conclusions: The results of this study indicate that the COVID-19 pandemic has had a significant impact on anesthesiologist burnout. The prevalence of burnout among anesthesiologists during the pandemic was significantly higher than before the pandemic, and certain demographic factors, such as age, gender, and years of experience, were associated with increased burnout. These findings suggest that anesthesiologists should be aware of the potential for burnout during the pandemic and take steps to mitigate the risk, such as engaging in self-care activities and seeking support from colleagues. Additionally, healthcare organizations should consider implementing strategies to reduce the risk of burnout among anesthesiologists, such as providing additional resources and support.

Global Health 2- Projecting carbon emissions with low fresh gas flow rates for inhalational anesthetic agents

Saad Khan[1], Matthew Lam[1], Harshaan Dhaliwal[1], Mark Reisbig[2], Cassandra Hays[1]

Creighton University School of Medicine[1] CHI Creighton University Medical Center[2]

Introduction: Volatile anesthetic gases such as sevoflurane, isoflurane, and desflurane are major culprits in the production of greenhouse gases. The healthcare industry contributes nearly 10% of greenhouse gas emissions in the United States [1]. Approximately 20 to 33% of hospital emissions are generated in the operating room, with 51% of operating room emissions a direct result of anesthetic gases [2]. The environmental harm of these volatile agents vary, with desflurane having a significantly longer atmospheric lifetime and a global warming potential (GWP) 2,540 times that of CO_2 [3]. These differences in GWP present an opportunity to evaluate the use of these gases in current practice with the aim of reducing hospital carbon emissions. At our institution, we analyzed emissions over a fixed period where desflurane use declined and projected further reductions in emissions if manufacturer suggested fresh gas flow (FGF) rates would be adopted.

Methods: Purchasing data was acquired from the pharmacy of a 400-bed academic medical center in the Midwest over a period of approximately 6 years. This data comes from a hospital that does not perform elective surgeries; case numbers were not affected by COVID-19 restrictions. Metric tons of carbon dioxide emissions ($MtCO_2e$) were calculated using formulas provided by the *Practice Greenhealth Anesthetic Gas Toolkit*: (# bottles x bottle volume x density x GWP x 0.002 = total $MtCO_2e$ of anesthetic gas). To account for variable potencies between gases, MTCO2e per MAC hour were calculated assuming FGF rates in 100% O_2 to represent $MtCO_2e$/MAC·hour (Table 1) [4]. Data were analyzed with linear regression and simple or mixed-model analyses of variance (ANOVA) with GraphPad Prism software. Projected changes in $MtCO_2e$ by adopting low, FDA suggested, fresh gas flow rates (FGF) assumed that current FGF at our institution reflects published national averages (Table 1) [5, 6].

Results: Over the observed period, there was a decline in volume of desflurane purchased ($p < 0.0001$), while there was an increase in the volume of sevoflurane purchased ($p < 0.0001$) (Figure 1). The rate of isoflurane purchasing remained stable. The reduction in purchasing led to an amplified reduction in monthly $MtCO_2e$ due to the high GWP of desflurane compared to sevoflurane and isoflurane (Figure 2). $MtCO_2e$ per MAC-hour of desflurane is higher than iso- and sevoflurane due to: greater MAC (6% vs 1.5 and 2%, respectively), and greater GWP (2,540 vs 510 and 130, respectively). Thus, the decrease in desflurane use drove a decrease in total $MtCO_2e$ ($p = 0.03$), despite stable MAC-hours ($p = 0.65$) during this time (Figure 3). Assuming a current average FGF rate of desflurane of 1.59 L/min, we determined the $MtCO_2e$ per MAC-hour of desflurane was 0.1, equivalent to driving a car 240 miles (Table 2) [7]. If FGF rates for desflurane are reduced to 0.5 L/min, we project a 68% reduction in emissions per MAC-hour. For sevoflurane, with an assumed average FGF rate of 2.34 L/min, reducing FGF to 1 L/min would lead to a 57% reduction in emissions per MAC-hour.

Conclusions: At our institution, reduced purchasing in desflurane led to subsequent reductions in generated emissions. The pollution profile and costliness of desflurane, and availability of alternative anesthetics such as sevoflurane, suggest that significant reduction or elimination of desflurane from the formulary would prove both environmentally and economically beneficial, as has been observed in the U.K [2]. Widespread adoption of low FGF rates in practice, as well as provider education on low FGF and anesthetic agent selection, will further reduce environmental harm from anesthetic gases, as shown in previous studies [8]. Human health and planetary health are intimately associated; thus we have a responsibility to our patients to reduce the carbon footprint of the healthcare industry by finding safe alternatives to desflurane use.

References: [1] PLoS One. 2016;11(6):e0157014.

[2] Lancet Planet Health. 2017 Dec;1(9):e381-e388.

[3] Br J Anaesth. 2020 Nov;125(5):680-692.

[4] Can J Anaesth. 1993 May;40(5 Pt 1):472-4.

[5] Anesthesiology. 2013 Apr;118(4):874-84

[6] Int J Anesth Anesth. 2018;5(1):064

[7] Can J Anaesth. 2019 Jul;66(7):838-839

[8] Anesth Analg. 2019 Jun;128(6):e97-e99

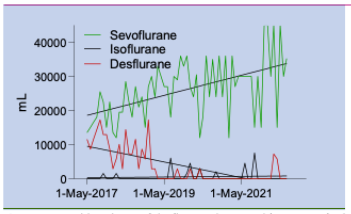

Figure 1. Monthly volume of desflurane decreased ($p < 0.0001$) while sevoflurane use increased ($p < 0.0001$). Isoflurane volume was unchanged ($p = 0.43$)

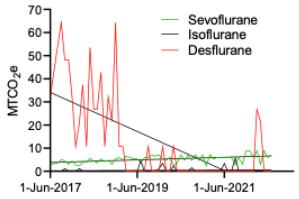

Figure 2. Trends in emissions followed those of volume purchased, with reduction in desflurane-related emissions ($p < 0.0001$) being amplified by its high global warming potential (GWP)

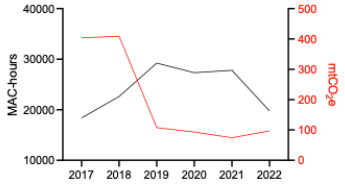

Figure 3. MAC-hours calculated using the FGF of each gas in Table 1. The number of cases or operating room hours were inaccessible, so we assume MAC-hours used will reflect surgical volume. The large decrease in desflurane-related emissions drove a decrease in total operating room emissions ($p = 0.03$) despite stable surgical volume ($p = 0.65$) and increased use of sevoflurane.

	FGF rate (L/min)		MAC
	Current	Minimal	
Desflurane	1.59	0.5	0.060
Isoflurane	2.34	1	0.015
Sevoflurane	2.33	1	0.020

Table 1. Published national average FGF rates that are assumed to reflect the institution's current practices and the FDA recommended minimum flow. MAC is the minimal alveolar concentration for each species of gas.

FGF	Current		Reduced	
	MTCO2e /MAC· hr	Car Miles	MTCO2e / MAC· hr	Car Miles
Desflurane	0.099	240.82	0.0310	75.73
Isoflurane	0.011	27.42	0.0050	11.72
Sevoflurane	0.001	3.64	0.0006	1.56

Table 2. Car mile equivalents of MTCO2e per MAC-hour of desflurane, isoflurane, and sevoflurane at current fresh gas flow rates compared to MTCO2e per MAC-hours with low flow rate adoption.

Liver

Liver 1- Functional mitral regurgitation in liver transplant recipients and its impact on post-transplant mortality

Do-Kyeong Lee[1], Hye-Mee Kwon[1], Young-Jin Moon[2], In-Gu Jun[2], Jun-Gol Song[3], Gyu-Sam Hwang[3]

Asan Medical Center, University of Ulsan College of Medicine[1] University of Ulsan College of Medicine, Asan Medical Center[2] Asan Medical Center, Department of Anesthesiology[3]

Introduction: In the current era, cardiovascular disease has been recognized as the leading cause of death early and late after liver transplantation (LT)[1, 2]. Mitral regurgitation (MR) is the most common valvular heart disease, moreover, high mortality and heart failure events are reported in functional MR[3]. We aimed to examine the prevalence and prognostic role of functional MR in LT recipients across the severity of liver disease at a large volume LT center.

Methods: Of consecutive 3,887 LT recipients who examined routine preoperative echocardiography at the our medical center between 2008 and 2019, we evaluated 449 (11.6%) patients with functional MR after exclusion of trivial and severe MR, mitral valve surgery, prolapse, annular calcification, and degenerative changes. Post-transplant all-cause mortality up to 12 years (median: 4.8 years) were followed, and 564 (14.5%) patients died after LT. Multivariate cox regression analysis was performed and hazard ratio (HR) was adjusted with age, sex, model for end-stage liver disease (MELD) score and revised cardiovascular risk index (RCRI).

Results: Patients with functional MR comprised 348 (9.0%) with mild MR and 101 (2.6%) with moderate MR. Functional MR remained significant after multivariable Cox analysis (P<0.001, adjusted HR: 1.55 [95% confidence interval;1.24 – 1.93]) and had lower overall survival rates of 75% vs 83.1% at 10 years compared to those without (log-rank P<0.001). Notably, when patients were grouped with MELD score of >35 and 20-35, survival rates at 10 years in patients with functional MR were significantly lower (51 % vs. 72.6%, P<0.001; 74.3% vs. 82.7%, P=0.036) compared to those without, whereas it was not significant in MELD score of < 20 group (82.3 % vs. 85%, P=0.13). (Figure)

Conclusions: This study demonstrates that pre-transplant functional MR is an independent determinant of death after LT proportionately with liver disease severity, raising the concerns that functional MR may mirror ventricular dysfunction or a surrogate in patients with advanced liver disease. Therefore, strategies attempting to reduce it need to be focused to improve survival after LT.

References: 1. Korean J Anesthesiol. 71(2): 85–91. 2018 Apr.

2. Eur Heart J Qual Care Clin Outcome. 6(4): 243-253. 2020 Oct.

3. J Am Heart Assoc. 11(1). 2022 Jan 4.

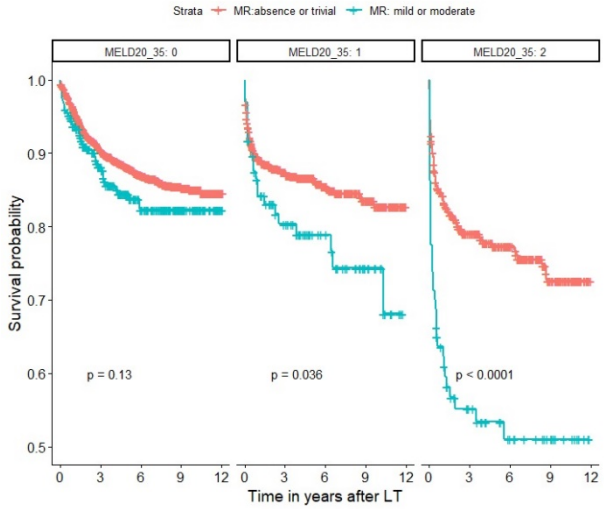

Liver 2- Mechanical Complications from Double-Cannulation of Central Venous Catheters in Patients Undergoing Liver Transplantation

Aaron Kurtti[1], Federico Arenas Quintero[1], Matthew Palascak[1], Bobby Nossaman[1]

University of Queensland - Ochsner Clinical School[1]

Introduction: Patients undergoing liver transplantation often require central vascular monitoring and reliable venous access via central venous (CV) catheters due to intraoperative hemodynamic instability.[1] Double-cannulation central venous catheters (DC-CVC) involves placement of two central lines into the same vein. Although mechanical complications have been reported following insertion of either CV or pulmonary artery (PA) catheters;[2-6] there is limited information regarding the incidence of DC-CVC complications.[7-9]
The purpose of this descriptive study is to report the incidences of mechanical complications following DC-CVC in patients undergoing liver transplantation.

Methods: Following IRB approval, 1,448 adult patients ≥18 years undergoing liver transplantation between 11/9/2012 through 6/6/2022 were included for study. Large-bore multi-lumen CVCs were initially placed in the right internal jugular vein with double-cannulation for subsequent insertion of a PA catheter under ultrasound guidance. Medical records were reviewed for mechanical complications occurring at any point during hospital admission including pneumothorax, site hematoma, arterial puncture, thrombosis, nerve injury, loss of guide wire, air embolism, and dysrhythmias. Absolute rates of these mechanical complications were calculated to estimate the safety profile.

Results: Initial analysis showed low rates of mechanical complications following insertion of CV and PA catheters at a single vascular access site. The most common complication was pneumothorax reported in 21 (1.5%) patients followed by site hematoma (7 events; 0.5%), arterial puncture (5 events; 0.4%), dysrhythmia (4 events; 0.3%), thrombosis (1 event; 0.1%), nerve injury (1 event; 0.1%), and loss of guide wire (1 event; 0.1%). Figure 1 depicts mean rates with 95% confidence intervals of observed DC-CVC compared to reported single cannula rates of mechanical complications. Rates of observed hematoma, arterial puncture, thrombosis, nerve injury, and dysrhythmia were significantly lower. Rates for pneumothorax, and loss of guide wire did not significantly differ.

Conclusions: The rates of mechanical complications for DC-CVC were found to be low, suggesting that DC-CVC vascular access can be safely used in patients undergoing liver transplantation.

References: Perioperative monitoring in liver transplant patients. *J Clin Exp Hepatol.* 2012;2(3):271–278

Anaesthesia for Liver Transplantation: An Update. J Crit Care Med (Targu Mures). 2020 May 6;6(2):91-100.

Pulmonary artery catheters: state of the controversy. J Cardiovasc Nurs. 2008 Mar-Apr;23(2):113-21

Complications of 1303 central venous cannulations. J R Soc Med. 1997 Jun;90(6):319-21.

Central line complications. Int J Crit Illn Inj Sci. 2015 Jul-Sep;5(3):170-8.

Complications associated with pulmonary artery catheters: a comprehensive clinical review. Scand J Surg. 2009;98(4):199-208.

Hazards in multiple cannulation of a single vein. Anaesthesia. 1985 Jul;40(7):700.

For complete list of references see attached document.

Figure 1:
Observed (DC-CVC) vs Reference (Single Catheter) Rates of Mechanical Complications

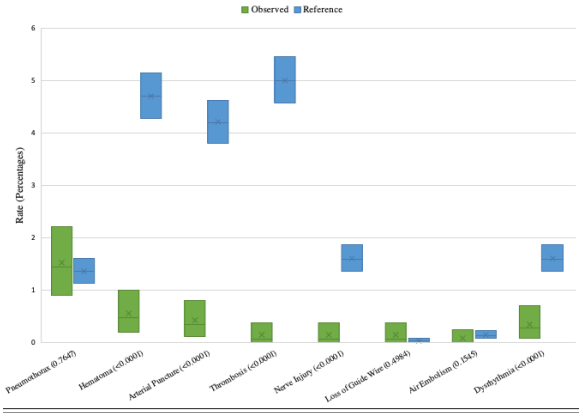

Figure 1: Significance (p-values) listed following mechanical complication on the x-axis. Box length represents 95% confidence interval. Rates and confidence intervals for reference values were calculated by converting reported frequency of complications to a patient population of 10,000 . Literature reference rates varied slightly, lowest reported available population rates of complications were used as a conservative estimate.

References: Pneumothorax[10], Hematoma[11], Arterial Puncture[12], Thrombosis[13], Nerve Injury[5], Loss of Guide Wire[14], Air Embolism[15], Dysrhythmia[4]

References

1. Singh A, Nasa V, Tandon M. Perioperative monitoring in liver transplant patients. *J Clin Exp Hepatol*. 2012;2(3):271–278
2. Brezeanu LN, Brezeanu RC, Diculescu M, Droc G. Anaesthesia for Liver Transplantation: An Update. J Crit Care Med (Targu Mures). 2020 May 6;6(2):91-100.
3. Frazier SK, Skinner GJ. Pulmonary artery catheters: state of the controversy. J Cardiovasc Nurs. 2008 Mar-Apr;23(2):113-21
4. Yilmazlar A, Bilgin H, Korfali G, Eren A, Ozkan U. Complications of 1303 central venous cannulations. J R Soc Med. 1997 Jun;90(6):319-21.
5. Kornbau C, Lee KC, Hughes GD, Firstenberg MS. Central line complications. Int J Crit Illn Inj Sci. 2015 Jul-Sep;5(3):170-8.
6. Evans DC, Doraiswamy VA, Prosciak MP, Silviera M, Seamon MJ, Rodriguez Funes V, Cipolla J, Wang CF, Kuvuturu S, Torigian DA, Cook CH, Lindsey DE, Steinberg SM, Stawicki SP. Complications associated with pulmonary artery catheters: a comprehensive clinical review. Scand J Surg. 2009;98(4):199-208.
7. Withington PS, Carter JA. Hazards in multiple cannulation of a single vein. Anaesthesia. 1985 Jul;40(7):700.
8. Reeves ST, Roy RC, Dorman BH, Fishman RL, Pinosky ML. The incidence of complications after the double-catheter technique for cannulation of the right internal jugular vein in a university teaching hospital. Anesth Anal 1995 Nov;81(5):1073-6.
9. Reeves ST, Baliga P, Conroy JM, Cleaver TL. Avulsion of the right facial vein during double cannulation of the internal jugular vein. J Cardiothorac Vasc Anesth. 1995 Aug;9(4):429-30.
10. Celik B, Sahin E, Nadir A, Kaptanoglu M. Iatrogenic pneumothorax: etiology, incidence and risk factors. Thorac Cardiovasc Surg 2009; 57:286.
11. Vats HS. Complications of catheters: Tunneled and nontunneled. *Adv Chronic Kidney Dis*. 2012;19:188–94.
12. Bowdle A. Vascular complications of central venous catheter placement: evidence-based methods for prevention and treatment. J Cardiothorac Vasc Anesth. 2014 Apr;28(2):358-68.
13. Kamphuisen PW, Lee AY. Catheter-related thrombosis: lifeline or a pain in the neck? Hematology Am Soc Hematol Educ Program. 2012;2012:638-44.
14. Vannucci A, Jeffcoat A, Ifune C, Salinas C, Duncan JR, Wall M: Retained guidewires after intraoperative placement of central venous catheters. Anaesth Analg 2013; 117:102–8
15. Vesely TM. Air embolism during insertion of central venous catheters. J Vasc Interv Radiol 2001; 12:1291.

Liver 3- The SATA multicenter Liver Transplant Outcomes in Anesthesia Database (Liver-TOAD): building the foundation for research collaboration in transplant anesthesia

Dieter Adelmann[1], Alexandra Anderson[2], Lorenzo De Marchi[3], Ana Fernandez-Bustamante[4], Kyota Fukazawa[4], Jiapeng Huang[4], Cale Kassel[4], Ryan Nazemian[4], Christine Nguyen-Buckley[5], Natali Smith[6], Elizabeth Townsend[7], Elizabeth Wilson[7], George Zhou[7]

University of California, San Francisco[1] Mayo Clinic Rochester[2] MedStar-Georgetown University Hospital[3] University of Colorado School of Medicine[4] UCLA Department of Anesthesiology and Perioperative Medicine[5] The Mount Sinai Hospital[6] University of Wisconsin School of Medicine and Public Health[7]

Introduction: There is currently no infrastructure to collect and share perioperative data for observational research in liver transplant (LT). Although patient and graft survival are reported to national organizations, this does not include perioperative metrics. Some transplant centers have established their own anesthesia databases, but data sharing for research is limited by differences in parameters collected and variable definitions, as well as administrative barriers regarding data sharing between institutions.
We report the development and deployment of the Society for the Advancement of Transplant Anesthesia (SATA) Multicenter Liver Transplant Anesthesia Outcomes Database (Liver-TOAD) to facilitate multicenter collaborations.

Methods: This multicenter database is based on a common set of variables defined in a shared data dictionary. Variables include data on fluid management, blood product usage, invasive monitoring, kidney injury, extubation, and ICU length of stay. The database can be deployed using a REDCap template provided to participating centers. Alternatively, existing local databases can be adapted to match the variable definitions agreed on by the group.
Data collected at each center will be linked to additional donor and recipient data from the Scientific Registry of Transplant Recipients (SRTR) on a yearly basis. Centers can opt in to share their de-identified dataset, which will be stored at the data coordinating center (University of California, San Francisco). Each participating center can request data for specified research projects (Figure 1). All centers agreed on bylaws governing data sharing and authorship for all publications resulting from Liver-TOAD.

Results: As of December 2022, 27 centers are collaborating on the project. 17 centers have received local institutional review board approval, and 13 centers have started data collection. The first merged dataset will be available for research in the fall of 2023.

Conclusions: Liver-TOAD will facilitate multicenter research in liver transplant anesthesia with the potential to positively impact patient outcomes. Centers all over the world are encouraged to join the initiative. Please reach out to the authors to learn more (dieter.adelmann@ucsf.edu).

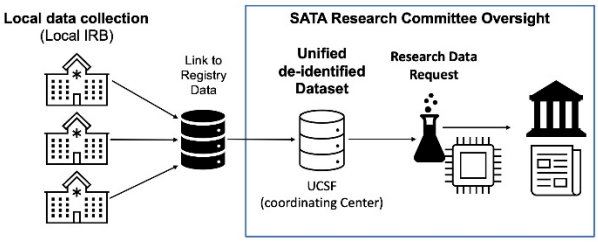

Neuroscience in Anesthesiology and Perioperative Medicine

Neuroscience in Anesthesiology and Perioperative Medicine 1- A Pilot Study of Incidence and Risk Factors Associated with Post-Anesthesia Care Unit Delirium

Alice Daramola[1], Bushra Yasin[1], Tuan Cassim[1], Oliver Isik[2], Paul Garcia[3]

Columbia Vagelos College of Physicians and Surgeons[1] Columbia University Vagelos College of Physicians & Surgeons[2] Columbia University[3]

Introduction: Delirium is an acute disorder of attention and cognition that is more common in older adults. Studies have shown that delirium can happen at various stages of the postoperative period; on the floor, in the intensive care unit (ICU), or even in the immediate post-surgical period in the post-anesthesia care unit (PACU). Given the aging surgical population and research indicating an association between postoperative delirium and adverse outcomes such as longer term cognitive and functional impairments, this is an area of concern for anesthesiologists.[1] Besides age, additional risk factors have been identified as predisposing individuals to develop delirium after surgery: e.g., case duration, severe illness, and previous stroke, cognitive impairment, or delirium.[2] Literature suggests that PACU delirium is associated with increased risk of developing subsequent postoperative delirium and the associated sequelae.[3] Previous studies have found an incidence of PACU delirium that ranges from 16-45%.[3,4]

Methods: Our study consisted of a convenience sample of older adult patients admitted to the PACU between December 2021 and August 2022 after undergoing general anesthesia for surgery. The sample was gathered as a quality improvement project and exempt from IRB oversight per institutional guidelines. Each patient was administered English or Spanish versions of two brief, validated screening tools for delirium. The confusion assessment method for the intensive care unit (CAM-ICU) and the three-minute diagnostic interview for the confusion assessment method (3D-CAM), were administered at least 15 minutes after arrival to the PACU. We also explored risk factors for PACU delirium via retrospective chart review. Group comparisons were made using chi square or Fisher's exact test and *t*-tests.

Results: A total of 152 adult patients who underwent anesthesia were included in our analyses (Figure 1). Thirty-nine out of 152 patients screened positive for delirium in the PACU by either measure. Of these 39 patients, 17 (44%) screened positive for both the CAM-ICU and the 3D-CAM (Figure 2). In our sample, the average age of both patient groups (delirium, no delirium) was similar (Table 1). PACU delirium was associated with, length of case ($p=0.0078$), and surgical severity ($p < 0.0001$) (Table 2). Although patients in the group with delirium received more phenylephrine (Figure 3), intraoperative phenylephrine exposure was not significantly associated with PACU delirium ($p = 0.06$).

Conclusions: PACU delirium is a relatively new concept that may be overlooked by anesthesiologists. Our analyses demonstrated an incidence of PACU delirium consistent with other studies. We failed to find an age association with PACU delirium in our study, likely due to the preponderance of aged patients in our sample. Two screening tools for delirium were used as there is no gold standard for diagnosing delirium in the PACU. Interestingly, there was incomplete overlap of the CAM-ICU and 3D-CAM in identifying delirium in our population. Different sensitivities of the CAM-ICU and 3D-CAM in identifying delirium in both the PACU and hospitalized patients has also been previously reported. Recent work by Banerji et al. (2022) found the 3D-CAM to be more sensitive to cognitive deficits in the PACU compared to the CAM-ICU.[4] Our study confirms that these measures may be attuned at picking up different aspects of delirium. Thus, a measure that is quick and easily given at the bedside in the PACU, yet comprehensive may be needed. Additionally, findings that undergoing major surgery may contribute to development of delirium could signal this as a stratification point for interventions aimed at reducing postoperative delirium in the future. Although, the relationship between intraoperative phenylephrine exposure and PACU delirium was not statistically significant, it may be clinically relevant. A proposed mechanism of delirium is that it is the result of a disruption in normal cortical integration.[5] This theory proposes that insults such as cerebral hypoperfusion and oxidative stress may contribute to disconnection of cortical networks. Similarly, phenylephrine administration has been shown to significantly reduce cardiac output and cerebral oxygenation. Our results are limited by the observational nature of this study, and thus future research aimed at investigating how intraoperative pharmacologic decision-making may impact development of delirium is needed.

References: 1. High risk of cognitive and functional decline after postoperative delirium, 26:26-31, 2008.

2. Delirium in elderly people, 383:911-22, 2014.

3. Post-anaesthesia care unit delirium: incidence, risk factors and associated adverse outcomes, 119:288-90, 2017.

4. Deconstructing delirium in the post anaesthesia care unit, 14, 2022.

5. An update on postoperative delirium: clinical features, neuropathogenesis, and perioperative management, 8:252-62, 2018.

Figure 1. PACU-Delirium Pilot Participant Diagram

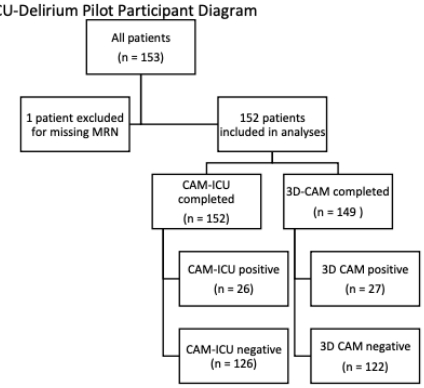

Figure 2. Venn Diagram of Positive Delirium Screen on CAM-ICU vs. 3D-CAM

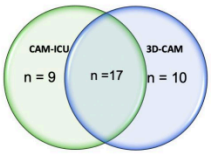

Figure 2 represents a Venn diagram of patients who screened positive for delirium in the post-anesthesia care unit (PACU) by the confusion assessment method for the intensive care unit (CAM-ICU) and/or the three-minute diagnostic interview for the confusion assessment method (3D-CAM).

Table 1. Patient demographics by delirium status

	All Participants (N= 152)	Delirium Positive (n=39)	Delirium Negative (n=113)	P value
Age mean(sd)	54.94 (17.84)	55.95 (17.56)	54.59 (18.00)	0.68
Gender n(%)				0.85
Female	75 (49.34)	20 (26.67)	55 (73.33)	
Male	77 (50.66)	19 (24.67)	58 (75.32)	
Race n(%)				0.69
White	76 (50)	17 (22.36)	59 (77.63)	
Black/African American	21 (13.8)	8 (38.09)	13 (61.90)	
Asian	3 (1.9)	1 (33.33)	2 (66.67)	
Other/combined	36 (23.6)	9 (25.0)	27 (75.0)	
Unknown/declined	16 (10.5)	4 (25.0)	12 (75.0)	
Ethnicity n(%)				0.55
Not Hispanic/Latino	100 (65.8)	23 (23)	77 (77)	
Hispanic/Latino	41 (26.9)	13 (31.70)	28 (68.29)	
Unknown/declined	11 (7.2)	3 (27.27)	8 (72.72)	

Table 2. Patient, surgical, and anesthetic factors by delirium status

	All Participants (N= 152)	Delirium Positive (n=39)	Delirium Negative (n=113)	P value
Assessment time, mean (sd)[A]	35.78 (26.39)	34.26 (22.32)	36.28 (27.66)	0.69
ASA Score n(%)				
< 3	81 (53.29)	18 (46.15)	63 (55.75)	
≥ 3	71 (46.71)	21 (53.84)	50 (44.25)	
Midazolam given n(%)	121 (79.60)	31 (79.49)	90 (79.65)	>0.999
Anesthesia protocol n(%)[B]				>0.999
Volatile	124 (89.20)	32 (88.89)	92 (89.32)	
TIVA	15 (10.79)	4 (11.11)	11 (9.73)	
Surgical Severity n(%)				<0.0001*
Major	59	27 (69.23)	32 (28.32)	
Minor	93	12 (30.77)	81 (71.68)	
Case duration, mean (sd)	125.8 (86.72)	157.4 (85.9)	114.9 (84.65)	0.0078*
Total opioid fentanyl equivalents, mean(sd)	192.5 (120.9)	236.9 (128.1)	177.2 (114.9)	0.0073*
Intraprocedural phenylephrine, n(%)[C]	77 (50.66)	25 (64.10)	52 (46.01)	0.0595

*statistically significant using alpha level of 0.05.
[A]data was not collected on time from arrival in PACU to administration of delirium assessments for nine patients.
[B]thirteen patients who did not receive general anesthesia were excluded from analyses.
[C]three patients who received blood products intraoperatively were excluded from analyses.

Figure 3. Graph of Total Intraoperative Phenylephrine by Delirium Status

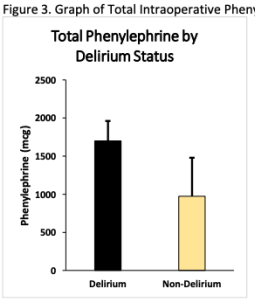

Figure 3 displays the total amount of phenylephrine administered to patients intraoperatively by whether they screened positive for delirium using the CAM-ICU and/or the 3D-CAM.

Neuroscience in Anesthesiology and Perioperative Medicine 2- A polydrug model of opioid and alcohol co-use identifies serotonin 2A receptor agonists as potential addiction therapeutics in rats

Jasper Heinsbroek[1], Joel Bonilla[1], Giuseppe Giannotti[1], Jamie Peters[2]

Washington State University[1] University of Colorado Anschutz Medical Campus[2]

Introduction: Polydrug use is common in human substance use disorders, and epidemiological studies indicate that opioid use disorder (OUD) patients often co-use alcohol. However, preclinical polydrug use models are lacking to screen novel potential therapeutics for addiction. We set out to establish a model of comorbid heroin and alcohol use that could be used to screen potential therapeutics.

Methods: Male and female Wistar rats were first exposed to either (12%) alcohol or control drinking conditions in their home cage for four weeks. Thereafter, rats were trained to lever press for either alcohol or heroin (separate groups), followed by extinction of drug seeking and a test for cued relapse. Next, rats were trained to self-administer the alternate reward (alcohol or heroin) on an alternate lever, and subsequently had to choose between these rewards. Rats were finally tested under progressive ratio conditions, which reveals the break point, or maximum effort (in lever presses) an animal is willing to expend for a single (heroin or alcohol) reward. All procedures were approved by the University of Colorado Anschutz Medical Campus Institutional Animal Care and Use Committee. Data were analyzed using t-tests or ANOVAs as appropriate.

Results: Whereas home-cage drinking condition did not impact choice between heroin and alcohol, rats with a history of alcohol self-administration were more likely to choose alcohol over heroin compared to rats with a history of heroin self-administration. The serotonin 2A receptor (5-HT2Ar) agonist, tabernanthalog (TBG), effectively reduced motivation for heroin and alcohol. A follow-up study revealed that the classical psychedelic and more selective 5-HT2Ar agonist, 2,5-Dimethoxy-4-iodoamphetamine (DOI), had comparable therapeutic effects in rats trained to self-administer both heroin and alcohol simultaneously (without prior home cage drinking).

Conclusions: Thus, the non-hallucinogenic TBG compound may be a promising therapeutic for OUD with comorbid alcohol use and potentially works through a 5-HT2Ar mechanism.

Neuroscience in Anesthesiology and Perioperative Medicine 3- Alterations in Amygdala Functional Connectivity in Juvenile Non-Human Primates 2 Years after Anesthesia Exposure during Infancy

Viola Neudecker[1], Viola Neudecker[1], Jose Perez-Zhogbi[1], Oscar Miranda-Dominguez[1], Katie Schenning[2], Lauren Martin[3], Gregory Dissen[4], Damien Fair[4]

Columbia University Medical Center[1] Oregon Health and Science University[2] Oregon National Primate Research Center -ARRS[3] ONPRC/OHSU[4]

Introduction: The latest clinical studies with prospective assessments indicate that early-in-life anesthesia exposure causes behavioral alterations later in life, but does not affect general intelligence. Preclinical studies, including those in non-human primates (NHPs), report functional alterations after early-in-life anesthesia exposure. Recently, we found that juvenile NHPs display decreased close social behaviors 2 years after early-in-life isoflurane exposure, but similar to clinical findings, the juveniles showed no cognitive impairments. Histopathological analysis of the juvenile NHP brains revealed increased gliosis in the amygdala, a brain region important for processing of social behaviors. Resting state functional connectivity MRI (rs-fcMRI) noninvasively allows the detection of alterations in functional connectivity (fc) of specific areas of the brain. However, whether early-in-life anesthesia exposure causes changes in fc of brain areas associated with social behavior remains unknown. We hypothesized that early-in-life isoflurane exposure of NHPs causes alterations in fc of the amygdala of the juvenile animals two years after the exposure.

Methods: Rs-fcMRI was performed in 2-year-old NHPs under light anesthesia, after early-in-life exposure to 5 hours of isoflurane, either one (1X), or three times (3X), or to room air only. The NHP brain was segmented into 82 regions of interest (ROIs). Based on blood-oxygen-level dependent (BOLD) contrast imaging data, amygdala-ROI fcs were determined. To identify differences in fc between the three groups we used ANOVA and Bonferroni correction for multiple comparison.

Results: We found significant differences in fc among groups for the left and right amygdala with the primary auditory cortex (A1). Specifically, the fc between the left amygdala and the right A1 was significantly different among the three groups, and post hoc analysis revealed significantly decreased fc in the 3X group compared to both, the control, and the 1X group. For the right amygdala, we found a significant difference in its fc with the left A1 among the three groups. Post-hoc testing revealed that the 3X group showed a significant increase in fc with the left A1 as compared to the 1X group, however this increase was not significant when compared to the control group.

Conclusions: Early-in-life anesthesia exposure of NHPs causes changes in the fc of their amygdala evident at the age of 2 years. Since the amygdala is critical for processing of social behaviors, alterations in its connectivities may contribute to impairments in social functioning.

Neuroscience in Anesthesiology and Perioperative Medicine 4- An immune signature of postoperative cognitive dysfunction (POCD), a prospective cohort study

Franck Verdonk[1], Julien Hedou[1], Gregoire Bellan[2], Ed Ganio[2], Ina Stelzer[2], Dorien Feyaerts[2], Masaki Sato[1], Adam Bonham[2], Kazuo Ando[3], Dyani Gaudilliere[3], Raphael Gaillard[3], Serge Molliex[3], Tarek Sharshar[3], Brice Gaudilliere[3]

Stanford University[1] SurgeCare SAS[2] Stanford University School of Medicine[3]

Introduction: Post-operative cognitive decline (POCD) is one of the most common postoperative complications in elderly patients undergoing major surgery. POCD has been associated with increased mortality, earlier retirement, and more frequent use of social financial assistance (1). Although there is currently no treatment for POCD, preventive approaches have been shown to mitigate the risk of POCD (2), requiring predictive algorithms to stratify patients at risk. While emerging preclinical evidence suggests that the systemic immune response to surgical trauma is a key pathobiological process driving POCD (3), studies in patients are critically lacking. Considering the complex, dynamic and multi-cellular systemic response to surgery (4), we employed an integrated approach combining the functional analysis of immune cell subsets with mass cytometry and the multiplex assessment of plasma proteins to provide a comprehensive survey of immune cell- trajectories differentiating patients with and without POCD and to build a robust predictive model identifying patients at risk for POCD.

Methods: Thirty-three patients were prospectively enrolled as part of a multicenter, randomized, placebo-controlled trial including 272 elderly patients undergoing major orthopedic surgery between March 2017 and May 2019 for whom cognitive status was evaluated. Blood samples collected over four timepoints before and after surgery: day of surgery (DOS) and postoperative days (POD) one, seven, and ninety were analyzed using a combination of single-cell mass cytometry and plasma proteomics. POCD was defined as a decline of one or more standard deviations in neuropsychological assessment at post-operative day seven (POD7) after surgery in comparison to preoperative assessment. We employed unsupervised clustering from correlation networks and univariate analyses to characterize the trajectory of immune cell distribution and signaling responses in patients with or without POCD. A stacked generalization (SG) predictive modeling approach combining immunological data and clinical data was applied to classify patients at risk for POCD before surgery.

Results: Unsupervised analysis of the high-dimensional immunological data collected before and after surgery identified cell-type and signaling-specific immune trajectories differentiating patients with and without POCD (***Figure 1***). Examination of the most prominent trajectory features revealed early exacerbation of JAK/STAT and dampening of inhibitory kB (IκB) and/nuclear factor κB (NF-κB) immune signaling responses to surgery in patients with POCD. Further analyses integrating immune cell responses, proteomic, and clinical data collected before surgery identified a robust predictive SG model that classified patients with and without POCD with excellent accuracy (AUC = 0.86, p = 2.2e-03, unpaired Mann–Whitney rank-sum test on the SG model cross-validated values).

Conclusions: The single-cell immune system analysis of elderly patients undergoing orthopedic surgery identified immunological trajectories differentiating patients with and without POCD, thereby revealing a peripheral immune signature of POCD. In addition, a multi-omic model integrating immunological and clinical data collected before surgery accurately predicted the later development of POCD, providing a promising strategy for future development of a diagnostic test for POCD that could guide the individualized care of elderly patients undergoing surgery.

References: (1) Boone, M. D. *et al.* Economic Burden of Postoperative Neurocognitive Disorders among US Medicare Patients. *JAMA Netw Open* (2020) doi:10.1001/jamanetworkopen.2020.8931.

(2) Humeidan, M. L. *et al.* Effect of Cognitive Prehabilitation on the Incidence of Postoperative Delirium Among Older Adults Undergoing Major Noncardiac Surgery: The Neurobics Randomized Clinical Trial. *JAMA Surg* (2020) doi:10.1001/jamasurg.2020.4371.

(3) Forsberg, A. *et al.* The immune response of the human brain to abdominal surgery. *Ann Neurol* **81**, 572–582 (2017).

(4) Gaudillière, B. *et al.* Clinical recovery from surgery correlates with single-cell immune signatures. *Sci Transl Med* **6**, (2014).

Figure 1

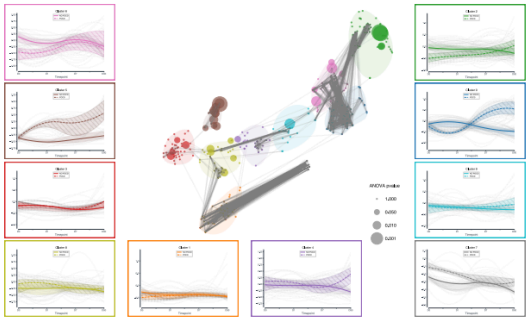

Visualization of the high-dimensional immunological dataset on a correlation network. Unsupervised analysis using k-mean clustering identified ten clusters of highly correlated immune features. Visualization of the high-dimensional immunological dataset on a correlation network. Unsupervised analysis using k-mean clustering identified ten clusters revealing differential immune trajectories in patients with and without POCD.

Neuroscience in Anesthesiology and Perioperative Medicine 5- Anesthetic modulation of single-unit and population dynamics in visual cortex

Duan Li[1], Duan Li[1], Shiyong Wang[2], Anthony Hudetz[3]

University of Michigan[1] The University of Michigan[2] University of Michigan[3]

Introduction: Neural dynamics is thought to support the brain's vast functional repertoire at multiple time scales. Neuronal groups form transient ensembles at subsecond time scale while brain regions display metastable activity patterns on the time scale of minutes. There is growing evidence for spontaneous shifts in large-scale brain states during anesthesia at constant effect-site drug concentration. What causes these state fluctuations in the absence of exogenous sensory stimulation? A possibility is that global dynamics can be traced back to local fluctuations of neuron firing but this hypothesis has not been tested. Here we investigate how individual cortical neurons participate in local population activity while undergoing spontaneous transitions at various anesthetic levels.

Methods: We recorded local field potential and unit activity from the primary visual cortex of 7 rats with chronically implanted 64-site microelectrode arrays. Anesthesia was produced with desflurane at steady-state inhaled concentrations 6%, 4%, 2% and 0% for 20 min each. Single-unit activity was identified using the clustering software Spiking Circus [1]. Distinct states of population activity were identified with the multiunit activity (MUA)-derived firing rate, temporal variability (as assessed by Lempel-Ziv complexity) and the percentage of time for which MUA rate was zero. Single units were classified into putative excitatory and inhibitory units based on the trough-peak time of spike waveform, and their activity were characterized by the autocorrelogram (ACG) and interspike interval (ISI) distribution across the MUA-derived states. To evaluate whether the firing patterns of individual neurons conform to population activity, we applied unsupervised clustering to the ISI histogram of individual single units and assessed the percentage of data where the population state membership was retained via ISI-based

classification.

Results: *k*-means cluster analysis of MUA activity showed five typical patterns. State 1 was mainly observed in the awake condition (0% desflurane), whereas States 2-5 did not consistently associate with any of the anesthetic concentrations. State 5 characterized by increased spike rate and complexity occurred mostly at 4% and 6% desflurane and thus was identified as a paradoxical state [2] (Figure 1). Single units tended to switch to burst spiking from State 1 to State 4, as evidenced by the decrease of ACG peak from 9.0 (6.0, 13.0) ms (median [interquartile range]) to 4.5 (4.0, 6.0) ms for putative excitatory neurons (p<0.001, Wilcoxon rank sum test), and from 17.5 (12.4, 22.1) ms to 8.3 (7.0, 12.5) ms for putative inhibitory neurons (p=0.004). Meanwhile, the neurons that exhibited a unimodal ISI distribution in State 1 demonstrated a bi- or multi-model distribution in State 2-5, which may imply a shift to bistable or multi-stable neuronal dynamics (Figure 2). Nevertheless, the spiking activity of individual neurons may not conform to population activity. Using a hierarchical cluster analysis of single unit activity, the population state membership was retained in 58.9 (48.7, 69.4) % of data across all the neurons and rats, though significantly higher than expected by chance ([100/5 states] %). As compared to putative inhibitory neurons, putative excitatory neurons seemed less probable to retain their multiunit cluster membership (59.6 [44.8, 73.9] % vs. 70.0 [49.6, 78.2] %, p<0.001) (Figure 3).

Conclusions: The firing pattern of neurons often deviate from their population cluster membership suggesting that local populations and individual neurons follow different spontaneous dynamics independent of the anesthetic depth. Differences in individual neuronal excitability or network connectivity may contribute to this phenomenon.

References:

1. Elife 7: e34518, 2018
2. J. Neurosci. 40(49):9440-54, 2020

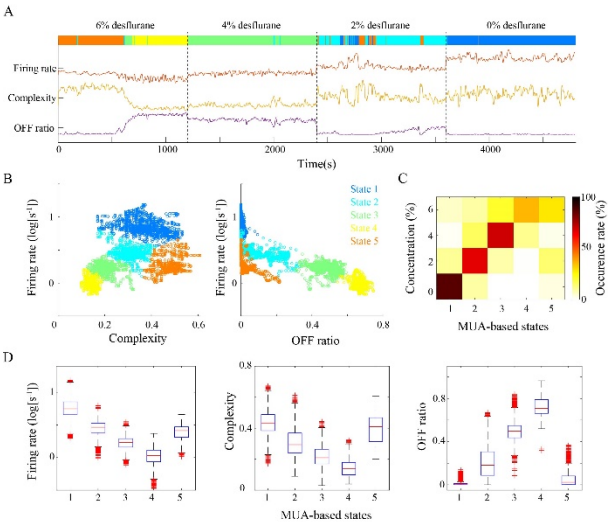

Figure 1. MUA-based state classification of cortical population activity. (**A**) Classification of population activity from a representative rat. Colors indicate different clusters (i.e. MUA-based states). (**B**) Scatterplots of the mean firing rate, temporal complexity and OFF ratio (the percentage of time for which MUA rate was zero) from the same rat. (**C**) The occurrence rate, i.e. the fraction of time spent in each cluster for each studied session (6% - 0% desflurane) across all rats. (**D**) State-dependent changes of the MUA features. The central line and edges of each box indicate the median and interquartile range across all time windows that were assigned in a certain cluster in all rats, while the whiskers extend to the most extreme values, and the outlier is marked as a red cross.

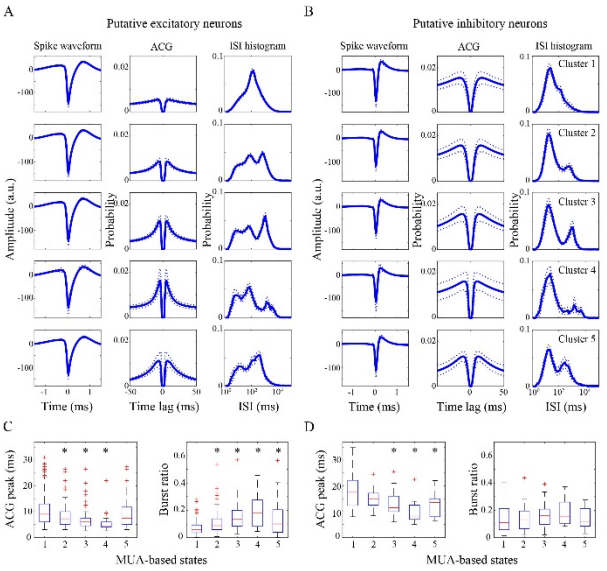

Figure 2. Spiking characterisitics of single units across the MUA-based states. (**A**, **B**)The averaged spike waveform, ACG and ISI distribution across all putative excitatory (A) and inhibitory neurons (B) from all rats (solid line: mean, dashed line: 95% confidence interval). (**C**, **D**) the peak of ACG and the burst ratio (defined as the number of ISIs <10 ms divided by the total number of ISIs) across all putative excitatory (C) and inhibitory neurons (D) from all rats. * indicates statistically significant difference relative to those in State 1 (p<0.05/4, Wilcoxon rank sum test). Units with firing rate <1 IIz in each state were excluded.

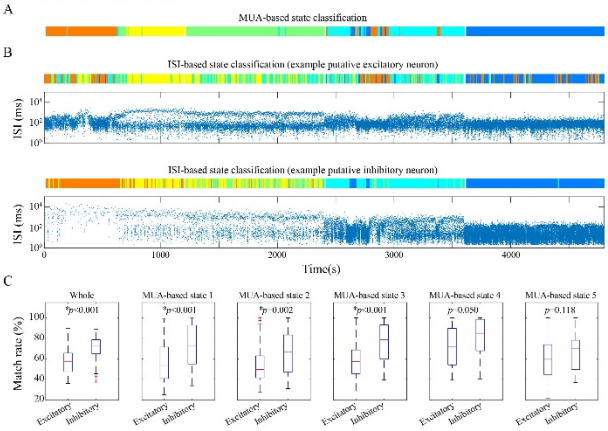

Figure 3. Individual neurons exhibit spontaneous dynamics substantially different from local population activity. (**A**) MUA-based state classification from the same rat as in Figure 1. (**B**) ISI-based state classification, and ISI scatterplots for an example putative excitatory neuron and an example putative inhibitory neuron from the same rat. (**C**) Using ISI-based classification, the match rate (i.e. the percentage of data where the population state membership was retained) across all putative excitatory or inhibitory neurons from all 7 rats, for the whole data, and the data in each MUA-based state respectively. * indicate significant difference between putative excitatory (N=147) and inhibitory neurons (N=38) (p<0.05/6, Wilcoxon rank sum test).

Neuroscience in Anesthesiology and Perioperative Medicine 6- $Ca_V3.1$ isoform of T-type calcium channels plays an important role in morphine-induced alterations in thalamic excitability and conditioned place preference in mice

Tamara Timic Stamenic[1], Slobodan Todorovic[1]

Department of Anesthesiology University of Colorado - Anschu[1]

Introduction: More than 750,000 people have died since 1999 from a drug overdose (http://wonder.cdc.gov). Opioids were involved in approximately 70% (46,802) of drug overdose deaths during 2018. Recent findings strongly suggest that the intralaminar nucleus of thalamus may be very important for various aspects of addiction (Li et al., 2018, Cover et al., 2019). The central medial nucleus of thalamus (CeM), a part of intralaminar nucleus has been recognized as a hub through which natural sleep and general anesthesia are initiated (Stamenic et al., 2019) but other CeM roles are not well studied. Low-voltage-activated T-type Ca^{2+} channels (T-channels) have a crucial role in regulating neuronal excitability, synaptic plasticity and oscillatory behaviors. Based on the structure of the α1 pore-forming subunit, these channels are classified into three isoforms: $Ca_V3.1$ (Cacna1g), $Ca_V3.2$ (Cacna1h), and $Ca_V3.3$ (Cacna1i) with different distributions in the central and peripheral neurons. We previously showed the important role of the $Ca_V3.1$ T-channels in CeM neuron excitability (Stamenic et al., 2018). The mechanisms underlying the role of T-channels in thalamic excitability and behavioral changes in vivo during morphine exposure are largely unknown.

Methods: We investigated the effects of acute (10 μM) and repeated (15 mg/kg i.p. 4 days) morphine exposure on $Ca_V3.1$ T-channels kinetics and excitability of CeM neurons in an ex vivo slice preparation. We also used mouse genetics in vivo to correlate the addictive effects of morphine with thalamic $Ca_V3.1$ T-channels using wild-type (WT), global $Ca_v3.1$ knock-out (KO) and CeM-selective $Ca_v3.1$ knock-down (KD) mutant mice.
To specifically investigate the contribution of $Ca_V3.1$ T-channels in the thalamus, for behavioral experiments we used mice with silenced cacna1g gene that encodes the $Ca_V3.1$ channel in the CeM: the method that consists of knocking down Cacna1g by injecting short hairpin RNA (shRNA).
The condioned place preference (CPP) test was performed in a custom-made 3-compartment apparatus with a transparent middle chamber and different visual patterns on the walls in the testing chambers. Here we used suboptimal morphine CPP protocol: 30 min baseline and testing sessions and 3 days of conditioning with 6 mg/kg morphine i.p. (60 min, Figure 3).

Results: Our results showed a reduction of T-channels currents (Figure 1) and inhibition of rebound firing in CeM neurons in WT animals (Figure 2) during acute morphine application. Morphine stabilizes inactive states of T-channels and shifts inactivation V_{50} significantly (Figure 1B), hence diminishes the "window" component of T-currents. Additionally, it reduces T-current density (shaded area on Figure 1C). In current-clamp experiments morphine reduced excitability of CeM neurons after both acute (Figure 2B, C) and repeated exposure (reduced tonic depolarization-induced firing frequency in WT animals measured at -60 mV). Also 10 μM morphine decreased action potential number in rebound burst after hyperpolarization (Figure 2D) in CeM neurons.
The CPP test is commonly used to explore the reinforcing effects of natural and pharmacological stimuli, including drugs of addiction. CPP occurs when a subject comes to prefer one place more than another because the preferred location was previously paired with rewarding events. Importantly, CPP has been demonstrated in many animal species, including humans. Our results with suboptimal morphine CPP, showed that both global deletion (KO animals) and CeM-specific reduction (KD mice) of $Ca_V3.1$ T-channels resulted in the animals being more sensitive to the rewarding effects of morphine (Figure 3, preference index calculated as the time in the morphine-paired side divided by the time spent in both testing chambers)).

Conclusions: The role of thalamus in the context of addiction and precise mechanisms involved in drug induced CPP are not well studied. Also, the potential role of T-channels in the brain circuits that regulate drug reward and seeking behavior remains relatively understudied. Here, we show for the first time the importance of the thalamic $Ca_V3.1$ T-channels in both morphine-induced neuronal excitability and morphine-induced CPP in mice.
Funding: This study was funded by grants from the National Institutes of Health, GRANT# R35GM141802 to SMT and GRANT# K01DA055258 to TTS

References: Li X et al. Role of anterior intralaminar nuclei of thalamus projections to dorsomedial striatum in incubation of methamphetamine craving. *J Neurosci* 2018; 38:2270–82

Cover KK et al. Activation of the Rostral Intralaminar Thalamus Drives Reinforcement through Striatal Dopamine Release. *Cell Rep* 2019; 26: 1389-1398.e3

Stamenic et al. Alterations in Oscillatory Behavior of Central Medial Thalamic Neurons Demonstrate a Key Role of CaV3.1 Isoform of T-Channels During Isoflurane-Induced Anesthesia. *Cereb Cortex* 2019; 29:1–18

Stamenic et al. Cytosolic ATP Relieves Voltage-Dependent Inactivation of T-Type Calcium Channels and Facilitates Excitability of Neurons in the Rat Central Medial Thalamus. *Eneuro* 2018; 102525:1–16

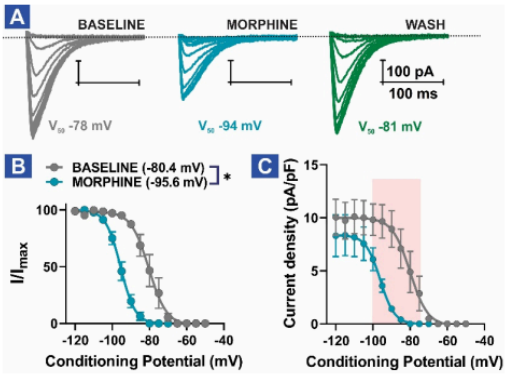

Figure 1. Voltage-dependent T-current inhibition by morphine (10 µM) in CeM neurons from WT mice. (A) Traces of T-current in a representative CeM neuron in control condtions (gray), after morphine (blue) and wash (green), recorded using a double-pulse protocol with 3.6-s-long prepulses to variable voltages (from −120 to −50mV in 5mV increment) – note that there is hyperpolarizing shift in inactivation V_{50} after morphine **(B)** Average normalized steady-state inactivation (I/I_{max}) curves with respective V_{50} values. **(C)** Reduction in T-current density after morphine application. **p<0.05, 2-tailed paired t-test or 2-way RM ANOVA, Sidak's post hoc (shaded area)*

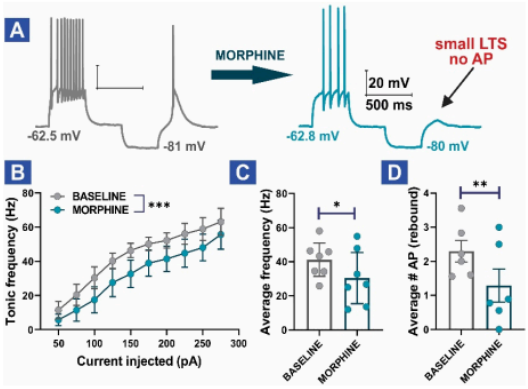

Figure 2. Acute morphine effect on CeM neuron excitability. (A) Representative traces from CeM neuron; baseline (gray) and after morphine (blue) – note that there is reduced tonic firing and drastically decreased LTS after hyperpolarization without rebound AP. Current injection depolarization (+100 pA) and hyperpolarization (-50 pA). Reduced tonic frequency in WT animals after acute morphine application across different current injections **(B)** and average **(C)**. Reduction of APs in rebound after morphine application **(D)**. **p<0.05, **p<0.01, ***p<0.001 2-way RM ANOVA, Sidak's post hoc or 2-tailed t-test*, N = 4 animals.

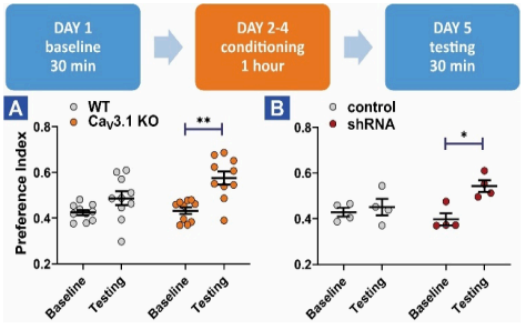

Figure 3. Schematic of the suboptimal morphine CPP protocol. Preference index in **(A)** WT and $Ca_V3.1$ KO male mice and **(B)** control (scrambled RNA) and $Ca_V3.1$ KD (Cacna1g shRNA) mice. **p<0.05, **p<0.01, 2-way RM ANOVA, Sidak's post hoc*

Neuroscience in Anesthesiology and Perioperative Medicine 7- Concurrent cerebral desaturation and EEG burst suppression in Cardiac Surgery patients

Rushil Vladimir Ramachandran[1], Alkananda Behera[1], Hibiki Orui[1], Zaid Hussain[1], Jordan Peck[1], Ajaykarthik Ananthakrishnan[1], Zenah Al-Dhamen[1], Priyam Mathur[2], Valerie Banner-Goodspeed[1], Jochen Muehlschlegel[3], Jean-Francois Pittet[4], Amit Bardia[4], Robert Schonberger[5], Edward Marcantonio[1], Kestas Kveraga[6], Balachundhar Subramaniam[7]

Beth Israel Deaconess Medical Center[1] BIDMC[2] BWH[3] Univ of Alabama at Birmingham[4] Yale School of Medicine Department of Anesthesiology[5] Beth Israel Deaconess Medical Center, Harvard Medical School[6] Harvard Medical School - Beth Israel Dea[7]

Introduction: The use of raw electroencephalogram (EEG) parameters as opposed to processed EEG is a promising development in the perioperative management of brain health. Intraoperative EEG burst suppression is associated with increased postoperative delirium (1). An algorithm combining processed EEG with cerebral oximetry was proposed to reduce burst suppression in a clinical case series (2). The incidence of simultaneous EEG burst suppression and cerebral desaturation is unknown.

Methods: In a multisite randomized controlled trial evaluating postoperative intravenous acetaminophen for the prevention of postoperative delirium, blinded EEG and cerebral oxygen desaturation was collected with the SEDLine monitor. We analyzed 13,577 intraoperative single site observations at one-minute intervals from 51 patients. The inclusion and exclusion criteria have been previously published (3). 6,825 minute interval observations were used for adjusted analysis. Burst suppression events were defined as observations with Suppression Ratio >0. Cerebral oximetry measurements were obtained from right and left cerebral hemispheres and desaturation events were defined as cerebral oximetry values <60% (4). Association between burst suppression and cerebral desaturation was analyzed using Pearson's Chi-squared test. Burst suppression was compared using the generalized linear mixed effect model with compound symmetry as the covariance matrix with cerebral desaturation, age, gender, BMI, and inhalational anesthetic concentration values as covariates.

Results: Of the 13,577-minute interval events, 21% had burst suppression and 47% had cerebral desaturations (either left or right, Table 1). Co-existing desaturation and burst suppression was seen in 12% of these events. Associations of burst suppression with only left or right sided cerebral desaturations are shown in Table 2. The odds of a significant burst suppression event having a co-existing cerebral desaturation (left or right) was 1.6 [1.5 - 1.8], $p < 0.01$) compared to events without burst suppression. On adjusted analysis, the association was still significant (OR 1.8 [1.5 - 2.3], $p < 0.001$), as shown in Table 3.

Conclusions: Significant association was seen between burst suppression events and cerebral desaturations in cardiac surgery patients. Further exploration is required with simultaneous monitoring of oxygen desaturation with routine EEG to determine causality of burst suppression (anesthetic vs. reduced perfusion).

References:

1. Intraoperative electroencephalogram suppression predicts postoperative delirium. Anesthesia and analgesia. 2016 Jan;122(1):234.
2. Patient management algorithm combining processed electroencephalographic monitoring with cerebral and somatic near-infrared spectroscopy: a case series. Canadian journal of anesthesia, 2019, Vol.66 (5), p.532-539
3. Scheduled Prophylactic 6-Hourly IV AcetaminopheN to Prevent Postoperative Delirium in Older CaRdiac SurgicAl Patients (PANDORA): protocol for a multicentre randomised controlled trialBMJ Open 2021;11: e044346.
4. Cerebral oximetry in cardiac anesthesia. J Thorac Dis. 2014 Mar;6 Suppl 1(Suppl 1): S60-9.

Figure 1: Association of Burst suppression events with means of left sided cerebral oximetry values (RSO2 A1)

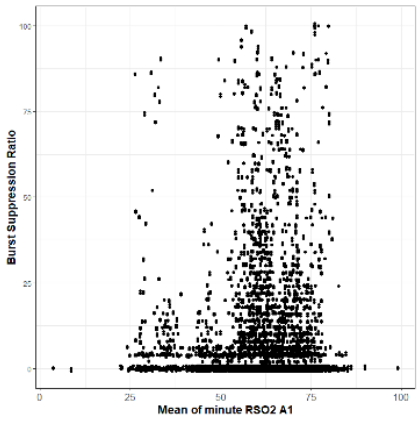

Figure 2: Association of Burst suppression events with means of right sided cerebral oximetry values (RSO2 A2)

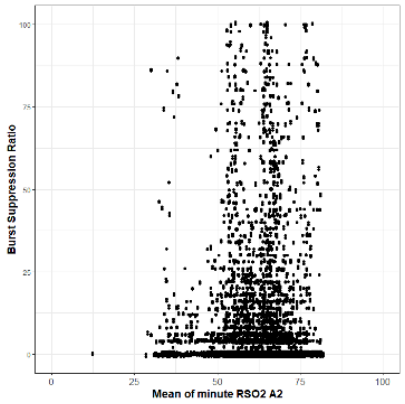

Table 1: Association of Burst suppression with cerebral desaturation on either side

	Events with Burst Suppression	Events without Burst Suppression	p value
Events with cerebral desaturation on either side	**1620 (12%)**	4726 (35%)	<0.001
Events with no cerebral desaturation on both sides	1247 (9%)	5984 (44%)	

Proportions were calculated with total number of observations as denominator

Table 2: Association of Burst suppression with cerebral desaturation only on the left or right side

	Events with Burst Suppression	Events without Burst Suppression	p value
Events with cerebral desaturation on the left side	**1086 (7.9%)**	3374 (25%)	<0.01
Events without cerebral desaturation on the left side	1786 (13%)	7337 (54%)	
Events with cerebral desaturation on the right side	**1247 (9.1%)**	3401 (25%)	<0.01
Events without cerebral desaturation on the right side	1676 (12%)	7445 (54%)	

Proportions were calculated with total number of observations as denominator

Table 3: Generalized linear mixed effect model with compound symmetry as the covariance matrix showing association between burst suppression and cerebral desaturation

Characteristic	OR[1]	95% CI[1]	p-value
Cerebral desaturation	1.8	1.49, 2.29	**<0.001**
Anesthesia concentration [every 0.1 % increase]	1.2	5.20, 9.25	**<0.001**
Age	1.1	0.97, 1.20	0.16
Gender			
Male	0.6	0.16, 2.08	0.41
BMI	1	0.91, 1.08	0.90

[1]OR = Odds Ratio, CI = Confidence Interval

Neuroscience in Anesthesiology and Perioperative Medicine 8- D1 dopamine receptor agonism restores locomotion without spatial memory recovery under isoflurane in rats

Michael Fettiplace[1], Kathleen Vincent[2], Angel Cho[3], Emmaline Dillon[4], Brendan Stapley[4], Victoria Stewart[4], Ken Solt[1]

Massachusetts General Hospital[1] Massachusetts General Hospital and Harvard Medical School[2] MGH[3] Brigham Young University[4]

Introduction: Stimulation of dopaminergic midbrain circuits restores arousal during general anesthesia[1] and prior reports suggest the utility of dopamine-receptor agonists as anesthetic reversal agents.[2] Midbrain dopaminergic neurotransmission also modulates hippocampal memory.[3] In this study we tested the hypothesis that dopaminergic agonists reverse the amnestic properties of isoflurane anesthesia in rats.

Methods: Our institutional animal care and use committee approved all experiments. We trained 16 Sprague-Dawley rats (8 male, 8 female, Charles River Labs) on a touchscreen task (Bussey-Saksida chamber, LaFayette Instruments).[4] Trial-unique nonmatching to location (TUNL) assesses if an animal can remember a touchscreen location (S) and choose a novel location (S') following a pre-specified delay when presented with both locations (S & S'). Behavioral training occurred in a step-wise fashion until animals consistently answered >80% correct at the furthest distances (D3) with a delay of 6 seconds (Figure 1). Other metrics of performance included overall performance and the ratio of independent TUNL trials (e.g. non-correction trials). Following training, we characterized the sex-dependent, distance-dependent and delay-dependent contributions to task performance. We evaluated the impact of an amnestic dose[5] of 0.25-0.35% isoflurane, delivered continuously in the behavioral chamber. Finally, we tested the effects of intravenous dextroamphetamine (a dopamine and norepinephrine releasing agent), atomoxetine (a norepinephrine reuptake inhibitor), and chloro-APB (a D1 dopamine receptor agonist) on task performance during continuous isoflurane delivery. Preliminary experiments demonstrated a need for 8 animals of each sex, based on a performance difference of ~=12% and standard deviation = 5% (power = 0.8, a =0.05) and anticipated 25% attrition. Statistical comparisons for multiple groups were performed with one-way analysis or variance with Holm-Sidak multiple comparison corrections. Multi-variate comparisons used mixed-models with Dunnett multiple comparison post-tests.

Results: Task acquisition correlated with the number of trials. D3 performance at a 6 second delay stabilized after 4500 trials (79±10% correct). Animals completed a variable number of trials per day from 37 (95% CI: 12 – 84) to 137 (30 – 191) translating into 33 to 121 days of training required to achieve consistent performance; after 60 days of training, underperforming animals were excluded (25%, no sex effect; Fisher-exact test p=0.57). Females completed 85±25 trials per day compared with 86±21 in males (p=0.88); comparisons between cage mates identified significant differences in all pairs (p<0.0001 Holm-Sidak multiple comparison). Increasing task-delay reduced all measures of performance with a reduction in percent correct at D3 from 82±3.5% (n=12) at 2.5 second delay to 47±4.3% at 36 seconds (n=12, p<0.0001, Mixed effects model) but no gender (p=0.3889) or subject effect (p=0.5261). D3 performance fit to a sigmoidal curve with half-maximal inhibitory time (IC50) of 16.5 seconds (R^2 = 0.43; Figure 2). Isoflurane reduced task performance at D3 from 80±2% to 58.6±6.0%, independent of task delay (Figure 3; ****p<0.0001) with return to 79±3% at 24 hours. Isoflurane also reduced physical activity based on beam breaks from 426±17 to 207±49 (p<0.0001) with a return to 425±22 at 24 hours. Treatment with intravenous dextroamphetamine (1 mg/kg, dAmph), chloro-APB (0.3 mg/kg, c-APB) or atomoxetine (1 mg/kg, atomox) did not improve task performance relative to controls (Figure 4, Mixed-effects model p=0.0045; Dunnett's multiple comparisons; **p=0.0038, ***p=0.0002, *p=0.039). Both dextroamphetamine (dAmph) and chloro-APB (c-APB) rescued locomotor activity as assessed by infrared beam breaks compared to baseline, whereas atomoxetine (atomox) did not (Figure 5, ANOVA p=0.0035; Dunnett's multiple comparisons; * p=0.01, ** p=0.003).

Conclusions: We characterized the effects of an amnestic dose of isoflurane and several arousal-promoting agents on a touchscreen task designed to test short-term spatial memory in rats. Treatment with dextroamphetamine or chloro-APB (but not atomoxetine) reversed locomotor deficits produced by 0.3% isoflurane without reversing amnesia. This suggests that elevated dopaminergic neurotransmission in the setting of residual isoflurane may cause hyperactive delirium in the postoperative setting.

References: 1. PNAS, 113 12826 – 12831, 2016

2. Anesthesiology, 118 30-39, 2013

3. PNAS, 113: 14835-14840, 2016

4. Neurobiol Learn Mem, 94, 341-352, 2010

5. Anesthesiology; 113, 1299-1309, 2010

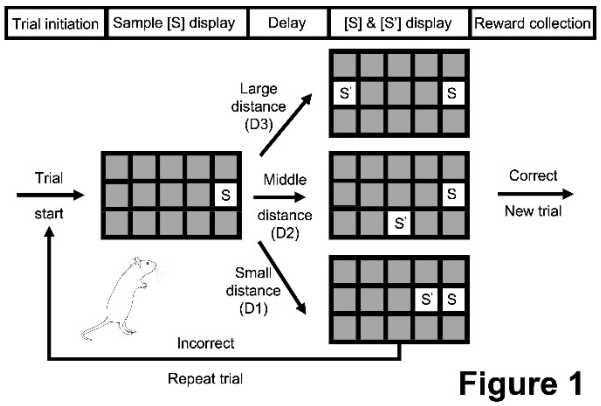

Figure 1

Figure 2

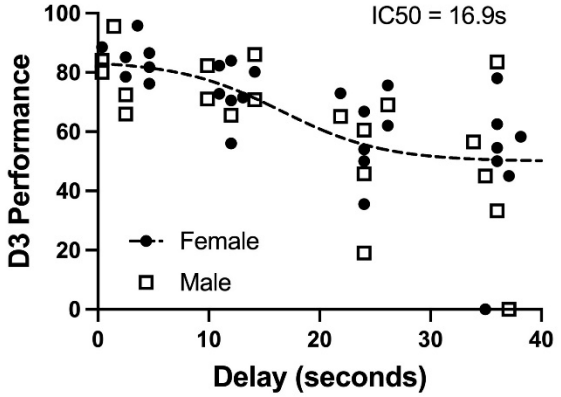

Figure 3

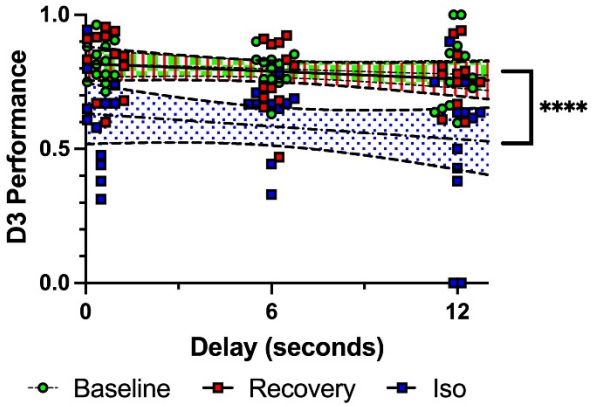

Figure 4

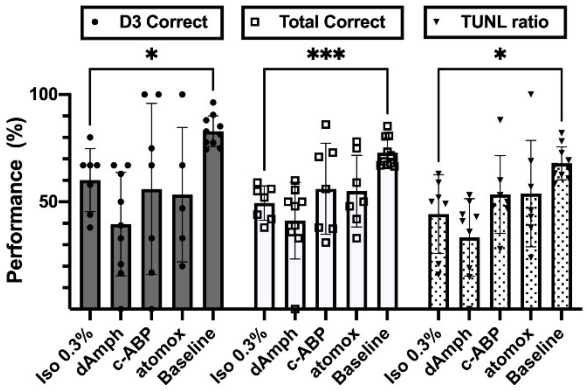

Figure 5

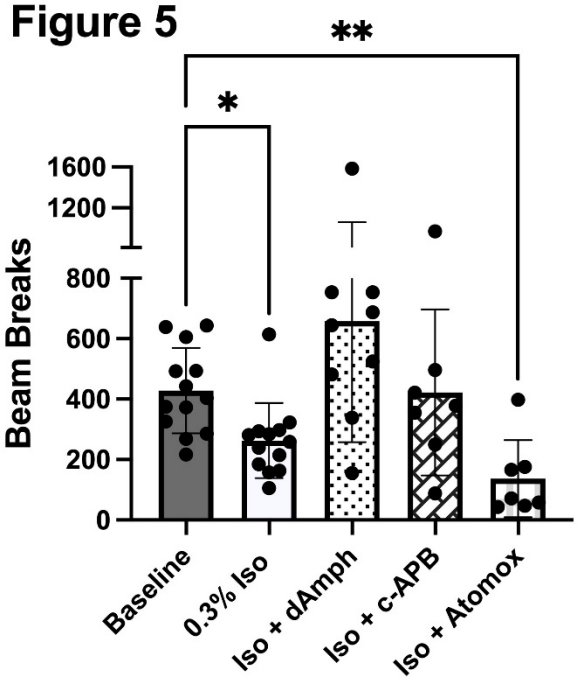

Neuroscience in Anesthesiology and Perioperative Medicine 9- Effect of Repeated Exposure to Sevoflurane on Electroencephalographic Alpha Oscillation in Pediatric Patients Undergoing Radiation Therapy

Rodrigo Gutierrez[1], Patrick Purdon[1], Antonello Penna[2], Jose Egaaña[2], Samuel Madariaga[2], Christ Devia[2], Felipe Maldonado[2]

Massachusetts General Hospital[1] Universidad de Chile[2]

Introduction: General anesthesia is required for pediatric who receive radiation therapy for the treatment of malignancies. This is a unique scenario, in which a developing brain is exposed to daily administration of general anesthetics for up to 5 weeks. We do not know whether and to what extent this repeated exposure to anesthetic drugs induces tolerance, defined as a decrease in the effect of the drug over time or the need to increase the dose to achieve the same effect[1]. Here we evaluate whether the repeated exposure to inhalational anesthesia leads to the development of tolerance in children undergoing radiation therapy.

Methods: We conducted an observational prospective study between November 2019 and August 2021 in the Instituto Nacional del Cancer (Santiago, Chile). Patients older than 1 y and younger than 6 y, with the diagnosis of cancer and indication to receive radiotherapy treatment under general anesthesia, were included. Exclusion criteria were previous treatment with radiotherapy, the need of propofol during anesthesia induction, and history of malignant hyperthermia. Anesthesia management was standardized before the start of the study to a sole sevoflurane agent for the entire procedure. EEG records were obtained with use of the SedLine monitor every 3 sessions. Power spectra were computed for each patient and session using the multitaper method. From each session spectrum, we calculated the relative power at each frequency band[2], as the ratio between the band power and the total power of the signal. Total power was calculated between 1 to 40 Hz. EEG frequency bands were defined as follow: delta (1 to 4 Hz), theta (4 to 8 Hz), alpha (8 to 12 Hz) and beta (12 to 30 Hz) power. As a clinical outcome, induction time was operationally stated as the time (in seconds) between the beginning of the induction and the time after LMA was successfully placed. Regarding the EEG outcomes, we define the theta relative power as a primary endpoint given previous evidence suggesting its association with inhalational anesthetic dose. Data were reported as means and SD or medians and IQR for continuous variables and frequencies and percentages for categorical variables. For group comparisons, we used a t-test or Mann-Whitney depending on the variable distribution. We fit individual and group level linear regression models to evaluate the correlation between the outcome and session. Finally, we build a linear mixed-effect model to evaluate the association between anesthesia session and both induction time and EEG spectral power at specific frequency bands. A p-value less than 0.05 was considered statistically significant. Sample size: We aimed to include all patients that meet our inclusion criteria during an 18-months period. Based on our historical volume of patients, we expected to enroll 20 patients over this time lapse, which is a similar sample size reported in previously[3,4]

Results: We included 19 patients in the analysis. Demographics and diagnoses are summarized in **Table 1**. Our mixed-effect model showed no correlation between the induction time and sessions of anesthesia (**Table 2**). This was also corroborated both, at individual level (**Figure 1A**) and at group level (**Figure 1B**). With regard the EEG analysis, our mixed-effect model indicate that only alpha relative power was inversely correlated with the number of anesthesia sessions (**Table 2**). We observed that only a subgroup of patients exhibited an inverse correlation between alpha relative power and anesthesia sessions (**Figure 2A**). Using a Gaussian mixture model (GMM) we found that the dataset was composed of 2 subpopulations, identified by their estimated individual slope (**Fig 2B-C, Fig 3**). One group had a mean slope near zero (Cluster 1), while the other group showed a negative slope, in agreement with the inverse correlation between the alpha relative power and anesthesia sessions (Cluster 2). No differences in clinical characteristics and baseline EEG features were found between patients in the two clusters.

Conclusions: Our results do not support the development of tolerance to sevoflurane in children undergoing repeated anesthesia exposure for radiation therapy. However, we found that a group of patients exhibited a reduction in the alpha relative power as function of anesthetic exposure. These results may have implications that justify further studies.

References: 1. Tolerance, withdrawal, and physical dependency after long-term sedation and analgesia of children in the pediatric intensive care unit. *Crit Care Med* 2000;28(6):2122-32

2. Electroencephalographic Alpha and Delta Oscillation Dynamics in Response to Increasing Doses of Propofol. *J Neurosurg Anesthesiol* 2022;34(1):79-83

3. Children undergoing repeated exposures for radiation therapy do not develop tolerance to propofol: clinical and bispectral index data. *Anesthesiology* 2004;100(2):251-4

4. Evaluation of propofol for repeated prolonged deep sedation in children undergoing proton radiation therapy. *Br J Anaesth* 2007;99(4):556-60.

Table 1. Baseline Demographic and Individual Characteristics of the Patients.

Subject	Age (years)	Sex	Weight (Kg)	Diagnosis	CMT	No. Sessions
1	4.2	M	18	Medulloblastoma	Y	33
2	3.9	M	22	Leukemia	Y	13
3	1.9	F	12	Wilms Tumor (lung)	Y	8
4	3.1	F	21	Wilms Tumor (abdominal)	Y	9
5	6.0	F	24	Wilms Tumor (abdominal)	Y	11
6	2.0	F	10	Ependymoma	N	26
7	5.9	M	21	Glioblastoma	N	29
8	3.0	F	14	Ependymoma	N	31
9	2.7	F	18	Ependymoma	Y	33
10	1.1	F	10	Ependymoma	N	31
11	2.5	F	16	Leukemia	Y	18
12	3.7	F	19	Leukemia	Y	9
13	2.8	M	16	Ependymoma	N	35
14	4.8	F	15	Wilms Tumor (kidney)	N	9
15	5.1	F	22	Leukemia	Y	9
16	3.1	F	15	Ependymoma	Y	33
17	5.2	F	16	Ewing's sarcoma	Y	31
18	4.6	F	17	Medulloblastoma	N	33
19	4.8	F	27	Osteochondroma (skull)	N	34

M: male, F: female, Kg: kilograms, CMT: chemotherapy

Table 2. Linear Mixed Effect Models Results

	Fixed Coefficient Estimate	SE	tStat	pValue	95% CIs	R^2
Clinical Outcome						
Outcome ~1 + Session + (1+Session | Subject) + (Session| Anesthetist)						
Induction Time	-0.6847	0.5605	-1.22	0.22	-1.787 – 0.418	0.29
Electroencephalographic Outcomes						
Outcome ~1 + Session + (1+Session | Subject) + (1+Session|Cluster)						
Delta Relative Power	0.0021	0.001	1.78	0.08	-0.0002 – 0.0045	0.46
Alpha Relative Power	-0.0018	0.001	-2.35	0.02	-0.0031 – -0.0010	0.51
Theta Relative Power	-0.00004	0.001	-0.07	0.93	-0.0011 – 0.0016	0.11
Beta Relative Power	-0.0004	0.0004	-1.13	0.26	-0.0014 – 0.0002	0.29

SE: Standard Error, CI: Confidence Interval.

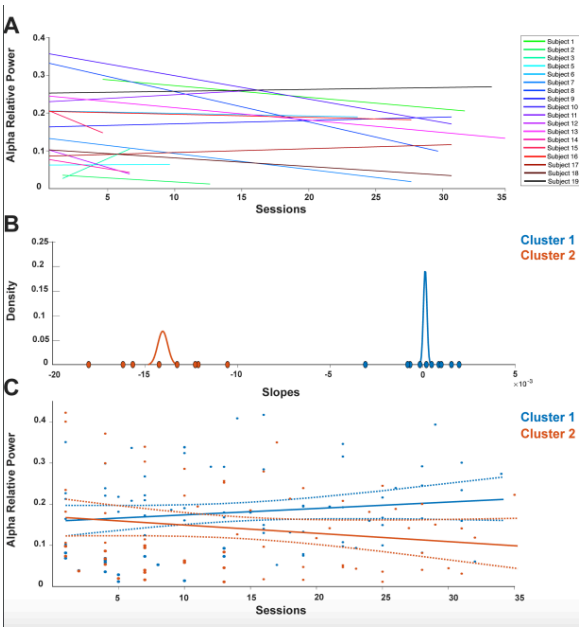

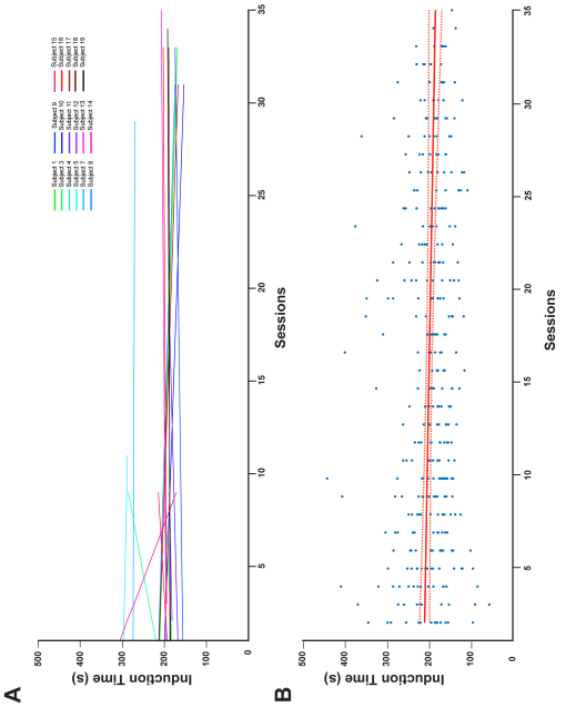

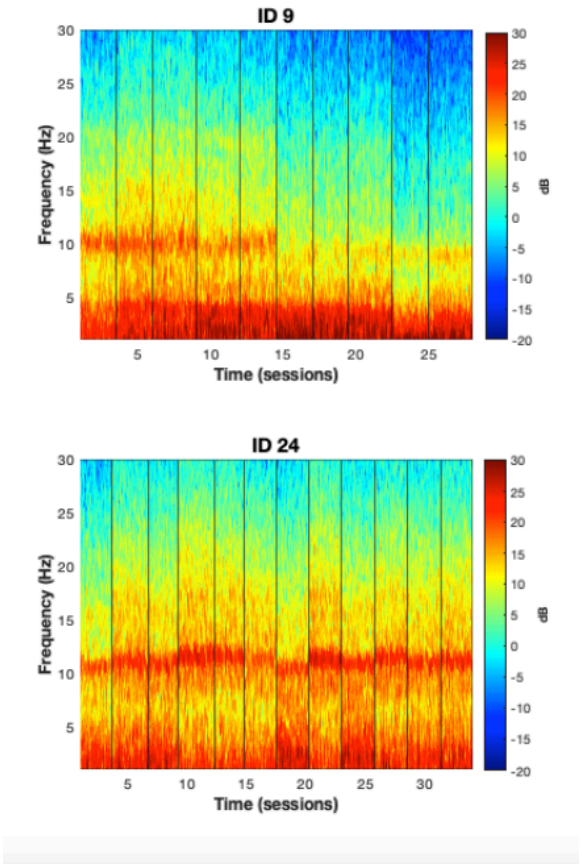

Neuroscience in Anesthesiology and Perioperative Medicine 10- Estrogen regulates myogenic tone in hippocampal arterioles by enhanced basal release of nitric oxide and endothelial SK_{Ca} channel activity

Fabrice Dabertrand[1]

University of Colorado Anschutz Medical Campus[1]

Introduction: Arteries and arterioles exhibit myogenic tone, a partially constricted state typically inhibited by isoflurane. Myogenic tone allows further constriction or dilation in response to moment-to-moment fluctuations in blood pressure. The vascular endothelium that lines the internal surface of all blood vessels controls a wide variety of essential functions, including the contractility of the adjacent smooth muscle cells by providing a tonic vasodilatory influence. Studies conducted on large (pial) arteries on the surface of the brain have shown that estrogen lowers myogenic tone in female mice by enhancing nitric oxide (NO) release from the endothelium, however, whether this difference extends to the intracerebral microcirculation remains ambiguous. The existing incomplete picture of sex differences in cerebrovascular physiology combined with a deficiency in treatments that fully restore cognitive function after cerebrovascular accidents places heavy emphasis on the necessity to investigate myogenic tone regulation in the microcirculation from both male and female mice. We hypothesized that sex-linked hormone regulation of myogenic tone extends its influence to the microcirculation level, and sought to characterize it in isolated arterioles from the hippocampus, a major cognitive brain area.

Methods: Using diameter measurements in pressure myography experiments, we measured lower myogenic tone responses in hippocampal arterioles from female than male mice at physiologically relevant pressures.

Results: By using a combined surgical and pharmacological approach, we found myogenic tone in ovarectomized (OVX) female mice matches that of males, as well as in endothelium-denuded arterioles. Interestingly, eNOS inhibition induced a larger constriction in female arterioles but only partially abolished the difference in tone. We identified that the remnant difference was mediated by a higher activity of the small-conductance Ca^{2+}-sensitive K^{+}(SK) channels.

Conclusions: Collectively, these data indicate that eNOS and SK channels exert greater vasodilatory influence over myogenic tone in female mice at physiological pressures.

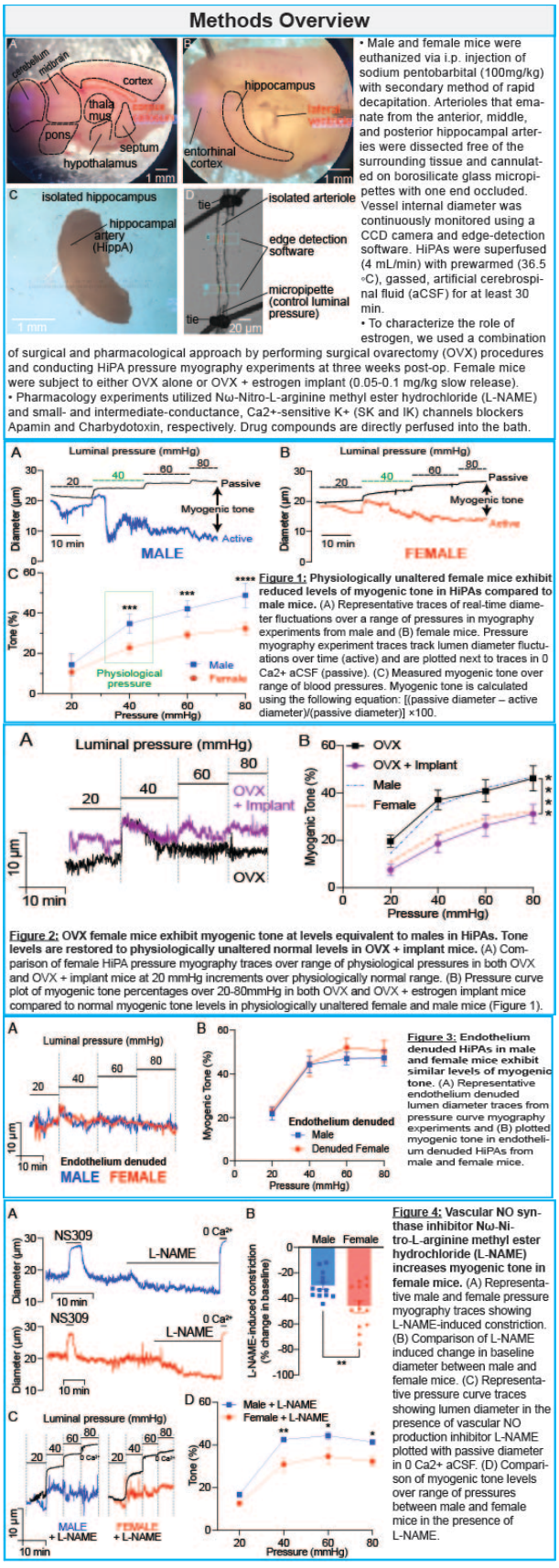

Neuroscience in Anesthesiology and Perioperative Medicine 11- Evaluating Speech and Language in The Post-Anesthesia Care Unit; Implications for Perioperative Neurocognitive Disorders

Meah Ahmed[1], Alice Daramola[2], Carla Troyas[3], Oliver Isik[4], Antara Banerji[4], Jamie Sleigh[5], Paul Garcia[6]

Columbia University Irving Medical Center[1] Columbia Vagelos College of Physicians and Surgeons[2] Technical University of Munich School of Medicine[3] Columbia University Vagelos College of Physicians & Surgeons[4] University of auckland[5] Columbia University[6]

Introduction: Precise mechanisms for the return of consciousness and baseline cognitive function after surgical anesthesia have eluded neuroscientists for decades [1]. Perioperative neurocognitive disorders (PND) can range from mild and transient confusion to persistent cognitive dysfunction [2]. Sometimes surgical recovery is characterized by brief, subacute, and self-resolving episodes of post-operative delirium (POD): a form of PND with an estimated incidence of 20-50% [3-4]. Identifying compromised neuroanatomic correlates for PND has proven to be difficult in part due to heterogeneity in phenotypes. Yet, binary assessments such as delirium screens (e.g., 3-D CAM) are the mainstay to evaluate PND in the post-anesthesia care unit (PACU). Essentially, these assessments rely on verbal instructions to determine cognitive abnormalities. Unfortunately, these assessments do not consider the production of speech and language which may provide initial insight into crucial brain networks that have potentially failed to appropriately recover from anesthesia. Characterized as aphasia, speech and language deficits can aid in the diagnosis of localized brain abnormalities for disorders such as stroke or TBI [5]. We hypothesized that speech and language deficits in the PACU may play an important role in identifying normal vs. abnormal sequential activation of brain networks during early anesthetic recovery, and help us gain insight into specific underlying neuroanatomic correlates at the bedside when brain imaging is not immediately feasible. In doing so, we developed an assessment evaluating cognitive domains specific to speech and language (figure 1). Each domain has neuroanatomic correlates indicative of cognitive dysfunction [6].

Methods: This is a planned interim analysis of an ongoing study with institutional IRB approval (IRB-AAAT7281). 39 patients undergoing elective surgeries with general anesthesia were considered (table 1). Participants were administered the speech and language assessment in the 48 hours before their scheduled surgery via telephone. Following anesthesia emergence (i.e., arousable to voice), a post-operative speech and language assessment was completed in the PACU. To avoid a learning effect, different versions of the assessment were utilized pre- and post-operatively. Assessments were conducted no sooner than 30 minutes after arrival in the PACU. All assessments were completed before the patients' discharge from the PACU.

The assessment examined cognitive domains pertaining to speech processing and production, namely, verbal fluency, auditory comprehension, objective naming, sentence repetition, and narrative production (scored in real-time by trained personnel) (figure 1). The Wilcoxon signed-rank test was used to evaluate for significant differences between pre- and post-operative performances for each domain ($p < 0.05$).

Results: There was a significant decrease in total word output between the pre- and post-operative verbal fluency assessments ($p = 4E-7$) (table 2). Each verbal fluency task (semantic and phonemic fluency) was separated into two 15-second epochs from its 30-second assessment. The total word output of each epoch showed a significant decrease between pre- and post-operative assessments (figure 2).
Interestingly, auditory comprehension and objective naming scores were not significantly different between the pre- and post-operative assessments, whilst sentence repetition scores revealed a significant deficit ($p = 0.01$) (table 2). Furthermore, narrative production scores between the pre- and post-operative assessments revealed a substantial decrease in fluency ($p = 8.9E-7$), content ($p = 9.6E-5$), and cohesion ($p = 0.005$) (table 2).

Conclusions: Speech and language assessments have been used to identify cerebral damage as a result of TBI, stroke, etc. Our study examined speech and language in the post-operative period, using an assessment originally developed to identify the neuroanatomic basis of specific aphasias [6]. Our results suggest that executive function governing speech and language can be impacted for patients in the PACU. Most pronounced deficits in fluency and narrative production domains, with conservation of comprehension and objective naming, are consistent with transcortical motor aphasia and underlying thalamic aphasia, which may reflect the residual effects of anesthesia on these important structures. Future studies that incorporate imaging may be useful to manifest or further speculate upon these findings for certain.

References: [1] General Anesthesia and Altered States of Arousal: A Systems Neuroscience Analysis, 34:601–28, 2011

[2] Recommendations for the nomenclature of cognitive change associated with anaesthesia and surgery, 121(5):1005-1012, 2018

[3] Early delirium after cardiac surgery: an analysis of incidence and risk factors in elderly (65 years) and very elderly (80 years) patients, 13:1061-1070, 2018

[4] Postoperative delirium: a 76-year-old woman with delirium following surgery, 308(1):73-81, 2012

[5] Aphasia and Aphasic Syndromes, 13: 133-148, 2021

[6] Acquired Speech and Language Disorders, 1-59, 1990

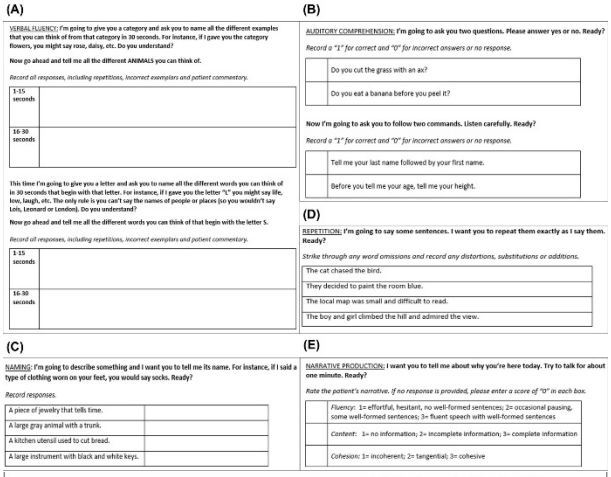

	All Patients in Study (39)
Age (mean years old)	59.51 (std± 13.8)
BMI (mean kg/m²)	28.84 (std± 7.55)
Surgery (mean minute duration)	131.18 (std± 86.1)
Anesthesia (mean minute duration)	202.95 (std± 97.8)
Sex (n,%)	
Males	14 (35.90%)
Females	25 (64.10%)
Type of surgery	
General	23 (58.97%)
Gynecologic	12 (30.77%)
Urologic	4 (10.26%)

	Preop Group Mean (std)	**Postop Group** (PACU) Mean (std)	**Difference** (Preop-Postop) Mean (std)	**p-value** Wilcoxon Signed Rank Test
VERBAL FLUENCY				
Naming animals (total words)	13.9 (4.0)	10.2 (3.4)	3 (5)	***0.000009**
Letters (total words)	10.1 (3.4)	6.8 (3.3)	3 (5)	***0.000002**
Overall word count	*24.0 (6.5)*	*17.1 (5.4)*	*7 (6.75)*	***0.0000004***
AUD. COMPREHENSION (0-4)	3.9 (0.3)	3.8 (0.5)	0.1 (0.5)	0.40
OBJECTIVE NAMING (0-4)	4 (0)	4 (0)	0 (0)	1
SENTENCE REPETITION (0-4)	3.7 (0.4)	3.3 (0.9)	0.4 (1.0)	***0.01**
DISCOURSE				
Fluency (0-3)	2.9 (0.3)	2.3 (0.5)	0.7 (0.5)	***8.9E-7**
Content (0-3)	2.9 (0.3)	2.4 (0.6)	0.4 (0.6)	***9.6E-5**
Cohesion (0-3)	2.9 (0.3)	2.6 (0.7)	0.3 (0.7)	***0.005**

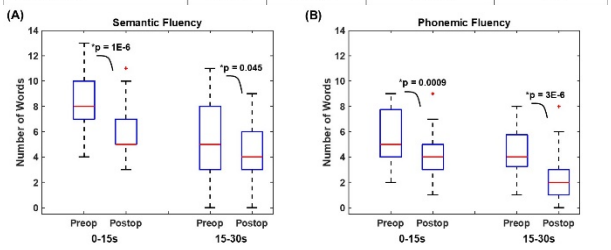

Neuroscience in Anesthesiology and Perioperative Medicine 12- Frequency-specific neurophysiological coactivation patterns during post-anesthetic recovery of consciousness and cognition

Duan Li[1], Duan Li[1], Michael Avidan[2], Max Kelz[2], Phillip Vlisides[2], George Mashour[3]

University of Michigan[1] Washington University in St Louis[2] University of Michigan[3]

Introduction: Understanding how the brain recovers from unconsciousness can inform neurobiological theories of consciousness and guide clinical investigation. Using general anesthesia as a controlled and reproducible model, previous studies have investigated the patterns of reemerging consciousness and cognitive functions [1-3], but the neurophysiological processes that underlie this process remain incompletely understood. We aimed to characterize the spatiotemporal dynamics of spontaneous brain activity during post-anesthetic recovery and further investigate the relationship of those dynamics to the reconstitution of consciousness and cognitive performance.

Methods: We re-analyzed electroencephalographic (EEG) data from 30 healthy participants who underwent induction of anesthesia with propofol followed by 3 h of isoflurane anesthesia at age-adjusted 1.3 minimum alveolar concentration [1, 4]. Upon recovery of consciousness, recurrent cognitive testing was performed for 3 h at 30-min intervals. Each testing session consisted of a battery of six neurocognitive tests including digit symbol substitution test (DSST, a test of cognitive throughput and visual scanning) and psychomotor vigilance test (PVT, a measure of vigilance and attention resistant to learning effects with repeat administration), followed by an eyes-closed resting-state session (Figure 1A). *k*-means clustering analysis was applied to the envelope data of scalp EEG signals to extract a set of recurring states. To further characterize the brain states, cortical sources were estimated using the weighted minimum norm estimation method, based on 128-channel EEG signals acquired from nine subjects. Temporal dynamics were evaluated by the state occurrence rate and transition probabilities between brain states. Spearman's rank correlation was used to assess the associations between state-dynamic measures and cognitive data in individual subjects.

Results: Excluding suppression, nine brain states were identified that represent frequency-specific spatial coactivation patterns (Figure 2B). After induction of propofol anesthesia, the temporal progression of brain states demonstrated a shifting trajectory that was reversed after the discontinuation of isoflurane anesthesia. Loss of consciousness was associated with the highest occurrence rate of beta activation patterns, while recovery of consciousness was associated with an increasing occurrence of the temporal gamma pattern (Figure 1C). Subjects that entered the anterior alpha state later (with the greatest activation in source-localized anterior cingulate cortex) (r=-0.627, p<0.001) and resided in the anterior alpha state for a longer time (r=-0.613, p<0.001) tended to recover consciousness more slowly and show a greater degree of impaired speed of DSST upon recovery (Figure 2A). At initial recovery, aside from changes in posterior alpha and anterior beta patterns, the state occurrence and transition dynamics were comparable to that of baseline, despite the impairment of cognitive performance. Importantly, the state dynamics of the anterior beta pattern (with the greatest activation in anterior cingulate cortex), but not other patterns, during the post-anesthetic resting-state sessions tracked the recovery of cognitive performance of DSST (accuracy: r=-0.543 [-0.786, -0.289], p<0.001; speed: -0.543 [-0.829, -0.371], p<0.001) and PVT (accuracy: -0.609 [-0.829, -0.303], p<0.001; speed: -0.600 [-0.786, -0.300], p<0.001) (Figure 2B).

Conclusions: The spatiotemporal-spectral dynamics of spontaneous EEG signals, especially anterior alpha and beta activation patterns, are associated with post-anesthetic recovery of consciousness and cognitive performance in healthy adults. These results support the hypothesis that anterior cortex is critical for the recovery of consciousness and cognition after general anesthesia and also advance our understanding of the neurophysiological signatures of perianesthetic neurocognitive function in surgical patients.

References:

1. eLife 10: e59525, 2021
2. Br J Anaesth 123(2): 206-218, 2019
3. Br J Anaesth S0007-0912(22)00028-9, 2022
4. Frontiers in Human Neuroscience 11: 284, 2017

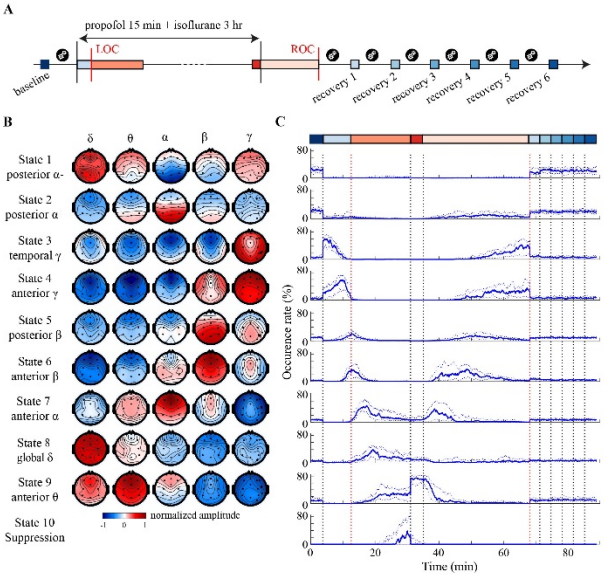

Figure 1. Experimental design and brain states. (**A**) Experimental design and timeline. The colored rectangles indicate the studied time periods, including 5-min eyes-closed resting-state baseline, induction, post-loss of consciousness period, last 5 min during maintenance period, emergence period and six 5-min eyes-closed resting-state sessions after recovery. (**B**) Besides suppression, nine brain states were identified by *k*-means clustering of the band-limited envelope data from 30 subjects that represent distinct spectral and spatial coactivation patterns in spontaneous cortical activity. (**C**) The temporal progression of occurrence rate of each brain state across the studied periods (solid line: median, dashed lines: the interquartile range across all subjects). For each subject, the occurrence rate of each brain state was calculated in 1-min windows at a step size of 1-s. The time spans during baseline, induction, post-loss of consciousness, maintenance, emergence, and each recovery period were rescaled. LOC, loss of consciousness. ROC, recovery of consciousness.

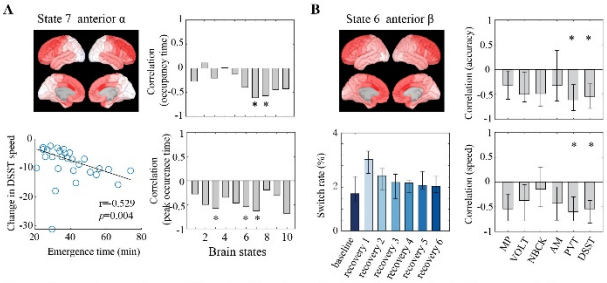

Figure 2. The spatiotemporal-spectral dynamics of spontaneous EEG signals are associated with post-anesthetic recovery of cognitive performance. (**A**) The emergence time and the occurrence of anterior alpha pattern during emergence are associated with the degree of disrupted speed in DSST upon recovery of consciousness. *indicates statistically significant correlation (p<0.05/10 brain states, Spearman's rank correlation). (**B**) The brain state dynamics of anterior beta pattern tracks the recovery of cognitive performance after general anesthesia in individual subjects. *indicates statistically significant correlation defined as (1) median correlation value larger than 0.5 (or smaller than -0.5), and (2) data distribution of correlation coefficients with median value statistically different from zero (Sign test, p<0.05/9 coactivation patterns). In A and B, the spatial characteristics of the brain states were shown by mapping the cluster centroids to source space using 9 subjects with high-density EEG recordings. PVT, Psychomotor Vigilance test. MP, Motor Praxis. VOLT, Visual Object Learning Test. NBCK, Fractal-2-Back. AM, Abstract Matching. DSST, Digital Symbol Substitution Test.

Neuroscience in Anesthesiology and Perioperative Medicine 13- GLUT1 reduction in the blood-brain barrier promotes cognitive impairment in aged surgical mouse model

Ying Chen[1], Raymond Chuen-Chung Chang[1], Gordon Wong[2]

The first affiliated hospital of Sun Yat-sen University[1] Department of Anaesthesiology University Of Hong Kong[2]

Introduction: Glucose transporter 1 (GLUT1) is essential for glucose transport from the periphery into the brain. Abnormal GLUT1 expression led to insufficient glucose metabolism [1]. Previously, GLUT1 downregulation was correlated with cognitive impairment in Alzheimer's disease, even emerged much earlier than cognitive symptoms [1, 2]. However, the implication whether GLUT1 was affected by surgery and involved in perioperative neurocognitive disorders has not been elucidated. Here, we investigated the role of GLUT1 in post-operative cognitive decline in aged surgical mouse model.

Methods: A laparotomy was subjected to aged male C57BL/6N mice under sevoflurane anesthesia and analgesia. Novel Objective Recognition test was used for cognitive function assessment. Expression of microvascular GLUT1 were evaluated by RT-PCR and Western blot. Hippocampal metabolic profiling was quantified by gas chromatography-tandem mass spectrometry. Intracerebroventricular administration of AAV9-ICAM2-GLUT1 was used for microvascular GLUT1 overexpression

Results: Using an abdominal surgery model in aged WT mice, we showed a significant decline in cognitive performance, along with GLUT1 reduction in the blood-brain barrier and diminished glucose metabolism, especially ATP level. Enhanced microvascular GLUT1 alleviated cognitive decline and improved metabolic profiles but did not directly retain ATP generation in the hippocampus.

Conclusions: GLUT1 reduction may contribute to cognitive deficits in aged surgical mice by affecting metabolic networks in the brain. It indicates the potential of GLUT1 to be one of therapeutic target of for postoperative cognitive decline

References: 1.Barros, L.F., et al., *Near-critical GLUT1 and Neurodegeneration.* J Neurosci Res, 2017. **95**(11): p. 2267-2274.

2. Szablewski, L., *Glucose Transporters in Brain: In Health and in Alzheimer's Disease.* J Alzheimers Dis, 2017. **55**(4): p. 1307-1320.

Neuroscience in Anesthesiology and Perioperative Medicine 14- Intracranial electrophysiological signatures of delirium in neurosurgical patients

Matthew Banks[1], Benjamin Hayum[1], Bryan Krause[1], Robert Sanders[1], Kirill Nourski[1]

University of Wisconsin[1]

Introduction: Post-operative post-ictal delirium (POD, PID) are acute disorders of consciousness characterized by confusion, fluctuating arousal, impaired executive function, and perceptual disturbances. POD is a harbinger of dementia and accelerated age-associated cognitive decline[1]. PID is a significant health concern in epilepsy and is a common complication of electroconvulsive therapy[2]. Thus, delirium is a major public health problem[3], yet its pathophysiology is poorly understood. The mechanisms underlying delirium and the degree to which these mechanisms overlap between POD and PID are unknown.
Epilepsy patients undergoing intracranial electroencephalographic (iEEG) monitoring prior to surgery for resection of seizure foci can experience both POD and PID, and thus are suitable subjects for mechanistic investigations. Network models suggest that these symptoms are secondary to disruptions in information flow within and between canonical brain networks[4,5]. Delirium-related changes in cortical activity and connectivity overlap with those of sleep and anesthesia (e.g., disrupted fronto-parietal connectivity[6,7], even though patients remain conscious. Here we report initial observations on spectral power and functional connectivity assayed from iEEG recordings in patients experiencing both POD and PID.

Methods: iEEG recordings were obtained from 19 adult neurosurgical patients implanted with electrodes in temporal, parietal, and frontal cortex to identify epileptic foci. Research protocols aligned with best practices[8]. Research participation did not interfere with acquisition of clinically necessary data, and participants could rescind consent for research without interrupting their clinical management.
POD was assessed daily or twice daily using the 3-Minute Diagnostic interview for Confusion Assessment Method (3D-CAM) or Confusion Assessment Method for the Intensive Care Unit (CAM-ICU) beginning 24 hours after surgery. PID was assessed immediately following seizures. Resting state data (~10 mins) were collected [1] following POD assessments at two time points: Early (40–70 hrs after surgery) and Late (140–320 hrs after surgery), [2] following PID assessments, [3] at a third time point >4 hrs after a seizure to serve as control, and [4] during overnight sleep recordings in a subset of subjects[9].
Electrodes were rejected if they corresponded to seizure foci, were excessively noisy, or located in white matter or outside the brain. Slow wave activity (1-4 Hz; SWA) was calculated using the demodulated band transform[10], and compared between different time points and according to delirium status. Resting state functional connectivity (RSFC) was calculated as alpha band (8-14 Hz) weighted phase lag index (wPLI)[10] and as orthogonalized g (30-50 Hz) power envelope correlations (g_{env}-corr)[11].

Results: SWA was elevated post-operatively in all patients, but POD+ patients tended to have higher SWA overall. Patients tended to have SWA post-ictally when they are PID+ compared to when they are PID-, but not compared to control. However, PID+ patients tend to have higher SWA overall. All patients tend to have higher g_{env}-corr and lower wPLI post-op, but POD+ patients tend to have higher higher g_{env}-corr and lower wPLI overall. We observed no consistent differences in RSFC for PID. Post-operative SWA was comparable to that observed in slow wave sleep all patients, but post-ictal SWA was lower than during sleep.

Conclusions: POD & PID delirium can be studied in neurosurgery patients with iEEG electrodes and may have overlapping underlying mechanisms. SWA when the patient is not delirious may be predictive of both POD and PID. Functional connectivity when the patient is not delirious may be predictive of POD, but not PID. Post-operative SWA wake is comparable to that in slow wave sleep post-operatively in all patients.

References: 1 J Gerontol A Biol Sci Med Sci 72, 1697-1702 (2017).

2 Psychiatry Clin Neurosci 63, 180-185 (2009).

3 Arch Intern Med 168, 27-32 (2008).

4 Med Hypotheses 77, 140-143 (2011).

5 Med Hypotheses 104, 80-85 (2017).

6 Br J Anaesth 125, 55-66 (2020).

7 Clin Neurophysiol 132, 246-257 (2021).

8 Neuron 110, 188-194 (2022).

9 Neuroimage 211, 116627 (2020).

10 J Neurosci Methods 261, 135-154 (2016).

11 Neuroimage 55, 1548-1565 (2011).

12 Nat Neurosci 15, 884-890 (2012).

Neuroscience in Anesthesiology and Perioperative Medicine

15- Intraoperative ketamine for prevention of postoperative neurocognitive disorders after major orthopedic surgery in elderly patients: a prospective multicenter randomized blinded placebo-controlled trial – the POCK study

Franck Verdonk[1], Pierre Lambert[1], Clément Gakuba[1], Anais Charles Nelson[1], Brice Gaudilliere[1], Tarek Sharshar[1], Raphael Gaillard[1], Serge Molliex[1]

Stanford University[1]

Introduction: Preventive anesthetic impact on the high rates of postoperative cognitive disorders in elderly patients is debated (1, 2, 3). The Prevention of postOperative Cognitive dysfunction by Ketamine (POCK) study aimed to assess the effect of ketamine on delayed neurocognitive recovery post-surgery.

Methods: This is a multicenter, randomized, quadruple-blind, prospective study. Patients ≥60 years undergoing major orthopedic surgery were randomly assigned in a 1:1 ratio to receive preoperative ketamine (0.5mg/kg) or placebo in random blocks of size 2 and 4 stratified according to study site, preoperative cognitive status (Montreal Cognitive Assessment score) and age. The primary outcome was the proportion of delayed cognitive recovery defined as a decline of one or more standard deviations in neuropsychological assessment according to the Diagnostic and Statistical Manual for Mental Disorders, fifth edition (DSM-5) on postoperative day 7. Secondary outcomes included the incidence of postoperative neurocognitive disorders three months after surgery and the incidence of delirium, anxiety, and depression seven days and three months after surgery. Statistical analyses were performed on an intention to treat basis using a logistic regression for binary outcomes.

Results: Of the 7,308 patients screened, 149 and 143 patients were randomly assigned to the ketamine and placebo groups, respectively. Delayed neurocognitive recovery occurred in 50 (38.8%) and 54 (40.9%) patients in the ketamine and placebo groups, respectively (OR [95%CI] 0.92 [0.56;1.51], p=0.73) (***Figure 1***). Incidence of postoperative neurocognitive disorders three months after surgery did not differ significantly between groups, nor did delirium, anxiety, apathy, and fatigue seven days and three months post-surgery. Depression was less frequent in the ketamine group three months after surgery (OR [95%CI] 0.34 [0.13-0.86]) (***Figure 2***).

Conclusions: A single bolus of intravenous ketamine does not prevent delayed neurocognitive recovery but may reduce postoperative depression in elderly patients scheduled for major orthopedic surgery.

References: (1) Alam A, Hana Z, Jin Z, *et al.* Surgery, neuroinflammation and cognitive impairment. *EBioMedicine* 2018;**37**:547–56. doi:10.1016/j.ebiom.2018.10.021

(2) Avidan MS, Maybrier HR, Abdallah A Ben, *et al.* Intraoperative ketamine for prevention of postoperative delirium or pain after major surgery in older adults: an international, multicentre, double-blind, randomised clinical trial. *The Lancet* 2017;**390**:267–75. doi:10.1016/S0140-6736(17)31467-8

(3) Hovaguimian F, Tschopp C, Beck-Schimmer B, *et al.* Intraoperative ketamine administration to prevent delirium or postoperative cognitive dysfunction: A systematic review and meta-analysis. *Acta Anaesthesiol Scand* 2018;**62**:1182–93. doi:10.1111/aas.13168

Figure 1

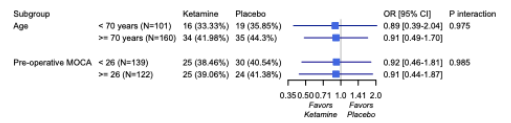

Subgroup analysis of delayed neurocognitive recovery within the 7 first days following surgery. Horizontal bars are 95% confidence intervals.

Figure 2

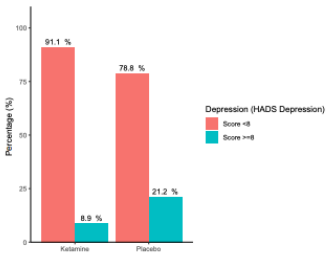

Percentage of patients 90 days after surgery with a Hospital and Anxiety Scale (HADS) depression score < or >= 8, depending on their treatment group.

Neuroscience in Anesthesiology and Perioperative Medicine 16- Isoflurane inhibits synaptic calcium reuptake in mouse neurons in an ATP-dependent manner

Phil Morgan[1], Sangwook Jung[1], Beatrice Predoi[1], Jan-Marino Ramirez[2], Margaret Sedensky[2]

University of Washington, Department of Anesthesiology[1] University of Washington[2]

Introduction: Dysfunction of mitochondrial complex I causes hypersensitivity to volatile anesthetics (VAs) in nematodes, flies, mice and humans.[1-4] NDUFS4 (complex I subunit)-KO mouse shows hypersensitivity to VAs and is a well-established model for mitochondrial disease.[5] VAs inhibited presynaptic function of excitatory neurons; however, it remained unclear what is the precise mechanism by which VAs exert effects on synaptic neurotransmission.[6] Recent work showed that isoflurane inhibits mitochondrial complex I, reduces ATP levels at presynaptic terminals, and inhibits synaptic vesicle endocytosis.[7] During neuronal activity, calcium also plays an important role in both exocytosis and endocytosis of synaptic vesicles.[8] Here, we investigated the effects of isoflurane on mitochondrial regulation of calcium levels in presynaptic terminals and whether rescue of ATP defects would alleviate any changes in calcium levels.

Methods: We performed live-cell optical imaging to measure changes in calcium levels during neuronal stimulations in presynaptic terminals from hippocampal neuronal cultures. Primary hippocampal cells from mouse pups (P0 or P1) were cultured and transfected with a construct containing VGlut1-GCaMP5 (to measure synaptic calcium levels). A CRE-recombinase construct was used to generate *Ndufs4* (KO) cultures. Each cell was co-transfected with a mCherry-synaptophysin (to identify synaptic boutons). To study the changes of calcium levels in presynaptic boutons during neuronal activity, live-cell images were obtained in presynaptic terminals at DIV 10–14 after transfection. Intense stimulations were elicited at 10Hz for 60s and images were acquired using an acquisition rate of once ever 10 seconds (0.1Hz). To analyze the fluorescence response to stimulation over time, the background-subtracted fluorescence at each time point was normalized to the total amount of fluorescence evoked by the stimulation. Decay times were calculated by fitting a first order exponential curve.

Results: Both WT and *Ndufs4*(KO) cultures showed increased calcium levels followed by a return to baseline (or overshoot) during stimulations in the absence of isoflurane (Not shown). However, exposure to isoflurane treatment at whole animal $2XEC_{50}$s slowed the return to baseline (measured by decay times) of calcium levels following the 2nd stimulation in boutons from both wildtype (**Figure, Table 1**) and *Ndufs4* (KO) (**Figure, Table 2**) cultures compared to unexposed controls. The addition of 30mM glucose alleviated the delayed return to baseline of calcium levels in the presence of isoflurane from both genotypes (**Figure, Tables 1,2**).

Conclusions: Isoflurane treatment inhibited a calcium removal during neuronal activity in the presynaptic boutons from both WT and *Ndufs4* (KO) cultures. Notably, lower concentrations of isoflurane (0.6%) inhibit the *Ndufs4(KO)* (**Figure, Table 2**) but not wildtype neurons (**not shown**). Previous work showed that the 0.6% isoflurane causes decreased ATP levels in the KO but not in wildtype and that ATP levels are rescued by 30mM glucose levels.[7] Here we find that 30mM glucose also rescued the inhibition of calcium removal, similar to the alleviation of the inhibition of synaptic endocytosis caused by isoflurane. Since it is known that 30mM glucose rescues ATP levels in the presence of isoflurane, we interpret these changes to represent isoflurane-dependent inhibition of ATP-dependent calcium removal from the synapse. Calcium levels may be upstream of the defect in endocytosis caused by isoflurane. Whether inhibition of endocytosis is a result of failure of calcium removal or an independent effect remains to be determined. We are planning to investigate which calcium removal pathways are affected by isoflurane and whether the failure of calcium removal leads to the defect in endocytosis.

References: 1. *Anesth*. 90**:**545, 1999. **2**. *PLoS One* 7:e42904, 2012. **3**. *Anesth Analg*. 133: 924, 2021. **4**. *Sci Rep.* 8: 2348, 2018. 5. *Cell Metab*. 7:312, 2008. 6. *Br J Anaesth.* 120:1019, 2018. 7. *Curr Biol.* 32:3016, 2022. **8.** *Proc Natl Acad Sci*. 119(20):e2111051119, 2022.

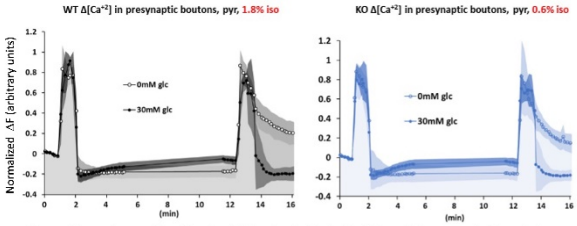

Figure. Changes in synaptic calcium levels following electrical stimulations of hippocampal cultures in the presence of isoflurane (1.8% for WT; 0.6% for KO) supplemented with pyruvate. 30mM glucose provoked a calcium removal during isoflurane exposure compared to no exogenous glucose. Left panel shows results in wildtype neurons at 1.8% isoflurane. Right panel shows results in *Ndufs4(KO)* neurons.

treatment	stim.	Decay time mean	SD	N	p values	t-test
(1) 0mM glucose, 0% isoflurane	1st	9.47	6.09	6		
	2nd	28.03	20.59	6		
(2) 0mM glucose, 0.6% isoflurane	1st	12.37	11.08	8	0.58	(1) vs (2)
	2nd	146.92	98.89	8	**0.014**	
(3) 30mM glucose, 0% isoflurane	1st	5.99	0.80	8	0.51	(3) vs (4)
	2nd	10.47	9.34	8	0.36	
(4) 30mM glucose, 0.6% isoflurane	1st	6.35	1.23	8	0.15	**(2) vs (4)**
	2nd	16.7	16.23	8	**0.0025**	

Table 2. Isoflurane/glucose effects on *Ndufs4(KO)* decay times. Effects of isoflurane and glucose on decay times following neuronal stimulation (10Hz, 60 seconds). Note the increased decay time following the second stimulations in the presence of 0.6% isoflurane (2) which was alleviated by the addition of 30mM glucose.

treatment	stim.	Decay time mean	SD	N	p values	t-test
(1) 0mM glucose, 0% isoflurane	1st	6.04	0.33	7		
	2nd	16.36	14.07	7		
(2) 0mM glucose, 1.8% isoflurane	1st	10.29	4.03	6	**0.017**	(1) vs (2)
	2nd	155.89	60.56	6	**0.0001**	
(3) 30mM glucose, 0% isoflurane	1st	6.06	0.64	6	0.84	(3) vs (4)
	2nd	8.20	6.25	6	0.25	
(4) 30mM glucose, 1.8% isoflurane	1st	6.31	2.91	8	0.052	**(2) vs (4)**
	2nd	15.59	13.92	8	**0.00003**	

Table 1. Isoflurane/glucose effects on wildtype decay times. Effects of isoflurane and glucose on decay times following neuronal stimulation (10Hz, 60 seconds). Note the increased decay time following the second stimulations in the presence of isoflurane (2) which was alleviated by the addition of 30mM glucose.

Neuroscience in Anesthesiology and Perioperative Medicine 17- Ketamine for Postoperative Avoidance of Depressive Symptoms: The K-PASS Feasibility Randomized Clinical Trial

Bradley Fritz[1], Bethany Pennington[1], Katie Dalton[1], Ben Palanca[2], Julie Schweiger[3], Logan Griffin[3], Wilberforce Tumwesige[3], Jon Willie, Nuri Farber[4]

Washington University in St Louis[1] Washington University School of Medicine in St. Louis[2] Washington University School of Medicine[3] Washington University[4]

Introduction: Postoperative depressive symptoms are associated with pain, readmission, death, and other undesirable outcomes [1-3]. Prior perioperative studies have shown rapid but transient antidepressant effects with ketamine, usually administered as 0.5 mg/kg over 40 minutes during or after surgery [4-7]. Longer infusions have yielded sustained antidepressant responses, lasting several weeks, in outpatients with treatment-resistant depression [8,9], but it is unknown whether a similar strategy can produce lasting antidepressant effects after surgery. The objective of this feasibility study is to determine whether it is possible to conduct a large randomized comparative effectiveness clinical trial to answer this question.

Methods: This single-center, double-blind, placebo-controlled feasibility randomized clinical trial includes patients aged 18 or older with a history of depression scheduled for inpatient surgery. Depression was detected using either a previous diagnosis documented in the electronic health record and/or an antidepressant on the home medication list.

After surgery, patients were randomized to receive either ketamine (load of 0.5 mg/kg over 10 minutes followed by infusion of 0.3 mg/kg/h) or an equal volume of normal saline. Initially, the infusion was given over 8 hours on postoperative day 1, to patients with planned intensive care unit (ICU) admission in accordance with local hospital policy regarding approved locations for ketamine infusions. In order to increase the number of eligible patients, the protocol was updated to remove the ICU inclusion criterion, to shorten the infusion duration to 3 hours allowing administration to occur in the post-anesthesia care unit, and to start the loading dose in the operating room immediately after extubation.

Depressive symptoms were measured using the Montgomery-Asberg Depression Rating Scale (MADRS) preoperatively and on post-infusion days 1, 2, 4, 7, and 14. The primary feasibility endpoints were the fraction of patients approached who enroll and were randomized, the fraction of randomized patients who completed the study infusion, and the fraction of randomized patients with MADRS scores at the scheduled time points.

Results: As of 12/07/2022, 19 patients have been randomized out of the target of 32. Characteristics of randomized patients are shown in Table 1. Under the original protocol, 1 patient was randomized out of 26 who were invited to participate (3.8%). Under the updated protocol, 18 patients have been randomized out of 84 who were invited (21% - Figure 1). Since launching the updated protocol, on average 1.5 patients have been randomized per week (Figure 2).

The study medication infusion was completed as planned in 18 out of 19 patients (95%). In one patient, the infusion was stopped early because the patient experienced a seizure followed by impaired consciousness (postoperatively from a neurosurgical procedure). Upon review, this adverse event was deemed unlikely to be related to the study medication. Psychotomimetic and organic side effects during the infusion have been minimal (Table 2).

MADRS assessments were completed at 98 of the 112 time points at which they were attempted (87.5%). Incomplete assessments were primarily related to patients not answering the telephone. Depressive symptom trajectory after surgery varied across patients, including some with increasing MADRS scores (worsening symptoms) and others with decreasing scores (improving symptoms – Figure 3).

Conclusions: Following the protocol changes, patient recruitment and medication administration appear to be highly feasible. Further adjustments to communication and patient engagement procedures are expected to improve the MADRS completion rate. Based on the current rate of progress, we expect to finish randomization in February 2023. Updated results will be provided at the meeting.

References: 1. *Clin J Pain.* 2013;29:392-399.

2. *J Behav Med.* 2008;31:281-290.

3. *Heart Vessels.* 2017;32:1458-1468.

4. *Psychiatry Res.* 2019;279:252-258.

5. *Brain Behav.* 2020;10:e01715.

6. *Anesth Analg.* 2002;95:114-118.

7. *Med Sci Monit.* 2020;26:e922028.

8. *World J Biol Psychiatry.* 2016;17:230-238.

9. *Psychopharmacology (Berl).* 2021;238:1157-1169.

Table 1. Characteristics of Randomized Patients (N = 19)

Variable	N (%)
Sex	
Female	16 (84%)
Male	3 (16%)
Race	
Black or African American	1 (5%)
White	18 (95%)
Ethnicity	
Not Hispanic or Latino	19 (100%)
Education	
Some High School	1 (5%)
High School or GED	6 (32%)
Some College	7 (37%)
College	5 (26%)
Living Situation	
Alone	3 (16%)
With Others	16 (84%)
Marital Status	
Single	7 (37%)
Married	10 (53%)
Divorced	2 (11%)
Employment Status	
Work Outside the Home	7 (37%)
Student	1 (5%)
Homemaker	2 (11%)
Retired	4 (21%)
Disabled	2 (11%)
Other	3 (16%)
Type of Surgery	
Cardiac Surgery	2 (11%)
Neuro Surgery	11 (58%)
Craniotomy	3 (16%)
Spine	8 (42%)
Vascular Surgery	6 (32%)
Thoracic Outlet Syndrome	5 (26%)
Lower Extremity Revascularization	1 (5%)
Baseline MADRS Score	
0-6 (no symptoms)	4 (21%)
7-19 (mild symptoms)	8 (42%)
20-34 (moderate symptoms)	7 (37%)
> 34 (severe symptoms)	0 (0%)

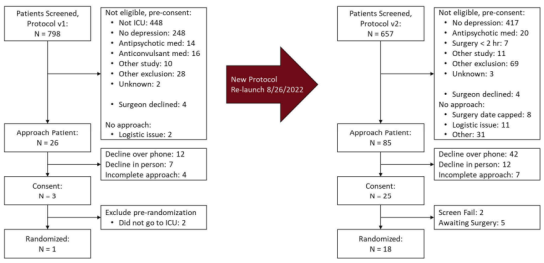

Figure 1. Flow diagram of patient recruitment under the original and updated protocols

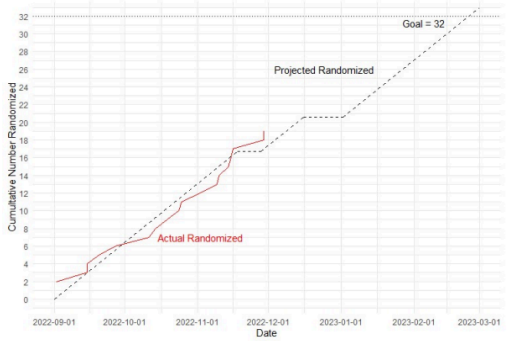

Figure 2. Cumulative number of patients randomized over time under the revised study protocol. The projected randomization (dotted line) assumes 1.5 patients randomized per week, with planned pauses in randomization around November and December holidays.

Table 2. Side Effects Reported During Infusion (N = 17)

Variable	Any	Minimal	Mild	Moderate	Severe
PATIENT-REPORTED					
Dizziness or lightheadedness	5	3	1	1	0
Headache	2	0	0	1	1
Heart beating fast or racing	0	0	0	0	0
Thinking feels foggy	10	5	2	2	1
Trouble with concentration or memory	6	1	2	2	1
Seeing double	2	1	0	0	1
Nausea	3	0	0	2	1
Vomiting	3	0	0	2	1
Tired or fatigued	14	1	2	4	7
Nystagmus	0				
Richmond Agitation and Sedation Scale					
-1 (Drowsy)	4				
0 (Alert and calm)	12				
+1 (Restless)	1				
STRUCTURED ASSESSMENTS	**Mean (SD)**				
Clinical Administered Dissociative State Scale *(range 0-24, higher is worse symptoms)*	0.9 (1.5)				
Components of Brief Psychiatric Rating Scale *(each item scored from 1 not present to 7 extremely severe)*					
Conceptual Disorganization	1.2 (0.5)				
Suspiciousness	1.0 (0)				
Hallucinatory Behavior	1.1 (0.2)				
Unusual Thought Content	1.0 (0)				

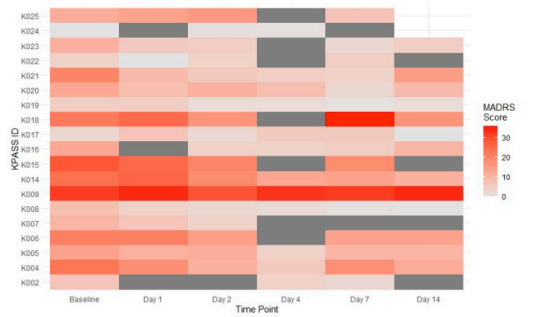

Figure 3. Montgomery-Asberg Depression Rating Scale (MADRS) scores for individual patients at baseline (preoperatively) and on days 1, 2, 4, 7, and 14 after the study medication infusion. Higher scores (darker colors) represent more severe symptoms. Dark gray squares are missing data. Blank squares represent patients still on follow-up at the time of abstract submission.

Neuroscience in Anesthesiology and Perioperative Medicine 18- Membrane Thickness Affects Pentameric Ligand Gated Ion Channel Activity and M4 Helix Structure

Brandon Tan[1], Wayland Cheng[2]

Washington University in St Louis[1] Washington University in St. Louis[2]

Introduction: Pentameric ligand gated ion channels (pLGICs) are a superfamily of ion channels involved in fast neural transmission and are the active sites of anesthetics. Some examples include the GABA(A) receptor and nicotinic acetylcholine receptor (nAchR). In the nAchR, it has been shown that thick membranes promote coupling of agonist binding to channel activation (1). However, the effect of membrane thickness on the ion transport activity of other pLGIC is not known and this effect may be generalized through the whole class of channels.
Methods: To investigate the effect of membrane thickness on ion channel activation, we reconstituted the model pLGIC, *Erwinia* ligand gated ion channel (ELIC), in liposomes consisting of di-monounsaturated phosphatidylcholine (PC) of varying acyl chain length (16-22), and assayed ion flux using a sequential mixing fluorescence quenching assay. In addition, we investigated the structural basis of ELIC sensitivity to membrane thickness by obtaining apo and agonist-bound structures of ELIC in a circularized nanodisc with di16:1PC, di20:1PC or di22:1PC using single particle cryo-EM.

Results: ELIC exhibited maximal agonist responses in di-20:1PC liposomes with a dramatic decrease in thinner or thicker membranes. To verify that differences in agonist responses are not a function of changes in channel orientation in the liposomes, we further assayed an ELIC construct with a quenchable fluorescent label in the N-terminal ECD. Minimal differences in the amount of outwardly facing channels were observed in different membrane conditions confirming that changes in agonist responses are primarily a function of channel activity.

In the agonist-bound structures, the membrane facing helix, M4, is poorly resolved in thin (di16:1PC) and thick (di22:1PC) membranes but clearly resolved in di20:1PC, indicating a correlation between the structure and dynamics of M4 and the optimal membrane thickness that supports channel function.

Conclusions: These findings indicate that ELIC function is promoted by thicker membranes and suggests that sensing of membrane thickness is mediated by M4, as has been proposed for the nAchR. Givent the findings of this study, it may be possible to develop novel anesthetics target sites exploiting changes in lipid composition since other mammalian pLGICs include anesthetic targets.

References: 1. Journal of Biological Chemistry. **284**(26): p. 17819-25. 2009

Membrane Thickness Affects ELIC Function

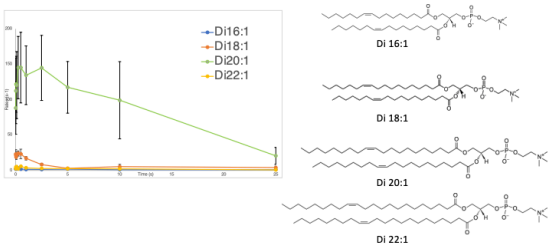

Orientation Not Affected by Liposomes

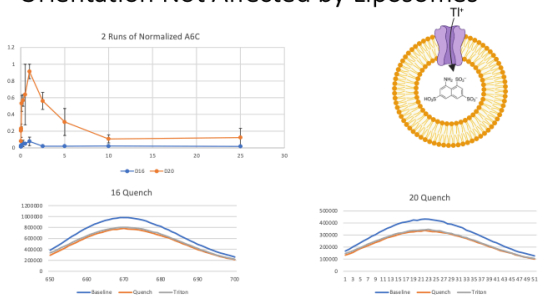

M4 Stabilization Correlated With Increased Function

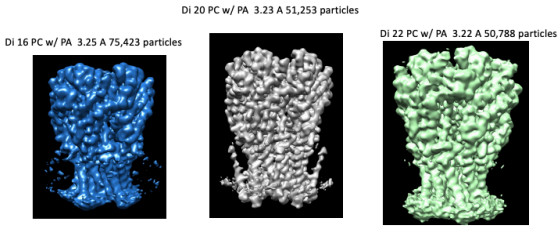

Neuroscience in Anesthesiology and Perioperative Medicine 19- Paradoxical Increases in Anterior Cingulate Cortex Activity During Volatile Anesthetic-Induced Analgesia in Mice

Jarret Weinrich[1], Madison Jewell[1], Cindy Liu[2], Christopher Andolina[2], Mikhail Nemenov[2], Mervyn Maze[2], Allan Basbaum[2]

UC San Francisco[1] University of California - San Francisco[2]

Introduction: General anesthetics are potent regulators of nociception and produce effects ranging from diminished or absent pain perception (i.e., analgesia) to the total abolition of nociceptive reflexes in response to ongoing surgical stimuli. However, general anesthetics do not always provide adequate analgesia, as even patients that retain consciousness under general anesthesia are still capable of experiencing pain. Importantly, pain is a conscious, multidimensional percept that is comprised of sensory-discriminative (i.e., location, intensity) and affective-motivational (i.e., unpleasantness) aspects. In the present studies in the mouse, we investigated the influence of volatile anesthetics on the processing of pain by the anterior cingulate cortex (ACC), a brain region that encodes affective-motivational, but not sensory-discriminative, features of the pain experience. Using *in vivo* calcium imaging, we monitored the activity of hundreds of ACC neurons during the presentation of a noxious stimulus and concurrent inhalation of volatile anesthetics in awake, freely moving mice. Our objective is to uncover the extent to which general anesthetics provide analgesia by altering the cortical processing of pain.

Methods: We tested mice during inhalation of medical air, or equipotent, subhypnotic concentrations of ISO (0.26%) or N_2O (60%), with equivalent concentrations of oxygen throughout (~21%). Stimuli were generated by a high-power infrared laser (LASMED Inc.) targeted to the hindpaw. Reflexive (withdrawals, shakes) and affective-motivational (licks) behaviors were recorded for each stimulus. Virally delivered, genetically encoded fluorescent reporters of neural activity were expressed in principle (excitatory) neurons (AAV1-CaMK2a-GCaMP6f). Fluorescence changes in GCaMP6f were monitored with an Inscopix nVista (v3) head-mounted miniscope. Imaging data were recorded and processed with Inscopix nVista and Inscopix Data Analysis software, respectively, and with custom-written MATLAB code.

Results: First, we assessed the analgesic effects of volatile anesthetics and found that both nitrous oxide and isoflurane significantly decreased laser-evoked affective-motivational behaviors while producing minimal decreases in stimulus-evoked reflexes. Next, we assessed the properties of laser-evoked ACC activity during inhalation of air and found stimulus responsive neurons that consistently increase their activity during the presentation of the laser stimulus. However, we found no change in stimulus-evoked activity (measured as integrated laser-evoked activity) between the air, isoflurane, and nitrous oxide conditions. Interestingly, isoflurane and nitrous oxide increase spontaneous (baseline pre-laser activity, measured as calcium transients over time). Lastly, when correlating stimulus-evoked neural activity with affective-motivational behaviors we found that the baseline pre-stimulus ACC activity, but not stimulus-evoked ACC activity, significantly correlated with the analgesic effects of volatile anesthetics (i.e., the reduction of licks) as compared to air.

Conclusions: We conclude that volatile anesthetics alter the processing of noxious stimuli by the ACC, thereby dampening the affective-motivational aspects of pain and producing analgesia. As expected, and in agreement with previous studies investigating the nociceptive properties of ACC neurons, we found neurons activated by noxious stimuli in the ACC. However, as decreases in ACC activity are generally associated with analgesia in both patients and animals, our finding that increased spontaneous ACC activity correlated with greater analgesia (as measured by a reduction in affective motivational-behaviors) was unexpected. Our findings suggest that the neural encoding of the perception of pain by the ACC results from the stimulus-evoked change in neural activity (i.e., fold change from baseline), and not the absolute level of neural activity (i.e., firing rate). Paradoxical to the established view of the contribution of the ACC to pain processing, by increasing the spontaneous (baseline) activity of the ACC, volatile anesthetics decrease the fold change in neural activity driven by a noxious stimulus, likely driving the reduced expression of affective-motivational pain behaviors. We suggest that selectively modulating the spontaneous activity ACC neurons, thereby disrupting pain processing, offers a promising objective measure for the development of novel general anesthetics with increased analgesic potency.

References: Basbaum et al, Cell, 139, 267-284, 2009

Neuroscience in Anesthesiology and Perioperative Medicine 20- Role of calcium fluxes from mouse astrocytes in emergence from general anesthesia

Phil Morgan[1], Miranda Howe[1], Sangwook Jung[1], Margaret Sedensky[2]

University of Washington, Department of Anesthesiology[1] University of Washington[2]

Introduction: The mechanism(s) by which volatile anesthetics (VAs) produce reversible loss of consciousness remains an unsolved mystery. Using genetic approaches, we demonstrated that mitochondrial complex I, an entry point of electrons into the mitochondrial electron transport chain, specifically controls the sensitivity of multiple species to VAs[1]. *Ndufs4(KO)*, a mouse defective in complex I function is extremely hypersensitive to VAs[2]. Surprisingly, an astrocytic-specific KO of NDUFS4 required a dose of halothane or isoflurane that was roughly half that of wild type animals to emerge from anesthesia while its induction concentration was identical to that of controls[3].
Norepinephrine (NE) is associated with arousal from anesthetics[4,5], and triggers calcium flux in astrocytes. Astrocyte calcium transients in turn affect the release of gliotransmitters[6] which are proposed to alter synaptic activity. We hypothesized that VAs inhibit mitochondrial activity at a lower concentration in *Ndufs4(KO)* astrocytes and disrupt mitochondrial calcium regulation, resulting in a defect in the release of gliotransmitters that control emergence. Here, we investigate how VAs impact calcium dynamics in wildtype and KO astrocytes.

Methods: Primary astrocytes were isolated from the whole brain homogenates of wildtype and *Ndufs4(KO)* P0-P2 mice. Astrocytes were grown in Pexidartinib for 7 days to suppress microglial growth. Astrocyte cultures were then differentiated with Dibutyryl-cAMP, incubated with Fluo-8AM for 30 mins (for calcium imaging) and then time-lapse images were recorded in the presence and absence of isoflurane. Astrocytes were perfused +/- 10uM NE throughout the course of imaging; 5 minutes baseline, 5 minutes +/- isoflurane, 5 minutes +/- NE (with continued +/- isoflurane). We compared changes in frequency and intensity of fluorescent signal of astrocytes +/- NE and +/- isoflurane. Results were non-normal and the effects of +/- isoflurane on the effects of NE alone were compared using the Wilcoxon signed rank test and significance was defined as $p<0.05$.

Results: In wildtype cultures, an increased ratio of cells exhibited calcium transient increases with NE exposure (D=1.2 +/-1.9), compared to untreated controls (**Figure 1, Table 1**). The ratio of maximal fluorescence with NE exposure also increased (D=0.72 +/-0.47) (**Figure 2**). In WT astrocytes isoflurane approached significance for suppression of the increase in frequency of calcium transients (NE D=1.20 +/-0.27, NE + 1.8% Iso D=0.19 +/-0.9, p=.053) (**Figure 1**) and strongly suppressed the maximal fluorescence (D=0.22 +/-0.11; p=.007) (**Figure 2, Table 2**) caused by NE. In WT astrocytes 0.6% isoflurane did not suppress the effects of NE on either the ratio of cells flashing (NE D=1.20 +/-0.27, NE + 0.6% Iso D=2.24 +/-0.33, p=0.037) or of the change in maximal fluorescence (D=0.60 +/-0.36; p=.572). The number of cells with calcium transients did not significantly increase for KO cultures exposed to NE. However, KO cells that did exhibit calcium transients had an increase in the ratio of maximal fluorescence during norepinephrine exposure compared to baseline (D=0.38 +/-0.11). Isoflurane was sufficient to prevent the increased fluorescence (D=0.22 +/-0.11; p=.004) (**Figure 2, Table 2**).

Conclusions: Here, we have established an *in vitro* model for studying Ca^{2+} signaling in astrocytes. Mitochondrial function impacts the ability of astrocytes to respond to NE when exposed to isoflurane. Calcium responses to NE are prevented by a lower concentration of isoflurane in KO cultures compared to wild-type cultures consistent with a role for astrocytes in emergence from anesthesia. Isoflurane concentrations that affect NE induced calcium transients in astrocytes are congruent with the whole animal EC_{50}s of wild type and *Ndufs4(KO)* mice. We are analyzing gliotransmitter concentrations (ATP, glutamate, cAMP) from cultured astrocytes to further probe the role of astrocytes in mediating emergence from VAs.

References: *Anesth 90*, 545-554, 1999. **2.** PLoS, 7(8)e42904, 2017. 3. *Anesth*, 130(3):423-434, 2019. **4.** *PNAS*, 109:18974, 2012. **5.** *Cereb Cortex*, 18(12):2789, 2008. **6.** *Novartis Found Symp*, 276:208, 2006.

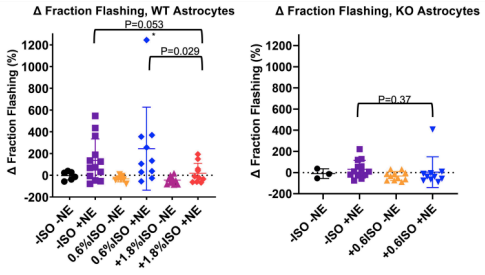

Figure 1. The changes in fraction of astrocytes flashing reflecting calcium concentrations in the presence or absence of 10uM norepinephrine (NE) and isoflurane. Curves from wildtype (Left) and *Ndufs4(KO)* (Right) astrocytes. L. The presence of 1.8% isoflurane trended to decreased flashing in wildtype astrocytes (Red). The presence of 0.6% isoflurane did not significantly decrease flashing in wildtype astrocytes (Blue). R. In *Ndufs4(KO)* astrocytes, the presence of 0.6% isoflurane did not flashing (Blue) in *Ndufs4(KO)* astrocytes nor did NE alone increase flashing (Purple).

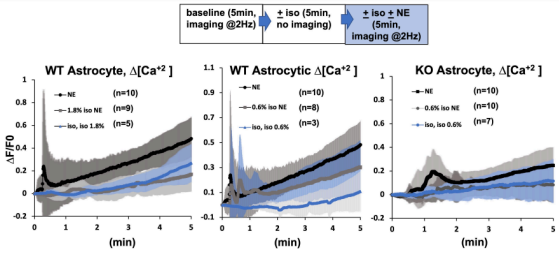

Figure 2. The changes in intensity of fluorescence reflecting calcium concentrations in astrocytes in the presence or absence of 10uM norepinephrine (NE). Dark black line in the absence of isoflurane. Grey and blue lines in the presence of isoflurane. Curves from wildtype (Left, Middle) and *Ndufs4(KO)* (Right) astrocytes. L. The presence of 1.8% isoflurane decreased intensity of fluorescence in wildtype astrocytes. M. The presence of 0.6% isoflurane did not significantly decrease intensity of fluorescence in wildtype astrocytes. R. The presence of 0.6% isoflurane did decrease intensity of fluorescence in *Ndufs4(KO)* astrocytes.

Genotype	Condition	Mean Δ Fraction Flashing	Standard Deviation	N
WT	-ISO -NE	-0.0311	0.393	6
WT	-ISO +NE	1.20* (c/w -ISO -NE)	1.97	13
WT	+0.6% ISO -NE	-0.331* (c/w -ISO -NE)	0.275	7
WT	+0.6% ISO +NE	2.45* (c/w -ISO +NE)	3.82	10
WT	+1.8% ISO -NE	-0.444** (c/w -ISO -NE)	0.356	10
WT	+1.8% ISO +NE	0.186 p=0.053 (c/w -ISO +NE)	0.916	10
KO	-ISO -NE	-0.1	0.459	3
KO	-ISO +NE	0.314	0.839	13
KO	+0.6% ISO -NE	-0.326*	0.421	11
KO	+0.6% ISO +NE	0.0366	1.45	10

Table 1. Change in number of astrocytes exhibiting calcium activity. Isoflurane (ISO) and norepinephrine (NE) concentrations as in Methods. WT, wildtype cells. KO, *Ndufs4(KO)* cells *= p<0.05, **=p<0.01

Genotype	Condition	Mean Δ Fluorescence	Standard Deviation	N
WT	NE	0.718	0.474	10
WT	iso+NE	0.224** (c/w NE)	0.112	9
WT	iso+iso	0.283	0.144	5
KO	NE	0.38	0.114	10
KO	iso+NE	0.219**	0.107	10
KO	iso+iso	0.171	0.137	7

Table 2. Change in maximal fluorescence of astrocytes exhibiting calcium activity. Isoflurane (ISO) and norepinephrine (NE) concentrations as in Methods. WT, wildtype cells. KO, *Ndufs4(KO)* astrocytes **=p<0.01 compared to NE treatment without isoflurane. ** indicates p<0.01

Neuroscience in Anesthesiology and Perioperative Medicine 21- Surgical anesthesia with propofol does not result in sleep debt accumulation in aged mice

Michal Jedrusiak[1], Navya Atluri[1], Nadia Lunardi[1]

University of Virginia[1]

Introduction: Prior studies have yielded conflicting results regarding the effects of propofol on sleep. Tung et al. found that propofol sedation affects sleep homeostasis in a fashion similar to naturally occurring sleep in adult rats. However, a follow-up study by Kelz and colleagues concluded that propofol does not dissipate a pre-existing sleep debt in Drosophila. We aimed to resolve these contrasting findings by characterizing EEG sleep-wake states in mice following exposure to a surgical plane of propofol anesthesia.

Methods: Twenty male and female C57BL/6J mice (18-20 months old, comparable to human age 60 to 70 years old) were implanted with electroencephalographic (EEG) and electromyographic (EMG) electrodes under sevoflurane anesthesia. After a minimum of one week of recovery, mice were randomly allocated to the propofol intralipid or control group. Propofol mice were intubated with a 22G intravenous cannula after a brief sevoflurane induction. Next, propofol infusion was started through a commercially-implanted jugular venous catheter and titrated to an EEG endpoint of delta waves for a total duration of 3 hours (Fig. 1). The average propofol infusion rate was 2.57 mg/kg/min. Mechanical ventilation was set to a FiO_2 of 100% and $ETCO_2$ of 35-45 mmHg measured via capnometry. Fig. 2 is a schematic of the anesthesia setup and physiologic monitoring during anesthesia. Intralipid mice received an equal volume of 10% intralipid administered via a jugular venous catheter for 3 hours, and breathed spontaneously. Control mice did not receive propofol or intralipid. Twenty-four hour-long EEG/EMG recordings were obtained at the conclusion of the infusion in all groups. Mice were kept on a 12 h light on; 12 h light off schedule throughout the experiments. Two-tailed unpaired t-test was used for statistical analysis. Data are presented as mean ± S.D. Statistical significance was set at $p < 0.05$. In the intralipid group, EEG dynamics data from one recording was excluded due to artifacts.

Results: Compared to control and intralipid mice, propofol mice spent less time in NREM sleep, and more time awake, during the 24 hours following infusion (Fig. 3A, p=0.026, p=0.001; Fig. 3B, p=0.008, p=0.006). REM sleep duration was not significantly changed in mice receiving propofol relative to control mice or to mice receiving intralipid (Fig. 3C, p=0.761, p=0.482). Time spent in NREM, awake, and REM sleep was not significantly different in intralipid mice compared to controls (Fig. 3A, p=0.107; Fig 3B, p=0.739; Fig 3 C, p=0.457).
Normalized power in the delta band during NREM sleep was also unchanged in anesthetized mice versus control or intralipid mice (Fig. 4, p=0.945, p=0.801). There was no difference in normalized delta power between intralipid and control groups (Fig 4, p=0.849).

Conclusions: Our findings suggest that in aged mice a 3 h long propofol anesthesia administered during the normal sleep phase and titrated to an EEG endpoint of delta waves does not result in sleep debt accumulation. Further analysis - including time block comparisons between post-anesthesia sleep, transitions between states, sleep bout frequency/duration and movement frequency - will be required to validate these preliminary data.

References:

1. Prolonged sedation with propofol in the rat does not result in sleep deprivation. Anesthesia and analgesia, 92(5), 1232–1236, 2001.

2. Recovery from sleep deprivation occurs during propofol anesthesia. Anesthesiology, 100(6), 1419–1426, 2004.

3. Sleep Homeostasis and General Anesthesia: Are Fruit Flies Well Rested after Emergence from Propofol?. Anesthesiology, 124(2), 404–416, 2016.

4. How to Translate Time? The Temporal Aspect of Human and Rodent Biology. Frontiers in neurology, 8, 92, 2017.

FIG. 1

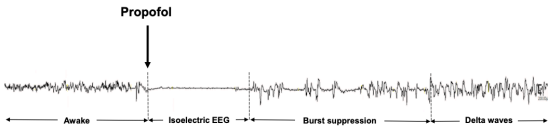

FIG. 2

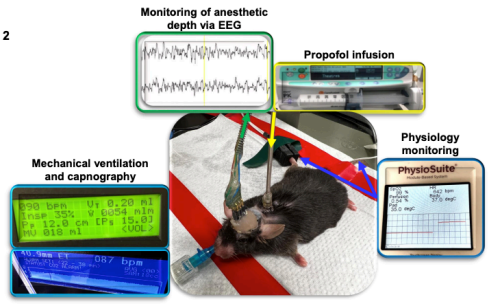

FIG. 3

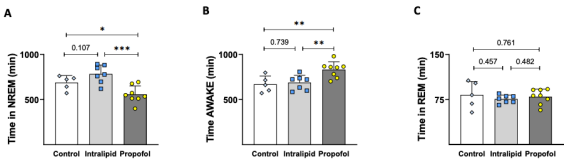
A
B
C
Time in NREM (min)
Time AWAKE (min)
Time in REM (min)
1000
500
150
75
*
**
***
0.107
0.739
0.761
0.457
0.482
Control
Intralipid
Propofol

FIG. 4

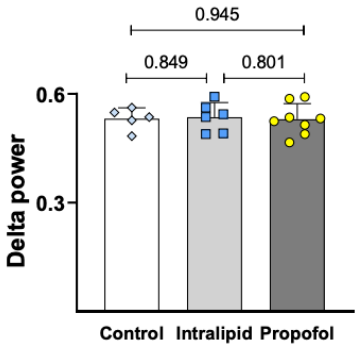
0.945
0.849
0.801
0.6
0.3
Delta power
Control
Intralipid
Propofol

Neuroscience in Anesthesiology and Perioperative Medicine 22- Systemic inflammation exacerbates sevoflurane-induced developmental neurotoxicity in rat neonates

Nemanja Useinovic[1], Stefan Maksimovic[1], Cole Liechty[1], Omar Cabrer[1]a, Nidia Quillinan[2], Vesna Jevtovic-Todorovic[3]

University of Colorado Anschutz Medical Campus[1] University of Colorado, Anschutz Medical Campus[2] University of Colorado[3]

Introduction: Over the past two decades, mounting preclinical and clinical evidence has increasingly shown that general anesthesia administered during the neonatal period induces acute neuronal apoptosis and behavioral deficits that persist through adulthood[1]. While the traditional approach in preclinical research is to study anesthesia-induced neurotoxicity in isolation, the clinical reality is that surgical scenarios which necessitate anesthesia in the first place are often accompanied by the underlying systemic inflammatory response. Despite this clinical commonality, the impact of the underlying inflammation is largely unknown. Therefore, we aimed to quantitatively assess the acute and chronic effects of underlying inflammation on sevoflurane-induced developmental neurotoxicity, and to assess the contribution of inflammasome pathway on hippocampal neuronal death.

Methods: Sprague Dawley rat pups at postnatal day 6 (PND6) were administered lipopolysaccharide (LPS, 1 µg/g) or phosphate-buffered saline (PBS) as an intraperitoneal injection. Twelve hours following LPS or vehicle, PND7 rat pups of either sex were randomly assigned to receive either 3% sevoflurane anesthesia or 30% oxygen carrier gas for a total of 3h. In a separate set of experiments, age-matched animals were further pretreated with Vx-765 (50 µg/g, two separate doses), a selective pharmacological inhibitor of caspase-1, or vehicle, administered 1h before LPS and 1h prior to beginning of anesthesia. To block microglial activation, we selected minocycline (40 µg/g, two doses) or PLX-5622 (65 µg/g, administered once daily for 3 consecutive days PND4-6), then treated with LPS and sevoflurane as previously described. For histomorphological evaluation and hippocampal interleukin levels quantification, animals were euthanized and brain samples collected 2h after the end of anesthesia. Animals designated for assessment of long-term functional outcomes were returned to home cages after anesthesia, weaned at PND28 and tested at 5-8 weeks of age using a battery of behavioral tests in memory and anxiety domains.

Results: Histomorphological quantification of acute neuronal injury in the subiculum revealed significant upregulation in activated caspase-3 and -9 positive neurons after either LPS or sevoflurane individual treatments, which was further exacerbated following combined LPS+sevoflurane administration. Furthermore, we observed a significantly higher degree of activated hippocampal microglia after LPS+sevoflurane treatment compared to either treatment alone. The injury induced by LPS+sevoflurane persisted into adulthood and manifested as significant, sex-specific behavioral deficits when tested at 5-8 weeks. Males treated with LPS+sevoflurane demonstrated significant impairments in learning and memory when tested in the contextual fear conditioning paradigm, whereas females who had undergone same treatment exhibited heightened anxiety when tested in the elevated zero maze. Both the LPS and LPS+sevoflurane treatments were associated with upregulated mRNA levels of caspase-1 and NLRP1, but not NLRP3, along with increased IL-1β hippocampal protein levels. In order to examine to role of microglia in the worsening of neuronal cell death, we introduced pharmacological knock-down of microglia via minocycline or PLX-5622 administration, then quantified cell death in the subiculum of treated animals. Our findings revealed significantly higher numbers of caspase-3 positive cells following either treatments, suggesting a potentially protective role of microglia in our model. Finally, inhibition of caspase-1 via Vx-765 pretreatment resulted in decreased caspase-3 and -9 immunoreactivity in LPS+sevoflurane treatment compared to vehicle-treated counterparts, which suggests that caspase-3 and -9 activation was driven, at least in part, by upstream caspase-1 mechanism.

Conclusions: Systemic inflammation accompanying neonatal anesthesia significantly worsens neuronal cell death, with sex-specific behavioral sequelae. NLRP1/caspase-1 inflammasome pathway appears to be an important molecular mechanism contributing to ensuing injury. Interference with microglial activation results in further worsening of neuronal apoptosis, suggesting a protective role of microglial cells. Pharmacological blockade of caspase-1 via Vx-765 administration significantly reduced neuroapoptosis in subiculum of animals treated with LPS+Sevoflurane, which could be a promising therapeutic strategy.

References: 1. Early exposure to common anesthetic agents causes widespread neurodegeneration in the developing rat brain and persistent learning deficits (2003) Br J Anaesth. 129(4):555-566

Neuroscience in Anesthesiology and Perioperative Medicine 23- The Impact of Surgery on Functional and Cognitive Outcomes after Traumatic Brain Injury: A TRACK-TBI Study

Christopher Roberts[1], Lindsay Nelson[1], Nancy Temkin[1], Athena Dong[1], Jason Barber[1]

Medical College of Wisconsin[1]

Introduction: Traumatic brain injury (TBI) is associated with persistent functional and cognitive deficits, which may be susceptible to secondary insults. The implications of exposure to surgery/anesthesia following TBI warrant investigation, given that surgery has been associated with neurocognitive disorders in children[1,2] and the elderly.[3,4] Annually, at least 69 million people across the globe sustain traumatic brain injuries (TBI),[5] and many have other injuries warranting surgical evaluation. Following a mild TBI (mTBI), ~50% of patients had surgery within 1 week of injury, and 5% had procedures and anesthesia *unrelated* to the traumatic event that caused their mTBI.[6] Based on these studies, there are millions of patients throughout the world who undergo potentially delayable procedures following TBI annually. The hypothesis of this study is that exposure to extracranial (EC) surgery, and consequently anesthesia, will worsen brain injury as measured by functional and cognitive outcomes following TBI.

Methods: This study is a retrospective, secondary analysis of the TRACK-TBI dataset, which is a prospective observational cohort study that enrolled patients from 18 level-1 trauma centers in the USA between February 2014 to August 2018. Subjects included in analysis were ≥ 17 years old, presented within 24 hours of trauma, admitted to an inpatient unit, had known Glasgow Coma Scale (GCS) and head computed tomography (CT) scan status, and did not undergo cranial surgery. Patients that underwent EC-surgery during the admission were compared to patients with no surgery in groups that had a peripheral orthopedic injury (OTC) or a TBI, classified as uncomplicated mild (GCS 13-15, negative CT; CT-mTBI), complicated mild (GCS 13-15, +CT scan; CT+mTBI), moderate/severe (GCS 3-12; m/sTBI). The primary outcomes were functional limitations (Glasgow Outcome Scale–Extended for all injuries [GOSE-ALL] and brain injury [GOSE-TBI]) and neurocognitive outcomes at 2-weeks and 6-months post-injury.

Results: Subjects (n=1835) were 69.9% male, mean (SD) age of 42.2 (17.8) with 1349 non-surgical and 486 EC-surgery patients (Figure 1). EC-surgery patients across all TBI severities had significantly worse GOSE-ALL scores at 2-weeks (Figure 2) and 6-months (Figure 3) compared to nonsurgical counterparts. At 6-months post-injury, m/sTBI and CT+mTBI patients who underwent EC-surgery had significantly worse GOSE-TBI scores (-1.11 [95% CI -0.68 to -1.53] and -0.39 [95% CI -0.01 to -0.77]), and performed worse on Trails B (30.1 [95% CI 11.9 to 48.2] and 26.3 [95% CI 11.3 to 41.2]) compared to non-surgical controls (Table 1 and Figure 4).

Conclusions: Exposure to EC-surgery/anesthesia is associated with adverse functional outcomes and executive functioning post-TBI. These medium-to-large effect sizes reflect patient deficits that impact quality of life. Most strikingly, the effect size for EC-surgery was comparable for GOSE-TBI and GOSE-ALL at 6-months post-injury, suggesting that EC-surgery may impact brain recovery following TBI. Importantly, cognitive deficits associated with EC-surgery were detected in the m/sTBI and CT+mTBI groups, but not the CT-mTBI or OTC groups, which is mildly reassuring since diagnosis of CT-mTBI in trauma inpatients is more likely to be overlooked due to subtle signs/symptoms.[7]

There are limited interventions during the perioperative period that can improve patient-oriented outcomes related to postoperative neurocognitive disorders (PNDs) beyond encouraging pre-rehabilitation and avoiding deleterious medications,[4,8,9] but fortunately the general population is not at risk of PNDs.[10-13] PNDs seem to be independent of the type of surgery or anesthesia,[10-12,14-16] suggesting that the surgical stress response[17] and patient specific factors may be the primary contributors to any neurological changes. Age and pre-existing cognitive deficits are the most consistent individual risk factors for PNDs,[18,19] such as delirium or prolonged postoperative cognitive dysfunction (POCD).

The unfavorable association found here warrants further studies into the mechanisms and clinical implications, which, if replicated, suggest EC-surgery/anesthesia might need to be included in the list of secondary insults following TBI. Likewise, TBI might need to be included in the list of non-modifiable patient factors, along with age and preclinical/diagnosed dementia, that increase the risk for PNDs.

References: 1. New England Journal of Medicine,2017. 376(10):p.905-907.

2. British Journal of Anaesthesia,2019. 122(6):p.716-719.

3. Journal of the American College of Surgeons,2016. 222(5):p.930-947.

4. Anesthesia & Analgesia,2018. 127(6):p.1406-1413.

5. Journal of Neurosurgery,2019. 130(4):p.1080-1097.

6. Mayo Clin Proc,2017. 92(7):p.1042-1052.

7. JAMA Netw Open,2018. 1(1):p.e180210.

8. JAMA,2021. 326(9):p.863-864.

9. JAMA Surg,2021. 156(2):p.148-156.

10. Cochrane Database of Systematic Reviews,2016. 2017(3).

11. JAMA,2022. 327(1):p.50.

12. New England Journal of Medicine,2021. 385(22):p.2025-2035.

13. JAMA,2022. 327(1):p.36-38.

14. Anesth Analg,2011. 112(5):p.1179-85.

15. Journal of Neurosurgical Anesthesiology,2014. 26(4):p.369-376.

16. JAMA,2021. 325(19):p.1955-1964.

17. Front Surg,2015. 2:p.43.

18. Anesthesiology,2016. 124(2):p.353-61.

19. Lancet,1998. 351(9106):p.857-61.

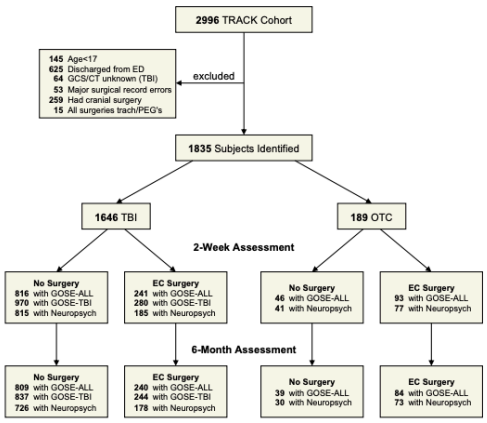

Figure 1. Recruitment and Retention Flow Chart.

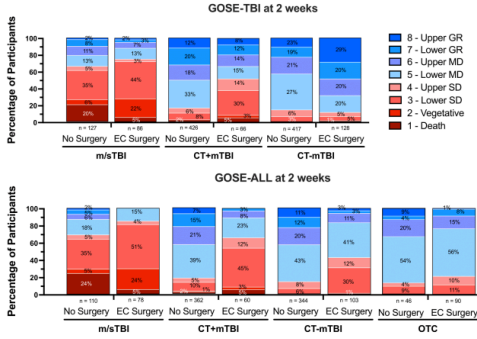

Figure 2. Functional Outcomes quantified using Glasgow Outcome Scale–Extended for brain injury (GOSE-TBI) and all injuries (GOSE-ALL) at 2-weeks post-injury based on injury group and exposure to extracranial surgery. **A)** GOSE-TBI at 2 weeks; **B)** GOSE-ALL at 2 weeks; Sample sizes of each subgroup are presented beneath the respective column with percentage for each injury group given within the column. Abbreviations: good recovery (GR), moderate disability (MD), severe disability (SD), mild TBI (negative computed tomography scan; -CT scan; CT-mTBI), complicated mild TBI (+CT scan; CT+mTBI), moderate to severe TBI (m/sTBI), orthopedic trauma control (OTC), extracranial (EC) surgery.

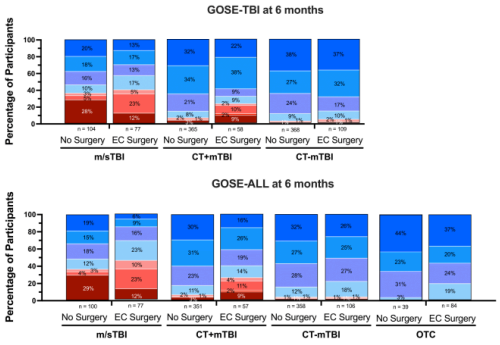

Figure 3. Functional Outcomes quantified using Glasgow Outcome Scale–Extended for brain injury (GOSE-TBI) and all injuries (GOSE-ALL) at 6-months post-injury based on injury group and exposure to extracranial surgery. **A)** GOSE-TBI at 6 months; **B)** GOSE-ALL at 6 months; Sample sizes of each subgroup are presented beneath the respective column with percentage for each injury group given within the column. Abbreviations: good recovery (GR), moderate disability (MD), severe disability (SD), mild TBI (negative computed tomography scan; -CT scan; CT-mTBI), complicated mild TBI (+CT scan; CT+mTBI), moderate to severe TBI (m/sTBI), orthopedic trauma control (OTC), extracranial (EC) surgery.

Table 1 -- Regression models for functional and neurocognitive outcomes excluding deaths occurring within 2 weeks of injury

6-months	GOSE-TBI		GOSE-ALL		Trails A[1]		Trails B	
	B (95% CI) Cohen's d	p	B (95% CI) Cohen's d	p	B (95% CI) Cohen's d	p	B (95% CI) Cohen's d	p
Injury Group	---	<.001	---	<.001	---	<.001	---	<.001
m/sTBI (vs. CT-mTBI)	-0.85 (-1.18, -0.52) -0.75 (-1.04, -0.46)	<.001	-0.80 (-1.17, -0.47) -0.67 (-0.97, -0.37)	<.001	9.00 (5.57, 12.42) 1.63 (1.01, 2.24)	<.001	18.3 (9.5, 27.0) 1.73 (0.90, 2.56)	<.001
CT+mTBI (vs. CT-mTBI)	-0.03 (-0.23, 0.17) -0.03 (-0.20, 0.15)	.782	0.00 (-0.21, 0.19) 0.00 (-0.18, 0.18)	.964	2.47 (0.24, 4.70) 0.45 (0.04, 0.85)	.030	3.44 (-3.81, 10.69) 0.33 (-0.36, 1.02)	.353
OTC (vs. CT-mTBI)	---	---	0.55 (0.14, 1.97) 0.05 (0.01, 0.18)	.009	-0.20 (-5.30, 4.90) -0.04 (-0.96, 0.88)	.939	-2.58 (-18.18, 13.02) -0.25 (-1.75, 1.25)	.761
Injury Group x Surgery[2]	---	.004	---	.005	---	.540	---	.002
EC-Surgery (m/sTBI)	-1.11 (-1.51, -0.69) -0.75 (-1.03, -0.46)	<.001	-1.24 (-1.68, -0.81) -0.67 (-0.91, -0.44)	<.001	1.63 (-0.57, 3.84) 0.13 (-0.04, 0.30)	.569	30.1 (19.2, 40.9) 0.70 (0.45, 0.95)	.001
EC-Surgery (CT+mTBI)	-0.39 (-0.72, -0.06) -0.27 (-0.52, -0.01)	.043	-0.48 (-0.85, -0.10) -0.24 (-0.43, -0.06)	.015	2.50 (-0.77, 5.78) 0.19 (-0.06, 0.45)	.287	26.1 (15.2, 37.1) 0.61 (0.36, 0.86)	.001
EC-Surgery (CT-mTBI)	-0.27 (-0.54, 0.00) -0.18 (-0.37, 0.00)	.051	-0.32 (-0.59, -0.04) -0.22 (-0.41, -0.03)	.023	-0.93 (-3.98, 2.12) -0.07 (-0.31, 0.16)	.546	1.09 (-9.68, 11.86) 0.03 (-0.25, 0.31)	.837
EC-Surgery (OTC)	---	---	-0.54 (-1.03, -0.04) -0.38 (-0.72, -0.03)	.027	-1.77 (-7.79, 4.25) -0.14 (-0.64, 0.35)	.555	2.92 (-14.19, 20.02) 0.07 (-0.38, 0.51)	.764
Age (per +1yrs)	-0.12 (-0.17, -0.08)	<.001	-0.13 (-0.18, -0.08)	<.001	3.56 (3.01, 4.10)	<.001	11.5 (9.7, 13.4)	<.001
Sex	-0.25 (-0.55, 0.06)	.005	-0.24 (-0.56, 0.07)	.005	1.11 (-2.75, 4.99)	.252	2.01 (-11.13, 15.15)	.522
Race	---	.001	---	.004	---	<.001	---	<.001
Injury Cause	---	.032	---	.014	---	.277	---	.499
Education Years (per +1yrs)	0.18 (0.10, 0.26)	.002	0.25 (0.17, 0.33)	<.001	-7.03 (-8.21, -5.85)	<.001	-23.26 (-27.29, -19.23)	<.001
ISS Non-Head/Neck	0.01 (-0.03, 0.05)	.243	-0.01 (-0.05, 0.03)	.156	0.05 (-0.09, 0.19)	.485	-0.18 (-0.63, 0.28)	.444

Functional and Neurocognitive Outcomes at 6-months post-injury quantified using GOSE-TBI, GOSE-ALL, Trail Making Test Part A and B (Trails A and B) classified by injury group and exposure to extracranial surgery (EC-Surgery). Standardized Cohen's d effect-size (reported in the same cell as B estimate), calculated as the reported B estimate divided by the standard deviation of the residuals, where values of 0.2, 0.5, and 0.8 are considered a small, medium, and large effects, respectively. B estimate and Cohen's d values (95% confidence interval).
[1] Trails A and B: values indicate number of seconds to complete so a lower score is faster/better; positive values represent poorer performance.
[2] Main effect of EC-Surgery is reflected in the Injury Group x EC-Surgery (CT-mTBI) contrasts and the model included main effect of surgery, which is reported here using contrasts.

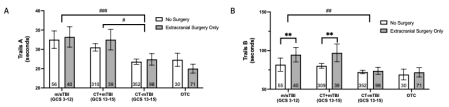

Figure 4. Cognitive Outcomes at 6-months post-injury. Executive functioning quantified using **A)** Trail Making Test Part A; and **B)** Trail Making Test Part B (Trails A and B; number of seconds to complete; lower score is faster/better) classified by injury group and exposure to extracranial surgery. Significance denoted by **p<0.01 for differences between non-surgical and EC-Surgery groups and by $^{\#}$p<0.05; $^{\#\#}$p<0.01; $^{\#\#\#}$p<0.001 for differences between injury groups; based on results from the interaction regression models. Graphs are mean +/- SEM with sample sizes displayed at bottom of each column.

Neuroscience in Anesthesiology and Perioperative Medicine 24- Acute hippocampal dysfunction following deep hypothermic cardiac arrest in a juvenile piglet model

Richard Ing[1], James Orfila[1], Jacob Basak[2], Srdjan Joksimovic[2], Suzanne Osario Lujan[2], Nidia Quillinan[3], Slobodan Todorovic[3], Jesse Davidson[3], Paco Herson[3]

University of Colorado[1] The University of Colorado School of Med[2] University of Colorado, Anschutz Medical Campus[3]

Introduction: Deep hypothermic cardiac arrest (DHCA) in heart surgery may cause brain injury. Changes in electroencephalogram (EEG) activity consistent with seizure activity are seen with DHCA in patients and may cause learning difficulties, delayed brain development.[1,2] A confounding factor is the concurrent use of anesthetic agents. Early-life exposure to anesthesia has been shown to cause neuronal injury and cognitive dysfunction in animal models.[3] We used a piglet model to assess the impact of DHCA on hippocampal brain injury, neuronal excitability, and synaptic plasticity while under anesthetic exposure.

Methods: This study was approved by the University of Colorado Institutional Animal Care and Use Committee. Specific pathogen-free (SPF) female pigs, 6-10 kg (8.33 ± 0.82 kg, Oak Hill Genetics®, Ewing IL, U.S.A.) were separated into a control group(C) with anesthetic exposure (n=3) and an experimental group with anesthetic exposure cardiopulmonary bypass (CBP) and DHCA (n=6). Isoflurane anesthesia at induction (5%) and maintenance (1-1.5%) was used. For the CBP/DHCA group, animals were cooled to 22° and DHCA for 75 mins. Animals were anesthetized for 4 hours, rewarmed, euthanized and brains removed. The C group piglets that were mechanically ventilated, cannulated for CPB and exposed to the same duration and amount of anesthesia as the experimental group. Immunohistochemical analysis of brain death tissue used an antibody that recognizes cleaved caspase-3 at 4 hrs post warming. Whole-cell patch clamp experiments were performed on CA1 neurons in the hippocampus to assess for neuronal excitability, and hippocampal brain slices were used to measure long-term potentiation (LTP) in the hippocampus.

Results: Histologic evidence of hippocampal slices showed no caspase-3 signal in either group, suggesting the lack of cell death in our model. Next, electrophysiologic analysis of hippocampal CA1 neurons from both experimental groups, found no difference in the resting and tonic firing rate. To test the effect of DHCA on hippocampal synaptic plasticity, extracellular field recordings of CA1 neurons were performed on brain slices. In control slices, a physiologic theta burst stimulation resulted in LTP that increased the slope of the excitatory post-synaptic potential to 167.5%±12.4% of baseline. In contrast, recordings obtained from post-DHCA brain slices demonstrated diminished LTP (123.1±8.7%, $p<0.05$ compared to control), demonstrating impaired synaptic plasticity with the DHCA procedure.

Conclusions: This study shows that DHCA causes deficits in hippocampal synaptic plasticity independent of anesthetic exposure. We did not observe any impact of DHCA on neuronal excitability or neuronal cell loss. These findings have important translational implications by demonstrating that DHCA produces functional changes in the brain independent of cell death.

References: 1. J Cardiothorac Vasc Anesth. 35:2875-2888, 2021.

2. Ann Thorac Surg. 106:1841-1846, 2018.3.

3. J Neurosci. 23:876-882, 2003.

Neuroscience in Anesthesiology and Perioperative Medicine 25- Acute Inhibition of Adrenergic Neurons Produces Sedation, Increases Anesthetic Sensitivity, and Increases Resistance to State Transitions in Mice

Andrew McKinstry-Wu[1], Paula Kwasniewska[1], Tim Jiang[1], Nathan Frick[1], Aden Mandel[1]

University of Pennsylvania[1]

Introduction: Central adrenergic signaling plays a significant role in sleep-to-wake transitions, with increases in locus coeruleus (LC) activity preceding transitions to arousal and LC stimulation able to induce those transitions. Animals lacking norepinephrine demonstrate increased sensitivity to volatile anesthetics, and stimulation of LC signaling has been shown to speed emergence (1, 2). Suppression of LC activity, however, has not been shown to have a sedative effect (3.) Here, we investigate the effect of inhibition of adrenergic signaling on behavioral measures of sedation, and on dynamic measures of anesthetic response at isoflurane steady-state.

Methods: *Pupillometry:* Dbh-Cre x stop-floxed hM4di mice (n=6) were sedated under 1.0% isoflurane and a digital camera trained on one eye. After a 10 min baseline, mice were given saline or 20 µg/ml deschlorclozapine (DCZ) I.P. Pupil size was analyzed using the video processing functions in Matlab 2022a. *Sedation Measures*: Mice previously trained on rotarod (n=17) were given IP DCZ or saline and evaluated on rotarod 20 minutes after injection, then placed in beam break cage for 1 hour. Temperature was recorded at baseline, after rotatrod testing, and after beam break testing
Righting Reflex (RR): Male and female mice were exposed to continuous steady-state isoflurane at population EC25 on four separate days while warmed to maintain temperature(n=17). The presence or absence of the righting reflex was checked every 3 minutes starting after 90 min of isoflurane exposure to assure pharmacokinetic equilibration. After 90 min of baseline evaluation, IP saline or DCZ was given and RR checks resumed after 5 minutes for an additional 90 min.
Data Analysis and Statistics: Markov matrix estimation and calculation of sensitivity and resistance to state transition (RST) was done using Matlab 2021a as described previously (4.) Statistical calculations used PRISM 9.5 or Matlab 2022a, using paired t-test, one-way ANOVA, or mixed-effect as appropriate with significance set at $p<0.05$.

Results: Dbh-Cre x stop-floxed hM4di mice showed significantly greater pupillary constriction (n=6, $p<0.05$) in response to DCZ than saline control, indicating a decrease in central adrenergic tone (Fig 1.) This same mouse line showed significant behavioral sedation in response to DCZ, evidenced by a decrease in forced and spontaneous movement ($p<0.0001$, Fig 2.) Mice given DCZ also showed a significant decrease in temperature after rotarod and beam break ($p<0.0001$, 3 degrees and 12 degrees difference.) At steady-state isoflurane, DCZ exposure significantly increased population EC to a median 77, compared with no change to saline ($p<0.0001$, Fig 4.) RST also significantly increased in response to DCZ ($p<0.05$, Fig 5.)

Conclusions: We show here for the first time behavioral sedation in response to inhibition of adrenergic neurons. Significant decrease in temperature in these unwarmed individuals may be a confounding factor in measuring sedation, and future experiments will look at behavioral sedation endpoints with warming. We show for the first time that acute adrenergic inhibition sensitizes animals to anesthetic hypnosis and show the first change in neural activity, rather than a pharmacologic intervention, that alters RST. This is evidence for control of RST by a neural population implicated in similar sleep-to-wake transitions. These results do not relate to temperature changes as mice were kept at constant temperature through chamber warming.

References: 1. PNAS. 111(10):3859-64. 2014.

2. Anesthesiology. 117(5):1006-17. 2012.

3. Prog Neuropsychopharmacol Biol Psychiatry. 90:264-276. 2019.

4. Br J Anaesth. 125(3):308-320. 2020.

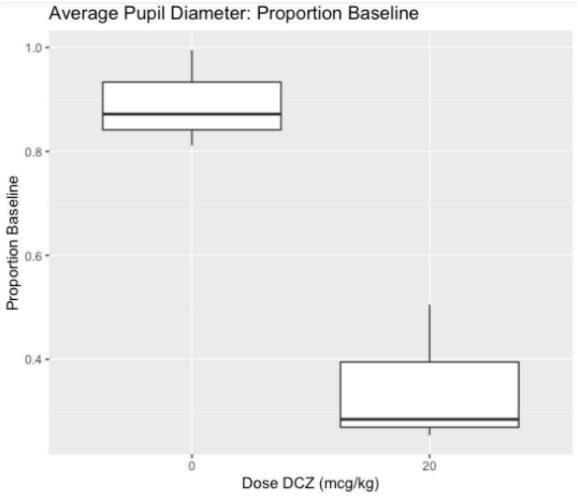

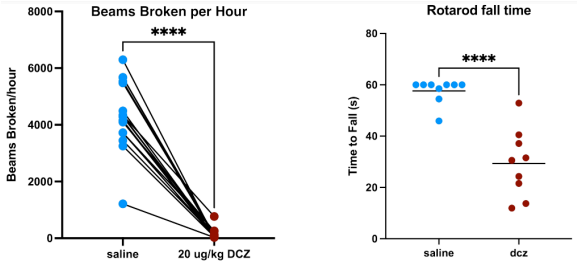

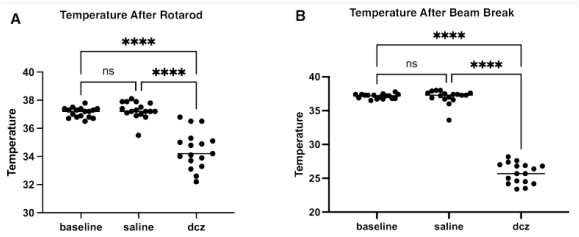
A
Temperature After Rotarod
****
ns
****
Temperature
40
38
36
34
32
30
baseline
saline
dcz
B
Temperature After Beam Break
****
ns
****
Temperature
40
35
30
25
20
baseline
saline
dcz

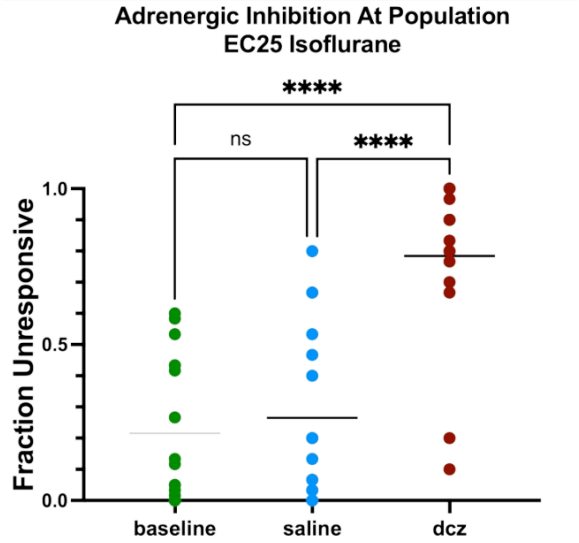
Adrenergic Inhibition At Population
EC25 Isoflurane
****
ns
****
Fraction Unresponsive
1.0
0.5
0.0
baseline
saline
dcz

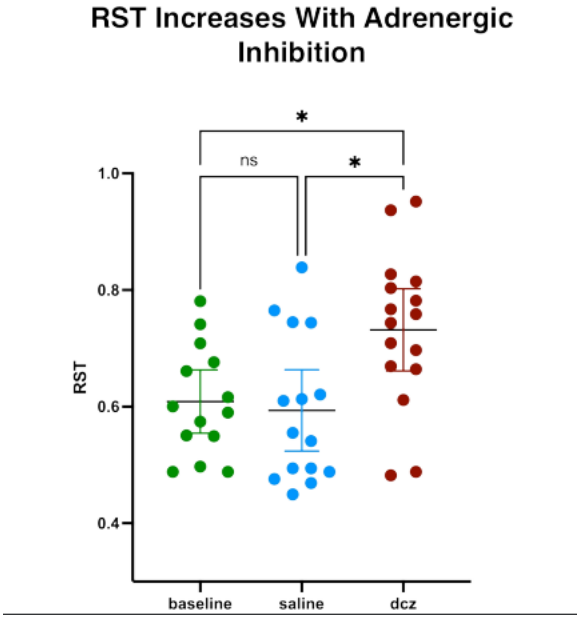
RST Increases With Adrenergic
Inhibition
*
ns
*
RST
1.0
0.8
0.6
0.4
baseline
saline
dcz

Neuroscience in Anesthesiology and Perioperative Medicine 26- Alternate electrode placement to facilitate frontal electroencephalography monitoring in sedated, critically ill patients

Oliver Isik[1], Vikas Chauhan[1], Brian Chang[1], Tuan Cassim[1], Morgan Graves[2], Meah Ahmed[2], Shobana Rajan[3], Paul Garcia[4]

Columbia University Vagelos College of Physicians & Surgeons[1] Columbia University Irving Medical Center[2] University of Texas Health Science Cente[3] Columbia University Medical Center[4]

Introduction: Frontal electroencephalography (EEG) monitoring provides key information on guiding sedation and analgesia in sedated patients, both in the operating room and the intensive care unit (ICU).[1, 2] However, the placement of continuous frontal EEG monitoring requires adequate space on patients' heads. In admitted patients with dressings or other monitors over the same space, or those in neurosurgical cases in which that space is part of the operating field, it is not feasible to place the electrodes in standard configuration. This study investigates the effect of several alternate electrode configurations on the frontal EEG spectrum in sedated, critically ill patients.

Methods: This study recruited ten patients receiving sedation in the surgical, neurosurgical, and cardiothoracic intensive care units. Per protocol, sedation was titrated to a Richmond Agitation-Sedation Scale score at or below negative 2. Given the potential for variability in noxious stimuli and hemodynamic changes in the operating room to affect the EEG, we favored stable ICU patients for this observational study. Frontal EEG was monitored using the Sedline™ electrode sensor placed in the standard configuration (bifrontal upright). Then, five alternate configurations were recorded, each for five minutes: bifrontal inverse, malar, lateral upright, lateral inverse, and semilateral (Figure 1). Tracings were processed to produce two minutes of artifact-free EEG per configuration for each participant. Participants without two minutes of artifact-free bifrontal upright tracing were not included for analysis; participants without two minutes of artifact free tracing for a single alternate configuration were included for analysis without that specific configuration. Average power spectral densities (PSDs) for each configuration with 95% confidence intervals were generated to compare the complete spectrum of each alternate configuration to that of bifrontal upright. Multiple numerical parameters were calculated to compare the frontal EEG spectrum across configurations: the spectral edge frequency (SEF), the frequency below which 95 percent of EEG power is located; the total EEG power in decibels; and the percentages of that total EEG power found in the delta (0.5-3.5 Hz), alpha (8-12 Hz), and beta (20-30 Hz) ranges. One-way ANOVA was used to evaluate potential differences between electrode configurations.

Results: Of the 10 participants enrolled in the study, seven had artifact-free EEG tracings in all configurations, and two others had artifact-free tracings in all configurations other than malar. Sample artifact-free EEG tracings and spectrograms in alternate configurations for one study participant are included in Figure 2. In the average PSDs, each alternate configuration had lower mean power across frequency bands relative to bifrontal upright, but the difference was never statistically significant (Figure 3). Regarding numerical outcomes, mean SEF in the alternate configurations differed from that in bifrontal upright by no more than 2 Hz ($p = 0.961$). In all configurations other than semilateral, SEF differed by no more than 0.3 Hz. Relative EEG power in the alternate configurations differed from bifrontal upright by no more than 2 percent in the delta ($p = 0.992$), alpha ($p = 0.998$) and beta ($p = 0.903$) bands. Total EEG power was reduced across alternate configurations ($p = 0.436$). Patient State Index™ (PSI) was not examined as it is intended for use in only the standard configuration.

Conclusions: Alternate configurations did not change SEF or relative delta, alpha, or beta power by a clinically significant amount, suggesting that the relative distribution of frequencies on the EEG spectrum is preserved. Total EEG power was decreased numerically and across frequencies on PSDs, but this decrease was not significant. Many alternate configurations involve placing part of the configuration lower on the face, and increased distance from the frontal cortex could explain the lower voltage recordings. Further research into the recorded total EEG power of alternate configurations is warranted. These results provide reassurance that these alternate electrode placements for the Sedline™ sensor are suitable alternatives to guide sedation and analgesia in anesthetized or critically ill patients when the standard configuration is not feasible.

References: 1. Clin Neurophysiol. 2021; 132 (3): 730-736.

2. Ann Intensive Care. 2021; 11 (1): 76.

Figure 1. Standard and alternate Sedline™ configurations used for comparison.

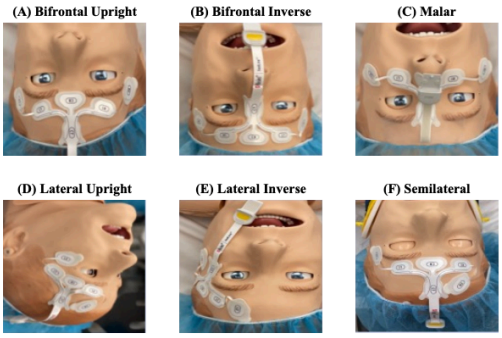

Figure 2. Artifact-free electroencephalogram (EEG) and processed spectrogram of one study participant in each of the electrode configurations.

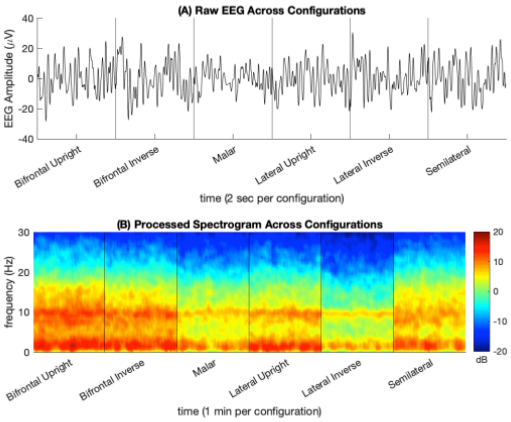

Figure 3. Average power spectral densities (PSDs) with 95% confidence intervals (CI) for each alternate configuration compared to the standard bifrontal upright configuration. Bif. = Bifrontal; Lat. = Lateral.

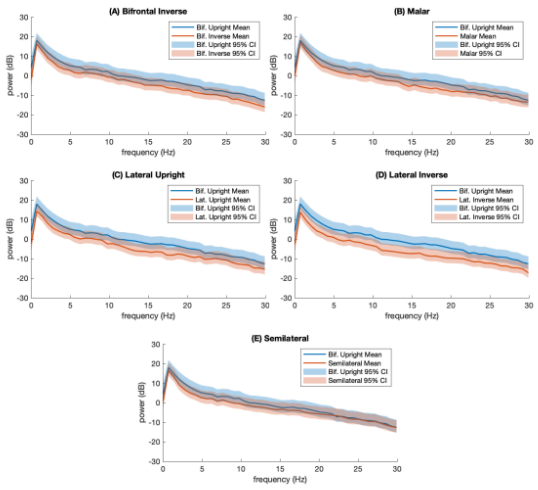

Table 1. Mean EEG parameters with standard deviations for standard and alternate configurations with *p*-values from one-way ANOVA.

Metric	Parameter Mean (Standard Deviation) by Configuration						*p*
	Bifrontal Upright	Bifrontal Inverse	Malar	Lateral Upright	Lateral Inverse	Semilateral	
Spectral Edge (Hz)	12.8 (5.1)	13.1 (4.8)	12.6 (4.9)	12.8 (5.2)	12.9 (4.8)	14.8 (5.4)	0.961
Total EEG Power (dB)	206 (200)	119 (89)	131 (127)	80 (60)	78 (93)	161 (204)	0.436
Relative Delta Power (%)	50.3 (10.5)	52.1 (8.2)	52.2 (9.7)	52.2 (7.4)	49.9 (7.9)	50.8 (12.0)	0.992
Relative Alpha Power (%)	8.1 (9.1)	6.7 (7.1)	7.6 (9.2)	7.5 (7.4)	7.2 (8.6)	6.3 (6.8)	0.998
Relative Beta Power (%)	1.5 (1.4)	1.7 (2.4)	1.6 (1.8)	2.0 (2.2)	2.3 (3.5)	2.9 (3.4)	0.903

Neuroscience in Anesthesiology and Perioperative Medicine 27- An Integrated Multi-Omic Analysis for Delirium Biomarkers: *Towards Definitive Case Identification after Cardiopulmonary Bypass*

Kwame Wiredu[1], Jason Qu[1], Isabella Turco[2], Katia Colon[2], Tina McKay[2], Oluwaseun Akeju[2]

Mass General Hospital[1] Massachusetts General Hospital[2]

Introduction: Postoperative delirium, a behavioral state characterised by an acute change in cognition and attention, occurs in 10 to 30% of patients older than 60 years recovering from cardiac surgery.[1, 2] It is associated with long-term cognitive deficits, prolonged hospitalization and institutionalization, and increased mortality, resulting in total attributable healthcare costs of approximately $32·9 billion annually.[3-5] Prognostic biomarkers may enable pre-emptive identification and targeted interventions of patients at highest risk for postoperative delirium. It may also advance our understanding of putatively linked inflammation, lipid metabolism, and tauopathy mechanisms underlying postoperative delirium. Biomarker studies of postoperative delirium have typically focused on a limited set of targeted proteins. However, the expression pattern of a limited set of proteins or lipids is unlikely to lend principled insights into the large-scale complex interactions underlying postoperative delirium. Here, we hypothesize that a multiomic (proteomic, lipidomic) approach that also integrates clinical data would enable new and innovative prognostic and diagnostic insights into postoperative delirium.

Methods: Using SOMAscan and tandem mass spectrometry, we comprehensively profiled serum from a nested case/control cohort of 86 subjects from the Minimizing ICU Neurological Dysfunction with Dexmedetomidine-induced Sleep trial [*n*(POD cases) = 38] at baseline and on post-operative day one. Important protein and lipid features were identified using penalized logistic regression (ElasticNet) and orthogonal projections to latent structures discriminant analysis (OPLS-DA), respectively. Stacked generalization modeling using h2oEnsemble algorithm[6, 7] to find optimal combination of predictive features from the clinical, proteomics and lipidomics data of study subjects was used to build prognostic and diagnostic classifier models to identify postoperative delirium cases at baseline and postoperative time points, respectively. Performance of each classifier was assessed using prediction accuracy, coefficient of determination, and area under receiver operator curve (AuROC) analyses. A comparative analysis to determine the putative postoperative delirium-sparing effects of dexmedetomidine was also performed.

Results: Relative to baseline levels, we found that postoperative delirium was associated with significant proteomic changes in inflammatory markers and enzymes involved in energy metabolism postoperatively (**Figure A).** Conversely, postoperative delirium was associated with a distinguishable lipidomic profile at baseline (**Figure B**). Consistent with this, the AuROC of proteomic biomarkers was higher postoperatively (84% vs. 74%), while the AuROC of lipidomic biomarkers was higher preoperatively (96% vs 100%). At both timepoints, the stacked generalization model outperformed each of the clinical, proteomic, or lipidomic models (AuROC = 100%, **figures C** and **D**). In a subgroup of patients who received dexmedetomidine, we observed a down-regulationof inflammatory markers (C-X-C motif chemokine 11 [CXCL11], interleukin-27 subunit beta [EBI3], and interleukin-1 receptor accessory protein [IL1RAP]) and an up-regulation of the antioxidant enzyme superoxide dismutase [SOD3] (**Figure E**), with a concomitant down-regulation of lipid species that correlate with several inflammatory proteins.

Conclusions: Our data suggest that lipidomic features may enable prognostic insights into postoperative delirium before surgery. Proteomic features, on the hand, have diagnostic relevance after surgery. We found that a multiomic approach may aid our understanding of the large-scale complex interactions that underlie postoperative delirium. Given that dexmedetomidine was associated with a reduced incidence of postoperative delirium in the parent study, current findings suggest a putative biological mechanism for the dexmedetomidine effect.

References:

1. Clinical interventions in aging, 2019. 14: p. 1095.
2. Anesth Analg, 2011. 112(5): p. 1202-11.
3. J Gerontol A Biol Sci Med Sci, 2017. 72(12): p. 1697-1702.
4. of the American College of Surgeons, 2015. 220(2): p. 136-148e1.
5. JAMA surgery, 2021. 156(5): p. 430-442.
6. H2O. ai Inc, 2016.
7. O'Reilly Media, Inc, 2016.

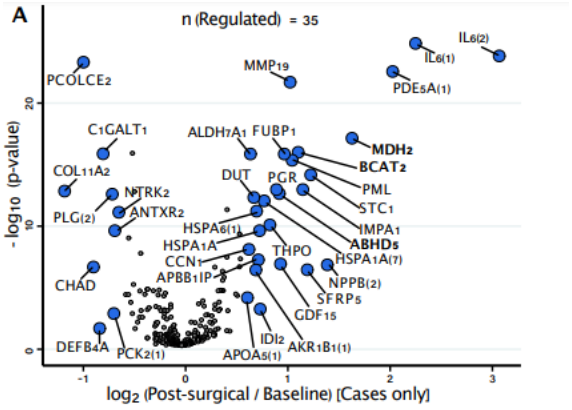

A. Volcano plot showing proteomic changes among POD cases at postsurgical time, relative to baseline levels.

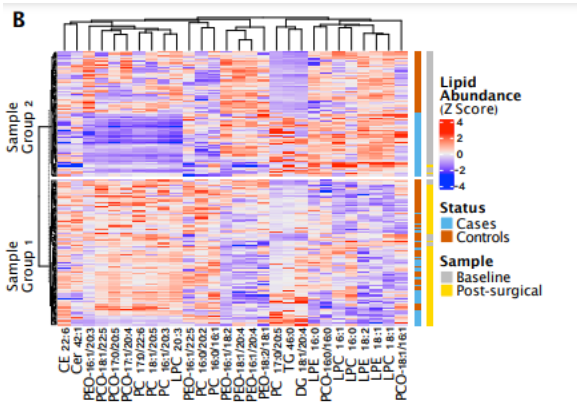

B. Heatmap illustration of lipidomic profiles of cases and controls at both baseline and post-surgical timepoints.

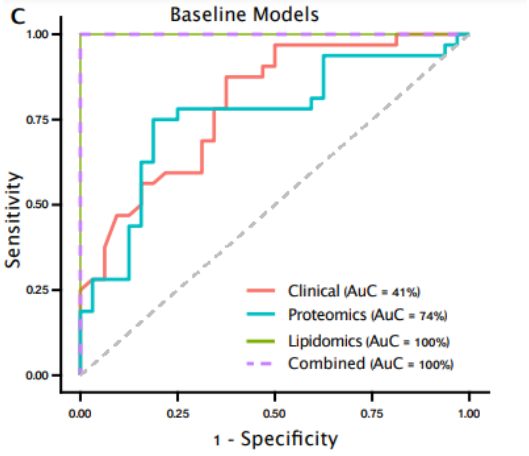

C. ROC curve of baseline classifiers.

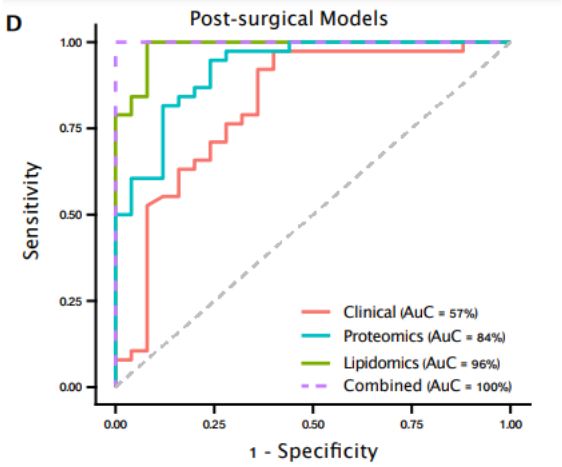

D. ROC curve of post-surgical classifiers.

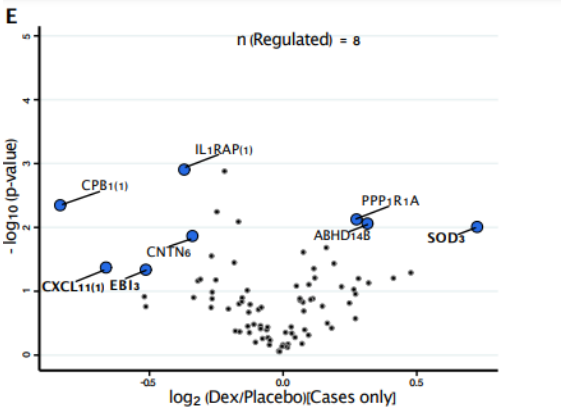

E. Volcano plot of proteomic changes among cases who received Dexmedetomidine compared to those who did not receive Dexmedetomidine

Neuroscience in Anesthesiology and Perioperative Medicine 28- Chronic Allergic Lung Inflammation Induced by Intranasal House Dust Mite Antigen Causes Suppression of Neuronal Activity in Mice

Maya Mikami[1], Mariam Trichas[1], Akihiro Kanaya[1], Kai Chen[1], Guang Yang[2], Charles Emala[2]

Columbia University[1] Columbia University Department of Anesth[2]

Introduction: Previously we have observed depressive-like behaviors in mice following the development of chronic allergic lung inflammation that potentially involved brain mast cell activation[1]. However, the specific brain regions that might be responsible for the observed behavioral changes were not identified. The anterior cingulate cortex (ACC) has been implicated in depression, and hypoactivity of this region is seen in the EEG of patients with depression[2]. In the current study, we tested our hypothesis that chronic allergic lung inflammation causes mast cell activation that affects neuronal activity in the ACC, leading to depressive-like behavior changes in mice.

Methods: All animal studies were approved by the institutional IACUC. Wild-type C57BL/6J and Thy1-GCaMP6 female mice were sensitized with intranasal house dust mite (HDM) antigen or control PBS for 6 weeks to induce chronic allergic lung inflammation. Intraperitoneal injection of control PBS or cromolyn sodium (50 mg/kg once a day, Sigma) were performed during HDM sensitization. For immunohistochemistry experiments, 7 µm brain paraffin slices were incubated with anti-chymase antibody (1:100, ab233103, Abcam). In vivo cortical calcium imaging was performed through cranial windows in head-restrained awake mice, and spontaneous calcium activity in the cortex was measured by two-photon microscopy analyzed with NIH ImageJ software. Statistical analysis was carried out using Kruskal-Wallis test with Dunn's multiple comparison.

Results: Coronal sections of frontal cortex showed that chymase expression was substantially increased in the ACC after 6 weeks of HDM treatment compared with PBS controls. The frequency of somatic calcium activity in ACC pyramidal neurons were reduced in HDM compared with PBS control group ($p<0.0001$). Intraperitoneal administration of cromolyn sodium, a mast cell stabilizing agent, during HDM sensitization inhibited this frequency reduction observed in HDM sensitized mice ($p<0.0001$). There was no significant change in the somatic calcium activity frequency from pyramidal neurons in the auditory cortex.

Conclusions: Chronic intranasal HDM sensitization caused increased chymase immunoreactivity in the ACC of the brain, indicating cerebral mast cell activation in this region. Somatic calcium activity in ACC pyramidal neurons was decreased after HDM sensitization compared with PBS control, and co-administration of intraperitoneal cromolyn prevented this HDM-induced hypoactivity. The observed decrease in ACC calcium activity was site specific, as there was no decrease in the auditory cortex. The activation of mast cells in ACC and decreased pyramidal neuronal activity may play a role in the depressive behaviors observed in mice after chronic HDM sensitization.

References:

1. J Neuroinflamation (2022) 19(1): 210.
2. Am J Psychiatry (2001) 158(3): 405-15.

Neuroscience in Anesthesiology and Perioperative Medicine 29- Enhanced Phasic GABA Inhibition Underlies Persistent Hippocampal Synaptic Plasticity Impairments Following Cerebral Ischemia

Nidia Quillinan[1], Amelia Burch[1], Joshua Garcia[1], Heather Caballes[1], Erika Tiemeier[1], Katharine Smith[1], Paco Herson[1]

University of Colorado, Anschutz Medical Campus[1]

Introduction: Excitatory-inhibitory (E/I) imbalance underlies perturbations in circuit function following numerous neurologic diseases, leading to cognitive and motor sequelae. In the context of cerebral ischemia, recent studies have demonstrated increased phasic GABA signaling in the peri-infarct region of the cortex during the chronic repair phase following stroke. Excitatory-inhibitory (E/I) imbalance in the hippocampus has yet to be explored in the repair phase following cerebral ischemia, despite ischemia-induced cognitive impairment as a major cause of disability worldwide. Here, we assessed GABAergic signaling in the hippocampal neurons following global cerebral ischemia (GCI) and tested the hypothesis that the oxidative stress-activated calcium channel TRPM2 regulates post-ischemic GABA signaling, resulting in changes is plasticity and repair.

Methods: Dissociated rat hippocampal neurons were exposed to 20-minute oxygen-glucose deprivation (OGD), fixed at 96 hours, and stained for GABAergic synaptic proteins, $GABA_A$ receptor g2 subunit, gephyrin, and vGAT. For *in vivo* experiments, adult male mice were subjected to 8 minutes of cardiac arrest followed by cardiopulmonary resuscitation to induce global cerebral ischemia. For whole-cell electrophysiology, acute hippocampal slices were prepared 7 days following cardiac arrest/cardiopulmonary resuscitation and spontaneous or evoked inhibitory post-synaptic currents (sIPSC and eIPSC respectively) were recorded in CA1 pyramidal neurons. For immunofluorescence, brains were perfusion fixed at 7 days following CA/CPR and staining was performed for gephyrin and vGAT. Clotrimizole or the novel peptide inhibitor, tat-M2NX, were used to inhibit TRPM2 ion channel function.

Results: CA/CPR and OGD increased density and clustering of GABAergic synaptic markers (22%-increase gephyrin, 25% g2, 30% vGAT; $p<0.05$). CA/CPR mice also exhibit increased sIPSC amplitude in CA1 neurons (sham: 58.5±4.5pA; CA/CPR: 91.2±8.2pA, $p<0.05$). Increased amplitude of inhibitory currents was also observed as a decrease in the E/I ratio of evoked synaptic responses. Inhibition of TRPM2 rapidly reduced clustering of GABAergic synapses and restored sIPSC amplitude to sham levels (66.25±6.0pA).

Conclusions: These data suggest enhanced phasic GABA signaling may be a significant contributor to long-term GCI-induced E/I imbalance and hippocampal dysfunction resulting from persistent TRPM2 activity. Thus, we highlight a novel mechanism by which enhanced phasic GABA signaling contributes to persistent hippocampal synaptic plasticity deficits following ischemia.

References: 1. Nakayama, S., et al., *Sexually Dimorphic Response of TRPM2 Inhibition Following Cardiac Arrest-Induced Global Cerebral Ischemia in Mice.* Journal of Molecular Neuroscience, 2013. **51**(1): p. 92-98.

2. Dietz, R.M., et al., *Reversal of Global Ischemia-Induced Cognitive Dysfunction by Delayed Inhibition of TRPM2 Ion Channels.* Transl Stroke Res, 2020. **11**(2): p. 254-266.

Neuroscience in Anesthesiology and Perioperative Medicine 30- Ischemia-induced hippocampus subregion specific alterations in mouse mitochondrial homeostasis

Tibor Kristian[1], Jordan Fick[1], Theodor Balog[1]

University of Maryland Baltimore[1]

Introduction: Mitochondrial homeostasis via mitochondrial dynamics and quality control is crucial to normal cellular functions. To determine the contribution of mitochondrial homeostasis to ischemic brain damage we examined the hippocampal region-specific and cell-type specific changes in mitochondrial dynamics and mitophagy following global brain ischemia. To this end we used our transgenic mouse model that expresses mitochondria targeted yellow fluorescence protein (mito-eYFP) either in neurons or astrocytes (Chandrasekaran et al, 2006).

Methods: Both neuron-, and astrocyte-specific mito-eYFP expressing mice were subjected to transient 10 min global cerebral ischemia. Following 2, 4, 24 hours and 3 days of recovery, the mice were perfusion-fixed or hippocampal samples were collected for further analysis by western blots. By utilizing serial z-sectioning with a Zeiss confocal microscope, we examined the morphological alterations of the entire mitochondrial network within the whole cell. Images were taken from the vulnerable CA1 and ischemia resistant dentate gyrus (DG) sub-region of the hippocampus. At the designated recovery time points, we examined the mitochondrial size distribution, total mitochondrial number, and total volume. Furthermore, the expression levels of proteins that regulate mitochondrial fission, fusion and proteins that are involved in mitophagy mechanisms were determined. The study was approved by the University of Maryland Baltimore Institutional Animal Care and Use Committee.

Results: Neuronal mitochondria in both CA1 and DG hippocampal subregions became fragmented following ischemia. This intense fragmentation of neuronal mitochondria was observed at 2 hours of reperfusion and persisted during the whole 3-day recovery period only in the vulnerable CA1 hippocampal sub-region. In ischemia resistant DG mitochondria were able to refuse at 3 days recovery. In CA1 neurons the total mitochondrial mass was decreased during reperfusion suggesting an activation of mitophagy. This notion was supported by dramatic increase in hippocampal PINK1 levels and co-localization of PARKIN, LC3 and lysosomal protein LAMP2 with mitochondria. At 2 hours of recovery, the PARKIN colocalization was observed only in the perinuclear region. At 3 days of recovery, we also observed PARKIN co-localization with mitochondria located in astrocytic processes. Interestingly, in DG neurons, the total mitocohndrial volume recover to pre-ischemic levels, hoiwver, in CA1 neurons the mitochohdrial mass was significantly reduced.

Conclusions: The presented data show that:

- There is a permanent fragmentation of neuronal mitochondria in ischemia vulnerable brain tissue.
- Mitochondria in ischemia resistant brain regions are able to re-fuse following ischemia-induced fragmentation.
- The total mitochondrial mass represented by total volume was significantly reduced by about 30% in the CA1 sector of the hippocampus. In ischemia-resistant DG, the mass reduction was transient.

References: Neuron-specific conditional expression of a mitochondrially targeted fluorescent protein in mice. J Neurosci, 26(51):1323-1327, 2006.

Neuroscience in Anesthesiology and Perioperative Medicine 31- Methylphenidate and D-amphetamine Produce Distinct Arousal States After High-dose Dexmedetomidine in Rats

Kathleen Vincent[1], Gwi Park[2], Brendan Stapley[3], Emmaline Dillon[3], Ken Solt[2]

Massachusetts General Hospital and Harvard Medical School[1] Massachusetts General Hospital[2] Brigham Young University[3]

Introduction: Dexmedetomidine (DEX) is an alpha-2A adrenergic receptor agonist that induces unconsciousness when administered at high doses. Because DEX has a long elimination half-life (~2 hours) in humans, a reversal agent would be clinically useful to terminate the effects of DEX as needed. The alpha-2 adrenergic receptor antagonist atipamezole is an efficacious reversal agent for DEX in animals, but it is not approved for human use. We recently reported that intravenous d-amphetamine, which causes synaptic dopamine and norepinephrine release, is a highly efficacious reversal agent for high-dose DEX in rats.[1] Similar to d-amphetamine, methylphenidate enhances dopaminergic and noradrenergic neurotransmission by inhibiting reuptake transporters for these arousal-promoting neurotransmitters. Unlike d-amphetamine, however, methylphenidate does not cause synaptic dopamine or norepinephrine release.[2] In this study, we tested the behavioral and neurophysiological effects of methylphenidate after the administration of DEX at a high dose sufficient to induce loss of righting (a standard proxy for unconsciousness). It is known that DEX attenuates dopamine concentrations in the shell of the nucleus accumbens (NAc),[3] which is an important downstream target of arousal-promoting dopaminergic neurotransmission.[4] Therefore, we also compared the activity of NAc neurons after administering DEX followed by methylphenidate or d-amphetamine.

Methods: All studies were conducted in adult Sprague-Dawley rats and approved by our Institutional Animal Care and Use Committee (protocol #2010N00026). First, an intravenous catheter was placed in the lateral tail vein under brief isoflurane anesthesia. After full recovery from isoflurane, DEX (50 µg/kg IV over 10 minutes) was administered to establish loss of righting. After the DEX infusion, methylphenidate (1mg/kg or 5 mg/kg IV) or saline (vehicle) was administered (n=8; 4 males, 4 females). Latency to return of righting reflex (RORR), a standard proxy for return of consciousness, was compared by RM-ANOVA. In a separate group of rats (n=4; 2 females and 2 males), frontal EEG electrodes (+1.5 anterior-posterior, +/-1.5 medial-lateral relative to bregma) were implanted under isoflurane anesthesia, postoperative analgesics were administered, and the animals recovered for a minimum of 7 days after surgery. On the day of an EEG experiment, the EEG was continuously recorded while DEX (50 µg/kg IV over 10 minutes) was administered, followed by methylphenidate or saline. Spectral analysis was performed on EEG recordings to assess neurophysiological changes. Finally, an additional group of rats (n=9; 5 females and 4 males) received DEX (50 µg/kg IV over 10 minutes) followed by d-amphetamine (3 mg/kg IV), methylphenidate (5 mg/kg IV) or saline (vehicle), and subsequently underwent perfusion with formalin. Using immunofluorescence, neural activity was assessed in the shell of the nucleus accumbens (NAc) and ventral tegmental area (VTA) by counting cells positive for expression of c-Fos, a marker of neuronal activity, and analyzed by a mixed-effects model.

Results: Latency to RORR following DEX was not significantly altered by methylphenidate ($F(1,9)= 2.588$, $p=.1387$)(Fig 1). EEG analysis revealed that methylphenidate transiently attenuated alpha power ($t(12)=7.045$, $p<.0001$) following DEX when compared with saline (Fig 2). Histological analysis revealed a significant interaction between drug condition and brain region on c-Fos expression ($F(2,6)=5.261$, $p=.0479$). Simple main effects with Dunnett's correction revealed that compared with saline, both d-amphetamine ($t(12)=3.577$, $p=.0071$) and methylphenidate ($t(12)=5.008$, $p=.0006$) significantly increased c-Fos expression in the medial shell of the NAc (Fig. 3). There was no significant difference in VTA c-Fos expression across any of the drug conditions.

Conclusions: Unlike d-amphetamine, methylphenidate does not accelerate emergence following unconsciousness induced by high-dose DEX in rats, despite a transient attenuation of EEG alpha power. Surprisingly, both d-amphetamine and methylphenidate increase activity in the medial shell of the NAc, suggesting that other downstream targets of arousal-promoting dopaminergic neurotransmission may be involved in the rapid reversal of DEX-induced unconsciousness by d-amphetamine.

References: 1. *Front Pharmacol,* **12**:668285, (2021).

2. *Neuropharmacology,* **57**:608-618, (2009).

3. *Brain Res,* **919**:132-138, (2001).

4. *Curr Biol,* **31**:1-10, (2021).

Fig 1

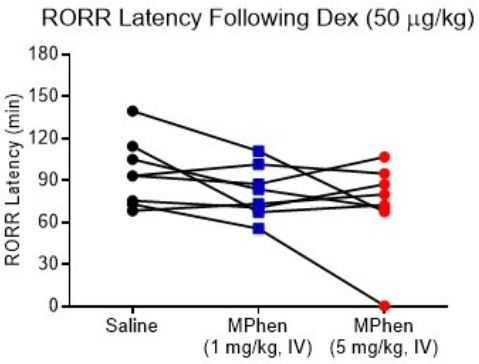

Fig 2

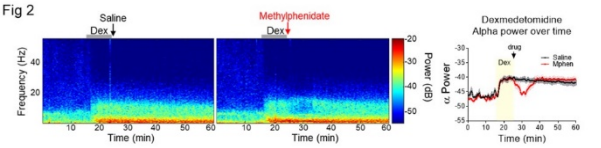

Fig 3

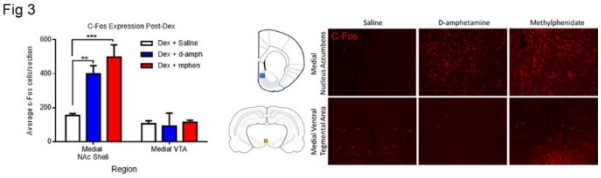

Neuroscience in Anesthesiology and Perioperative Medicine 32- Midazolam suppression of place cells and spatial engrams is independent of a5-$GABA_A$ receptors on pyramidal neurons

Mengwen Zhu[1], Mark Perkins[2], Richard Lennertz[1], Robert Pearce[1]

University of Wisconsin-Madison[1] UW-Madison Dept of Anesthesiology[2]

Introduction: The amnestic property of midazolam contributes to its widespread use in the perioperative period and for procedural sedation. Like other benzodiazepines, midazolam exerts its effects through modulation of $GABA_A$ receptors. However, the specific receptor subtypes and cellular targets that contribute to the suppression remain unclear. A recent study reported that midazolam can suppress long-term potentiation, an *in vitro* cellular model of memory, through allosteric modulation of either a1- or a5-subunit-containing $GABA_A$Rs.[1] Immunohistochemical studies indicate that a5-$GABA_A$Rs are concentrated in the hippocampus, and modulation of a5-$GABA_A$Rs has been linked to suppression of learning and memory by the prototypical GABAergic general anesthetic etomidate.[2] To test the role of a5-$GABA_A$Rs in midazolam-induced amnesia, in the present study we used calcium imaging in freely exploring mice to assess effects of midazolam on place cell formation and spatial engrams as neural correlates of contextual memory in wild-type mice (WT) and in mice with selective knockout of a5-$GABA_A$Rs from pyramidal neurons (a5-pyr-KO).

Methods: Under IACUC approval, AAV carrying the genetically encoded calcium fluorescent indicator GCaMP6f driven by CaMKIIa promoter was injected into the CA1 region of the hippocampus of 5 WT (C57BL/6J), 5 pseudo-WT (p-WT, floxed a5 allele), and 4 a5-pyr-KO mice. 2-3 weeks later, an integrated GRIN lens with baseplate was implanted over dCA1, to which a miniature endoscopic camera (Inscopix nVoke) was attached to capture the underlying calcium dynamics. Mice were first screened for stable and sufficient (> 100 active cells) cellular activities in an arena that allows for synchronized recording of hippocampal calcium dynamics and mouse behavior (Noldus EthoVision). Qualified mice were then tested in a series of paired 10-min recording sessions. We measured place cells that formed upon novel context exposure during the first session (Day1), and the recurrence/remapping of spatial engram during the second session (Day2). 40 minutes prior to Day1, mice were injected intraperitoneally with either saline (control) or midazolam (0.25 and 1.25 mg/kg).

Calcium imaging recordings were analyzed in two stages using Inscopix Data Processing Software (IDPS v1.8.0) and custom-written MATLAB (2021a) functions. In the first stage, raw recordings were preprocessed, motion corrected, and DF/F transformed in preparation for cell and calcium event detection using CNMFe algorithm. Identified cells were longitudinally registered and assigned a global ID. In the second stage, calcium imaging data were combined with behavioral data to compute place cell formation based on mutual information between firing rate and mouse position, and spatial engram stability based on rate-map (RM) and population-vector (PV) correlations between Day1 and Day2 spatially modulated firing rates. Statistical analyses were done using a linear mixed effects model within RStudio.

Results: All mice used in this study passed our minimum screening criteria, with up to 800 cells captured in a single field of view. Upon novel context exposure, mice actively explored the arena for ~8 out of 10 min. Detected cells showed an average event rate of 0.12 Hz. In all genotypes, midazolam dose-dependently reduced exploratory activity ($p<0.0001$), but even at the highest dose (1.25 mg/kg) they still actively explored the arena for ~3 min, and calcium event rates were unchanged ($p>0.5$). In WT mice, 1.25 mg/kg reduced place cell formation ($p<0.05$), and both 0.25 and 1.25 mg/kg significantly suppressed spatial engram stability ($p<0.01$) (Fig. A, i-iii). Similarly, in both a5-pyr-KO and p-WT mice, 1.25mg/kg strongly suppressed place cell formation ($p<0.001$) and spatial engram stability as indicated by RM and PV correlations ($p<0.05$). There were no significant interactions between genotype (p-WT vs. a5-pyr-KO) and drug condition (saline vs. 1.25 mg/kg) (Fig. B, i-iii).

Conclusions: Since eliminating a5-$GABA_A$Rs from pyramidal neurons did not influence the dose-dependence of place cell and spatial engram suppression by midazolam, we conclude that a5-$GABA_A$Rs on pyramidal neurons do not mediate midazolam suppression of contextual memory. Instead, either a5-$GABA_A$Rs expressed on interneurons,[3] or other subtypes of $GABA_A$Rs, are responsible. Experiments with mice lacking interneuronal a5-$GABA_A$Rs are underway and should reveal which explanation is correct.

References:

1. Anesthesiology 136(6): 954-969, 2022
2. J. Neurosci. 26:3713-3720, 2006
3. bioRxiv doi: 10.1101/2022.03.03.482912, 2022.

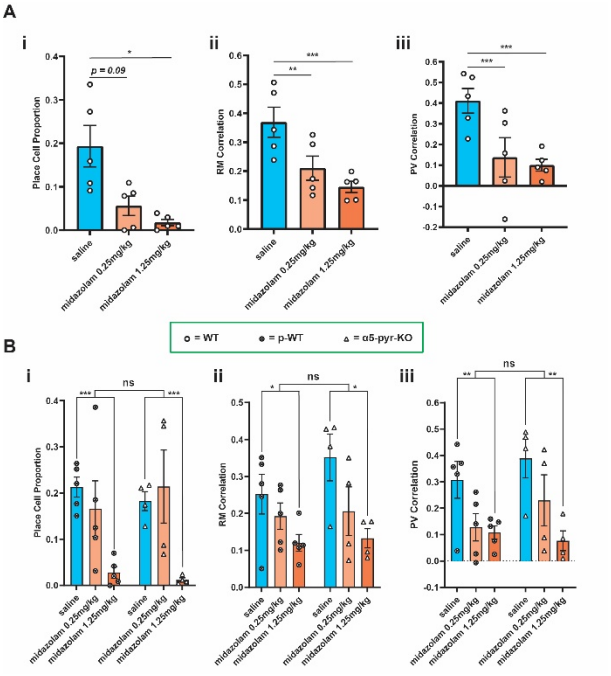
A
i
ii
iii
Place Cell Proportion
RM Correlation
PV Correlation
p = 0.09
saline
midazolam 0.25mg/kg
midazolam 1.25mg/kg
B
○ = WT
● = p-WT
△ = α5-pyr-KO
ns

Neuroscience in Anesthesiology and Perioperative Medicine 33- Modulation of human memory and pain by diverse anesthetic agents: A randomized placebo-controlled crossover 7 Tesla functional MRI study in healthy young adults

Keith Vogt[1], Sujatha Nallama Reddy[1], Courtney Kozdron[2], Alex Burlew[2], Steven Shafer[3], Howard Aizenstein[3], Lynne Reder[3], James Ibinson[1], Julie Fiez[1]

University of Pittsburgh[1] University of Pittsburgh[2] Stanford University[3]

Introduction: Anesthetic and analgesic agents are well-known to impair performance on distinct cognitive tasks [1, 2]. Though important prior work has demonstrated how memory and fear learning areas in the brain may be modulated by specific drugs [3], less attention has been given to these questions during the concomitant experience of pain [4]. We developed a novel paradigm with periodic painful stimulation during an auditory memory encoding task, which more closely reflects clinical conditions under which anesthetics are used. This experimental framework was used to study the effects of three different agents using high-field functional MRI (fMRI).

Methods: This is an interim analysis of data from an ongoing trial (NCT04062123) comparing propofol, dexmedetomidine, and fentanyl. Healthy adults age 40 and under were recruited; two in-scanner sessions were followed by next-day memory testing. During both scan sessions, subjects received a crystalloid infusion. In one session, a constant effect-site concentration was targeted using stanpumpR (steveshafer.shinyapps.io/stanpumpR). Subjects were blinded and randomized to propofol[5] 1.0 mcg/ml, dexmedetomidine[6] 0.15 ng/ml, or fentanyl[7] 0.9 ng/ml (effect-site concentrations). ASA pre-anesthesia fasting guidelines and standard monitoring were employed. An electric nerve stimulator was connected to the left index finger, and current was titrated in advance to 7/10 intensity on a numerical rating scale. Subjects listened to a series of 80 words (divided across two 8-min scans); each word was repeated 4 times in succession during a 6 s window. In a novel auditory memory task, subjects were instructed to create a mental picture involving the word and add more detail as the word repeated. Thirty of the words were accompanied by a 2 s painful shock during the latter half of the 6 s window. Ratings of pain intensity and unpleasantness were obtained at the end of each scan. Blood oxygen-weighted images (1 s temporal resolution, 2 mm isotropic spatial resolution) were obtained at 7 T, using a custom head coil[8]. Next-day Remember-Know[9] recognition memory testing determined recollection and familiarity, against a background of 80 additional words not previously-heard. FMRI analysis was performed with SPM12 (fil.ion.ucl.ac.uk/spm/), after correction for magnetic field inhomogeneity and physiologic noise[10]. Group contrast maps for saline minus drug were thresholded at $p < 0.001$.

Results: Light sedation was achieved in most subjects, though two were unresponsive to voice under propofol. The lowest pain ratings and next-day memory performance, averaged across subjects, are shown in Fig 1. Pain ratings trended toward decreasing along expected analgesic effect of the 3 drugs. Memory performance was highly variable across subjects, with decrements in average value seen to match expected amnestic profile (propofol > dexmedetomidine > fentanyl).

The left side of Fig 2 shows drug-associated differences in pain-related brain activity. All drugs reduced activation in the posterior insula bilaterally, though different subregions of the insula were affected by each agent. Dexmedetomidine was associated with an increase in right anterior insula activation. Propofol and dexmedetomidine, but not fentanyl, reduced activation in a similar location in the anterior cingulate.

The right side of Fig. 2 shows drug differences for items successfully encoded (recognized as familiar at testing). Propofol and fentanyl, but not dexmedetomidine, reduced activity in the right amygdala. Propofol and dexmedetomidine, but not fentanyl, reduced activity in the right hippocampus. One surprising finding was increased activity under all drugs in the right mid-parahippocampus. Notably, no modulation of left-sided medial temporal lobe memory structures was detected with any drug.

Conclusions: These preliminary results show an intriguing pattern of differential brain activation across distinct anesthetics that is not obviously predicted by similar behavioral data and observer level of sedation. Just as these drugs have nuanced clinical features in their cognitive effects, fMRI activation in brain regions characteristically involved in pain and memory are not universally inhibited. Each drug studied exhibited a distinct pattern of brain modulation that can have bi-directionality and laterality differences. Further characterization of these brain activation differences is anticipated with final analysis of data from this trial.

References: 1. Anesthesiology 2009;110:295-312.

2. Anesthesiology 1997;87:749-64.

3. Br J Anaesth 2015;115 Suppl 1:i104-i13.

4. Anesthesiology 2021;135:69-82.

5. Br J Anaesth 2018;120:942-59.

6. Anesthesiology 1993;78:813-20.

7. Anesthesiology 1990;73:1091-102.

8. PloS one 2019;14:e0209663.

9. Consciousness and cognition 2012;21:1435-55.

10. NeuroImage 2007;37:90-101.

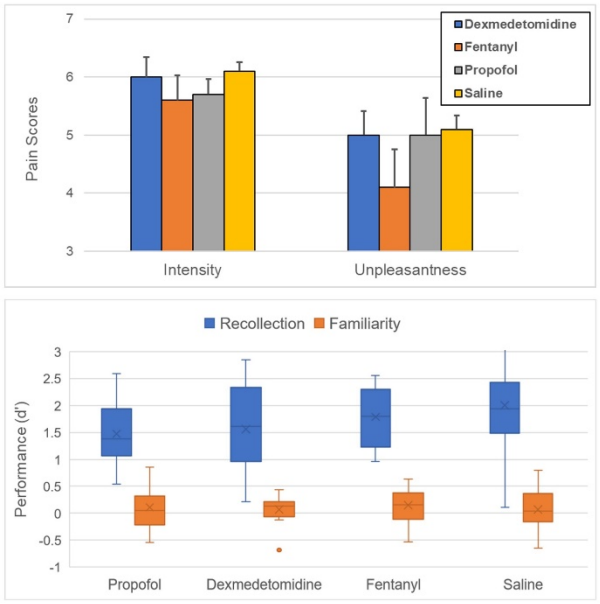

Fig 1. Behavioral results across drug condition. The top panel shows nadir pain intensity and unpleasantness scores during the experiment, using a (0-10) numerical rating scale. Bars indicate standard error. The bottom panel shows, in Box & Whisker format, next-day recognition memory performance, using the standardized metric d' (d-prime), a Z-score-like measure indicating standard deviations above/below chance performance (d'=0). Whiskers indicate 1.5 times the inter-quartile range.

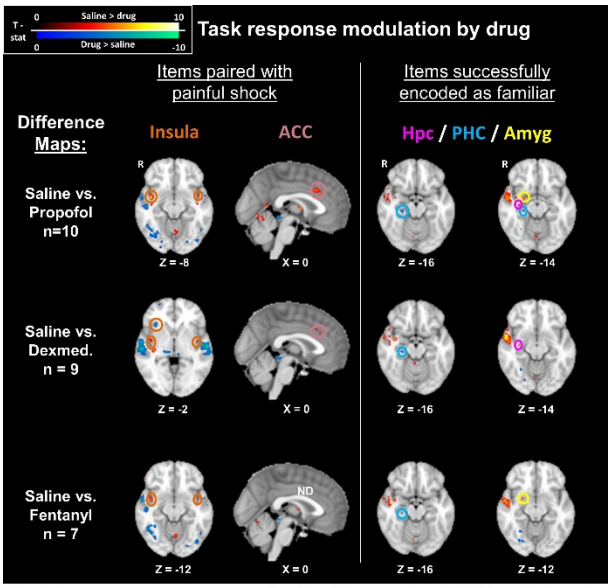

Fig 2. Group average contrast maps showing differences ($p < 0.001$) in task-related brain activation between saline and drug sessions (by row, as labelled). The left two columns show activation changes in pain-processing areas, focused on experimental items paired with painful shock. The right two columns show changes in medial temporal lobe memory systems, for items successfully recognized as familiar, based on next-day testing.

Legend: T-stat= T-statistic, ACC = anterior cingulate cortex, Hpc= hippocampus, PHC= parahippocampus, Amyg= amygdala, vs =versus, Dexmed= dexmedetomidine, ND= no difference. z and x refer to slice coordinates in the MNI-152 brain.

Neuroscience in Anesthesiology and Perioperative Medicine 34- Predicting Sedation Level using Surface and Intracranial EEG with Convolutional Neural Networks during Emergence from Anesthesia

Lichy Han[1], David Purger[1], Sarah Eagleman[1], Casey Halpern[1], Vivek Buch[1], Babak Razavi[1], Kimford Meador[1], David Drover[2]

Stanford University[1] Stanford Medical Center[2]

Introduction: Accurate assessment of the level of sedation under anesthesia is necessary to optimize the balance between overmedication and awareness while enabling timely emergence from anesthesia. Electroencephalography (EEG) has become an increasingly common tool to assess brain states during anesthesia [1]. However, surface EEG frequently contains artifactual sources of electrical signal, obscuring the underlying brain activity [2]. Comparing simultaneous intracranial and surface EEG can provide additional insight into neurophysiological patterns associated with different clinical sedation levels.

Methods: Seven patients with medically refractory epilepsy underwent placement of intracranial electrodes under general anesthesia for localization of epileptic foci. During emergence from anesthesia, intracranial EEG, surface EEG, and Observer's Assessment of Alertness/Sedation (OAA/S) scores [3] were recorded simultaneously. We constructed a convolutional neural network (CNN) to predict OAA/S scores of 0-2 (unresponsive) versus 3-5 (responsive) at every second of recording using the previous 5 seconds of scalp and intracranial EEG data (Figure 1). We trained our model using 70% of our patients with 5-fold cross validation for parameter optimization. We tested the model on the remaining independent 30% and examined the layers to gain further insight into predictive features learned by our model.

Results: Our model yielded an area under the receiver operating curve of 0.991 on the training data, 0.986 on the validation data, and 0.722 on the test data. This corresponded to an accuracy of 97.4%, 97.1%, and 78.5% respectively. In our test patients, the prediction probability corresponds well with the OAA/S score during final emergence from anesthesia and may detect lightening events (Figure 2). Applying the weights from the first layer of filters from the intracranial CNN enables examination of features automatically extracted by the model. The filters from the first layer appear to focus on different frequency bands, similar to what may be intuitively extracted by a human observer (Figure 3). These frequency-based features suggest that their combination in subsequent convolutional layers yields predictive power in intracranial EEG.

Conclusions: Deep learning models can extract spectral features from raw surface and intracranial EEG data for the continuous monitoring of sedation level in real time. In turn, these models may reveal electrophysiological patterns characterizing the underlying brain states to facilitate sedation assessment and personalized titration of anesthesia in the operating room.

References: 1. A primer for EEG signal processing in anesthesia. Anesthesiology. 89(4):980-1002. 1998.

2. Artifact and recording concepts in EEG. J Clin Neurophysiol. 28(3):252-63. 2011.

3. Validity and reliability of the Observer's Assessment of Alertness/Sedation Scale: study with intravenous midazolam. J Clin Psychopharmacol. 10(4):244-51. 1990.

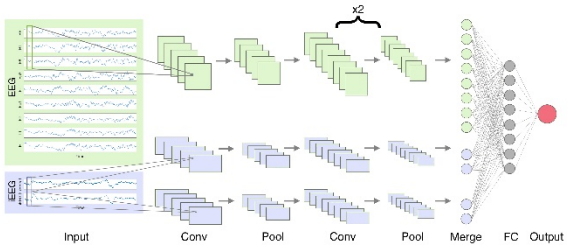

Figure 1. CNN architecture. Nine channel surface EEG and two channels of iEEG were analyzed using a 3-layer CNN on each input. Max pooling layers were used between convolutional layers for downsampling, and dropout was used to limit overfitting. The separate convolutional networks for surface and intracranial EEG were then flattened and concatenated. The merged data were then inputted into a fully connected (FC) layer followed by classification with the sigmoid function to produce the final output.

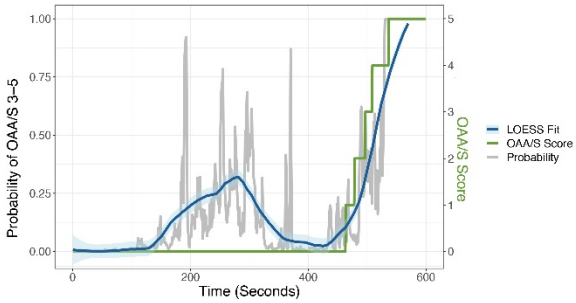

Figure 2. Prediction probability (gray) with overlying locally estimated scatterplot smoothing (LOESS, blue) for one of the test group patients during emergence from anesthesia, with the actual OAA/S score in green. Close to the end of emergence, the probabilities correspond well with the OAA/S score. Interval lightening of the brain state prior to the end (~200-375 seconds) is predicted by our model, though with average probabilities below 0.5 and thus may not be reflected in the OAA/S score.

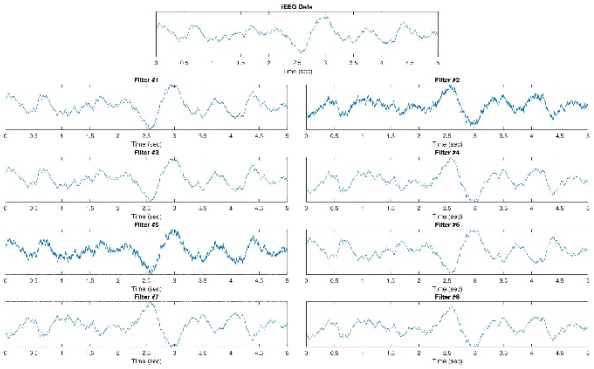

Figure 3. Application of the 8 filters from the first convolutional layer on intracranial EEG data (raw data shown on top). The filters consist of weights that extract features from the data corresponding to improved model prediction. These weights have then been applied to the raw data to visualize transformations learned by the machine. Different filters appear to be focused on different frequency ranges (higher frequencies in filters 2 and 6), with some filters also examining inversions of the data (filters 2, 4, 7, and 8).

Neuroscience in Anesthesiology and Perioperative Medicine 35- Preoperative cognitive impairment and intraoperative burst suppression duration in older cardiac surgical patients – A potential link?

Alkananda Behera[1], Hibiki Orui[1], Rushil Vladimir Ramachandran[1], Zaid Hussain[1], Ajaykarthik Ananthakrishnan[1], Jordan Peck[1], Ziena Al-Dhamen[2], Priyam Mathur[2], Valerie Banner-Goodspeed[1], Jochen Muehlschlegel[3], Jean-Francois Pittet[4], Amit Bardia[4], Robert Schonberger[5], Edward Marcantonio[1], Kestas Kveraga[6], Balachundhar Subramaniam[7]

Beth Israel Deaconess Medical Center[1] BIDMC[2] BWH[3] Univ of Alabama at Birmingham[4] Yale School of Medicine Department of Anesthesiology[5] Beth Israel Deaconess Medical Center, Harvard Medical School[6] Harvard Medical School - Beth Israel Deacon[7]

Introduction: Postoperative delirium (POD) is common in older cardiac surgery patients and is associated with a prolonged hospital stay as well as increased morbidity and mortality (1). Older patients are also at greater risk of having pre-existing cognitive impairment, which is associated with a higher incidence of postoperative neurocognitive disorders (2). With the advent of raw EEG analysis replacing processed EEG parameters, current research suggests that electroencephalogram (EEG) burst suppression (BS) incidence and duration (BSD) may predict postoperative delirium (3). Literature correlating preoperative risk factors with BS is still sparse (2) and thereby the underlying mechanisms of this important public health problem is not completely understood. Our purpose was to explore the relationship between preoperative cognitive impairment and intraoperative BSD in this vulnerable patient population, aiming to potentially link an important risk factor with EEG parameters that predict POD.

Methods: This is a secondary analysis of an ongoing, multi-center, triple blinded, randomized trial evaluating postoperative intravenous acetaminophen for the prevention of postoperative delirium (4). Enrolled patients are >=60 years old and undergoing elective CABG and/or valve surgery under cardiopulmonary bypass. For our analysis, baseline characteristics of 108 study participants were collected from a single academic medical center. Preoperative cognition was assessed using the validated MoCA (Montreal Cognitive Assessment) screening tool, scored out of 30, and t-MoCA (telephone version), scored out of 22. Participants were categorized into the following 2 study groups – normal (MoCA score >=26, t-MoCA >=19) and abnormal cognition. Participants with abnormal cognition were identified as having preoperative cognitive impairment. Patients received institutionally standard anesthesia and surgery care. Intra-operative frontal electroencephalogram (EEG) was recorded passively. 91 patients out of 108 had clean raw EEG data available for analysis. Burst suppression was identified with a recursive variance estimation algorithm (5) and its total duration was computed per patient in minutes. The burst suppression ratio (SR) was the summed duration of burst suppression segments relative to the overall length of intraoperative EEG recordings analyzed. Relevant intraoperative parameters were assessed between the 2 groups using the Wilcoxon rank sum test. Association between the intraoperative burst suppression duration and the baseline cognitive assessment was analyzed using multiple linear regression controlling for age, race, hypertension, diabetes, intraoperative total fentanyl and propofol dose, total surgical duration spent in mean arterial pressure (MAP) <65 mmHg, and end tidal anesthesia concentration.

Results: Baseline characteristics of the study participants are presented in Table 1. No statistically significant difference was noted between the 2 groups in terms of intraoperative sedative/hypnotics, surgery/EEG duration, total time spent in MAP<65mmHg and end tidal anesthesia concentration (Table 2). Unadjusted analysis for the association of BSD and SR with the two MoCA categories didn't achieve statistical significance as graphically represented in Figures 1 and 2 respectively and corroborated in Table 2. Adjusted analysis (Table 3) for the relationship between the baseline cognitive assessment and the BSD was not significant (p = 0.12). Age and end tidal anesthesia concentrations were significantly associated with BSD (Beta 2.6; 95% CI 0.08, 5.1; p =0.045 and Beta 19, 95% CI 4.7, 34, p=0.017 respectively).

Conclusions: Preoperative cognitive impairment was not found to be associated with intraoperative burst suppression in our study. Age and end tidal anesthesia concentrations were found to be significantly associated with BSD. Future efforts should be directed at looking into other EEG variables (spectral edge frequency, alpha band power etc.) along with BS.

References:

1. Review articles: postoperative delirium: acute change with long-term implications. Anesth Analg. 2011 May;112(5):1202-11.
2. ENGAGES Research Group. Preoperative Cognitive Abnormality, Intraoperative Electroencephalogram Suppression, and Postoperative Delirium: A Mediation Analysis. Anesthesiology. 2020 Jun;132(6):1458-1468.
3. Electroencephalogram Burst-suppression during Cardiopulmonary Bypass in Elderly Patients Mediates Postoperative Delirium. Anesthesiology. 2020 Aug;133(2):280-292.
4. Scheduled Prophylactic 6-Hourly IV AcetaminopheN to Prevent Postoperative Delirium in Older CaRdiac SurgicAl Patients (PANDORA): protocol for a multicentre randomised controlled trialBMJ Open 2021;11:e044346 #NCT04093219
5. Real-time segmentation of burst suppression patterns in critical care EEG monitoring. J Neurosci Methods. 2013 Sep 30;219(1):131-41.

Table 1: Baseline characteristics of study participants

Characteristic	Abnormal, N = 61[1]	Normal, N = 47[1]
Age	70.84 (6.40)	69.47 (6.34)
Gender		
Female	20 (33%)	12 (26%)
Male	41 (67%)	35 (74%)
Calculated BMI	27.61 (5.94)	29.21 (4.92)
Race		
Caucasian	54 (89%)	45 (96%)
Non-Caucasian	6 (9.8%)	1 (2.1%)
Unknown	1	1
Smoking status		
Nonsmoker	29 (48%)	21 (45%)
Smoker	32 (52%)	26 (55%)
Hypertension	54 (89%)	40 (85%)
Diabetes	23 (38%)	12 (26%)

[1]Mean (SD); n (%)

Table 2 : Comparison between two study groups

Characteristic	Normal, N = 40[1]	Abnormal, N = 51[1]	p-value[2]
BSD	10.8 (5.19, 24.89)	13.38 (5.89, 32.20)	0.4
BSmeans	0.05 (0.02, 0.11)	0.04 (0.02, 0.14)	0.6
Propofol [mg]	120 (80, 150)	100 (80, 150)	0.4
MAP<65mmHg_ duration	135 (87.5, 153.0)	108 (88.0, 131.5)	0.4
End tidal anesthetic concentration	0.69 (0.6, 0.75)	0.69 (0.61, 0.78)	0.6
Surgery duration (min)	239.2 (209.3, 299,0)	239.2 (209.3, 306.48)	0.2

[1]Median (IQR)

[2]Wilcoxon rank sum test

Fig.1 Unadjusted analysis: Association between burst suppression duration and MoCA category

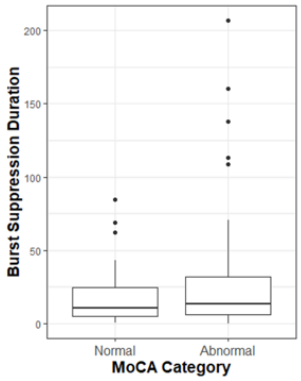

Fig.2: Unadjusted analysis: Association between burst suppression ratio and MoCA category

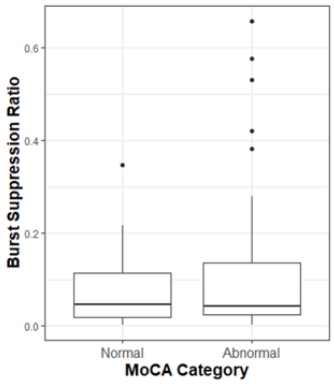

Table 3: Adjusted analysis for confounding variables

Characteristic	Beta	95% CI[1]	p-value
MoCA category			0.12
Abnormal	25	-7.9, 57	
Age	2.6	0.08, 5.1	**0.045**
Race			
Non-Caucasian	-2.7	-79, 73	0.94
Hypertension			
Yes	-42	-93, 8.8	**0.091**
Diabetes			
Yes	29	-23, 81	0.23
Fentanyl [mcg]	0.05	-0.16, 0.26	0.60
Propofol [mg]	-0.21	-0.59, 0.17	0.24
Total MAP duration <65mmHg [min]	-0.44	-1.2, 0.28	0.19
End tidal anesthetic concentration [units in 0.1]	19	4.7, 34	**0.017**

[1]CI = Confidence Interval

Neuroscience in Anesthesiology and Perioperative Medicine 36- Resting-state functional connectivity changes with propofol, dexmedetomidine, and fentanyl in healthy young adults: A randomized placebo-controlled comparative study using 7 Tesla MRI

Keith Vogt[1], Alex Burlew[1], Sujatha Nallama Reddy[1], Courtney Kozdron[2], Sheri Wang[2], Steven Shafer[3], Howard Aizenstein[3], James Ibinson[1], Julie Fiez[1]

University of Pittsburgh[1] University of Pittsburgh[2] Stanford University[3]

Introduction: Distinct anesthetic and analgesic agents are known to impact different aspects of human cognition [1,2]. However, the changes in whole-brain functional connectivity under these drugs that produce the observed cognitive effects are less well-known. Here we demonstrate differences in resting-state connectivity across different sedative agents, using data from high-resolution 7 Tesla MRI. Behavioral testing data obtained in the same session helps to characterize changes in cognitive state.

Methods: This is an interim analysis of data collected in an ongoing clinical trial (NCT04062123) comparing propofol, dexmedetomidine, and fentanyl in healthy adult participants age 40 and under. Data were drawn from two in-scanner sessions; during both, subjects received a crystalloid carrier infusion. In one of the sessions, a steady-state effect-site concentration of an anesthetic was targeted (either propofol[3] 1.0 mcg/ml, dexmedetomidine[4] 0.15 ng/ml, or fentanyl[5] 0.9 ng/ml) using stanpumpR (steveshafer.shinyapps.io/stanpumpR). ASA pre-anesthesia fasting guidelines and standard monitoring were employed, and drug administration was blinded to subjects. A brief battery of cognitive tasks was performed just before the resting-state scan, to characterize impairments in motor, executive, and memory function. Notably, this resting state data was obtained after a separate experimental epoch in which painful stimulation was used, however subjects were explicitly informed that no further painful stimulation would occur during this scan. Blood oxygen-weighted images (1 s temporal resolution, 2 mm isotropic spatial resolution, 8 min scan) were obtained at 7 T using a custom head coil[6]. Correction for magnetic field inhomogeneity and physiologic noise correction (using CompCor[7]) were performed. Analysis was performed with Conn toolbox (https://www.conn-toolbox.org/) and SPM12 (fil.ion.ucl.ac.uk/spm/); group results were thresholded for $p < 0.001$. Regions of interest (ROIs) from the Harvard-Oxford brain atlas were used for parcellation.

Results: Fig. 1 shows the average group behavioral performance across the three tasks. Motor slowing was most pronounced under dexmedetomidine. More unexpectedly, performance on the 3-back task and explicit memory encoding were also worst with dexmedetomidine. Fig. 2 shows connectivity changes for saline versus propofol (n=14 datasets); Fig. 3 shows saline versus dexmedetomidine (n=13 datasets). Preliminary results for fentanyl were limited by the small number of datasets (n=4) available for analysis at the time of submission, and no significant group-level connectivity changes were detected. A legend for the brain region abbreviations in the connectome rings is included as Fig. 4. Notably, few changes in connectivity are shared between propofol and dexmedetomidine, despite being at similar levels of observer-assessment of sedation. Under drug, compared to saline, both increases (cool colors) and decreases (warm colors) in connectivity were seen. Though few specific connectivity changes were shared between drugs, long-range and cross-modal changes in connectivity between anatomically-distant and functionally-distinct brain structures were seen with both propofol and dexmedetomidine.

Conclusions: At equi-sedative doses of mechanistically-distinct anesthetics, key differences were quantified in this preliminary analysis. Both performance on behavioral tasks spanning different cognitive domains and the underlying brain connectivity changes differed across drugs. This methodology demonstrates the ability to profile sedative drug effects using systems-level neuroscience data. Further clarification of these effects is anticipated with complete reporting of study results.

References: 1. Anesthesiology 2009;110:295-312.

2. Anesthesiology 1997;87:749-64.

3. Br J Anaesth 2018;120:942-59.

4. Anesthesiology 1993;78:813-20.

5. Anesthesiology 1990;73:1091-102.

6. PloS one 2019;14:e0209663.

7. NeuroImage 2007;37:90-101.

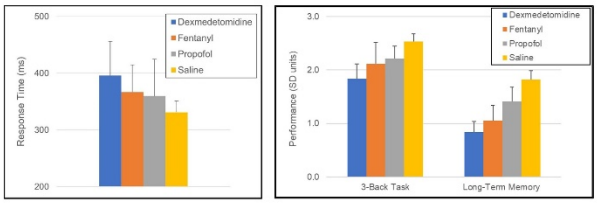

Fig. 1. Behavioral task performance characterized before resting-state MRI scan. Left panel shows changes in average response times after hearing a tone. Right panel shows performance on the 3-back task (demonstrating working memory capacity) and the long-term memory task, using the normalized signal detection metric, d-prime, which is in standard deviation (SD) units above chance performance. Error bars indicated standard error.

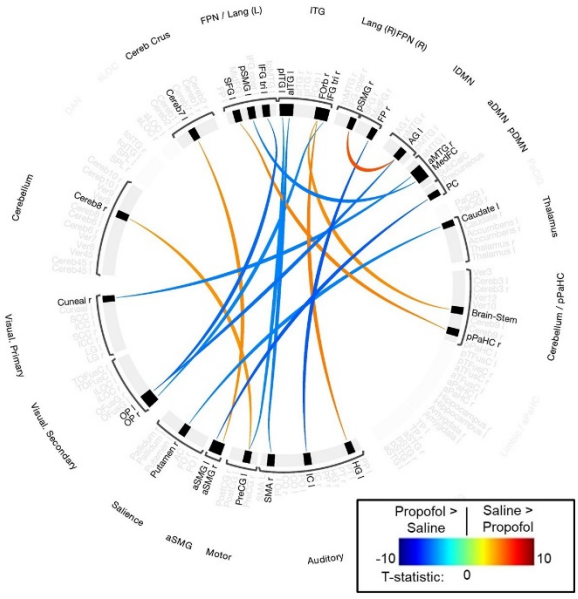

Fig. 2. Connectome ring showing changes in functional connectivity between anatomical regions of interest for saline versus propofol contrast.

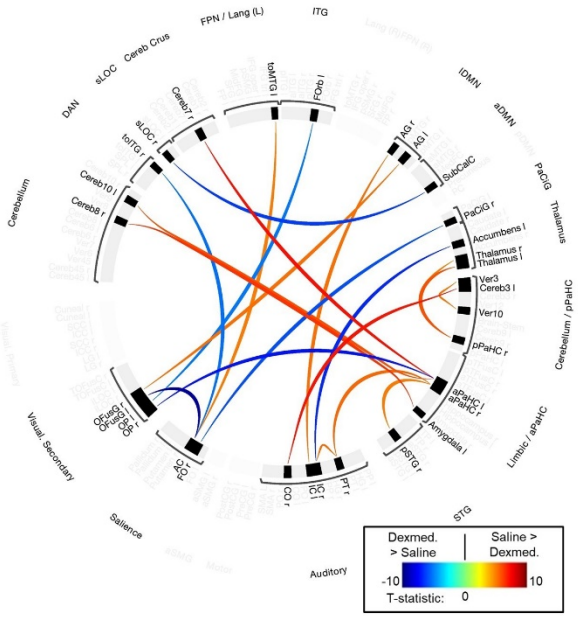

Fig. 3. Connectome ring showing changes in functional connectivity between anatomical regions of interest for saline versus dexmedetomidine contrast.

Fig 4. - Region of Interest legend for connectome rings
l = left, r = right
FP (Frontal Pole), IC (Insular Cortex), SFG (Superior Frontal Gyrus), MidFG (Middle Frontal Gyrus), IFG tri (Inferior Frontal Gyrus, pars triangularis), IFG oper (Inferior Frontal Gyrus, pars opercularis), PreCG (Precentral Gyrus), TP (Temporal Pole), aSTG (Superior Temporal Gyrus, anterior division), pSTG (Superior Temporal Gyrus, posterior division), aMTG (Middle Temporal Gyrus, anterior division), pMTG (Middle Temporal Gyrus, posterior division, toMTG (Middle Temporal Gyrus, temporooccipital part), aITG (Inferior Temporal Gyrus, anterior division), pITG (Inferior Temporal Gyrus, posterior division), toITG (Inferior Temporal Gyrus, temporooccipital part), PostCG (Postcentral Gyrus), SPL (Superior Parietal Lobule), aSMG (Supramarginal Gyrus, anterior division), pSMG (Supramarginal Gyrus, posterior division), AG (Angular Gyrus), sLOC (Lateral Occipital Cortex, superior division), iLOC (Lateral Occipital Cortex, inferior division), ICC (Intracalcarine Cortex), MedFC (Frontal Medial Cortex), SMA (Juxtapositional Lobule Cortex -formerly Supplementary Motor Cortex-), SubCalC (Subcallosal Cortex), PaCiG (Paracingulate Gyrus), AC (Cingulate Gyrus, anterior division), PC (Cingulate Gyrus, posterior division), Precuneous (Precuneous Cortex), Cuneal (Cuneal Cortex), FOrb (Frontal Orbital Cortex), aPaHC (Parahippocampal Gyrus, anterior division), pPaHC (Parahippocampal Gyrus, posterior division), LG (Lingual Gyrus), aTFusC (Temporal Fusiform Cortex, anterior division), pTFusC (Temporal Fusiform Cortex, posterior division), TOFusC (Temporal Occipital Fusiform Cortex), OFusG (Occipital Fusiform Gyrus), FO (Frontal Operculum Cortex), CO (Central Opercular Cortex), PO (Parietal Operculum), PP (Planum Polare), HG (Heschl's Gyrus), PT (Planum Temporale), SCC (Supracalcarine Cortex), OP (Occipital Pole), Cereb (Cerebellar Crus), Ver (Cerebellar Vermis).

Neuroscience in Anesthesiology and Perioperative Medicine 37- Sexually Amygdala Dysfunction Following Cardiac Arrest and Cardiopulmonary Resuscitation

Nidia Quillinan[1], Jose Vigil[1], Erika Tiemeier[1], Paco Herson[1]

University of Colorado, Anschutz Medical Campus[1]

Introduction: Modern medical advances have greatly increased the chance of surviving an ischemic event such as cardiac arrest or stroke. With more people surviving and recovering from these ischemic insults, it is becoming apparent that survivors experience long-term effects as it relates to brain function. We have previously identified cognitive dysfunction in a mouse model of global cerebral ischemia (GCI) which has been attributed to hippocampal neurodegeneration and impaired hippocampal plasticity. However, no study has attempted to identify amygdala dysfunction after GCI, despite clinical evidence of emotional dysfunctions, such as anxiety and PTSD. Given these clinical findings, it is important to identify the effect that GCI has on the amygdala, the emotional center of the brain. I hypothesize GCI results in deficits in amygdala dependent learning tasks and circuit specific deficits of long-term potentiation (LTP).

Methods: Experimental GCI was induced in adult (8-12 week) C57BL6 mice via cardiac arrest and subsequent cardiopulmonary resuscitation (CA/CPR). CA/CPR was induced for 8 minutes and subsequent resuscitation by epinephrine injection, ventilation and mild chest compressions. Neuronal injury was evaluated at 3 days after CA/CPR by Fluorojade staining in coronal brain sections. Seven days post GCI, the amygdala-dependent delay fear conditioning paradigm was used to assess amygdala-dependent learning and memory. Synaptic plasticity was evaluated by performing LTP recordings in the basolateral amygdala.

Results: We observed no acute cell death within the amygdala. Behavioral testing revealed that only male mice displayed a background contextual fear deficit (Male:74.05% sham freezing vs. 47.2% CACPR freezing). Also, only male mice displayed a diminished cued fear response (52.4% sham freezing vs. 26.6% in CACPR). Similarly, plasticity involving cortical inputs to the basolateral amygdala was impaired only in males (143.6% of baseline in controls vs. 110.9% of baseline in CACPR). Interestingly intra-amygdala recordings revealed no disruption of LTP in this circuit.

Conclusions: These results support the role of the amygdala in cognitive-affective impairments after CA despite a lack of neuronal cell death in this brain region. We have revealed a sexually dimorphic deficit in amygdala-dependent fear learning and memory that provide new insights into the role that biological sex plays in mediating brain dysfunction following CA. Our results also suggest a sex- and circuit-specific deficit in synaptic plasticity within the amygdala that correlates with behavioral outcomes in males. We will continue to unravel the mechanisms by which this sexually dimorphic impairment occurs.

References: Orfila, J. E., et al. (2018). "Cardiac Arrest Induces Ischemic Long-Term Potentiation of Hippocampal CA1 Neurons That Occludes Physiological Long-Term Potentiation." Neural Plast **2018**: 9275239.

Orfila, J. E., et al. (2014). "Increasing small conductance Ca2+-activated potassium channel activity reverses ischemia-induced impairment of long-term potentiation." Eur J Neurosci **40**(8): 3179-3188.

Neuroscience in Anesthesiology and Perioperative Medicine 38- Synaptic metabolic vulnerability is cell- and phenotype-specific in hippocampal neurons from rats

Daniel Cook[1], Timothy Ryan[1]

Weill Cornell Medicine[1]

Introduction: The human central nervous system (CNS) has a high metabolic demand, consuming 20% of the body's oxygen despite constituting only 2% of body mass.[1] Interruptions in the supply of fuel to the brain impair CNS function within minutes and may lead to permanent dysfunction. The release of chemical neurotransmitters from nerve terminals during synaptic vesicle recycling is a substantial metabolic load to neurons, and impaired synaptic metabolism leads to arrest of vesicle endocytosis.[2] However, the determinants of metabolic vulnerability of neurons and individual nerve terminals are not well understood. Here, we used a genetically-encoded, fluorescent biosensor of synaptic vesicle recycling, synaptophysin-pHluorin (sy-pH), expressed in excitatory and inhibitory neurons in dissociated hippocampal cultures to compare the ability of individual nerve terminals to sustain synaptic vesicle recycling during fuel deprivation. We demonstrate that the metabolic vulnerability of neurons is both cell- and phenotype-specific and not fully explained by the metabolic load of synaptic vesicle recycling.

Methods: Protocols were approved by Weill Cornell Medicine IACUC. Dissociated hippocampal neurons from postnatal day 0-2 Sprague-Dawley rats of both sexes were plated on coverslips. Transfection occurred on day in vitro (DIV) 6-8 with sy-pH under either CaM kinase II (CaMKII) or DLX promoter to drive expression in glutamatergic or GABAergic neurons, respectively. Experiments were performed on DIV 14-21. Images were acquired with a laser-illuminated epifluorescence microscope and Andor iXon+ EMCCD. Coverslips were loaded onto a custom chamber, maintained at 37°C, and perfused with Tyrode's solution buffered with HEPES to pH 7.4 and containing glucose 1 mM or no glucose. Action potentials (APs) were elicited with 1 ms field depolarizations to generate 100 APs in 2 s every 22 s. At the end of experiments, Tyrode's solution with equimolar replacement of NaCl with NH_4Cl was perfused to alkalinize intracellular sy-pH to normalize ΔF to the total releasable pool of vesicles. ImageJ was used to calculate fluorescence with local background subtraction. To facilitate robust single nerve terminal analysis, terminals were excluded if ΔF was less than 3 standard deviations (SDs) of the pre-stimulus baseline ($\sigma_{pre\text{-}stim}$) or if ΔF with NH_4Cl was less than 5 $\sigma_{pre\text{-}stim}$. The criteria to define arrest of synaptic vesicle recycling are 1) 2 sequential AP responses in which recovery of fluorescence is less than half the recovery of the initial stimulus or ΔF less than σpre-stim and 2) over half of subsequent stimuli must meet either of these criteria. Statistical analysis was performed with Prism v8 with significance defined as $p < 0.05$.

Results: Nerve terminals from excitatory neurons were divided into quartiles (Q1-4) of release probability quantified by the initial $\Delta F/\Delta F_{NH4Cl}$ in glucose. Increasing synaptic vesicle exocytosis was associated with earlier failure of synaptic vesicle recycling ($p < 0.0001$, log-rank test, n = 1012 terminals from 7 neurons; Figure 1). However, considering only terminals in the first quartile (Q1) of synaptic vesicle exocytosis, substantial heterogeneity exists between neurons in the ability to sustain vesicle recycling during fuel deprivation ($p < 0.0001$, log-rank test, n = 89 – 216 terminals from 7 neurons; Figure 2). Comparison of inhibitory to excitatory neurons demonstrated a modest improvement in synaptic vesicle recycling during glucose deprivation ($p < 0.0001$, log-rank test, n = 1012 and 878 terminals from 7 and 6 neurons of excitatory and inhibitory neurons, respectively; Figure 3). Because inhibitory neurons exhibit increased exocytosis ($p < 0.0001$, Mann Whitney test; Figure 4), grouping terminals by quartiles of exocytosis of excitatory neurons demonstrates the relative improvement of inhibitory neurons in sustaining synaptic vesicle recycling ($p < 0.0001$ for each comparison, t-test with Bonferroni correction).

Conclusions: We demonstrate that release probability is a determinant of metabolic vulnerability. However, terminals with similar release probability differ between neurons in their ability to sustain synaptic vesicle recycling during fuel deprivation. Moreover, inhibitory neurons are more metabolically resilient to fuel deprivation compared to excitatory neurons. These results support that the metabolic vulnerability of neurons is both cell- and phenotype-specific and not fully explained by the metabolic load of synaptic vesicle recycling.

References: 1. Am J Physiol 1981; 241(3): 203-12

2. Neuron 2020; 105(4): 678-87

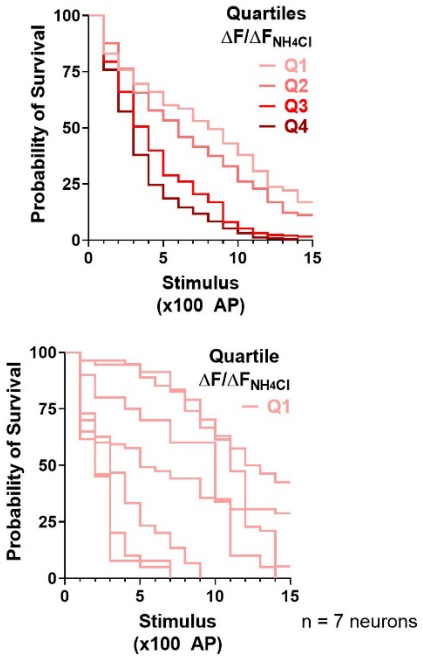

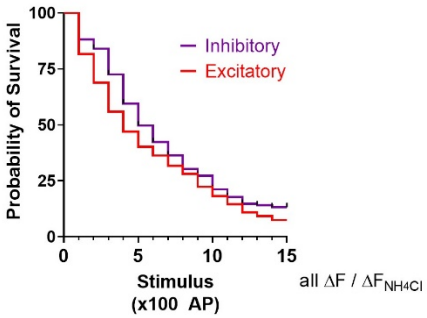

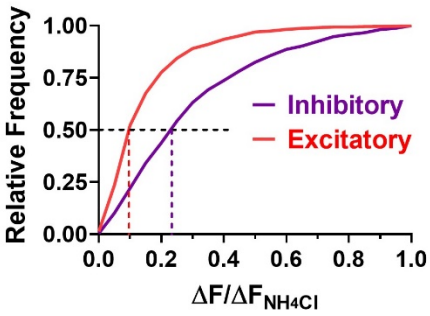

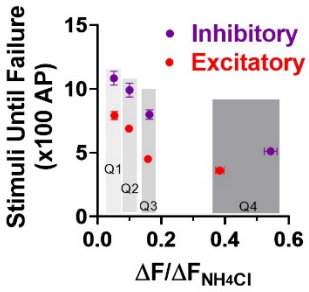

Neuroscience in Anesthesiology and Perioperative Medicine 39- The effect of the patient's age on the spectral electroencephalographic characteristics during an ultra-slow propofol induction

David Obert[1], Matthias Kreuzer[1], Gerhard Schneider[1], Fernando Zurita[2], Luis Cardenas[3], Pablo Sepúlveda[4]

Technical University of Munich, School of Medicine[1] Hospital San José Osorno[2] Hospital Base Osorno[3] Hospital Base San José de Osorno /Universidad Astral Chile[4]

Introduction: Due to the demographic change the health care system will be challenged by a growing number of elderly patients requiring general anesthesia within the next years. Since age is an independent risk factor for adverse postoperative neurocognitive outcome it is of utmost importance to improve anesthetic management and to adjust drug dosing to the individual patient characteristics.
As recommended by the European Society of Anesthesiology and Intensive Care processed electroencephalographic (EEG) parameters should be used to titrate anesthetic (1). However, all neuromonitoring indices are based on the analysis of the spectral composition of the EEG which is influenced by the patient's age (2). For this reason, the index values might not be accurate for the elderly potentially resulting in drug overdosing which might induce an EEG pattern called burst suppression. Burst suppression is characterized by suppression phases interspersed with cortical activity and seems to be associated with adverse patient outcome. Especially older patients are prone to demonstrate a burst suppression pattern (3). In addition, pharmacokinetics and pharmacodynamics (PKPD) of drugs also vary with patient's age making it particularly challenging to titrate anesthetics in this patient collective and to design accurate PKPD models. One well-established target controlled infusion (TCI) model was developed by Schnider based on 24 volunteers with only seven of them >70 years (4). To evaluate the effect of the patient's age on the spectral composition of the EEG during an ultra-slow propofol induction we performed a post-hoc analysis.

Methods: In our analysis we included 26 young (<65 years of age) and 25 old (≥65 years of age). All patients gave written informed consent to participate in the study. The young patients received propofol with a flow rate of 10 mg/kg/h, the elderly with a flow rate of 8 mg/kg/h. Every 30 seconds patients were assessed for loss of responsiveness (LOR) to tactile stimulus. Upon LOR we switched from a flow rate based to a TCI mode (Schnider) and kept the calculated effect site concentration (Ce) at LOR stable. After LOR we started a remifentanil infusion using the Minto model with a target concentration of 4.5 ng/ml. During induction we recorded a frontal EEG using the SEDLine® monitor. In order to evaluate the EEG dynamics throughout the observation period, we calculated the power spectral density (PSD) using the *pwelch* function with a frequency resolution of 0.7 Hz for 5 s EEG segments with a 4 s overlap. We also calculated the nPSD, i.e., the PSD divided by its total power in the 0.7 to 30 Hz range. We displayed the averaged courses of the nPSD over time as density spectral arrays (DSA). We divided the induction period into two sections: start propofol to LOR and LOR +300seconds. We normalized the former one to adjust for the different time periods till LORR. For the evaluation of differences in the DSA, we used the Mann–Whitney U test. We also calculated the total mass of propofol at LOR. Results are displayed as median [1st quartile; 3rd quartile].

Results: The median age of the patients in the young group was 50 [36; 57] and 75 [72; 79] years in the old group. The elderly received significantly less propofol (1.06 [0.89; 1.26] vs 1.35 [1.16; 1.70] mg/kg body weight; p<0.001), but the time from start propofol till LOR did not differ significantly (480 [390; 660] vs 420 [473; 597] seconds; p=0.905). No patient showed a burst suppression pattern. During the induction and also 5 minutes after LOR the younger patients demonstrated a significantly higher power across all frequency bands (delta, theta, alpha, and beta). Correlating the age with the absolute power using a linear regression, we found a significant decrease across all frequency bands. However, the composition of the spectrum did not change significantly with the patient's

age. This was shown by calculating the normalized power distribution. There was no significant in- or decrease in the frequency bands after normalization.

Conclusions: Our analyses will help to understand age-dependent physiologic changes in pharmacodynamics in correlation with (processed) EEG parameters. Detailed knowledge of these changes will allow an individual titration of anesthetics resulting in an improved patient care by reducing drug overdosing and consequently the incidence of adverse postoperative outcomes.

References:

1. C. Aldecoa et al. *Eur J Anaesthesiol* **(2017),** 34:192-214.

2. M. Kreuzer et al. *Anesthesiology* **(2020),** 132:1003-1016.

3. P. L. Purdon et al. *Br J Anaesth* **(2015),** 115 Suppl 1:i46-i57.

4. T. W. Schnider et al. *Anesthesiology* **(1999),** 90:1502-1516.

Neuroscience in Anesthesiology and Perioperative Medicine 40-

Understanding the synaptotoxic role of soluble amyloid beta in a mouse model of acute post-stroke cognitive impairment

Jacob Basak[1], Macy Falk[1], Danae Mitchell[1], Kelley Coakley[1], Nidia Quillinan[2], James Orfila[2], Paco Herson[2]

The University of Colorado School of Med[1] University of Colorado, Anschutz Medical Campus[2]

Introduction: Chronic cognitive impairment and dementia are prevalent among stroke survivors[1-3]. Understanding the cellular mechanisms mediating ischemia-induced neuronal dysfunction is critical for developing diagnostic tools and treatment strategies that can be implemented in the intensive care unit and hospital setting to improve the long-term cognition of stroke survivors. The molecular mechanisms underlying post-stroke cognitive impairment are poorly defined, but may involve perturbations in pathways involved in both neurodegeneration and oxidative stress. Specifically, synaptic dysfunction after stroke may be directly mediated by alterations in the levels of amyloid beta (Aβ), the peptide that accumulates in the brains of Alzheimer's disease (AD) patients. In this study, we use the transient middle cerebral artery occlusion (MCAo) model in mice to evaluate how a large vessel stroke affects soluble Aβ levels in the brain and to determine if altering the production of Aβ during the recovery period improves hippocampal plasticity. We also looked at whether TRPM2, an ion channel regulated by oxidative stress that we have previously shown to be critical in regulating the brains response to ischemia[4-5], plays a role in regulating Aβ levels after an MCAo stroke.

Methods: All animal use procedures were approved by the University of Colorado Institutional Animal Care and Use Committee. An ELISA assay was used to quantify soluble Aβ40 and 42 from the hippocampus and cortex of brains collected from wild-type adult mice or TRPM2$^{-/-}$ mice (8-12 weeks) 7 days after recovery from a transient MCAo (60 min) stroke. To measure the level and activity of the Aβ-generating enzyme BACE1 (β-site APP cleaving enzyme 1), we stained tissue from the MCAo mice with a BACE1 antibody and measured the amount of BACE1 activity using a fluorogenic-based BACE1 activity assay, respectively. Finally, to determine the effects of decreasing Aβ levels via BACE1 inhibition on hippocampal synaptic function, we treated both sham and MCAo mice on day 7 with a known BACE1 inhibitor (verubecestat, 30 mg/kg). Extracellular field recordings of CA1 neurons were then performed in acute hippocampal slices and long-term potentiation (LTP) was assessed to evaluate for synaptic plasticity[6].

Results: Soluble Aβ40 and Aβ42 levels were increased in the ipsilateral hippocampus in MCAo mice 7 days after the injury when compared to sham-treated mice (71.1% increase for Aβ40, $p = 0.04$; 91.7% increase for Aβ42, $p=0.03$). Non-statistically significant increases in both soluble Aβ40 and Aβ42 were observed in the ipsilateral MCAo cortex compared to the sham cortex. We also analyzed the level and activity of BACE1, an enzyme that generates Aβ in the brain. We found that BACE activity is increased by approximately 50% in the ipsilateral hippocampus of the MCAo mice, with no changes in BACE expression levels. LTP recordings obtained in brain slices from mice 7 days after the MCAo injury exhibited impairment in LTP (166±10.4% in sham versus 124±10.4% versus in MCAo hippocampus). Mice treated with the BACE1 inhibitor verubecestat demonstrated a significant increase in LTP in both sham (225±22.6%) and MCAO mice (219±18.5%). Finally, we measured Aβ levels and BACE activity after a MCAo stroke in TRPM2 knock-out mice and found no statistically significant increases in either of these parameters.

Conclusions: Our data highlights that a transient MCAo stroke leads to increases in soluble Aβ40 and Aβ42 in the hippocampus of the injured brain via a mechanism that requires the presence of TRPM2. We also directly show that activation of BACE1 activity occurs after a MCAo stroke, and inhibition of BACE1 activity rescues stroke-induced deficits in hippocampal synaptic plasticity. Taken together, these data provide a potential molecular pathway linking ischemia to altered neurodegeneration and oxidative stress after a large vessel stroke and suggest that increased Aβ levels may lead to synaptic and cognitive deficits seen in patients with post-stroke cogntive dysfunction. We anticipate that these findings will stimulate future studies investigating the role of Aβ in other areas of acute brain ischemia that are relevant to both the ICU and operative environment.

References: 1. S. T. Pendlebury, P. M. Rothwell. *Lancet Neurol* **8**, 1006-1018 (2009).

2. D. A. Levine *et al*. *JAMA* **314**, 41-51 (2015).

3. P. Schaapsmeerders *et al. Stroke* **44**, 1621-1628 (2013).

4. I. Alim, L. Teves, R. Li, Y. Mori, M. Tymianski, et al. *J Neurosci* **33**, 17264-17277 (2013).

5. T. Shimizu *et al. Exp Neurol* **283**, 151-156 (2016).

6. J. E. Orfila *et al. J Cereb Blood Flow Metab* **39**, 1005-1014 (2019).

Obesity

Obesity 1- Comparing Different Inhalational Anesthetics on Bariatric Patient Postoperative Outcomes and Environmental Impact

Briana Kossbiel[1], Alberto Uribe[2], Mahmoud Abdel-Rasoul[1], Sabrena Noria[3], Vidya Raman[4]

The Ohio State University[1] The Ohio State University Wexner Medical Center[2] The Ohio State University, Wexner Medical Center[3] OSU[4]

Introduction: Climate action and sustainability are increasingly recognized topics in medicine as 5-8% of the carbon footprint is from healthcare (1-3). Operating rooms contribute approximately 50% of a single hospital's footprint with the greatest share coming from the use of inhaled anesthetics (4). These highly fluorinated gases include sevoflurane, isoflurane, and desflurane which are not only greenhouse gases, but also ozone-depleting (3-5). Desflurane has been noted to have approximately 50 times the global warming impact compared to other agents. For instance, one hour of desflurane use is equated to the same environmental impact of driving a car for 155 miles (6-8).

Multiple studies have looked at the use of these volatile agents individually and in combination, but there is limited data on their environmental impact when used in patients with obesity (defined as a body mass index (BMI) > 30). There are many considerations for the delivery of anesthetics to this population. For example, a higher BMI has been shown to increase lipid soluble anesthetic uptake, leading to the need to deliver a greater amount of anesthetic to sustain a constant alveolar concentration (7).

The purpose of this study was to both to calculate the environmental impact of the total anesthetic gas used for each individual patient to approximate environmental cost and define differences in the length of post anesthesia care unit (PACU) and hospital stay in patients undergoing bariatric surgery when they received different anesthetic gases intraoperatively.

Methods: A retrospective chart review of 1546 adult subjects who underwent bariatric surgery between January 1, 2018 and April 30, 2022. Exclusion criteria included pregnancy, minors, and cases not done under general anesthesia. Data collected included weight, BMI, ASA classification, total surgical and anesthesia length, anesthetic gas used, metric tons carbon dioxide equivalent used per hour, length of PACU stay, and length of hospital stay.

The collected data was summarized with median for continuous variables and frequency for categorical variables. Kruscal-Wallis Tests were used to test differences in continuous outcomes between inhalation agents while chi-squared or Fisher's exact tests were used for categorical variables where relevant. Hypothesis testing was conducted at a 5% Type 1 error rate. The environmental impact and cost were calculated used the app, Gassing Greener. Statistical Analysis was conducted using SAS version 9.4 (SAS Institute, Cary, NC).

Results: When stratified by the agent used, there was no statistically significant difference between the variables of age and ASA. Controversially, there was a statistically significant difference among sex, weight, BMI, ASA status, length of anesthesia and length of surgery **[Table 1].** Although desflurane was used less in bariatric surgeries, sevoflurane was used more frequently in subjects with increased ASA classification.

The median metric tons carbon dioxide equivalent (MTCO2E) produced per hour for sevoflurane and isoflurane were similar among all groups. On the other hand, when desflurane was used as the sole anesthetic or in combination, the median MTCO2E produced per hour was significantly higher than the other groups (desflurane 11.32 [8.07, 15.44] vs. sevoflurane 0.35 [0.26, 0.46] or Isoflurane 0.41 [0.29, 0.64], p value <0.0001) **[Table 2 and Figure 1].**

Lastly, the use of sevoflurane compared to desflurane in subjects with obesity undergoing bariatric surgery was not associated with increased length of stay in the PACU or hospital. However, it was associated with a significantly lower carbon footprint and economic cost despite being used more frequently for sicker patients while having properties that make it more soluble.

Conclusions: Our results suggest that the use of desflurane compared to other agents resulted in a higher carbon footprint. Studies in different patient populations should be done to replicate the findings with our study in the bariatric patient population. Anesthesia providers are best positioned to reduce the negative impact our daily practice has on the environment by proactively examining these issues and changing practice accordingly. This is of extreme importance with our growing obese patient population and our changing climate.

References:

1. Addressing climate change and its effects on human health: A call to action for medical schools. 2021;96(3):324-328.

2. Climate change: challenges and opportunities to scale up surgical, obstetric, and anesthesia care globally. 2020;4(11):e538-543.

3. Environmental footprint of anesthesia: More than inhaled anesthetics! 2021;135:937-939.

4. Greening the operating room. 2018;216(4):683-688.

5. The carbon footprint of operating theatres: a systematic review. 2022;272(6):986-995.

6. Environmental implications of anesthetic gases. 2012;59(4):154-588.

7. Obesity modestly affects inhaled anesthetic kinetics in humans. 2008;107(6):1864-1870.

8. University of Nebraska Medical Center. Newroom - Strategic anesthetic selection reduces enviromental impact, costs. 2021.

Table 1. Demographics and surgery variables

Variables	Sevoflurane (n=964)	Desflurane (n=458)	Isoflurane (n=32)	Sev + Des (n=40)	Sev + Iso (n=5)	Des + Iso (n=2)	Total (n=1546)	P-Value
Age, years, Median [IQR]	43 [36,52]	44 [35,53]	44.5 [34, 52.5]	47 [36.5, 53.5]	49 [36, 54]	63 [51, 75]	44 [36,52]	0.4538
Sex, Female, N (%)	803 (83.30%)	350 (76.42%)	24 (75%)	43 (75%)	5 (51.58%)	2 (100%)	1246 (80.6%)	0.0128
Weight, kg, Median [IQR]	282 [233.35, 325.05]	296.57 [263.38, 343.6]	274.2 [251.2, 321.5]	313.8 [261.98, 357.75]	295 [273.5, 309.8]	299.35 [293.2, 305.5]	289.4 [254.8, 331.5]	<0.0001
BMI, units, Median [IQR]	46.29 [41.91, 51.65]	47.94 [42.88, 53.42]	45.76 [42.06, 50.14]	49.49 [44.21, 56.37]	43.95 [40.89, 49.87]	50.37 [33.48, 67.26]	46.69 [41.2, 52.56]	0.0001
ASA (I/II/II/IV)	1/228/718/16	0/84/371/3	0/7/25/0	0/7/49/4	0/3/2/0	0/0/2/0	1/331/1183/26	0.2177
Length of anesthesia, min, Median [IQR]	142 [115, 169]	137.5 [110, 167]	127.0 [98, 158]	157 [128, 189.5]	148 [138, 171]	280 [231, 329]	140.5 [115, 168]	0.0016
Length of surgery, min, Median [IQR]	87 [63, 113.5]	83 [62, 113]	71.5 [55, 113.5]	103 [72.5, 138]	86 [77, 124]	223 [175, 271]	86 [63, 117]	0.0082

Legend: IQR= Interquartile range, N= Number of subjects, BMI= body mass index, ASA= The American Society of Anesthesiologists physical status, Sev= sevoflurane, Des= desflurane, Iso= isoflurane

Table 2. Primary and secondary outcomes

Variables	Sevoflurane (n=964)	Desflurane (n=458)	Isoflurane (n=32)	Sev + Des (n=40)	Sev + Iso (n=5)	Des + Iso (n=2)	Total (n=1546)	P-Value
Length of PACU stay, min, Median [IQR]	105 [82, 142]	98 [79, 128]	102.5 [83, 115]	103 [86, 145]	91 [83, 114]	101 [100, 102]	102 [81, 139]	0.1765
Hospital stay, days, Median [IQR]	3 [2, 3]	3 [3, 3]	3 [2.5, 3]	3 [3, 3]	3 [3, 3]	5.5 [4, 7]	3 [2, 3]	0.2559
Metric tons carbon dioxide equivalent (MTCO2E) per hour, Median [IQR]	0.35 [0.29, 0.48]	11.92 [8.07, 15.44]	0.41 [0.29, 0.64]	4.39 [2.39, 9.1]	0.35 [0.28, 0.39]	15.28 [7.62, 22.95]	0.45 [0.3, 7.92]	<0.0001

Legend: IQR= Interquartile range, N= Number of subjects, Sev= sevoflurane, Des= desflurane, Iso= isoflurane

Figure 1. The MTCO2E (carbon footprint) per hour for each group

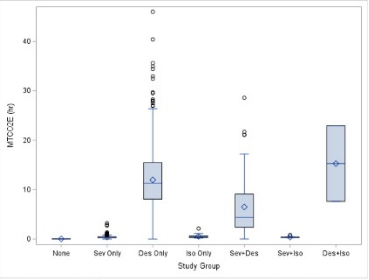

Legend: MTCO2E (hr)= Metric tons carbon dioxide equivalent per hour, Sev= sevoflurane, Des= desflurane, Iso= isoflurane

Disclaimer: The project described was supported by Award Number UL1TR002733 from the National Center for Advancing Translational Sciences. The content is solely the responsibility of the authors and does not necessarily represent the official views of the National Center for Advancing Translational Sciences or the National Institutes of Health.

Obstetric Anesthesiology

Obstetric Anesthesiology 1- Behavioral and neuropsychological outcomes in children after exposure to labor epidural analgesia

Oliver Isik[1], Shaqif Junaid[1], Ling Guo[1], Deven Lackraj[1], Ruth Landau[2], Caleb Miles[2], Craig Pennell[2], Britta von Ungern Sternberg[2], Andrew Whitehouse[2], Guohua Li[3], Caleb Ing[2]

Columbia University Vagelos College of Physicians & Surgeons[1] Columbia University Irving Medical Cente[2] Columbia University[3]

Introduction: The potential effect of labor epidural analgesia (LEA) on child neurodevelopment is still being investigated. An association between mothers who receive LEA and later development of autism spectrum disorder in their children was reported,[1] while several subsequent studies reported either no association or slightly elevated risks that could be explained by unmeasured confounding.[2-4] This study explores the association between maternal LEA and child behavioral and neuropsychological assessments, accounting for a wide range of sociodemographic and perinatal variables.

Methods: This study evaluates participants from the Raine Study, a multigenerational birth cohort of children born between 1989 and 1992 in Perth, Australia. Children born via vaginal delivery from a singleton pregnancy were included for analysis. The primary outcome was the Child Behavior Checklist (CBCL) evaluated at age 10, with higher scores indicating more behavioral problems. To adjust for confounding, 73 sociodemographic and clinical covariates were identified. Multiple imputation was used to impute any missing covariate data. To account for differences in children exposed to LEA, the predicted probability of LEA exposure conditional on all covariates was calculated and applied to Inverse Probability of Treatment Weights (IPTW). We aimed for standardized differences in covariate means below 0.1 following IPTW. To account for missing outcome data, censoring conditional on all covariates and exposure status was calculated and applied to Inverse Probability of Censoring Weights (IPCW). As a primary analysis, the association between LEA and CBCL scores was evaluated using linear regression with IPTW and IPCW. Three secondary analyses were performed. The risk of clinical deficit based on LEA exposure was evaluated using modified Poisson regression with IPTW and IPCW, where clinical deficits were defined as CBCL scores above 60.[5] In mothers who received LEA, a multivariable linear regression evaluated the association between duration of LEA exposure and CBCL scores. Where significant score differences were observed, mediation analysis evaluated the role of fever during labor requiring antibiotics and oxytocin for augmentation of labor.[6] The same analyses were applied to secondary outcomes: Clinical Evaluation of Language Fundamentals (CELF), Peabody Picture Vocabulary Test (PPVT), McCarron Assessment of Neuromuscular Development (MAND), Raven's Colored Progressive Matrices (CPM), Symbol Digit Modality Test (SDMT), and Autism Spectrum Quotient (AQ). AQ was assessed between child ages 19 and 20; other assessments were evaluated at age 10. Higher AQ scores indicate more autistic tendencies, whereas for other secondary outcomes, higher scores indicate better performance.

Results: Of 2180 children included for analysis, 850 (39.0%) were exposed to LEA (Figure 1). Covariates for exposed and unexposed children were evaluated, with a subset of covariates displayed in Table 1. Appropriate balance in all covariates following IPTW is displayed in Figure 2. For the primary outcome, LEA-exposed children had higher (worse) scores on the CBCL Total (+1.66 points; 95% confidence interval [CI] 0.49, 2.83; $p = 0.006$), Internalizing (+1.33; 95% CI 0.20, 2.45; $p = 0.021$), and Externalizing (+1.26; 95% CI 0.18, 2.34; $p = 0.022$) assessments. Exposure was not associated with an increased risk for clinical deficit (Table 2), nor was increased LEA duration associated with CBCL performance (Table 3). Fever and oxytocin for augmentation of labor did not mediate observed increases in CBCL scores. Regarding the secondary outcomes, while exposed children had worse scores in some of the outcomes (Table 2), increased LEA exposure duration was not associated with worse scores (Table 3). Fever and oxytocin for labor augmentation also did not mediate the observed differences.

Conclusions: Children exposed to LEA performed worse on the CBCL assessment at age 10 but had no increased risk for clinical deficit, suggesting a lack of clinical significance in the observed differences. Differences were seen in some secondary outcomes, but are small and should be interpreted with caution. It should be noted that higher concentrations of local anesthetic were used in the era that these epidurals were performed. That longer LEA duration and thus exposure to higher doses of local anesthetic was not associated with worse scores may argue against toxicity of local anesthetic medications.

References: 1. JAMA Pediatr. 2020; 174 (12): 1168-1175.

2. JAMA Pediatr. 2021; 175 (7): 698-705.

3. JAMA. 2021; 326 (12): 1170-1177.

4. JAMA. 2021; 326 (12): 1178-1185.

5. Anesth Analg. 2021; 133 (3): 595-605.

6. Neonatology. 2020; 117 (3): 259-270.

Zoom out udy flow with inclusion and exclusion criteria.

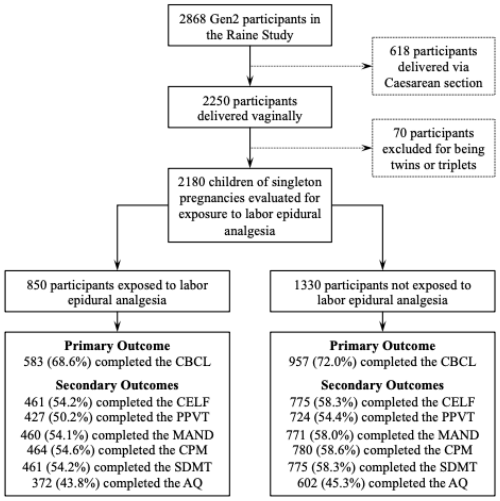

Figure 2. Standardized mean differences (SMD) in covariates for each imputed dataset before and after inverse probability of treatment weighting.

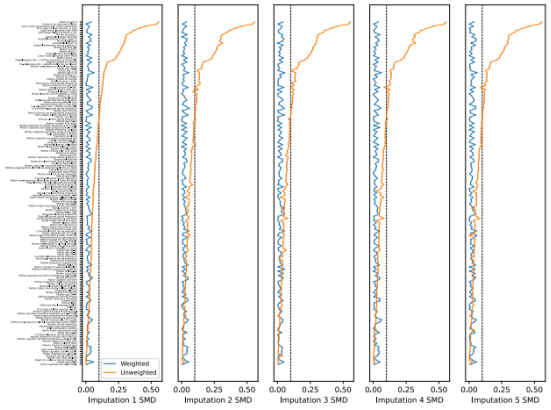

Table 1. Selected sociodemographic and clinical covariates in exposed and unexposed study participants.

	No LEA (%) $n = 1330$	LEA (%) $n = 850$
Parental Sociodemographic Characteristics		
Mother's age ≥ 35 years	166 (12.5)	85 (10.0)
Father's age ≥ 35 years	312 (23.5)	141 (16.6)
Mother's race White	1153 (86.7)	772 (90.8)
Mother native to Australia	775 (58.3)	518 (60.9)
Family income ≥ $24,000	673 (50.6)	456 (53.6)
Maternal Health Characteristics		
Treated for asthma	180 (13.5)	156 (18.4)
Treated for epilepsy	22 (1.7)	26 (3.1)
Treated for anemia	339 (25.5)	280 (32.9)
Maternal Antenatal Characteristics		
Mother primiparous	506 (38.0)	550 (64.7)
Attended antenatal classes	518 (38.9)	491 (57.8)
Hospital admission during pregnancy	243 (18.3)	258 (30.4)
Pre-eclampsia during pregnancy	240 (18.0)	260 (30.6)
Used prescription medications during pregnancy	215 (16.2)	184 (21.6)
Used paracetamol (acetaminophen) during pregnancy	150 (11.3)	113 (13.3)
Maternal Perinatal Characteristics		
Received prostaglandins during labor	31 (2.3)	66 (7.8)
Labor onset via induction of labor	355 (26.7)	418 (49.2)
Received oxytocin for induction of labor	198 (14.9)	322 (37.9)
Duration of first stage of labor ≥ 12 hours	43 (3.2)	125 (14.7)
Child Neonatal Characteristics		
Child Sex Male	666 (50.1)	436 (51.3)
Neonatal birthweight ≥ 4000 grams	107 (8.0)	92 (10.8)
Post-Exposure Mediators		
Received antibiotics for fever ≥ 37.4 °C during labor	11 (0.8)	58 (6.8)
Received oxytocin for augmentation of labor	56 (4.2)	212 (24.9)

Table 2. Score differences and relative risks of crossing a threshold for clinical deficit for primary and secondary outcomes. Each score and relative risk is adjusted by inverse probability of treatment weighting and inverse probability of censoring weighting.

Domain	Outcome	Adjusted Mean Score Difference Est. (95% CI)	*p*	Adjusted Relative Risk of Clinical Deficit aRR (95% CI)	*p*
Primary Outcome					
Behavior	CBCL Total	1.66 (0.49, 2.83)	0.006	1.12 (0.77, 1.62)	0.547
	CBCL Internalizing	1.33 (0.20, 2.45)	0.021	1.25 (0.88, 1.77)	0.209
	CBCL Externalizing	1.26 (0.18, 2.34)	0.022	1.07 (0.7, 1.63)	0.762
Secondary Outcomes					
Language	CELF Total	-1.05 (-2.81, 0.71)	0.242	1.04 (0.71, 1.52)	0.848
	CELF Receptive	-1.19 (-2.98, 0.60)	0.191	1.11 (0.75, 1.65)	0.588
	CELF Expressive	-0.19 (-1.97, 1.60)	0.837	1.04 (0.72, 1.5)	0.825
	PPVT	-0.82 (-2.21, 0.57)	0.245	1.14 (0.79, 1.65)	0.489
Motor	MAND	-1.72 (-3.34, -0.09)	0.038	1.44 (1.01, 2.06)	0.046
Cognition	CPM Total	-0.33 (-0.75, 0.08)	0.117	1.13 (0.79, 1.63)	0.498
	SDMT Written	-1.32 (-2.21, -0.44)	0.003	1.45 (1.02, 2.06)	0.037
	SDMT Oral	-1.55 (-2.72, -0.37)	0.010	1.54 (1.06, 2.24)	0.025
Autism	AQ	0.61 (-0.09, 1.30)	0.087	0.88 (0.38, 2.01)	0.759

Table 3. Score difference per additional hour of labor epidural analgesia exposure in children with recorded durations, adjusted by multivariable linear regression including all 73 covariates.

Domain	Outcome	Participants (%) $n = 828$	Adjusted score difference per additional hour of LEA Est. (95% CI)	*p*
Primary Outcome				
Behavior	CBCL Total	573 (69.2)	0.08 (-0.25, 0.40)	0.632
	CBCL Internalizing	573 (69.2)	0.03 (-0.29, 0.36)	0.834
	CBCL Externalizing	573 (69.2)	0.09 (-0.21, 0.39)	0.562
Secondary Outcomes				
Language	CELF Total	454 (54.8)	0.68 (0.15, 1.21)	0.012
	CELF Receptive	456 (55.1)	0.78 (0.23, 1.34)	0.005
	CELF Expressive	454 (54.8)	0.48 (-0.05, 1.02)	0.077
	PPVT	420 (50.7)	0.16 (-0.25, 0.57)	0.456
Motor	MAND	453 (54.7)	-0.08 (-0.57, 0.41)	0.742
Cognition	CPM	457 (55.2)	0.05 (-0.08, 0.17)	0.493
	SDMT Written	455 (55.0)	0.07 (-0.19, 0.33)	0.600
	SDMT Oral	454 (54.8)	0.06 (-0.28, 0.40)	0.721
Autism	AQ	368 (44.4)	0.09 (-0.16, 0.34)	0.497

Obstetric Anesthesiology -2 Changes in coagulation Functions of Pregnant Women with Thalassemia in South China: A Retrospective Cohort Study

Chaoxuan Dong[1], Li Zhang[2], Xi Tan[3], Wenyi Sun[3], Hao Zhou[3]

The First Affiliated Hospital of Jinan U[1] The International School of Jinan University[2] The First Affiliated Hospital of Jinan University[3]

Introduction: Thalassemia is a hereditary hemolytic anemia with a high incidence in South China. (1) Previous studies show that the patients with thalassemia is hypercoagulable.(2) During pregnancy, physiological hypercoagulability is considered as an adaptive mechanism to protect pregnant women from childbirth hemorrhage.(3) But changes in coagulation functions beyond the common range would leave some severe risks in epidural analgesia for vaginal delivery and Cesarean delivery anesthesia. This Study is to clarify the exact changes of main maternal coagulation functions in the pregnant women with thalassemia.

Methods: This is a retrospective cohort study of 405 singleton pregnant women (Gestational age >37weeks) admitted in a tertiary hospital of South China between June 2018 and October 2018. (Table 1) Main blood coagulation indexes were compared between pregnant women with thalassemia and non-thalassemia in the early (the first trimester) and late (the third trimester) pregnancy. The parameters include Hemoglobin (Hb) concentration, red blood cell distribution width (RDW), fibrinogen (FB), prothrombin time (PTs), thrombin time (TTs), activated partial thromboplastin times (APTTs), international normalized ratio (INR) and platelet count (PLT). Distribution normality was determined using Shapiro-Wilk test. Mean (standard deviation [SD]) and median (inter-quartile range [IQR]) were used for description of normally and non-normally distributed quantitative variables, respectively. Normally distributed values were compared using independent samples Student's t-test, whereas the ManneWhitney U test was used for non-normally distributed values. The X2 test was used to analyze the differences between categorical variables.

Results: The study includes 405 patients among which 53 patients were diagnosed with thalassemia and 352 patients were with non-thalassemia. (Figure 1) Hb concentration in pregnant women with thalassemia was lower than that in pregnant women without thalassemia in both early (105.1 (95.7~114.4g/L) VS 119.8 (113.6~126.1g/L), p<0.001) and late pregnancy (106 (99~114g/L) VS 117 (110~124g/L), p<0.001). RDW were significantly higher in the thalassemia group whether in early (15.4 (14.7~16.3%) VS 13.4(13.0~14.0%), p<0.001) or late pregnancy (15.3(14.7~16.2%) VS 13.9(13.4~14.6%), p<0.001). Women with thalassemia have shorter TTs in the early pregnancy than those without thalassemia (14.8(14.4~15.3) VS 15.1(14.7~15.6), P<0.01). Platelet counts of pregnant women with thalassemia are significantly higher than those without thalassemia during the early pregnancy (252(218~296) VS 226(193~255), P <0.001) and the late pregnancy (246(208~292)VS 211(181~245), P<0.001). No significant difference was found in APTTs, PTs, FIB and INR between the thalassemia group and the non-thalassemia group during the early pregnancy and the late pregnancy, respectively. Significant decreases in APTTs, PTs, and INR were observed in the thalassemia and the non-thalassemia groups (P<0.01), while significant increase in TTS and FB concentration (P<0.01). The non-thalassemia group had a significant decrease in the PLT during late pregnancy (P<0.01), which no significant difference was found in the thalassemia group between the early and the late pregnancies (P>0.05). In the thalassemia group, significant less APTTs (P<0.05) and more (P <0.05) in FB were found during the early pregnancy than those during the late pregnancy. (Figure 2 and 3)

Conclusions: Pregnant women with thalassemia have a stronger coagulation function than those without thalassemia. During the early pregnancy through the late pregnancy, coagulation function is gradually increased, but more significant in the thalassemia pregnant women. Therefore, based on the data of patients included in this study, thalassemia induced changes in coagulation functions lead to a hypercoagulable state, which does not significantly affect spinal anesthesia during the vaginal and the Cesarean-section delivery.

References:

1. BMC Public Health,14:905, 2014
2. Blood, 99(1):36-43, 2002
3. *Thrombosis Research,*114(5-6):409–414, 2004

Table 1: Descriptive statistics of baseline data and perinatal outcome in thalassemia and non-thalassemia group. Abbreviations: IVF-ET: In Vitro Fertilization and Embryo Transfer. BMI, kg/m^2(IQR): in thalassemia group n=53 and in non-thalassemia group n=349

	Thalassemia (n=53)	Non-thalassemia (n=352)	p value
Baseline data			
Pregnancy (IQR)	2 (1~2)	2 (1~3)	0.364
Parity (IQR)	1 (1~2)	1 (1~2)	0.997
Gestational week (IQR)	39 (38~39)	39 (38~40)	0.455
Delivery mode			0.268
Vaginal delivery	39 (73.6%)	232 (65.9%)	
Caesarean section	14 (26.4%)	120 (34.1%)	
Age,yr (IQR)	28 (27~32.5)	29 (27~32)	0.614
BMI kg/m^2 (IQR)	25.2 (24.1~28.2)	25.2 (23.5~27.6)	0.514
Pregnancy with anemia	10 (18.9%)	20 (5.7%)	0.002**
IVF-ET	0 (0%)	3 (0.9%)	1.000
Hepatitis B carriers	4 (7.6%)	30 (8.5%)	1.000
Scarred uterus	9 (17.0%)	62 (17.6%)	0.910
Uterine leiomyomas	2 (3.8%)	16 (4.5%)	1.000
Hyperthyroidism	1 (1.9%)	6 (1.7%)	1.000
Hypothyroidism	3 (5.7%)	16 (4.5%)	0.992
Abnormal pregnancy histories	0 (0%)	7 (2.0%)	0.601
Fetal body weight (±SD)	3.16 (±0.39)	3.20 (±0.39)	0.450
Perinatal outcome			
Fetal macrosomia	0 (0%)	12 (3.4%)	0.352
Low birth weight infant	2 (3.8%)	6 (1.7%)	0.631
Abnormal placenta	5 (9.4%)	17 (4.8%)	0.292
Battledore placenta	3 (5.7%)	9 (2.6%)	0.419
Velamentous placenta	2 (3.8%)	2 (0.6%)	0.085
Placental abruption	0 (0%)	3 (0.9%)	1.000
Placenta previa	0 (0%)	3 (0.9%)	1.000
Premature rupture of membranes	16 (30.2%)	69 (19.6%)	0.078
Fetal distress	2 (3.8%)	23 (6.5%)	0.637
Nuchal cord	16 (30.2%)	109 (31.0%)	0.909
Torsion of umbilical cord	1 (1.9%)	19 (5.4%)	0.447
Neonatal asphyxia	0 (0%)	3 (0.9%)	1.000
Polyhydramnion	3 (5.7%)	8 (2.3%)	0.336
Oligohydramnion	0 (0%)	13 (3.7%)	0.315
Amniotic fluid turbidity	2 (3.8%)	23 (6.5%)	0.637
Postpartum hemorrhage	3 (3.9%)	16 (3.4%)	1.000

Figure 1: Flowchart of study population

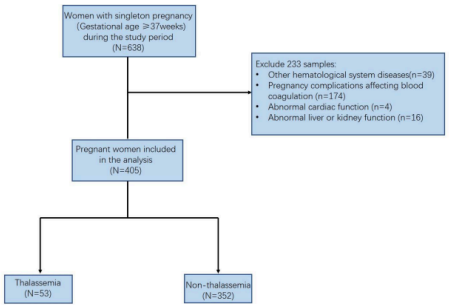

Figure 2: Changes in APTT, PT, TT, Fb, INR, Hb, RDW and PLT in the thalassemia and the non-thalassemia groups during the early pregnancy and the late pregnancy, respectively

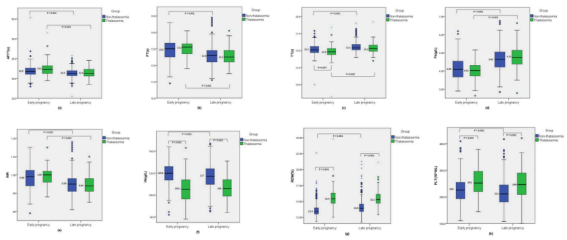

Figure 3: Changes in APTT, PT, TT, Fb, INR, Hb, RDW and PLT from the early pregnancy to the late pregnancy between the thalassemia and the non-thalassemia groups.

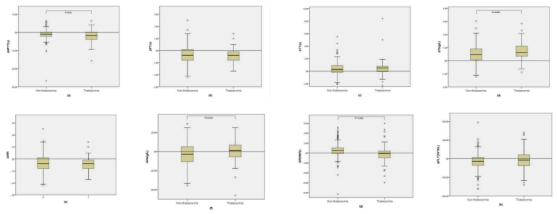

Δ: changes=the value in late pregnancy- the value in early pregnancy

Pain Mechanisms

Pain Mechanisms 1- β-Caryophyllene inhibits monoacylglycerol lipase activity and increases 2-arachidonoyl glycerol levels in vivo: a new mechanism of endocannabinoid-mediated analgesia?

Jost Klawitter[1], Wiebke Weissenborn[1], Iuliia Gvon[2], MacKenzie Walz[3], Jelena Klawitter[3], Cristina Sempio[3], Sonja Joksimovic[3], Touraj Shokati[3], Ingo Just[3], Uwe Christians[3], Slobodan Todorovic[3]

University of Colorado[1] CU Anschutz[2] UC Denver Anschutz Medical Campus[3]

Introduction: Pain is a pervasive problem that affects millions of Americans each year. Over recent years the prescription of pain medications including opioids has skyrocketed. However, there has been very little progress, innovation or new approved drugs in the field of pain[1]. Previous studies have shown that β-Caryophyllene (BCP) is an effective analgesic in some chronic and inflammatory pain models[2]. However, the mechanisms of BCP-induced analgesia are not well studied. Here, we tested the efficacy of BCP in an acute post-surgical pain model and evaluated its effect on the endocannabinoid system. In this study, we investigated the analgesic properties of BCP on surgically induced hyperalgesia using plantar incision of the hind paw in rats[3], which is a rodent model considered to be similar in context to the underlying mechanisms and the development of human post-operative pain[4].

Methods: Efficacy of BCP was tested in an acute postsurgical pain model. Adult Sprague-Dawley rats were treated with vehicle, 10, 25, 50, and 75 mg/kg BCP that was injected intra-peritoneally (i.p.). Time-dependent paw withdrawal responses (PWR) to mechanical stimuli were evaluated using von Frey filaments. BCP levels were determined in tissue (paw, spinal cord, and brain) and plasma using an HPLC-MS-based approach. An assay for the analysis of 14 endocannabinoids including 2-arachidonoylglycerol (2-AG) was applied to plasma and tissues samples using an HPLC-MS-based approach[5]. A novel mass spectrometry-based approach for the evaluation of monoacylglycerol lipase (MAGL) activity in vitro and in vivo was developed and validated. Using this approach, we evaluated the effect of BCP on MAGL activity in vitro. We also used heavy isotope labeled (deuterium) MAGL substrate to evaluate the MAGL activity ex vivo in spinal cord tissue incubations.

Results: We found that BCP elicits a dose-dependent anti-hyperalgesia in incised paws (two-way RM ANOVA, interaction: $p = 0.022$; treatment: $F(1,6) = 7.62$, $p = 0.033$). Importantly, unincised left paws showed no significant changes in the paw withdrawal rates after BCP treatment in any study groups at any time point. These data demonstrate for the first time the efficacy of BCP to selectively reduce pain in incised paws using this post-surgical pain model (figure 1). In contrast, baseline PWRs in the contralateral un-incised paws were not affected in the same animals. We also observed dose-dependent increase in the 2-AG levels of about 3-fold after administration of BCP as compared to vehicle controls (see figure 2A). Incubations of spinal cord tissue homogenates from BCP-treated rats with isotope-labeled 2-arachidonoylglycerol-d8 revealed a significantly reduced formation of the isotope-labeled MAGL product arachidonic acid-d8 (AA-d8) as compared to vehicle controls indicating MAGL enzyme inhibition. Vehicle controls showed an AA-d8 formation rate of 3.76 ± 0.96 pg·mg^{-1}·min^{-1}. The values for the treatment groups were 3.56 ± 1.01, 3.16 ± 0.57, 2.99 ± 1.12 and 2.58 ± 0.73 pg·mg^{-1}·min^{-1} ($p = 0.036$) for the 10, 25, 50, and 75 mg/kg treatment groups, respectively. In vitro MAGL enzyme activity assessment using 2-AG as the substrate revealed an IC_{50} of 14 µM for MAGL inhibition using BCP (see figure 2B). These concentrations of BCP were exceeded in plasma, as well as in spinal cord and brain tissues as determined by HPLC-MS assessments in vivo.

Figures.

Figure 1: β-Caryophyllene (BCP) in the post-surgical pain model. Paw withdrawal response (PWR) for BCP for the incised paw. Data are represented as mean ± SEM. ***significant ($p<0.001$) by ANOVA with Sidak's post hoc test.

Figure 2. Changes in 2-arachidonoylglycerol (2-AG) and MAGL activity with sesquiterpenes. A. BCP induces a dose-dependent increase in circulating 2-AG levels. B. BCP also showed a dose dependent inhibition of MAGL activity *in vitro* (IC50 = 14.4 µM). The BCP levels observed in plasma, paw and spine tissue are indicated by arrows). All data are presented as mean ± STD.

Conclusions: BCP was originally hypothesized to be a selective CB2 receptor agonist[6], but several studies have been unable to confirm BCP binding to CB2 receptors[7]. We examined the ability of BCP to modulate the endocannabinoid system. These data showed that BCP inhibits MAGL activity in vitro, ex vivo and in vivo causing 2-AG levels to rise. Since the endocannabinoid 2-AG is a CB1 and CB2 receptor agonist, we propose the 2-AG-mediated cannabinoid receptor activation may contribute to BCP's mechanism of analgesia,

References:

1. A future without chronic pain: neuroscience and clinical research. Cerebrum 2012, 2012:7.
2. Plant Natural Sources of the Endocannabinoid (E)-beta-Caryophyllene: A Systematic Quantitative Analysis of Published Literature. 2020, 21(18).
3. Characterization of a rat model of incisional pain. 1996, 64:493-502.
4. Postoperative pain-from mechanisms to treatment. 2017, 2(2).
5. Analysis of 14 endocannabinoids and endocannabinoid congeners in human plasma using column switching high-performance atmospheric pressure chemical ionization liquid chromatography-mass spectrometry. 2021, 413(12):3381-3392.
6. Beta-caryophyllene is a dietary cannabinoid. 2008, 105(26):9099-9104.
7. Terpenoids Commonly Found in Cannabis sativa Do Not Modulate the Functional Activity of Delta(9)-THC at Human CB1 and CB2 Receptors. 2019, 4(3):165-176.

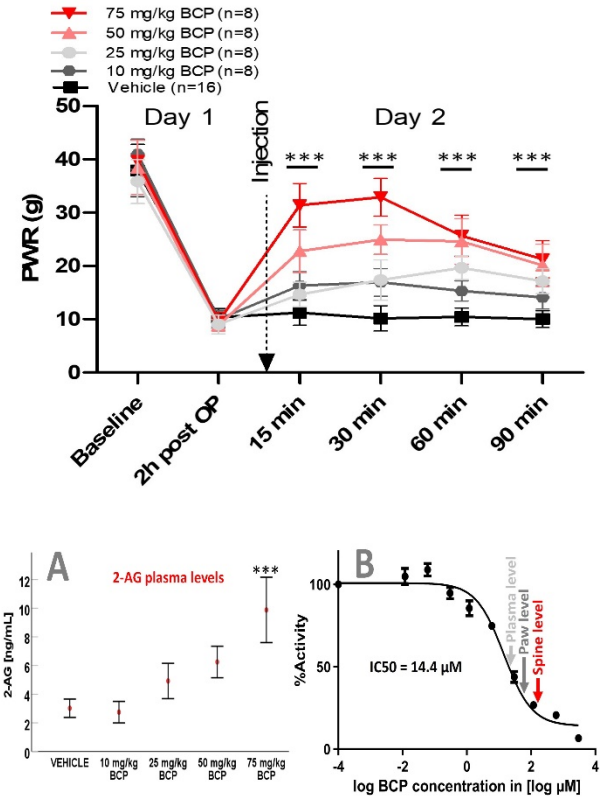
75 mg/kg BCP (n=8)
50 mg/kg BCP (n=8)
25 mg/kg BCP (n=8)
10 mg/kg BCP (n=8)
Vehicle (n=16)
Day 1
Injection
Day 2
***
***
***
***
PWR (g)
50
40
30
20
10
0
Baseline
2h post OP
15 min
30 min
60 min
90 min
A
2-AG plasma levels
***
2-AG [ng/mL]
12
10
8
6
4
2
0
VEHICLE
10 mg/kg BCP
25 mg/kg BCP
50 mg/kg BCP
75 mg/kg BCP
B
%Activity
100
50
0
IC50 = 14.4 µM
Plasma level
Paw level
Spine level
-4
-2
0
2
4
log BCP concentration in [log µM]

Pain Mechanisms 2- TRPV1-expressing Cell-Specific Nrf2 Overexpression Protects Against Mechanical Allodynia in a Chronic Femoral Arterial Occlusive Mouse Model

Oliver Kitzerow[1], Irving Zucker[1], Hanjun Wang[1]

University of Nebraska Medical Center[1]

Introduction: Peripheral arterial disease (PAD) is a progressive atherosclerotic disorder that is estimated to impact >200 million people worldwide. Higher physical activity levels are associated with better overall survival rate and slower decline of functional capability; however, ischemia and intermittent claudication, a hallmark symptom of PAD, severely limits physical activity in PAD patients. The neural mechanisms that produce pain and dysfunction in PAD remain unknown. In our previous pilot study, we found increased pro-inflammatory macrophage infiltration/activation within the lumbar DRGs at the chronic stage of PAD, indicating neural inflammation. In parallel, our pilot data also suggested upregulated protein expression of nuclear factor erythroid 2-related factor (Nrf2) in lumbar DRGs at the chronic stage of PAD. Nrf2 is a transcription factor that mediates the cellular response to oxidative stress and inflammation. We believe that the purpose of upregulated Nrf2 protein in lumbar DRGs is to counteract the influence of neural inflammation in DRG neurons post PAD. However, the compensatory response by an intrinsic DRG system may not be potent enough to antagonize exogenous neural inflammation evoked by PAD. Therefore, in the current study, we hypothesized that selective overexpression of Nrf2 by knockout (KO) of its negative regulator Keap1, in mouse TRPV1-expressing DRG neurons improves symptoms of pain post PAD.

Methods: We have developed a novel endovascular femoral artery occlusion rodent model in which a catheter is inserted within the femoral artery to the aortic bifurcation. Previous animal models of PAD require multiple surgeries or do not chronically reduce blood flow to the hindlimb. To validate our model, we have assessed hindlimb perfusion using Scanning Laser Doppler in 9 occlusive mice and 6 sham-surgery mice **(Figure 1)**. Mice were examined in the prone position and sedated with continued administration of isoflurane (1.5%) while laser measurements were being collected. Hair and shaving create artifact during the scan, so only the hind paw was used for statistical analysis in which contralateral and ipsilateral paws of the catheter placement were compared. In combination with our PAD animal model, we developed a TdTom/Keap1 double KO (DKO) **(Figure 2)** in TRPV1 expressing neurons by crossing TdTom-floxed/Keap1-floxed and TRPV1-cre founders. To determine the effects of TRPV1 specific Nrf2 overexpression on pain sensitivity, we collected *in vivo* pain behavioral data 4 days, 1-, 2-, 3-, and 4-weeks after femoral arterial occlusion in 16-week-old male and female mice with and without PAD. Von Frey hairs were used to evaluate mechanical threshold while Hargreaves test was utilized for thermal thresholds. Differences between treatments were determined using a mixed-effects model for repeated-measures ANOVA. For comparison between two groups both Tukey and Bonferroni corrections for multiple comparisons were used with $P<0.05$ being statistically significant.

Results: The endovascular catheter greatly reduced blood flow to the hind paw up through 6 weeks. Recovery of flow can start to be seen at 6 weeks but remained significantly reduced (**Figure 1**). Following occlusion, wild type floxed-PAD mice showed significant mechanical allodynia at 4 days when compared to floxed-Sham. The observed sensitivity continued through 4 weeks with only slight improvement from the 4-day timepoint. When compared to floxed-PAD, Keap1-KO mice had higher mechanical thresholds at all timepoints after PAD **(Figure 3A)**. Consistent with other reports showing that PAD does not induce thermal sensitivity, floxed-PAD nor Keap1-KO mice with PAD exhibited altered thermal thresholds when compared to floxed-Sham mice **(Figure 3B)**. However, slight but significant differences were observed between Keap1-KO and floxed-PAD mice at 4 days which may suggest that Nrf2 can protect against thermal hypersensitivity although, this conclusion is obscured by the high fluctuations of thermal responses in floxed-PAD mice. Female Keap1-KO mice revealed similar trends and were not different from their male Keap1-KO counterparts **(Figure 3C and 3D)**.

Conclusions: The current study provides evidence that our endovascular catheter animal model provides a reliable and easy chronic PAD model for research. It also shows that Nrf2 targeting serves a protective role against mechanical allodynia and may provide potential therapy to reduce claudication and increase physical activity in PAD patients.

References: Development of a two-stage limb ischemia model to better simulate human peripheral artery disease, *Sci Rep* 10, 3449, 2020

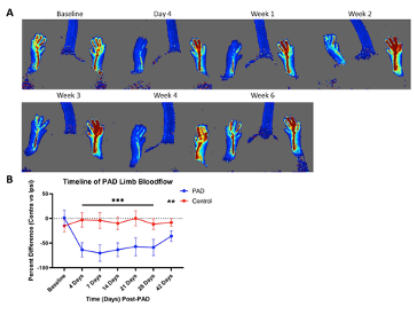

Figure 1. Representative Laser Doppler Scans showing the time course of reduced blood flow indicated by blue pixels in the ipsilateral hind paw of the endovascular catheter **(A)**. Time course analysis of blood flow comparing the contralateral and ipsilateral paws **(B)**. Mean± SD. n=6-9 per group. $P<0.01$ (**) and $P<0.001$ (***).

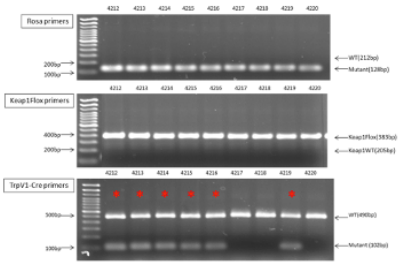

Figure 2. Representative PCR gels confirming desired genotype of mutant strain, TdTom-floxed$^{+/+}$ Keap1-floxed$^{+/+}$ and TRPV1-cre$^{+/-}$ indicated by the red stars.

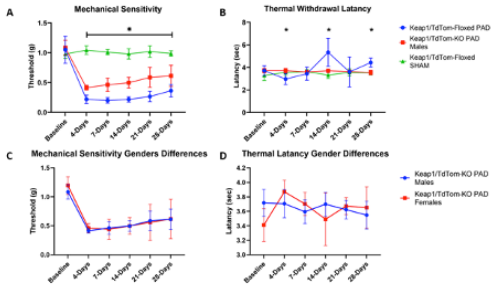

Figure 3. Mechanical sensitivity measured by Von Frey behavioral assessment of male mice. **(A)**. Thermal sensitivity measured by Hargreaves behavioral assessment of male mice. **(B)**. Mechanical sensitivity measured by Von Frey behavioral assessment comparing the differences of male and female mice **(C)**. Thermal sensitivity measured by Hargreaves behavioral assessment comparing the differences of male and female mice **(D)**. Mean± SD. n=4-12 per group. P<0.05 (*) being statistically significant when Keap1-KO is compared to Keap1-floxed.

Pain Mechanisms 3- Behavioral Analysis of Neuropathic Pain in Mice via Machine Learning

Chia-Chen Liang[1], Shiming Yang[1], Weihua Ding[1], Liuyue Yang[1], Jing Zhu[1], Shiqian Shen[2], Peter Hu[3], Wei Chao[3]

University of Maryland, Baltimore[1] Massachusetts General Hospital[2] University of Maryland School of Medicine[3]

Introduction: Pain testing of animal behavior often relies on trained personnel to conduct standard assays. Such testing processes could be laborious and prone to biases. Besides, the presence of testers might affect animal behavior and confound data interpretation. Here we develop a computer vision technique based on machine learning to identify behavioral changes in a mouse pain model to establish technical feasibility of automated behavior assessment.

Methods: Thirty-three videos were recorded from eleven pairs (male and female) of mice with 1) trigeminal neuralgia (TN) procedure or 2) sham procedure on day 0, 7 and 21. For each pair of mice, only male mice were subjected to TN or sham procedure and the female mice were not. To analyze the "mating" behavior between male and female mice, we extracted several features from the videos – 1) moving speed and direction, 2) their relative distance and relative speed, 3) moving direction and 4) the total body area of two mice (Figure 2). To obtain the training data to build a machine learning model, independent human video reviewers watched the videos and identified each mating action with episodes and duration. A mating episode is one continuous mating event with a specific start time and end time. Duration is the elapse of an episode time in seconds. We developed a computer vision analysis system based on Logistical Regression (LR) and Random Forest (RF) method to analyze the mouse mating behavior (both duration and episode) from the videos. Then, based on the algorithm-generated duration and episodes, we used the Area Under the Curve of the Receiver Operating Characteristic (AUROC) to evaluate the prediction values in a new set of mice after TN or sham procedures.

Results: Among the eleven pairs of mice, six pairs of mice were used for the training model development. the other five pairs were used as model testing data sets, of which three pairs were in the TN group and two pairs were in the sham group. Pearson correlation between human records and RF's estimations were duration (0.61) and episode (0.75) (Table 1). Using the duration estimated by machine learning methods (RF and LR), we could predict mice with TN or sham in the testing dataset with AUROC of 1.00 (95%CI: 1.00-1.00) by using RF method and 0.67 (95%CI: 0.13-1.00) by using LR method. Using estimated episodes, we achieved AUROC of 1.00 (95%CI: 1.00-1.00) by using RF method and 0.79 (95%CI: 0.47-1.00) by using LR method (Figure 2). Overall, RF method is consistently better than LR method. Moreover, both human and computer-based vision analysis revealed a significant decreased mating episodes and duration in TN mice compared to sham mice.

Conclusions: Machine learning-based vision analysis predicts animal mating behavior changes in a mouse pain model with high AUROC. The study provides a proof-of-concept that computer-based vision analysis is feasible in assessing complex pain-related behavior.

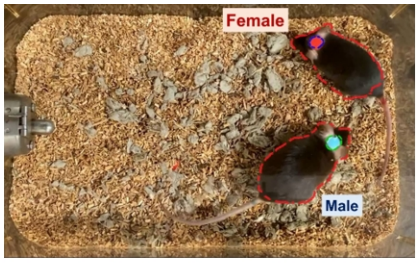

Figure 1. Tracking mice movement and body area by color detection. Recognize male (blue head dot) and female (red head dot) mice, then detect two mice body area (red contours).

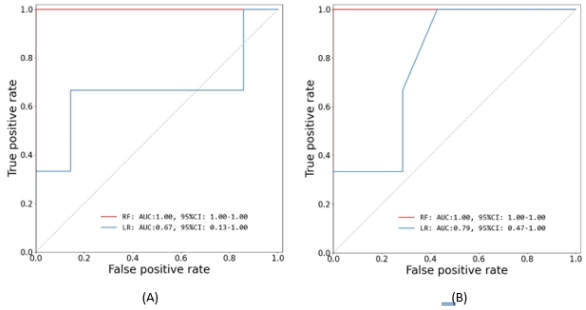

Figure 2. AUROCs of classification (trigeminal neuralgia TN procedure or sham procedure) results produced by estimated duration and episode for testing data. (A) Duration. (B) Episode.

Table 1. Pearson correlation of duration and episode for testing data.

Method	Duration	Episode
Human label vs Random Forest	**0.61**	**0.75**
Human label vs Logistic Regression	0.39	-0.20

Pain Mechanisms 4- Direct application of a novel neuroactive steroid, (3α,5α)-3-hydroxy-13,24-cyclo-18,21-dinorchol-22-en-24-ol (CDNC24) on the rat dorsal root ganglia alleviates post-incisional pain through GABAergic modulation

MacKenzie Walz[1], Nemanja Useinovic[2], Vesna Jevtovic-Todorovic[3], Douglas Covey[4], Slobodan Todorovic[4]

UC Denver Anschutz Medical Campus[1] University of Colorado Anschutz Medical Campus[2] University of Colorado[3] Washington University in St. Louis[4]

Introduction: The role of $GABA_A$ modulation in both the spinal cord and dorsal root ganglia (DRG) of rodents in nociception was previously studied in chronic preclinical pain models, however similar studies in an acute incisional model are lacking[1,2]. Previous studies have demonstrated the importance of GABA modulation in neuropathic pain and the downregulation of the $GABA_A$ α_2 subunit following sciatic nerve injury model in rats[1]. It has also been shown that some neuroactive steroids potentiate GABA currents, block T-type calcium currents, or both, which shows potential therapeutic benefit to acute and neuropathic pain[2]. For this reason, we used a novel neuroactive steroid and positive modulator of neuronal $GABA_A$ receptors (3α,5α)-3-hydroxy-13,24-cyclo-18,21-dinorchol-22-en-24-ol (aka CDNC24). This compound was previously shown to be an ineffective analgesic in an acute incisional pain model with intrathecal application, however, has yet to be studied with a direct application to the DRG[3]. The main goal of this study is to investigate the changes in $GABA_A$ α_2 subunit expression within the dorsal root ganglia (DRG) after plantar skin incision in rats and determine potential therapeutic benefit of direct DRG application of the $GABA_A$ modulator CDNC24.

Methods: This study was approved by the Institutional Animal Care and Use Committee. Acute incisional pain was induced in Sprague Dawley female adult (3-month-old) rats and mechanical threshold was measured using electronic Von Frey for both hind paws in triplicates before and after incision and compound application. Incision pain was induced by a plantar longitudinal incision in the right hind paw while the animal was under 2.5% Isoflurane. At the same time as the paw incision surgery in treated animals, a midline incision was made in the L4-6 spinal level, the laminar bone of L5 was exposed, and a 0.49mm hole was drilled directly above the DRG. A blunt needle was then used to apply CDNC24 directly onto the L5 DRG. Thirty nanograms or 100 nanograms (3α,5α)-3-hydroxy-13,24-cyclo-18,21-dinorchol-22-en-24-ol (CDNC24) or equal volume (30 microL) of vehicle (25% 2-hydroxypropyl-beta-cyclodextrin), was applied in a blinded manner. Western blot analysis was performed on acutely dissected lumbar DRGs (L4-L6) collected on post-operative day (POD) 2 or 10. The DRG samples were pooled, separated on SDS-polyacrylamide gels by electrophoresis, and transferred to PVDF membranes. The membranes were probed overnight with anti-$GABA_A$ α_2 receptor subunit antibody, and β-actin-HRP antibody was used as loading control. Statistical significance of behavioral data was analyzed by multiple unpaired t-tests, and Western blot data was analyzed using paired t-tests.

Results: Post-incisional hyperalgesia in naive animals lasted for approximately 5 days, with POD 2 showing the most pronounced mechanical hyperalgesia (n=15). Mechanical thresholds recovered back to baseline level by POD 10. Western blot analysis showed about 25% (±10%) reduced protein expression of the $GABA_A$ receptor α_2 subunit in the ipsilateral side on POD 2 (n=12). In contrast, no difference in expression of the α_2 subunit was seen in sham incised animals (n=12) or in incised animals at POD 10 (n=15). Direct DRG application of CDNC24 effectively alleviated hyperalgesia at 30 ng /30 microL (n=7) on POD 1, and at 100 ng /30 microL dose (n=8) up to POD 4 when compared to vehicle. In contrast, CDNC24 applied to sham incised animals did not show any difference in mechanical thresholds.

Conclusions: Overall, we show that the acute incisional pain model induced a downregulation of the α_2 subunit of $GABA_A$ receptors in ipsilateral DRG that coincided with most intense periods of hyperalgesia. Application of CDNC24 to the DRG dose-dependently diminished hyperalgesia up to POD 4. Since we previously have shown no effective analgesic effect of CDNC24 when administered intrathecally in the same pain model, this argues for specificity of $GABA_A$ modulation by CDNC24 in the DRG. We conclude that the $GABA_A$ receptor modulation in the DRG plays an important role in pathophysiology of post-operative hyperalgesia and represents a promising target for novel pain therapies.

References:

1. Obradovic AL, et al., *Anesthesiology.* 2015; 123(3):654-67.
2. Pathirathna S, et al., *Pain*. 2005; 114(3):429-443.
3. Tat QL, et al., *Cells.* 2020; 9(12):2674.

This research is funded by NIH Grant 1 R35 GM141802 and VA Merit Award I01 BX004763 to SMT.

Pain Mechanisms 5- Effects of persistent inflammation on the endocannabinoid system and cannabinoid CB1 receptors (CB1Rs) in rat periaqueductal gray (PAG)

Susan Ingram[1], Basile Coutens[1], Courtney Bouchet[1]

University of Colorado Anschutz Medical Campus[1]

Introduction: Cannabinoid-targeted pain therapies are increasing with expansion of cannabis legalization. The cannabinoid 1 receptor (CB1R) is one of the most highly expressed GPCRs in the brain and is primarily localized to presynaptic terminals, where its activation inhibits neurotransmitter release. CB1Rs are activated by exogenous and endogenous ligands. Here we examine the effects of exogenous cannabinoid agonists and the endocannabinoid system on synaptic transmission in the periaqueductal gray (PAG), part of the descending pain modulatory circuit. We compare cannabinoid signaling in the PAG of Sprague-Dawley rats between naïve and persistent inflammation induced by Complete Freud's adjuvant (CFA) injected into the hindpaw.

Methods: Brain-slices for whole-cell patch-clamp recordings from ventrolateral PAG neurons were prepared from adult male and female Sprague Dawley rats (postnatal day 30-60) or rats injected with Complete Freund's Adjuvent (CFA) into one hindpaw to induce inflammation for 5-7 days. The effects of exogenous CB1R agonists on evoked GABAergic inhibitory synaptic currents (eIPSCs) and miniature inhibitory synaptic currents (mIPSCs) were assessed and compared between treatments. Endocannabinoid activation of CB1Rs was assessed using a depolarization-induced synaptic inhibition (DSI) protocol (5 s depolarization to +20 mV). Comparisons between recordings in naïve and CFA-treated rats were analyzed using parametric and nonparametric analyses as appropriate.

Results: Persistent inflammation in male and female Sprague-Dawley rats increases tonic endocannabinoid signaling and presynaptic CB1R desensitization, resulting in significantly reduced inhibition of GABA release in slices from CFA-treated rats. The exogenous CB1R agonist WIN55212 (WIN; 3 uM) inhibits eIPSCs by 57 ± 5%. CFA-induced inflammation significantly attenuated WIN inhibition (18 ± 4%; t14 = 5.34; p = 0.0002). There were no effects of CB2R agonists. G protein-coupled receptors are desensitized following phosphorylation by G protein receptor kinase (GRK). The GRK inhibitor Compound 101 (1 uM) reversed the reduced inhibition in slices from CFA-treated rats back to baseline, without an effect in slices from naïve rats (2-way ANOVA: main effect of Cmp101: $F(1,13) = 7.6$; $p = 0.016$). The DSI protocol was used to assess endocannabinoid signaling. Maximal inhibition induced with DSI in recordings from naïve rats (41 ± 6%) is similar to 37 ± 4% inhibition observed in recordings from CFA-treated rats. After 30s, eIPSC amplitudes return close to baseline (14 ± 5% inhibition) in naïve but stays inhibited 37 ± 5% in recordings from CFA treated rats (2-way repeated-measures ANOVA: interaction DSI x CFA: $F(1,24) = 14.3$; $p = 0.0009$), indicating prolonged activity of endocannabinoids in the PAG of CFA-treated rats. Further studies determined that 2-arachidonylglycerol (2-AG) was the primary endocannabinoid released during inflammation. Preliminary studies fnd that corticosterone inhibits eIPSCs in the PAG and this inhibition is blocked by CB1R antagonists. Ongoing studies will examine the role of corticosterone in the adaptations involved in the PAG of inflamed rats.

Conclusions: The results indicate that CB1Rs targeted by exogenous cannabinoid agonists may signal via different effectors compared to endocannabinoids in the ventrolateral PAG or that there are substantial differences inefficacy of endocannabinoids compared to exogenous cannabinoids requiring fewer spare receptors. The potentiated inhibition of GABA release in PAG synapses in inflamed rats may be a compensatory mechanism to relieve pain or may contribute to the hyperalgesia observed with persistent inflammation. Further studies will attempt to answer this important question. These adaptations with inflammation in the cannabinoid system have important implications for the future development of cannabinoid-focused therapies.

Pain Medicine

Pain Medicine 1- Patient-Physician Dynamics and Opioid Prescription in Pain Management of Prostate Cancer

Lulu Wei[1], Ruoyu Wang[1], Christopher Alessandro[1], Samuel Yim[2], Rose Calixte[2], Andrew Winer[2], Ketan Shevde[2]

SUNY Downstate Health Sciences University[1] SUNY Downstate[2]

Introduction: Opioid therapy is a pain management option for patients with prostate cancer. Few studies have investigated how social factors may affect opioid prescription in prostate cancer patients. Racial differences in opioid prescription rates have been found and postulated to be driven by greater practitioner mistrust towards non-White patients (1-3). However, this disparity was not seen in a study of prostate cancer patients (4). Our study's goal is to investigate another underexplored social factor, quality of patient-physician communication, and elucidate possible associations between communication quality and opioid prescription prevalence among prostate cancer patients.

Methods: We used the Agency for Healthcare Research and Quality's Medical Expenditure Panel Survey (MEPS) data from 2014-2017 to create a national cohort of 367 patients with prostate cancer. We collected information on demographics, health care access, global rating of health (0-10 scale), self-reported limitation from pain, and opioid prescription data. Patient ratings of how often the doctor would listen, explain, show respect, spend enough time, and provide easily understandable instructions were examined. Factors relating to opioid use were found by multivariable analysis in SAS®.

Results: 114 of 367 (31%) prostate cancer patients were prescribed opioids. Opioid prescriptions were more likely in younger patients (OR = 0.93, 95% CI [0.89, 0.96]) and in those who reported pain that limited the ability to perform normal work (OR = 1.72, 95% CI [1.34, 2.21]). There were no significant differences in opioid prescription by race when compared to non-Hispanic white, marital status, US-born status, US region, or insurance coverage. Additionally, no significant differences were found by patient-physician interaction quality. Patient ratings of their general health, health care received, and ability to overcome illness without medical help were similar in prostate cancer patients regardless of opioid status.

Conclusions: Opioid prescription rates in prostate cancer are associated with younger age and pain that limits the ability to work. No significant differences were found by race, which is consistent with prior studies, nor were there differences by patient-physician social factors. This suggests that more objective measures of significant pain, such as pain limiting the ability to work in younger patients, may lessen physician mistrust and bias regarding opioid prescriptions for prostate cancer patients. Further research is needed to elucidate the role of physician mistrust in this cohort.

References: 1. Racial differences in opioid use for chronic nonmalignant pain. J. Gen. Intern. Med. 20(7), 593–598 (2005).

2. Trends in opioid prescribing by race/ethnicity for patients seeking care in US emergency departments. JAMA 299(1), 70–78 (2008).

3. Prospective, observational study of pain and analgesic prescribing in medical oncology outpatients with breast, colorectal, lung, or prostate cancer. J. Clin. Oncol. 30(16), 1980–1988 (2012).

4. Disparities in prescription of opioids among prostate cancer patients of various racial groups. Pain Management, 9(3), 273–281 (2019).

5. Sample Designs of the Medical Expenditure Panel Survey Household Component, 1996–2006 and 2007–2016. Methodology Report #33. January 2019.

Pain Medicine 2- State-space ERP: A novel signal processing method to estimate pain-evoked response and opioid-induced analgesia

Rodrigo Gutierrez[1], Rodrigo Motefusco-Siegmund[1], Proloy Das[1], Alonso Blanch[1], Antonello Penna[2], Daniel Rojas-Libano[2], Patrick Purdon[1], Gonzalo Rivera-Lillo[2], Jose Egaña[2]

Massachusetts General Hospital[1] Universidad de Chile[2]

Introduction: Post-surgical pain is a major contributor to chronic pain, opioid dependence, and opioid substance abuse (1-2). While anesthesiologists have many tools for treating surgical and post-operative pain, they have no tools to monitor how well their treatments might be working, making it difficult if not impossible to accurately and reliably treat nociception during surgery and minimize post-operative pain (3).

It is well-known that painful stimuli generate event-related potentials (ERPs) that can be measured at the scalp by averaging waveforms from repeated stimuli generated by a variety of methods including electrical stimulation (4). These ERPs are challenging if not impossible to use for anesthesia monitoring because they are very small, between ~1 to 5 microvolts, and are overshadowed by background electroencephalogram oscillations that are 10- to 100-fold larger in amplitude during general anesthesia or sedation.

In the present study we evaluated a novel signal processing method to estimate ERPs that are associated with pain and analgesia.

Methods: Volunteers were recruited at the University of Chile. They all provided written informed consent. Recordings were performed in the operative room under standard continuous monitorization. At arrival, a left forearm vein was cannulated using a 22G infusion catheter. Each subject received oxygen via a Venturi mask. **Protocol:** After EEG, monitorization, and oxygenation were installed, two ring electrodes were placed in the middle finger of the right hand separated by 3 cm. Stimulation was performed using a direct current stimulator (DS7A, Digitimer Ltd, Hertfordshire, UK). Pain was measured using the Numeral Rating Scale (NRS) from 0 (no pain) to 10 (worst pain imaginable) For each subject four intensities were defined in order to elicit a given amount of pain in the NRS. I1 = 1; I2 = 2-3; I3 = 4-5; I4 = 6. Similarly, the analgesic concentrations needed to elicit mild (pain reduction of 1 in the NRS), moderate (2-3 reduction) and intense (4 or more) analgesia were defined for each subject. Stimuli consisted of triplets (S1-S2-S3) of the same intensity (**Figure 1**). In the no-analgesia sessions 20 trains/triplets at each of the four intensities (I1-I4) were delivered in random order for a total of 80 trains. In the analgesia experiments 20 trains at each intensity were delivered at each of the three levels of analgesia (A1-A3) for a total of 60 trains. Stimuli within a triplet were separated by 1 s. Time interval between triplets was 20 s. Subjects were trained to wait 3-5 seconds after stimulation and then rate verbally the intensity of pain elicited by each of the 3 stimuli. **ERP and EEG analysis:** The raw EEG data is bandpass filtered between 0.5 Hz to 30Hz, followed by downsampling to 64Hz. Data preprocessing is done using MNE-Python 1.0.3. The individual channels were visually inspected for artifacts and marked as bad. The data from the Cz channel after average referencing is used for SS-ERP analysis. Our SS-ERP algorithm employs a multi-level model that represents persistent oscillatory background signals distinct from evoked responses, making it possible to separate these two components and dramatically reduce the uncertainty in the ERP estimate. The event-related time series are modeled as a convolution between ERP waveforms, h, and discrete events, e (modeled as impulses), and the observed EEG signal is then represented as the sum of background and ERP components with an observation noise term.

Results: Ten volunteers were included in the study, mean age was 26.3 years (SD 6.7), 3 of them (30%) were females, and everyone were healthy (ASA 1). The average ERP are presented in **Figure 2**. At baseline condition we identified an ERP composed by a negative deflection around 100 ms and a positive deflection around 250 ms. The amplitude of both components is correlated with the intensity of the stimuli. Under mild level of analgesia, we observed an overall reduction in the amplitude of the ERPs. Under moderate level of analgesia, the lower intensities do not longer elicit an evoked response, while the highest intensity elicit a lower-amplitude ERP. Notably, the narrow confidence intervals generated with our state space allow us to discriminate each intensity-associated evoked response.

Conclusions: Here we report a novel method to estimate the pain ERP, that it is indeed able to discriminate different stimuli intensities, and at the same time is modified distinctively by different levels of analgesia.

References:

1. Transition from acute to chronic pain after surgery. Lancet. 2019 Apr 13;393(10180):1537-1546.
2. Electroencephalography During Nociceptive Stimulation in Chronic Pain Patients: A Systematic Review. Pain Med. 2020 Dec 25;21(12):3413-3427.
3. Objective monitoring of nociception: a review of current commercial solutions. Br J Anaesth 2019, 123: 312-321
4. Determinants of laser-evoked EEG responses: pain perception or stimulus saliency?. J Neurophysiol. 2008 Aug;100(2):815-28

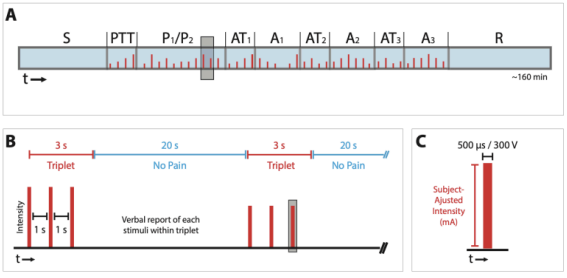

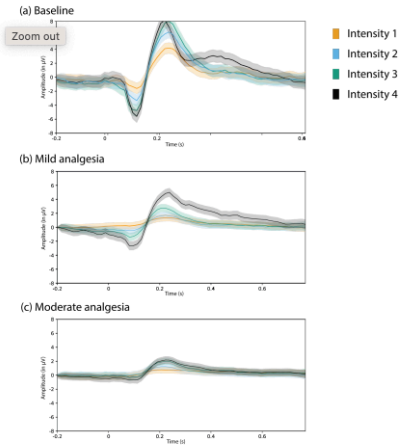
(a) Baseline
Zoom out
Intensity 1
Intensity 2
Intensity 3
Intensity 4
(b) Mild analgesia
(c) Moderate analgesia

Pain Medicine 3- The Value of Stakeholder Voices in Clinical Trial Design: The Comparing Analgesic Regimen Effectiveness and Safety for surgery (CARES) Trial

Sarah Clark[1], Kendall Dubois[1], Rachel McDuffie[2], Kellie McFarlin[3], Simon Haroutounian[3], Mary Neff[3], Duminda Wijeysundera[4], Jennifer Waljee[4], Chad Brummett[4], Karim Ladha[5], Mark Bicket[5]

University of Michigan[1] Washtenaw County Prosecutor's Office[2] Henry Ford Health System[3] St Michael's Hospital[4] University of Toronto[5]

Introduction: There is debate among patients and experts that opioid-free analgesic regimens may result in poor pain relief as patients recover at home from surgery. While some argue that the harms outweigh the benefits for opioids prescribed after low-risk surgery, little rigorous evidence exists comparing non-steroidal anti-inflammatory drugs (NSAIDs) and opioid analgesics on their safety and ability to relieve postoperative pain. To address this gap, we designed the Comparing Analgesic Regimen Effectiveness and Safety for surgery (CARES) Trial to compare two clinically relevant analgesic prescribing regimens (NSAIDs or opioids) up to six months after discharge from surgery at 4 sites throughout the US and Canada. Given the diverse communities that have an interest in this question, we recruited and engaged with a team of key partners in research to ensure the study design and conduct represented relevant perspectives that would maximize the value of study results. Here, we examine the organization of these partners on the Stakeholder Advisory Board and ways in which their engagement has contributed to the design and conduct of the trial.

Methods: CARES is a pragmatic randomized clinical trial designed to compare the effectiveness of two prescribing strategies over 6 months that will randomize 900 adults undergoing laparoscopic cholecystectomy, inguinal hernia repair, or breast lumpectomy to either prescriptions for NSAIDs (n=450) or opioids (n=450) after discharge from surgery. The CARES Trial draws on longstanding reciprocal relationships between key partners, patients, and investigators. We recruited a Stakeholder Advisory Board to provide input and collaborate throughout the research process. Stakeholders provided input into key decisions regarding CARES building on the principles of reciprocal relationships, co-learning, and partnerships via quarterly meetings, online surveys, and other purposeful feedback.

Results: The Stakeholder Advisory Board includes five key partners who are Patients with Lived Experience (PWLE) with backgrounds and experiences that reflect each of the communities at the four study sites as well as each of the three types of surgical procedures included in CARES. Five other partners represent other key domains including a community organization focusing on mental health needs, the Detroit Mental Health Leadership Team; surgeons who perform the three types of procedures that participants undergo in CARES;a professional organization, the American College of Surgeons; a payer group, Blue Cross Blue Shield of Michigan; and a pain research group, the US Association for the Study of Pain. Together, these ten stakeholders have been involved from the initial stages of study development and will continue to guide the conduct and reporting of the study through the final stages of CARES. Specifically, members of the Stakeholder Advisory Board have individually and collectively collaborated on various aspects spanning the formulation of research questions to determining outcomes, including refining outcome measures of postoperative pain and safety, offering input on approaches to analysis of results tailoring language and phrasing in the informed consent document, shaping opt-in/opt-out language for participants to receive study results, and enhancing designs to engage participants with recruitment materials, study communication, and outcome assessments.

Conclusions: Some patients and experts argue that opioid-free analgesic regimens may result in poor pain relief as patients recover at home after surgery. Other patients and experts argue that the harms outweigh the benefits for opioids prescribed after low risk-surgery. Our Patient Partners and other key advocates have voiced that evidence gaps on how to best treat pain after discharge from surgery are important to close. Specifically, they have said that CARES will provide powerful reassurance about whether avoiding opioids is possible and appropriate. Risks that matter to patients exist for both NSAID (indigestion, stomach upset) and opioid analgesic regimens (sedation, constipation, misuse of leftover pills, addiction).1-11 CARES has potential to meaningfully impact patient care choices by producing evidence to fill critical knowledge gaps regarding the comparative effectiveness and safety of NSAID-versus opioid-based analgesic regimens.

References:

1. JAMA Surg. 2017;152(6):1-9. doi:10.1001/jamasurg.2017.0504
2. Am J Surg. Published online March 2021. doi:10.1016/j.amjsurg.2021.03.044
3. Br J Anaesth. 2001;86(2):272-274. doi:10.1093/bja/86.2.272
4. Br J Anaesth. 2004;92(5):681-688. doi:10.1093/bja/aeh123
5. Anesth Analg. 1991;73(2):190-198. doi:10.1213/00000539-199108000-00013
6. J Pain. 2010;11(11):1095-1108. doi:10.1016/j.jpain.2010.02.007
7. JAMA Surg. 2017;152(11):1066-1071. doi:10.1001/jamasurg.2017.0831
8. Syst Rev. 2020;9(1):1-15. doi:10.1186/s13643-020-01393-8
9. JAMA Psychiatry. 2014;71(7):821. doi:10.1001/jamapsychiatry.2014.366
10. Can J Addict. 2010;1(2):9-13.
11. Humphreys K, Caulkins J, Felbab-Brown V. What the US and Canada can learn from other countries to combat the opioid crisis. Brookings. Published 2020. Accessed January 19, 2021. https://www.brookings.edu/blog/order-from-chaos/2020/01/13/what-the-us-and-canada-can-

learn-from-other-countries-to-combat-the-opioid-crisis/

Pain Medicine 4- A new animal model of trigeminal neuralgia

Shiqian Shen[1], Jianren Mao[2], Weihua Ding[2], Liuyue Yang[1]

Massachusetts General Hospital[1] Massachusetts General Hospital, Harvard Medical School[2]

Introduction: Trigeminal neuralgia (TN) is a classical neuropathic pain condition with distinct clinical characteristics. Modeling TN in rodents proves challenging. Our goal is to develop an animal model that could recapitulate key clinical features of TN.

Methods: We performed comparative skull base anatomical studies with human and rodent skulls. Addiiontally. we investigated if a skull base foramen could allow trigeminal nerve root impingement to create TN-like behavior in animals. Moreover, we examined the primary somatosensory cortex neural dynamics underlying pain-like behavior.

Results: We performed comparative anatomical studies of skull base in humans and rodents and found a foramen that allowed for trigeminal nerve root accessed. Taking advantage of this access, we developed a rodent model of TN and observed distinct pain-like behaviors in rodents, including paroxysmal pain attackes and altered eating behavior secnodary to dental pain. As such, this model recapitulated key clinical features of TN. We further optimized the model by examining a dose range of impingement as well as validated the model in different animal strains/species. Importantly, when compared with a trigeminal neuropathic pain model (infraorbital nerve chronic constriction injury, IoN-CCI), this model was associated with significantly higher numbers of c-Fos positive cells in the primary somatosensory cortex (S1), unraveling robust cortical activation in the FLIT model. Using intravital two-photon calcium imaging, unique population dynamics of S1 neurons were present, revealing differential implication of cortical activation in different pain models.

Conclusions: Taken together, we developed a clinically relevant rodent model of TN with a potential to facilitate pain research and therapeutics development.

References: Ahn DK, Lim EJ, Kim BC, Yang GY, Lee MK, Ju JS, Han SR, Bae YC. Compression of the trigeminal ganglion produces prolonged nociceptive behavior in rats. European journal of pain 2009;13(6):568-575.

Yeomans DC, Klukinov M. A rodent model of trigeminal neuralgia. Methods Mol Biol 2012;851:121-131.

Pain Medicine 5- Identification of Persistent Postoperative Opioid Use from Clinical Notes via a Natural Language Processing Engine

Eri Seng[1], Soraya Mehdipour[2], Sierra Simpson[3], Rodney Gabriel[3]

University of California San Diego School of Medicine[1] University of California, San Diego[2] University of California San Diego[3]

Introduction: The opioid epidemic continues to be a serious issue for the US, causing more than 564,000 deaths from overdoses between 1999 and 2020, an eight-fold increase over that period.[1] Preoperative opioid use was found to be the strongest predictor for persistent opioid use following surgery, imparting a greater than 4-fold risk.[2,3] A substantial 20%-70% of patients that undergo multilevel spine surgery have preoperative opioid use, and 29%-45% of patients who underwent spine surgery continued to use opioids 12 months after surgery.[2–5] Natural language processing (NLP) is a branch of artificial intelligence capable of extracting clinically relevant information from free-text narratives in medical notes. Access to this previously inaccessible data can quickly identify at-risk patients from unstructured text from clinical notes for targeted outreach, and aid in the analysis of large datasets to further investigate the risk factors for persistent postoperative opioid use.[6–9] The primary objective of this study was to demonstrate the ability of an NLP engine to review clinical postoperative spine surgery notes and accurately identify a significant portion of patients' opioid use status, as compared to manual review by anesthesiologists.

Methods: Notes from all patients that underwent major spine surgery were collected from 3 different surgeons at our institution. For each patient, the postoperative spine surgery follow-up notes (≥ 2 months after surgery) were extracted from the institution's electronic health record system. The follow-up dates of service occurred between November 2015 and December 2021, and ranged from 2 months to 12 months after the surgery date, prioritizing earlier notes if there were multiple visits. A Named Entity Recognition (NER) model, provided by KAID Health, extracted relevant entities from the medical notes and mapped them to medical concepts. Each concept is assigned an attribute flag based on the context in which the concept reference is present, such as allergy history and family history, to modulate the references as truly present or not. A list of concepts related to opioids, such as the drug class, generic drug names, and brand names (Table 1), was used to filter the output of the model. Patients with a reference to a concept in the list were presumed to have a positive presence of opioids (Table 2), unless negated by an attribute flag (Table 3). The final output was a table of patients and their opioid use status derived from the postoperative follow-up visit note. The NLP's assessment of opioid status was compared to the anesthesiologists' review (Figure 1).

Results: A single free-text note from the outpatient orthopedic spine surgery follow-up visit was collected and inputted into the NLP engine for each patient. Patients without a follow-up visit greater than or equal to 2 months from the date of surgery were excluded, resulting in a final total of 1160 patients. The NLP correctly identified patients who were still taking opioids in 792 of 834 cases (95.0%), and correctly identified those not taking opioids in 281 of 326 cases (86.2%). The sensitivity, specificity, positive predictive value, and negative predictive value were 95.0%, 86.2%, 94.6%, 87.0%, respectively (Table 4).

Conclusions: In this proof-of-concept study, the NLP engine was able to extract relevant clinical information to accurately identify patients' opioid use status. Clinicians can utilize the NLP engine to efficiently screen their patient population for persistent opioid use, improving clinical care and workflows by reducing the need for chart review, and increasing operational efficiency.[10] On a broader level, institutions can quickly assess their postoperative cases across all departments to ensure patients are receiving proper surveillance for risk factors for development of chronic opioid use. Co-morbidities such as behavioral and pain disorders can be more easily followed-up on to ensure all patient-level factors are being addressed.[11] Future studies will need to assess the NLP engine's ability to evaluate additional clinical information before these automated tools can be integrated within both clinical and research workflows.

References:

1. CDC Wonder, 2021
2. JAMA Netw Open, 3, e207367, 2020
3. Anesth Analg, 127, 247-254, 2018
4. Spine J, 18, 1974-1981, 2018
5. Spine, 42, 1405-1411, 2017
6. Nat Rev Genet, 13, 395-405, 2012
7. J Allergy Clin Immunol, 145, 463-469, 2020
8. J Am Med Inform Assoc, 27, 457-470, 2020
9. Linguist Philos Investig, 19, 93, 2020
10. Ann Fam Med, 15, 419-426, 2017
11. JAMA Surg, 152, e170504, 2017

Table 1 – List of example concepts screened for to catch the presence of opioids

Categories	Concepts
Drug class	Opioids
	Opiates
	Narcotic pain medications
Generic drug name	Codeine
	Hydrocodone
	Naloxone
	Naltrexone
	Morphine
	Oxycodone
	Tramadol

Table 2 – Sample of opioid concepts captured and noted as present

Text	Start Character	Label	Sentence	Patient ID	Date of Service	CUI	Trigger	Attribute	Present
Oxycodone	1704	Drug	Oxycodone 10 mg tablet	NA	NA	C0030489			1
Oxycodone-acetaminophen	2364	Drug	Oxycodone-acetaminophen 10-325 mg tablet	NA	NA	C0717368			1
Tramadol	1497	Drug	Continues with tramadol 50 mg up to 4 tabs a day	NA	NA	C0040610			1
Narcotic pain medication	6743	Treatment	We counseled that patient should continue to try to wean off the narcotic pain medication	NA	NA	C0002771			1
Oxycodone	498	Drug	Pain improving, though requesting more oxycodone	NA	NA	C0030049			1

Table 3 – Sample of opioid concepts captured and noted as not present

Text	Start Character	Label	Sentence	Patient ID	Date of Service	CUI	Trigger	Attribute	Present
Opioids	1367	Treatment	Denies taking any opioids	NA	NA	C0242402	Denies	Negate	0
Narcotic pain medications	1136	Treatment	Patient continues to take gabapentin for pain, but is no longer taking narcotic pain medications	NA	NA	C0002771	No	Negate	0
Hydromorphone	1930	Drug	Hydromorphone Anaphylaxis	NA	NA	C0728755		Allergy	0
Oxycodone	2185	Drug	Patient has followed up with pain management and has completely weaned off oxycodone	NA	NA	C0030049	Weaned	History	0

Figure 1 – NLP pipeline. The top half of this figure illustrates the process of curating the codes of interest. The bottom half of this figure illustrates the process of extracting relevant clinical information from the notes, encoding the concepts, and then filtering the output to determine opioid use status. cNLP, clinical natural language processing; CUI, concept unique identifier; EMR, electronic medical record; NER, named entity recognition; UMLS, Unified Medical Language System

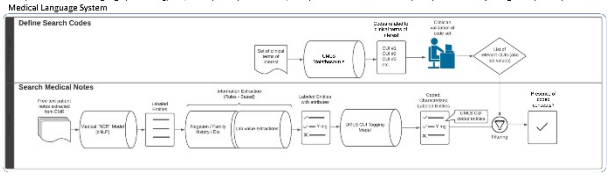

Table 4 – Contingency table displaying the comparison of the NLP model and the true situation as determined by the anesthesiologists' review. The sensitivity, specificity, positive predictive value (PPV), and negative predictive value (NPV) are below. NLP, natural language processing

NLP	Truth (as determined by anesthesiologists' review)	
	No opioid	Opioid
No opioid	281	42
Opioid	45	792

Sensitivity	95.0%
Specificity	86.2%
PPV	94.6%
NPV	87.0%

Pain Medicine 6- Intrathecal oxytocin for neuropathic pain: A randomized, controlled, blinded, cross-over clinical trial

James Eisenach[1], Regina Curry[2], Timothy Houle[2]

Wake Forest School of Medicine[1] Atrium Health Wake FOrest Baptist Medical Center[2]

Introduction: Preclinical data demonstrate that activation of supraspinal to spinal oxytocin pathways dampens hypersensitivity from in neuropathic injury, as does intrathecal injection of oxytocin [1]. The purpose of this study is to investigate the effect of intrathecal oxytocin compared to placebo on pain and hypersensitivity in individuals with chronic neuropathic pain using a randomized, controlled, double-blind cross-over study.

Methods: Following local IRB and FDA approval and trial registration and after obtaining informed consent, individuals between ages of 18 and 70 years with neuropathic pain caudal to the umbilicus for at least 6 months received two blinded intrathecal injections of either 100 mcg oxytocin or saline in a 3 mL volume, separated by at least 7 days, with the order of injections randomized. Ongoing neuropathic pain at rest using a visual analog scale (VAS) and areas of hypersensitivity were measured at intervals for 4 hours. The primary outcome was VAS pain, analyzed by linear mixed effects model with random intercepts at the level of participant. Secondary outcomes were verbal pain intensity scores at defined intervals for 7 days and areas of hypersensitivity and elicited pain for 4 hr after injections, analyzed by the same method. Safety was assessed via systematic measures, including QTc interval, serum sodium, neurological examination, and noninvasive vital sign monitoring, and queries at defined intervals up to 6 months after study. A sample size of 40 was determined to detect a minimum clinically meaningful difference in VAS of 0.7

Results: The study was stopped early after completion of only 5 of 40 subjects due to slow recruitment and funding limitations. Three subjects were men and 2 were Black and 3 were white. All subjects had peripheral neuropathy (3 from diabetes, 1 from chemotherapy, and 1 after surgery for osteosarcoma), with pain in feet and/or legs. Hypersensitivity was present in 4 subjects. There were no adverse events associated with intrathecal injections with the exception of mild headache or backache in three individuals, 2 after saline and 1 after oxytocin. Pain intensity prior to injection was 4.75 ± 0.99 and modeled pain intensity decreased more after oxytocin (to 1.61 ± 0.87) than after placebo (to 2.49 ± 0.87; p=0.003; Figure 1A). Daily pain scores were also lower in the week following injection of oxytocin than saline (2.53 ± 0.89 vs 3.66 ±0.89; p=0.001; Figure 1B) and pain during this time was lower in all 5 individuals after oxytocin than saline, regardless of injection order (Figure 2). Hypersensitivity and elicited pain in the hyperalgesic area differed between oxytocin and placebo by <18% in opposite directions depending on modality tested.

Conclusions: Intrathecal oxytocin produced no objective or subjective symptoms or signs, similar to findings in 62 healthy volunteers and surgical patients [2,3]. Pain intensity scores decreased more by oxytocin than placebo in 100% of the subjects in 4 hours after injection and for the following week, and in both cases the difference exceeded the predefined minimum clinically meaningful difference. The effect size of oxytocin was large (>75% reduction in pain: Figure 1), and there was no evidence of unblinding due to adverse events or subjective sensations. Despite the use of a rigorous study design and statistical analysis, however, failure to recruit more than a small fraction of the planned enrollment limits these findings to encouraging further research rather than definitively testing the proposed hypothesis.

References: 1. Neurosci Biobehav Rev 55:53;2015

2. Anesthesiology 122:407;2015

3. PAIN doi:10.1097/j.pain.0000000000002810;2022

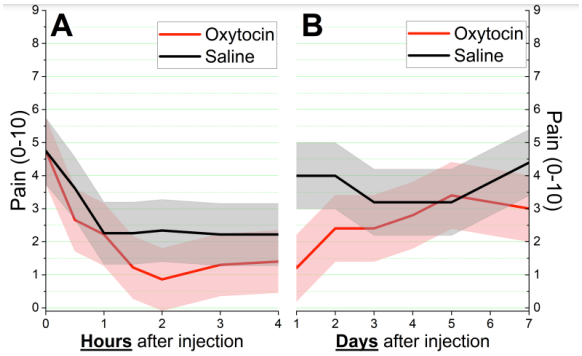

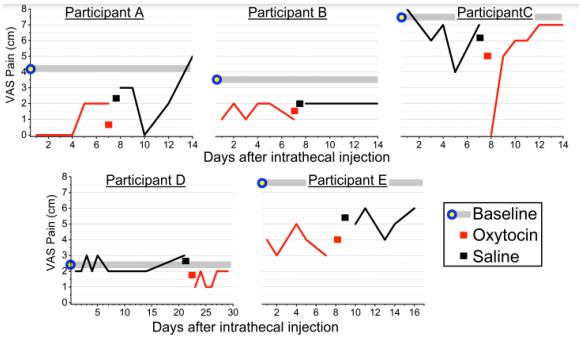

Pain Medicine 7- Perioperative opioid stewardship: a service evaluation of persistent postoperative opioid use at a tertiary healthcare institution

Harry Griffiths[1], Liam Taylor[1], Lexy Sorrell[1], Joanne Hosking[1], Mark Rockett[1], Daniel Martin[2]

Peninsula Medical School[1] University of Plymouth[2]

Introduction: Unwarranted chronic opioid use after surgery, known as persistent postoperative opioid use (PPOU), is a significant public health concern associated with misuse, dependence, and fatal or non-fatal adverse events.[1-3] A recent systematic review of 33 studies and 1,922,743 surgical patients concluded that the pooled rate of PPOU was 6.7% (95% CI, 4.5-9.8), thus the potential for opioid-related harm is evident, of which surgery is an important stimulus.[3] In addition, rates of opioid-related deaths and emergency admissions are increasing in the UK, particularly in Scotland; at present, Scotland's opioid use trajectory risks mirroring that of the US, where an opioid crisis is well-established, and is currently deemed the greatest outlier in Europe.[4] However, despite growing concern, just three studies have evaluated PPOU in the UK, each with methodological limitations which prevent meaningful interpretation to inform modern risk reduction strategies.[3] Consequently, UK expert consensus guidelines on perioperative opioid stewardship were published in 2021 calling for more primary studies due to the paucity of data.[1]

Methods: We performed a service evaluation at a tertiary healthcare institution using a retrospective cohort design. Adult (≥18 years) patients who underwent one of the top ten elective or emergent surgical procedures during 1-31 August 2021 were included. Preadmission and postadmission opioid use and patient demographics were extracted from primary care electronic medical records (EMR), intraadmission opioid use and naloxone requirements from were determined from hospital EMR. Hence, patients with neither primary care nor hospital EMR available were excluded. Opioid prescription (OP) data were converted to oral morphine equivalent (OME) doses (mg day^{-1}) for comparisons. Concordant with other literature, opioid use within preoperative days 180-0 was categorised into opioid-naïve (no OPs), opioid-exposed (≥1 OP), and chronic users (continuous OPs without an interruption exceeding 30 days).[1] PPOU was defined within postoperative days 90-180 as ≥1 OP for opioid-naïve or exposed patients, and any baseline increase in OME for chronic users.[1] Demographics were summarised with descriptive statistics. Associations were tested using Pearson's chi-sqaured (c^2), Fisher's Exact test, and Mann-Whitney U tests according to sample size and distribution, with statistical significance set at $p < .05$ (two-tailed).

Results: 162 patients underwent elective or emergency surgery during August 2021 and were identified to determine eligibility. 18 patients were excluded: 13 died within six postoperative months and 5 were missing a full dataset, resulting in 144 patients for analysis. Of these, 135 (93.8%) had hospital data available, 114 (79.2%) had primary care data available, and 102 (70.8%) had a full dataset. 14/114 (12.3%) were classified as having PPOU, of which 7 (50%) were opioid-naïve, 1 (7.1%) was opioid-exposed, and 6 (42.9%) were chronic opioid users prior to surgery. Significant variables associated with PPOU were depression ($c^2 = 13.655$, $p < .001$), antidepressant use ($c^2 = 4.765$, $p = .029$), anxiety ($p = .043$), preadmission overdose ($p = .041$), opioid-naïve status ($c^2 = 11.622$, $p = .003$), and chronic user status ($p < .001$). Preadmission OME (median [IQR], non-PPOU, 0 [40.0]; PPOU, 0.29 [13.46]) and postadmission OME (non-PPOU, 0 [70.0]; PPOU, 20.82 [25.5]) were associated with PPOU (both $p < .001$). Just one patient (0.7%) required naloxone during admission.

Conclusions: These preliminary findings have identified local rates of PPOU and factors which are associated. To our knowledge, this is the first attempt to quantify PPOU across multiple surgical disciplines within the UK. Our incidence rate of PPOU is comparable to previous work, where associations with depression and antidepressant use are also described.[2, 3] Moreover, chronic opioid use prior to surgery is a well-known risk factor for PPOU, which was associated in our study.[1-3] However, further demographic associations were not possible due to our sample size lacking statistical power for such variables, thus providing scope for further work. Regardless, our aim was to evaluate the study area and elucidate the potential magnitude of PPOU in response to recent guidelines, where more data are warranted.[1] As highlighted in these guidelines, high-risk patients should be identified before surgery to inform patient-centred pain strategies and support moderated, judicious opioid prescribing perioperatively.

References: 1. Srivastava D, Hill S, Carty S, Rockett M, Bastable R, Knaggs R, et al. 2021;126(6):1208-16.

2. Larach DB, Hah JM, Brummett CM. 2022;136(4):594-608.

3. Lawal OD, Gold J, Murthy A, Ruchi R, Bavry E, Hume AL, et al. 2020;3(6):e207367.

4. van Amsterdam J, Pierce M, van den Brink W. 2021;43(1).

Figure 1: Recruitment flowchart

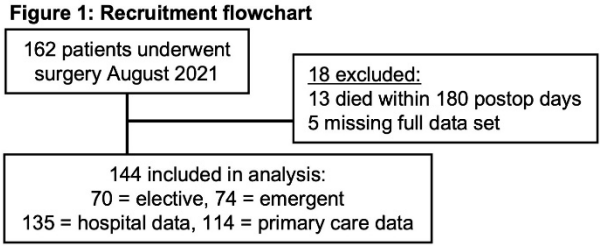

Table 1: Patient demographics.			
	PPOU		
Characteristic	No (n = 100)	Yes (n = 14)	*p*-value
Sex			
Male	62 (62)	7 (50)	
Female	38 (38)	7 (50)	.390*
Age, median (range [IQR])	70.5 (19-96 [24])	64.5 (29-86 [18])	.329‡
Ethnicity			
White British	81 (81)	12 (85.7)	
Other	19 (19)	2 (14.3)	.992*
Type of surgery			
Elective	52 (52)	7 (50)	
Emergent	48 (48)	7 (50)	.888*
Length of stay, days, median (range [IQR])	6.0 (0-50 [8])	5.5 (1-22 [7])	.927‡
Required ICU	5 (5)	1 (7.1)	.743*
Discharge			
Home	99 (99)	14 (100)	
Non-home	1 (1)	0 (0)	.707*
Cancer	27 (27)	7 (50)	.083*
Ischaemic heart disease	33 (33)	4 (28.6)	1.0°
Arthritis	19 (19)	3 (21.4)	1.0°
Chronic lung disease	13 (13)	4 (28.6)	.221°
Diabetes	21 (21)	2 (14.3)	.731°
Depression	11 (11)	7 (50)	**< .001***
Anxiety	8 (8)	4 (28.6)	**.043°**
Other psychological diagnosis	4 (4)	2 (14.3)	.163°
Alcohol usage	10 (10)	3 (21.4)	.207°
Smoking	28 (28)	5 (35.7)	.583*
Substance abuse	3 (3)	1 (7.1)	.418°
Preadmission overdose	1 (1)	2 (14.3)	**.041°**
Benzodiazepines	4 (4)	2 (14.3)	.158°
Antidepressants	13 (13)	5 (35.7)	**.029***
GABA drugs	6 (6)	2 (14.3)	.255°

PPOU = persistent postoperative opioid use, ICU = intensive care unit, IQR = interquartile range. All values are no. (%) unless otherwise stated under Characteristics.
* = Chi-squared test
° = Fisher's exact test
‡ = Mann-Whitney U test

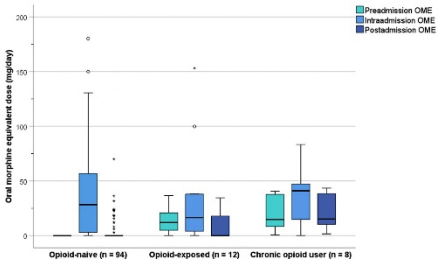

Figure 2: Boxplots of OME before, during, and after admission for patients who were opioid-naïve, opioid-exposed, or chronic users before surgery. Solid lines = medians, boxes = IQR, whiskers = range, stars and dots = outliers.

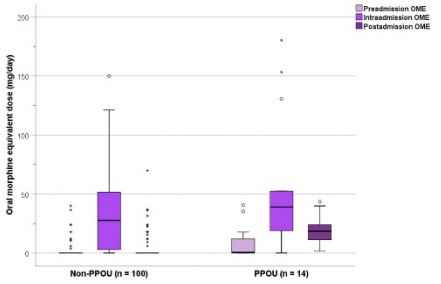

Figure 3: Boxplots of OME before, during, and after admission for patients who were either classified as PPOU or not. Solid lines = medians, boxes = IQR, whiskers = range, stars and dots = outliers.

Pain Medicine 8- Preoperative Predictors of Prolonged Opioid Use in the 6 Months Following Total Knee Arthroplasty

Daniel Larach[1], Miklos Kertai[1], Frederic Billings[2], Sara Anderson[1], Gregory Polkowski[1], Andrew Shinar[1], Ginger Milne[1], Puneet Mishra[1], Stephen Bruehl[1]

Vanderbilt University Medical Center[1] Vanderbilt University[2]

Introduction: Prolonged postoperative opioid use increases risk for new post-procedural opioid use disorder.[1] Although large retrospective database studies examining persistent post-surgical opioid use rates are available,[2] lack of systematic prospective data examining risk factors for persistent opioid use represents a significant research gap.[3] This study evaluated preoperative phenotypic factors predicting prolonged postoperative opioid use while controlling for contemporaneous pain intensity (a confound rarely addressed) and with and without controlling for influence of preoperative opioid use (a known predictor of prolonged use).

Methods: We performed a secondary analysis of a prospective observational cohort undergoing total knee arthroplasty (TKA) at an academic medical center between 2017-2021 with 6-week and 6-month follow-up. Subjects were osteoarthritis patients aged ≥55 undergoing unilateral TKA. In addition to assessing the impact of preoperative opioid use, we hypothesized *a priori* based on prior mechanistic and clinical literature that the following preoperative factors would predict more prolonged postoperative opioid use: greater lifetime opioid exposure; prior positive subjective opioid responses (e.g., euphoria); greater depression, catastrophizing, and anxiety; more widespread pain, pain interference, and central sensitization (indexed by punctate temporal summation); and greater sleep disturbance. Primary outcome was days/week of opioid use at 6 weeks and 6 months postoperatively.

Given the opioid use outcome distributions, primary analyses used generalized linear models specifying a negative binomial distribution, and adjusted for sex, age, and body mass index, as well as past-24-hour worst pain intensity assessed contemporaneously with opioid use outcomes (to evaluate opioid use beyond that attributable to postoperative pain). To evaluate combined predictor models, significant phenotype predictors in primary analyses were subjected to principal components analysis. Two factors were extracted: a negative affect/sleep disturbance/pain-related factor (NA factor) and an opioid-related factor. These factors and preoperative opioid use were tested as predictors of daily versus non-daily opioid use in receiver operating characteristic curve analyses, with area under the curve (AUC) indicating predictive accuracy.

Results: Primary opioid outcome data were available for 108 of 113 patients in the final cohort (mean age 67.4 [SD 6.91], 63.9% female); 12 (11.3%) and 6 (5.6%) patients used opioids daily at 6 weeks and 6 months, respectively. At 6 weeks, greater preoperative opioid use (aOR 3.83 [95% CI 1.58-9.31]), cumulative opioid exposure (aOR 1.52 [1.22-1.89]), depression (aOR 1.11 [1.06-1.15]), catastrophizing (aOR 1.05 [1.03-1.08]), anxiety (aOR 1.03 [1.01-1.06]), pain interference (aOR 1.07 [1.02-1.12]), sleep disturbance (aOR 1.07 [1.03-1.11]), and central sensitization (aOR 1.43 [1.17-1.76]) were significantly associated with more days/week of opioid use. At 6 months, significant predictors of greater days/week of opioid use included: greater preoperative opioid use (aOR 307.19 [24.86-3796.07]), cumulative opioid exposure (aOR 19.26 [3.36-110.54]), depression (aOR 1.14 [1.06-1.22]), catastrophizing (aOR 1.10 [1.05-1.15]), anxiety (aOR 1.06 [1.02-1.11]), pain interference (aOR 1.11 [1.03-1.21]), sleep disturbance (aOR 1.18 [1.09-1.27]), central sensitization (aOR 2.20 [1.47-3.28]), and prior euphoric response to opioids (aOR 1.85 [1.08-3.18]; **Table 1**). At 6-week follow-up, the predictors identified above (except anxiety) remained significant even after controlling for preoperative opioid use. At 6-month follow-up, cumulative opioid exposure, catastrophizing, pain interference, and sleep disturbance remained significant predictors after adjusting for preoperative opioid use. In multivariable predictor models, the NA factor most accurately predicted 6-week daily opioid use (AUC=0.84; **Figure 1**). A combined predictive model incorporating NA factor scores, opioid-related factor scores, and preoperative opioid use showed near-perfect predictive accuracy at 6 months (AUC=0.97; **Figure 2**).

Conclusions: Preoperative psychosocial, pain-related, and opioid-related phenotypic characteristics predicted prolonged opioid use following TKA. Future risk stratification algorithms should incorporate these predictors as well as preoperative opioid use to optimally predict risk for persistent postoperative opioid use.

References: 1. Ann Surg 2022;10.1097/sla.0000000000005372.

2. Anesthesiology 2020;132:1528-39.

3. Anesthesiology 2020;132:1304-6.

Table 1. GLM analyses of prospective preoperative predictors of days per week of opioid use at post-TKA follow-up.

	6-Week Follow-Up					6-Month Follow-Up				
Preoperative Predictor	Beta	SE	P value	Adj OR	95% CI	Beta	SE	P value	Adj OR	95% CI
Preoperative Opioid Use	**1.344**	**0.452**	**.003**	**3.83**	**1.58, 9.31**	**5.727**	**1.283**	**<.001**	**307.19**	**24.86, 3796.07**
HOME-Euphoric Response	-0.020	0.163	.902	0.98	0.71, 1.35	**0.615**	**0.276**	**.026**	**1.85**	**1.08, 3.18**
HOME-Opioid Exposure	**0.417**	**0.113**	**<.001**	**1.52**	**1.22, 1.89**	**2.958**	**0.892**	**<.001**	**19.26**	**3.36, 110.54**
CES-D	**0.101**	**0.022**	**<.001**	**1.11**	**1.06, 1.15**	**0.130**	**0.035**	**<.001**	**1.14**	**1.06, 1.22**
CATS	**0.053**	**0.013**	**<.001**	**1.05**	**1.03, 1.08**	**0.091**	**0.024**	**<.001**	**1.10**	**1.05, 1.15**
STAI	**0.031**	**0.015**	**.035**	**1.03**	**1.01, 1.06**	**0.060**	**0.023**	**.009**	**1.06**	**1.02, 1.11**
MBM	-0.030	0.047	.520	0.97	0.89, 1.06	0.095	0.071	.183	1.10	0.96, 1.26
PROMIS Pain Interference	**0.065**	**0.023**	**.005**	**1.07**	**1.02, 1.12**	**0.108**	**0.040**	**.007**	**1.11**	**1.03, 1.21**
PROMIS Sleep Disturbance	**0.063**	**0.020**	**.001**	**1.07**	**1.03, 1.11**	**0.163**	**0.039**	**<.001**	**1.18**	**1.09, 1.27**
Temporal Summation of Pain	**0.360**	**0.105**	**<.001**	**1.43**	**1.17, 1.76**	**0.786**	**0.204**	**<.001**	**2.20**	**1.47, 3.28**

Note: Analyses of the continuous days per week of opioid use outcome specified a negative binomial distribution. Significant results are highlighted in bold text. TKA = Total Knee Arthroplasty, HOME = History of Opioid Medical Exposure, CES-D = Center for Epidemiological Studies Depression Scale, CATS = Catastrophizing Scale, STAI = State Trait Anxiety Inventory, MBM = Michigan Body Map.
Each analysis was adjusted for sex, age, body mass index, and contemporaneous past-24-hour worst pain intensity.

Figure 1. ROC curves displaying classification accuracy of preoperative opioid use and factor analysis-derived combined phenotype predictors of subsequent daily opioid use versus non-daily opioid use at 6 weeks post-TKA.

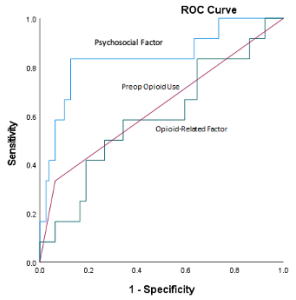

Figure 2. ROC curves displaying classification accuracy of preoperative opioid use and factor analysis-derived combined phenotype predictors of subsequent daily opioid use versus non-daily opioid use at 6 months post-TKA.

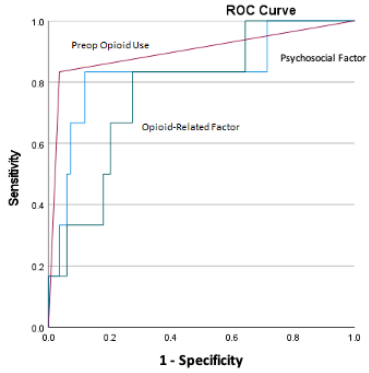

Pain Medicine 9- The Impact of the COVID-19 Pandemic on Opioid Overdose Deaths Among Racial Groups in the United States

Richie Chu[1], Sai Sarnala[1], Thanh Doan[1], Tina Cheng[1], Annabel Chen[2], Gloria Kim[3], Armaan Jamal[3], Robert Huang[3], Malathi Srinivasan[3], Latha Palaniappan[3], Eric Gross[4]

Stanford Center for Asian Health Research and Education[1] Stanford University[2] Stanford University School of Medicine[3] Stanford Medical Center[4]

Introduction: In 2017, the U.S. Department of Health and Human Services declared the opioid epidemic a public health crisis.[1] Subsequently, the COVID-19 pandemic has caused an increase in opioid overdose deaths, but how opioid overdose deaths have impacted different racial communities during the COVID-19 pandemic remains unclear.[2] Our objective is to understand how the COVID-19 pandemic impacted the prevalence and intention of opioid overdose deaths among racial groups.

Methods: We used data from the National Vital Statistics System Mortality component (NVSS-M) from 2019 to 2020 to examine opioid overdose underlying cause of deaths among Non-Hispanic Whites; Non-Hispanic Blacks; Non-Hispanic Asian American and Pacific Islanders (AAPI); and Hispanics. We conducted an observational, cross-sectional study looking at differences between these racial groups 10 months before the start of COVID-19 pandemic (May 2019-February 2020, n = 61411) and 10 months after the start of the COVID-19 pandemic (March 2020-December 2020, n = 78968). Underlying causes of death due to opioid overdose deaths were based on the International Statistical Classification of Diseases and Related Health Problems, Tenth Revision (ICD-10). We used the following ICD-10 codes: X40-44 (unintended overdose), X60-64 (suicide), X85 (homicide), and Y10-Y14 (intent undetermined). We calculated and compared opioid overdose crude mortality rates per 100,000 people based on state population using 2019 and 2020 American Community Survey data.

Results: Comparing 10 months before and after the start of the COVID-19 pandemic, all racial groups, Non-Hispanic Whites, Non-Hispanic AAPI, Hispanics, and Non-Hispanic Blacks experienced increases in opioid overdose deaths (24%, 35.94%, 37.11%, and 41%, respectively). The percentage of intentional self-harm opioid overdose deaths still remained the highest in the Non-Hispanic AAPIs (at 11.43%). We also found that somewhat surprisingly, the proportion of intentional self-harm opioid overdose deaths decreased by 1-3% for all racial groups relative to percentages prior to the COVID-19 pandemic.

Conclusions: Our findings suggest that the COVID-19 pandemic has drastically, but variably, increased opioid overdose deaths across all racial groups in the United States. In particular, minority groups (Non-Hispanic Black, Non-Hispanic AAPI, and Hispanic) experienced 12% to 22% higher increases in opioid overdose deaths compared to Non-Hispanic Whites. Despite a small decrease, Non-Hispanic AAPIs remain the racial group with the highest proportion of intentional self-harm opioid overdose deaths. Further prospective studies are warranted to elucidate the causes of the varying effects of the pandemic on opioid overdose deaths by racial group and by geographic region. Understanding what communities were most vulnerable and affected by opioid-related mortality during the COVID-19 pandemic can hone public health interventions and policies to address this growing issue.

References: 1. Haffajee RL, Frank RG. Making the Opioid Public Health Emergency Effective. JAMA Psychiatry. 2018;75(8):767-768. doi:10.1001/jamapsychiatry.2018.0611

2. Hedegaard H, Miniño AM, Spencer MR, Warner M. Drug overdose deaths in the United States, 1999–2020. NCHS Data Brief, no 428. Hyattsville, MD: National Center for Health Statistics. 2021. DOI: https://dx.doi.org/10.15620/cdc:112340external icon.

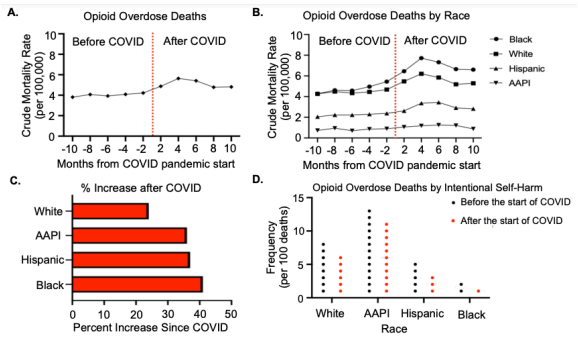

Figure. U.S. opioid overdose deaths 10 months before and 10 months after the start of the COVID pandemic *For **A** and **B**, the vertical red line is the start of the COVID-19 pandemic in March 2020. The left of the red line are the 10 months before and to the right of the line is the 10 months after the start of the COVID pandemic. **A.** Crude opioid overdose deaths per 100,000. **B.** Crude opioid overdose mortality rate per 100,000 by racial group. **C.** Percent increases in opioid overdose deaths since the start of the COVID-19 by race. **D.** Frequency of intentional self-harm deaths per 100 opioid overdose deaths.

Patient Blood Management

Patient Blood Management 1- Effect Analysis of Antifibrinolytics in Coronary Artery Bypass Surgery: Tranexamic Acid versus Epsilon-Aminocaproic Acid

Daniel Raza[1], Bradford Seem[2], Brad Skene[2], Ethan Sheinbaum[2], David Allain[2], Cara Bevinetto[2], Logan Kosarek[2], David Broussard[2], George Gilly[2], Jay Trusheim[3], Jacob Lessing[3], Christopher Owen[3], Jason Falterman[3], Bobby Nossaman[3]

Tulane University School of Medicine - - New Orleans, LA[1] Ochsner Clinical School[2] Ochsner Health[3]

Introduction: Intra and post-operative bleeding can worsen outcomes in patients undergoing coronary artery bypass surgery (CABG).[1] Antifibrinolytic agents, tranexamic acid (TXA) and epsilon-aminocaproic acid (ε-ACA) reduce intraoperative bleeding.[2] We evaluated the efficacy of TXA and ε-ACA on perioperative bleeding in patients undergoing CABG.

Methods: Our retrospective cohort study analyzed the medical records of 630 patients who underwent CABG from July 2021 to July 2022 at all surgical centers under one hospital system. The selection of patients was for both on-pump and off-pump CABG procedures. The outcomes of interest included estimated blood loss, intraoperative cell saver, intraoperative and postoperative chest tube drainage at 24 and 48 hours, and intraoperative and postoperative administration of blood products at 24 and 48 hours. TXA was used in 275 patients (44% CI 39-48%), ε-ACA was used in 167 patients (27% CI 23-30%), and 188 patients (30% CI 26-34%) did not receive antifibrinolytic therapy for surgery. Measures of effect size were developed with standardized mean differences.[3] JMP 16.2 (SAS Institute, Cary, NC) was utilized for all statistical analyses.

Results: Following Institutional Review Board approval, all patients who underwent CABG from July 2021 – July 2022 were included in our study. Three patients were excluded for not undergoing the procedure. TXA was associated with lower estimated blood loss (EBL) and cell-saver administration volumes compared to both ε-ACA and the control groups. Post-operative drainage at 24 hours was lower in TXA compared to ε-ACA and control. Intraoperative blood transfusions were higher with antifibrinolytics compared to patients given no antifibrinolytics. At 24 hours, lower blood transfusions were observed in the control group, while no relationship was found 48 hours after surgery. Results are shown in table 1.

Conclusions: TXA was more effective in reducing estimated blood loss, cell-saver, and post-operative drainage when compared to ε-ACA. Patients who received antifibrinolytics had a relatively higher risk for intraoperative blood transfusions in CABG. Although the use of antifibrinolytics has been extensively studied, standardized guidelines for using antifibrinolytics, patient risk profiles, and transfusion thresholds need to be established to optimize health outcomes.[4]

References:

1. "Effects of Tranexamic Acid on Postoperative Bleeding and Related Hematochemical Variables in Coronary Surgery: Comparison between On-Pump and Off-Pump Techniques. 128(1):83-91, 2004.
2. Comparison of Effectiveness of Tranexamic Acid and Epsilon-amino-Caproic-Acid in Decreasing Postoperative Bleeding in Off-pump CABG Surgeries: A Prospective, Randomized, Double-blind Study. 23(1): 65–69, 2020.
3. Using Effect Size or Why the P Value Is Not Enough. 4(3):279-82, 201.
4. The effect of tranexamic acid in blood loss and transfusion volume in adolescent idiopathic scoliosis surgery: a single-surgeon experience. 7(3):245-249. 2013.

Table 1. Comparisons of Antifibrinolytic Therapy in Patients Undergoing CABG

Outcomes		No Antifibrinolytic (Control)	Antifibrinolytics			
			Tranexamic Acid	TXA Std. Mean Difference	ε-Aminocaproic Acid	ε-ACA Std. Mean Difference
Estimated Blood Loss (ml), median [CI]		500 [200-600]	200 [100-200]	0.63	500 [250-500]	-0.34
Cell Saver (ml), median [CI]		515 [400-690]	412 [286-600]	0.42	530 [425-750]	-0.33
Post-operative Drainage (ml), median [CI]	POD 0	560 [370-800]	450 [305-675]	0.34	615 [480-870]	-0.27
	POD 1	335 [220-490]	225 [158-410]	0.34	356 [240-565]	-0.27
Intraoperative Blood Transfusion (units)		0.6 [0.4-0.8]	1.5 [1.1-2.0]		1.0 [0.74-1.4]	
Post-operative Blood Transfusion (units)	POD 0	0.8 [0.6-1.0]	1.1 [0.8-1.4]		1.1 [0.8-1.5]	
	POD 1	1.1 [0.7-1.6]	0.8 [0.6-1.1]		1.1 [0.8-1.7]	

Note: Continuous variables are reported as median [interquartile ranges 25% - 75%]. Dichotomous variables are reported as relative risk [95% confidence intervals]; Standardized differences were based upon means or proportions when divided by their pooled standard deviations.
ε-Aminocaproic Acid; POD: Post-operative Day; TXA: Tranexamic Acid; Std. Mean Difference: Standardized Mean Difference.

Patient Blood Management 2- ROTEM® Analysis of Sodium Citrate Toxicity Effect in Cardiac Surgical Patients: An In Vitro Study

Anthony Wang[1], Jeremy Reeves[1], Alberto Uribe[1], Mahmoud Abdel-Rasoul[2], Amy Baumann[3], Victor Davila[4]

The Ohio State University Wexner Medical Center[1] The Ohio State University[2] The Ohio State University Wexner Medical Center / The James[3] Ohio State University Medical Center[4]

Introduction: Cardiovascular surgeries often involve blood transfusions, with cardiac valve replacements and coronary artery bypass grafts demonstrating the highest risk of blood transfusion requirements among all cardiac surgeries [1].

Calcium (Ca^{2+}) plays a significant role in coagulation and platelet adhesion due to its activation effect of clotting factors and function in stabilizing fibrinogen and platelets at the damaged endothelium [2]. Hypocalcemia is a common event during massive transfusion of blood products; this is caused by the chelation (coordinated bond) of serum Ca^{2+} and citrate [2]. Sodium citrate is a blood anticoagulant that sequesters ionized Ca^{2+} in blood, and it is often used in blood products. Each unit of packed red blood cells or fresh frozen plasma holds approximately 3 grams of citrate anticoagulant as a preservative; this is rapidly cleared by a healthy individual's liver in 5 minutes [2]. However, in a patient with hemorrhagic shock, the rapid infusion of blood products and decreased hepatic clearance could lead to citrate clearance impairment [2]. Therefore, citrate overdose is known to cause hypocalcemia-induced coagulopathy with potentially fatal effects.

Rotational thromboelastometry (ROTEM®) is a novel point-of-care (POC) testing device that provides an accurate assessment of the coagulation status and supports guided selection of anticoagulation therapy as needed, reducing then the transfusion and bleeding-associated complications during or after cardiac surgery [3]. However, the 3.2 % sodium citrate plastic vacutainer tubes used to perform ROTEM tests may delay the diagnosis of citrate-induced hypocalcemia and coagulopathy in this surgical population. This study aimed to identify significant dose-dependent changes on ROTEM®'s INTEM (intrinsic pathway), EXTEM (extrinsic pathway), and fibTEM (fibrinogen availability) assays at toxic citrate doses previously shown to cause significant hypocalcemia and coagulopathy [4,5].

Methods: After IRB approval, we conducted a prospective, in vitro, pilot study that enrolled ten adult patients scheduled to undergo elective major cardiac surgery from June 2022 through August 2022.

In the morning prior to surgery, blood was obtained from each of the ten patients and deposited in three 3 mL plastic vacutainer tubes. Each tube contained 0.3 mL of 3.2% sodium citrate (the standard ROTEM test tube). Subsequently, each tube received an additional 0 µL, 50 µL or 150 µL dose of 3.2% sodium citrate and a complete ROTEM® test was performed. Clotting Time (CT), Clot Formation Time (CFT), α-angle, Maximum Clot Firmness (MCF), Clot Firmness 10 minutes after CT (A10), and Maximum Lysis (ML) were measured in ROTEM® EXTEM, INTEM, and fibTEM. A linear mixed effects model with random intercepts was used to compare means between the treated and baseline samples.

Results: Overall, there were few significant effects of a toxic plasma concentration of citrate found in the ROTEM® results for early ROTEM® parameters among all tubes. The intrinsic pathway (INTEM) had a significant decrease in coagulation time (seconds) when comparing the 0 µL with the 50 µL tubes (173.9 [156.7-191.1] vs. 155.6 [138.4-172.8], p-value 0.0462, respectively) [Table 1]. In addition, when comparing maximum lysis (ML%) in the 0 µL vs. 50 µL or 150 µL tubes, there was a significant decrease in the ML% from the EXTEM assays (ML % 6.2 [3.8-8.6] vs 4.3 [1.9-6.7] and 3.5 [1.1-5.9], p-value 0.0031 and <0.0001 respectively) and INTEM assays (ML % 6.1 [3.7-8.5] vs 4.6 [2.2-7.0] and 3.7 [1.3-6.1], p-value 0.0041 and <0.0001 respectively) [Table 1]. Lastly, the fibrinogen availability assay had a significant increase in MCF mm when comparing the 0 µL with the 50 µL tubes (19.1 [14.1-24.1] vs. 20.8 [15.8-25.8], p-value 0.043, respectively) [Table 1].

Conclusions: The results from our study suggest that there were few significant effects of a toxic plasma concentration of citrate found in the ROTEM® results for early ROTEM® parameters among all tubes. There was a slightly lower rate of clot lysis, but this would only be detectable after allowing a full 60-minute run of the ROTEM® graph. Therefore, these results do not support the use of ROTEM® for the diagnosis of citrate toxicity.

References:

1. Br J Surg. 2020; 107(13):e642-e643.
2. J of Surg Res. 2016; 202(1):182-187.
3. J Cardiothorac Vasc Anesth. 2012; 26(6):1083-93.
4. J Cardiothorac Vasc Anesth. 2004; 18(5):581-586.
5. Perfusion. 2018; 33(7):577-583.

Table 1. Comparison of means between ROTEM® parameters of 0 µL (baseline) and 50 µL of additional 3.2% sodium citrate treatment, and between baseline and 150 µL of additional 3.2% sodium citrate treatment.

ROTEM® analysis, median IQR	Baseline	50 µL Citrate Ca.	150 µL Citrate Ca.	Baseline vs 50 µL p-value	Baseline vs 150 µL p-value
Ex-tem®					
CT, s (normal range, 38-79)	92.4 (53.7, 131.1)	62.6 (23.9, 101.3)	66.2 (27.5, 104.9)	0.2741	0.3351
CFT, s (normal range, 34-159)	107.9 (50.9, 164.9)	139.4 (82.4, 196.4)	90.8 (33.8, 147.8)	0.4088	0.6516
A10, mm (normal range, 43-65)	53.2 (46.1, 60.3)	49.2 (42.1, 56.3)	54.5 (47.4, 61.6)	0.2567	0.7079
MCF, mm (normal range, 50-72)	60.9 (54.1, 67.7)	57.9 (51.1, 64.7)	63.5 (56.7, 70.3)	0.3604	0.4266
ML, % (normal range, 0-15)	6.1 (3.7, 8.5)	4.6 (2.2, 7.0)	3.7 (1.3, 6.1)	0.0041	<.0001
In-tem®					
CT, s (normal range, 100-240)	173.9 (156.7, 191.1)	155.6 (138.4, 172.8)	167.0 (149.8, 184.2)	0.0462	0.4301
CFT, s (normal range, 30-110)	91.3 (62.3, 120.3)	84.0 (55.0, 113.0)	84.8 (55.8, 113.8)	0.5657	0.6087
A10, mm (normal range, 44-66)	54.4 (48.0, 60.8)	52.8 (46.4, 59.2)	54.2 (47.8, 60.6)	0.3364	0.9031
MCF, mm (normal range, 50-71)	61.3 (55.1, 67.5)	60.1 (53.9, 66.3)	62.4 (56.2, 68.6)	0.3822	0.4223
ML, % (normal range, 0-15)	6.2 (3.8, 8.6)	4.3 (1.9, 6.7)	3.5 (1.1, 5.9)	0.0031	<.0001
Fib-tem®					
A10, mm (normal range, 7-23)	17.6 (13.2, 22.0)	18.8 (14.4, 23.2)	17.8 (13.4, 22.2)	0.1731	0.8158
MCF, mm (normal range, 9-25)	19.1 (14.1, 24.1)	20.8 (15.8, 25.8)	19.9 (14.9, 24.9)	0.043	0.3191

Legend: **ROTEM**= rotational thromboelastometry, **Ex-tem**= blood clot formation initiated via the extrinsic coagulation cascade, **In-tem**= blood clot formation via the intrinsic coagulation cascade, **Fib-tem**= blood clot formation via the extrinsic coagulation cascade, platelets inhibited, **CT**= clotting time, **CFT**= clot formation time, **A10**= amplitude of clot firmness 10 minutes after CT, **MCF**= maximum clot firmness, **ML**= maximum lysis.

Patient Blood Management 3- Racial disparities in the association between preoperative anemia and postoperative morbidity and mortality

Oluwadara Nafiu[1], Christian Mpody[2], Joseph Tobias[2]

Carle Illinois College of Medicine[1] Nationwide Children's Hospital[2]

Introduction: Preoperative anemia is associated with a heightened risk of morbidity and mortality, although little is known on the differential impact of preoperative anemia on babies of different race and ethnicity.[1] We evaluated whether racial differences exist in the association between preoperative anemia and postoperative morbidity and mortality.

Methods: We performed a retrospective cohort study of neonates (≤ 30 days) from the American College of Surgeons National Surgical Quality Improvement Program for Pediatrics (NSQIP-P), who underwent inpatient pediatric surgery between 2012 and 2019. We included patients in the analytical sample if they had preoperative anemia, defined as a hematocrit < 40% (Youden J index). We excluded babies who received a preoperative blood transfusion. We compared the risk-adjusted rates of 30-day postoperative mortality and morbidity for the two racial groups.

Results: We identified 13,004 anemic neonates of whom 17.8% were black. In the presence of anemia, babies of black race were significantly more likely to develop postoperative complications than their white counterparts (35.9% versus 31.4%; odds ratio [OR], 1.30; 95% confidence interval [CI], 1.10-1.53; P < 0.01). In particular, black patients had a significantly higher rate of postoperative pulmonary complications (8.7% versus 6.8%; OR, 1.40; 95% CI, 1.06-1.85; P = 0.019). No statistically significant difference was found between the two racial groups with respect to 30-day mortality.

Conclusions: We compared the risk-adjusted incidences of postoperative mortality and morbidity between racial groups in the presence of preoperative anemia. We found that race appears to be an important determinant of postoperative complications. Our findings may have important policy implications, such as accounting for race in the management of preoperative anemia. Further research is warranted into identifying the reasons for these differences and determining strategies for minimizing the differential impact of preoperative anemia between children of different races.

References: Goobie SM, Faraoni D, Zurakowski D, DiNardo JA. Association of preoperative anemia with postoperative mortality in neonates. JAMA Pediatrics. 2016;170(9):855.

Table 1. Characteristics of 13,004 neonates of Black or White race who underwent surgical procedures at NSQIP-participating hospitals between 2012 and 2019.

	White	Black	Total
	n (%)	n (%)	n (%)
Study population	**9199 (70.74)**	**3805 (29.26)**	**13004 (100)**
Male sex	5482 (59.60)	2,198 (57.78)	7,680 (59.07)
Emergency case status	1392 (15.13)	553 (14.53)	1945 (14.96)
Preoperative sepsis	435 (4.73)	245 (6.44)	680 (5.23)
Preterm birth	6,771 (73.61)	3,117 (81.92)	9,888 (76.04)
Current pneumonia	22 (0.84)	12 (1.30)	34 (0.96)
Cardiac risk factors	4,991 (54.26)	2,285 (60.05)	7,276 (55.95)
Chronic lung disease	2,717 (29.54)	1,647 (43.29)	4,364 (33.56)
CNS abnormality	2,188 (23.79)	1,118 (29.38)	3,306 (25.42)
Congenital malformation	4,579 (49.78)	1,558 (40.95)	6,137 (47.19)
Pulmonary abnormality	1,636 (17.78)	578 (15.19)	2,214 (17.03)

Abbreviations: CNS, central nervous system; NSQIP, National Surgical Quality Improvement Program.

Table 2. Perioperative complications in neonates of Black and White race.

	White	Black	Non-adjusted		Adjusted	
	n (%)	n (%)	OR (95% CI)	P-value	OR (95% CI)	P-value
30-day mortality	218 (2.69)	100 (3.16)	1.18 (0.93, 1.50)	0.18	0.99 (0.64, 1.53)	0.961
Post-operative complications	1,826 (31.40)	821 (35.85)	1.22 (1.10, 1.35)	<0.01	**1.30 (1.10, 1.53)**	**<0.01**
Unplanned reoperation	856 (9.31)	376 (9.88)	1.07 (0.94, 1.21)	0.31	1.10 (0.83, 1.45)	0.501
Wound complications	226 (2.46)	105 (2.76)	1.12 (0.89, 1.42)	0.32	1.56 (0.90, 2.69)	0.111
Pulmonary complications	397 (6.82)	200 (8.72)	1.30 (1.09, 1.56)	<0.01	**1.40 (1.06, 1.85)**	**0.019**
Renal complications	21 (0.23)	5 (0.13)	0.56 (0.22, 1.53)	0.27	0.81 (0.21, 3.14)	0.763
Neurological complications	97 (1.05)	45 (1.18)	1.12 (0.79, 1.60)	0.52	1.16 (0.56, 2.40)	9.689
Cardiovascular complications	126 (1.37)	78 (2.05)	1.51 (1.13, 2.00)	<0.01	1.11 (0.61, 2.03)	0.725
Septic complications	217 (2.36)	100 (2.63)	1.12 (0.88, 1.42)	0.363	0.89 (0.52, 1.52)	0.670

Statistically significant values are indicated in bold. Abbreviations: OR, odds ratio; CI, confidence interval.

Patient Blood Management 4- The Impact of Intraoperative vs Postoperative Allogeneic Red Blood Cell Transfusions on Postoperative Complications in Pediatric Patients with Neuromuscular Scoliosis Undergoing Posterior Spinal Fusion

Michael Green[1], Scott Luhmann[2], Julie Drobish[3]

Washington University in St Louis School of Medicine[1] Washington University School of Medicine[2] Washington University[3]

Introduction: Neuromuscular scoliosis (NMS) patients undergoing posterior spinal fusion (PSF) are a complex and fragile patient population that usually require blood transfusions both during and after surgery, and are at high risk for postoperative complications.[1] Relatively little is known about how transfusion timing can impact the incidence of complications after surgery.[2] Our primary goals were to determine the perioperative transfusion requirements and corresponding hemoglobin levels of this patient population, and to describe the postoperative complications. Furthermore, we sought to determine whether the timing of packed red blood cell (pRBC) transfusions correlated to postoperative complications in this cohort of pediatric patients.

Methods: In this retrospective cohort study, we analyzed patients with NMS who had undergone PSF at our institution between 5/2017 and 11/2022. We collected demographic data including age, weight, and preoperative diagnoses. Other data points collected included length of surgery, estimated blood loss (EBL), preoperative, intraoperative, and postoperative hemoglobin (Hgb) levels until postoperative day 5, blood product transfusions during and after surgery, and postoperative complications. Specifically, complications were defined as respiratory complications (hypoxia, pneumonia, respiratory failure, pulmonary edema, and tracheitis), infectious complications (sepsis, surgical site infections, cellulitis, meningitis, spine infections, and pneumonia), other (seizures and hemodynamic instability), and death. Patients were analyzed in three groups: 1) first pRBC transfusion occurring intraoperatively (Group 1), 2) first pRBC transfusion occurring postoperatively (Group 2), and 3) no pRBC transfusions required (Group 3). Continuous variable data are presented as mean (SD). Statistical analysis was performed between groups using t-test, with p-values <0.05 considered statistically significant.

Results: A total of 52 cases were identified for inclusion based on NMS diagnosis and PSF surgery date between May 2017 and November 2022; three patients were excluded from analysis due to incomplete data. The mean age at the time of surgery was 13.7 (2.7) years, the mean weight was 36.8 (12.1) kg, the mean length of surgery was 5.2 (0.9) hours, and the mean EBL was 448 (224) ml.
Our transfusion data analysis showed that 80% received pRBC either intraoperatively or postoperatively, and 20% did not receive any transfusion. Among the 39 who were transfused, 31% were transfused intraoperatively, 5% were transfused immediately post-op, 54% were transfused on post-op days 1 or 2, and 11% were transfused after post-op day 2. (Fig.1)
The overall post-op complication rate was 52%, with 25% respiratory complications, 23% infectious complications, 13% other complications, and 2% died.
The postoperative infection rate in Group 1 (transfused intraoperatively) was 8%, in Group 2 (transfused postoperatively) was 39%, and in Group 3 (no transfusion) was 0%. (Fig.2) The infection complication rate of Group 1 compared to Group 3 was not significantly different ($p=0.34$), while Group 2 compared to Groups 1 and 3 were significantly different ($p=0.019$ & $p<0.001$ respectively).
We further analyzed the intraoperative Hgb nadir in Groups 1, 2, and 3, and found the means to be 7.0 (1.3), 9.4 (1.3), and 10.4 (1.9) g/dL, respectively. By plotting the intraoperative nadir (Fig.3), we found that patients with Hgb 8.2-10.2 g/dL were rarely transfused in the operating room but frequently required transfusions postoperatively, and had a high incidence of infectious complications.

Conclusions: We discovered a statistically significant association between postoperative transfusions and postoperative infections, whereas no statistically significant association exists between intraoperative transfusions or no transfusions and postoperative infections. Furthermore, an intraoperative Hgb nadir between 8.2 and 10.2 g/dL was predictive for a postoperative transfusion in this population 80% of the time, with only 10% being spared an exposure to blood products. Therefore, our data suggest that intraoperative transfusion may be safer than postoperative transfusion in terms of infectious complications, and that the intraoperative Hgb threshold for transfusion should perhaps be raised to 10.2 g/dL in this patient population so that the patients who would otherwise receive blood postoperatively could receive it instead intraoperatively. This theory would require further prospective study.

References: [1] J Neurosurg Spine. 2016 Oct;25(4):500-508.

[2] Global Spine J. 2019 Jun;9(4):434-445.

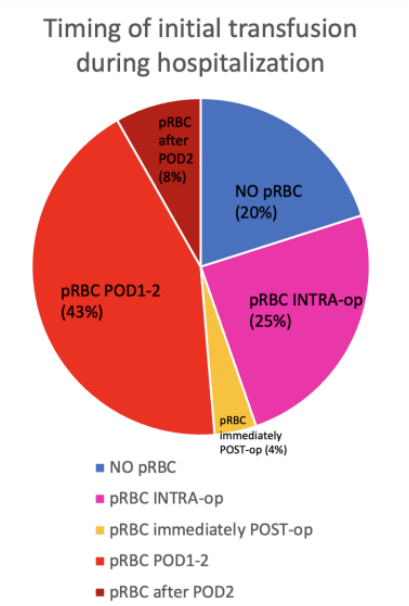
Timing of initial transfusion during hospitalization
pRBC after POD2 (8%)
NO pRBC (20%)
pRBC INTRA-op (25%)
pRBC POD1-2 (43%)
pRBC immediately POST-op (4%)
NO pRBC
pRBC INTRA-op
pRBC immediately POST-op
pRBC POD1-2
pRBC after POD2

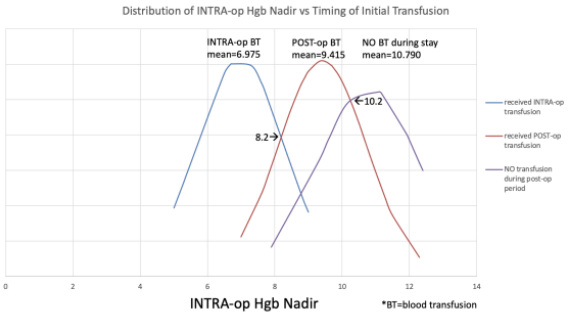
Distribution of INTRA-op Hgb Nadir vs Timing of Initial Transfusion
INTRA-op BT mean=6.975
POST-op BT mean=9.415
NO BT during stay mean=10.790
8.2
10.2
received INTRA-op transfusion
received POST-op transfusion
NO transfusion during post-op period
0
2
4
6
8
10
12
14
INTRA-op Hgb Nadir
*BT=blood transfusion

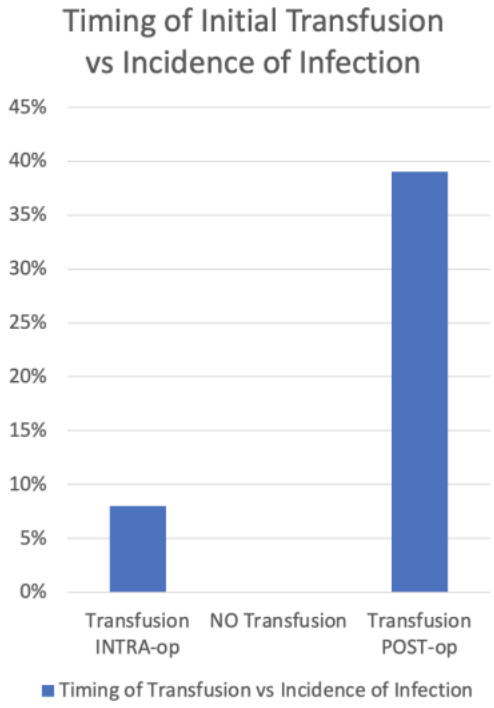
Timing of Initial Transfusion vs Incidence of Infection
45%
40%
35%
30%
25%
20%
15%
10%
5%
0%
Transfusion INTRA-op
NO Transfusion
Transfusion POST-op
Timing of Transfusion vs Incidence of Infection

Patient Blood Management 5- Trends in Gender of Authors of Patient Blood Management Publications from 2017-2021

Katherine Forkin[1], Caroline Render[1], Steven Staffa[2], Susan Goobie[3]

University of Virginia Health System[1] Boston Children's Hospital[2] Boston Children's Hospital, Harvard Medical School[3]

Introduction: Patient blood management (PBM) is an important aspect of thoughtful, targeted patient care that optimizes goal-directed transfusions while minimizing risks to patients. Diverse representation in this field may help bring varying perspectives to improve patient care. Miller and colleagues[1] reviewed gender-based trends among two anesthesiology journals and found female first authors increased over the 15-year period, particularly when the senior author was also female, noting mentorship plays a major role in advancement of female academic anesthesiologists. A recent study of two high impact journals (JAMA and NEJM) also demonstrated an under-representation with no evidence of improvement over time of female authorship.[2] Assessing trends of authorship in PBM publications may identify gender inequities and help in advocating for womens' involvement in PBM-related studies. We hypothesized there are fewer female compared to male first and last authors among recent PBM publications.

Methods: We reviewed manuscripts from 10 high-impact anesthesiology and blood transfusion medicine journals from 2017-2021 using 19 keywords to identify PBM-related articles. Each article title was reviewed independently by the researchers to determine whether it met inclusion criteria. Gender of the first and last author of each publication was identified by using a software program for the most common names. Gender that could not be idenfitied through this process was determined by querying institutional websites and professional social networks (e.g. ResearchGate). Any publication where gender of the first and/or last author could not be determined was excluded from analysis. Trends over time were assessed using the Cochran-Armitage test.

Results: 2,467 publications met inclusion criteria of the 2,873 yielded by the initial search. Gender of the first and last author were identified for 2,384 of the articles which were included in the final analysis. 42.8% of the total publications featured a female first author [Fig 1] with the highest being JAMA (48.7%), Transfusion (48.1%), and Eur J Anesth (44.0%), and the lowest being Br J. Anaesth (24.1%), Anesth Analg (24.4%), and Anaesthesia (26.1%). 32.0% of the publications featured a female last author (Fig 1) with the highest being Transfusion (36.9%), Anaesthesia (31.8%), and Eur J Anesth (30.6%) and the lowest being Anesth Analg (18.3%), Anesthesiology (18.6%), and Br J Anaesth (23.5%). 57.6% of publications had either a first or last author who was female while 16.3% of publications had both female first and last authors. 32.6% of PBM articles with only one author was female. Female first authorship did not change significantly over the study period (P=0.115) [Fig 2]. Similarly, female last authorship did not change significantly over this time (P=0.119). There was no significant difference from 2017-2021 in the percentage of PBM articles with a female first or last author, with a female first and last author, or with a female single author (P=0.089, P=0.055, and P=0.226, respectively).

Conclusions: The percentage of female first and last authorship in PBM publications from 2017-2021 was less than 50%. Gender equality in PBM authorship was identified as an area for improvement. High impact journals should lead the way with editors appointed as diversity, equity, and inclusion champions and should evaluate their data frequently to assess for gender equity. Female mentorship and sponsorship remain important in promoting gender equity in PBM authorship.

References: 1. Miller J, Chuba E, Deiner S, et al. Trends in Authorship in Anesthesiology Journals. Anesth Analg. 2019;129(1):306-310.

2. Abdalla M, Abdalla M, Abdalla S, Saad M, Jones DS, Podolsky SH. The Under-representation and Stagnation of Female, Black, and Hispanic Authorship in the Journal of the American Medical Association and the New England Journal of Medicine. J Racial Ethn Health Disparities. 2022; 1–10.

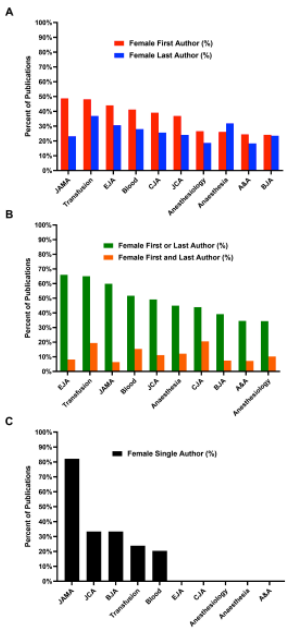

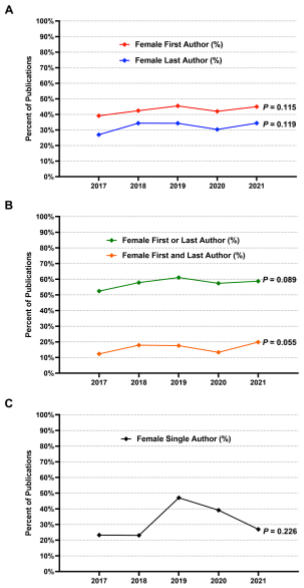
A
Female First Author (%)
Female Last Author (%)
P = 0.115
P = 0.119
B
Female First or Last Author (%)
Female First and Last Author (%)
P = 0.089
P = 0.055
C
Female Single Author (%)
P = 0.226
Percent of Publications
100%
90%
80%
70%
60%
50%
40%
30%
20%
10%
0%
2017
2018
2019
2020
2021

Patient Safety

Patient Safety 1- Association of intraoperative opioid dose and clinical adverse outcomes: a hospital registry study

Simone Redaelli[1], Aiman Suleiman[1], Dario von Wedel[1], Sarah Ashrafian[2], Ricardo Munoz[3], MITRA KHANY[3], Catriona Stewart[3], John Hertig[4], Guanqing Chen[4], Sarah Nabel[4], Maximilian Schaefer[5], Satya Krishna Ramachandran[6]

Beth Israel Deaconess Medical Center, Harvard Medical School[1] Beth Israel Deaconess Medical Center[2] BIDMC[3] Butler University[4] Beth Israel Deaconess Medical Center & H[5] Harvard Medical School[6]

Introduction: Preventable adverse drug events and harmful errors when administering inpatient injectable medications result in more than one million hospitalizations per year [1]. Intraoperative opioid use has been associated with postoperative respiratory complications [2] and increased risk of readmission in surgical patients [3]. In this study, we hypothesized that higher doses of intraoperatively administered opioids are associated with higher risk of relevant patient safety events, defined according to the National Coordinating Council for Medication Error Reporting and Prevention (NCC MERP) classification [4].

Methods: This retrospective study included 182,109 adult patients who underwent general anesthesia at an academic tertiary healthcare center in Massachusetts, USA, between 2010 and 2020 and received intraoperative fentanyl, hydromorphone or morphine. Patients who had an American Society of Anesthesiology physical status >4, underwent cardiac procedure or were kept intubated after surgery were excluded. The primary exposure was the intraoperative opioid dose, categorized as: fentanyl >0-50 mcg, >50-100 mcg, and >100 mcg; hydromorphone >0-0.5 mg, >0.5-1 mg, and >1 mg; and morphine >0-2 mg, >2-4 mg, and >4 mg. Opioid categories were chosen according to available ready-to-administer (RTA) syringes or their clinically reasonable combinations. The primary outcome, according to the NCC MERP categories, was defined as a patient safety event that resulted in temporary harm to the patient and required intervention (Category E). The secondary outcomes included harm to the patient that required hospitalization (Category F, investigated only in outpatients); permanent patient harm (Category G), and need of interventions necessary to sustain life (Category H). Detailed components of the outcomes are presented in **Table 1**. Multivariable logistic regressions were applied, adjusting for a *priori* defined patient characteristics and comorbidities, as well as intraoperative factors and any additional opioid.

Results: Out of 182,109 included patients, 119,113 received fentanyl, 71,483 hydromorphone, and 8,906 morphine (**Figure 1**). The median (IQR) dose was 100 mcg (100-200) for the fentanyl cohort, 1 mg (0.6-1.2) for the hydromorphone cohort and 5 mg (4-8) for the morphine cohort. The primary outcome, Category E events, was observed in 19,916 (16.7%), 14,332 (20.1%), and 1,500 (16.8%) patients of the fentanyl, hydromorphone, and morphine cohort. Patients characteristics and distribution of variables according to the intraoperative opioid administered are presented in **Table 2**. In adjusted analysis, fentanyl was associated with higher risk of Category E at a dose of 50-100 mcg (aOR=1.65 [1.56-1.76], P<0.001, adjusted risk difference [ARD] 2%) and >100 mcg doses (aOR=1.58 [1.49-1.68], P<0.001, ARD 3%). Hydromorphone was not associated with the outcome at doses of 0.5-1 mg, while it was at doses >1 mg (aOR=1.13 [1.06-1.20], P<0.001, ARD 2%). Morphine was associated with an increased in risk Category E, both at doses of 2-4 mg (aOR=1.32 [1.07-1.62], P<0.01, ARD 3%) and >4 mg (aOR=1.44 [1.20-1.74], P<0.001, ARD 5%). Estimated risks of Category E per dose of opioids in oral morphine equivalents are presented in **Figure 2**. In secondary analyses, risk of Category F was increased for all fentanyl and hydromorphone doses, while only high morphine doses (>4 mg) were associated with higher risk of this outcome. No association among all the opioid doses and Category G was observed. The risk of Category H was increased in high (>100 mcg) fentanyl doses. No association with Category H was observed for morphine. Detailed results of adjusted analyses for secondary outcomes are summarized in **Table 3**.

Conclusions: Higher opioid doses were associated with increased risk of Category E safety events. Clinicians should carefully titrate the intraoperative opioid dose to decrease the incidence of adverse outcomes.

References:

1. National burden of preventable adverse drug events associated with inpatient injectable medications: healthcare and medical professional liability costs. Am Health Drug Benefits. 2012 Nov;5(7):1-10.
2. Effects of low-dose intraoperative fentanyl on postoperative respiratory complication rate: a pre-specified, retrospective analysis. Br J Anaesth. 2019 Jun;122(6):e180-e188.
3. Association between intraoperative opioid administration and 30-day readmission: a pre-specified analysis of registry data from a healthcare network in New England. Br J Anaesth. 2018 May;120(5):1090-1102.
4. Severity-indexed, incident report-based medication error-reporting program. Am J Hosp Pharm. 1991 Dec;48(12):2611-6.

Category E
• post-extubation desaturation • postoperative nausea and vomiting needing rescue treatment in PACU • postoperative somnolence or sedation needing nursing observation or administration of naloxone
Category F *(This category applies only to outpatients)*
• delayed discharge from PACU (LOS ≥120 minutes) with defined clinical cause • unplanned admission: booked outpatients who required unplanned admission • delayed discharge from hospital, defined as LOS >75th percentile • readmission within 30 days after hospital discharge (all cause)
Category G
• cardiac arrest within 7 days postoperatively • stroke within 7 days postoperatively
Category H
• unplanned intubation • unplanned ICU admission (all causes)

Table 1. Detailed components of the primary and secondary outcomes, defined according to the National Coordinating Council for Medication Error Reporting and Prevention. PACU, post-anesthesia care unit; LOS, length of stay

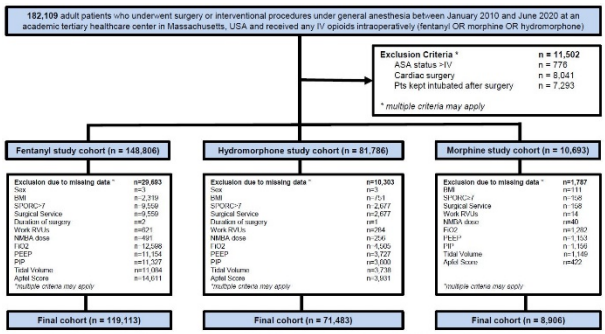

Figure 1. Study flow diagram indicating numbers of patients excluded due to exclusion criteria and missing data. IV, intravenous; ASA, American Society of Anesthesiology; Pts, patients; BMI, Body Mass Index; SPORC, Score for the Prediction of Postoperative Respiratory Complications; RVU, Relative Value Units; NMBA, Neuromuscular Blocking Agent; FiO2, Fraction of Inspired Oxygen; PEEP, Positive End Expiratory Pressure; PIP, Peak Inspiratory Pressure.

	Fentanyl N=119,113	Hydromorphone N=71,483	Morphine N=8,906
Age, years	58.0 (45.0 - 67.0)	58.0 (45.0 - 66.0)	54.0 (41.0 - 65.0)
Sex			
Female	51,850 (43.6%)	29,453 (41.1%)	3,983 (47.4%)
BMI, kg/m2	27.4 (25.0 - 31.0)	27.9 (26.1 - 32.3)	27.4 (24.0 - 32.1)
ASA physical status			
1	14,191 (11.9%)	7,366 (10.3%)	1,196 (13.3%)
2	67,889 (48.6%)	36,248 (58.7%)	4,519 (50.7%)
3	43,239 (36.3%)	28,105 (39.3%)	2,861 (33.6%)
4	3,824 (3.2%)	1,741 (2.4%)	210 (2.4%)
Year of surgery			
2010	10,478 (8.8%)	2,339 (3.3%)	1,913 (21.5%)
2011	11,366 (9.5%)	4,169 (5.8%)	1,736 (19.4%)
2012	12,214 (10.3%)	4,589 (6.3%)	2,268 (25.4%)
2013	13,098 (10.9%)	6,854 (9.5%)	1,142 (12.8%)
2014	12,346 (10.4%)	6,909 (12.5%)	379 (4.2%)
2015	12,371 (10.4%)	9,268 (13.0%)	66 (1.1%)
2016	11,430 (9.6%)	9,823 (13.7%)	18 (0.7%)
2017	10,810 (9.1%)	9,275 (13.0%)	124 (1.4%)
2018	11,661 (9.7%)	8,231 (8.7%)	1,134 (12.7%)
2019	10,666 (8.9%)	6,161 (11.4%)	35 (0.3%)
2020	2,833 (2.4%)	2,149 (3.5%)	6 (0.1%)
Charlson Comorbidity Index	0.0 (0.0 - 2.0)	0.0 (0.0 - 2.0)	0.0 (0.0 - 2.0)
Chronic heart failure	5,484 (4.6%)	2,786 (3.9%)	280 (3.1%)
Smokers	12,886 (10.8%)	8,562 (12.0%)	909 (9.6%)
OSAS	7,777 (6.5%)	4,592 (6.4%)	473 (5.3%)
Obstructive pulmonary disease	29,286 (24.6%)	17,126 (24.0%)	2,071 (23.3%)
Restrictive pulmonary disease	5,051 (4.2%)	2,495 (3.4%)	396 (4.3%)
SPORC3T	4,595 (3.9%)	2,258 (3.2%)	319 (3.6%)
Type of surgery			
Colorectal	3,229 (2.7%)	3,340 (4.7%)	292 (3.3%)
Dentistry	395 (0.3%)	275 (0.4%)	29 (0.3%)
Otorhinolaryngology	5,266 (4.4%)	1,897 (2.7%)	319 (3.6%)
Ophthalmology	229 (0.2%)	19 (0.0%)	n.a.
General	16,515 (13.9%)	9,094 (12.7%)	1,841 (20.7%)
Gastrointestinal	66 (0.1%)	8,602 (12.2%)	n.a.
Gynecology	14,031 (11.8%)	4,823 (6.8%)	1,022 (11.5%)
Neurosurgery	6,868 (5.8%)	18,961 (26.5%)	351 (3.9%)
Orthopedics	29,586 (24.8%)	8,687 (9.6%)	2,114 (23.8%)
Plastic	8,091 (6.8%)	176 (0.2%)	729 (8.2%)
Podiatry	590 (0.5%)	3,183 (4.5%)	42 (0.5%)
Surgical Oncology	4,900 (4.1%)	2,963 (4.1%)	371 (4.2%)
Thoracic	6,381 (5.4%)	1,671 (2.3%)	346 (3.9%)
Transplant	2,594 (2.2%)	2,842 (4.0%)	139 (1.6%)
Trauma	4,695 (3.4%)	4,349 (6.1%)	347 (3.9%)
Urology	10,793 (9.0%)	2,457 (3.4%)	595 (6.7%)
Vascular	5,542 (4.7%)	21,656 (29.8%)	367 (4.1%)
Emergency surgery	8,799 (7.4%)	5,360 (7.5%)	929 (10.4%)
Duration of surgery, min	126.0 (84.0 - 186.0)	167.0 (113.0 - 224.0)	143.0 (100.0 - 201.0)
Work RVU	12.1 (7.0 - 17.9)	15.8 (10.5 - 21.6)	14.4 (9.4 - 19.5)
Fentanyl, mcg	180.0 (100.0 - 280.0)	168.0 (25.0 - 205.6)	180.0 (100.0 - 280.0)
Morphine, mg	0.0 (0.0 - 0.0)	0.0 (0.0 - 0.0)	5.0 (4.0 - 5.0)
Hydromorphone, mg	0.0 (0.0 - 0.6)	1.0 (0.6 - 1.2)	0.0 (0.0 - 0.0)
Ketamine administration	8,120 (7.7%)	5,363 (13.1%)	395 (4.4%)
Dexmedetomidine administration	1,752 (1.5%)	1,762 (2.5%)	191 (1.9%)
Regional anesthesia (adjuvant)	12,989 (10.9%)	6,145 (8.6%)	670 (7.5%)
Age-adjusted MAC, %	1.0 (0.8 - 1.1)	1.0 (0.8 - 1.2)	1.0 (0.8 - 1.2)
Non-depolarizing NMBA, EDS95	1.7 (0.0 - 2.8)	2.3 (1.3 - 3.3)	2.0 (0.8 - 3.0)
Succinylcholine administration	44,441 (37.3%)	25,376 (35.5%)	4,216 (47.3%)
Neostigmine dose, mg/kg	0.0 (0.0 - 3.0)	2.0 (0.0 - 3.0)	2.0 (0.0 - 3.0)
Sugammadex use	12,494 (10.4%)	10,999 (14.8%)	473 (5.3%)
Crystalloid and colloid infusion, mL	1680.0 (700.0 - 1908.0)	1190.0 (600.0 - 1708.0)	1280.0 (600.0 - 1700.0)
Vasopressor dose, mg norepinephrine equivalents	0.0 (0.0 - 0.1)	0.0 (0.0 - 0.1)	0.0 (0.0 - 0.0)
Apfel Score			
Risk of PONV Low (10-20%)	34,448 (28.9%)	19,136 (26.8%)	2,366 (26.6%)
Risk of PONV Moderate (40%)	48,382 (40.6%)	28,470 (41.1%)	3,988 (41.4%)
Risk of PONV Severe (60%)	25,699 (21.5%)	16,137 (22.6%)	2,003 (22.5%)
Risk of PONV Very Severe (80%)	10,674 (9.0%)	6,800 (9.5%)	852 (9.6%)
Number of administered antiemetics			
0	10,073 (8.5%)	3,817 (5.3%)	814 (9.5%)
1	50,599 (42.5%)	28,264 (39.5%)	3,969 (47.2%)
2	48,190 (40.5%)	31,479 (44.0%)	3,892 (47.5%)
3	8,913 (7.5%)	7,212 (10.1%)	834 (9.4%)
4	936 (0.8%)	696 (1.0%)	84 (1.1%)
5	41 (0.0%)	23 (0.0%)	7 (0.1%)
6	n.a.	1 (0.0%)	n.a.
Minutes of mean arterial pressure below 55 mmHg	0.0 (0.0 - 2.0)	1.0 (0.0 - 3.0)	1.0 (0.0 - 3.0)
FiO$_2$, %	56.0 (50.5 - 64.0)	56.0 (51.0 - 61.3)	54.5 (48.5 - 60.0)
PEEP, cmH$_2$O	4.1 (2.5 - 5.1)	5.0 (2.5 - 5.1)	4.0 (2.5 - 5.0)
PIP, cmH$_2$O	19.3 (15.2 - 24.0)	20.8 (17.2 - 25.3)	21.0 (17.0 - 25.3)
Tidal Volume, mL	522.0 (431.5 - 592.0)	535.5 (471.0 - 597.0)	540.0 (484.5 - 620.0)

Table 2. Patient characteristics and distribution of variables. Data are presented as median (IQR) for continuous measures, and n (%) for categorical measures. BMI, Body Mass Index; ASA, American Society of Anesthesiology; OSAS, Obstructive Sleep Apnea Syndrome; SPORC, Score for the Prediction of Postoperative Respiratory Complications; RVU, Relative Value Units; MAC, minimal alveolar concentration; NMBA, Neuromuscular Blocking Agent; EDS5, amount of NMBD required to reduce twitch height by 95%; PONV, postoperative nausea and vomit; FiO_2, Fraction of Inspired Oxygen; PEEP, Positive End Expiratory Pressure; PIP, Peak Inspiratory Pressure; n.a., not applicable.

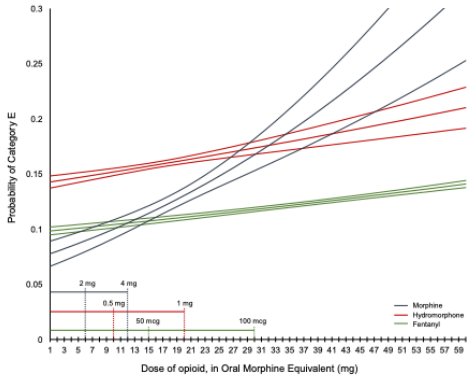

Figure 2. Estimated risk of postoperative Category E in patients who received fentanyl (in green), hydromorphone (in red) and morphine (in blue), stratified by oral morphine equivalent dose. The adjusted risk estimates with corresponding 95% confidence intervals for Category E are presented.

		Category F			Category G			Category H		
	n (%)	aOR (95% CI)	p-value	ARD (%)	aOR (95% CI)	p-value	ARD (%)	aOR (95% CI)	p-value	ARD (%)
Fentanyl	**119,113 (100)**									
>0-50 mcg	12,328 (10.4)	*Ref*	*Ref*	*Ref*	*Ref*	*Ref*	*Ref*	*Ref*	*Ref*	*Ref*
>50-100 mcg	52,194 (43.8)	1.19 (1.13 - 1.26)	<0.001	3	1.16 (0.31-4.33)	0.83	-	1.12 (0.96-1.31)	0.15	-
> 100 mcg	54,591 (45.8)	1.39 (1.30 - 1.48)	<0.001	6	0.42 (0.10-1.88)	0.26	-	1.28 (1.09-1.50)	<0.01	1
Hydromorphone	**71,483 (100)**									
>0-≤0.5 mg	16,774 (23.5)	*Ref*	*Ref*	*Ref*	*Ref*	*Ref*	*Ref*	*Ref*	*Ref*	*Ref*
>0.5-≤1 mg	33,945 (47.5)	1.18 (1.09 - 1.27)	<0.001	2	0.59 (0.17-1.98)	0.39	-	0.91 (0.83-1.00)	0.06	-
>1 mg	20,764 (29.0)	1.54 (1.37 – 1.73)	<0.001	5	1.17 (0.25-5.45)	0.84	-	0.86 (0.77-0.96)	<0.01	-0.6
Morphine	**8,906 (100)**									
>0-2 mg	1,105 (12.4)	*Ref*	*Ref*	*Ref*	-	-	-	*Ref*	*Ref*	*Ref*
>2-4 mg	2,430 (27.3)	1.08 (0.81 - 1.44)	0.60	-	-	-	-	0.77 (0.49-1.22)	0.27	-
> 4 mg	5,371 (60.31)	1.50 (1.13 – 1.97)	<0.01	5	-	-	-	1.04 (0.69-1.58)	0.84	-

Table 3. Association of intraoperative opioids dose and Category F, Category G, and Category H. aOR, adjusted odd ratio; ARD, adjusted risk difference. Logistic regression model for association between morphine dose and Category G was not applicable due to absence of the outcome in this population. Category F was investigated only in outpatients. Study population for this outcome was 60,368 for fentanyl cohort (9,362 [15.5%], >0-50 mcg; 30,566 [50.6%], >50-100 mcg; 20,440 [33.9%], >100 mcg); 27,553 for hydromorphone (8,434 [30.6%], >0-0.5 mg; 14,111 [51.2%], >0.5-1 mg; 5,008 [18.2%], >1 mg) and 3,424 for morphine (513 [15.0%], >0-2 mg; 1,068 [31.2%], >2-4 mg; 1,843 [53.8%], >4 mg).

Patient Safety 2- 30-Day Mortality Following Various Types of Surgical Procedures: The Contributing Role of Hypotension as Assessed by the SLUScoreiars

Wolf Stapelfeldt[1], Cristina Barboi[1]

Richard L. Roudebush VA Medical Center[1]

Introduction: Periods of intraoperative hypotension have been associated with a greater risk of adverse outcome after non-cardiac surgery, including 30-day mortality. A novel score, the SLUScore (range 0-31), was designed to quantify the portion of total risk that is independently attributable to hypotension, after adjustment for age, co-morbidity and case duration[1]. As originally conceived, the SLUScore was not adjusted for the type of surgical procedure, raising questions about its uniform applicability across surgical specialties. Therefore, the present study was designed to examine in retrospective analysis across various CPT-code-defined surgical specialty areas the incidence and severity of hypotension as quantified by the SLUScore as well as the percent increase in the odds of 30-day mortality *per SLUscore increment* and the odds of death associated with the average SLUScore of patients experiencing hypotension (SLUScore >0).

Methods: With IRB approval, institutional databases were queried for adult non-cardiac, non-obstetric surgical procedures performed during the years from 2011 to 2021 at Indiana University Medical Center, including CPT codes, patient age, co-morbidities (for the calculation of the Charlson score), case duration, 30-day mortality (obtained from the State of Indiana) and minute-to-minute mean arterial blood pressure (MAP) data for the calculation of the patients' final SLUScores as previously described[1]. Only procedures whose CPT codes could be uniquely allocated as exclusively belonging to exactly one of 10 major surgical procedure type groupings were included (see Table 1). Patient records were analyzed for raw 30-day mortality; age; case duration; Charlson score as well as the incidence (%) and severity (average) of a SLUScore >0. Logistic regression was utilized to ascertain the percent increase in the odds of 30-day mortality *per SLUScore increment*. The contribution of hypotension in increasing the odds of death within 30 days was estimated as (1+percent increase per SLUScore increment)^averageSLUScore>0. P<0.05 was considered indicating statistical significance.

Results: A total of 274,062 cases were identified as uniquely belonging to one of ten surgical specialty areas, experiencing an average 30-day mortality of 1.06%, ranging from a low of 0.16% (Gynecology) to a high of 4.64% (Thoracic Surgery). The detection of significant hypotension (a SLUScore >0) varied from a low of 7.6% (NORA) to a high of 46% (Orthopedics) in incidence and a low of an average of 9.2 (NORA) to one of 16.6 (Vascular Surgery) in magnitude. Based on basically similar percent increases in the odds of 30-day mortality *per SLUScore increment* (except for NORA) certain specialties exhibited a role of hypotension associated with an apparently greater contribution to adverse outcome, particularly in General Surgery, Orthopedic Surgery, Neurosurgery, Gynecology and Vascular Surgery (Table 1).

Conclusions: The present data suggest that while differences exist in the incidence and severity of hypotension, no surgical specialty area seems to be spared from an adverse impact associated with each *increment of the SLUScore*. Certain specialties with overall higher risk contribution of hypotension appear to hold greater promise for allowing the potential benefit of hypotension prevention strategies to be studied and related prospective clinical effectiveness trials to be performed.
The study was supported by a Population Health Fellowship Grant (Dr. Cristina Barboi) from the Indiana Clinical and Translational Sciences Institute (CTSI), Indianapolis, IN.

References: 1) The SLUScore: A Novel Method for Detecting Hazardous Hypotension in Adult Patients Undergoing Noncardiac Surgical Procedures. Anesth Analg. 2017 Apr; 124(4): 1135–1152.

	N	Raw Mortality	Age	Duration	Charlson	%SLU>0	avSLU>0	Incr. odds per SLU inc	Incr. odds att. to hypotension	
All	274,062	1.06%	55.5	92.3	1.4	26.7%	13.6			
NORA	70,775	1.03%	58.1	37.8	1.5	7.6%	9.2	3.7%		1.4
GI Surgery	51,934	0.90%	51.7	115.9	1.2	25.0%	12.4	4.8%		1.8
EYE/ENT	7,241	0.36%	54.4	76.4	0.8	26.1%	12.7	6.8%		2.3
THORACIC	8,046	4.64%	58.9	104.0	2.7	29.1%	13.5	6.6%		2.4
GU	29,956	0.91%	58.0	98.9	1.7	27.7%	12.0	8.0%		2.5
GenSurg	25,510	0.57%	53.4	117.4	1.7	39.9%	13.8	8.2%		3.0
ORTHO	43,452	0.77%	57.6	106.0	1.0	46.0%	15.7	7.7%		3.2
Neuro	3,388	1.18%	55.5	133.9	1.2	39.6%	13.9	9.4%		3.5
GYNE	19,087	0.16%	43.6	106.7	0.5	22.0%	11.4	11.8%		3.5
VASCULAR	14,673	3.38%	62.3	147.0	3.4	43.8%	16.6	8.0%		3.6

Patient Safety 3- Effect of Simulated Blood Pressure Elevation During Hypotensive Noncardiac Surgical Procedures Upon 30-Day All-Cause Postoperative Mortality As Projected By The Sluscore

Wolf Stapelfeldt[1], Murray du Plessis[2], Philip Leaning[3], Mark Leaning[4]

Richard L. Roudebush VA Medical Center[1] Medical Devices Testing and Evaluation Centre, QEHB[2] Directed Systems Limited[3] Directed Systems Inc[4]

Introduction: Intraoperative hypotension has been identified as being closely associated with adverse postoperative outcome after non-cardiac surgery. While a period of 15 minutes below a of MAP of 65 has been adopted as a quality metric for identifying patient populations at greater risk for adverse outcome[1], this criterion by itself is of modest use in guiding the hemodynamic management of individual patients, particularly ones that may already have exceeded this threshold. Based on the premise that progressively worse outcome has been shown to be attributable to progressively worse cumulative hypotensive exposures (in terms of severity and duration of hypotension below a MAP of 75, as reflected in the patient's SLUScore[2]), the present study was designed to track the estimated increment of 30-day all-cause mortality odds as projected by the contemporaneous SLUscore over the course of the surgical procedure and appraising the theoretical impact of simulated interventions (blood pressure elevation of varying magnitude) instituted at various points of time in response to the detection of hypotension.

Methods: With institutional approval the minute-to-minute mean arterial pressure (MAP) trajectories of adult non-cardiac anesthetics performed at the Queen Elizabeth Hospital in Birmingham, UK, were electronically captured using the HDA clinical decision support data acquisition and analysis platform (Directed Systems, Cambridge UK). The native records of hypotensive patients with expected increased 30-day mortality as projected by a final SLUScore >0[2] were selected for further off-line analysis. This consisted of the concurrent tracking of the estimated increment in 30-day all-cause mortality odds as projected by the contemporaneous SLUScore (contemp. SLUScore) during each minute of the case, calculated as $1.05^{\text{contemp.SLUScore.}}$ Four different time points were selected to define onset of hypotension and trigger a simulated intervention by elevating MAP by an increment of 1-10 mm Hg throughout the remainder of the case: 1) the first occurrence of MAP dropping below 65 (for at least 1 minute); 2) the time by which 10 minutes had accumulated below a MAP of 65; 3) the time the ePreop31 criterion[1] was met (15 min accumulated below a MAP of 65); 4) the time of SLUScore transition from 0 to 1. The projected final end-of-case odds increments of projected hypotension-attributable mortality ($1.05^{\text{finalSLUScore}}$) under the native and the various simulated conditions were examined for statistical differences using ANOVA, $p<0.05$ considered significant.

Results: Of 30 MAP records acquired, 10 exhibited a final SLUScore >0 (projecting a mortality odds increment attributable to hypotension) and were utilized for a total of 40 simulations each: 10 MAP elevations (1-10 mm Hg, for example, see figure 1, panel A) instituted at the 4 different trigger times (for example, see figure 1, panel B). Projected odds of 30-day all-cause mortality were lower the larger and earlier a simulated intervention was initiated ($p<0.002$ throughout). The final SLUScore-projected odds increment of mortality attributable to hypotension under these various native and simulated conditions are summarized in figure 2.

Conclusions: These simulations suggest that hypotensive patients' outcomes might be significantly improved through MAP elevations of manageable magnitude. While this benefit would be expected to be the greater the earlier such interventions were to occur and the larger their size, significant improvements might still be expected as a result of even modest blood pressure elevation instituted at a later time, despite the common MAP variability that is typical for many surgical cases. Actual patient benefit of the proposed simulated strategy remains to be examined in future prospective randomized clinical effectiveness trials analogous to the proposed SLUScore trial[3]. The present simulation study was supported by the NIHR Trauma Management MedTech Co-operative, funded by the National Institute of Health & Care Research (NIHR), and by Innovate UK.

References: 1) Anesthesia Quality Institute, Internal Improvement Measures, IIM025: ePreop 31: Intraoperative Hypotension among Non- Emergent Noncardiac Surgical Cases, 2020.

2) The SLUScore: A Novel Method for Detecting Hazardous Hypotension in Adult Patients Undergoing Noncardiac Surgical Procedures Anesth Analg 2017: pp 1135-1152

3) Prospective, randomised trial of alerting to extended hypotensive exposures on long-term outcome following adult non-cardiac surgical procedures: the SLUScore trial (NCT02217969). Protocol 14PRT/4102. The Lancet

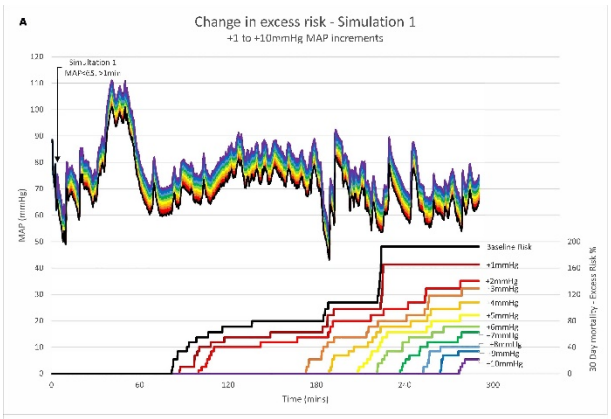
A
Change in excess risk - Simulation 1
+1 to +10mmHg MAP increments
MAP (mmHg)
Time (mins)
30 Day mortality - Excess Risk %
Baseline Risk
+1mmHg
+2mmHg
+3mmHg
+4mmHg
+5mmHg
+6mmHg
+7mmHg
+8mmHg
+9mmHg
+10mmHg

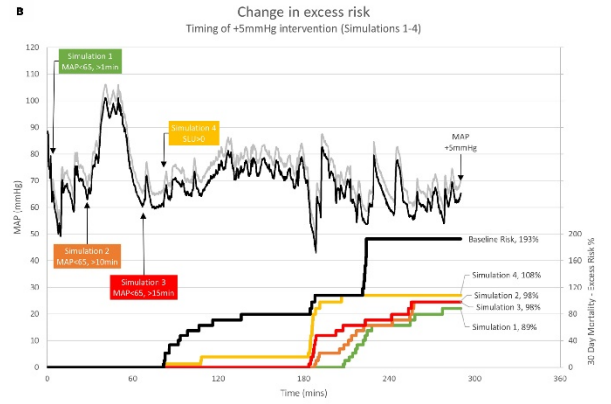
B
Change in excess risk
Timing of +5mmHg intervention (Simulations 1-4)
Simulation 1
MAP<65, >1min
Simulation 2
MAP<65, >10min
Simulation 3
MAP<65, >15min
Simulation 4
SLU>0
MAP
+5mmHg
Baseline Risk, 193%
Simulation 4, 108%
Simulation 2, 98%
Simulation 3, 98%
Simulation 1, 89%
MAP (mmHg)
Time (mins)
30 Day Mortality - Excess Risk %

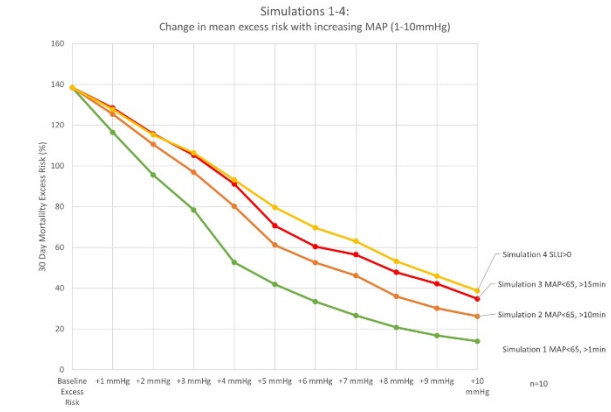
Simulations 1-4:
Change in mean excess risk with increasing MAP (1-10mmHg)
30 Day Mortality Excess Risk (%)
Baseline Excess Risk
+1 mmHg
+2 mmHg
+3 mmHg
+4 mmHg
+5 mmHg
+6 mmHg
+7 mmHg
+8 mmHg
+9 mmHg
+10 mmHg
n=10
Simulation 4 SLU>0
Simulation 3 MAP<65, >15min
Simulation 2 MAP<65, >10min
Simulation 1 MAP<65, >1min

Pediatric Anesthesiology

Pediatric Anesthesiology 1- Objective Analysis of Awake Infant Spinal and Caudal Epidural Anesthesia Using Surface Electromyography

Samuel Aldous[1], Dylan Casey[1], Jonathan Riddell[1], Emmett Whitaker[2]

Larner College of Medicine at the University of Vermont[1] University of Vermont[2]

Introduction: Spinal anesthesia (SA) and general anesthesia (GA) with caudal epidural anesthesia (CEA) are safe and effective alternatives to GA alone.[1; 2] Despite the clear advantages of awake SA in infants, its use remains uncommon, largely due to concerns about its limited duration. Historically, the clinical characteristics of these anesthetic techniques have been described subjectively, and no study has objectively characterized infant SA versus CEA. Surface electromyography (sEMG) is a safe, inexpensive, and non-invasive method to study the behavior of neural blockade. The goal of this observational study was to objectively define the rate of onset, maximum effect, and duration of infant SA versus CEA using continuous sEMG.

Methods: Infants undergoing surgery with awake SA (n=13) or GA + CEA (n=5) were recruited. Anesthetic technique was selected based upon patient and surgical factors. SA (0.5% bupivacaine 1 mL with clonidine 1 mcg/kg) or CEA (0.25% bupivacaine 1 mL/kg with clonidine 1 mcg/kg) were used. Electrodes were attached to the patient at T2, right T8 (T8R), left T8 (T8L), and L2 (**Figure 1**). Data collection began in the preoperative area and ended at return of lower extremity motor function. Raw signal data were processed using custom MATLAB scripts (https://github.com/dylantcasey/EMG). The rate of onset was calculated as the mean derivative value for each myotome in the first 15 and 60 seconds after SA and CEA administration, respectively. The maximum difference was determined by identifying the lowest mean sEMG signal per channel when applying a moving mean of 20 seconds. The rate of onset and maximum difference data were converted from decibels (logarithmic scale) to % change (scalar scale) to allow for comparison between groups/myotomes and normalization of data. We assessed approximate block duration by calculating the time between SA/CEA administration and when sEMG signal intensity for each myotome remained above 50% of its maximum difference (calculated as above. Techniques were compared using student's t-tests and were considered statistically significant when $p<0.05$.

Results: The average age and weight for the groups were 7.3 months and 8.0 kg (SA) and 15.2 months and 10.8 kg (CEA). Exclusion criteria were infection, spinal cord abnormality, or allergy to bupivacaine/clonidine. The sEMG raw signal tracings revealed a visually apparent decrease in power after block administration (SA and CEA) and resolution of block at the end of the case **(Figures 2 and 3)**. Remarkably, the rate of onset of SA compared to CEA was 13-28 fold faster than CEA depending on the myotome. The rate of block onset was significantly faster in SA when compared to CEA **(Figure 4A)**, and the maximum decrease in sEMG power was significantly greater in SA patients when compared to CEA (all myotomes, **Figure 4B**). In addition, we found that the rate of onset of SA was consistent with anatomical expectations (L2>T8>T2). The SA group had a near complete attenuation of sEMG signal at each myotome, while CEA achieved a maximum signal attenuation of approximately 60% at T8. Approximate block duration in SA patients averaged 90 minutes, with no statistical difference between myotomes. While CEA had a larger time from anesthetic administration to 50% return of sEMG signal, its duration in comparison to SA was not statistically significant (**Figure 5**).

Conclusions: This preliminary study establishes feasibility and proof-of-concept for the efficacy of sEMG to characterize neural blockade in infants. Our current understanding is that the duration of SA in infants is approximately 45 minutes[3]. Our results indicate that this is a substantial underestimate, as we measured a 50% resolution at approximately 90 minutes. It is likely that the sensory block lasts much longer, suggesting that awake SA can be used for much longer cases (e.g., hypospadias repair). Our results also confirm and quantify what has been clinically observed about infant SA. For example, in comparison to CEA, SA is significantly faster in onset and provides a much denser block, suggesting that it is superior technique for use in awake infants. In contrast to our expectations, the time to 50% resolution of block in SA vs. CEA was similar, suggesting that their duration is similar. Taken together, these data support the use of awake SA in infants and should reassure the pediatric anesthesiologist that this technique results in a long-lasting, rapid onset, dense surgical anesthetic.

References: 1. *Anesthesia & Analgesia* 102, 67-71, 2006.

2. *The Lancet Respiratory Medicine* 5, 412-425, 2017.

3. *Journal of Anaesthesiology Clinical Pharmacology* 30, 2014.

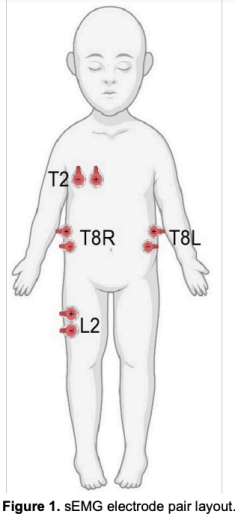

Figure 1. sEMG electrode pair layout.

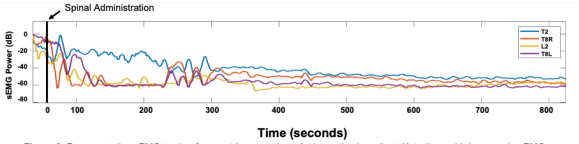

Figure 2. Representative sEMG tracing for onset in an awake spinal anesthesia patient. Note the rapid decrease in sEMG power seconds after spinal administration. Consistent with the expected anatomic spread of local anesthetic given injection at L3-4, muscle tone at L2 and T8 reach near maximal signal decrease in the first 120 seconds, while T2 takes significantly longer to reach maximal effect. Temporary upward deflections in power reflect patient movement.

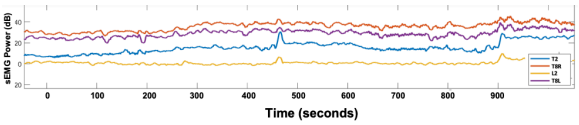

Figure 3. Representative sEMG tracing for resolution of block in a caudal block patient under general anesthesia at the end of the case. Note the gradual increase in sEMG over the course of approximately 15 minutes. As expected, sEMG at L2 remains low during this period and would be expected to increase as the block further resolves.

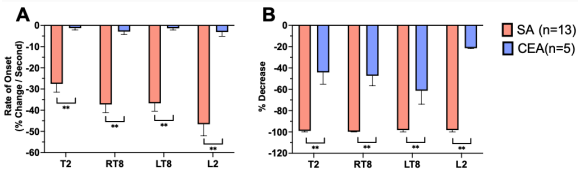

Figure 4. Comparison of rate of onset and maximum effect of SA vs. CEA by myotome. A, initial rate of onset (% change in sEMG per second) over the first several seconds (approximately 15 sec for SA patients; 60 sec for CEA patients) after anesthetic administration. Rate of onset was significantly faster at each myotome for SA when compared to CEA. B, maximum % decrease in sEMG power for the entire case by myotome. SA caused a significantly larger % decease in sEMG at each myotome when compared to CEA. **p<0.01, student's t test.

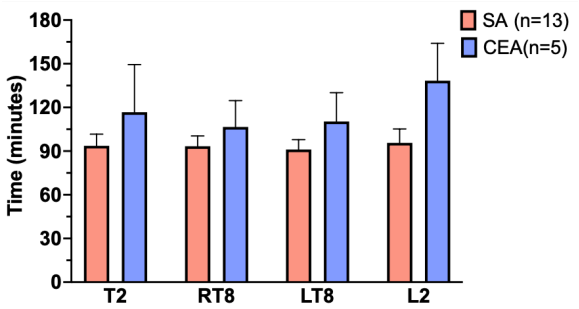

Figure 5. Time to 50% increase in sEMG from maximum effect baseline for SA vs. CEA by myotome. Consistent with what is experienced clinically in patients who receive SA, 90 minutes elapsed before sEMG power increased by 50%. Though a greater amount of time elapsed before 50% resolution in CEA patients, it was not statistically significant at any myotome.

Pediatric Anesthesiology 2- A Retrospective Study of Pain Intensity Among Pediatric Inpatients at a Single-Center in the U.S.

Thomas Anderson[1], Elizabet De Souza[1]

Stanford University School of Medicine[1]

Introduction: Poorly controlled pain is associated with worsened patient outcomes. Acute pain is a common complaint among hospitalized patients. Investigations of pain prevalence for adult patients have suggested that moderate-to-severe pain remains a common issue for inpatients, but fewer investigations of pediatric patients exist in the recent literature.

Methods: This is a retrospective chart review of all inpatients at a single academic children's hospital during twelve 24-hour periods in 2021 (one 24-hour period per month). Outcomes were assessed over the 24-hour analysis period, separately for patients in the intensive care units and on the non-intensive care inpatient floors. The primary outcome was any presence of moderate/severe pain (i.e., any pain score ≥4). Secondary outcomes were: pain prevalence (i.e., any pain score >0), mean pain score (categorized: 0-<1= no pain, 1-<4=mild pain, 4-<7=moderate pain, 7-10= severe pain), the continuous presence of pain (i.e., no pain score <1), mean pain score separately for daytime (7am to 7pm) and nighttime (7pm to 7am), number of recorded pain scores, analgesic type (opioid, non-opioid) and analgesic administration details (scheduled, as needed).

Results: Of 1355 patients on a non-intensive care inpatient floor during analysis periods, 23.5% had at least one moderate or severe pain score during the 24-hour analysis period, 56.4% had only pain scores of 0, 77.5% had a mean pain score <1, and 4.0% had pain scores >0 at all time points assessed. Analgesics were received by 42.4% of non-intensive care patients: non-opioids only in 24.7%, a combination of opioids and non-opioids in 13.1%, and opioids only in 4.6%.

Of 485 patients in the intensive care unit during analysis periods, 58.6% had at least one moderate or severe pain score during the 24-hour analysis period, 17.5% had only pain scores of 0, 63.1% had a mean pain score <1, and 0.4% had pain scores >0 at all time points assessed. Analgesics were received by 74.2% of the patients in the intensive care unit: a combination of opioids and non-opioids in 47.8%, non-opioids in 17.7%, and opioids only in 8.7%.

Conclusions: In a retrospective study at a single-center, the prevalence of at least one moderate-to-severe pain score among pediatric inpatients during a 24-hour period was greater than 20% for non-intensive care patients, and greater than 50% for patients in intensive care units. However, mean pain scores were less than one for the majority (>60%) of patients in both settings. Additionally, non-opioid analgesic administration was common. Future studies may focus on identification of variables associated with pediatric inpatients at high risk of moderate-to-severe pain as well as pain prevention and reduction strategies.

Table 2: Results

	Regular inpatient floor		ICU	
	n	(%)	n	(%)
Moderate/severe pain at any point?				
No	1036	(76.5)	201	(41.4)
Yes	319	(23.5)	284	(58.6)
Pain at any point?				
No	764	(56.4)	85	(17.5)
Yes	591	(43.6)	400	(82.5)
Mean pain score				
0-<1	1050	(77.5)	306	(63.1)
1-<4	260	(19.2)	174	(35.9)
4-<7	38	(2.8)	5	(1.0)
7-10	7	(0.5)	0	(0)
Always in pain?				
No	1301	(96.0)	483	(99.6)
Yes	54	(4.0)	2	(0.4)
Analgesia?				
None	780	(57.6)	125	(25.8)
Opioids	62	(4.6)	42	(8.7)
Non-opioids	335	(24.7)	86	(17.7)
Opioids and non-opioids	178	(13.1)	232	(47.8)
Mean pain score, day				
0	1050	(77.6)	291	(60.6)
1-<4	245	(18.1)	179	(37.3)
4-<7	46	(3.4)	10	(2.1)
7-10	12	(0.9)	0	(0)
Mean pain score, night				
0	977	(78.5)	290	(65.5)
1-<4	216	(17.4)	148	(33.4)
4-<7	41	(3.3)	5	(1.1)
7-10	10	(0.8)	0	(0)
Opioid administration (when given)				
Scheduled only	94	(39.2)	64	(23.4)
PRN only	81	(33.8)	39	(14.2)
Scheduled and PRN	65	(27.1)	171	(62.4)
Non-opioid administration (when given)				
Scheduled only	299	(58.3)	211	(66.4)
PRN only	144	(28.1)	41	(12.9)
Scheduled and PRN	70	(13.6)	66	(20.8)
Number of painscores, median(IQR)	7	(5,9)	24	(17,27)
Analgesia by PCA?				
No	1330	(98.2)	482	(99.4)
Yes	25	(1.9)	3	(0.6)
Total	1355		485	

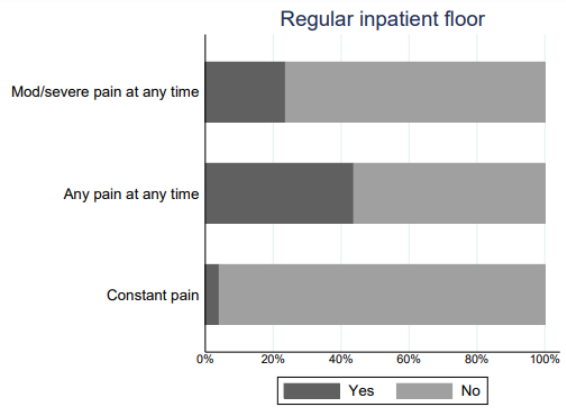

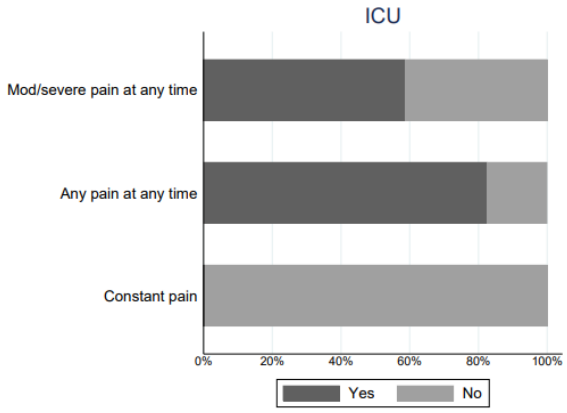
ICU
Mod/severe pain at any time
Any pain at any time
Constant pain
0%
20%
40%
60%
80%
100%
Yes
No

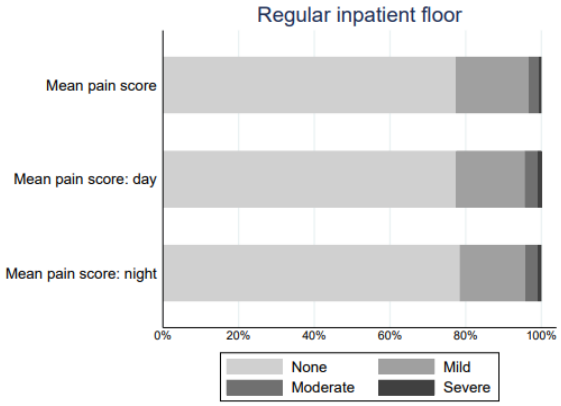
Regular inpatient floor
Mean pain score
Mean pain score: day
Mean pain score: night
0%
20%
40%
60%
80%
100%
None
Mild
Moderate
Severe

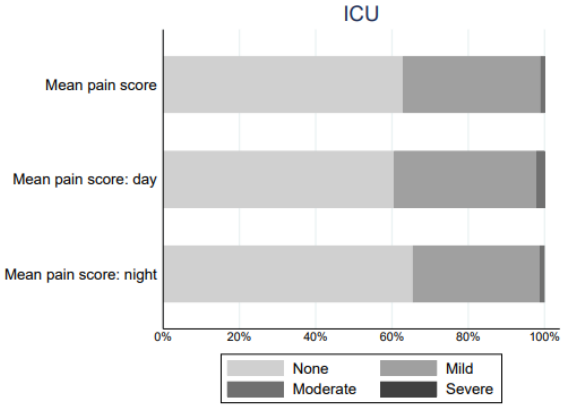
ICU
Mean pain score
Mean pain score: day
Mean pain score: night
0%
20%
40%
60%
80%
100%
None
Mild
Moderate
Severe

Pediatric Anesthesiology 3- Defining severe Pediatric Post-tonsillectomy Pain Using Plasma Untargeted Metabolomics

Christian Mpody[1], Joseph Tobias[1], Olubukola Nafiu[1]

Nationwide Children's Hospital[1]

Introduction: Approximately 583,000 tonsillectomies are performed every year in the United States, making these some of the most common surgical procedures in children. Despite universal administration of intraoperative opioid analgesia, 3 out of 5 children undergoing tonsillectomy ± adenoidectomy (T&A) reports moderate to severe pain upon recovering from anesthesia. However, the underlying molecular basis of this differential pain experience is presently unknown. This gap in knowledge means that therapies are poorly targeted and often unsuccessful. Here, we utilized an untargeted metabolomic approach to identify candidate molecules that may influence the frequency and severity of post-tonsillectomy pain (PTP) in children.

Methods: After institutional IRB approval, we prospectively enrolled children (4-18 years of age) undergoing T&A and performed an untargeted metabolite assay on venous blood samples collected upon completion of surgery (before the patient emerged from anesthesia). We performed principal component analysis and orthogonal partial least-squares discriminant analysis to discover and validate the different metabolomic profiles between children with severe PTP (numeric pain score ≥7) and those with mild PTP (numeric pain score ≤3.

Results: The study cohort included 35 patients. We identified 8 metabolites that were significantly different between children with severe PTP and those with mild PTP: Phenylacetic Acid, Methylxanthine, Hydroxyl-L-proline, Bilirubin, and CAR51-100. Multivariable partial least-squares discriminant analysis revealed a visible separation between groups, with a minor overlap of the 95% confidence ellipses (Fig. 1), although the permutation test did not reach a statistical significance (P-value=0.419).

Conclusions: To the best of our knowledge, this is the first study to assess whether specific metabolomes are identifiable across subpopulations defined by severity of PTP in children. We found difference in the metabolome between mild and severe PTP. These findings could improve our understanding of the molecular pathways and mechanisms that regulate pediatric postoperative pain, and thus help identify future molecular targets to improve the treatment of pain. Although further studies are needed to validate our findings, they support the possibility of the developing "personalized analgesic" regimens for the management of PTP, which could be transferable to other pediatric surgical procedures.

References: Aroke EN, Powell-Roach KL. The Metabolomics of Chronic Pain Conditions: A Systematic Review. Biol Res Nurs. 2020 Oct;22(4):458-471. doi: 10.1177/1099800420941105. Epub 2020 Jul 15. PMID: 32666804; PMCID: PMC7802026.

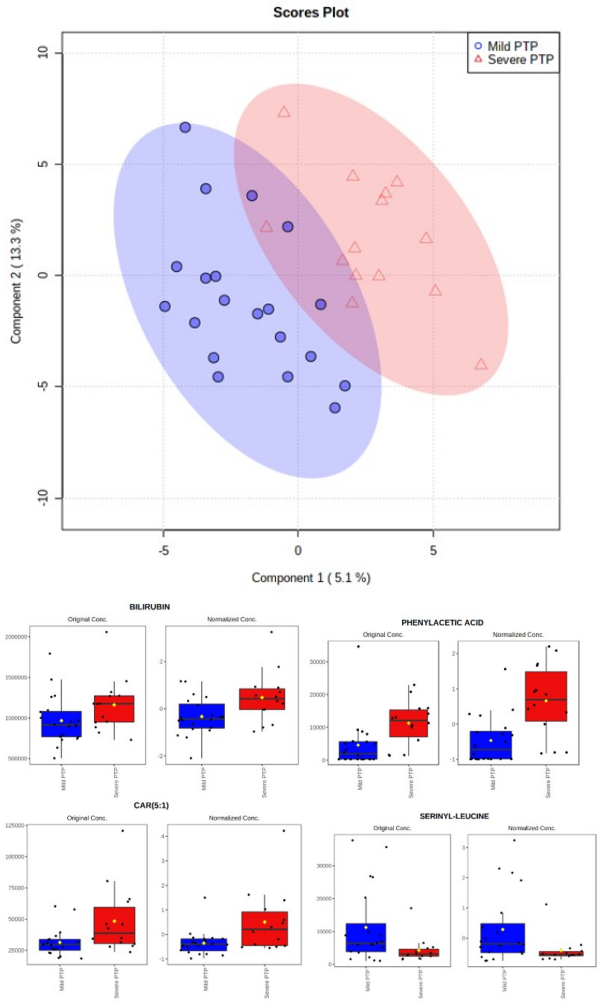

Pediatric Anesthesiology 4- Long term effects of general anesthesia exposure during early life on the excitability and plasticity of thalamocortical networks in mice

Vasilije Tadic[1], Slobodan Todorovic[1]

CU Anschutz Medical Campus[1]

Introduction: It has been shown that the exposure to general anesthetics (GA) during the critical periods of development in rodent and mammalian brains can cause a widespread neurodegeneration, including in the thalamus[1]. However, lasting effects of an early exposure to GA to neuronal function is not well studied. Here, we focused on the thalamocortical (TC) network which consists of mutually interconnected neurons of somatosensory cortex, ventrobasal (VB) thalamic nuclei, and reticular thalamic nucleus (NRT). It is well known that rhythmic oscillations of TC network are important for normal sensory processing, cognitive functions and consciousness[2]. We studied the excitability of intact TC network, as well as intrinsic excitability and synaptic plasticity of the neurons of VB thalamus in adult mice that were treated with GA in early life.

Methods: Mice pups were exposed at postnatal day (PND) 7 to either GA (treated group) or mock anesthesia (control group) for 6 hours (n=62). Being commonly used in clinical practice, Sevoflurane was the anesthetic of choice (3% for the first 2h of exposure; 2.4% for the other 4h) and mock anesthesia for the control group consisted of regular air supplemented with 30% O_2. Approximately at PND 65 – PND 80, the surviving animals from both groups (n=34) were implanted with cortical electroencephalogram (EEG) electrodes and recordings were obtained 15 minutes before and 45 minutes after the intraperitoneal (IP) application of gamma-butyrolactone (GBL), a drug used in research for its ability to induce a characteristic spike-wave discharge (SWD) pattern on EEG[3]. In ensuing voltage-clamp recordings, we studied properties of T-type calcium currents (T-currents) of VB neurons (n=15 control; n=25 treatment). A voltage-gated sodium channel blocker, tetrodotoxin (TTX), was applied to the external solution in order to prevent the generation of action potentials. Synaptic plasticity of the VB neurons was next evaluated by the voltage-clamp recordings of spontaneous inhibitory postsynaptic currents (sIPSCs). For the isolation of GABA receptor mediated currents, glutamate receptors antagonists NBQX and AP-5 were applied to the external solution. Postsynaptic inhibitory activity was observed in the form of spontaneous events, which were analyzed based on their frequency, amplitude and decay time.

Results: We found that there was a significant increase in cumulative SWD duration of about 2-fold in the first 30 minutes after the GBL application ($p<0.001$) in treated (n=15) vs. control (n=19) groups. Interestingly, we observed significant sex-dependent increase in SWDs only in GA-treated female mice. In ensuing voltage-clamp recordings, we studied properties of T-type calcium currents (T-currents) of VB neurons (n=15 control; n=25 treatment). We demonstrated that peak T-current densities were significantly increased in the GA group compared to the control group for about 40%. In addition, the half-maximal inactivation voltage (V_{50}) showed a significant depolarizing shift of about 3 mV in the GA group ($p<0.05$), without significant changes in voltage-dependent activation. Spontaneous inhibitory postsynaptic events in the GA group (n=18) were 70% more frequent ($p<0.005$) compared to the control group (n=11). Average event amplitude was significantly higher (about 65%) in the GA group compared to the control group ($p<0.0005$). No significant differences were observed in decay time of the events between the groups.

Conclusions: Based on our experiments, we conclude that there is a chronic hyperexcitability of TC networks in mice that were exposed to GA during early life. Increased frequency and amplitude of sIPSCs in VB thalamic neurons in GA treated group indicate that there is a stronger inhibitory input coming from the GABAergic neurons of NRT, which represents the main inhibitory structure in the thalamus and mainly projects to the VB nuclei. The increased inhibitory activity of NRT neurons, as well as the altered biophysical properties and increased T-current densities of VB neurons significantly contribute to the observed hyperexcitable state. The mechanisms responsible for these changes are still to be determined in our future experiments.

References: [1] Jevtovic-Todorovic V, Olney JW. PRO: Anesthesia-induced developmental neuroapoptosis: status of the evidence. *Anesth Analg.* 2008 Jun;106(6):1659-63;

[2] Sherman SM. Thalamic relays and cortical functioning. *Prog Brain Res.* 2005;149:107-26;

[3] Snead OC 3rd. gamma-Hydroxybutyrate model of generalized absence seizures: further characterization and comparison with other absence models. *Epilepsia.* 1988 Jul-Aug;29(4):361-8;

Acknowledgment: Supported by NIH grant 1 R35 GM141802

Pediatric Anesthesiology 5- Clinical, Demographic, and Technical Factors Associated with Pediatric Arterial Line Insertion First Attempt Success and Ultrasound Use in the Operating Room

Frank Yanko[1], John Hajduk[2], Eric Cheon[3], Heather Ballard[3]

Northwestern University Feinberg School of Medicine[1] Ann & Robert H. Lurie Children's Hospital of Chicago[2] Lurie Children's Hospital[3]

Introduction: Arterial catheterization is a common medical intervention that enables continuous hemodynamic monitoring and blood sampling. Multiple arterial catheter placement attempts are associated with increased vascular, neurologic, and thrombotic complications[1,2]. Complication rates in large pediatric studies have been reported to be 10.3% and 33%[3,4]. Though ultrasound has been shown to decrease the number of attempts to place an intraarterial catheters, few studies have examined what clinical and demographic factors are associated with ultrasound use and first attempt success for placement of intraarterial catheters[5]. The aim of the study was to identify clinical, demographic, and technical factors associated with arterial line insertion first attempt success and ultrasound use in the operating room.

Methods: We performed a retrospective analysis of prospectively collected data from pediatric patients who had arterial lines inserted in the operating room at an academic tertiary care children's hospital from January 2018 to March 2022. We measured associations among patients who had arterial line insertion first attempt success and ultrasound use with clinical, demographic, and technical factors.

Results: 3,946 arterial line insertions were analyzed after excluding 168 placements for not having the outcome variable or placement outside the OR. Multivariable analysis showed significantly higher odds of first attempt success was associated with cardiac surgery versus all other specialties, pediatric surgery (OR: 0.56, 95% CI:0.40-0.77, p<0.001), neurosurgery (OR: 0.38, 95% CI: 0.28-0.53, p<0.001), orthopedic surgery (OR: 0.31, 95% CI: 0.22-0.44, p<0.001), later time (weeks, OR: 1.002, 95% CI: 1.0002-1.0003, p: 0.022), palpation technique relative to ultrasound (OR: 0.75, 95% CI: 0.60-0.95, p=0.019), CRNA (OR: 3.64, 95% CI: 2.45-5.40, p<0.001) and trainee (OR: 2.94, 95% CI: 2.45-3.54, p<0.001) versus anesthesiologist placing the arterial line, and radial artery versus other locations (femoral, brachial, dorsalis pedis) (OR: 0.20, 95% CI: 0.14-0.30, p<0.001). Multivariable analysis showed significantly higher use of ultrasound was associated with neonate (OR: 9.6, 95% CI: 4.1-22.5, p<0.001), infant (OR: 6.98, 95% CI: 4.67-10.42, p<0.001), toddler (OR: 6.10, 95% CI: 3.8-9.8, p<0.001), and child (OR: 2.0, 95% CI: 1.7-2.5, p<0.001) age categories compared to teenager, ASA status III (OR: 1.62, 95% CI: 1.11-2.38, p=0.013), ASA IV (OR: 1.87, 95% CI: 1.11-3.16, p=0.019) compared to ASA I, cardiac surgery relative to all other specialties; pediatric surgery (OR: 0.48, 95% CI: 0.3-0.7, p<0.001), neurosurgery (OR: 0.27, 95% CI: 0.18-0.40, p<0.001), orthopedic surgery (OR: 0.38, 95% CI: 0.25-0.58, p<0.001), later time (weeks, OR: 1.009, 95% CI: 1.007-1.01, p<0.001), and anesthesiologist relative to CRNA (OR: 0.48, 95% CI: 0.33-0.69, p<0.001).

Conclusions: First attempt success was associated with cardiac surgery, later time, palpation technique, non-anesthesiologist placement, and radial artery location. Ultrasound use was associated with younger age groups, ASA III and IV status, cardiac surgery, later time, and anesthesiologist placement.

References: 1. Arterial catheters as a source of bloodstream infection: a systematic review and meta-analysis. 42:1334-9, 2014.

2. Insertion, management, and complications associated with arterial catheters in paediatric intensive care: A clinical audit. 33:326-332, 2019.

3. Complications associated with arterial catheterization in children. 9:5, 2008.

4. Pediatric arterial catheters: Complications and associated risk factors. 53:794-797, 2018.

5. Femoral arterial cannulation performed by residents: a comparison between ultrasound-guided and palpation technique in infants and children undergoing cardiac surgery 26:823-30, 2016.

Table 1. Multivariable logistic regression to Evaluate Patient Demographic, Clinical, and Technical Factors Associated with First Attempt Success

	Odds Ratio	95% CI	P-value
Age Category			
Teenager	Reference		
Child	1.1	0.88 - 1.36	0.407
Toddler	1.39	1 - 1.94	0.053
Infant	0.77	0.59 - 1.01	0.056
Neonate	0.83	0.55 - 1.26	0.39
Sex			
Female	Reference		
Male	1.06	0.91 - 1.27	0.375
Race			
White non-Hispanic	Reference		
White Hispanic	0.95	0.68 - 1.33	0.768
Black non-Hispanic	0.94	0.74 - 1.2	0.632
Other	0.88	0.73 - 1.06	0.186
Patient Class			
Outpatient	Reference		
Inpatient	1.14	0.93 - 1.39	0.219
ASA Physical Status			
I	Reference		
II	0.77	0.52 - 1.13	0.179
III	0.95	0.65 - 1.38	0.795
IV	1.24	0.78 - 1.95	0.361
Congenital Heart Dx	1.27	0.98 - 1.65	0.07
Prematurity	0.83	0.56 - 1.24	0.361
Renal Disease	1.1	0.85 - 1.41	0.473
Trisomy 21	0.75	0.49 - 1.14	0.174
Surgical Subspecialty			
Cardiac Surgery/Cardiology	Reference		
Pediatric Surgery	0.56	0.4 - 0.77	<0.001
Neurosurgery	0.38	0.28 - 0.53	<0.001
Orthopedic Surgery	0.31	0.22 - 0.44	<0.001
Other	0.79	0.6 - 1.05	0.101
Time (weeks)	1.002	1.0002 - 1.003	0.022
Ultrasound Use Any Attempt	0.75	0.6 - 0.95	0.019
Practitioner Type			
Attending Anesthesiologist	Reference		
CRNA	3.64	2.45 - 5.4	<0.001
Trainee	2.94	2.45 - 3.54	<0.001
Artery Location			
Radial	Reference		
Ulnar	0.76	0.53 - 1.11	0.15
Other (femoral, DP, brachial)	0.2	0.14 - 0.3	<0.001

Abbreviations: ASA, American Society of Anesthesiologists; CRNA, certified registered nurse anesthetist; Ref, reference

Table 2. Multivariable logistic regression to Evaluate Patient Demographic, Clinical, and Technical Factors Associated with Ultrasound Use

	Odds Ratio	95% CI	P-value
Age Category			
Teenager	Reference		
Child	2.04	1.65 - 2.52	<0.001
Toddler	6.1	3.81 - 9.75	<0.001
Infant	8.96	4.67 - 10.42	<0.001
Neonate	9.8	4.1 - 22.48	<0.001
Sex			
Female	Reference		
Male	0.93	0.77 - 1.13	0.461
Race			
White non-Hispanic	Reference		
White Hispanic	0.85	0.56 - 1.28	0.428
Black non-Hispanic	0.93	0.7 - 1.23	0.603
Other	0.96	0.78 - 1.2	0.739
Patient Class			
Outpatient	Reference		
Inpatient	1.09	0.86 - 1.39	0.455
ASA Physical Status			
I	Reference		
II	1.3	0.88 - 1.91	0.189
III	1.62	1.11 - 2.36	0.013
IV	1.87	1.11 - 3.16	0.019
Congenital Heart Dx	1.19	0.87 - 1.62	0.282
Prematurity	0.56	0.28 - 1.11	0.097
Renal Disease	1.02	0.75 - 1.38	0.92
Trisomy 21	1.35	0.62 - 2.94	0.452
Surgical Subspecialty			
Cardiac Surgery/Cardiology	Reference		
Pediatric Surgery	0.46	0.31 - 0.73	<0.001
Neurosurgery	0.27	0.18 - 0.4	<0.001
Orthopedic Surgery	0.38	0.25 - 0.58	<0.001
Other Services	0.47	0.32 - 0.68	<0.001
Time (weeks)	1.009	1.007 - 1.01	<0.001
Ultrasound Use In Any Attempt	Not Included		
Practitioner Type			
Attending Anesthesiologist	Reference		
CRNA	0.46	0.33 - 0.69	<0.001
Trainee	1.05	0.84 - 1.31	0.664
Artery Location			
Radial	Reference		
Ulnar	1.55	0.74 - 3.22	0.235
Other (femoral, DP, brachial)	0.74	0.39 - 1.44	0.377

Abbreviations: ASA, American Society of Anesthesiologists; CRNA, certified registered nurse anesthetist; Ref, reference

Pediatric Anesthesiology 6- Effect of intraoperative dexmedetomidine on post anesthesia care unit length of stay and costs in pediatric patients

Omid Azimaraghi[1], Maira Rudolph[2], Elie Salloum[3], Maya Dohne[1], Juliane Beier[4], Hilana Lewkowitz-Shpuntoff[4], Terry-Ann Chambers[4], Jerry Chao[5], Matthias Eikermann[5], William Jackson[1]

Montefiore Medical Center[1] Department of Anesthesiology, Montefiore Medical Center[2] Montefiore Medical Center, Department of Anesthesiology[3] Montefiore Health Center[4] Montefiore-Einstein[5]

Introduction: Dexmedetomidine is frequently used off-label in pediatric anesthesia. (1,2,3) However, potential adverse effects of the drug in pediatric populations, including prolonged sedation, have not been well characterized. A previous study by our group showed prolonged post anesthesia care unit (PACU) stay in adult ambulatory patients receiving dexmedetomidine. (4) We hypothesized that intraoperative dexmedetomidine use in pediatric patients is associated with delayed discharge from PACU and increased health care costs.

Methods: We analyzed data from all pediatric patients (age < 13 years) who underwent procedures requiring anesthesia between 2016-2021 at a health care network in New York, USA. We excluded children with American Society of Anesthesiologists (ASA) physical status classification of 5 or greater, and records with missing data for confounding variables. The primary exposure was the use of intraoperative dexmedetomidine versus no dexmedetomidine administration. The primary outcome was postoperative length of stay (PLOS), defined as the time of arrival in PACU until discharge as measured in minutes.
In secondary analyses, we assessed potential effect modification of the primary association by patient- and procedure-related factors, including younger age (under 2 years), a shorter surgical duration (≤1 hours) and admission type (ambulatory versus inpatient). After the results of these analyses became available, we built a composite variable to depict a set of patients with the highest impact and re-evaluated a possible effect modification using this composite variable.
Further, we studied the association of intraoperative dexmedetomidine use and direct hospital costs defined as variable and fixed costs directly associated with patient-care-related activities. Differences in direct hospital costs (in USD) were calculated using the geometric means in direct hospital costs across the groups and the coefficients obtained from the multivariable regression model.
A Multivariable generalized linear model was applied. Analyses described in this manuscript were adjusted for potential confounding variables including, demographics information, other drugs administered perioperatively, and medical risk factors. Variables related to acuity such as surgical service, relative value units, emergency status, duration of surgery, fluid- and red blood cell unit resuscitation volume, and vasopressor dose were also included in the primary model. All analyses were performed in Stata (Version SE 16.0, Stata Corp LLC, College Station, TX).

Results: The final study cohort included 19,658 pediatric patients. Overall, 72.4%(n=14,254) patients received intraoperative dexmedetomidine (Table 1, Figure 1). The median PLOS in patients who received dexmedetomidine was 131 minutes compared to 113 minutes in patients who did not receive dexmedetomidine (adjusted absolute difference [ADadj] 16.1 min; 95%CI 14.5-17.6; p < 0.001).
The primary effect of dexmedetomidine administration on PLOS was magnified in surgeries of under 1 hr duration (ADadj 30.3 min; 95%CI 26.3-32.4; p < 0.001), children younger than 2 years (ADadj 19.4 min; 95%CI 16.1-22.5; p < 0.001), children undergoing ambulatory surgeries (ADadj 18.4 min; 95%CI 16.5-20.2; p < 0.001) and the high impact group(younger than 2 years undergoing short procedures in the ambulatory setting)(ADadj 32min; 95%CI 26.2-36.3; p < 0.001)(p for interaction<0.001). (Figure 2).
Analysis of direct costs showed increased direct hospital costs in patients receiving dexmedetomidine compared to those who did not (adjusted model estimate: 1.05;95%CI1.02-1.08)(ADadj 500 USD; 95%CI 244-764; p< 0.001). (5-7)

Conclusions: Intraoperative administration of dexmedetomidine in pediatric patients undergoing anesthesia is associated with a prolonged PACU length of stay. This effect is magnified in shorter procedures, younger children, and those undergoing ambulatory surgery. These findings suggest that dexmedetomidine may prolong postanaesthetic sedation and lead to longer stays and increased costs. The beneficial effects of dexmedetomidine (quieter, sleeping child in the recovery room) need to be considered in the context of these side-effects.

References: 1.Paediatr Drugs. 2022 May;24(3):247-257.

2.Drug Des Devel Ther. 2019 Mar 15;13:897-905

3.Paediatr Anaesth. 2018 Jul;28(7):632-638

4. J Clin Anesth. 2021;72

5. British Journal of Anaesthesia. 2022 In press

6.Anaesth, 2022, 15940, doi:10.1111/anae.15940, In press.

7.British Journal of Anaesthesia. 2022 In press

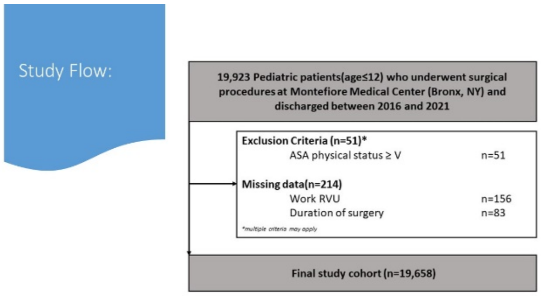

Table 1: Cohort characteristics

	No Dexmedetomidine N=5,404	Dexmedetomidine N=14,254	Standard difference
Age (years), mean ± SD	5.3 ± 4.0	5.3 ± 3.4	-0.00497
Gender, n (%)			
Male	3,294 (61.0%)	9,009 (63.2%)	0.04635
Female	2,110 (39.0%)	5,245 (36.8%)	
BMI (kg m⁻²), mean ± SD	18.2 ± 5.8	18.7 ± 29.7	-0.02567
ASA Status, median (IQR)	2.0 [1.0 - 2.0]	2.0 [1.0 - 2.0]	0.00714
Congestive heart failure, n (%)	161 (3.0%)	161 (1.1%)	0.13068
Malignancy, n (%)	180 (3.3%)	316 (2.2%)	0.06787
HIV, n (%)	1 (0.0%)	1 (0.0%)	0.01017
Diabetes mellitus, n (%)	22 (0.4%)	58 (0.4%)	0.01523
Renal disease, n (%)	71 (1.3%)	163 (1.1%)	0.01546
Rheumatologic disease, n (%)	7 (0.1%)	10 (0.1%)	0.00091
Coronary artery disease, n (%)	66 (1.2%)	67 (0.5%)	0.08052
Asthma, n (%)	1,007 (18.6%)	2,755 (19.3%)	0.01769
Malignant hyperthermia	0 (0.0%)	3 (0.0%)	0.02052
Seizure, n (%)	443 (8.2%)	824 (5.8%)	0.09490
Cystic fibrosis, n (%)	0 (0.0%)	1 (0.0%)	0.01185
Anemia, n (%)	625 (11.6%)	1,245 (8.7%)	0.09385
Muscular dystrophy, n (%)	24 (0.4%)	47 (0.3%)	0.01843
Obstructive sleep apnea	35 (0.6%)	217 (1.5%)	0.08451
Neurocognitive disorders	690 (12.8%)	1,965 (13.8%)	0.02938
Respiratory infection 30d prior, n(%)	218 (4.0%)	575 (4.0%)	0.00000
Admission status, n (%)			
Ambulatory	3,868 (71.6%)	11,200 (78.6%)	0.21202
Same day admission	753 (13.9%)	1,917 (13.4%)	
Inpatient	783 (14.5%)	1,137 (8.0%)	
Emergency surgery, n (%)	339 (6.3%)	343 (2.4%)	0.19064
Year of surgery, n (%)			
2016	1,294 (23.9%)	1,262 (8.9%)	0.54842
2017	1,486 (27.5%)	3,129 (22.0%)	
2018	1,239 (22.9%)	3,199 (22.4%)	
2019	776 (14.4%)	3,335 (23.4%)	
2020	417 (7.7%)	2,167 (15.2%)	
2021	192 (3.6%)	1,162 (8.2%)	
Duration of surgery, mean ± SD	79.5 ± 66.7	87.8 ± 58.3	-0.13290
Fluids (ml), mean ± SD	175.3 ± 284.5	225.2 ± 254.6	-0.18475
Norepinephrine dose, mean ± SD	0.0 ± 0.0	0.0 ± 0.0	0.00338
Surgical service, n (%)			
Cardiology	239 (4.4%)	220 (1.5%)	0.46883
Gastroenterology	815 (15.1%)	1,048 (7.4%)	
General Surgery	868 (16.1%)	1,692 (11.9%)	
Maxillofacial surgery	121 (2.2%)	934 (6.6%)	
Neurosurgery	88 (1.6%)	117 (0.8%)	
Ophthalmology	163 (3.0%)	378 (2.6%)	
Orthopedics	525 (9.7%)	1,054 (7.4%)	
Others	322 (6.0%)	613 (4.3%)	
Otorhinolaryngology	1,630 (30.2%)	5,734 (40.2%)	
Urology	633 (11.7%)	2,472 (17.3%)	
Neuromuscular blocking agents, n (%)	751 (13.9%)	1,583 (11.1%)	0.08448
Intra-op benzodiazepines, n (%)	654 (12.1%)	1,028 (7.2%)	0.16827
Intraoperative opioids, n (%)	3,507 (64.9%)	9,362 (65.7%)	0.01646
Opioid dose, median (IQR)	3.0 [0.0 - 10.0]	3.0 [0.0 - 7.5]	0.06175
MAC age adjusted, median (IQR)	1.0 [0.8 - 1.3]	1.0 [0.9 - 1.2]	0.04596

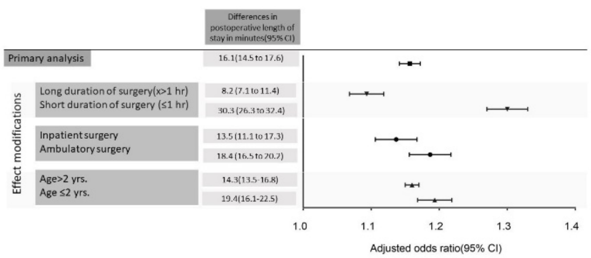

Figure 2: Effect modification Analysis. The association between intraoperative dexmedetomidine administration and postoperative length of stay was magnified in patients who underwent ambulatory surgery and in patients who underwent shorter procedures and age≤2 yrs. Statistical analyses were performed using a multivariable generalized linear model of the gaussian family with identity link adjusted for confounding variables. Adjusted model estimates are reported for regression analyses as results of the exponential transformation of model coefficients.

Pediatric Anesthesiology 7- Neonatal ketamine exposure impairs infrapyramidal bundle pruning and causes lasting synaptic hyperexcitability in hippocampal CA3 neurons

Michelle Near[1], Omar Hoseá Cabrera[1], Stefan Maksimovic[1], Nemanja Useinovic[1], Nidia Quillinan[2], Slobodan Todorovic[2], Vesna Jevtovic-Todorovic[3]

University of Colorado Anschutz Medical Campus[1] University of Colorado, Anschutz Medical Campus[2] University of Colorado[3]

Introduction: In experimental settings general anesthetics (GA) have been associated with widespread neurodegeneration in developing rodent and non-human primate brains (Bittigau et al., 2002). The initial cell death during peak stages of synaptogenesis is followed by extensive damage to nervous system tissue and cognitive impairments later in life. During the developmental stage, in which pediatric GA exposure occurs, long axon collaterals are pruned as part of neurogenesis and proper development. During stereotyped axonal pruning, axons that transiently innervate neurons are eliminated as development proceeds (O'Leary and Stanfield, 1986). We hypothesize that this axonal pruning may be disrupted by ketamine exposure early in life leading to alterations in the infrapyramidal bundle (IPB) of the hippocampus.

Methods: To examine changes in CA3 neuron synaptic excitability, male and female CD1 mouse pups at postnatal day (PND) 7 were exposed to of ketamine or vehicle then observed at PND 20, 30, and 40 during peak stages of IPB pruning. The pups were injected intraperitoneally every 90 minutes with 40 mg/kg ketamine to maintain sedation over a 6 hour period. Following exposures, hippocampal sections were analyzed with immunohistochemistry to quantify stereotyped axonal pruning of the IPB. We stained with calbindin to find the normalized IPB length for each animal which was calculated as the length of the IPB divided by the length of CA3. Dual labeling of the tissue with synaptoporin, to mark mossy fibers, and PSD-95, a glutamatergic excitatory neuron scaffolding protein, was assessed to determine the functionality of synapses formed. To understand how these neurons impacted synaptic excitability, we measured the frequency of miniature postsynaptic potentials (mEPSCs) in hippocampal CA3 neurons with patch-clamp electrophysiology. We plotted the cumulative frequencies, amplitudes, and rise times to assess the alterations to synaptic glutamate levels and analyzed Semaphorin 3F expression to examine a possible mechanistic route for changes to axonal remodeling.

Results: Treated groups displayed IPB further extension into regions of the hippocampus, were thicker, and were more numerous than vehicle groups. At PND 30, IPB length was 20% shorter in vehicle groups compared to ketamine while at PND 40 this difference increased to 30%. To determine the functionality of synapses in unpruned IPBs we jointly labeled tissue with synaptoporin to mark synaptic vesicles and calbindin to label mossy fibers. We found extensive staining for both labels in ketamine groups which contrasted the minimal immunofluorescence in vehicle groups. Our previous studies have shown reduced BDNF levels in ketamine exposed neonatal mice leading us to analyze modifications to the levels of Semaphorin 3F and the resulting impact on the routes of synaptic development in the central nervous system. In order to understand how changes to these neurons impacted synaptic excitability we measured miniature postsynaptic potentials (mEPSCs) in hippocampal CA3 neurons with patch-clamp electrophysiology. Measurements of mEPSC frequency in CA3b neurons of ketamine groups compared to those treated with vehicle showed increased values and a leftward shift in the cumulative frequency of the interevent interval. In the ketamine groups the average amplitude of mEPSCs was also increased and we found a shortened rise time of mEPSC events compared to the vehicle group.

Conclusions: These results suggested neonatal exposure to ketamine led to synaptic hyperexcitability in hippocampal neurons of the CA3 region in concert with the diminishing of axonal pruning. Our data also indicated a greater number of synapses onto the target cell with an increased probability of glutamate release. Along with the well documented potential for neurodegeneration as a result of GA, we propose that the disruption of development in the IPB indicates dysregulation of circuitry which could correlate with the observed cognitive impairments persisting into adulthood.

References: 1. Bittigau P, Sifringer M, Genz K, Reith E, Pospischil D, Govindarajalu S, Dzietko M, Pesditschek S, Mai I, Dikranian K, Olney JW, Ikonomidou C (2002) Antiepileptic drugs and apoptotic neurodegeneration in the developing brain. Proc Natl Acad Sci 99:15089–15094 Available at: https://www.pnas.org/content/99/23/15089 [Accessed July 27, 2021].

2. O'Leary DDM, Stanfield BB (1986) A transient pyramidal tract projection from the visual cortex in the hamster and its removal by selective collateral elimination. Dev Brain Res 27:87–99.

Pediatric Anesthesiology 8- Pediatric Anesthesia Outcomes in Underserved Communities: An Epidemiological Analysis from 2000 to 2022

Faisal Elali[1]

SUNY Downstate Health Sciences University[1]

Introduction: The purpose of this epidemiological study is to examine the pediatric anesthesia outcomes in patients living in underserved communities from 2010 to 2022. Anesthesia is a critical component of pediatric care, and it is important to understand the outcomes of anesthesia in underserved communities. This study will use a database to analyze the outcomes of pediatric anesthesia in underserved communities. Additionally, this study will examine the differences in outcomes based on the type of anesthesia used, the patient's age, and the type of procedure.

Methods: The data for this study was collected from a database of pediatric anesthesia outcomes from 2010 to 2022. The database used was the American Society of Anesthesiologists (ASA) Pediatric Anesthesia Outcomes Database. The database included information on the type of anesthesia used, the patient's age, the type of procedure, and the outcome of the procedure. The data was analyzed to determine the outcomes of pediatric anesthesia in underserved communities. The data was analyzed to determine the outcomes of pediatric anesthesia in underserved communities. Descriptive statistics were used to summarize the data and chi-square tests were used to examine differences in outcomes based on the type of anesthesia used, the patient's age, and the type of procedure.

Results: The results of the study showed that the outcomes of pediatric anesthesia in underserved communities were generally favorable. The study included a total of 500 patients. The majority of patients (80%) experienced successful outcomes with no complications. The most common type of anesthesia used was general anesthesia (60%), followed by regional anesthesia (30%) and sedation (10%). The most common type of procedure was orthopedic surgery (50%), followed by dental surgery (30%) and other procedures (20%). The average length of the procedure was 2.5 hours. The average length of recovery was 1.5 hours. The chi-square tests revealed that there were no significant differences in outcomes based on the type of anesthesia used ($p = 0.45$), the patient's age ($p = 0.78$), or the type of procedure ($p = 0.32$).

Conclusions: The results of this study indicate that pediatric anesthesia outcomes in underserved communities are generally favorable. The majority of patients experienced successful outcomes with no complications. This study provides important information about the outcomes of pediatric anesthesia in underserved communities and can be used to inform future research and clinical practice. Additionally, this study suggests that there are no significant differences in outcomes based on the type of anesthesia used, the patient's age, or the type of procedure. The findings of this study suggest that pediatric anesthesia is a safe and effective procedure for patients living in underserved communities. Further research is needed to better understand the outcomes of pediatric anesthesia in underserved communities and to identify potential areas for improvement.

Pediatric Anesthesiology 9- The Effect of Just-In-Time Rapid Cycle Deliberate Practice (JIT-RCDP) Simulation Training on Pediatric Anesthesia Trainee Cognitive Task Load During Infant Intubation

Stephen Flynn[1], Mary Lyn Stein[1], James Peyton[2], Raymond Park[3], Steven Staffa[1], Rachel Bernier[1], Karina Lukovits[1], Samuel Kim[1], Ivy Pham[1], Julia Clarke[1], Peter Weinstock[1], Pete Kovatsis[1]

Boston Children's Hospital[1] Boston Children's Hospital[2] Harvard Medical School[3]

Introduction: Performing neonatal and infant tracheal intubation is a core anesthetic skill. It is usually taught at academic medical centers by experienced pediatric anesthesiologists during patient care via guided instruction. Increasingly, these training environments are of higher acuity. Recent infant intubation studies reveal competency gaps in first-attempt success between attendings and trainees;[1] and multiple attempts are associated with more complications.[1] We hypothesize that mental workload, defined by the cost of accomplishing mission requirements experienced by a human operator,[2] is high among novices while intubating neonates/infants. This is important because a high mental workload increases errors in medicine and other high-risk industries like aviation.[3,4] We initiated Just-In-Time Rapid Cycle Deliberate Practice (JIT-RCDP) airway coaching as a potential method to mitigate trainee mental workload and improve infant laryngoscopy performance.

Methods: Study Design – ClinicalTrials.gov registered and IRB-approved non-crossover, prospective, non-blinded randomized control trial. Anesthesia trainees were block-randomized to the experimental vs. control group for intubation of children≤12 months. *Inclusion criteria*: Trainees assigned to infants ≤12 months with an ASA-PS of I-III and pre-planned endotracheal intubation. *Exclusion criteria*: Infants ≤12 months with known or suspected difficult intubations/critical airways, a diagnosis of complex congenital heart disease, a pre-existing oxygen requirement, an artificial airway *in situ*, or COVID-19. The experimental group underwent a JIT-RCDP *in situ* simulation on an infant manikin within one hour of patient intubation. The session simulated the planned intraoperative intubation (DL or VL). The JIT-RCDP coaching approach was embedded with critical laryngoscopy steps. Latitude exists in JIT-RCDP sessions to remedy trainee-specific laryngoscopy pitfalls.[5] In addition, three study team coaching insights to solve laryngoscopy uncertainty were shared during intra-session microdebriefs. The experimental trainees proceeded with their scheduled cases after two successful mannikin intubations or after ten minutes had elapsed. The control group had no interventions. All trainees performed up to five separate infant intubations to examine a dose effect. After each intubation, the trainee completed the NASA-Task Load Index (TLX) survey (Cronbach α coefficient. >0.80) (Figure 1) to examine the cognitive load of the intubation. *Statistical analysis:* The study was powered for first-attempt intubation success as the primary outcome. Raw NASA-TLX score domains (mental, physical, and temporal demand, performance, effort, and frustration) were secondary outcomes. The raw NASA-TLX continuous scores were compared using Generalized Estimating Equations (GEE).

Results: From August 1, 2020, to April 30, 2022, 153 trainees were enrolled (70 experimental, 83 control). A total of 515 intubations were performed (232 experimental, 283 control). Raw NASA-TLX scores for six domains are summarized in the Table. Statistical significance between groups favoring the intervention was demonstrated for mental demand, temporal demand, effort, and frustration and was not significant for physical demand or performance. Very high control group average scores of 58 and 58.6 were seen in the mental demand and effort domains, respectively.

Conclusions: The baseline cognitive workload among pediatric anesthesia trainees who intubate neonates/infants was very high for mental demand and effort domains and high in temporal demand, as demonstrated by control group NASA-TLX workload domain scores of 50 or higher. Scores in this range are associated with errors across many industries. In this study, JIT-RCDP significantly improved these cognitive workload domains for novice infant laryngoscopists. This training method may empower young providers near the limits of performance ability and reduce errors that lead to subsequent intubation failure.

References: 1. *Lancet,* 396(10266),1905-1913, 2020.

2. Human Mental Workload, 139-183, 1988.

3. *Simul Healthc,* 14(2), 96-103, 2019.

4. *Practical Radiation Oncology*, 3, e171-177, 2013.

5. *Simul Healthc.* 15(5), 356-362, 2020.

NASA Task Load Index

Hart and Staveland's NASA Task Load Index (TLX) method assesses work load on five 7-point scales. Increments of high, medium and low estimates for each point result in 21 gradations on the scales.

Name	Task	Date

Mental Demand — How mentally demanding was the task?
Very Low — Very High

Physical Demand — How physically demanding was the task?
Very Low — Very High

Temporal Demand — How hurried or rushed was the pace of the task?
Very Low — Very High

Performance — How successful were you in accomplishing what you were asked to do?
Perfect — Failure

Effort — How hard did you have to work to accomplish your level of performance?
Very Low — Very High

Frustration — How insecure, discouraged, irritated, stressed, and annoyed wereyou?
Very Low — Very High

Table – Raw NASA-TLX Data

NASA Task Load Index - Comparison of Experimental and Control Arms

Domain	Experimental Group (n=231)	Control Group (n=283)	Coefficient or Odds Ratio for Experimental Group (ref. = control)	95% CI	P value
Mental Demand					
Score (0-100)	48 ± 24.5	58 ± 23.3	-9.5	(-16, -3)	**0.004***
Score ≥ 55	107 (46.3%)	177 (62.5%)	0.54	(0.32, 0.92)	**0.023***
Physical Demand					
Score (0-100)	33 ± 20.7	29.8 ± 18.5	-3.2	(-8.2, 1.8)	0.212
Score ≥ 55	37 (16%)	54 (19.1%)	0.77	(0.42, 1.43)	0.412
Temporal Demand					
Score (0-100)	36.2 ± 31	45.8 ± 31	-9.1	(-16.1, -2.1)	**0.011***
Score ≥ 55	66 (28.6%)	111 (39.2%)	0.63	(0.39, 1.04)	0.07
Performance					
Score (0-100)	23.9 ± 16.6	26.9 ± 17.1	-2.9	(-6.6, 0.7)	0.113
Score ≥ 55	12 (5.2%)	17 (5%)	0.84	(0.36, 1.94)	0.683
Effort					
Score (0-100)	47.9 ± 23.9	58.6 ± 20.5	-10.2	(-16, -4.4)	**0.001***
Score ≥ 55	104 (45%)	174 (61.5%)	0.53	(0.32, 0.87)	**0.013***
Frustration					
Score (0-100)	23.8 ± 19.9	31 ± 24.2	-7.1	(-12.6, -1.7)	**0.01***
Score ≥ 55	25 (10.8%)	58 (20.5%)	0.46	(0.26, 0.83)	**0.009***

Values are self-scored by the trainee for each intubation.
Data are expressed as mean (standard deviation) or n (%).
P values were calculated using Generalized Estimating Equations (GEE) modeling to account for multiple intubations per trainee.
*Statistically significant.

Figure 2 – NASA-TLX Graphic Representation including Redline Cutoff of 55.

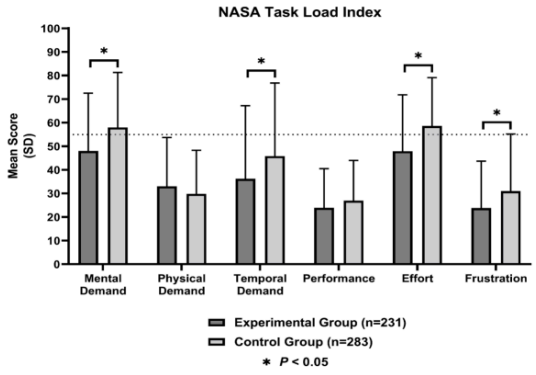

Pediatric Anesthesiology 10- The Utilization of Vasopressor Infusions During Pediatric Liver Transplantation and Association with Postoperative Outcomes

Ashley Bartels[1], Laura Gilbertson[2], Joelle Karlik[1], Katie Liu[1]

Emory University/Children's Healthcare of Atlanta[1] Emory University[2]

Introduction: Pediatric patients undergoing liver transplantation frequently require vasopressor infusions (1). While vasopressors may have a detrimental effect on graft function, there is limited data on the effect of intraoperative vasopressor use on postoperative outcomes (2). In this retrospective study, we aimed to evaluate the use of intraoperative vasopressor infusions during pediatric liver transplantation and its association with postoperative outcomes. We hypothesized that perioperative vasopressors result in untoward postoperative outcomes such as increased length of stay, infection, and graft dysfunction.

Methods: Following IRB approval, we evaluated 173 records which included all patients who underwent a liver transplant at our campus from January 1, 2014 to June 1, 2021. The vasopressor group was characterized as any patient who had a vasopressor infusion utilized for a minimum of 15 consecutive minutes intraoperatively. Re-exploration was defined as any patient who required a subsequent surgical procedure during the hospitalization to evaluate for arterial or venous thrombosis, decreased arterial or venous flow, elevated liver enzymes, or other concerning symptoms. Postoperative infection was defined as infection requiring additional antibiotic coverage and/or fever of unknown origin. To compare baseline characteristics, two-sample t- test and Wilcoxon rank-sum test were utilized. A multivariable regression model was used to ascertain the correlation between vasopressor infusion use and postoperative outcomes, with ordinal logistic regression used for comparison of number of infusions.

Results: 173 patients were analyzed, with 134 (77.5%) meeting criteria for the vasopressor infusion group. Baseline patient characteristics were similar between the two groups with the exception of patients presenting from home were less likely to require a vasopressor infusion. Intraoperative variables including surgical duration, total crystalloids administered, and final pH were similar between groups. The no vasopressor infusion group had significantly more patients who were able to be extubated post-op. The other significant difference was in length of stay, which was shorter in the no vasopressor infusion group. When broken down by type of infusion, the use of a norepinephrine resulted in significantly longer length of stay than any other type of vasopressor (5.58 days). Also, the total number of infusions used had no effect on outcomes.

Conclusions: Pediatric liver transplantation frequently requires vasopressor use. Often, the utilization of these infusions is limited to a short period during the intraoperative course. Our results show that patients not requiring any vasopressor infusion are more likely to be extubated immediately postoperatively and had a shorter length of stay (6.15 days), but there was no significant difference between other postoperative outcomes such as graft dysfunction or infection. Interestingly, we found that the use of a norepinephrine infusion resulted in a significant increase in length of stay. We also found that there was no difference in postoperative outcomes by the total number of vasopressors used.

In patients undergoing pediatric liver transplantation, intraoperative vasopressor infusion is associated with an increase in length of stay, but not with other postoperative complications such as graft dysfunction or infection. The use of a norepinephrine infusion is associated with an increased length of stay as compared with other types on vasopressors.

References: 1. Diagnosis, Incidence, Predictors and Management of Postreperfusion Syndrome in Pediatric Deceased Donor Liver Transplantation. Annals of Transplantation 23; 334-344 (2018)

2. Predictors of Patient and Graft Survival Following Pediatric Liver Transplantation: Long-term Analysis of More Than 300 Cases from Single Centre. Pediatric transplantation 26.1 (2022)

Table: Association between types of vasopressor infusions and postoperative outcomes

Type of Infusion	Re-exploration OR	95% CI	P-Value	Re-transplant OR	95% CI	P-Value	Post-op Infection OR	95% CI	P-Value	Post-op Death OR	95% CI	P-Value	PICU LOS OR	95% CI	P-Value	Hospital LOS OR	95% CI	P-Value
Epinephrine	0.65	0.31, 1.37	0.3	1.17	0.27, 6.04	0.8	0.90	0.38, 2.31	0.9	0.64	0.06, 4.06	0.6	0.10	-2.69, 2.89	0.94	-0.08	-3.81, 3.36	0.97
Norepinephrine	1.23	0.57, 2.61	0.6	0.83	0.08, 2.48	0.5	2.36	1.00, 5.63	0.051	1.95	0.32, 17.3	0.5	3.17	0.34, 5.99	0.028	5.58	2.09, 9.07	0.002
Dopamine	0.67	0.25, 1.60	0.4	1.19	0.17, 5.69	0.8	1.00	0.35, 2.71	>0.9	1.29	0.06, 11.0	0.8	1.17	-2.03, 4.36	0.47	2.12	-1.82, 6.06	0.29
Vasopressin	0.65	0.18, 1.89	0.5	2.26	0.31	0.3	1.11	0.29, 3.39	0.9	2.29	0.11, 20.0	0.5	1.46	-2.45, 5.36	0.46	2.57	-2.25, 7.39	0.29

Table: Association between total number of vasopressor infusions and postoperative outcomes

	Re-exploration	95% CI	P-Value	Re-transplant	95% CI	P-Value	Post-op Infection	95% CI	P-Value	PICU LOS (days)	95% CI	P-Value	Hospital LOS (days)	95% CI	P-Value
# of Infusions															
4	0.00	NA	>0.9	0.00	NA	>0.9	0.00	NA	>0.9	2.65	-15.08, 20.37	0.77	-0.94	-25.85, 17.98	0.72
3	0.43	0.06, 1.76	0.3	1.76	0.08, 19.5	0.7	1.18	0.24, 4.55	0.8	0.65	-4.06, 5.35	0.79	2.45	-3.37, 8.28	0.41
2	1.06	0.44, 2.52	0.9	1.73	0.28, 13.5	0.6	1.47	0.56, 3.96	0.4	0.34	-2.92, 3.59	0.84	0.52	-3.51, 4.55	0.8
0	1.27	0.49, 3.23	0.6	1.71	0.20, 14.8	0.6	0.52	0.11, 1.88	0.4	-3.79	-7.44, -0.14	**0.04**	-6.15	-10.67, -1.63	**0.008**
1	Reference														

*The use of 1 vasopressor was used as the reference point for logistic regression model

Pediatric Anesthesiology 11- Using Real Word Data to Examine Neurodevelopmental Outcome Following Prenatal Opioid Exposure

Lena Sun[1], Michael Kuzniewicz[1], Samuel Pimentel[2], Cynthia Campbell[2], Lisa Croen[3], Sandra Comer[3], Cynthia Salorio[3], Monique Hedderson[3], Sherian Li[3], Eileen Walsh[3], Jacquelin Narula[1]

Columbia University[1] University of California, Berkeley[2] Kaiser Permanente Division of Research[3]

Introduction: The use of Real-World Data (RWD), derived from multiple sources during the delivery of health care to many different different patient populations, is increasingly being used to generate Real World Evidence (RWE) for improving health care[4]. Neonatal opioid withdrawal syndrome (NOWS) is a significant public health problem in the U.S and its incidence has risen dramatically with the onset of the opioid epidemic[5-8]. Very few longitudinal outcome studies of NOWS infants exist, particularly those reporting neurodevelopmental outcomes. Clinical trials to follow up these children are extremely difficult since many of these children have challenging familial environments and depressed socioeconomic conditions. To elucidate neurodevelopmental outcomes in this vulnerable group of children, we sought to create a RWD dataset leveraging available data sources from the Kaiser Permanente Northern California (KPNC) health care delivery system.

Methods: The Kaiser Permanente Northern California (KPNC) healthcare delivery system serves a large and socioeconomically diverse pediatric population in Northern California. The RWD data sources for our study include the unique clinical and data resources that capture all healthcare encounters in comprehensive administrative records and cEHR as well as pharmacy data from 2010-2019, and data from the KPNC Autism Registry. We also obtained additional demographic data from the California birth registry and the California Developmental Disability Services (DDS) dataset. A birth cohort was created for all live births that were ≥ 35 weeks gestational age between 2010-2019. NOWS infants were identified using prespecified ICD-9-CM and/or ICD-10-CM diagnostic codes (P779.5, P96.1, P96.2, P04.49 in first 7 days of life), together with antenatal maternal urinary drug screens, and maternal prescription records from pharmacy for all opioids and other substances. Excluded were those infants transferred out of KPNC, with congenital malformations, and with hypoxic ischemic encephalopathy. Selective chart reviews were performed to ascertain accurate assignment of the birth cohort infants to the NOWS and un-exposed groups. Neurodevelopmental outcomes for the study that examined after age 24 months were autism spectrum disorder, behavioral disorders, cognitive disorders, developmental disorders, and depression/anxiety/psychiatric disorders.

Results: The study received IRB approval at KPNC. There were a total of 376,930 infants in the birth cohort (3,266 NOWS and 340,515 unexposed). One or more urinary drug screen results were available for each infant in the study. Pharmacy data provided information related to prenatal opioid exposure from opioid prescriptions. Birth registry data provided additional demographic information regarding race, ethnicity, and parental education. The CA DDS dataset provided confirmation or additional information related to autism spectrum disorder, cognitive disorders, and cerebral palsy.

Conclusions: We were able to create a RWD dataset that is demographically comparable to the broader California population, leveraging rich data sources from the KPNC health care delivery system, the KPNC Autism Registry, and birth registry and DDS data from the state of California. Our ongoing study will generate RWE using this RWD with NOWS infants from a more diverse socioeconomic background, and with exposure data that have more detailed information regarding prenatal opioid exposure in terms of types of opioids, frequency, duration, and time of exposure during pregnancy.

References: 1. Early Hum Dev **128**: p. 69-76, 2019

2. Pediatrics 2018. **142**(3), 2018

3. Vaccine **39**(29): p. 3814-3824, 2021

4. JAMA Pediatr, 2021. **175**(10): p. 1077-1079, 2021

5. Am J Public Health, **83 Suppl**: p. 1-32, 1993

6. JAMA Pediatr**170**(11): p. 1110-1112, 2016

7. MMWR Morb Mortal Wkly Rep **65**(31): p. 799-802, 2016

8. Pediatrics **137**(5), 2016

Pediatric Anesthesiology 12- When direct laryngoscopy fails. Comparing rescue techniques: video laryngoscopy versus flexible intubation in the Pediatric Difficult Intubation Registry

Mary Lyn Stein[1], Julia Heunis1, Steven Staffa[1], Raymond Park[2], James Peyton[3], John Fiadjoe[3], Pete Kovatsis[1]

Boston Children's Hospital[1] Harvard Medical School[2] Boston Children's Hospital[3]

Introduction: Flexible intubation (FI) has long been considered the gold standard for difficult airway management; however, video laryngoscopy (VL) has gained favor for its ease of use and high success rates. We conducted this study to examine the use of each device type to rescue failed DL and to compare success rates and complications rates. We hypothesized that \ with the technological advancements in VL, failed DL is more frequently rescued with VL than FI in pediatric patients enrolled in Pediatric Difficult Intubation Registry (PeDI-R). Secondarily, we hypothesized that VL and FI would not differ in success rates or complication rates when used to rescue a failed DL. We also hypothesized the standard Mac/Miller blade VL (SVL) and hyperangulated VL (HAVL) would have similar success rates when used to rescue a failed DL.

Methods: The PeDI-R is a prospectively collected multicenter international registry of pediatric patients with difficult DL. Demographic and medical data are collected from clinicians caring for patients using an online submission form. We reviewed all cases from August 2012 – May 2022 and identified cases where FI or VL was attempted following failed DL. Demographic and medical data are collected from clinicians caring for patients using an online submission form. Patients who had attempts with both FI and VL were excluded from the analysis. Data are presented as median (IQR) and number (%). Statistical analyses used the Wilcoxon rank sum test, the Chi-square test, or Fisher's exact test. A p-value < 0.05 was considered statistically significant.

Results: DL failed in 1440 patients with a median age of 4 years and weight of 13kg (Table 1). VL was more likely to be used to rescue a failed DL than flexible intubation (1291/1440 (90%) VL vs 149/1440 (10%) FI, p<0.001). VL was used in older (4 vs 2 years, p = 0.03), larger (14.2 vs 10.5 kg, p = 0.04) patients. First-attempt success (61% VL vs. 60% FI), eventual success (87% VL vs. 88% FI), and overall complications (19% VL vs. 21% FI) did not differ between the techniques (Table 2). DL persistence (>2 DL attempts) was similar between groups (23% vs. 20%). Airway activation was more common in the FI group than the VL group (5% vs. 2%, p = 0.02). In a subgroup analysis of SVL versus HAVL, SVL was less likely to be used to rescue a failed DL than HAVL (437/1291 (34%) SVL vs, 854/1291 (66%) HAVL, p<0.001). The rates of first-attempt success and eventual success were higher with SVL (first-attempt success 68% SVL vs 58% HAVL

Conclusions: In a cohort of pediatric patients with difficult airways, VL was chosen much more frequently (90% of cases) as a rescue intubation technique after failed DL than was FI. Both techniques had similar success and complication rates, although the rate of airway activation was lower in the VL group. Within the VL group, success rates were higher using a standard blade than a hyperangulated blade. The nature of registry data limits the ability to draw definitive conclusions from this study. A prospective randomized trial of VL versus FI is warranted to guide practice, training, and inform equipment purchasing decisions.

References: 1. Fiadjoe JE, Nishisaki A, Jagannathan N, et al. Airway management complications in children with difficult tracheal intubation from the Pediatric Difficult Intubation (PeDI) registry: a prospective cohort analysis. Lancet Respir Med 2016;4(1):37-48.

2. Garcia-Marcinkiewicz AG, Kovatsis PG, Hunyady AI, et al. First-attempt success rate of video laryngoscopy in small infants (VISI): a multicentre, randomised controlled trial. Lancet 2020;396(10266):1905-1913.

3. Peyton J, Park R, Staffa SJ, et al. A comparison of videolaryngoscopy using standard blades or non-standard blades in children in the Paediatric Difficult Intubation Registry. Br J Anaesth 2021;126(1):331-339.

Table 1.

	PeDI-R with failed DL	VL following failed DL	FI following failed DL	p-value
Number of patients (excluding crossover patients)	1440	1291 (90%)	149 (10%)	**<0.001**
Age (years)	4 (0.5, 12.5)	4.1 (0.6, 12.5)	2.1 (0.3, 10.9)	**0.03***
Weight (kilograms)	13.7 (5.8, 33.5)	14.2 (6, 33.6)	10.5 (4.5, 30)	**0.04***
ASA-PS	n=1436	n=1288	n=148	
I	55 (4%)	50 (4%)	5 (3%)	
II	380 (27%)	344 (27%)	36 (24%)	
III	858 (60%)	765 (60%)	93 (63%)	0.9
IV	140 (10%)	126 (10%)	14 (10%)	
V	3 (0.2%)	3 (0.2%)	0 (0%)	
Emergency status	85/1436 (6%)	77/1288 (6%)	8/148 (5%)	0.9
Criteria for registry entry?				
1 – Poor DL view by attending	957 (67%)	842 (65%)	115 (77%)	**0.003***
2 – Limited mouth opening	65 (5%)	57 (4%)	8 (5%)	0.535
3 – Failed DL in last 6 months	96 (7%)	89 (7%)	7 (5%)	0.387
4 – Anticipated difficulty, attending DL defined	445 (31%)	412 (32%)	33 (22%)	**0.02***
Abnormal physical exam?	405/1437 (28%)	382/1288 (30%)	23 (15%)	**<0.001***
Identified genetic syndrome?	798 (55%)	695 (54%)	103 (69%)	**<0.001***
Anticipated difficulty?	851 (59%)	743 (58%)	108 (73%)	**<0.001***
Initial clinician managing the airway	N=1437	N=1288	N=149	
Trainee (1)	754 (53%)	683 (53%)	71 (48%)	
CRNA (2)	224 (16%)	199 (16%)	25 (17%)	
Attending anesthesiologist (3-7)	402 (28%)	358 (28%)	44 (30%)	**<0.001***
Otolaryngologist (8)	19 (1%)	10 (1%)	9 (6%)	
Other (9, 10)	38 (3%)	38 (3%)	0 (0%)	
Total number of attempts with DL	2 (1, 2)	2 (1, 2)	2 (1, 2)	0.4
DL persistence (> 2 attempts with DL)	330 (23%)	301 (23%)	29 (20%)	0.3

*Denotes statistical significance.
Data are presented as median (IQR) and number (%). Statistical analyses used the Wilcoxon rank sum test, the Chi-square test, or Fisher's exact test. A p-value < 0.05 was considered *statistically significant.

Abbreviation	Meaning
ASA-PS	ASA Physical Status Classification
DL	direct laryngoscopy
FI	flexible intubation
PeDI-R	Pediatric Difficult Intubation Registry
VL	video laryngoscopy

Table 2.

Outcome	VL following failed DL	FI following failed DL	p-value
Number of patients	1291 (90%)	149 (10%)	**<0.001**
First attempt success with technique	793 (61%)	90 (60%)	0.8
Eventual success	1125 (87%)	131 (88%)	0.8
Surgical or failed airway	2 (0.2%)	0 (0%)	0.9
Total number of attempts	3 (2, 4)	3 (2, 4)	0.6
Any complications?	241 (19%)	32 (22%)	0.5
Death	6 (0.5%)	1 (0.7%)	0.5
Cardiac arrest	19 (2%)	1 (0.7%)	0.7
Hypoxemia	117 (9%)	16 (11%)	0.6
Airway activation (bronchospasm and/or laryngospasm)	26 (2%)	8 (5%)	**0.02***
Subgroup analysis by VL type			
	SVL following failed DL	**HAVL following failed DL**	
Number of patients	437 (34%)	854 (66%)	**<0.001***
First attempt success with technique	297 (68%)	496 (58%)	**0.001***
Eventual success	393(90%)	732 (86%)	**0.03***

*Denotes statistical significance.
Data are presented as median (IQR) and number (%). Statistical analyses used the Wilcoxon rank sum test, the Chi-square test, or Fisher's exact test. A p-value < 0.05 was considered *statistically significant.

Abbreviation	Meaning
ASA-PS	ASA Physical Status Classification
DL	direct laryngoscopy
FI	flexible intubation
HAVL	hyperangulated blade video laryngoscopy
PeDi-R	Pediatric Difficult Intubation Registry
SVL	standard Macintosh/Miller blade video laryngoscopy
VL	video laryngoscopy

Perioperative Anesthesia

Perioperative Anesthesia 1- Impact of the difference between preoperative blood pressure measured in the ward and pre-induction blood pressure on the postoperative outcomes in non-cardiac surgery

Jin-*Young Kim[1], Sang-Wook Lee[1], Sung-Hoon Kim[1], Woo-Young Seo[1], Seongyong Park[2], Hyun-Seok Kim[2], Dong-Kyu Kim[2], Jaewon Jang[2], Hyungjun Park[2]*

Asan Medical Center, University of Ulsan College of Medicine[1] Asan Medical Center[2]

Introduction: There are cases in which the blood pressure measured in the ward of a surgical patient is different from the blood pressure measured before induction of anesthesia. It is not known how the difference between baseline blood pressure measured in the ward and blood pressure measured immediately before induction of anesthesia in the operating room affects postoperative outcomes. This study aims to investigate the relationship between these blood pressure differences and postoperative outcomes.

Methods: This study included 65,854 patients (18 years of age and older) who were admitted to a single tertiary institution for non-cardiac surgery between March 1, 2019, and February 28, 2021, for study analysis (Figure 1). The data used in the study were automatically collected through the electronic medical record (EMR) system, analyzed retrospectively, and used for analysis after being anonymized, so the IRB exempted the informed consent of the patients. Data included patient demographic information, surgical details, ward, and operating room blood pressure data, and postoperative outcome data. The demographic information of the patient includes age, sex, height, weight, and body mass index (BMI), and the surgery information includes the name of the operation and the surgical department. Ward blood pressure is defined as the average value of non-invasive blood pressure measured within 24 hours before surgery, and pre-induction blood pressure refers to the blood pressure measured immediately before anesthesia induction in the operating room. Postoperative clinical outcomes for analysis in this study were in-hospital 30-day mortality, and acute kidney injury (AKI). The most recent consensus on the definition and stages of AKI was made by the Kidney Disease: Improving Global Outcomes (KDIGO) Foundation in 2012. Blood pressure difference and induced blood pressure were divided into 8 groups according to data distribution and converted into categorical variables for analysis. Analysis was performed by applying a univariate logistic regression model to analyze the effect of blood pressure data on outcome data. We also performed an analysis of adjustment by applying a multivariate logistic regression model to correct for the influence of other variables on the outcome.

Results: As a result of the analysis, the systolic blood pressure, mean blood pressure, and pulse pressure showed a tendency to increase the risk of death at 30 days as the pre-induction blood pressure was lower than the ward blood pressure. Figure 2 shows the correlation between various blood pressure differences and 30-day mortality as an odds ratio. Diastolic blood pressure and mean blood pressure increased the 30-day risk of death when pre-induction blood pressure was higher than ward blood pressure, but the risk decreased for systolic blood pressure and pulse pressure. In all types of blood pressure, if pre-induction blood pressure is lower than ward blood pressure, the risk of 30-day mortality tends to increase. For AKI, the risk of developing AKI was reduced when pre-induction blood pressure was higher than ward blood pressure, but the risk of AKI tends to increase when pre-induction blood pressure was lower than ward blood pressure Figure 3 shows the correlation between various blood pressure differences and AKI as an odds ratio.

Conclusions: This study showed that the difference between pre-induction blood pressure measured in the operating room before induction of anesthesia and preoperative blood pressure measured in the ward could affect surgical outcomes such as 30-day mortality and AKI. Therefore, in the case of patients with a large difference between pre-induction and preoperative blood pressure in the ward, careful patient management, and hospital resource allocation are required during the preoperative period.

References: 1. Sanders RD, et al. Perioperative Quality Initiative consensus statement on preoperative blood pressure, risk and outcomes for elective surgery. *Br J Anaesth* 2019; **122:** 552-62.

2. Abdelmalak BB, et al. The association between preinduction arterial blood pressure and postoperative cardiovascular, renal, and neurologic morbidity, and in-hospital mortality in elective noncardiac surgery: an observational study. *J Hypertens* 2018; **36:** 2251-9.

3. van Klei WA, et al. Relationship Between Preoperative Evaluation Blood Pressure and Preinduction Blood Pressure: A Cohort Study in Patients Undergoing General Anesthesia. *Anesth Analg* 2017; **124:** 431-7.

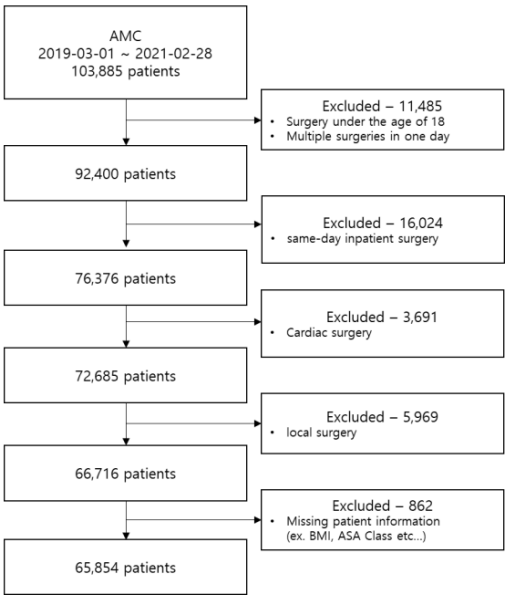
AMC
2019-03-01 ~ 2021-02-28
103,885 patients
Excluded – 11,485
Surgery under the age of 18
Multiple surgeries in one day
92,400 patients
Excluded – 16,024
same-day inpatient surgery
76,376 patients
Excluded – 3,691
Cardiac surgery
72,685 patients
Excluded – 5,969
local surgery
66,716 patients
Excluded – 862
Missing patient information
(ex. BMI, ASA Class etc...)
65,854 patients

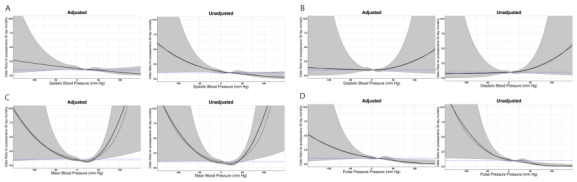
A
Adjusted
Unadjusted
B
Adjusted
Unadjusted
C
Adjusted
Unadjusted
D
Adjusted
Unadjusted

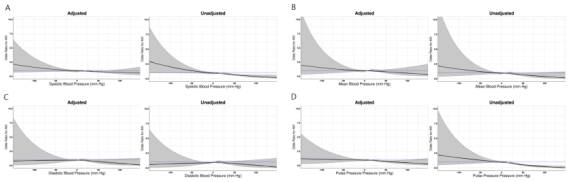
A
Adjusted
Unadjusted
B
Adjusted
Unadjusted
C
Adjusted
Unadjusted
D
Adjusted
Unadjusted

Perioperative Anesthesia 2- A Machine Learning Approach Utilizing Radiological Findings to Estimate Surgical Case Duration for Open Reduction and Internal Fixation of Radial Fractures

Fernanda Pacheco[1], Rodney Gabriel[2], Brenton Alexander[3]

University of California, San Diego School of Medicine[1] University of California San Diego[2] UC San Diego[3]

Introduction: Accurate predictions of surgical case durations are critical to maintaining operating room (OR) efficiency. Current hospital methods for case-time predictions may utilize historical data from electronic medical records (EMRs) and surgeon input, but may not factor in significant patient, provider, or system variables.[1] As a result, EMR and surgeon-generated case time estimates are potentially prone to over and under-estimation, leading to loss of valuable OR time.[2] In recent years, machine learning (ML) has been introduced as a method for generating more accurate surgical case time predictions. Additionally, incorporating radiologic findings in ML models to predict radial fracture repair times has not been studied. Thus, the objective of our study was to develop ML models that incorporate preoperative imaging reads to predict radial fracture open reduction and internal fixation (ORIF) case times.

Methods: This was a single-center, retrospective study of 236 cases identified to have undergone ORIF of radial fractures from 2018 to 2020. After exclusion (e.g., missing radiology reports), 201 cases were included in the final analysis (**Table 1**). The primary outcome measurements obtained from preoperative radiological findings included: imaging type (CT or x-ray), fracture displacement, tilt/angulation, intra- or extra-articular, comminution, impaction, ulnar styloid fracture, additional ulnar fracture, and surgery redo status. Additional patient and procedure variables obtained from the EMR were also included in the model.

We then implemented three machine learning approaches in R Studio[3] for predicting actual skin times: multivariable linear regression using all features, multivariable linear regression with feature selection (based on a combination of forward selection and backwards elimination using Akaike Information Criterion), and multilayer perceptron neural networks. The average root mean squared error (RMSE) and mean absolute error (MAE) were calculated via 5-fold cross-validation. The model performances were then compared to a baseline model, which utilized scheduled skin times to estimate actual skin time. These scheduled skin times were based on the average of the last three times this procedure was performed from that surgical provider.

Results: The median [quartile] scheduled skin minutes was 85 [65, 90] minutes. The median [quartile] actual skin minutes was 67 [55, 86] minutes. The majority of the study population had intra-articular fracture, fracture displacement, fracture tilt/angulation, fracture comminution, fracture impaction, and ulnar styloid fracture.

Initially, multivariable linear regression with all features was implemented, in which features such as preoperative utilization of CT-imaging (+6.3 minutes), intra-articular fractures (+10.2 minutes), redo surgery (+33.3 minutes), and surgeon (-16.9 minutes) had the most impact (**Table 2**). Next, a multivariable linear regression model using feature selection was implemented, in which 7 features remained in the model, including preoperative utilization of CT-imaging, intra-articular fracture on imaging, ulnar styloid fracture on imaging, redo surgery, patient weight, scheduled skin times, and surgical provider (**Table 3**). Lastly, a neural network model was developed, in which all features served as inputs. The neural network consisted of one hidden layer and 100 hidden nodes. Using 5-fold cross-validation, the average RMSEs for the baseline, multivariable linear regression with all features, multivariable linear regression with feature selection, and neural network were 33.7, 24.9, 16.3, and 14.2 minutes, respectively; while the MAEs were 26.1, 19.6, 12.7, and 10.9 minutes, respectively (**Figure 1**).

Conclusions: Compared to the institution's standard method of case-time predictions, our ML models had improved prediction accuracy, with the neural network model having the best performance. Our results demonstrate the potential for ML incorporating radiologic findings to improve OR scheduling efficiency. Further studies are necessary to validate this ML method in other surgical subspecialties.

References:

1. Production Planning & Control, 2013. 24(10-11), 891-902.
2. Journal of the American College of Surgeons, 2019. 229(4), 346-354.
3. RStudio: Integrated Development for R. RStudio, PBC, Boston, MA.

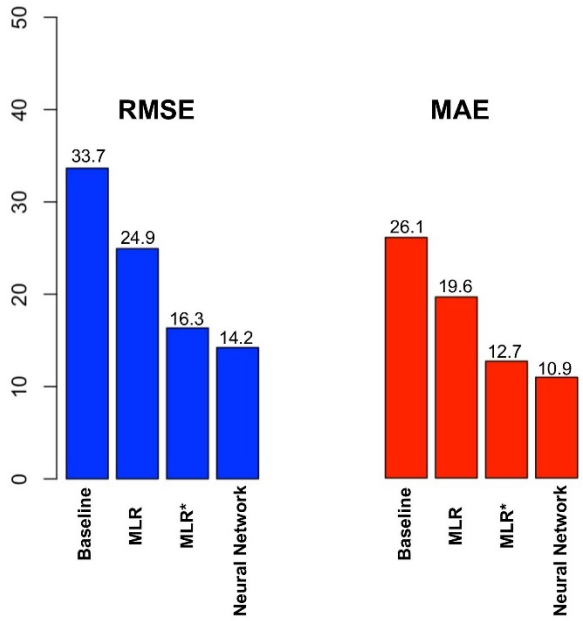

Features	Estimate	Standard Error	P-value
Preoperative Utilization of CT-Imaging Radiological Findings	6.25	2.75	0.02
Displacement	-1.94	4.74	0.68
Tilt/Angulation	-0.42	4.47	0.93
Intra vs. Extra-articular Fracture	10.23	4.99	0.04
Comminuted	2.67	4.64	0.57
Ulnar Fracture	-0.53	3.04	0.86
Ulnar Styloid Fracture	5.57	4.47	0.21
Impacted	2.81	4.25	0.51
Redo Surgery	33.29	16.68	0.04
ASA PS Classification Score			
1		Reference	
2	-2.69	5.52	0.63
3	-11.74	7.56	0.12
Age (years)	0.04	0.15	0.81
Weight (kg)	0.32	0.13	0.01
Male Sex	3.49	5.21	0.51
Scheduled Skin Time	0.23	0.12	0.04
Surgeon			
other		Reference	
A	-16.93	7.21	0.02
B	3.59	6.85	0.61

Table 2. Feature estimates based multivariable linear regression modeling actual surgical skin time using all available features
Abbreviations:
ASA PS, American Society of Anesthesiologists
CT, computed tomography

Features	n	%
Total	201	
Preoperative Utilization of CT-Imaging Radiological Findings	44	21.9
Displacement	141	70.1
Tilt/Angulation	127	63.2
Intra vs. Extra-articular Fracture	156	77.6
Comminuted	138	68.7
Ulnar Fracture	13	6.5
Ulnar Styloid Fracture	116	57.7
Impacted	104	51.7
Redo Surgery	3	1.5
ASA PS Classification Score		
1	68	33.8
2	101	50.2
3	32	15.9
Age (years), median [quartile]	55 [34, 63]	
Weight (kg), median [quartile]	75.8 [64.8, 86.1]	
Male Sex	74	36.8
Scheduled Skin Time, median [quartile]	85 [65, 90]	
Surgeon		
other	22	10.9
A	83	41.3
B	96	47.8

Table 1. Baseline characteristics of study population
Abbreviations:
ASA PS, American Society of Anesthesiologists
CT, computed tomography

Features	Estimate	Standard Error	P-value
Preoperative Utilization of CT-Imaging Radiological Findings	6.48	2.67	0.02
Intra vs Extra-Articular Fracture	11.34	4.79	0.02
Ulnar Styloid Fracture	5.78	4.01	0.15
Redo Surgery	31.32	16.38	0.06
Weight (kg)	0.32	0.12	0.007
Scheduled Skin Minutes	0.22	0.11	0.05
Surgeon			
Other		Reference	
A	-18.48	7.02	0.009
B	1.91	6.64	0.77

Table 3. Feature estimates based multivariable linear regression modeling actual surgical skin time using selected features. The features were chosen based on a combination of backwards elimination and forward selection based on the Akaike Information Criterion.
Abbreviations:
ASA PS, American Society of Anesthesiologists
CT, computed tomography

Perioperative Anesthesia 3- An Analysis of Intraoperative Fibrinolysis following Introduction of Goal-Directed Coagulation Management Guidelines during Liver Transplantation

Alan Boiangu[1], Aaron Kurtti[2], Matthew Palascak[2], Daniel Arango[2], Bryan Evans[2], William Daly[2], Brian Fish[2], Donald Ganier[2], Joseph Koveleskie[2], Shaun Yockelson[2], Ramona Nicolau-Raducu[2], Bobby Nossaman[2]

Ochsner Medical Center[1] University of Queensland - Ochsner Clinical School[2]

Introduction: Cirrhosis impedes synthesis of functional hemostatic proteins resulting in significant hemorrhagic diathesis during liver transplantation (1). In 2018, the International Liver Transplant Society proposed coagulation management guidelines to assist liver transplantation centers (2). The purpose of this study was to measure outcomes following introduction of a version of these treatment guidelines when assayed by thromboelastrogram (TEG) immediately following liver transplantation (3, 4).

Methods: Following IRB approval, all adult (≥18 years of age) patients with end-stage liver disease undergoing liver transplantation were entered into this study. Intraoperative TEGs assessed changes in the incidence of fibrinolysis following introduction of goal-directed coagulation management guidelines (5). Key associations with 95% confidence intervals (CI) were analyzed with Chi-square tests with the associated probability value for statistical significance set at the more stringent value of <.005 to minimize for the risk of false discovery rates (6). Effect size for this model was analyzed with risk differences with CI (7). Predictive accuracy of this model was analyzed with misclassification rates.

Results: Analysis of variance of the incidence of fibrinolysis (LY-30 >8%) following introduction of goal-directed coagulation management guidelines during liver transplantation are shown in Table 1. In this study of 1464 patients, 285 patients underwent goal-directed coagulation management guidelines (Table 1). The incidence of fibrinolysis immediately following liver transplantation decreased from 23.2% to less than 3% with a risk reduction of -20.6% (Table 1). This reduction in fibrinolysis due to chance was less than 1 in 10,000 (Table 1). The predictive accuracy of this model was 80.6%.

Conclusions: The results from this preliminary study suggest an important clinical improvement in the incidence of fibrinolysis as detected by TEGs following introduction of the goal-directed coagulation management guidelines in this patient population.

References: Coagulation during and after orthotopic transplantation of the human liver. Arch Surg. 1969;98(1):31-4.

Perioperative Coagulation Management in Liver Transplant Recipients. Transplantation. 2018;102(4):578-92.

Thromboelastogram monitoring in the perioperative period of hepatectomy for adult living liver donation. Liver Transpl. 2004;10(2):289-94

Epsilon-Aminocaproic Acid Has No Association With Thromboembolic Complications, Renal Failure, or Mortality After Liver Transplantation. J Cardiothorac Vasc Anesth. 2016;30(4):917-23.

Comparison between thrombelastography and thromboelastometry in hyperfibrinolysis detection during adult liver transplantation. Br J Anaesth. 2016;116(4):507-12.

Redefine statistical significance. Nature Human Behaviour. 2018;2(1):6-10.

Using Effect Size-or Why the P Value Is Not Enough. J Grad Med Educ. 2012;4(3):279-82.

Table 1 Contingency Table of the Incidence of Fibrinolysis during Liver Transplantation following Introduction of Goal-directed Coagulation Management Guidelines

	Fibrinolysis by TEG Assessment		
Patients, n (%)	Yes	No	Totals
GDCMG	7 (2.6)	260 (97.4)	267
Control	278 (23.2)	919 (76.8)	1197
Totals	285	1179	1464

n (%): counts and percentage; Risk Difference in the incidence of fibrinolysis decreased -20.6% with a 95% confidence interval [-23.7 to -17.5%] following introduction of Goal-Directed Coagulation Management Guidelines (GDCMG) during liver transplantation. Likelihood Chi-Square=81.0, P<.0001. P values <.005 are statistically significant (6).

Perioperative Anesthesia 4- An immune signature of Surgical Site Infections (SSI), a retrospective study with a novel machine learning pipeline for biomarker identification

Franck Verdonk[1], Julien Hedou[1], Ivana Marić[1], Gregoire Bellan[2], Jakob Einhaus[2], Dyani Gaudilliere[2], Adam Bonham[2], Martin Angst[3], Brice Gaudilliere[3], Amélie Cambriel[4]

Stanford University[1] SurgeCare SAS[2] Stanford Medicine[3] Department of anesthesia, Stanford University[4]

Introduction: Surgical Site Infections are some of the most devastating, costly, and common surgical complications after surgery. The ability to accurately predict SSI is critical as it will guide high-quality surgical decision-making, including optimizing preoperative interventions and timing of surgery. However, existing risk prediction tools for the prediction of SSI perform poorly. In a prospective study of 43 patients, our group previously identified strong immune correlates of SSI from the combined plasma and single-cell proteomic analysis of blood samples collected after surgery (1). Here, we performed a retrospective study in 96 patients undergoing abdominal surgery to identify pre-operative immune responses predictive of SSI from the analysis of peripheral blood samples collected before surgery.

Methods: Blood samples collected before surgery were analyzed using a combined single-cell (mass cytometry) and plasma proteomic (SomaScan) approach. Samples were selected from a larger cohort using a frequency-matching procedure to minimize the effect of confounders on identified immunological biomarkers. The analysis combines two omics datasets, a plasma proteomic dataset and a mass cytometry dataset containing four omics sublayers. STABL, a novel machine learning analysis for the analysis of high-dimensional multi-omic data is applied to merge the sublayers into a final model with a unique set of features selected from each sublayer.

Results: STABL identifies a model of SSI with good predictive performance (Area Under the Curve = 0.74), improving on current clinical scales performance. Notably, patients at risk for SSI showed increased MyD88 signaling (e.g., pMAPKAPK2 signal) in response to LPS in myeloid cell subsets such as granulocytes, which resonates with selected features from the proteomic dataset, including increased levels of pro-inflammatory cytokines IL-1b and CCL3 or the stress response protein HSPH1. While IL-1b and HSPH1 represent classic mediators of acute response to inflammation and are released, among others, by activated neutrophils, CCL3 mediates initial recruitment of neutrophils to sites of inflammation (2,3). (***Figure 1***)

Conclusions: These new findings emphasize the potential of STABL to discover predictive biomarkers that link multiple omics data layers with high biological plausibility and provide an avenue for efficient diagnostic and therapeutic development. Informative features of the SSI classification are readily interpretable biologically and the model points at coordinated bulk and single-cell proteomic features that are consistent with previously unrecognized innate immune system mechanisms, conducive to infection after surgery.

References: (1) ***Ann Surg*** 2022 Mar 1;275(3):582-590. Integrated Single-cell and Plasma Proteomic Modeling to Predict Surgical Site Complications: A Prospective Cohort Study. Kristen K Rumer et al.

(2) ***Nat Immunol*** 2021 Jan;22(1):2-6.Trained immunity, tolerance, priming and differentiation: distinct immunological processes. Maziar Divangahi et al.

(3) ***J Immunol*** 2007 Jan 15;178(2):1164-71. MyD88-dependent and MyD88-independent pathways in synergy, priming, and tolerance between TLR agonists. Aranya Bagchi et al.

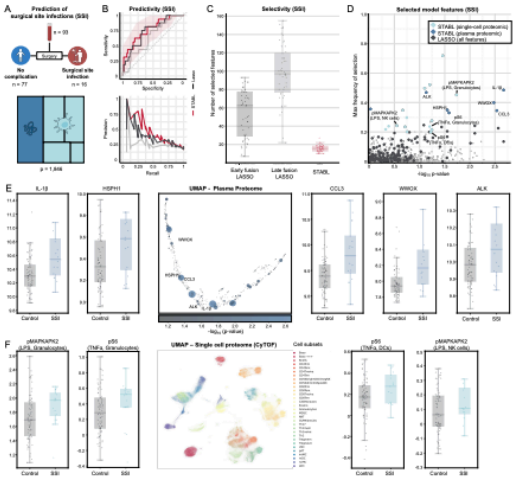

Figure 1
STABL identifies candidate biomarkers from newly generated multi-omics data. A. A multiomic dataset was generated with a combination of proteomics and immune cell omics data. In total, 93 samples were collected. Among them, 16 patients suffered from a surgical site infection. **B.** From the collected data, an integrated model was computed using either early fusion LASSO, late fusion LASSO, or STABL. Predictive performance was comparable with an Area Under the Receiver-Operator Curve (AUROC) of 0.74 for STABL. The Area Under the Precision-Recall Curve is also shown (AUPRC) **C.** For each model, using a Monte Carlo Cross-Validation (CV) framework, the average number of features is assessed. STABL is the most selective algorithm with a median of 16 features selected, compared to 59 for early fusion and 97 for late fusion. **D.** Plotting the maximum frequency of selection from STABL against the -log10 pvalue using a univariate Mann-Whitney test statistics procedure, the features selected above the threshold display improved reliability in STABL compared to the LASSO. **E.** UMAP of the plasma proteomic molecular features. Each node's color and size represent the strength of the association with the outcome. The top hits from STABL are represented with boxplots: IL-1B, HSPH1, CCL3, WWOX, and ALK. **F.** UMAP of the single-cell proteome representing the data at the cellular level. Each color corresponds to a sub-cell type after cell gating. Similarly, the top hits are represented using boxplots: pMAKAPK2 after LPS stimulation in Granulocytes, pS6 after TNF alpha stimulation in Granulocytes, pS6 after TNF alpha stimulation in Dendritic Cells, and pMAPKAPK2 after LPS stimulation in Natural Killer Cells.

Perioperative Anesthesia 5- Are Sex Discordances between the Anesthesia Provider and Patient Associated with Adverse Postoperative Outcomes?

Dario von Wedel[1], Laetitia Chiarella[2], Elena Ahrens[3], Denys Shay[3], Luca Wachtendorf[4], Simone Redaelli[1], Aiman Suleiman[1], Ricardo Munoz[5], Sarah Ashrafian[3], Eva-Lotte Seibold[1], Stephen Woloszynek[3], Guanqing Chen[3], Valerie Banner-Goodspeed[3], Maximilian Schaefer[6]

Beth Israel Deaconess Medical Center, Harvard Medical School[1] Director, Center for Anesthesia Research Excellence (CARE).[2] Beth Israel Deaconess Medical Center[3] Montefiore Medical Center[4] BIDMC[5] Beth Israel Deaconess Medical Center & Hospital[6]

Introduction: Previous studies have raised concerns of poorer patient outcomes when there is discordance between the sex of the surgeon and their patients [1]. We investigated whether anesthesia provider-patient sex discordances are associated with adverse postoperative outcomes.

Methods: This retrospective study included adult patients who underwent anesthesia care at an academic tertiary healthcare center in Massachusetts, USA, between 2008 and 2020. The primary exposure was anesthesia provider-patient sex discordance, defined as opposite-sex constellation between the patient and primary anesthesia provider in the room. The primary outcome was a composite of major postoperative complications (including myocardial infarction, stroke, pneumonia, need of mechanical ventilation, renal failure, cardiac arrest, pulmonary embolism, atrial fibrillation, and shock), readmission, or mortality within 30 days [2, 3]. In secondary analyses, potential effect modification of the primary association by surgeon sex was assessed. We conducted analyses stratified by patient sex to differentiate the effect of sex discordance in male compared to female patients. Multivariable-adjusted mixed-effects logistic regression was applied for all models, including individual anesthesia and surgical providers as crossed random effects, while adjusting for patient demographics and characteristics (age, sex, BMI, comorbidities, and socioeconomic factors), as well as provider factors (experience, sex of anesthesia and surgical provider) as fixed effects (**Figure 1**). With an exploratory intent, random effect variances and model residuals were used to calculate intraclass correlation (ICC), further quantifying provider-related variance in the primary outcome.

Results: 368,877 patient cases (206,962 [56.1%] female; **Figure 2**, **Table 1**) were included. 182,811 (49.6%) cases were performed by female providers. 181,573 (49.2%) patients received care by a primary anesthesia provider of the opposite sex (**Table 1**). The primary composite outcome was observed in 39,495 (11.5%) patients (components are shown in **Table 1**). There was no association between anesthesia provider-patient sex discordance and the primary outcome (aOR, 0.99; 95% CI, 0.97-1.01, p=0.36), and no interaction with surgeon sex was found (p-interaction=0.93). Furthermore, anesthesia provider-patient sex discordance was not associated with individual components of the primary outcome, including major postoperative complications (aOR, 0.97; 95% CI, 0.94-1.01, p=0.12), readmission to the hospital (aOR, 1.00; 95% CI, 0.97-1.02, p=0.91) or mortality (aOR, 1.01; 95% CI, 0.94-1.08, p=0.83) within 30 days. The results of the primary analysis were confirmed after stratification by patient sex (aOR, 0.99; 95% CI, 0.96-1.03, p=0.64 in female and aOR, 0.99; 95% CI, 0.96-1.03, p=0.61 in male patients). Compared to surgical providers, the individual effects of anesthesia providers with regard to the primary outcome were marginal (ICC 5.7% for surgical vs. 0.1% for anesthesia providers; **Figure 3**).

Conclusions: In contrast to the effect of discordances between surgeon and patient sex, discordances between the anesthesia provider and their patient were not associated with adverse postoperative outcomes. This might be explained by a smaller effect of the individual anesthesia provider and potentially a higher fraction of female providers.

References: [1] Association of Surgeon-Patient Sex Concordance With Postoperative Outcomes. JAMA Surg. 2022 Feb 1;157(2):146-156.

[2] Association Between Handover of Anesthesia Care and Adverse Postoperative Outcomes Among Patients Undergoing Major Surgery. JAMA. 2018 Jan 9;319(2):143-153.

[3] Outcomes of Daytime Procedures Performed by Attending Surgeons after Night Work. N Engl J Med. 2015 Aug 27;373(9):845-53.

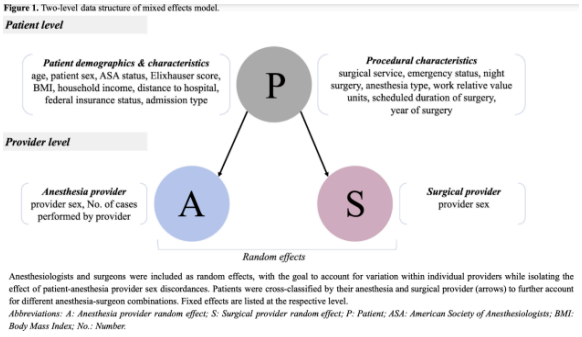

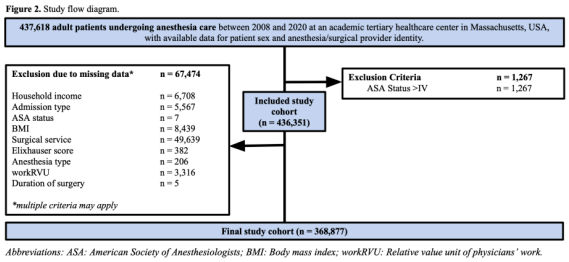

Figure 3. Provider-related variability in 30-day composite outcome across individual anesthesiologists and surgeons.

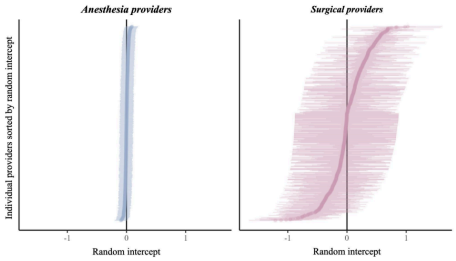

Sorted random intercepts of individual providers are shown by group. Random intercepts for anesthesia and surgical providers were obtained from the primary adjusted mixed effects model, including adjustment for markers of procedural severity. Variance among anesthesiologists was marginal when compared to surgeons (intraclass correlation [ICC] 0.1% vs. 5.7%).

Table 1. Patient characteristics by anesthesia provider-patient sex discordance.

	Cases with anesthesia provider-patient sex concordance n=187,304	Cases with anesthesia provider-patient sex discordance n=181,573	Standardized difference
Patient characteristics			
Age, years	58.0 (45.0 - 69.0)	58.0 (45.0 - 69.0)	0.00
Sex, female	104,100 (55.6%)	102,862 (56.7%)	-0.02
ASA physical status			0.00
1	19,371 (10.3%)	18,235 (10.0%)	
2	83,834 (44.8%)	81,107 (44.7%)	
3	69,910 (37.3%)	69,669 (38.4%)	
4	14,189 (7.6%)	12,502 (6.9%)	
Elixhauser Comorbidity Score	4 (0 - 13)	4 (0 - 13)	0.00
Body mass index, kg/m^2	27.2 (23.7 - 31.6)	27.2 (23.7 - 31.6)	0.00
Estimated household income, USD	$4,170.0 ($4,526.0 - 105,061.0)	$4,034.0 ($4,136.0 - 104,928.0)	0.00
Residing within 10 miles of hospital	87,068 (46.5%)	84,458 (46.5%)	0.00
Federal insurance status	64,485 (34.4%)	63,152 (34.8%)	0.00
Admission type			0.00
Ambulatory	102,149 (54.5%)	99,063 (54.6%)	
Same day admission	52,523 (28.0%)	51,257 (28.2%)	
Inpatient	32,632 (17.4%)	31,253 (17.2%)	
Provider characteristics			
Anesthesia provider sex, female	104,100 (55.6%)	78,711 (43.3%)	0.24
Surgical provider sex, female	35,209 (18.8%)	32,923 (18.1%)	0.01
Total cases performed by anesthesia provider	635 (304 - 1,135)	619 (297 - 1,086)	0.02
Procedural characteristics			
Surgical service			-0.01
Cardiac	6,620 (3.5%)	5,411 (3.0%)	
Colorectal	3,900 (2.1%)	3,854 (2.2%)	
Cardiology	1,131 (0.6%)	1,005 (0.6%)	
Dental, oral	354 (0.2%)	342 (0.2%)	
Ear, nose, throat	4,342 (2.3%)	4,272 (2.4%)	
Eye	7,870 (4.2%)	7,198 (4.0%)	
General surgery	27,719 (14.8%)	27,332 (15.1%)	
Gastrointestinal	19,751 (10.5%)	19,669 (10.8%)	
Gynecology	27,205 (14.5%)	25,480 (14.0%)	
Neurosurgery	5,941 (3.2%)	5,835 (3.2%)	
Orthopedics	33,291 (17.8%)	33,597 (18.5%)	
Plastic	9,224 (4.9%)	8,558 (4.7%)	
Podiatry	3,574 (1.9%)	3,507 (1.9%)	
Surgical oncology	5,877 (3.1%)	5,025 (2.8%)	
Thoracic	7,676 (4.1%)	7,731 (4.3%)	
Transplant	3,516 (1.9%)	3,497 (1.9%)	
Trauma, surgical critical care	4,129 (2.2%)	4,188 (2.3%)	
Urology	8,974 (4.8%)	9,027 (5.0%)	
Vascular	6,210 (3.3%)	5,965 (3.3%)	
Emergency status	13,911 (7.4%)	13,513 (7.4%)	0.00
Anesthesia care type			0.00
General anesthesia	113,558 (60.6%)	109,436 (60.3%)	
Monitored anesthesia care	69,077 (36.9%)	67,397 (37.1%)	
Regional anesthesia	4,669 (2.5%)	4,738 (2.6%)	
Work relative value units	8.3 (4.8 - 15.6)	8.1 (4.7 - 15.4)	0.01
Scheduled duration of surgery, min	120 (62 - 180)	120 (60 - 180)	0.00
Night surgery	12,142 (6.5%)	11,983 (6.6%)	0.00
Year of surgery			-0.01
2008	11,780 (6.3%)	11,440 (6.3%)	
2009	12,706 (6.8%)	12,202 (6.7%)	
2010	13,383 (7.1%)	12,504 (6.9%)	
2011	13,924 (7.4%)	13,586 (7.5%)	
2012	14,226 (7.6%)	14,390 (7.9%)	
2013	15,075 (8.0%)	14,543 (8.0%)	
2014	16,285 (8.7%)	15,153 (8.3%)	
2015	17,279 (9.2%)	16,273 (9.0%)	
2016	18,906 (10.1%)	17,943 (9.9%)	
2017	17,868 (9.5%)	17,482 (9.6%)	
2018	17,391 (9.3%)	17,405 (9.6%)	
2019	15,047 (8.0%)	15,072 (8.3%)	
2020	3,434 (1.8%)	3,580 (2.0%)	
Outcome components			
Major complication within 30 days	9,267 (4.9%)	8,644 (4.8%)	0.01
Readmission within 30 days	13,669 (7.3%)	13,247 (7.3%)	0.00
Mortality within 30 days	1,941 (1.0%)	1,858 (1.0%)	0.00

Data are expressed as frequency (prevalence in %), or median (interquartile range [25th-75th percentile]). Comorbidities were defined using International Classification of Diseases (9th/10th Revision, Clinical Modification [ICD-9/10-CM]) diagnostic codes.

ASA: American Society of Anesthesiologists; USD: United States Dollars.

Perioperative Anesthesia 6- Elevated Plateau Pressures in patients with BMI >25 kg/m^2 during low tidal volume mechanical ventilation

Cristian Rosa-Carrasquillo[1], Maria Crespo[1], Allan Reyes-Sullivan[1], Hector Torres-Perez[1]

University of Puerto Rico[1]

Introduction: Several studies have shown the protective benefits of maintaining the plateau pressure (Pplat) during low tidal volume mechanical ventilation (Vt; 6 ml/kg) at a certain threshold to avoid complications like atelectasis or barotrauma, with the latter being significantly associated with Pplat greater than 35 cm H2O [1]. In obesity and other conditions with increased chest wall stiffness, however, the Pplat may substantially overestimate the distending pressure of the lung [2]. Although limiting Pplat during mechanical ventilation helps in decreasing ventilator-associated lung injury, currently there is no defined threshold below which further reduction would result in improved outcomes in these patients [2]. Specifically, the association between body mass index (BMI) and Pplat has not been fully described, and there are no specific values attributed to obesity as a determinant of Pplat. Quantification of Pplat could elucidate the role that obesity plays in the mechanically ventilated lung and aid us in implementing strategies that not only avoid overdistension injury, but also atelectasis. To determine if obesity is associated with Pplat, we investigated the relationship between BMI and Pplat in mechanically ventilated patients undergoing elective surgery.

Methods: In this cross-sectional study, we assessed 581 non-trauma patients aged >21, with ASA physical status I, II, and III undergoing general anesthesia under mechanical ventilation in a tertiary medical institution from 2017 to 2022. Patient height, weight, and sex were initially obtained to measure real body weight (RBW) and calculate their ideal body weight (IBW) to estimate Vt. Five minutes after neuromuscular blockade, the ventilation parameters were assessed using standard ASA monitoring procedures. In continuous mandatory ventilation (CMV), peak pressure, Pplat and ETCO2 values were then assessed for IBW and RBW. Student's t-tests were performed, with equal or unequal variances, to determine an association between body mass index (BMI; < 25 kg/m^2, ≥ 25kg/m^2) and Pplat according to the calculated Vt for IBW or RBW.

Results: Results showed a positive correlation between the BMI and the Pplat values. When using RBW to calculate Vt, Pplat for patients with BMI>25 kg/m^2 was significantly higher than that for patients with BMI <25 kg/m^2 (18.7 ± 5.8 cmH2O vs. 13.0 ± 3.5 cmH2O, respectively, p<0.0001). When using IBW to calculate Vt a similar pattern was observed, 14.1 ± 3.8 cmH2O in patients with BMI>25 kg/m^2, and 12.3 ± 8.5 cmH2O in patients with BMI <25 kg/m^2 (p<0.02). Moreover, in patients with BMI <25 kg/m^2, no significant difference was observed in Pplat when using Vt calculated from RBW or IBW (13.0 ± 3.5 cmH2O vs. 12.3 ± 8.5 cm H20, respectively, p=0.39). In contrast, in patients with BMI>25 kg/m^2, Pplat was higher in the RBW group than in the IBW group (18.7 ± 5.8 cmH2O vs. 14.1 ± 3.8 cmH2O, respectively, p< 0.001). The fact that a significant difference was observed in Pplat values between RBW and IBW groups only in patients with BMI>25 kg/m^2, indicates that in addition to body weight, other variables should be considered as potential contributors to changes in Pplat. A reduction in lung compliance secondary to increased external pressure on the chest wall as a physiological effect of obesity may be a potential mechanism underlying this effect.

Conclusions: The current study suggests that in patients with BMI<25 kg/m^2, Vt may be determined using either RBW or IBW without significantly altering Pplat. In patients with BMI>25 kg/m^2, however, additional factors which may affect ventilation should be considered prior to selecting RBW or IBW to calculate Vt. In conclusion, BMI has a positive correlation with the Pplat values under low Vt ventilation and could probably mean that patients with decreased chest wall compliance are being sub-optimally ventilated.

References: [1]. Mark A. Warner, Bela Patel, in Benumof and Hagberg's Airway Management, 2013

[2]. William Henderson MD, Najib T. Ayas MD, MPH, in Murray and Nadel's Textbook of Respiratory Medicine (Sixth Edition), 2016

[3]. "The Acute Respiratory Distress Network: Ventilation with lower tidal volumes as compared with traditional Volumes for Acute Lung Injury and the Acute Respiratory Distress Syndrome." The New England Journal of Medicine, Volume 342, number 18, 2000.

Perioperative Anesthesia 7- History of COVID-19 and baseline lung mechanics in surgical patients: A hospital registry study

Aiman Suleiman[1], Simone Redaelli[1], Ricardo Munoz-Acuna[1], Elena Ahrens[2], Tim Tartler[3], Sarah Ashrafian[2], May Hashish[1], Daniel Talmor[2], Elias Baedorf Kassis[1], Maximilian Schaefer[4], Valerie Banner-Goodspeed[2]

Beth Israel Deaconess Medical Center, Harvard Medical school[1] Beth Israel Deaconess Medical Center[2] Center for Anesthesia Research Excellence[3] Beth Israel Deaconess Medical Center & Hospital[4]

Introduction: A variety of long-term pulmonary manifestations, ranging from dyspnea to fibrotic lung damage, have been reported after Coronavirus Disease 2019 (COVID-19) infection [1-3]. Fibrotic changes of the lung were observed three months after hospital discharge in approximately 20-60% of survivors [4]. In critically ill patients, a history of mechanical ventilation due to COVID-19 has led to a persistently lower respiratory system compliance [5]. The impact of a previous COVID-19 infection on pulmonary mechanics in patients receiving mechanical ventilation in the operating room (OR) has not yet been described. We hypothesized that a history of COVID-19 infection is associated with a decreased baseline respiratory system compliance in surgical patients.

Methods: In this retrospective hospital study, we analyzed adult surgical patients undergoing general anesthesia between January 1st, 2020 and March 31st, 2022 at a tertiary healthcare network in Boston, US. We excluded patients with an American Society of Anesthesiologists (ASA) physical status >IV, laryngoscopic surgeries, and patients who came intubated to the OR. The primary exposure was a history of COVID-19 infection, defined using COVID-19 polymerase chain reaction test results within or outside our healthcare network and International Classification of Diseases (ICD-10-CM) diagnostic codes. The primary outcome was baseline respiratory system compliance (ml/cmH_2O), calculated from minute-by-minute recordings of driving pressure and tidal volume recorded over the first 10 minutes post-intubation. In the primary analysis, we used a multivariable negative binomial regression model adjusted for patients' baseline characteristics and pre-intubation drugs to test the association between a previous history of COVID-19 and a change in baseline respiratory system compliance. Furthermore, we explored the association between a history of COVID-19 strain ($Alpha_1$, $Alpha_2$, Delta and Omicron, determined by timing of infection relative to strain predominance) and baseline respiratory system compliance, as well as an association of time since COVID-19 infection and baseline respiratory system compliance.

Results: 17,035 cases were included in the final cohort (*Figure 1*). 1,213 (7.1%) patients had a history of COVID-19. *Table 1* summarizes the baseline characteristics and the pre-intubation drug doses by history of COVID-19. The median (IQR) baseline respiratory system compliances were 39.0 (29.3-48.8) and 40.2 (31.1-50.6) ml/cmH_2O in patients who had a history of COVID-19 versus those who did not. Our primary analysis showed that a previous history of COVID-19 infection was significantly associated with a marginally lower baseline respiratory system compliance (incidence rate ratio [IRR] 0.96; 95%CI 0.95-0.98; p<0.001), which reflects an adjusted difference of a 1.5 ml/cmH_2O lower compliance in the COVID-19 group. When differentiating COVID infections by surges and respective variants, patients who had a history of COVID-19 during the $Alpha_1$, $Alpha_2$ and Delta surges had a lower baseline respiratory system compliance [(IRR 0.97; 95%CI 0.94-0.99; p=0.02), (IRR 0.95; 95%CI 0.93-0.98; p=0.001), (IRR 0.95; 95%CI 0.91-0.99; p=0.02), respectively] compared to patients without history of COVID-19 (*Table 2*). There was no difference in baseline respiratory system compliance between patients without prior COVID-19 infection and infection during the Omicron surge. The number of patients with a positive COVID-19 test per surge with corresponding adjusted baseline respiratory system compliance over time using fractional polynomial modeling is presented in *Figure 2*. No association was found between time difference of COVID-19 infection to surgery and baseline respiratory system compliance (IRR 0.99; 95%CI 0.99-1.00, p=0.89).

Conclusions: A previous history of COVID-19 infection during the $Alpha_1$, $Alpha_2$ and Delta strains irrelevant to time difference to surgery was associated with a measurable, but likely clinically irrelevant, lower baseline respiratory compliance. Patients with COVID-19 infection during the Omicron surges were not affected. Further studies on the clinical significance of these findings are warranted.

References: [1] Extrapulmonary manifestations of COVID-19. Nat Med. 2020 Jul;26(7):1017-1032

[2] 6-month consequences of COVID-19 in patients discharged from hospital: a cohort study. Lancet. 2021 Jan 16;397(10270):220-232

[3] Persistent Symptoms in Patients After Acute COVID-19. JAMA. 2020 Aug 11;324(6):603-605

[4] A prospective study of 12-week respiratory outcomes in COVID-19-related hospitalisations. Thorax. 2021 Apr;76(4):402-404

[5] Respiratory Mechanics in a Cohort of Critically Ill Subjects With COVID-19 Infection. Respir Care. 2021 Oct;66(10):1601-1609

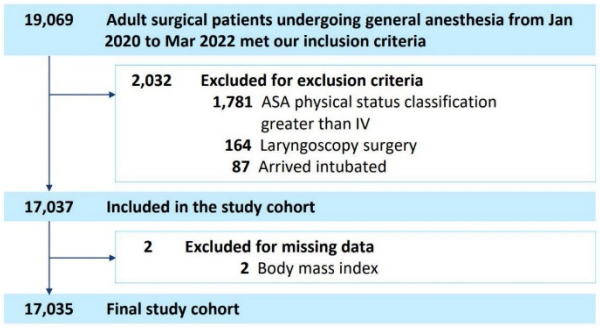

Figure 1. Study flowchart.

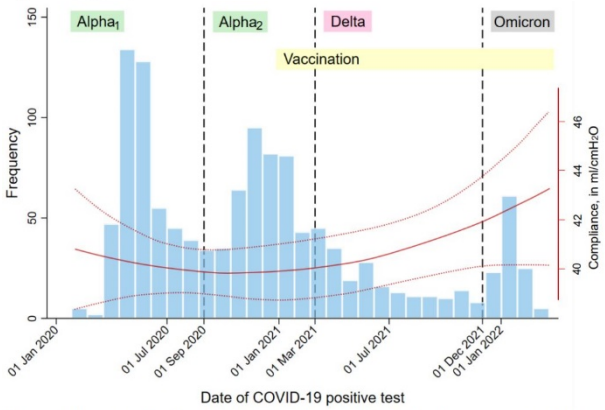

Figure 2. Number of patients per surge with baseline respiratory system compliance plotted over time using fractional polynomial modeling (95%CI).

Table 1. Patients' characteristics and pre-intubation factors per history of COVID-19 with standardized differences.

	No COVID-19 N=15,822	COVID-19 N=1,213	SD
Age, years	56.5 ± 17.0	54.4 ± 16.9	0.13
BMI, kg/m²	28.4 ± 6.6	29.0 ± 7.0	-0.08
Sex			-0.10
Female	9,168 (57.9%)	748 (61.7%)	
ASA physical status	2.0 (2.0 - 3.0)	3.0 (2.0 - 3.0)	-0.15
Smoking history	5,240 (33.1%)	347 (28.6%)	0.10
Obstructive lung disease	3,542 (22.4%)	343 (28.3%)	-0.14
OSA	2,352 (14.9%)	202 (16.7%)	-0.05
Chronic heart failure	1,426 (9.0%)	154 (12.7%)	-0.12
Charlson Comorbidity Index	1.0 (0.0 - 3.0)	2.0 (0.0 - 5.0)	-0.21
Total pre-intubation ND-NMBA ED_{95}	1.7 (0.0 - 2.6)	1.8 (0.0 - 2.7)	-0.04
Total pre-intubation opioid dose, mg OME	30.0 (0.0 - 30.0)	30.0 (0.0 - 30.0)	-0.00
Total pre-intubation lidocaine dose, mg/kg	0.5 (0.3 - 0.7)	0.5 (0.3 - 0.7)	0.06
Total pre-intubation succinylcholine dose, mg/kg	0.0 (0.0 - 0.0)	0.0 (0.0 - 0.0)	0.05
Laryngeal mask airway	2,635 (16.7%)	206 (17.0%)	-0.01
Quartiles of the pandemic			-0.43
Jan-Mar/2020	2,979 (18.8%)	5 (0.4%)	
Apr-Jun/2020	805 (5.1%)	99 (8.2%)	
Jul-Sep/2020	1,701 (10.8%)	101 (8.3%)	
Oct-Dec/2020	1,730 (10.9%)	148 (12.2%)	
Jan-Mar/2021	1,518 (9.6%)	162 (13.4%)	
Apr-Jun/2021	1,950 (12.3%)	204 (16.8%)	
Jul-Sep/2021	1,822 (11.5%)	140 (11.5%)	
Oct-Dec/2021	1,830 (11.6%)	138 (11.4%)	
Jan-Mar/2022	1,487 (9.4%)	216 (17.8%)	

Patient characteristics and distribution of variables. Data are presented as median (IQR) for continuous measures, and n (%) for categorical measures. BMI, body mass index; ASA, American Society of Anesthesiologists; OSA, obstructive sleep apnea; ND-NMBA, nondepolarizing neuromuscular blocking agents; ED95, effective dose in 95% of population; OME, Oral Morphine Equivalent.

Table 2. The association between a history of COVID-19 per surge of the pandemic ($Alpha_1$, $Alpha_2$, Delta and Omicron) and change in baseline respiratory system compliance.

Outcome	Ref (no COVID-19: 15,822)	Surges dates	Adjusted analysis		ARD
			IRR (95%CI)	*P-value*	
Baseline respiratory system compliance in ml/cmH_2O	$Alpha_1$ (n=462)	*(1/18/2020-8/31/2020)*	0.97 (0.94-0.99)	0.02	-1.4
	$Alpha_2$ (n=436)	*(9/1/2020-2/28/2021)*	0.95 (0.93-0.98)	0.001	-2.0
	Delta (n=197)	*(3/1/2021-11/30/2021)*	0.95 (0.91-0.99)	0.02	-2.1
	Omicron (n=118)	*(12/1/2021-3/31/2022)*	1.01 (0.95-1.07)	0.74	-

ARD, adjusted risk difference in units of outcome; IRR, incidence rate ratio.

Perioperative Anesthesia 8- Identifying Patient-Centered Psychological and Social Support Needs After Traumatic Birth: A Qualitative Study

Minhnoi Wroble Biglan[1], Taylor Roberts[2], Emma Nowakowski[2], Thomas Troyan[2], Minhnoi Wroble Biglan[1], Sarah Kroh[2], Priya Gopalan[2], Patricia Dalby[2], Grace Lim[1]

University of Pittsburgh[1] Magee Women's Hospital[2]

Introduction: Emergency deliveries for maternal or fetal health reasons can increase maternal risk for postpartum depression (PPD) and post-traumatic stress disorder (PTSD)[1, 2, 3]. Nearly one-third of people describe their birth experience as traumatic[4] and rates of PPD and PTSD postpartum are high (14% & 4%, respectively) in these cohorts[1, 4, 5]. However, among patients who have self-identified as having had a traumatic birth, little is known about patient-centered priorities for post-birth support. We conducted a qualitative study amongst subjects in the postpartum period who self-reported a recent traumatic birth experience to gain insight into their perspectives on optimizing post-birth psychosocial support.

Methods: The study was IRB approved and informed consent was given by all subjects. Individual semi-structured interviews (IDIs) with people who gave birth within the last year, had a labor emergency that resulted in an emergency cesarean delivery or an assisted vaginal birth, and self-identified as having had a traumatic experience were enrolled. Subjects completed two pre-interview surveys: the Stanford Acute Stress Reaction Questionnaire and the Post Traumatic Stress Disorders (PTSD) Checklist, Civilian Version. Interviews included open-ended discussions about the situations within labor and delivery that improved or worsened their experience, perceived support by staff following their experience, and whether they felt it would be appropriate to routinely refer people having emergency deliveries to psychiatric consultation for follow up.

Results: A total of eight subjects participated in all procedures. Some subjects (37.5%) had a history of anxiety, depression, or PTSD prior to their traumatic birth experience (Tables 1-4). Most subjects reported high levels of depression (M =63.5, SD = 41.23) and half met criteria for PTSD (M = 44, SD = 18.02) after their delivery experience (Tables 1-4). Seventy-five percent of the subjects indicated feelings of anxiety, depression, or PTSD during the IDIs. Results from the IDIs included increased risk of PPD in subjects with stressor outside of the pregnancy (i.e., single parenting or spousal abuse) and subjects who had previous prenatal or peripartum medical concerns (i.e., neonatal health issue, previous infant death). Expectations of the birthing process, communication between clinical care and support staff during and after the traumatic delivery, and subjects' perceptions of clinical quality of communication affected the birthing experience greatly. Subjects desired to be offered referrals to social support and psychiatric services after experiencing emergency deliveries, although many indicate they may not immediately accept the offer. Subjects also desired closure about the event from their obstetricians immediately after the event. Subjects reported that some of the most distressing features of the emergency event included seeing distress amongst the healthcare team, being physically manipulated or moved (e.g., running them from a room to an operating room, moving their legs or changing their positions), and minimal communication directly with the subjects as the medical teams were working with each other.

Conclusions: Our findings support that people self-reporting traumatic birth expect to have the event acknowledged by health care providers, and to be followed for mental health screening. Opportunities for enhanced patient-centered care and communication during emergencies were identified. Key areas for improvement include 1.) improvement of education in the prenatal period on alternative birth plans; 2.) improvement of communication of clinical staff to patients during emergent events; 3.) provision of emotional support following a patient's traumatic birth experience; 4.) specific, PPD and PTSD-relevant conversations regarding emotional response to delivery within the postpartum hospital stay; and 5.) and psychiatric follow up in women who undergo traumatic birth who have a history of mental health disorders, or had a previous traumatic prenatal or birth experience.

References: Post-Traumatic Stress Disorder Following Childbirth. (2021). *BMC Psychiatry*, 21(155).

The Prevalence of Posttraumatic Stress Disorder during Pregnancy and Postpartum Period. (2018). *Journal of Family Medicine and Primary Care.* 7(1), 220-223.

Postpartum Depression: Etiology, Treatment, and Consequences for Maternal Care. (2016). *Hormones and Behavior.* 77, 153-66.

Women's Descriptions of Childbirth Trauma Relating to Care Provider Actions and Interactions. (2017). *BMC Pregnancy and Childbirth.* 17 (21).

Maternal PTSD During the Perinatal Period. A systematic Review. (2018). *Journal of Affective Disorders*. 1(224), 8-3.

Psychosocial Predictors of Postpartum Posttraumatic Stress Disorder in Women with a Traumatic Childbirth Experience. (2018). *Frontier Psychiatry.* 9(348).

Table 1: *Patient Demographics*

Characteristics	Patients	
	N	(SD)
Mean Age in Years	27.6	(5.5)
	N	(%)
Race		
White/Caucasian	6	(75)
Black/African American	2	(25)
Asian	0	(0)
Pacific Islander	0	(0)
American Indian/Alaskan	0	(0)
Ethnicity		
Hispanic	0	(0)
Non-Hispanic	8	(100)
Prior Mental Health Illness	3	(37.5)
Past Medical History		
Hypertension	1	(12.5)
Substance use disorder	0	(0)
Smoking/tobacco use	1	(12.5)
Diabetes Mellitus	1	(12.5)
Asthma	3	(37.5)
Obesity (BMI>40)	1	(12.5)
No past medical history	2	(25)
Other[a]	4	(50)
Past Pregnancy History		
Gestational Diabetes	1	(12.5)
Preeclampsia	2	(25)
Previous Traumatic Births	4	(50)

[a]Other specified: premature rupture of the membranes, muscinouscystadenoma, pyelonephritis, anemia, ADHD, prolactinoma, embryonic demise, recurrent pregnancy loss

Table 2. *Obstetric, Labor & Delivery Outcomes*

Characteristics	Patients	
	N	(SD)
Mean APGAR 1 Minute	7.1 (1.6)	(1.6)
Mean APGAR 5 Minutes	8.5 (1.4)	(1.4)
	N	(Range)
Median Gravidity	1.5	(1-6)
Median Parity	1.5	(1-3)
Mean Gestational Age at Delivery in weeks	39	(2 weeks 1 day)
	N	(%)
Need for Induction		
Yes	5	(62)
No	3	(37)
Epidural Anesthesia		
Yes	7	(87.5)
No	1	(12.5)
Reason for Condition Obstetrics		
Fetal Bradycardia	7	(87.5)
Cord Prolapse	0	(0)
Maternal Emergency	0	(0)
Abruption	0	(0)
Suspected Uterine Rupture	0	(0)
Large for Gestational Age	1	(12.5)
Mode of Delivery		
Vaginal	0	(0)
Assisted Vaginal	3	(37)
Cesarean	5	(62)
NICU Need for Infant		
Yes	1	(12.5)
No	7	(87.5)

Table 3

PCL-C PTSD Screening Pre-Interview Survey

PLC-C PTSD Screening	Patients	
	N	(%)
Little to No Severity of PTSD (%)	3	(37.5)
Some PTSD Symptoms (%)	0	(0)
Moderate to Moderately High Severity of PTSD (%)	1	(12.5)
High Severity of PTSD (%)	4	(50)

Note. PCL-C PTSD Screening Scale Ranges: 17-29 - little to no severity, 28-29 - some PTSD symptoms, 30-44 - moderate to moderately high severity of PTSD symptoms, 45-85 - high severity of PTSD symptoms (Boston University, n.d.).

Table 4

SASRQ Pre-Interview Survey

Stanford Acute Stress Reaction Questionnaire	Patients	
	N	(%)
How disturbing was this event to you?		
Not at all disturbing	0	(0)
Somewhat disturbing	1	(12.5)
Moderately disturbing	1	(12.5)
Very disturbing	3	(37.5)
Extremely disturbing	3	(37.5)
On how many days did you experience any of the above symptoms of distress?		
No days	0	(0)
One day	1	(12.5)
Two days	0	(0)
Three days	2	(25)
Four Days	1	(12.5)
Five or more days	4	(50)

Note. A score ≥40 indicates a moderate to high sensitivity to predicting PTSD symptoms (Lötvall et al., 2022).

Perioperative Anesthesia 9- Impact of preoperative uni- or multimodal prehabilitation on postoperative morbidity: a systematic review and meta-analysis

Franck Verdonk[1], Benjamin Choisy[1], Amélie Cambriel[1], Julien Hedou[1], Marie-Pierre Bonnet[1], Jérémie Lefevre[1], Thibault Voron[1], Dyani Gaudilliere[1], Cindy Kin[1], Brice Gaudilliere[1]

Stanford University[1]

Introduction: Postoperative complications occur in up to 43% of cases, resulting in increased morbidity and economic burden (1). Prehabilitation (prehab) could increase patients' pre-operative health and improve postoperative outcomes (2). However, reported results of prehab are contradictory (3,4). The objectives of this systematic review are to evaluate the effects of prehab on postoperative outcomes in patients undergoing elective surgery.

Methods: We performed a systematic review and meta-analysis of randomized controlled trials published between January 2006 and January 2021 comparing prehab programs lasting ≥ 14 days to "standard of care" (SOC) and measuring postoperative complications. Database searches were conducted in four databases: PubMed, CINAHL, EMBASE, PsycINFO. Primary outcome was effect of uni and multi-modal prehab on 30-day complications, secondary outcomes were length of stay (LOS) and pain.

Results: Twenty-four studies (including 1984 patients randomized in a 1:1 ratio) met the inclusion criteria. The average methodological study quality was moderate. There was no difference between prehab and SOC groups for postoperative complications (OR 0.98; 95%CI [0.82; 1.17]; p=0.09; I^2=36%) (***Figure 1***), total hospital LOS (MD -0.13 days; 95%CI [-0.56; 0.28]; p=0.53; I^2=21%), or postoperative pain. The Intensive Care Unit (ICU) LOS was significantly shorter in the prehab group (MD -0.57 days; 95%CI [-1.10; -0.04]; p=0.03; I^2=46%) (***Figure 2***). Separate comparison of uni- and multi-modal prehab showed no difference in complications or hospital LOS.

Conclusions: Prehab reduces ICU LOS compared with SOC in elective surgery patients but has no effect on overall complications or total LOS, regardless of modality. Prehab programs should be more homogeneous and targeted to those patients most likely to benefit.

References: (1) W.J. O'Brien, Association of Postoperative Infection With Risk of Long-term Infection and Mortality, JAMA Surg. 155 (2020) 61–68. https://doi.org/10.1001/jamasurg.2019.4539.

(2) C. Gillis,Pre-operative nutrition and the elective surgical patient: why, how and what?, Anaesthesia. 74 (2019) 27–35.

(3) D.I. McIsaac, Prehabilitation Knowledge Network, Prehabilitation in adult patients undergoing surgery: an umbrella review of systematic reviews, Br. J. Anaesth. 128 (2022) 244–257.

(4) J. Moran, E. The ability of prehabilitation to influence postoperative outcome after intra-abdominal operation: A systematic review and meta-analysis, Surgery. 160 (2016) 1189–1201

Figure 1

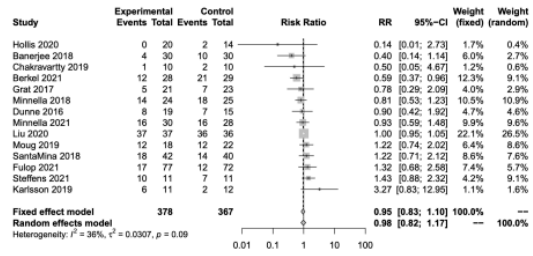

Impact of prehabilitation on postoperative complications according to the Clavien-Dindo classification

Abbreviations: CI: confidence interval; Control: standard of care group; Events: number of complications; Experimental: prehab group; Total: total number of patients; Weight: study weight

Figure 2

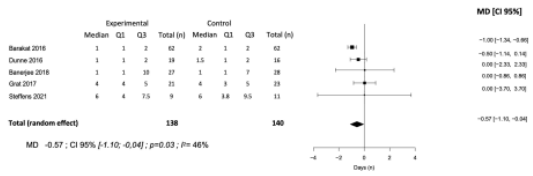

Impact of prehabilitation on critical care unit length of stay

Abbreviations: CI: confidence interval; Control: standard of care group; Experimental: prehab group; MD: median difference; Q1: first quartile (25%); Q3: third quartile (75%); Total: total number of patients

Perioperative Anesthesia

10- Intraoperative monitoring of high-sensitivity troponin I level during liver transplantation and its impact on post-transplant mortality

Sookeun Nam[1], Kyoung-Sun Kim[1], Hye-Mee Kwon[1], Young-Jin Moon[1], In-Gu Jun[2], Jun-Gol Song[2], Gyu-Sam Hwang[2]

Asan Medical Center, University of Ulsan College of Medicine[1] University of Ulsan College of Medicine, Asan Medical Center[2]

Introduction: Cardiovascular disease death is the leading cause of early and late post-liver transplant (LT) mortality in the current era. Although hemodynamic perturbation during LT is prevalent, severity of intraoperative myocardial injury detected by high sensitivity cardiac TnI (hs-cTnI) and its clinical relevance for predicting post-LT mortality remains undetermined [1],[2]. We aimed to investigate prevalence and severity of myocardial injury during LT and sought the relevant threshold level of hs-cTnI for the prediction of post-LT mortality at a large volume LT center.

Methods: We retrospectively evaluated 3,330 consecutive LT patients between 2008 and 2019 who routinely measured intraoperative hs-cTnI levels (the 99th percentile upper reference limit [99%URL] =0.040 ng/mL, lower limit=0.006 ng/mL) during LT. Peak intraoperative hs-cTnI level was determined among the three pre-anhepatic, anhepatic, and neohepatic hs-cTnI levels. Liver disease severity was evaluated with model for end-stage liver disease (MELD) score. Intraoperative peak hs-cTnI threshold level for predicting 1-year all-cause mortality was chosen by maximally selected rank statistics with the smallest log-rank P value.

Results: Within 1 year, 250 (7.5%) patients died after LT. Intraoperative hs-cTnI level ranged 0.006 to 39.3 ng/mL (median 0.068 ng/ml) and patients exceeding 1- (0.04 ng/ml) and 10-times 99%URL (0.4 ng/ml) were 64.6% and 7.5%, respectively. hs-cTnI threshold level for 1-year mortality were 8.2 times 99%URL (0.328 ng/ml). In patients exceeding 10 times 99%URL,1-year mortality was 12.4% versus 7.1% in those without (P=0.004), whereas in subgroup analysis with MELD score of > 30, those mortality rates increased greatly (35.6 % vs. 15.6%, P=0.002), respectively.

Conclusions: High hs-cTnI levels, suggesting pre- or intraoperative myocardial injury, were identified frequently during LT surgery. Particularly, patients exceeding 10 times 99%URL of Hs-cTnI need urgent myocardial investigation and management perioperatively to enhance post-LT survival, especially when MELD score of >30.

References: [1] Association of Postoperative High-Sensitivity Troponin Levels With Myocardial Injury and 30-Day Mortality Among Patients Undergoing Noncardiac Surgery. JAMA. 2017 Apr 25;317(16):1642-1651.

[2] Elevated High-Sensitivity Troponin I During Living Donor Liver Transplantation Is Associated With Postoperative Adverse Outcomes. Transplantation. 2018 May;102(5):e236-e244.

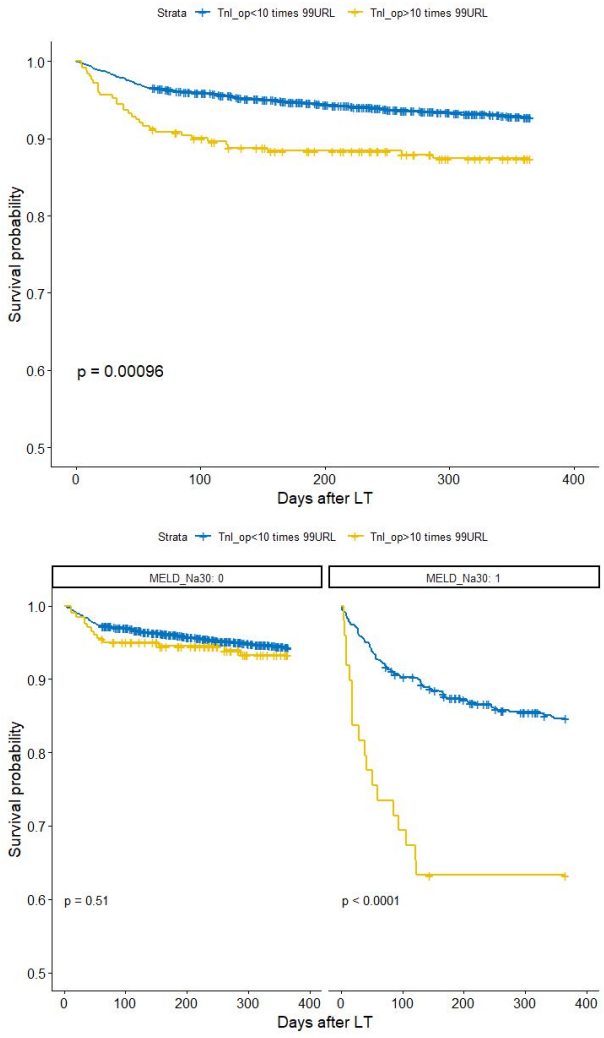

Perioperative Anesthesia

11- Intraoperative Triple Low and Low MAP-BIS States are Associated with Post-Operative ICU Delirium: a retrospective analysis

Brian Reon[1], Mike Schnetz[1], Keith Vogt[2]

UPMC[1] University of Pittsburgh[2]

Introduction: Post-operative delirium (POD) is a common postoperative complication, occurring in up to 52% of noncardiac surgical patients, and is a significant cause of increased mortality and morbidity (1,2). While general risk factors for POD have been identified, such as age, surgical duration, intraoperative hypotension and pre-operative cognitive function, there are many potential modifiable and unmodifiable risk factors contributing to POD that have not been well studied (3,4). The triple low state (TLS) is a composite metric of concurrent low bispectral index (BIS), MAC and MAP values, which has been associated with increased morbidity in postoperative patients and could represent a state of poor physiologic reserve (5). Double low states (DLS) are simultaneously low values of two of the aforementioned variables. This retrospective study aimed to determine whether intraoperative TLS or DLS are associated with POD.

Methods: This retrospective study included non-cardiac and non-liver transplant surgical patients within the UPMC multi-hospital health system from 2016 – 2020 who had Intensive Care Delirium Screening Checklist (ICDSC) delirium scores measured during an ICU stay. Patients were included in our analysis if there was no evidence of pre-op delirium, based on having a ICDSC greater than 3. The presence of a TLS was determined by patients simultaneously having a BIS value < 45, MAP < 75 and MAC < 0.8. Propensity score matching was performed on TLS and non-TLS cohorts with 3:1 matching. Multivariable logistic regression was then performed to determine the effect of TLS events (binary classifier) on the development of POD. Covariates included in our logistic regression model included age, gender, ASA physical status, whether the surgical case was an emergency, operative team surgical specialty, hospital site and the presence of a TLS or DLS event during the procedure. Dose-dependency of TLS events on POD incidence was determined by separating patients into 15-minute bins based on cumulative TLS duration.

Results: Of the 5016 patients that met our inclusion criteria, 3,299 patients remained following propensity score matching. Of those remaining patients, 37 % had intraoperative TLS events. Average TLS duration within the TLS cohort was 36.1 minutes. There was a higher incidence of POD in the TLS subgroup, 24.4%, compared to patients without TLS events, 15.6% (Figure 1). Multivariable logistic regression analysis demonstrated increased odds ratio of POD for both TLS (1.7 [1.40 – 2.07]) and low MAP-BIS (1.31 [1.02 – 1.70], (Figure 3). TLS events, but not low MAP-BIS events demonstrated a duration-dependent increase in delirium incidence when comparing patients based on cumulative low-state duration (Figure 4). TLS events occur uniformly throughout the procedural period, with a noted increase in TLS event frequency immediately prior to the procedural start (Figure 5).

Conclusions: In a retrospective, multi-hospital surgical population with post-op ICU admission, we identified a large group patients who had TLS and DLS events intraoperatively. Multivariate logistic regression demonstrated that patients experiencing either TLS or MAP-BIS DLS events intraoperatively were more likely to experience POD. This association was not demonstrated with the other DLS combinations. Furthermore, increasing cumulative duration of TLS events was associated with progressive increases in delirium incidence. These associations may reflect either causal effects or unmasking of pre-existing vulnerability (or both). Importantly, this study lays the framework for larger studies to evaluate the potential role of TLS and other modifiable and non-modifiable perioperative factors to help risk stratify patients for the development of POD.

References:

1. Am J Surg (2017) 214:1036-1038
2. BMC Geriatrics (2020) 20:40
3. JAMA Surg (2021) 156(5):430-442.
4. Sci Rep (2020) 10:9232
5. Anesthesiology (2012) 116:1195-203.

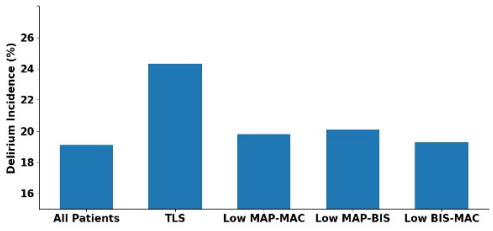

Figure 1) Delirium Incidence in Patients with TLS or DLS events

Characteristics	TLS	No TLS
Total Patients	1224	2075
Surgical Site		
PUH	585 (47.8 %)	878 (42.4 %)
SHY	250 (20.4 %)	449 (21.6 %)
MHP	137 (11.2 %)	267 (12.9 %)
PAS	231 (18.9 %)	419 (20.2%)
MUH	21 (1.7 %)	62 (2.9 %)
Year		
2016	171 (14 %)	276 (13.4 %)
2017	278 (22.7 %)	465 (22.4 %)
2018	339 (27.7 %)	543 (26.1 %)
2019	300 (24.5 %)	553 (26.7 %)
2020	136 (11.1 %)	238 (11.4 %)
Age	66.6	65.3
Sex		
Female	523 (42.7 %)	891 (42.9%)
Male	701 (57.3 %)	1184 (57.1%)
ASA		
5	26 (2 %)	29 (1.4 %)
4	588 (48 %)	797 (38.4 %)
3	562 (45.9 %)	1151 (55.5 %)
2	48 (3.9 %)	98 (4.7 %)
Emergency	447 (36.5 %)	599 (28.9 %)
Procedure Length	331.9	335.6
Surgical Specialty		
Thoracic	502 (41 %)	782 (37.7 %)
General Surgery	231 (18.9 %)	330 (15.9 %)
Vascular	140 (11.4 %)	221 (10.7 %)
Surgical Oncology	103 (8.4 %)	225 (10.8 %)
Orthopaedic	114(9.3 %)	190 (9.2 %)
Neurosurgery	32 (2.6 %)	109 (5.3 %)
Urology	28 (2.3 %)	71 (3.4 %)
ENT	17 (1.4 %)	63 (3 %)
Other	57 (4.7 %)	84 (4.1 %)

Figure 2)
Characteristics of the groups with and without triple-low state (TLS) events.

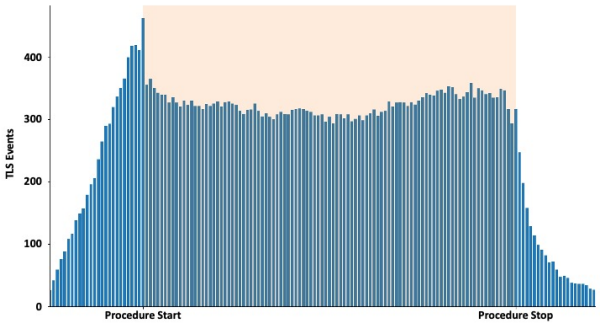

Figure 5) Number of TLS events plotted vs time in the anesthesia record. Procedural period normalized to 100 bins

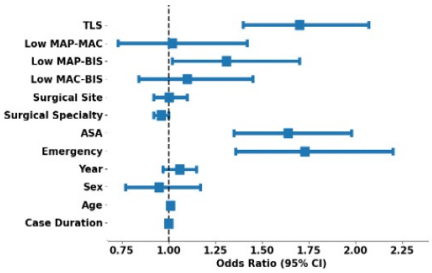

Figure 3) Logistic Regression Analysis of Factors from Figure 1

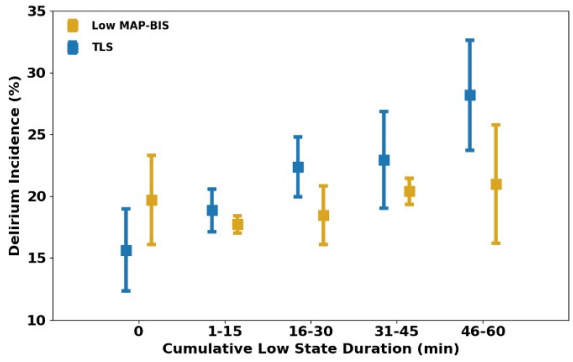

Figure 4) Cumulative TLS Duration Association with POD

Perioperative Anesthesia 12- Reddit Users' Questions and Concerns about Anesthesia

Khalid El-Jack[1], Korey Henderson[2], Lauren Southwick[3], Anietie Andy[3]

Perelman School of Medicine[1] Perelman School of Medicine at University of Pennsylvania[2] Penn Medicine[3]

Introduction: Patients utilize social media in search of support networks. Reddit is one of the most popular social media sites and allows users to anonymously connect. Anesthesia patients are actively using Reddit to discuss their treatment options and experiences within the medical system. This study explores the use of the platform Reddit by patients undergoing a procedure requiring anesthesia.

Methods: Posts published on an active Reddit forum on Anesthesia (i.e., */r/Anesthesia*) were used. Big Query was used to collect posts from */r/Anesthesia*. We collected 3,288 posts published between December 2015 and August 2019. We collected a control group of 3,288 posts from a Reddit forum not related to Anesthesia. Using latent Dirichlet allocation (LDA) we extracted 20 topics from our data set. The LDA topic themes most associated with posts in */r/Anesthesia* compared to the control group were determined.

Results: LDA analysis of posts in */r/Anesthesia* relative to a control group produced 6 distinct categories of posts (Table 1). The posts most associated with */r/Anesthesia* when compared to a control group were posts belonging to the "Physician-Patient Experience" category (Cohen's d= 0.389) while the posts least associated with */r/Anesthesia* were from the "Uncertainties" category of posts (Cohen's d= 0.147). Example experiences from members of the */r/Anesthesia* forum highlight subjective experiences of patients undergoing anesthesiology.

Conclusions: The language used on social media can provide insights into an individual's experience with anesthesia and inform physicians about patient concerns. Anesthesiologists are poised to address these concerns and prevent anonymous misinformation by providing verified physician insights on the forum */r/Anesthesia*.

References: Chen J, Wang Y. Social Media Use for Health Purposes: Systematic Review. J Med Internet Res. 2021;23(5):e17917. Published 2021 May 12. doi:10.2196/17917

Sumayyia, Marar D et al. "Health information on social media. Perceptions, attitudes, and practices of patients and their companions." Saudi medical journal vol. 40,12 (2019): 1294-1298. doi:10.15537/smj.2019.12.24682

Table 1: Latent Dirichlet Allocation Topics associated with */r/Anesthesia* Posts with Correlated Words Used to Highlight the Topic and Redacted Illustrative Examples

Category/Theme	Operational Definition	Cohen's D	Correlated Words	Redacted Illustrative Posts
Patient-Physician Experience	Posts surrounding relationships between members of the care team and patients	0.389	Anesthesia, surgery, procedure, sedation, anesthesiologist, patient, anesthetic, surgeon, pain, experience	Hello everybody, I underwent a procedure this morning while sedated. I came and read the pinned post in this subreddit since I had been worrying about it for weeks, and it truly helped me relax. I generally struggle with quite severe anxiety relating to my health. While getting ready this morning, I was still a little on edge, but my amazing and caring anesthesiologist basically informed me that given my health, she wouldn't even bother describing extreme risks; she only said that I might feel nauseous and have a sore throat after. I was asleep with one of the nurses holding my hand, and when I awoke, I was overjoyed. After roughly 4 hours of being awake, I feel great! The fear of the unknown made me worried, but I now get that it is truly okay. Thank you for your help across this forum.
Medication	Posts surrounding medication administration	0.365	Patient, risk, blood, propofol, dose, patients, anesthetics, pressure, drug, higher	Why does the white IV fluid hurt when it is inserted? I'm not sure what it was, but it quickly reached my brain and knocked me out in minutes Too bad it HURT LIKE HELL on my arm. Has Reynaud's been linked to this? I really struggle with that. What was this fluid, and why did they claim that some feel pain with it and others don't?
Health Care Infrastructure	Posts including various members of healthcare industry as a whole	0.336	CRNA, work, practice, school, medical, experience, states, nurse, job, hospital	I am currently completing a respiratory therapy AA program in California. I am very interested in pursuing anesthesia of some kind, and I am deciding between going to medical school to become an anesthesiologist, moving out of state to become an anesthesiology assistant, or returning to nursing school after I graduate from respiratory school and possibly pursuing a CRNA in the future. Can someone please describe the distinctions between the roles in terms of autonomy and the duties of each job?
Procedures	Posts surrounding specific procedures requiring anesthesia administration	0.304	Surgery, pain, block, body, nerve, heart, hospital, hours, spinal, epidural	I'm going to have a tummy tuck, and I read an article about someone who had general anesthesia and woke up, but they were paralyzed from the medication given along with the general anesthetic, so they couldn't tell anyone they were awake. I'm very scared right now! This surgery takes six hours! I hope I don't wake up during any of it, but if I do, I'd like to know how to let someone know so they can put me back to sleep!
Personal Inquiries	Posts including direct questions regarding anesthesia	0.201	Question, future, important, making, fact, learn, true, difficult, situation, personal	I have a cardiac problem and have a procedure tomorrow. I'm seeking feedback before scheduling this sedated procedure. For the last few years, I've experienced a persistent cough, shortness of breath, and periodic chest discomfort that feels like a heart attack (along with pain in my left arm, jaw, and back), as well as irregular heartbeats while lying down.... I'm worried that because I'm unsure of whether I have a problem or not, I won't know whether I should be sedated for the surgery until I get more information. Even though it's a colonoscopy and not surgery, I'm worried.
Uncertainties	User posts regarding patient worries and fears	0.147	I'm, don't, shit, stop, smoking, give, smoke, week, anxiety, die	Help me. I spent three weeks without doing any drugs. A friend of mine invited me out to drinks last Thursday (also something I must stop, but anyway). I let him know that I stopped doing drugs and that I needed to keep clean (especially for two weeks) since I am scheduled to undergo major surgery on April 15... Does anyone here have any information on whether I should be able to have the surgery? Has anyone ever smoked meth and felt sick afterwards?

Perioperative Anesthesia 13- STABL enables reliable and selective biomarker discovery in predictive modeling of high dimensional omics data

Franck Verdonk[1], Julien Hedou[1], Ivana Marić[1], Gregoire Bellan[2], Jakob Einhaus[2], Dyani Gaudilliere[2], Francois-Xavier Ladant[2], Ina Stelzer[2], Dorien Feyaerts[2], Amy Tsai[1], Adam Bonham[2], Martin Angst[3], Nima Aghaeepour[3], David Stevenson[1], Robert Tibshirani[1], Brice Gaudilliere[1]

Stanford University[1] SurgeCare SAS[2] Stanford Medicine[3]

Introduction: High-content omics technologies and sparse machine learning algorithms have transformed the biomarker discovery process. However, the translation of computational results into a clinical use case scenario remains challenging. A rate-limiting step is the rigorous choice of reliable biomarker candidates among a host of biological features included in multivariate models (1,2,3). We propose STABL, a machine learning framework that unifies the biomarker discovery process with the multivariate predictive modeling of clinical outcomes by choosing a reliable and selective set of biomarkers.

Methods: We benchmark STABL against the LASSO using synthetically generated datasets containing known informative and non-informative features. To investigate the impact of different training conditions, we examine variations in the number of observations, in the number of total features, and in the number of informative features (***Figure 1***). We also evaluate STABL's performance against four independent clinical omics datasets featuring complex classification (preeclampsia vs. normotensive pregnancy, severe vs. mild COVID-19, presence vs. absence of a Surgical Site Infection [SSI]) and regression (prediction of the pregnancy days remaining before labor (4)) scenarios.

Results: The results from the synthetic modeling show that STABL achieves better selectivity and reliability performances compared to the LASSO or stability selection algorithms. The set of chosen features is closer to the set of informative features, both in terms of cardinality and intersection. In addition, the predictive performance of STABL on the synthetic data is preserved in comparison to standard sparse algorithm algorithms. STABL also improves the reliability and selectivity of features in real-world single omics and multi-omics studies. For each case study, the identification of a manageable number of reliable biomarkers greatly facilitates the interpretation of the multivariate predictive model. While prior analyses of these datasets required post-hoc univariate data exploration, STABL reveals reliable biomarkers which alleviates the need for further analyses (***Figure 2***). This is particularly pertinent in the case of multi-omics datasets where a predictive model utilizes features from different biological systems.

Conclusions: Evaluation of STABL on synthetic datasets and four independent clinical studies demonstrates improved biomarker reliability and selectivity compared to sparse algorithms at similar predictive performance. STABL readily extends to double- and triple-omics data integration tasks, identifying a more reliable and selective set of biomarkers than state-of-the-art early- and late-fusion sparse algorithms, thereby facilitating the biological interpretation and clinical translation of complex multi-omics predictive models.

References: (1) Tibshirani, R. Regression Shrinkage and Selection Via the Lasso. *J. R. Stat. Soc. Ser. B Methodol.* **58**, 267–288 (1996).

(2) Meinshausen, N. & Buehlmann, P. Stability Selection. Preprint at https://doi.org/10.48550/arXiv.0809.2932 (2009)

(3) Candes, E., Fan, Y., Janson, L. & Lv, J. Panning for Gold: Model-X Knockoffs for High-dimensional Controlled Variable Selection. Preprint at https://doi.org/10.48550/arXiv.1610.02351 (2017)

(4) Stelzer, I. A. *et al.* Integrated trajectories of the maternal metabolome, proteome, and immunome predict labor onset. *Sci. Transl. Med.* **13**, eabd9898 (2021)

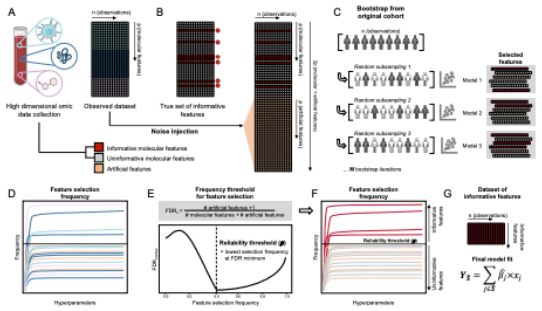

Fig 1 | Overview of the STABL algorithm. A. An original dataset of size n x p is obtained from the measurement of p molecular features in each one of the n observations (samples). **B.** Among the observed features, some are informative, and others are uninformative. p artificial features, all uninformative by construction, are injected into the original dataset to obtain a new dataset of size n x $2p$. **C.** M bootstrap iterations are performed from the original cohort of size n. At each iteration m, LASSO models varying in their regularization parameter λ are fitted on the subsample, which result in $S_{\lambda,m}$ sets of selected features. **D.** In total, for a given λ, M sets are generated. The fraction of sets in which feature i is present defines the feature selection frequency $\pi_i(\lambda)$. Plotting $\pi_i(\lambda)$ against λ yields a stability path graph. Features whose maximum frequency over λ is above a frequency threshold (t) are selected in the final model. **E.** STABL computes the reliability threshold (ρ), by minimizing the estimate of the FDRc. The FDRc estimate is constructed on the premise that the probability of selection of artificial features is, on average, the same as for uninformative original features. **F-G.** A reliable set of features with a selection frequency superior to ρ (i.e. a feature set with the lowest upper bound to the FDR) is included in a final predictive model.

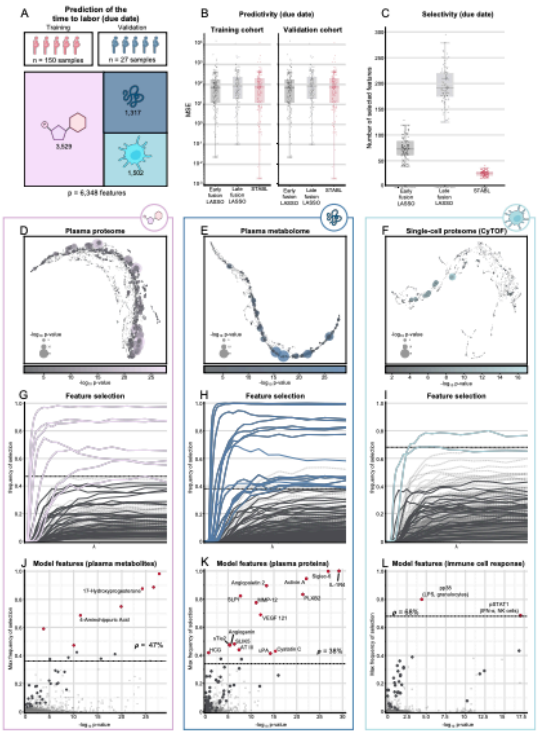

Fig. 2 | STABL's performances on multi-omics data integration. A. The case study is that of time-to-labor prediction, and STABL is compared to the two main methods currently used to analyze multi-omics datasets: early- and late-fusion Lasso. Performances are contrasted on three dimensions: predictivity, selectivity, and reliability. The initial cohort comprises 177 individuals, of whom 27 are held for validation. The features come from three different datasets: a proteomics dataset (1,317 features), a metabolomics dataset (3,529 features) and a mass cytometry dataset (1,502 features). **B.** The MSE measures predictivity through Monte-Carlo cross-validation. As shown on the boxplots of the results, STABL's predictivity performances are comparable to early- and late-fusion, both on the training and validation cohorts with quasi-identical median MSE and IQR. **c.** Selectivity, as measured by the number of features ultimately selected by the algorithm, is assessed through repeated cross-validation, whose results are displayed in boxplots. STABL outperforms early- and late-fusion on that dimension with a median number of selected features of 26 for STABL vs. 73 for early fusion and 192 for late-fusion. **D-F.** To give an overview of the data, every feature is represented on a U-map by a dot whose size and color are a function of the p-value of its coefficient in a univariate model. This is done for each dataset: metabolomics (d), proteomics (e) and CyTOF (f). **G-I.** The selection process by STABL is displayed by plotting the stability path alongside the reliability threshold θ: only those features whose maximal frequency of selection is above the threshold are selected by the algorithm. Again, this is done for each dataset, metabolomics (g), proteomics (h) and CyTOF (i), as the reliability threshold is specific to each omics sublayer. **J-l.** Finally, the maximum frequency of selection of each feature is plotted against its p-value in a univariate model for each omics sublayer: metabolomics (j), proteomics (k) and CyTOF (l). Features selected by STABL are colored in purple. On each plot, a label displays the name of features whose role has been demonstrated in other studies.

Perioperative Anesthesia 14- The influence of intraoperative opioid administration on postoperative pain and opioid requirements

Laura Santa Cruz Mercado[1], Ran Liu[1], Kishore Bharadwaj[1], Jasmine Johnson[1], Rodrigo Gutierrez[2], Proloy Das[2], Gustavo Balanza Villegas[2], Hao Deng[2], Akriti Pandit[2], Tom Sonte[3], Teresa MacDonald[2], Caroline Horgan[1], Si Long Tou[1], Timothy Houle[1], Edward Bittner[1], Patrick Purdon[2]

Beth Israel Deaconess Medical Center[1] Massachusetts General Hospital[2] MGH dept of Anesthesia, Critical Care, and Pain Medicine[3]

Introduction: Opioids administered to treat post-surgical pain are a major contributor to the opioid crisis, leading to chronic use and use disorder in a significant fraction of patients.[1,2,3,4] Initiatives to promote opioid-free or opioid-sparing approaches to perioperative pain management have led clinicians to reduce opioid administration in the operating room.[5,6,7] However, since the effects of intraoperative opioid usage on postoperative pain and opioid requirements are not well understood, this reduction could have unforeseen consequences that are overall detrimental for postoperative pain outcomes.
Objective: To characterize the relationship between intraoperative opioid usage and postoperative pain and opioid requirements

Methods: Design: Retrospective cohort study.
Setting: Quaternary care academic medical center
Participants: Adult patients who underwent non-cardiac surgery with general anesthesia.
Exposure: Intraoperative fentanyl and intraoperative hydromorphone average effect site concentration estimated using Pk/Pd models.
Main Outcomes and Measures: The primary study outcomes were the maximal pain score during the Post Anesthesia Care Unit (PACU) stay and the cumulative opioid dose, quantified in morphine milligram equivalents (MME), administered during the PACU stay. We also evaluated medium- and long-term outcomes associated with pain and opioid dependence.

Results: The study cohort contained a total of 61,250 surgical cases. Statistical models were fitted on the propensity-weighted dataset to characterize the effect of intraoperative opioid exposures on primary and secondary outcomes. Increased intraoperative fentanyl and intraoperative hydromorphone were both associated with reduced maximum pain scores in the PACU. Both exposures were also associated with a reduced probability and reduced total dosage of opioid administration in the PACU. We found that increased fentanyl administration in particular led to decreased frequency of uncontrolled pain, decreased chronic pain at 3-months, decreased opioid prescriptions at 30-, 90-, and 180-days, and decreased persistent opioid use, without significant increases in side-effects.

Conclusions: Our results show that intraoperative opioid administration has significant short- and long-term effects on post-operative pain and opioid outcomes. Contrary to prevailing trends, reduced opioid administration during surgery may have the unintended consequence of increasing postoperative pain and opioid consumption. Our analysis suggests that significant improvements in long-term outcomes might be achieved by optimizing opioid administration during surgery.

References: 1. Chronic Opioid Use After Surgery: Implications for Perioperative Management in the Face of the Opioid Epidemic. *Anesthesia & Analgesia*. 2017;125(5):1733-1740; 2. Risk of Prolonged Opioid Use Among Opioid-Naïve Patients Following Common Hand Surgery Procedures. *The Journal of Hand Surgery*. 2016;41(10):947-957.e3; 3. Chronic Opioid Usage in Surgical Patients in a Large Academic Center. *Ann Surg*. 2017;265(4):722-727; 4.Rates of opioid misuse, abuse, and addiction in chronic pain: a systematic review and data synthesis. *PAIN*. 2015;156(4):569-576; 5. A Review of Opioid-Sparing Modalities in Perioperative Pain Management: Methods to Decrease Opioid Use Postoperatively. *Anesthesia & Analgesia*. 2017;125(5):1749-1760.

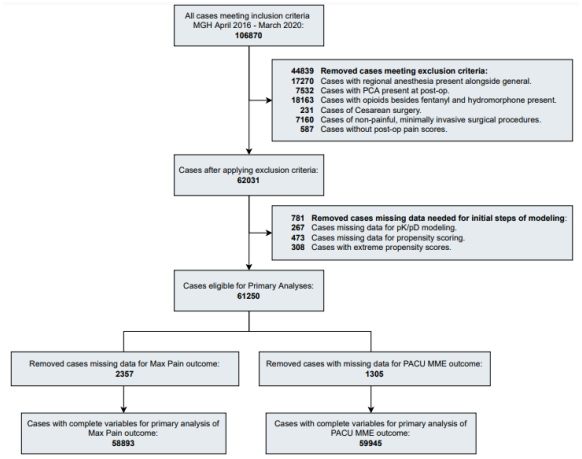

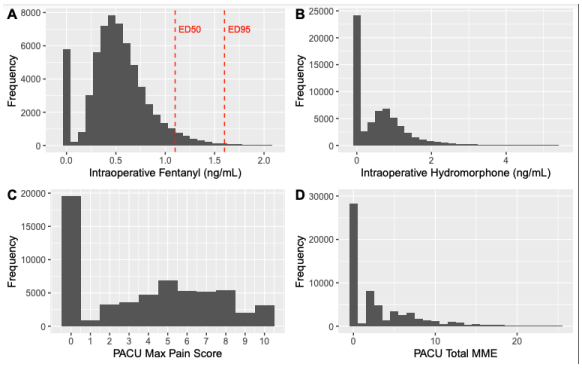

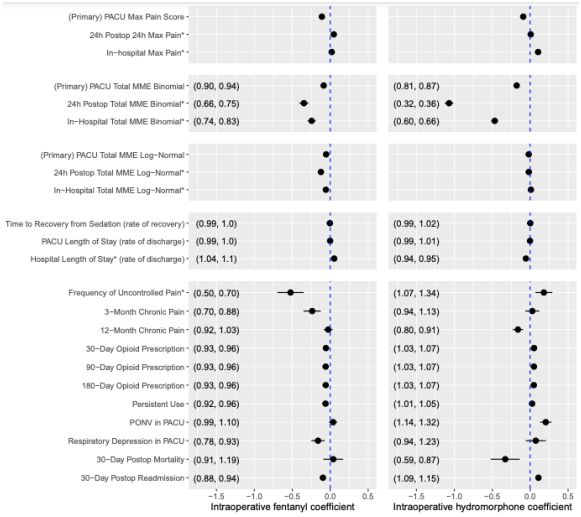
(Primary) PACU Max Pain Score
24h Postop 24h Max Pain*
In−hospital Max Pain*
(Primary) PACU Total MME Binomial
(0.90, 0.94)
(0.81, 0.87)
24h Postop Total MME Binomial*
(0.66, 0.75)
(0.32, 0.36)
In−Hospital Total MME Binomial*
(0.74, 0.83)
(0.60, 0.66)
(Primary) PACU Total MME Log−Normal
24h Postop Total MME Log−Normal*
In−Hospital Total MME Log−Normal*
Time to Recovery from Sedation (rate of recovery)
(0.99, 1.0)
(0.99, 1.02)
PACU Length of Stay (rate of discharge)
(0.99, 1.0)
(0.99, 1.01)
Hospital Length of Stay* (rate of discharge)
(1.04, 1.1)
(0.94, 0.95)
Frequency of Uncontrolled Pain*
(0.50, 0.70)
(1.07, 1.34)
3−Month Chronic Pain
(0.70, 0.88)
(0.94, 1.13)
12−Month Chronic Pain
(0.92, 1.03)
(0.80, 0.91)
30−Day Opioid Prescription
(0.93, 0.96)
(1.03, 1.07)
90−Day Opioid Prescription
(0.93, 0.96)
(1.03, 1.07)
180−Day Opioid Prescription
(0.93, 0.96)
(1.03, 1.07)
Persistent Use
(0.92, 0.96)
(1.01, 1.05)
PONV in PACU
(0.99, 1.10)
(1.14, 1.32)
Respiratory Depression in PACU
(0.78, 0.93)
(0.94, 1.23)
30−Day Postop Mortality
(0.91, 1.19)
(0.59, 0.87)
30−Day Postop Readmission
(0.88, 0.94)
(1.09, 1.15)
−1.5
−1.0
−0.5
0.0
0.5
Intraoperative fentanyl coefficient
Intraoperative hydromorphone coefficient

Perioperative Anesthesia 15- Using Venous Excess Ultrasound (VExUS) grading to assess perioperative volume status among patients undergoing non-cardiac surgeries: a comprehensive pilot study

Justin Magin[1], Jacob Wrobel[2], Xinming An[2], David Flynn[3], Duncan McLean[3], Stuart Grant[3]

University of North Carolina School of Medicine[1] UNC Chapel Hill School of Medicine[2] UNC School of Medicine[3]

Introduction: Perioperative fluid balance can impact the rate of complications following surgery[1,2]. These post-operative complications are linked to increased patient morbidity and mortality[3]. The VExUS grading system is a standardized point-of-care ultrasound (POCUS)-based, comprehensive method to assess volume status by incorporating measurements of the inferior vena cava along with doppler scans of the hepatic, portal, and intrarenal veins[4]. High VExUS scores have been associated with acute kidney injury (AKI) after cardiac surgeries[4] and have been used in intensive care units to guide medical decision making in patients undergoing clinical deterioration[5]. The use of VExUS grading has yet to be studied in the perioperative setting for routine management of post-operative patients. Therefore, our primary outcome was to describe the incidence of perioperative volume overload using VExUS score and determine feasibility of using VExUS perioperatively. Additionally, we aimed to assess whether grading perioperative fluid status using VExUS can identify patients at risk for 30-day post-operative complications.

Methods: We conducted a single center, prospective study with enrollment from June to August 2022. The study population included non-critically ill adults undergoing major, non-cardiac surgery. Patients were scanned at the bedside and were not ventilator dependent at time of scans. Patients were scanned pre-operatively, early post-operatively (PACU), and 24-hours post-operatively. Volume overload was stratified by VExUS scoring protocol as either Grade 0 (no congestion), Grade 1 (mild congestion), Grade 2 (moderate congestion), or Grade 3 (severe congestion)[4]. ASA scores were assigned by American Society of Anesthesiologists Physical Status Classification standards[6]. American College of Surgeons National Surgical Quality Improvement Program (ACS NSQIP) risks for complication and 30-day post-operative outcomes were retrospectively captured for multivariate analyses using R statistical computing[7,8]. VExUS grades were treated as ordinal variables and Kruskal-Wallis rank sum test was used to test the associations. This work was supported by grant number T35-DK007386 from the National Institutes of Health, as well as institutional funding.

Results: The cohort included 69 patients with a median age of 62 (48, 67). 41 (59%) identified as female and 46 (67%) identified as white. Median ASA score was 3 (1, 4) and median length of stay (LOS) was 2 days (1, 4). Of the 66 available PACU scans, positive VExUS grades were observed in 29 (44%) patients, from which 22 (33%) were identified with Grade 1 congestion and 7 (11%) had Grade 2 congestion. At the 24-hour timepoint (n=63), 31 (49%) had a positive VExUS grade with 20 (32%) patients scoring Grade 1 and 11 (17%) scoring Grade 2. Of the 56 patients that were Grade 0 before surgery, 28 (50%) had at least one post-operative scan with volume overload. Interestingly, no patients at any timepoints received a Grade 3: severe congestion score. There were 22 (32%) patients that had at least one NSQIP complication within the 30-day post-operative period. Notably, 11 (16%) patients developed an AKI. Trends show that those that developed an AKI may have had higher VExUS scores, however, upon analyzing all timepoints we did not observe a statistically significant signal. Moreover, higher VExUS scores were also not associated with increased risk of all-cause 30-day complications. Age, sex, race, ASA score, and LOS were also not associated with all-cause complications nor AKI.

Conclusions: VExUS grading is a useful and feasible bedside tool to assess for volume overload during the perioperative period. Volume overload had a relatively high incidence that increases over the perioperative timeline. In our study, VExUS was not associated with all-cause 30-day complications nor AKI. Further studies should be designed to describe associations between perioperative factors and increases in VExUS grading. Moreover, larger prospective studies should assess for complication risk factors after non-cardiac surgeries.

References: 1. *J Anaesthesiol Clin Pharmacol*. 2019;35:S29-S34

2. *Dis Esophagus*. 2021;34(7).

3. *Anesth Analg*. 2021;133(2):393-405.

4. *Ultrasound J*. 2020; 12:16.

5. *Ultrasound J*. 2021;13(1):32.

6. ASA Physical Status Classification System. Accessed 2022.

7. *J Am Coll Surg*. 2009;208(6):1009-1016.

8. R Statistical Computing. Accessed 2022.

Figure 1. VExUS grading trends over study timepoints

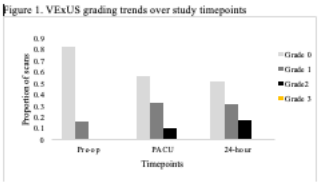

Figure 2. VExUS grading over timepoints stratified by presence of 30-day complications

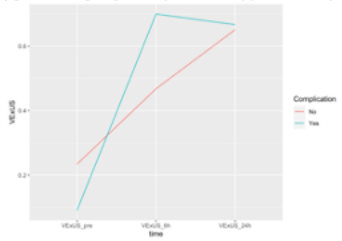

Figure 3. VExUS grading over timepoints stratified by presence of AKI

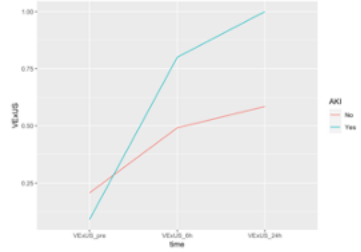

Perioperative Anesthesia 16- Utility of donor management goals during organ recovery procedures from deceased organ donors

Emily Vail[1], Mitchell Plesser[1], Rebekah Chun[2], Juliana Quin[2], Sarah Hamimi[3], Maureen Banigan[3]

University of Pennsylvania[1] University of Pennsylvania, Perelman School of Medicine[2] Perleman School of Medicine at the University of Pennsylvani[3]

Introduction: Donor management goals (DMGs) are physiologic and laboratory endpoints used to guide clinical management of deceased organ donors after diagnosis of brain death.[1] Observational research has found associations between the number of DMGs achieved and the number of organs recovered for transplant.[2] While several DMGs (including mean arterial pressure (MAP) and serum glucose) may be plausibly measured and achieved in the operating room, their utility as treatment endpoints and predictors of successful organ recovery has not been established. Therefore, we aimed to describe factors associated with measurement and achievement of intraoperative DMGs during organ recovery procedures, and to determine whether DMG achievement is associated with the number of organs transplanted per donor.

Methods: Retrospective study of adults with brain death who underwent organ recovery procedures in a US academic healthcare system, Jan 2017 – Dec 2022. Living donors and donors after cardiac death were excluded. Study data were extracted from electronic anesthesia records (EPIC systems, Verona, WI) and combined with donation outcomes data from the local organ procurement organization (Gift of Life Donor Program, Philadelphia, PA). To determine the feasibility and utility of DMG monitoring during organ recovery, we determined which DMGs were recorded, and achieved, for each donor, then calculated recording and achievement rates overall. For each type of organ transplanted, we determined rates of DMG recording and achievement among those donor subgroups. We determined associations between the number of DMGs recorded, the number achieved, and the number of organs transplanted per donor using unadjusted Poisson regression. This work was supported by a Pilot Grant from the University of Pennsylvania McCabe Foundation.

Results: In a cohort of 103 organ donors, median number of DMGs recorded intraoperatively was 7 (range 2-7 per donor, out of 9 goals). MAP (100% of donors), vasopressor administration (100%), and urine output (89.3%) were most frequently recorded (Table 1). Central venous pressure and left ventricular ejection fraction were not recorded in any donors. Only 54.2% of cohort patients had recorded intraoperative laboratory values (4 DMGs), with most recorded values in heart (82.9%) and lung (87.9%) donors. Donors with all 7 recorded DMGs were younger than those with at least one unrecorded DMG (44.9 years (IQR 30.5, 57.5) vs. 59.1 (IQR 48.0, 68.6), $p<0.001$). There were no discernable trends in recording or achieving the most prevalent goals by year of organ donation.

79 donors (76.7%) achieved at least one DMG; 4 donors (3.9%) achieved 7. DMG achievement varied by organ subgroup, with higher median numbers of DMGs achieved in heart, lung, and pancreas donors (Table 2). Among the most consistently recorded DMGs in the cohort, goals for low-dose vasopressors were achieved in 52 (50.5% of cohort donors), MAP in 20 (19.4%), and urine output in 43 (41.8%). Both the number of DMGs recorded and the number of DMGs achieved were associated with the number of organs transplanted from each donor (incident rate ratio (IRR) for DMG recording 1.17, 95% CI 1.11-1.24, Fig 1; IRR for DMG achievement 1.20, 95% CI 1.16-1.25; Fig 2).

Conclusions: In a cohort of deceased donors after brain death, we observed low rates of DMG recording and achievement during organ recovery procedures. Substantial missing data in available anesthesia records suggests that clinical management goals developed for the intensive care unit may not be feasibly applied in the OR. Observed variation in intraoperative monitoring and laboratory testing may be attributable to differences between individual anesthesiologists and differences in intraoperative management when specific organs are recovered. Although we observed differences in the primary outcome when DMGs were recorded, and achieved, analyses did not account for differences in donor characteristics between groups. Despite limitations, our finding that common measures of organ perfusion (MAP and urine output) were not achieved in most donors during organ recovery procedures suggests opportunities to improve intraoperative management.

References: [1] Malinoski D et al. Achieving donor management goals before deceased donor procurement is associated with more organs transplanted per donor. *J Trauma*. 2011; 71:990:995.

[2] Malinoski D et al. The impact of meeting donor management goals on number of organs transplanted per donor: results from the UNOS Region 5 prospective donor management goals study. *Crit Care Med*. 2012; 40:2773-2780.

FIGURE 1. Association between intraoperative recording of donor management goals (DMGs)[1] and number of organs transplanted from decreased organ donors after brain death

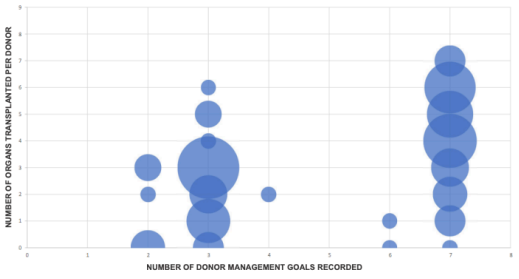

n=103 deceased organ donors after brain death
Size of each bubble is proportional to number of cohort donors with each combination of DMGs recorded and organs transplanted
Maximum possible number of DMGs recorded is 9. Maximum possible number of solid organs transplanted is 8.

[1] Malinoski D et al. Achieving donor management goals before deceased donor procurement is associated with more organs transplanted per donor. J Trauma. 2011; 71:990:995.

FIGURE 2. Association between intraoperative achievement of donor management goals (DMGs)[1] and number of organs transplanted from decreased organ donors after brain death

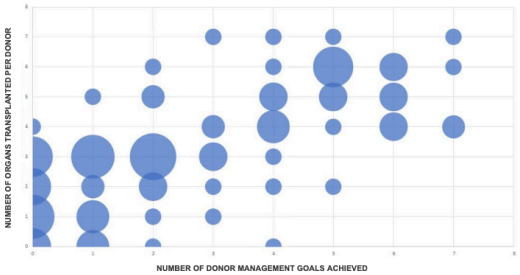

n=103 deceased organ donors after brain death
Size of each bubble is proportional to number of cohort donors with each combination of DMGs recorded and organs transplanted
Maximum possible number of DMGs achieved is 9. Maximum possible number of solid organs transplanted is 8.

1. Malinoski D et al. Achieving donor management goals before deceased donor procurement is associated with more organs transplanted per donor. J Trauma. 2011; 71:990:995.

TABLE 1. Intraoperative recording of donor management goals (DMGs)

Organ Donated	All Donors	Heart	Lung	Kidney	Liver	Pancreas
n (%) of cohort donors	103 (100)	35 (34.0)	33 (32.0)	75 (72.8)	83 (80.6)	7 (7.6)
Donor Management Goal						
Central venous pressure (CVP) 4-10mmHg, *n* (%)	0 (0)	0 (0)	0 (0)	0 (0)	0 (0)	0 (0)
Left ventricular ejection fraction (LVEF) > 50%	0 (0)	0 (0)	0 (0)	0 (0)	0 (0)	0 (0)
Mean arterial pressure 60-100 mmHg, *n* (%)	103 (100)	35 (100)	33 (100)	75 (100)	83 (100)	7 (100)
Low-dose vasopressors, *n* (%) [a]	103 (100)	35 (100)	33 (100)	75 (100)	83 (100)	7 (100)
Urine output 0.5 - 3 mL/kg/hr, *n* (%)	92 (89.3)	35 (100)	33 (100)	71 (94.7)	78 (94.0)	7 (100)
Arterial blood gas, pH 7.3-7.45, *n* (%)	54 (52.4)	29 (82.9)	29 (87.9)	35 (46.7)	48 (57.8)	7 (100)
PaO2: FiO2 ≥ 300, *n* (%)	54 (52.4)	29 (82.9)	29 (87.9)	44 (58.7)	48 (57.8)	7 (100)
Serum glucose ≤ 150 mg/dL, *n* (%)	55 (53.4)	30 (85.7)	29 (87.9)	44 (58.7)	49 (59.0)	7 (100)
Serum sodium 135-155 mEq/L, *n* (%)	54 (52.4)	29 (82.9)	29 (87.9)	44 (58.7)	48 (57.8)	7 (100)
All DMGs values recorded, *n* (% of donors) [b]	52 (50.4)	29 (82.9)	29 (87.9)	44 (58.7)	47 (56.6)	7 (100)

[a] Defined as ≤1 pressor administered, either dopamine ≤ 10 mcg/kg/min, norepinephrine ≤ 10 mcg/min, or phenylephrine ≤ 60 mcg/min.
[b] Excluding CVP and LVEF (not recorded in any cohort donor).

TABLE 2. Intraoperative achievement of donor management goals (DMGs)

Organ Donated	All Donors	Heart	Lung	Kidney	Liver	Pancreas
n (%) of cohort donors	103 (100)	35 (34.0)	33 (32.0)	75 (72.8)	83 (80.6)	7 (7.6)
Donor Management Goal						
Central venous pressure (CVP) 4-10mmHg, *n* (%)	0 (0)	0 (0)	0 (0)	0 (0)	0 (0)	0 (0)
Left ventricular ejection fraction (LVEF) > 50%	0 (0)	0 (0)	0 (0)	0 (0)	0 (0)	0 (0)
Mean arterial pressure 60-100 mmHg, *n* (%)	20 (19.4)	9 (25.7)	9 (27.3)	19 (25.3)	19 (25.3)	1 (14.3)
Low-dose vasopressors, *n* (%)[a]	52 (50.5)	25 (71.4)	26 (78.3)	43 (57.3)	46 (55.4)	5 (71.4)
Urine output 0.5 - 3 mL/kg/hr, *n* (%)	43 (46.7)	22 (62.9)	19 (57.6)	34 (45.3)	37 (44.6)	4 (57.1)
Arterial blood gas, pH 7.3-7.45, *n* (%)	38 (70.4)	26 (74.3)	27 (81.8)	35 (46.7)	38 (45.8)	7 (100)
PaO2: FiO2 ≥ 300, *n* (%)	44 (81.5)	24 (68.6)	28 (84.9)	38 (50.7)	40 (48.2)	6 (85.7)
Serum glucose ≤ 150 mg/dL, *n* (%)	26 (47.3)	20 (57.1)	19 (57.6)	24 (32.0)	25 (30.1)	5 (71.4)
Serum sodium 135-155 mEq/L, *n* (%)	41 (75.9)	25 (71.4)	24 (72.7)	35 (46.7)	39 (47.0)	6 (85.7)
All DMGs values achieved, *n* (% of organ donors)[b]	4 (3.9)	3 (8.6)	3 (9.1)	4 (5.3)	4 (4.8)	1 (14.3)
DMGs achieved per donor, median (IQR)	**2 (1, 4)**	**5 (3, 6)**	**5 (4, 6)**	**3 (1, 5)**	**3 (1, 5)**	**5 (4, 6)**

[a] Defined as ≤1 pressor administered, either dopamine ≤ 10 mcg/kg/min, norepinephrine ≤ 10 mcg/min, or phenylephrine ≤ 60 mcg/min.
[b] Excluding CVP and LVEF given the absence of recording in all cohort patients.

Perioperative Anesthesia 17- Association between Pulmonary Hypertension and Sickle Cell Disease Depending on Genotype, Age, and Sex

Ksenia Ershova[1], Ditha Nanditha[1], Jack Fox[1], Nandita Perumal[1], Nicholas Kassebaum[1]

UW[1]

Introduction: Pulmonary hypertension (PH) is associated with an increased risk of perioperative mortality after non-cardiac surgery. One review reported a 3.5-8% mortality rate in patients with PH [1], which is 2-4 times higher than 1.8%, the rate of perioperative mortality reported for the general population [2]. PH is also a common complication of sickle cell disease (SCD), experienced by 10-33% of patients depending on the method of measurement [3]. While SCD is well-recognized as a perioperative risk factor related to acute anemia and vaso-occlusive events, PH is another major consideration for potential complications. Among SCD patients, PH was found to be an independent risk factor for mortality where, for every 10mm Hg increase in mean pulmonary artery pressure, the likelihood of death increases 1.7 times [3]. This study aimed to evaluate the association between PH and SCD by genotype, age, and sex at the population level in the United States.

Methods: We conducted a retrospective case-control analysis using data from the IBM Truven Health MarketScan Commercial and Medicare Supplemental claims database for years 2015-2019. We included patients who had at least 6 months of continuous insurance coverage. Patients with non-SCD chronic hemolytic anemias and pregnant women were excluded. PH was defined as having at least one inpatient or two outpatient visits with a PH-related ICD-10 code. SCD genotypes included HbSS, HbSC, HbS/β-thalassemia (HbSth), and all other genotypes (HbOs), which were identified based on ICD-10 codes. Odds ratios (ORs) quantified how strongly PH (outcome) is associated with SCD (exposure) and were calculated for each subgroup combination of age, sex, and SCD genotype.

Results: 49,138,203 patients were included in the analysis, 18,310 of which were diagnosed with SCD, and 65,335 were diagnosed with PH. ORs ranged between 4.2 and 717.7 with a median of 43.7 [Q1Q3: 17.3, 99.9]. Men had higher median OR than women, (75.8 [Q1Q3: 28.7, 110.6] vs. 34.7 [Q1Q3: 11.9, 97.3], Figures 1 and 2. The most significantly elevated ORs were roughly between ages of 15 to 45 for both sexes. Across genotypes, the highest median OR was in HbSS genotype, 55.0, and the lowest was in HbSth, 28.1; in HbOs and HbSC genotypes, ORs were 53.1 and 34.1 respectively.

Conclusions: Evaluating a large cohort of patients, we found that SCD is associated with a substantial increase in the likelihood of PH, by 1-2 orders of magnitude, especially in younger men. Because of the well-established perioperative risk associated with PH, this finding highlights the need to routinely consider, and potentially screen for, PH in any person with SCD who is proposed for a procedure with sedation or under general anesthesia.

References: 1. "Focused Review of Perioperative Care of Patients with Pulmonary Hypertension and Proposal of a Perioperative Pathway." 2018. *Cureus* 10 (1): e2072

2. "Association between Complications and Death within 30 Days after Noncardiac Surgery." 2019. *CMAJ: Canadian Medical Association Journal Journal de l'Association Medicale Canadienne* 191 (30): E830–37.

3. "Sickle Cell Disease: At the Crossroads of Pulmonary Hypertension and Diastolic Heart Failure." 2020. *Heart* 106 (8): 562–68.

Fig. 1. ORs describing the association between SCD and PH by age and genotype among men

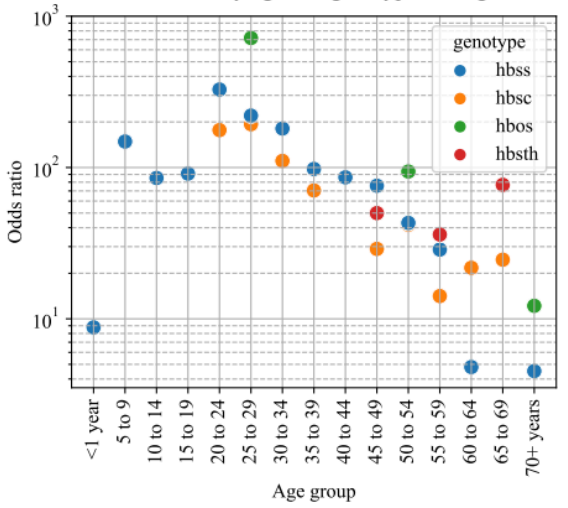

Fig. 2. ORs describing the association between SCD and PH by age and genotype among women

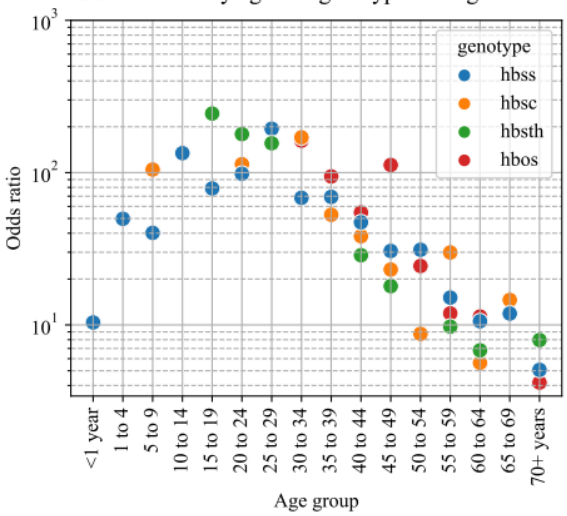

Perioperative Anesthesia 18- Comparison and validation of two methods for the determination of sevoflurane consumption during general anesthesia for non-cardiac surgery

Federico Ciardi[1], Megan Abbott[1], Samuel Smith[1], Lucinda Everett[1]

Massachusetts General Hospital[1]

Introduction: Volatile anesthetics (VA) are potent greenhouse gasses that contribute significantly to the total carbon footprint of healthcare institutions. Approximately, 2% sevoflurane delivered in an equal mix of oxygen and air at 2 L/min for 1 hour produces an equivalent to 2.87 $kgCO_2$ or driving a car 11.27 km. Tracking VA consumption may impact decision making to reduce departmental greenhouse gas emissions. The gold standard technique to measure VA consumption is to weigh vaporizers before and after administration, which cannot be deployed widely. One widely cited algorithm (Biro equation, Eqn. 1) calculates consumed VA volume retrospectively based on fresh gas flow (FGF) and VA concentration[1]. The proprietary Drägerwerk AG & Co. KGaK (Dräger) Gas Consumption Analytics software contains another algorithm that reports 'Cumulated Sevoflurane Consumption' (CSC) by their anesthesia machines. Our aim is to compare and validate both algorithms against the gold standard to evaluate their applicability.

Equation 1. Reproduced from Biro, P. (2014). Acta Anaesthesiologica Scandinavica, 58(8), *968–972.*

Methods: Over a two-week period during July 2022, sevoflurane consumption was measured in pediatric and adult non-cardiac operating rooms at large urban academic medical center. VAs were delivered according to local standards of care using the Dräger Apollo® equipped with Dräger Vapor® 2000 vaporizers. Prior to the start of a procedure, the vaporizer was detached from the Apollo® and weighed using a scale (Precision Balance PCB, Kern & Sohn GmbH, Balingen, Germany). Weights were collected in triplicate and averaged. After conclusion of the procedure average sevoflurane vaporizer weights were again measured, and the difference converted to fluid VA volume. Inputs for the Biro equation were pulled from the electronic medical record (EMR). The Dräger CSC variable was recorded for each case. Pearson correlation coefficients (r) were calculated, and Bland-Altman (BA) plots were constructed to assess statistical agreement between measurement techniques.

Results: Of cases in which volatile anesthetics were used (n=38) the median volume of sevoflurane consumed was 29.44 mL (IQR 31.64). The Biro equation was shown to have r = 0.973 (n = 38), and a bias of -3.84 mL (SD 5.59, Lower LOA -14.80 Upper LOA 7.12). The Dräger CSC was shown to have r = 0.985 (n = 32), and a bias of +1.05 mL (SD 4.00, Lower LOA -6.78 Upper LOA 8.89). BA plots of agreement are shown in figure 1.

Figure 1. Bland-Altman plots demonstrating degree of agreement between measured VA consumption and calculated consumption by the Biro equation (top) and Dräger CSC parameter (bottom).
LOA = limit of agreement.

Conclusions: The Biro equation was shown to underestimate consumption by 13.0%, and inspection of the BA plot suggests that a systematic proportional bias exists. These data agree with a prior study assessing the method on the same vaporizer[2]. CSC appears to have performed better; the bias was shown to be +3.6%, and differences evenly distributed between the limits of agreement even at greater consumption volumes. Further, the Biro equation results in greater error as VA consumption increases. This may be explained by more leak during longer cases or at higher FGF, or by greater patient uptake. Independent analysis of Dräger consumption software on the Zeus anesthesia machine was conducted by Dehouwer et al yielding similar results[3]. The CSC calculation incorporates more data derived from sensors in the anesthesia machine, accounting for factors such as patient uptake, circuit leak, waste gas scavenging and internal dead space, which may account for its superior accuracy in measuring consumed VA.

References: 1.Biro P. Calculation of volatile anaesthetics consumption from agent concentration and fresh gas flow. *Acta Anaesthesiol Scand*. 2014;58(8):968-972. doi:10.1111/aas.12374

2. Biro P, Kneschke O, Theusinger OM. Accuracy of calculated volatile agent consumption from fresh gas content. *Acta Anaesthesiol Scand*. 2015;59(5):619-624. doi:10.1111/aas.12487

3. Dehouwer A, Carette R, de Ridder S, de Wolf AM, Hendrickx JFA. Accuracy of inhaled agent usage displays of automated target control anesthesia machines. *J Clin Monit Comput*. 2016;30(5):539-543. doi:10.1007/s10877-015-9746-z

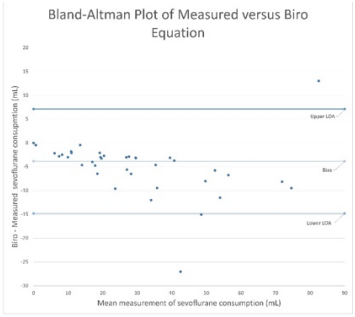

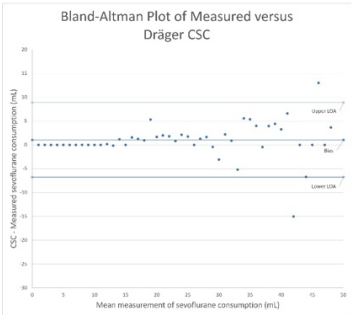

$$Fluid\ VA\ (mL) = \frac{FGF\ (L/\min) * VA\ conc.\ (Vol\%) * Anesthetic\ duration\ (\min)}{saturated\ gas\ volume\ (mL/mL) * 100\ (Vol\%)}$$

Perioperative Anesthesia 19- Differential association of recreational cannabis use or cannabis use disorder with major adverse cardiovascular and cerebrovascular events after surgery

Sarah Ashrafian[1], Elena Ahrens[1], Ricardo Munoz[2], Luca Wachtendorf[3], Denys Shay[1], Aiman Suleiman[4], Simone Redaelli[4], Dario von Wedel[4], Laetitia Chiarella[5], Guanqing Chen[5], Kevin Hill[1], Maximilian Schaefer[6]

Beth Israel Deaconess Medical Center[1] BIDMC[2] Montefiore Medical Center[3] Beth Israel Deaconess Medical Center, Harvard Medical school[4] Director, Center for Anesthesia Research Excellence (CARE).[5] Beth Israel Deaconess Medical Center & Hospital[6]

Introduction: In recent years, the prevalence of reported cannabis use among surgical patients has dramatically increased [1]. Previous studies suggested that surgical patients with a diagnosis of cannabis use disorder have an increased risk of cardiovascular and cerebrovascular events (MACCE) after surgery [2–4]. However, it is unclear whether these results apply to patients with "simple" recreational cannabis use [5]. We investigated the association between reported recreational cannabis use as well as cannabis use disorder and MACCE after surgery.

Methods: Adult patients who underwent non-cardiac procedures between 2008 and 2020 at a tertiary academic hospital in Massachusetts, USA were included in this retrospective study. Patients with ASA status ≥ V, transplant surgery, pre-interventionally admitted to the ICU, or patients with a previous prescription of medical cannabinoids were excluded. The primary exposure was recreational cannabis consumption, defined as self-reported use based on structured nursing and physician interviews or a diagnosis of cannabis use disorder, identified through International Classification of Diseases (9th/10th Revision, Clinical Modification [ICD-9/10-CM]) diagnostic codes. The primary outcome was MACCE within one year after surgery, defined as a diagnosis of stroke, cardiac arrest, acute heart failure, myocardial infarction or coronary artery revascularization. Multivariable logistic regression analysis adjusted for patient characteristics, socio-economic factors, pre-existing comorbidities, pre-procedural drug prescriptions as well as anesthesia-related and procedural characteristics was applied.

Results: 288,923 patients were included in the analysis (**Figure 1**). 21,117 (7.3%) were identified as cannabis users (**Table 1**), of whom 17,184 (81.4%) used cannabis recreationally and 3,933 (18.6%) had a diagnosed cannabis use disorder. 6,635 (2.3%) patients had MACCE within one year after surgery, out of which 302 (4.9%) were recreational cannabis users and 144 (2.3%) had a diagnosed cannabis use disorder. In adjusted analyses compared to non-users, a diagnosis of cannabis use disorder was associated with an increased risk of MACCE within one year after surgery (adjusted odds ratio [ORadj] 1.26; 95%CI 1.05–1.51; p=0.015). However, there was no association between recreational cannabis consumption and MACCE compared to non-users (ORadj 1.02; 95%CI 0.90–1.15; p=0.79). These findings were reflected when investigating the association between cannabis use and major cardiovascular events within one year postoperatively (**Figure 2**), while there was no association between recreational cannabis consumption or cannabis abuse disorder and stroke within one year following surgery (**Figure 2**).

Conclusions: While patients with a cannabis use disorder were at increased risk of MACCE after surgery, this association was not found for patients with "simple" recreational cannabis use. These differential effects might explain equivocal results among previous studies and should be considered when interpreting cannabis-associated risk of adverse cardiovascular and cerebrovascular events.

References: [1] Socioeconomic factors, psychiatric disorders and substance abuse associated with cannabinoid use in surgical patients, et al. Anesthesia and Analgesia. 2022; 963

[2] Cannabis Use Disorder and Perioperative Outcomes in Major Elective Surgeries: A Retrospective Cohort Analysis, Anesthesiology 2020; 132(4):625–35.

[3] Marijuana use and mortality following orthopedic surgical procedures, Subst Abuse 2019; 40(3):378–82.

[4] Cannabis Abuse and Perioperative Complications Following Inpatient Spine Surgery in the United States, Spine 2021; 46(11):734–43.

[5] Cumulative Lifetime Marijuana Use and Incident Cardiovascular Disease in Middle Age: The Coronary Artery Risk Development in Young Adults (CARDIA) Study, Am J Public Health 2017; 107(4):601–6.

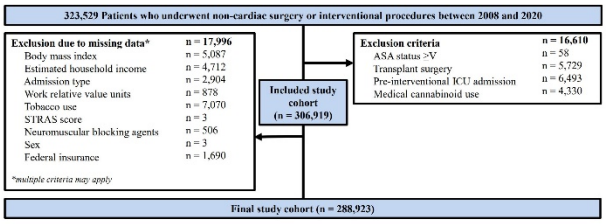

Figure 1. Study flow diagram indicating number of patients due to exclusion criteria and missing data.
Abbreviations: ASA: American Society of Anesthesiologists; ICU: Intensive care unit; STRAS: Stroke after surgery.

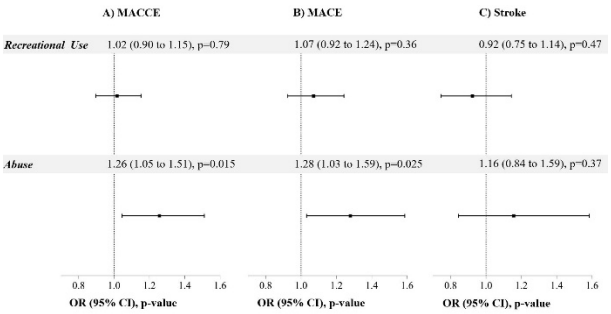

Figure 2. Association of recreational cannabis use or cannabis use disorder and outcomes.
A separate multivariable logistic regression model adjusting for patient demographics and characteristics as well as intraoperative factors was used for each outcome.

	No Cannabis consumption n=267,806	Cannabis consumption n=21,117	Standardized difference
Demographics			
Age, [years]	57 ± 16	47 ± 15	0.616
BMI [kg/m²]	27.2 (23.7 - 31.6)	26.8 (23.4 - 31.4)	0.035
Sex	158,498 (59.2%)	8,423 (39.9%)	0.393
Estimated household income	84,170.0 (64,559.0 - 105,061.0)	78,664.0 (57,649.0 - 96,514.0)	0.208
Federal insurance	88,488 (33.0%)	6,276 (29.7%)	0.072
Preoperative factors			
ASA physical status			0.036
1	28,780 (10.7%)	2,496 (11.8%)	
2	132,177 (49.4%)	10,394 (49.2%)	
3	100,077 (37.4%)	7,792 (36.9%)	
4	6,772 (2.5%)	435 (2.1%)	
Chronic heart failure	12,690 (4.7%)	723 (3.4%)	0.066
Diabetes mellitus	37,249 (13.9%)	2,403 (11.4%)	0.076
Artrial fibrillation	18,939 (7.1%)	933 (4.4%)	0.114
Arterial hypertension	106,950 (39.9%)	7,185 (34.0%)	0.123
Dyslipidemia	95,517 (35.7%)	5,940 (28.1%)	0.162
Coronary artery disease	40,871 (15.3%)	2,328 (11.0%)	0.126
STRAS score	6 (4 - 10)	5 (2 - 9)	0.270
Preoperative drug prescription			
Preoperative opioid prescription	44,777 (16.7%)	5,294 (25.1%)	-0.206
Betablocker	21,842 (8.2%)	1,368 (6.5%)	0.064
Diuretic	29,578 (11.0%)	1,695 (8.0%)	0.103
Calcium channel blocker	14,617 (5.5%)	963 (4.6%)	0.041
Angiotensin 1 receptor blocker	9,590 (3.6%)	454 (2.1%)	0.086
ACE inhibitor	19,494 (7.3%)	1,403 (6.6%)	0.025
Statins	33,813 (12.6%)	1,911 (9.0%)	0.115
Aspirin	26,835 (10.0%)	1,823 (8.6%)	0.048
Comorbidities			
COPD	21,637 (8.1%)	1,986 (9.4%)	-0.047
Cancer	50,739 (18.9%)	3,543 (16.8%)	0.057
Liver disease	4,628 (1.7%)	790 (3.7%)	-0.124
Renal disease	14,870 (5.6%)	996 (4.7%)	0.038
Anemia within 1 year prior	39,781 (14.9%)	3,290 (15.6%)	-0.020
Depression	41,503 (15.5%)	5,182 (24.5%)	-0.227
Anxiety	31,432 (11.7%)	4,207 (19.9%)	-0.226
Schizoaffective disorder	686 (0.3%)	142 (0.7%)	-0.061
Schizophrenia	889 (0.3%)	151 (0.7%)	-0.053
Psychosis	2,308 (0.9%)	352 (1.7%)	-0.072
History of drug use without cannabis	15,724 (5.9%)	4,309 (20.4%)	-0.441
Tobacco use	119,043 (44.5%)	14,597 (69.1%)	-0.514
Procedure characteristics			
Duration of surgery, median (IQR) (min)	77 (43 - 140)	82 (43 - 148)	-0.043
Type of surgery			-0.016
Colorectal surgery	6,619 (2.5%)	761 (3.6%)	
Dental, oral surgery	200 (0.1%)	57 (0.3%)	
Ear, nose, throat surgery	7,250 (2.7%)	656 (3.1%)	
Ophthalmologic surgery	14,209 (5.3%)	393 (1.9%)	
General surgery	42,324 (15.8%)	3,054 (14.5%)	
Gastrointestinal surgery	32,287 (12.1%)	2,995 (14.2%)	
Gynecological surgery	40,130 (15.0%)	2,453 (11.6%)	
Neurological surgery	7,852 (2.9%)	917 (4.3%)	
Orthopedic surgery	49,708 (18.6%)	4,622 (21.9%)	
Plastic surgery	14,313 (5.3%)	1,372 (6.5%)	
Podiatric surgery	5,599 (2.1%)	400 (1.9%)	
Oncological surgery	9,923 (3.7%)	484 (2.3%)	
Thoracic surgery	11,230 (4.2%)	825 (3.9%)	
Trauma, surgical critical care	3,473 (1.3%)	302 (1.4%)	
Urologic surgery	15,118 (5.6%)	1,283 (6.1%)	
Vascular surgery	7,571 (2.8%)	543 (2.6%)	
Admission type			-0.039
Ambulatory	173,625 (64.8%)	13,443 (63.7%)	
Same day admission	70,910 (26.5%)	5,541 (26.2%)	
Inpatient	23,271 (8.7%)	2,133 (10.1%)	
Work RVU	7.7 (4.7 - 14.5)	7.4 (4.4 - 15.0)	-0.0004
Crystalloid and colloid infusion, median (IQR) (ml)	700 (400 - 1,000)	700 (400 - 1,100)	-0.026
Units of packed red blood cells	0.0 (0.0 - 0.0)	0.0 (0.0 - 0.0)	0.032
Opioid dose, median (IQR) (mg oral morphine equivalents)	18.8 (0.0 - 42.0)	25.0 (0.0 - 49.5)	-0.086
Non-depolarizing NMBA, median (IQR) (ED95)	0.0 (0.0 - 1.8)	0.0 (0.0 - 2.1)	-0.082
Neostigmine dose, median (IQR) (mg/kg)	0.0 (0.0 - 1.5)	0.0 (0.0 - 1.0)	0.018
Vasopressor dose, median (IQR) (mg norepinephrine equivalents)	0.0 (0.0 - 0.0)	0.0 (0.0 - 0.0)	0.003
Minutes of mean arterial pressure below 55 mmHg, median (IQR)	0.0 (0.0 - 1.0)	0.0 (0.0 - 1.0)	0.010
Age-adjusted mean alveolar concentration of inhalation anesthetics, median (IQR)	0.8 (0.0 - 1.0)	0.8 (0.0 - 1.0)	-0.070
Sugammadex use	13,278 (5.0%)	1,801 (8.5%)	-0.143

Table 1. Patient characteristics by cannabis use. Data are expressed as frequency (prevalence in %), or median (interquartile range [IQR, 25th-75th percentile]). Comorbidities were defined using International Classification of Diseases (9th/10th Revision, Clinical Modification [ICD-9/10-CM]) diagnostic codes.
ASA: American Society of Anesthesiologists; ACE: Angiotensin-converting enzyme; BMI: Body mass index; COPD: Chronic obstructive pulmonary disease; ED95: Median effective dose required to achieve a 95% reduction in maximal twitch response from baseline; IQR: Interquartile range; MAP: Median arterial blood pressure; NMBA: Neuromuscular blocking agents; RVU: Relative value units; STRAS: Stroke after surgery.

Perioperative Anesthesia 20- Higher intercellular adhesion molecule-1 suppression by high-density lipoproteins is associated with a lower risk of postoperative acute kidney injury

Zoe Leuthner[1], Patricia Yancey[1], MacRae MD[2], Loren Smith[3]

Alabama College of Osteopathic Medicine[1] Vanderbilt University School of Medicine[2] Vanderbilt University Medical Center[3]

Introduction: Postoperative acute kidney injury (AKI) is common after cardiac and vascular surgery and is associated with an increased risk of chronic kidney disease (CKD) development, advancement and death. A higher preoperative high density lipoprotein (HDL) concentration is associated with a reduced risk of postoperative AKI.[1] In animals, one intravenous dose of HDL directly before renal ischemia reduces renal intercellular adhesion molecule-1 (ICAM-1) expression, renal neutrophil infiltration, renal oxidative damage, and AKI.[2] Further, in vivo administration of antibodies against ICAM-1 can reduce ischemic AKI, supporting the role of ICAM-1 in AKI.[3] Individual patients' HDL has a varying ability to suppress ICAM-1. We hypothesized that cardiac and vascular surgery patients with higher preoperative HDL capacity to suppress endothelial ICAM-1 would have lower postoperative sICAM-1 concentrations and a lower risk of postoperative AKI.

Methods: After obtaining IRB approval, we prospectively recruited 100 adult patients undergoing major, elective surgery on the heart and/or large blood vessels. To enrich our cohort for our outcome of interest, AKI, we recruited patients with an eGFR<60. Plasma samples were collected at induction of anesthesia and immediately after surgery. HDL cholesterol concentration (HDL-C) was determined using a selective enzymatic hydrolysis method. To quantify each patient's HDL ability to suppress endothelial ICAM-1, equal volumes of ApoB-depleted patient serum were incubated with human umbilical vein endothelial cells for 30 minutes before the addition of 8 ng/mL TNF-a. After an additional 5 hours of incubation, total RNA was collected, cDNA was synthesized, and RT-PCR was performed to quantify ICAM-1 mRNA. ICAM-1 suppression was calculated as a percent based on a TNF-a only control sample. A commercially available ELISA assay was used to measure postoperative sICAM-1 concentrations. Multivariable logistic regression was used to estimate the association between HDL ICAM-1 suppression and AKI.

Results: In this patient population, HDL cholesterol concentration did not correlate with HDL ICAM-1 suppression capacity (Spearman's R=0.05, p=0.64). Apolipoprotein A-I concentration, however, a major protein component of HDL known to have anti-inflammatory capacity, did correlate with HDL ICAM-1 suppression capacity (Spearman's R= 0.29, p=0.004). Higher preoperative HDL capacities to suppress endothelial ICAM-1 *in vitro* were correlated with lower postoperative plasma concentrations of sICAM-1 in study subjects (Spearman's R= -0.30, p=0.003). After adjustment for known AKI risk factors, including age, sex, BMI, preoperative kidney function, hypertension, diabetes mellitus, exposure to cardiopulmonary bypass, and intraoperative red blood cell transfusion volume, a higher preoperative HDL ability to suppress endothelial ICAM-1 was associated with a lower risk of AKI (OR 3.4 (95% CI 1.3-9.0), p=0.016, Figure). HDL-C concentration was not independently associated with postoperative AKI (OR 1.03 (95% CI 0.98-1.08), p=0.19) possibly due to CKD-induced HDL dysfunction.

Conclusions: In a previously published clinical trial, eight weeks of fenofibrate treatment in healthy humans with low HDL increased HDL and reduced plasma sICAM-1 concentrations,[4] demonstrating that pharmacological treatments, which raise HDL, can reduce sICAM-1 concentrations. Novel HDL-based therapeutics are being developed that also suppress endothelial ICAM-1 expression. Our data show that cardiac and vascular surgery patients with higher preoperative HDL capacity to suppress endothelial ICAM-1 have lower sICAM concentrations after surgery and a lower risk of postoperative AKI. HDL-based treatments may be promising new therapeutics for postoperative AKI.

References:

1. *J Am Heart Assoc*. 2017;6(12):e006975.
2. *J Am Soc Nephrol*. 2003;14(7):1833-1843.
3. *Atherosclerosis*. 2010;212(2):392-397.
4. *Arterioscler Thromb Vasc Biol*. 2002;22(4):656-661.

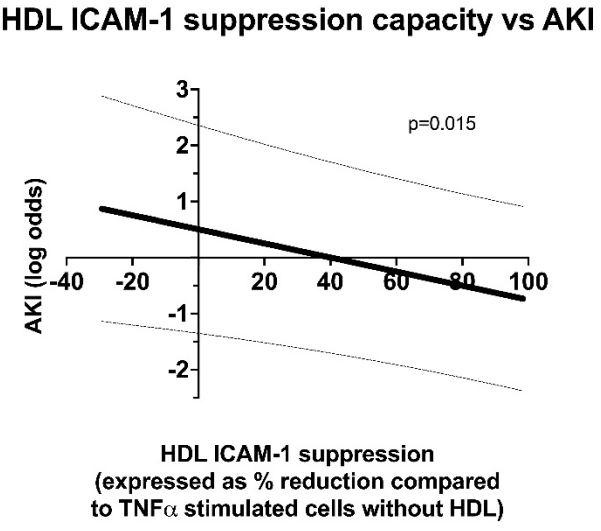

Perioperative Anesthesia 21- Intraoperative hemodynamic management of organ donors after neurologic determination of death

Emily Vail[1], Mitchell Plesser[1], Rebekah Chun[2], Juliana Qin[2], Sarah Hamimi[3], Maureen Banigan[1]

University of Pennsylvania[1] University of Pennsylvania, Perelman School of Medicine[2] Perleman School of Medicine at the University of Pennsylvania[3]

Introduction: Most transplanted organs in the US are from deceased donors after brain death. Loss of sympathetic tone following brain death frequently leads to profound vasoplegia and hypotension, organ hypoperfusion and decreased graft viability. Indeed, clinical management guidelines for deceased organ donors recommend mean arterial blood pressure (MAP) > 60 mmHg.1,2 During organ recovery procedures, donor hypotension may be compounded by insensible fluid losses, bleeding, and surgical manipulation, potentially reducing organ perfusion and function after transplant. To characterize this problem, we investigated the incidence and severity of hypotension during organ procurement procedures, described intraoperative hemodynamic management of organ donors after NDD, and evaluated the association between intraoperative hypotension and number of organs transplanted per donor (OTPD).

Methods: Retrospective study of adults who underwent organ recovery in a single healthcare system, Jan 2017 – Dec 2022. Living organ donors and donors after cardiac death were excluded. Study data were extracted from electronic anesthesia records (EPIC, WI) and combined with donation outcomes data from the local organ procurement organization (Gift of Life, PA). Variables of interest included donor demographics, hemodynamic monitoring, and vasopressor medication use (described by vasoactive inotropic score (VIS)3), overall and in subgroups defined by transplanted organ type. To quantify hemodynamic instability in donors, we calculated hypotensive burden, the percent of intraoperative recorded MAP values < 60 mmHg from anesthetic start to aortic cross-clamp time, to account for both time and severity of hypotension for each donor. We examined potential associations between hypotensive burden (stratified into higher and lower than cohort median values) and OTPD, as well as urine output (UOP) and arterial lactate, using Wilcoxon Rank-Sum tests. Work was supported by a pilot grant from the University of Pennsylvania McCabe Foundation.

Results: In a cohort of 103 deceased organ donors, arterial MAP was measured and recorded in 98% of cohort patients (the remainder via noninvasive measurements). The median hypotensive burden was 4.7 % [range 0–40.3] which did not vary by donated organ (Table 1). 91.3% of donors received vasoactive medications. Despite this, MAP exceeded 60 mmHg at all measured time points in only 19.4%. Phenylephrine was the most used vasoactive agent (63.1% of donors). Liver donors received more vasopressors than other organ subgroups (median VIS 2.5 [IQR 0, 5.6]). Measures of end-organ perfusion were recorded in the majority of donors with UOP available from 89.3% and arterial lactate from 52.4%.

326 organs were successfully transplanted from cohort donors with a median of 3 [IQR 2, 5] OTPD. Donors with hypotensive burdens below the cohort median had lower VIS (1.8 [IQR 0, 4.5] vs 3.8 [IQR 0, 10.5], p=0.01), and higher UOP (2.3 [IQR, 0.6, 5.4] vs 1.3 mL/kg/hr [IQR 0, 2.8], p=0.04, Table 2). Donors with lower than median hypotensive burdens donated more transplanted organs than donors with higher hypotensive burdens (4 [IQR 3, 6] vs. 2 [IQR 1, 3], p <0.001, Fig 1).

Conclusions: Despite guidelines recommending maintenance of normotension during organ procurement and frequent use of vasopressors, intraoperative hypotension remains common. In this small retrospective cohort, we defined hypotensive burden, a novel descriptor of the duration and severity of intraoperative hypotension, and identified significant associations between this measure and UOP, an indicator of end-organ perfusion, and OTPD. While these relationships are physiologically plausible and well-described4 in living patients, our finding that donors with lower than median hypotensive burdens received fewer vasopressors than patients with more hypotension suggests that factors other than treatment of hypotension (e.g., severity of illness) contributed to observed results. Other unmeasured donor characteristics, including age and comorbid disease, also influence the likelihood that individual organs will be recovered for transplant. Future work is necessary to evaluate the impact of intraoperative hypotension on graft function and to validate hypotensive burden as a predictor of donation outcomes.

References: (1) Kotloff R et al. Crit Care Med. 2015; 43:1291-325

(2) Souter M et al. Semin Cardiothorac Vasc Anesth 2018; 22:211-222

(3) Gaies M et al. Pediatr Crit Care Med. 2010; 11:234-238

(4) Salmasi, V et al. Anesthesiology. 2017; 126:47-65

FIGURE 1. Association between hypotensive burden during organ recovery procedures and number of organs transplanted from cohort organ donors

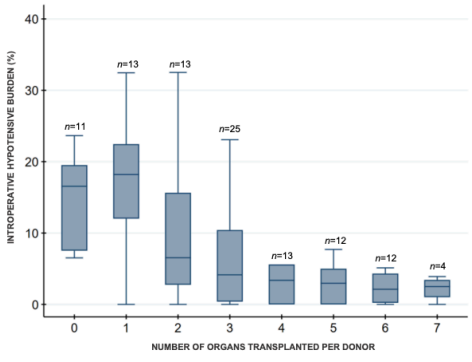

TABLE 1. Intraoperative hypotensive burden and hypotension management among cohort donors, stratified by type of organ donated

	All Donors (*n*=103)	**Heart Donors** (*n*=35)	**Lung Donors** (*n*=33)	**Liver Donors** (*n*=83)	**Kidney Donors** (*n*=75)	**Pancreas Donors** (*n*=7)
Age (yr), median (IQR)	53.4 (34.9, 64.9)	36.0 (26.2, 49.8)	42.5 (30.4, 52.8)	51.5 (32.9, 60.4)	48.6 (33.8, 58.3)	25.6 (19.7, 26.2)
Hypotensive burden %, median (IQR)	**4.7 (1.0, 15.2)**	**3.4 (0, 5.6)**	**2.6 (0, 4.6)**	**3.3 (0.4, 8.6)**	**3.3 (0, 8.3)**	**3.0 (1.1, 3.9)**
Mean arterial blood pressure > 60 mmHg at all measured time points from anesthesia start to aortic cross clamp, *n* (%)	20 (19.4)	9 (25.7)	9 (27.3)	20 (24.1)	19 (25.3)	1 (14.3)
Received vasopressors, *n* (%) [a]	94 (91.3)	32 (91.4)	30 (90.9)	76 (91.6)	67 (89.3)	7 (100)
Phenylephrine infusion, *n* (%)	65 (63.1)	21 (60.0)	22 (66.7)	51 (61.5)	45 (60.0)	4 (57.1)
Epinephrine infusion, *n* (%)	17 (16.5)	1 (2.9)	3 (9.1)	14 (16.9)	12 (16.0)	0 (0)
Vasopressin infusion, *n* (%)	39 (37.9)	18 (51.4)	16 (48.5)	33 (39.8)	34 (45.3)	6 (85.7)
Vasoactive Inotropic Score, median (IQR) [b]	2.7 (0, 6.5)	1.9 (0, 3.8)	1.3 (0, 2.7)	2.5 (0, 5.6)	1.9 (0, 4.8)	1.2 (0, 2.6)
Intraoperative Fluids						
Crystalloid (mL/kg), median (IQR)	8.3 (1.9, 19.7)	11.8 (5.6, 21.5)	13.8 (7.7, 21.9)	9.3 (2.1, 21.5)	9.3 (2.0, 19.9)	11.5 (5.7, 21.5)
Received packed red blood cells, *n* (%)	7 (6.8)	3 (8.6)	2 (6.1)	7 (8.4)	7 (9.3)	1 (14.3)
Received albumin, *n* (%)	21 (20.4)	11 (3.4)	14 (42.2)	19 (22.9)	19 (25.3)	3 (42.9)
Markers of end-organ perfusion						
Urine output, mL/kg/hr, median (IQR) [c]	1.6 (0.5, 4.1)	1.7 (0.8, 2.6)	1.9 (0.8, 2.9)	1.8 (0.6, 4.4)	2.1 (0.9, 5.2)	2.4 (1.2, 7.1)
Lactate value measured, *n* (%)	54 (52.4)	29 (82.9)	29 (87.9)	48 (57.8)	44 (58.7)	7 (100)
Lactate (mmol/L), median (IQR)	1.9 (1.2, 2.9)	1.5 (1.2, 2.7)	1.3 (1.1, 2)	1.6 (1.2, 2.8)	1.6 (1.2, 2.6)	1.2 (0.8, 1.3)

[a] Use of infusion or bolus dose of vasopressor (dopamine, norepinephrine, epinephrine, vasopressin, phenylephrine, milrinone, or dobutamine) any time from anesthesia start to aortic cross clamp
[b] Vasoactive Inotropic Score = dopamine dose (mcg/kg/min) + dobutamine dose (mcg/kg/min) + 100 × epinephrine dose (mcg/kg/min) + 100 × norepinephrine dose (mcg/kg/min) + 10,000 × vasopressin dose (units/kg/min) + 10 × milrinone dose (mcg/kg/min)
[c] Data available from 92 out of 103 donors

TABLE 2. Associations between intraoperative hypotensive burden, measures of end-organ perfusion, and number of organs transplanted per donor

	All Donors (*n*=103)	**Hypotensive Burden Below Cohort Median** (<4.7%, *n*=51)	**Hypotensive Burden Above Cohort Median** (≥4.7%, *n*=52)	***p***
Age (yr), median (IQR)	53.4 (34.9, 64.9)	47.9 (32.7, 57.8)	58.7 (45.7, 67.7)	**0.003**
Received vasopressor(s), *n* (%) [a]	94 (91.3)	45 (88.2)	49 (94.2)	0.28
Vasoactive Inotropic Score, median (IQR) [b]	2.7 (0, 6.5)	1.8 (0, 4.5)	3.8 (0, 10.5)	**0.01**
Total crystalloid (mL/kg), median (IQR)	8.3 (1.9, 19.7)	5.4 (0, 21.7)	6.8 (0, 17.7)	0.33
Received packed red blood cells, *n* (%)	7 (6.8)	3 (5.9)	4 (7.9)	0.71
Received albumin, *n* (%)	21 (20.4)	13 (25.5)	8 (15.4)	0.20
Urine output, mL/kg/hr, median (IQR) [c]	1.6 (0.5, 4.1)	2.3 (0.64, 5.4)	1.3 (0, 2.8)	**0.04**
Lactate value measured, *n* (%)	54 (52.4)	32 (62.8)	22 (42.3)	0.04
Lactate (mmol/L) median (IQR)	1.9 (1.2, 2.9)	1.5 (1.2, 2.6)	2.3 (1.4, 3.5)	0.08
Organs transplanted per donor, median (IQR)	**3 (2, 5)**	**4 (3, 6)**	**2 (1, 3)**	**<0.001**

[a] Use of infusion or bolus dose of vasopressor (dopamine, norepinephrine, epinephrine, vasopressin, phenylephrine, milrinone, or dobutamine) any time from anesthesia start to aortic cross clamp
[b] Vasoactive Inotropic Score = dopamine dose (mcg/kg/min) + dobutamine dose (mcg/kg/min) + 100 × epinephrine dose (mcg/kg/min) + 100 × norepinephrine dose (mcg/kg/min) + 10,000 × vasopressin dose (units/kg/min) + 10 × milrinone dose (mcg/kg/min)
[c] Data available from 92 out of 103 donors

Perioperative Anesthesia 22- Paravertebral Block for Robotic-Assisted Partial Nephrectomy: A Retrospective Review

Aditi Verma[1], Jordan Dutcher[1], Christine Moshe[2], Anna Shapiro[2], Steven Porter[1], David Thiel[2], Ryan Chadha[2]

Mayo Clinic[1] Mayo Clinic Florida[2]

Introduction: Robotic-assisted partial nephrectomies have become an increasingly common method for treating small renal masses[1]. As surgical techniques continue to evolve, new interest in regional nerve blocks has emerged for managing post-operative pain, although their use in these minimally invasive urologic procedures is not well established[2]. The primary aim of this study was to assess the analgesic efficacy of the paravertebral block (PVB) on post-operative pain scores and intra and post-operative opioid consumption in patients undergoing robotic-assisted partial nephrectomies. The secondary aim was to assess the impact on length of post-anesthesia care unit (PACU) and hospital stay.

Methods: This study is an Institutional Review Board approved retrospective analysis of patients who underwent elective robotic-assisted partial nephrectomies by a single surgeon from November 2018 to April 2022. Patients who required conversion to an open procedure or use of patient-controlled analgesia post-operatively were excluded from this study. All 200 patients who met inclusion criteria received general anesthesia and intraoperative opioids at the discretion of the anesthesia provider. 81 of these patients received an adjunctive paravertebral block, while the remaining 119 patients served as our control group. The paravertebral blocks were performed under ultrasound guidance in the thoracic region using 0.5% ropivacaine. Data was collected from the electronic medical record on demographic information, surgical type, intra and post operative opioid use (in IV morphine equivalents), post- operative pain scores (in verbal numerical rating scale), post-anesthesia care unit, and hospital length of stay. Data analysis was performed to obtain means (standard deviations) and frequency counts (%) as appropriate.

Results: A total of 200 patients were included in this study, of which, 81 patients received a paravertebral block, and 119 patients did not. There were no significant differences between the studied groups regarding age, sex, body mass index, American Society of Anesthesiology classification, anesthesia type (volatile vs total intravenous), and estimated blood loss (Table 1). There was also no significant difference between the two groups in post-operative pain scores (Table 2), IV morphine equivalents doses of opioid consumption (Table 3), or length of stay (Table 4).

Conclusions: The addition of a paravertebral block did not significantly improve post-operative pain scores, reduce IV morphine equivalent doses of intra or post-operative opioids, or decrease length of PACU or hospital stay. Therefore, paravertebral blocks are not recommended for optimization of post- operative pain following a robotic-assisted nephrectomy, as they are associated with increased risk and maintain comparable results.

References:

1. Ghani, Khurshid R et al. “Practice patterns and outcomes of open and minimally invasive partial nephrectomy since the introduction of robotic partial nephrectomy: results from the nationwide inpatient sample.” The Journal of urology vol. 191,4 (2014): 907-12.
2. Baik, Ji Seok et al. “Thoracic paravertebral block for nephrectomy: a randomized, controlled, observer-blinded study.” Pain medicine (Malden, Mass.) vol. 15,5 (2014): 850-6.

Table 1: Demographic Properties

	PVB group (n=81)	Control Group (n=119)
Age (years)	58.09 (11.9)	59.44 (12.1)
Sex (% male)	65.43	65.55
Sex (% female)	34.57	34.45
BMI	31.31 (5.7)	29.19 (5.4)
ASA score	2.63 (0.5)	2.68 (0.6)
Anesthesia type: volatile (%)	93.83	91.60
Anesthesia type: TIVA (%)	6.17	8.40
Estimated Blood Loss (mL)	243.27 (252.67)	177.65 (216.69)

The results are expressed as means (standard deviations) where appropriate.

Table 2: Outcome parameters comparing the PACU and Floor pain scores on a 10-point scale

	PVB group (n=81)	Control Group (n=119)
PACU initial pain score	3.46 (3.7)	3.64 (3.9)
PACU minimum pain score	2.82 (3.1)	2.32 (3.1)
PACU maximum pain score	5.68 (3.4)	6.42 (3.0)
PACU average pain score	4.35 (3.0)	4.69 (2.7)
Floor minimum pain	1.02 (1.6)	1.31 (1.8)
Floor maximum pain	8.44 (1.3)	7.59 (1.9)
Floor average pain score	4.92 (1.4)	4.60 (1.5)

The results are expressed as means (standard deviations) where appropriate.

Table 3: Outcome parameters comparing the total IV morphine equivalent consumption

	PVB group (n=81)	Control Group (n=119)
Intraop total morphine equivalent dose (mg)	32.38 (8.9)	31.21 (9.8)
PACU total morphine equivalent dose (mg)	4.32 (5.2)	6.40 (6.5)
Floor morphine equivalent dose (mg)	38.48 (24.69)	31.34 (26.5)

The results are expressed as means (standard deviations) where appropriate.

Table 4: Outcome parameters comparing the PACU and hospital length of stay

	PVB group (n=81)	Control Group (n=119)
PACU length of stay (min)	53.53 (39.7)	71.03 (34.9)
Hospital length of stay (days)	1.95 (1.7)	1.92 (1.0)

The results are expressed as means (standard deviations) where appropriate.

Perioperative Anesthesia 23- Patient Race and Census-Tract Level Disadvantage Predict Adherence to Antiemetic Prophylaxis

Cameron Jacobson[1], Nathan Pace[2], Jiuying Han[1], Neng Wan[2], Michael Andreae[3], John Pearson[4]

University of Utah[1] Univ of Utah - SOM[2] University of Utah - Department of Anesthesiology[3] University of Utah School of Medicine[4]

Introduction: Social determinants of health (SDOH) vary by domain (i.e., identity, wealth, education, etc.) at different social levels (i.e., patient, family, neighborhood, state, etc.). SDOH contribute significantly to health care disparities[1,2]. Previous work has shown that SDOH influence perioperative risk-adjusted administration of antiemetic prophylaxis (RAAP)[3]. We extended this work with a retrospective analysis of RAAP in our institution's patients found within the Multicenter Perioperative Outcomes Group (MPOG.org) EHR registry. MPOG data currently lacks SDOH. We enriched the registry data with census-tract level SDOH by linking patient addresses to "Neighborhood Disadvantage" (ND), a neighborhood deprivation index in the National Neighborhood Data Archive (NaNDA)[4]. Our null hypothesis was that patient Race and census-tract level ND influenced antiemetic prophylaxis, after adjusting for postoperative nausea and vomiting (PONV) risk in a Bayesian hierarchical multivariable regression model, modelling individual anesthesiologists' RAAP administration.

Methods: We extracted the MPOG PONV-05 quality improvement metric[5] in a 2021 cohort of anesthesia cases that included a composite, ordinal PONV risk score, the number of interventions (antiemetic classes, choice of anesthesia TIVA vs. volatile, etc.), anonymized individual provider ID, and Race (White, NonWhite, and Unknown). The PONV composite risk score included all accepted risk factors for PONV, namely patient sex, history of PONV, smoking status, opioid use for postoperative pain, duration of inhalational anesthesia, age < 50, and selected procedure types.
After appropriate IRB review and approval, we obtained patient home addresses on the date of surgery from our institution's data warehouse. We geocoded addresses to latitude and longitude coordinates and matched them to census tracts using ArcGIS (ESRI, Inc.); we extracted the census-tract level ND (a weighted composite of income, education, ethnicity, etc.) from the 2008–2017 NaNDA data set[4]. ND is a continuous [0, 1] variable; increasing values reflect higher levels of disadvantage.
We estimated a Bayesian hierarchical multivariable ordinal regression model with the number of RAAP interventions regressed on the fixed effects Race, census-tract level ND, and PONV risk score plus the crossed random effects of census tract and anonymized responsible anesthesiologist. An informative student t distribution was used as the prior with estimation and evaluation in the R *brms*[6–8] and *bayestestR*[9] packages. This posterior distribution allowed direct probability statements and plots using conditional expectation.

Results: After exclusions, the analyzed cohort contained 21,879 cases (White 17,359, NonWhite 2,093, Unknown 2,477). Most patients had a 3–5 risk score (84%, 18,369/21,879). About 3/4th of patients (77%, 16,948/21,879) received two or three antiemetic interventions. Stable regression models were obtained. All fixed effects had Bayesian (Maximum A Posteriori) p-values less than 0.005. Patients of White Race received more interventions; there was a linear increase of interventions for higher PONV risk score. As NaNDA "Neighborhood Disadvantage" increased, the probability of receiving two or three interventions decreased and the probability of receiving zero or one intervention increased; this was consistent across all three Race levels. Figure 1 illustrates the effect of ND (x-axis) on RAAP. If ND had no association with RAAP, then the probability (y-axis) to receive interventions (level 0–5+ color bands) should be flat, neither increasing nor decreasing with changes in ND. Instead, the probability of receiving more interventions (e.g., green 2 or blue 3) decreased with increasing neighborhood deprivation (ND). Additionally, White Race patients had a higher probability of receiving more interventions than NonWhite.

Conclusions: Our retrospective analysis of our institution's MPOG electronic health records linked to a NaNDA deprivation index demonstrate perioperative process disparity, in that patient Race and a census-tract level neighborhood deprivation index predict risk adjusted antiemetic prophylaxis. This analysis demonstrates the need for institutions, regulators, and healthcare quality associations to analyze these factors in their assessment of provider and institutional performance.

References:

1. Journal of Health and Social Behavior [Internet]. 1995;80-94
2. Public Health Rep. 2003;118(4):287-92
3. Anesthesia and Analgesia. 2018 Feb;126:588-599
4. National neighborhood data archive (NaNDA): Socioeconomic status and demographic characteristics of census tracts, unites states, 2008-2017 [Internet]
5. PONV-05 ASPIRE measure specification. 2022
6. Journal of Statistical Software. 2017;80(1):1-28
7. The R Journal. 2018;10(1):395-411
8. Journal of Statistical Software. 2021;100(5):1-54
9. Journal of Open Source Software. 2019;4(40):1451

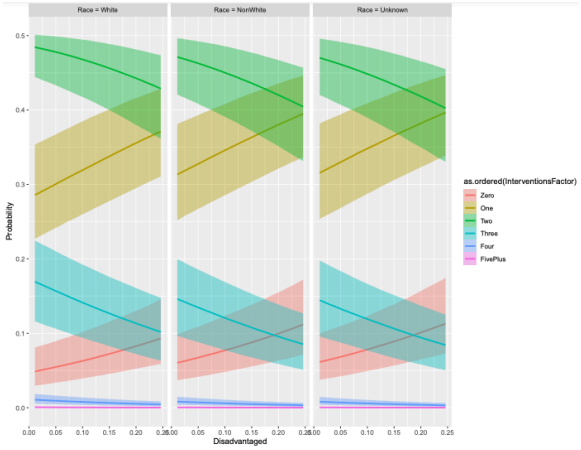
Race = White
Race = NonWhite
Race = Unknown
Probability
Disadvantaged
as.ordered(InterventionsFactor)
Zero
One
Two
Three
Four
FivePlus

Perioperative Anesthesia 24- Perioperative Risk Factors Associated with Unplanned Escalation of Care after Post-Anesthesia Care Unit Discharge

Andrew Barker[1], Brant Wagener[1], Ryan Melvin[1], Ryan Godwin[2]

University of Alabama at Birmingham[1] The University of Alabama at Birmingham[2]

Introduction: Following Post-Anesthesia Care Unit (PACU) discharge, a number of patients require unexpected escalations in clinical care leading to transfer to intermediate care or the intensive care unit (ICU) setting. This study seeks to determine modifiable risk factors before PACU admission and apply Artificial Intelligence/Machine Learning to predict patients that require escalations in clinical care to provide more effective patient care in the perioperative period.

Methods: We collected data from all non-cardiac surgical patients discharged from the PACU between 2016 and 2019. Escalation of care was defined as patient transfer from the inpatient floor to either an intermediate care unit or ICU within 3 midnights of PACU discharge. A Credit scorecard modeling system was then applied as a set pre- and post-processing step layered on top of logistic regression. Continuous variables were binned into discrete categories and extant categorical variables were grouped using weight-of-evidence (WoE) binning. Post-regression, WoE values were translated from model coefficients to scorecard points. Elastic-net regularized logistic regression served as both a variable selection method and hedge for colinear variables. The final scorecard model range of values was enforced upon the model by solving a mixed-integer programming problem.

Results: The following variables indicate a significant odds ratio: gender, age, BMI, Race, oxygen saturation, supplemental oxygen, HR, SBP, MAP, RR, pain score, Aldrete score, CKD, AKI, low albumin, crystalloid volume administered, HCO3, Hgb, platelets, temperature, emergency procedure, surgical duration, presence of arterial line, and transfused blood products. Many of the top risk factors were simply the missingness of charted vital sign data within the last hour before discharge, suggesting immediately modifiable behavior that may improve patient outcomes. When applying the credit scorecard model to the clinical model, the best candidate model's predictive ability places it in the acceptable range (AUC of 0.75) on holdout data. In holdout data, there was a statistically significant ($p<0.01$) relationship between the model's suggested score bins and the fraction of actual escalations that occurred for patients falling within those bins.

Conclusions: Several risk factors were identified as being associated with escalation in care after PACU discharge. The ability to understand the modifiable risk factors that lead to increased patient risk of an escalation of care with 3 midnights of PACU discharge may lead to improved perioperative optimization and bed utilization. This would translate to improved patient outcomes and more efficient bed flow.

References: Zou, H., and Hastie, T. (2005). Regularization and Variable Selection via the Elastic Net. J. R. Stat. Soc B 67 (2), 301–320.

Helling TS, Martin LC, Martin M, Mitchell ME. (2014) Failure events in transition of care for surgical patients. J Am Coll Surg. Apr;218(4):723-31.

Street M, Phillips NM, Mohebbi M, Kent B. (2017) Effect of a newly designed observation, response, and discharge chart in the Post Anaesthesia Care Unit on patient outcomes: a quasi-experimental study in Australia. BMJ Open. Dec 3;7(12):e015149.

Gender	Aldrete Score
Age	CKD
BMI	AKI
Race	Albumin
Oxygen Saturation	Crystalloid Volume Administered
Supplemental Oxygen	Bicarbonate
Heart Rate	Hemoglobin
Systolic Blood Pressure	Platelets
Mean Arterial Pressure	Temperature
Respiratory Rate	Emergency procedure Status
Pain Score	Surgical Duration
Presence of Arterial Line	Transfusion of Blood Products

Table 1. Variables with a significant odds ratio indicating increased risk within the predictive model.

Perioperative Anesthesia 25- Previous COVID-19 and postoperative respiratory complications in surgical Patients: a hospital registry study

May Hashish[1], Ricardo Munoz-Acuna[1], Simone Redaelli[1], Aiman Suleiman[1], Dario von Wedel[1], Sarah Ashrafian[2], Valerie Banner-Goodspeed[2], Elias Baedorf Kassis[1], Maximilian Schaefer[3]

Beth Israel Deaconess Medical Center, Harvard Medical School[1] Beth Israel Deaconess Medical Center[2] Beth Israel Deaconess Medical Center & Hospital[3]

Introduction: There are equivocal data with regards to the clinical relevance of a previous infection with COVID-19 in patients undergoing surgery and general anesthesia. Reports from initial COVID-19 surges documented that COVID-19 infections increased the risk of postoperative respiratory complications (PRC) [1-3]. Other studies did not find increased risk of PRC in patients whose surgery was shortly delayed for a positive COVID-19 test [4,5]. In addition, there are concerns about chronic pulmonary changes that might be associated with impaired recovery and higher risk of prolonged hospitalization, especially after early COVID-19 infections [6]. In this study, we investigated whether a previous COVID-19 infection is associated with increased risk of postoperative respiratory complications, and whether this differed by the associated variant and time since infection.

Methods: In this hospital registry study, we included adult surgical patients from January 1st, 2020 to March 31st, 2022 who underwent surgical procedures with general anesthesia at a tertiary healthcare center in Massachusetts. We excluded patients with American Society of Anesthesiologists physical status (ASA) class > IV, cardiac surgeries and patients kept intubated after surgery. The primary exposure was any previous COVID-19 infection, defined by a positive COVID-19 polymerase chain reaction (PCR) tests within or outside the institution, or presence of International Classification of Diseases (10th Revision, Clinical Modification [ICD-9/10-CM]) diagnostic codes. The primary composite outcome was postoperative respiratory complications (PRC), defined as peripheral pulse oximetry <90% within 10 minutes after extubation, postoperative reintubation or emergent non-invasive ventilation within seven days after surgery. Multivariable logistic regression adjusted for a priori defined confounder model that included patient demographics, comorbidities, as well as intraoperative and surgical factors was applied. In secondary analyses, we tested the association between any history of COVID-19 and PRC, based on variants associated with the date of positive testing (Alpha1, Alpha2, Delta and Omicron).

Results: We included 28,828 patients in our final cohort (Figure 1). 1,472 (5.11%) patients suffered PRC and 2,254 (7.8%) patients had a previous COVID-19 infection. Table 1 summarizes patient characteristics and variables distribution according to the presence of a previous COVID-19 infection.

In the primary analysis, there was no association between a previous COVID-19 infection and PRC (adjusted odds ratio (ORadj) 0.92; 95%CI 0.70-1.21; p=0.56). Further, there was no association between the length of the time between the day of COVID-19 positive test and date of surgery with PRC (ORadj 0.999; 95%CI 0.997-1.00; p=0.63). We further did not find any association between individual associated variants and PRC (Table 2). Effect modification analysis showed that the primary association was further not modified by high risk surgical procedures (general surgery, thoracic surgery, transplant or neurosurgery, p-for-interaction=0.95).

Conclusions: A previous COVID-19 infection is not a risk factor of PRC in surgical patients, irrespective of the time interval between diagnosis and date of surgery, or the associated variant.

References:

1. J Clin Anesth. 2021 Nov;74:110409
2. Surgery. 2021 Feb;169(2):264-274
3. Ann Surg. 2022 Feb 1;275(2):247-251
4. Br J Anaesth. 2022 May;128(5):e311-e314
5. J Surg Oncol. 2021 Mar;123(4):823-833
6. Thorax. 2021 Apr;76(4):402-404

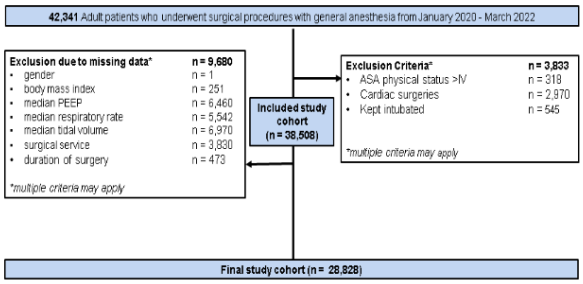

Figure 1. Study flow diagram.

ASA: American Society of Anesthesiologists; PEEP: Positive end-expiratory pressure.

Table 1. Patients' characteristics and distribution of variables per history of COVID-19 with standardized differences.

	No previous COVID-19 infection	Previous COVID-19 infection	Standardized Difference
	(N= 26,574)	(N= 2,254)	
Age, years	56.6 ± 17.0	54.7 ± 16.6	0.11
Sex			-0.08
Female	12,450 (46.9%)	971 (43.1%)	
Male	14,124 (53.1%)	1,283 (56.9%)	
BMI, kg/m2	28.9 ± 8.0	30.2 ± 9.1	-0.08
ASA physical status			-0.26
1	1,800 (6.8%)	77 (3.4%)	
2	11,897 (44.8%)	829 (36.8%)	
3	11,241 (42.3%)	1,113 (49.4%)	
4	1,636 (6.2%)	235 (10.4%)	
smoking	8,915 (33.5%)	784 (34.8%)	-0.025
Obstructive pulmonary disease	6,527 (24.6%)	713 (31.6%)	-0.09
OSA	4,468 (16.8%)	461 (20.5%)	-0.16
Charlson Comorbidity Index	2.0 (0.0 - 4.0)	3.0 (1.0 - 7.0)	-0.31
Congestive Heart Failure	2,939 (11.1%)	367 (16.3%)	-0.15
Non-depolarizing NMBA, (ED95)	2.3 (0.0 - 3.8)	2.2 (0.0 - 4.0)	0.01
Succinylcholine dose, (mg)	0.0 (0.0 - 80.0)	0.0 (0.0 - 0.0)	0.03
Neostigmine dose, (mg/kg)	0.0 (0.0 - 0.0)	0.0 (0.0 - 0.0)	0.02
Sugammadex dose, (mg)	200.0 (0.0 - 200.0)	200.0 (0.0 - 200.0)	-0.03
Vasopressor dose, (mg norepinephrine equivalents)	0.0 (0.0 - 0.1)	0.0 (0.0 - 0.1)	0.02
opioids dose, (mg OME	36.9 (25.0 - 59.0)	38.6 (25.0 - 61.1)	0.03
Crystalloid and colloid infusion (ml)	900.0 (600.0 - 1250.0)	800.0 (600.0 - 1200.0)	0.06
Units of packed red blood cells	0.0 (0.0 - 0.0)	0.0 (0.0 - 0.0)	0.00
PEEP (cmH2O)	5.0 (5.0 - 5.1)	5.0 (5.0 - 5.0)	-0.01
Respiratory Rate (breaths per min)	12.0 (11.0 - 14.0)	12.0 (11.0 - 14.5)	-0.01
Tidal Volume (mL)	466.0 (409.0 - 515.0)	461.3 (404.0 - 510.0)	0.08
Type of surgery			0.05
Colorectal	1,139 (4.3%)	78 (3.5%)	
Dentoral	190 (0.7%)	8 (0.4%)	
ENT	1,486 (5.6%)	187 (8.3%)	
Eye	101 (0.4%)	10 (0.4%)	
General surgery	3,317 (12.5%)	224 (9.9%)	
Gastrointestinal	562 (2.1%)	62 (2.8%)	
Gynecological	3,160 (11.9%)	366 (16.2%)	
Neurosurgery	1,655 (6.2%)	176 (7.8%)	
Orthopedic	5,460 (20.5%)	351 (15.6%)	
Plastic	2,072 (7.8%)	154 (6.8%)	
Podiatry	101 (0.4%)	8 (0.4%)	
Surgical oncology	1,020 (3.8%)	80 (3.5%)	
Thoracic	1,809 (6.8%)	202 (9.0%)	
Transplant	520 (2.0%)	89 (3.9%)	
Urology	2,697 (10.1%)	195 (8.7%)	
Vascular	1,284 (4.8%)	64 (2.8%)	
Other	1 (0.0%)	0 (0.0%)	
Emergency procedures	2,707 (10.2%)	224 (9.9%)	-0.00
Duration of surgery, median (IQR) (min)	137.0 (89.0 - 214.0)	132.0 (82.0 - 210.0)	0.00
Quarter of year			-0.29
Jan to March 2020	3,367 (12.7%)	5 (0.2%)	
April to June 2020	1,482 (5.6%)	205 (9.1%)	
July to Sep 2020	3,154 (11.9%)	198 (8.8%)	
Oct to Dec 2020	3,069 (11.5%)	277 (12.3%)	
Jan to March 2021	2,746 (10.3%)	304 (13.5%)	
April to June 2021	3,518 (13.2%)	367 (16.3%)	
July to Sep 2021	3,282 (12.4%)	249 (11.0%)	
Oct to Dec 2021	3,188 (12.0%)	258 (11.4%)	
Jan to March 2022	2,768 (10.4%)	391 (17.3%)	

Data are expressed as frequency (prevalence in %), or median (interquartile range [25th-75th percentile]) or mean and standard deviation.
ASA: American Society of Anaesthesiologists; OSA: Obstructive sleep apnea; NMBA: neuromuscular blocking agents; ED95: Median effective dose required to achieve a 95% reduction in maximal twitch response from baseline; PEEP: positive end-expiratory pressure.

Table 2. Association between history of COVID-19 per associated variant of the pandemic (Alpha$_1$, Alpha$_2$, Delta and Omicron) and postoperative respiratory complications.

Outcome	COVID-19	Surges dates	Adjusted analysis	
			*OR (95%CI)**	*P-value*
	No history of COVID-19 (n=26,574)	*Ref*	*Ref*	*Ref*
Postoperative respiratory complications	Alpha$_1$ (n=907)	(*1/18/2020-8/31/2020*)	1.07 (0.73-1.59)	0.74
	Alpha$_2$ (n=772)	(*9/1/2020-2/28/2021*)	0.92 (0.58-1.46)	0.73
	Delta (n=353)	(*3/1/2021-11/30/2021*)	0.91 (0.46-1.80)	0.79
	Omicron (n=222)	(*12/1/2021-3/31/2022*)	0.43 (0.15-1.23)	0.12

** OR, Odds ratio, CI, confidence interval*

Perioperative Anesthesia 26- Rectus femoris muscle cross-sectional area measured by ultrasound is associated with postoperative recovery metrics following deceased-donor kidney transplantation

Nicholas Mendez[1], Michael Bokoch[1], Dieter Adelmann[1], Elaine Ku[1], Kerstin Kolodzie[2]

University of California, San Francisco[1] UCSF Medical Center at Mt Zion[2]

Introduction: Low skeletal muscle mass is known to occur in patients with kidney failure as chronic kidney disease and dialysis accelerate muscle wasting.[1] Previous studies have demonstrated that low skeletal muscle mass is associated with increased postoperative morbidity and mortality across various surgical populations.[2, 3]However, this association remains poorly characterized in patients with kidney failure undergoing kidney transplantation.[1] Measurement of the rectus femoris cross-sectional area (CSA) by ultrasound has recently been described as a simple, low cost, noninvasive point-of-care technique for quantifying muscle mass at bedside.[3] Herein we aim to evaluate the ability of the ultrasound-measured rectus femoris CSA as a measure of muscle mass to predict short-term outcomes specifically in patients undergoing kidney transplantation.

Methods: After obtaining written informed consent, eligible patients admitted for a deceased-donor kidney transplant at our center were enrolled in this prospective cohort study between 2019-2020. The CSA of the rectus femoris muscle was set as the primary predictor and measured by a skilled ultrasonographer before transplant. Measurements were taken using a wide linear-array transducer with patients in the Semi-Fowler's position and legs in passive extension. Primary outcome was days alive and at home (DAH) within 30 days of transplant, with the category of 27 or more DAH representing the expected course based on a 3-day anticipated hospital length of stay without readmission.[4] Any in-hospital surgical complications, assessed according to the Clavien-Dindo classification, were recorded and evaluated as a secondary outcome measure.[5] Wilcoxon rank-sum test was used to assess the association between the rectus femoris CSA and the examined short-term outcome variables using Stata version 17 (Stata Corp., USA).

Results: Of the 38 patients enrolled, two ultimately did not undergo transplantation. The median CSA measurements of the 36 analyzed patients was 4.82cm^2 [interquartile range 4.18-6.05]. Twenty-three (63.9%) patients experienced fewer than the expected 27 DAH. A lower rectus femoris CSA was significantly associated with the number of DAH after surgery (p=0.046), Figure 1. Rectus femoris CSA was also significantly associated with the occurrence of postoperative surgical complications, with 13 (36.1%) patients experiencing at least one complication according to the Clavien-Dindo classification (p=0.024), Figure 2.

Conclusions: In our cohort, the rectus femoris CSA measured by point of care ultrasound is associated with short-term outcomes following kidney transplantation, including DAH within 30 days of surgery and the occurrence of at least one surgical complication. Further research should investigate whether interventions such as presurgical physical prehabilitation or nutritional optimization can increase muscle mass as tracked by ultrasound and lead to improved post-transplant outcomes.

References:

1. Sarcopenia in chronic kidney disease: what have we learned so far? J Nephrol, 2021. **34**(4): 1347-72.
2. Preoperative Point-of-Care Ultrasound to Identify Frailty and Predict Postoperative Outcomes: A Diagnostic Accuracy Study. Anesthesiology, 2022. **136**(2): 268-78.
3. Can Sarcopenia Quantified by Ultrasound of the Rectus Femoris Muscle Predict Adverse Outcome of Surgical Intensive Care Unit Patients as well as Frailty? A Prospective, Observational Cohort Study.Ann Surg, 2016. **264**(6): 1116-24.
4. Days at Home after Surgery: An Integrated and Efficient Outcome Measure for Clinical Trials and Quality Assurance. EClinicalMedicine, 2019. **11**: 18-26.
5. The Clavien-Dindo classification of surgical complications: five-year experience. Ann Surg, 2009. **250**(2): 187-96.

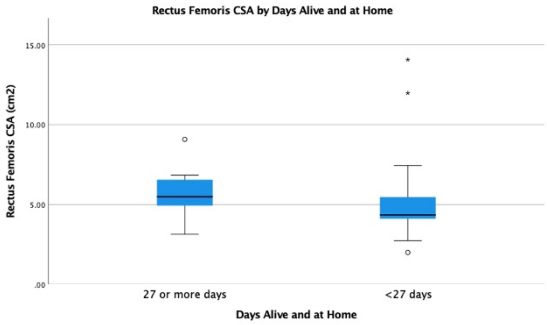

Figure 1: Association between DAH within 30 days of transplant and the rectus femoris CSA as measured by ultrasound (p=0.046). Error bars represent 95% confidence intervals, circles represent mild outliers (25th percentile – 1.5*IQ or 75th percentile + 1.5*IQ), and asterisks represent extreme outliers (25th percentile – 3*IQ or 75th percentile + 3*IQ).

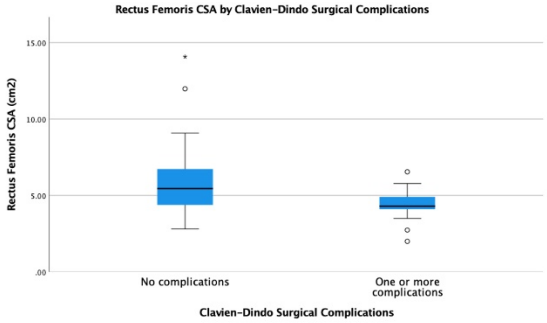

Figure 2: Association between the occurrence of any surgical complications after transplant by the Clavien-Dindo classification and the rectus femoris CSA as measured by ultrasound (p=0.024). Error bars represent 95% confidence intervals, circles represent mild outliers (25^{th} percentile – 1.5*IQ or 75^{th} percentile + 1.5*IQ), and asterisks represent extreme outliers (25^{th} percentile – 3*IQ or 75^{th} percentile + 3*IQ).

Perioperative Anesthesia 27- Validation and comparison of comorbidity indices using administrative data of patients undergoing surgery or interventional procedures

Denys Shay[1], Elena Ahrens[1], Dario von Wedel[2], Ricardo Munoz[3], Guanqing Chen[3], Maximilian Schaefer[4]

Beth Israel Deaconess Medical Center[1] Beth Israel Deaconess Medical Center, Harvard Medical School[2] BIDMC[3] Beth Israel Deaconess Medical Center & Hospital[4]

Introduction: Comorbidity-based prediction tools have been proposed to facilitate patient-level assessment of mortality risk following hospitalization [1,2]. These tools have further become essential for confounder adjustment in epidemiological studies. We aimed to compare established comorbidity indices when using administrative data in a surgical patient population.

Methods: Hospitalized patients aged ≥18 years who underwent surgical or interventional procedures between 2005 and 2020 at a tertiary healthcare center in Massachusetts, USA, were included. The Charlson Comorbidity Index [1], the Elixhauser Comorbidity Index [2], and the Combined Comorbidity Score [3] were compared with regards to prediction of the primary outcome, 30-day mortality. Discriminative ability was quantified by the area under the receiver operating characteristic curve (AUROC), and calibration was assessed using Brier scores and reliability plots. In secondary analyses, we compared the score performances in predicting in-hospital, 7-day, 90-day, 180-day, and 365-day mortality.

Results: 514,282 patients were included, of which 5,849 (1.1%) died within 30 days [Table 1]. The Elixhauser Comorbidity Index showed the best discriminative ability with an AUROC of 0.85 (95% confidence interval [CI] 0.85–0.85) and was superior in predicting 30-day mortality compared to the Combined Comorbidity Score (AUROC, 0.82 [95% CI 0.82–0.83]) and the Charlson Comorbidity Index (AUROC, 0.80 [95% CI 0.79–0.80]) (p<0.001, respectively) [Figure 1]. Similarly, the Elixhauser Comorbidity Index was superior in predicting in-hospital, 7-day, 90-day, 180-day, and 365-day mortality (p<0.001, respectively). Our primary findings were confirmed in subgroups, including analyses in 166,974 patients aged ≥65 years (AUROC, 0.78 [95% CI 0.77–0.79] for the Elixhauser Comorbidity Index, compared to the Combined Comorbidity Score, AUROC, 0.75 [95% CI 0.75–0.75] and the Charlson Comorbidity Index, AUROC, 0.71 [95% CI 0.70–0.72]) and in 219,806 patients with an ASA physical status classification ≥3 (Elixhauser Comorbidity Index, AUROC, 0.75 [95% CI 0.74–0.75], compared to the Combined Comorbidity Score, AUROC, 0.71 [95% CI 0.71–0.72] and the Charlson Comorbidity Index, AUROC, 0.67 [95% CI 0.67–0.68]), p<0.001, respectively. The Elixhauser Comorbidity index was further superior in subgroups by admission status (ambulatory, same-day admission, and inpatient), surgical complexity (based on tertiles of work relative value units), and in high-complexity cases, including cardiothoracic and abdominal surgery.

Conclusions: While all comorbidity indices predicted 30-day mortality with good discrimination, the Elixhauser Comorbidity Index showed the best performance and may therefore be used preferentially in epidemiologic studies using hospital registry data in surgical populations.

References: [1] A new method of classifying prognostic comorbidity in longitudinal studies: development and validation. J Chronic Dis;40(5):373-83. 1987

[2] Comorbidity measures for use with administrative data. Med Care;36(1):8-27. 1998

[3] A combined comorbidity score predicted mortality in elderly patients better than existing scores. J Clin Epidemiol;64(7):749-59. 2011

Figure 1. Comparison of areas under the receiver operating characteristic curve.

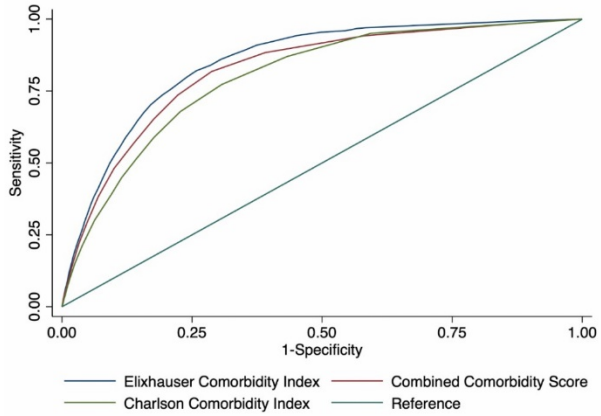

Table 1. Patient characteristics and distribution of variables by 30-day mortality.

	No 30-day mortality	30-day mortality	Standardized difference
	n=508,433	n=5,849	
Patient characteristics			
Age, years	55.1 ± 17.2	68.5 ± 14.8	-0.838
Sex, female (n=514,265)	294,980 (58.0%)	2,548 (43.6%)	0.292
Body mass index, kg/m^2 (n=502,397)	28.4 ± 6.8	27.6 ± 7.4	0.112
ASA physical status classification (n=514,102)	2 (2-3)	4 (3-4)	-1.747
Surgical service (n=393,011)			-0.273
Cardiac	11,777 (3.0%)	384 (9.2%)	
Colorectal	8,955 (2.3%)	53 (1.3%)	
Cardiology	2,363 (0.6%)	51 (1.2%)	
Dental, oral	1,170 (0.3%)	12 (0.3%)	
Ear, nose, throat	10,546 (2.7%)	36 (0.9%)	
Eye	20,182 (5.2%)	27 (0.6%)	
General surgery	49,535 (12.7%)	436 (10.4%)	
Gastrointestinal	13,843 (3.6%)	106 (2.5%)	
Gynecology	58,247 (15.0%)	212 (5.1%)	
Neurosurgery	14,622 (3.8%)	423 (10.1%)	
Orthopedic	82,348 (21.2%)	451 (10.8%)	
Plastic	22,840 (5.9%)	32 (0.8%)	
Podiatry	9,432 (2.4%)	34 (0.8%)	
Surgical oncology	11,728 (3.0%)	31 (0.7%)	
Thoracic	17,722 (4.6%)	613 (14.7%)	
Transplant	9,138 (2.4%)	281 (6.7%)	
Trauma, critical care	8,746 (2.2%)	545 (13.0%)	
Urology	23,065 (5.9%)	67 (1.6%)	
Vascular	12,573 (3.2%)	385 (9.2%)	
Charlson Comorbidity Index			
Myocardial infarction	23,805 (4.7%)	1,160 (19.8%)	-0.475
Congestive heart failure	51,721 (10.2%)	2,255 (38.6%)	-0.701
Peripheral vascular disease	54,602 (10.7%)	1,832 (31.3%)	-0.522
Cerebrovascular disease	40,555 (8.0%)	1,400 (23.9%)	-0.447
Dementia	6,787 (1.3%)	298 (5.1%)	-0.214
Chronic pulmonary disease	103,102 (20.3%)	1,800 (30.8%)	-0.243
Rheumatic disease	17,176 (3.4%)	320 (5.5%)	-0.102
Peptic ulcer disease	20,321 (4.0%)	610 (10.4%)	-0.251
Mild liver disease	70,436 (13.9%)	1,597 (27.3%)	-0.338
Diabetes without chronic complication	108,737 (21.4%)	2,139 (36.6%)	-0.340
Diabetes with chronic complication	45,396 (8.9%)	1,030 (17.6%)	-0.258
Hemiplegia or paraplegia	7,902 (1.6%)	390 (6.7%)	-0.260
Renal disease	50,293 (9.9%)	1,848 (31.6%)	-0.556
Any malignancy	104,585 (20.6%)	2,427 (41.5%)	-0.464
Moderate or severe liver disease	14,181 (2.8%)	798 (13.6%)	-0.403
Metastatic solid tumor	30,174 (5.9%)	1,432 (24.5%)	-0.535
AIDS/HIV	1,839 (0.4%)	25 (0.4%)	-0.011
Elixhauser Comorbidity Index			
Congestive heart failure	51,721 (10.2%)	2,255 (38.6%)	-0.701
Cardiac arrhythmias	107,423 (21.1%)	3,340 (57.1%)	-0.793
Valvular disease	90,728 (17.8%)	1,998 (34.2%)	-0.379
Pulmonary circulation disorders	26,433 (5.2%)	1,227 (21.0%)	-0.481
Peripheral vascular disorders	52,909 (10.4%)	1,827 (31.2%)	-0.531
Hypertension, uncomplicated	232,060 (45.6%)	3,845 (65.7%)	-0.413

Table 1. Patient characteristics and distribution of variables by 30-day mortality (continued).

	No 30-day mortality	30-day mortality	Standardized difference
	n=508,433	n=5,849	
Hypertension, complicated	59,147 (11.6%)	1,915 (32.7%)	-0.525
Paralysis	7,902 (1.6%)	390 (6.7%)	-0.260
Neurodegenerative disorders	41,360 (8.1%)	1,404 (24.0%)	-0.443
Chronic pulmonary disease	103,102 (20.3%)	1,800 (30.8%)	-0.243
Diabetes, uncomplicated	104,555 (20.6%)	1,994 (34.1%)	-0.307
Diabetes, complicated	53,015 (10.4%)	1,210 (20.7%)	-0.286
Hypothyroidism	82,293 (16.2%)	1,170 (20.0%)	-0.099
Renal failure	49,964 (9.8%)	1,837 (31.4%)	-0.553
Liver disease	72,049 (14.2%)	1,889 (32.3%)	-0.439
Peptic ulcer disease, no bleeding	16,632 (3.3%)	391 (6.7%)	-0.157
AIDS/HIV	1,839 (0.4%)	25 (0.4%)	-0.011
Lymphoma	13,008 (2.6%)	306 (5.2%)	-0.139
Metastatic cancer	30,174 (5.9%)	1,432 (24.5%)	-0.535
Solid tumor without metastasis	95,040 (18.7%)	2,195 (37.5%)	-0.429
Rheumatoid arthritis/collagen vascular diseases	28,498 (5.6%)	473 (8.1%)	-0.098
Coagulopathy	43,100 (8.5%)	2,522 (43.1%)	-0.862
Obesity	94,113 (18.5%)	1,049 (17.9%)	0.015
Weight loss	57,104 (11.2%)	1,717 (29.4%)	-0.463
Fluid and electrolyte disorders	134,502 (26.5%)	4,469 (76.4%)	-1.154
Blood loss anemia	15,816 (3.1%)	376 (6.4%)	-0.156
Deficiency anemia	59,615 (11.7%)	949 (16.2%)	-0.130
Alcohol abuse	30,474 (6.0%)	833 (14.2%)	-0.276
Drug abuse	23,516 (4.6%)	386 (6.6%)	-0.086
Psychosis	13,753 (2.7%)	153 (2.6%)	0.006
Depression	120,790 (23.8%)	1,598 (27.3%)	-0.082
Combined Comorbidity Score			
Alcohol abuse	27,984 (5.5%)	761 (13.0%)	-0.261
Any tumor	100,178 (19.7%)	2,344 (40.1%)	-0.456
Cardiac arrhythmias	98,654 (19.4%)	3,069 (52.5%)	-0.734
Chronic pulmonary disease	102,611 (20.2%)	1,788 (30.6%)	-0.240
Coagulopathy	43,100 (8.5%)	2,522 (43.1%)	-0.862
Complicated diabetes	51,393 (10.1%)	1,172 (20.0%)	-0.280
Congestive heart failure	56,041 (11.0%)	2,273 (38.9%)	-0.680
Deficiency anemia	109,744 (21.6%)	2,029 (34.7%)	-0.295
Dementia	4,990 (1.0%)	207 (3.5%)	-0.173
Fluid and electrolyte disorders	134,199 (26.4%)	4,448 (76.0%)	-1.145
Hemiplegia	7,443 (1.5%)	379 (6.5%)	-0.259
HIV/AIDS	1,801 (0.4%)	23 (0.4%)	-0.006
Hypertension	238,812 (47.0%)	4,192 (71.7%)	-0.520
Liver disease	51,774 (10.2%)	1,490 (25.5%)	-0.408
Metastatic cancer	30,174 (5.9%)	1,432 (24.5%)	-0.535
Peripheral vascular disease	50,673 (10.0%)	1,741 (29.8%)	-0.512
Psychosis	37,574 (7.4%)	291 (5.0%)	0.100
Pulmonary circulation disorders	21,609 (4.3%)	1,046 (17.9%)	-0.445
Renal failure	49,867 (9.8%)	1,839 (31.4%)	-0.555
Weight loss	28,692 (5.6%)	1,286 (22.0%)	-0.488

Abbreviations: ASA: American Society of Anesthesiologists; AIDS: Acquired immunodeficiency syndrome; HIV: Human immunodeficiency virus.

Perioperative Anesthesia 28- Volatile anesthetic dose and postoperative delirium in older patients: A hospital registry study

Elena Ahrens[1], Denys Shay[1], Aiman Suleiman[2], Ricardo Munoz[3], Luca Wachtendorf[4], Haobo Ma[4], Guanqing Chen[4], Maximilian Schaefer[5]

Beth Israel Deaconess Medical Center[1] Beth Israel Deaconess Medical Center, Harvard Medical school[2] BIDMC[3] Montefiore Medical Center[4] Beth Israel Deaconess Medical Center & Hospital[5]

Introduction: Intraoperative cerebral hypoperfusion and hypoxemia have been linked to an increased risk of postoperative delirium (1, 2). Volatile anesthetics exert competing effects on potential mechanisms of postoperative delirium, including hypotension but also dose-dependent vasodilation of cerebral vessels and reduction in cerebral metabolism (3). In this study, we investigated whether volatile anesthetic dose is associated with the risk of postoperative delirium.

Methods: Hospitalized patients ≥60 years who underwent general anesthesia with volatile anesthetics for non-cardiac and non-neurosurgical procedures between 2006 and 2020 at a tertiary healthcare center in Massachusetts, USA, were included. The primary exposure was the intraoperatively administered dose of volatile anesthetics, expressed as average age-adjusted minimum alveolar concentration (MAC). The primary outcome was delirium within 7 days after surgery. Multivariable logistic regression analyses adjusted for patient characteristics, comorbidities and other intraoperative factors including hypotension were applied.

Results: 54,667 patients were included (**Figure 1**), of whom 1,144 (2.1%) developed delirium (**Table 1**). The median (interquartile range) average age-adjusted MAC of inhalational anesthetics was 0.85 (0.68–1.02) in patients with and 0.89 (0.70–1.03) in patients without delirium. In adjusted analyses, higher doses of volatile anesthetics were associated with a lower risk of 7-day delirium (adjusted odds ratio [OR_{adj}] 0.91; 95%CI 0.86–0.97; p=0.003, per each 0.2 increase in average age-adjusted MAC, **Figure 2**). These findings were independent from patients' predicted average age-adjusted MAC of inhalational anesthetics (p-for-interaction=0.30), and independent from adjusting for the occurrence of hypotension, defined as the duration of mean arterial blood pressure <55 mmHg. They were further confirmed after adjustment for patients' predicted duration of intra-procedural hypotension (OR_{adj} 0.90; 95%CI 0.85–0.96; p=0.001, per each 0.2 increase in average age-adjusted MAC).

Conclusions: Higher doses of volatile anesthetics were associated with a lower risk of postoperative delirium even when adjusted for patients' risk of hypotension and predicted age-adjusted MAC, based on markers of comorbidity and frailty.

References: (1) Dose-dependent relationship between intra-procedural hypoxaemia or hypocapnia and postoperative delirium in older patients. Br J Anaesth. 2022 Sep 30:S0007-0912(22)00501-3.

(2) Association Between Intraoperative Arterial Hypotension and Postoperative Delirium After Noncardiac Surgery: A Retrospective Multicenter Cohort Study. Anesth Analg. 2022 Apr 1;134(4):822-833.

(3) Direct cerebrovasodilatory effects of halothane, isoflurane, and desflurane during propofol-induced isoelectric electroencephalogram in humans. Anesthesiology. 1995 Nov;83(5):980-5.

Table 1. Patient characteristics and distribution of variables.

	No delirium	Delirium	Standardized difference
	n = 53,523	n = 1,144	
Demographics and comorbidities			
Age, years	71.2 ± 8.2	76.1 ± 9.5	-0.555
Gender, female	28,060 (52.4%)	576 (50.3%)	0.042
Body mass index, kg/m²	28.4 ± 6.4	27.1 ± 6.6	0.203
Charlson Comorbidity Index	2 (0 – 3)	1 (0 – 3)	0.028
ASA physical status	3 (2 – 3)	3 (3 – 4)	-0.724
Smoking	7,243 (13.5%)	176 (15.4%)	-0.053
Alcohol abuse	1,077 (2.0%)	36 (3.1%)	-0.072
Drug abuse	486 (0.9%)	12 (1.0%)	-0.014
Anemia	13,089 (24.5%)	293 (25.6%)	-0.026
Procedure- and anesthesia-related factors			
Duration of surgery, minutes	161 (115 – 232)	180 (121 – 302)	-0.327
Emergency surgery	6,520 (12.2%)	397 (34.7%)	-0.551
Work relative units	17.6 (11.9 – 23.5)	19.7 (14.6 – 26.4)	-0.329
Crystalloid and colloid infusion, ml	1,250 (800 – 2,000)	1,600 (1,000 – 3,000)	-0.429
Units of packed red blood cells			-0.334
0	49,815 (93.1%)	908 (79.4%)	
1	1,655 (3.1%)	68 (5.9%)	
>1	2,053 (3.8%)	168 (14.7%)	
Short acting opioid dose, mg OME	37.5 (25.0 – 62.5)	37.5 (25.0 – 62.5)	-0.108
Long acting opioid dose, mg OME	6.8 (0.0 – 17.0)	3.4 (0.0 – 17.0)	0.072
Non-depolarizing NMBA, ED_{95}	2.1 (1.1 – 3.2)	2.8 (1.7 – 4.3)	-0.404
Neostigmine dose, mg/kg	2.0 (0.0 – 3.0)	0.0 (0.0 – 3.0)	0.281
Vasopressor dose, mg norepinephrine equivalents	0.1 (0.0 – 0.3)	0.3 (0.1 – 0.9)	-0.100
Minutes of MAP below 55 mmHg	1 (0 – 3)	2 (0 – 6)	-0.269
Regional or neuraxial anesthesia	2,809 (5.2%)	122 (10.7%)	-0.201
Longest consecutive time of SpO_2 <90%, minutes	0 (0 – 0)	0 (0 – 0.5)	-0.207
Longest consecutive time of $etCO_2$ <25 mmHg, minutes	0 (0 – 1)	0 (0 – 1)	-0.243
Midazolam administration	36,153 (67.5%)	593 (51.8%)	0.324
Nitrous oxide administration	25,646 (47.9%)	407 (35.6%)	0.252
Total propofol dose, mg/kg	160.0 (120.0 – 200.0)	150.0 (92.7 – 200.0)	-0.023

Data are expressed as frequency (prevalence in %), or median (interquartile range [25th-75th percentile]). *ASA: American Society of Anesthesiologists; ED_{95}: Median effective dose required to achieve a 95% reduction in maximal twitch response from baseline; MAP: mean arterial blood pressure; NMBA: Neuromuscular blocking agents; OME: Oral morphine equivalents; SpO_2: Peripheral oxygen saturation; $etCO_2$: end-tidal carbon dioxide pressure.*

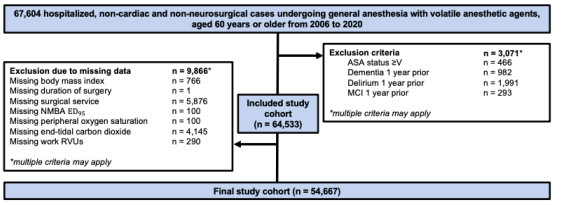

Figure 1. Study flow diagram.
ASA: American Society of Anesthesiologists; ED_{95}: median effective dose required to achieve a 95% reduction in maximal twitch response from baseline; NMBA: neuromuscular blocking agents; work RVUs: work Relative Value Units; MCI: mild cognitive impairment.

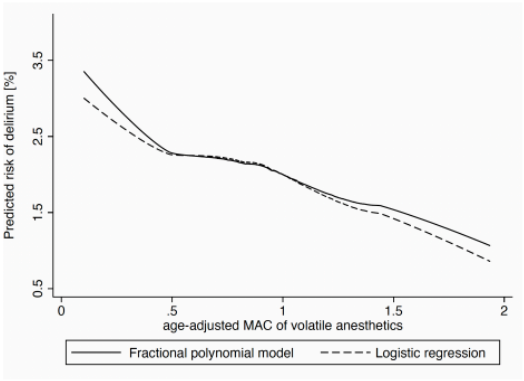

Figure 2. Primary analysis.

Predicted risk of delirium as a function of age-adjusted minimum alveolar concentration (MAC) of volatile anesthetics, estimated from logistic and fractional polynomial regression analysis

Regional Anesthesia

Regional Anesthesia 1- Effectiveness of Erector Spinae Plane Block in Patients Post-midline Sternotomies: A Systematic Review and Meta-analysis

Mohamed Fayed[1], Nimesh Patel[2], Wissam Maroun[3], John Mitchell[4], Patrick Forrest[2], Nicholas Yeldo[3]

Henry Ford Hospital[1] Henry Ford Health System[2] Henry Ford Health[3] Henry Ford Health, Michigan State University CHM[4]

Introduction: With advancements in the field of regional anesthesia, there is a shift in paradigm away from the liberal use of opioids towards multimodal analgesic techniques. The erector spinae plane block (ESPB) emerged as a relatively new player in regional anesthesia for managing thoracic pain. In 2016, it was first detailed by Forero et al. as a sensory block acting at the dorsal and ventral rami of the thoracic spinal nerves [1]. Many studies have demonstrated the analgesic effectiveness and comprehensive opioid-sparing advantages of ESPB in numerous surgical specialties [2,3]. Nonetheless, there remains to be a gap in knowledge and critical appraisal of clinical data relating to ESPB in cardiac surgery patients, especially the limited number of patients in each published study.
In this meta-analysis, we aim to investigate postoperative pain management and other outcomes, including ventilation days in cardiac surgery patients with post-midline sternotomies who received ESPB compared to standard care.

Methods: This systematic meta-analysis used the Preferred Reporting Items for Systematic Reviews and Meta-Analysis (PRISMA) statement guidelines. The search engine used MEDLINE, Embase, Web of Science, Cochrane Library, and ClinicalTrials.gov.
Interventions and Comparators: Intervention was defined as Erector Spinae Plane Block. Comparators were no regional technique performed.
Outcomes: The primary outcome was opioid consumption and pain relief. Secondary outcomes were ICU time, hospital length, postoperative nausea and vomiting (PONV), mechanical ventilation time, rescue analgesia, and ambulation time.
Weighted mean difference (WMD) and 95% confidence interval (CI) were calculated and reported for continuous outcomes, and odds ratio with 95% CI for dichotomous variables. The standardized mean difference was used to determine the effect measure for continuous outcomes measured in different scales. The inverse variance model was used for continuous data, and the dichotomous data, the Mantel-Haenszel model, was used. All data were analyzed with the random effects model to generalize the findings. Heterogeneity between studies was evaluated with I^2 statistics with thresholds of low (25-50%), moderate (50-75%), and high (>75%). A p-value of <0.05 was considered statically significant. All statistical analysis was performed using Comprehensive Meta-analysis Version 3.

Results: Screening results: A total of 3264 articles were identified through a literature search. A total of 192 articles were evaluated for full-text review, resulting in 178 being omitted (figure 1). One thousand eight hundred one records were excluded for duplicates, and an additional 1271 articles were excluded after a review of titles and abstracts. The final results are: 4 studies were RCTs, and 3 Non-RCT trials (Prospective, Retrospective matched control, and Consecutive patient-matched control) (Table 1).
Primary outcome: Intraoperative opioid use: a significant reduction of intraoperative IV fentanyl for sternotomy patients of WMD -445 mcg (95% CI, -814 to -75, p = 0.018, I2 = 99.9) Figure2). Pain scores: ESPB on postsurgical pain at 0 h following surgery displayed a significant effect, with WMD of -1 (95% CI, -1.7 to -0.6, p < 0.001, I2 = 74.2). An analysis of pain scores at 4-6 hours postoperatively was conducted, which showed a WMD of -1 (95% CI, -1.7 to -0.2, p = 0.018, I2 = 83.7) in the ESPB group.
Secondary outcomes: sternotomy patients have significantly less mechanical ventilation time (mean difference -2.4 hours), ICU duration (mean difference -22.3 hours), and PONV OR 0.39 (table 2).

Conclusions: This meta-analysis demonstrates that ESPBs offer several advantages post-cardiac surgery, including decreased postoperative and intraoperative opioid use, lower pain, shorter mechanical ventilation time, decreased ICU duration, and reduced postoperative nausea and vomiting.

References: 1. *The Erector Spinae Plane Block: A Novel Analgesic Technique in Thoracic Neuropathic Pain.* Reg Anesth Pain Med, 2016. **41**(5): p. 621-7.

2. *Erector Spinae Plane Block in Abdominal Surgery: A Meta-Analysis.* Front Med (Lausanne), 2022. **9**: p. 812531.

3. *Erector spinae plane block for postoperative analgesia in breast and thoracic surgery: A systematic review and meta-analysis.* J Clin Anesth, 2020. **66**: p. 109900.

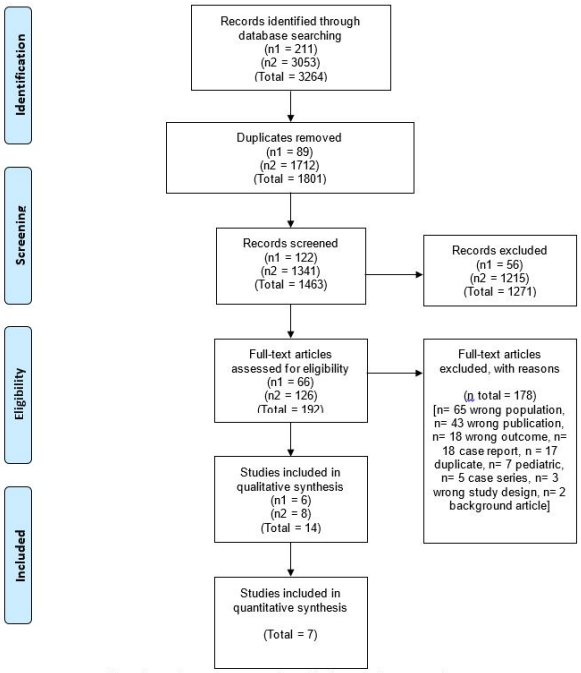

Figure 1: PRISMA flow chart of erector spinae plane block in cardiac surgical patients.

Outcome	Studies Included	Odds Ratio or Mean Difference (95% CI) or Standardized Mean Difference (95% CI)	P-value for statistical significance	I^2 test for heterogeneity
ICU duration (hr)	4	-22.3 (-31.7 to -13.0)	P <0.0001	97.3
Mechanical ventilation time (hr)	7	-2.4 (-3.2 to -1.5)	P <0.0001	96.4
Hospital length of stay (day)	2	-2.7 (-3.7 to -1.7)	P <0.0001	0
Time to ambulation (hr)	3	-11.0 (-28.7 to 6.6)	P =0.220	99.8
Rescue analgesia (Hedge's g)	5	-1.03 (-4.6 to 2.5)	P =0.57	98.6
PONV	3	0.21 (0.1 to 0.6)	P =0.006	0

Table 2: Secondary Outcomes

Abbreviation: hr, hour, PONV: post-operative nausea and vomiting, CI: confidence interval

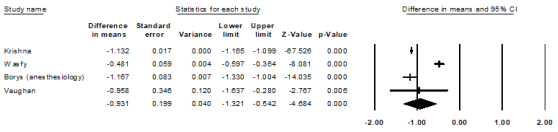

Figure 3 ICU duration in days

Authors	Year	Study design	Treatment Group (n)	Control group (n)	Local Anesthetic	Primary outcome	Secondary Outcomes
Krishna, S., et al.	2019	RCT	ESPB SS at T6 (n= 53)	Conventional Treatment paracetamol & tramadol (n= 53),	Ropivacaine 0.375% (20-25cc)(3 mg/kg)	NRS	perioperative fentanyl usage
Ozgur, L., et al.	2022	RCT	ESPB SS at T4-5 (n= 25)	Sham block), 0.5 ml/kg NS (n=25)	Bupivacaine 0.25% (0.5 ml/kg) and dexamethasone (8 mg)	Morphine requirement	Perioperative opioids use, extubation times, VAS scores, duration of first PCA bolus dose requirement, rescue analgesia, mobilization times.
Athar, M., et al	2021	RCT	ESPB SS at T5 (n= 15)	Sham block 20 ml NS (n= 15)	Levobupicacaine 0.25% (20 cc)	Postoperative analgesic requirement	Time to first rescue analgesic, NRS, duration of mechanical ventilation
Bashir, S., et al.	2021	RCT	ESPB Catheter at T5 (n=20)	multimodal IV analgesia (n=20)	Bupivacaine 0.25%, [15 ml bolus followed by 8 cc/h for 48 hours]	VAS score	perioperative opioids requirement, time to extubation, ICU stay
Macchia, P., et al.	2019	Consecutive, patient-matched, controlled before-and-after study	ESP catheter (n=47)	IV morphine, 0.5mg/h and IV nefopam 100 mg/24h (n=20)	**Bolus:** Ropivacaine (Bolus 0.25 ml/kg 5mg/ml **Infusion:** Ropivacaine Intermittent automatic boluses q6h of 2mg/ml	opioids consumption	pain at rest and during mobilization, time to extubate, early mobilization, blood pressure variations
Bona, M., et al.	2020	Prospective cohort	ESPB SS (n=29)	Standard care (n=28)	Ropivacaine 0.375% 0.2 ml/kg	postoperative mechanical ventilation time	ICU and hospital stay, postoperative drainage time, postoperative troponin-T level, pain severity, total opioid consumption
Vaughan, B., et al.	2021	Retrospective Cohort, matched control	Bilateral ESPB Catheter (n=28)	Control (n=50)	**Bolus:** Ropivacaine 0.5% 20ml **Infusion:** Ropivacaine 0.2% 3-7 ml/hr, started in ICU for max 5 days	opioids consumption	non-opioid analgesic consumption, time to extubation, ICU LOS, hospital LOS, pain scores

Table 1 RCT and Non-RCT trials.

Abbreviations: ESPB: erector spinae plan block, n: number, SS: Single shot, NS: normal Saline, IV: intravenous, NRS: Numeric pain rating, VAS: visual analogue scale, ICU: intensive care unit LOS: length of stay.

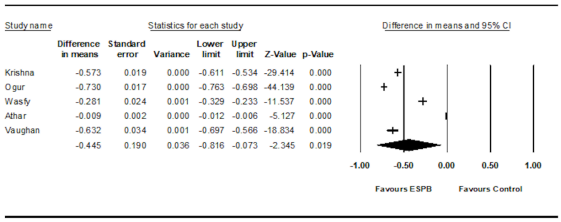

Figure 2 Intraoperative opioid consumption (IV fentanyl equivalent microgram)

Regional Anesthesia 2- Enhanced Recovery after Surgery: Epidural Analgesia for Gynecologic Procedures at an Academic Medical Center

Tiffany Chan[1], Kristina Michaud[2], Troy Davis[2], Paul Demarco[2]

University of Virginia[1] University of Virginia Health System[2]

Introduction: First-line treatment for locally advanced cervical cancer is primary chemoradiation. Interstitial brachytherapy[1] is the application of radiation to a localized area and typically results in adequate cervical regression within two to five weeks of therapy[2], while sparing surrounding normal tissue from radiation damage. However, brachytherapy poses a physical and emotional challenge as patients are expected to lie flat and still while perineal treatment needles remain in place for multiple brachytherapy sessions over three days. Previously, our academic medical center relied on intravenous opioid therapy alone as the main analgesic modality for these patients. Intravenous opioids cause undesirable side effects (e.g., nausea, pruritus) and may provide inadequate analgesia during this sustained period of time. The use of epidural analgesia has been reported[3-8] in other surgical patients with promising results. We developed a new Enhanced Recovery after Surgery (ERAS) protocol that introduces epidurally administered local anesthetic as the mainstay of analgesia and seeks to standardize a best practice for the pre-, intra- and post-operative management of patients undergoing cervical interstitial brachytherapy at our institution.

Methods: We performed a retrospective chart review of patients who underwent interstitial cervical brachytherapy at a single-center academic medical institution from 2018-2022. Patients identified as brachytherapy candidates by the gynecologic oncology and radiation oncology services following ERAS implementation in March 2022 were offered continuous epidural analgesia (CEA) as described below and enrolled in the present study. Statistical analysis was performed using unpaired t-tests with a significance level of $\alpha = 0.05$. Metrics include pain score, overall satisfaction with analgesia, location of pain, total amount of opioid administered, use of multimodal analgesia (e.g., acetaminophen, cyclobenzaprine, fentanyl, gabapentin, hydromorphone, ketamine, ketorolac, and oxycodone), and number of emesis occurrences.

CEA intervention: Patient is referred to the pre-anesthesia clinic and evaluated for spinal abnormalities, comorbid neurologic disorders, and coagulopathies or use of anticoagulant or antiplatelet medications. Barring contraindications, a mid- to lower lumbar epidural catheter is placed by the anesthesiologist immediately prior to the first session of brachytherapy. An epidural infusion of 0.125% bupivacaine or 0.2% ropivacaine is then initiated and continued postoperatively. Supplemental analgesic medications are available to the patient as needed for breakthrough pain. The infusion is discontinued just prior to transporting the patient to their last session, and the catheter is removed after completion of brachytherapy.

Results: A total of 16 patients were included at the time of submission. Twelve patients received intravenous opioid analgesia without epidural analgesia (conventional therapy group), including patient-controlled intravenous analgesia (PCA) or nurse-administered opioid therapy. Three patients received an epidural as the primary mode of analgesia (CEA intervention group). The average patient age was 66.9 ± 8.96 years in the conventional group, compared to 68 ± 7.81 years in the intervention group. Origins of gynecologic cancer within the conventional group were endometrial (50%), vaginal (33.3%), ovarian (8.3%), and rectal (8.3%). All 3 cancers in the intervention group were of vaginal origin (100%). Pain scores were initially higher in the conventional group, with complete timeline as illustrated in Figure 1 and Table 1. Average use of intravenous hydromorphone was higher in the conventional group ($p = 0.043$), while average use of intravenous fentanyl was higher in the intervention group ($p = 0.034$); multimodal analgesic usage was not significantly different between groups (Table 2). No episodes of emesis were recorded in either group.

Conclusions: Our initial data support lower pain scores overall with conventional opioid therapy, although epidural therapy may provide superior analgesia early in admission. We observed a trend toward more adjunct analgesia use in the conventional group. Limitations of our pilot study are low power, inconsistent documentation of outcome variables, and inadequate control for baseline pain score, baseline analgesic usage, and dosing weight. We aim to continue the ERAS protocol and improve sample size for more robust statistical analysis in the future.

References:

1. *Semantic Scholar*, 1970.
2. *Int J Radiat Oncol Biol Phys*, vol. 87, p. 111, 2013.
3. *Journal of Clinical Anesthesia*, vol. 35, pp. 509-515, 2016.
4. *Anaesthesia and Intensive Care*, vol. 26, pp. 165-172.
5. *Current Opinion in Anaesthesiology*, vol. 30, pp.736-742.
6. *The Journal of the American Society of Anesthesiologists*, vol. 28, pp. 592-622.
7. *Journal of the American Medical Association*, vol. 290, pp. 2455-2463.
8. *British Journal of Anaesthesia*, vol. 87, pp. 47-61.

Table 2. Multimodal analgesic medication use, total amount administered over entire 72-hour length of stay

	'Traditional' PCA Group	Epidural Group	P-value
acetaminophen	1083.3 mg (992.9)	1950 mg (2579.6)	0.343
oxycodone	3.3 mg (10.1)	0 (0)	0.587
hydromorphone (IV)	0.775 mg (0.582)	0 (0)	0.043
fentanyl	22.93 mcg (39.1)	100 mcg (90.14)	0.034*
ketamine	4.17 mg (9.96)	0 (0)	0.578
ketorolac	9.23 mg (13.3)	0 (0)	0.228
cyclobenzaprine	1.25 mg (4.33)	0 (0)	0.635
gabapentin	200 mg (692.8)	0 (0)	0.635

Figure 1. Pain scores reported over time

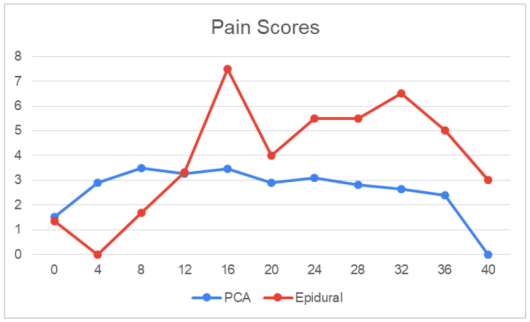

X-axis label: time of hospital admission in hours
Y-axis label: patient reported pain score out of 10

Table 1. Pain scores reported over time

	Traditional PCA	Epidural	p-value
0h	1.5 (2.6)	1.3 (2.3)	0.921
4h	2.9 (2.7)	0 (0)	0.101
8h	3.5 (2.3)	1.7 (2.9)	0.247
12h	3.3 (2.8)	3.3 (3.5)	0.975
16h	3.5 (2.3)	7.5 (0.7)	0.036*
20h	2.9 (3.0)	4 (1.4)	0.635
24h	3.1 (2.3)	5.5 (3.5)	0.225
28h	2.8 (2.3)	5.5 (2.1)	0.165
32h	2.6 (2.9)	6.5 (0.7)	0.11
36h	2.4 (2.3)	5 (1.4)	0.209
40h	0	3	n/a

Regional Anesthesia 3- Local anesthetic dosing and toxicity of truncal catheters: A systematic review and regression analysis

Michael Fettiplace[1], Brittani Bungart[1], Lana Joudeh[1]

Massachusetts General Hospital[1]

Introduction: Truncal local-anesthetic catheters arose following the popularization of paravertebral catheters by Sabanathan and colleagues in 1988.[1] Despite more than 30 years of use, the characterization of dosing is sparse. Expert recommendations advise a 400 mg daily limit of bupivacaine[2], 770 mg daily limit of ropivacaine (package insert) and 0.1-0.3 mg/kg/hr in pediatrics[3]. As such, we conducted a systematic review to characterize the dose, administration details and complications of two of the most frequent truncal blocks: the paravertebral block (PVB) and the transversus abdominis plane (TAP) block.

Methods: Institutional Review Board exempted full review. The study was registered in PROSPERO. We conducted a systematic review of the literature and identified studies of PVB or TAP catheters using bupivacaine or ropivacaine and extracted data including concentration and volume of bolus, infusion and breakthrough doses along with duration, complications, adjuvants, local anesthetic systemic toxicity and toxic blood levels. Bolus dose, infusion dose, and cumulative 24 hour doses were calculated on a patient specific level in Matlab. Statistical analysis in Prism compared numerical data with t-tests or Mann Whitney-U tests for dosing comparisons. Linear regression was conducted on a patient level to identify contributors to 24 hour dose based on R^2 and convergence of slope term; subsequent multiple-linear regression incorporated terms on an infusion level in a step-wise fashion based on R^2 and p-value while maintaining multicollinearity variance inflation factor <4.0 and normality of residuals.

Results: Screening identified 548 articles on PubMed and 932 articles on Europe PMC. Following exclusions, we extracted data from 252 papers with data from 32 pediatric studies, 108 adult bupivacaine studies and 121 adult ropivacaine studies with a total of 6802 adult patients and 331 pediatric patients. Mean adult dosing for bupivacaine over 24 hours was 6.0 mg/kg (95%CI 2.1 – 13.6) and maximum was 7.5mg/kg (2.1 – 13.4, n=3223) translating to 420mg and 525mg in a 70 kg patient (**Figure 1**). Mean adult dosing for ropivacaine over 24 hours was 7.75 mg/kg (95%CI 2.1-16.1, n=3579) and maximum was 9.3mg/kg (95%CI: 2.2.-19.6) translating to 543mg and 651mg in a 70 kg patient (**Figure 1**). Multiple-linear regression of adult data converged (261 degrees of freedom, R^2 =0.95) with normal residuals (D'Agostino K^2 = 0.23, p=0.89) and multiple factors contributing to the 24 hour dose (**Table 1**). Patient weight, age, on-demand delivery, PVB vs. TAP, duration of infusion and level did not contribute to 24 hour dose. Mean pediatric dosing for bupivacaine over 24 hours was 0.29 mg/kg/hr (0.12 – 1.0, n=172, **Figure 2**) and maximum dosing was 0.5 mg/kg/hr (0.12 – 1.0). Mean pediatric dosing for ropivacaine over 24 hours was 0.5 mg/kg/hr (range: 0.2 – 0.68, n=213, **Figure 2**) and maximum dosing was of 0.5 mg/kg/hr (0.2 – 0.75). Multiple-linear regression converged (42 degrees of freedom, R^2 = 0.89) with normal residuals (D'Agostino K2 = 2.0, p=0.37) and multiple factors contributing to the 24 hour dose (**Table 2**). On demand use, infusion rate, year of publication and patient age of less than 6 months did not contribute to dose. There were 29 reports of toxicity, 17 from ropivacaine in adults, 12 from bupivacaine in adults and 0 in pediatrics with at least 67 additional reports of toxic blood levels (**Table 3**). Excluding case reports, toxicity occurred in 26 of the 6939 patients (0.4%) with symptoms of toxicity ranging from tinnitus to death. A disproportionate amount of toxic events occurred in cardiac cases (n=11) and at least two cases occurred following breakthrough dosing.

Conclusions: Mean total dosing of bupivacaine and ropivacaine in the published literature frequently exceeded recommendations with linear regression indicating modifiable risk factors for high dose. Given the expansion of truncal regional anesthesia,[4] patient safety would benefit from more specific dosing recommendations including weight-based dosing, break-through dosing and recommendations about continuous infusion versus intermittent bolus methods. Data also indicate the need for prospective evaluation about safe dosing of intermittent bolus catheters (based on their lower total doses) and dosing in high risk groups including cardiac surgery patients who may suffer from reduced cardiac output or hepatic dysfunction elevating the risk of toxicity.

References: 1.) Annals of Thoracic Surgery 1988; 46:425–6

2.) Reg Anesth Pain Med 2004; 29:564–75

3.) Reg Anesth Pain Med 2018; 43:211–6

4.) Reg Anesth Pain Med 2016; 41:621–7

Figure 1

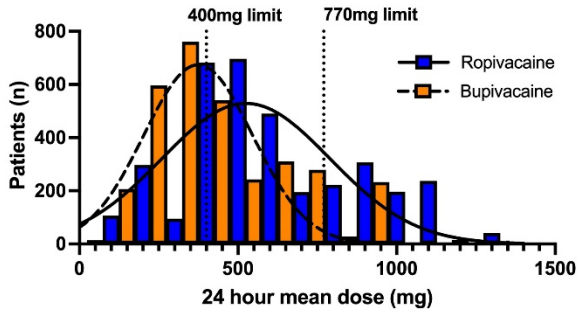

Figure 2

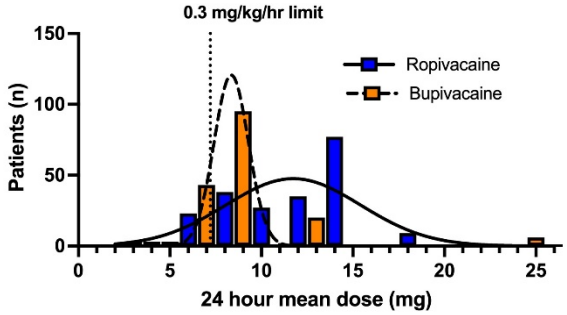

Table 1: Multiple linear regression analysis for 24 hour dosing in adult catheters

Variable	Estimate (mg/kg)	P-value	Variance inflation factor	R^2 with other variables
Mean Infusion rate (mL/kg/hr)	34 (31 - 37)	<0.0001	2.9	0.65
Mean Infusion conc (%)	15 (14 - 16.7)	<0.0001	2.8	0.64
Laterality (bilateral)	1.1 (0.66 - 1.6)	<0.0001	1.8	0.44
Drug (Bupivacaine)	-1.4 (-1.7 - -1.0)	<0.0001	1.7	0.42
Delivery (Intermittent)	-1.6 (-2.0 - -1.2)	<0.0001	1.6	0.37

Table 2: Multiple linear regression analysis for 24 hour dosing in pediatric catheters

Variable	Estimate (95% CI)	P-value	Variance inflation factor	R^2 with other variables
Mean weight (kg)	-0.08 (-0.12 - -0.03)	0.0009	3.9	0.74
Mean bolus concentration (%)	7.5 (2.1 - 12.9)	0.0072	3.4	0.71
Mean infusion concentration (%)	46.48 (33 - 60)	<0.0001	3.4	0.70
Drug (Ropivacaine)	2.1 (0.44 - 3.7)	0.014	1.8	0.45
Laterality (bilateral)	2.9 (0.2 - 5.5)	0.036	1.76	0.43

Table 3: Local anesthetic systemic toxicity and toxic local anesthetic levels

Group	*# patients (% of total)*	*Max 24 hour mg/kg [95%CI]*	*Max 24 mg for 70kg pt. [95%CI]*	*Peak concentration range (mg/L)*	*Peak time (hours)*
Local anesthetic systemic toxicity					
Ropivacaine	17 (0.5%)	13.8 [4.8-19.2]	966 [336-1344]	2.2 - 9	48 [1 - 48]
Bupivacaine	12 (0.4%)	13.3 [12.1-13.6]	931 [847-952]	8	63.5 (58.5 – 68)
Toxic blood levels					
Ropivacaine	34 (0.9%)	12 [12 - 19.2]	840 [840 – 1344]	2.2 – 4.5	24 [6-48]
Bupivacaine	28 (0.9%)	12.9 [5.1 – 13.5]	903 [357 – 945]	2.1 – 9.27	48 [15 – 72]
Pediatric	5 (1.3%)	7.25 [7.25 – 13.25]	-	2.81 – 3.14	42 [24 – 53]

Regional Anesthesia 4- Associations of Race and Hospital with Regional Nerve Block for Treatment of Postoperative Pain in Total Knee Arthroplasty: A Retrospective Analysis Using Medicare Claims

Anjali Dixit[1], Gabriel Sekeres[1], Edward Mariano[1], Stavros Memtsoudis[2], Eric Sun[1]

Stanford University School of Medicine[1] HSS/ Anesthesiology[2]

Introduction: Regional anesthesia for total knee arthroplasty (TKA), one of the most common surgeries in the United States,[1] has been deemed high priority by national and international societies.[2,3] Standardized administration of nerve blockade for TKA is well-substantiated,[3,4] and its use can serve as an important measure of anesthesia-related healthcare equity.[5] Specifically, evaluating whether Black patients receive lower-quality anesthetic care when undergoing TKA is critical given other known disparities experienced by this surgical population.[6-9] Further, given that the hospital where patients access care is a known driver of disparities on other performance metrics,[10] it is also important to understand the magnitude to which race and/or hospital may drive existing anesthesia-related healthcare disparities.
This study therefore 1) assessed whether racial disparities existed in the provision of regional nerve blocks for primary TKA in Black compared to White patients, and 2) estimated the extent to which variability in block administration was attributable to race or hospital. We hypothesized that Black patients would be less likely to receive regional blocks, and that variability in block administration would more likely be attributable to hospital rather than race.

Methods: We used healthcare claims for Medicare fee-for-service patients who underwent primary TKA between 1/1/2011 and 12/31/2016. Our sample included 733,406 surgeries. Our primary outcome was a composite representing receipt of any peripheral or neuraxial block (including femoral, lumbar plexus, spinal, epidural, or other peripheral block). Our primary exposure was self-reported race (White, Black, and Other).[11]
We used multivariable logistic regression to estimate the association between race and receipt of block, adjusting for demographic characteristics, Elixhauser comorbidities, and year. We next further adjusted for hospital and compared this model to the prior using a likelihood ratio test and computing partial eta-squared for hospital to evaluate the extent to which variability in block rate was attributable to hospital. We converted odds ratios to predicted probabilities for ease of interpretation.

Results: Our final sample consisted of 733,406 primary TKAs, of which 665,036 (90.7%) were performed on patients who were White, 34,821 (4.7%) on patients who were Black, and 33,549 (4.6%) on patients categorized as Other. Given poor validity of the "Other" category,[11] we focused our analyses on patients identified as White and Black. Approximately 52% of White and Black patients each received any regional nerve block and there was therefore no significant difference in unadjusted rate of block receipt.
Figure 1 shows unadjusted and adjusted predicted probabilities of receipt of any block by racial group. Black patients did not have statistically different probabilities of receiving a block compared to White patients after accounting for demographic variables, comorbidities, and year in Model 1 (52.5% Black vs. 52.1% White, p=0.216). These probabilities remained insignificant after accounting for hospital fixed effects in Model 2 (53.5% Black vs 52.7% White, p=0.174). A likelihood ratio test comparing Model 2 to Model 1 rejected the null hypothesis that these two models were the same (p<0.001). The partial eta-squared of hospital fixed effects in Model 2 was 0.42 relative to an R-squared of 0.42, implying that hospital where the surgery took place accounted for the vast majority of variation in block administration out of all variables included in the model. **Figure 2** illustrates this hospital-level variability in block administration by depicting the unadjusted rates of block administration by hospital plotted against the percent of White patients treated at that hospital.

Conclusions: We found no racial disparity in administration of regional nerve blocks for postoperative analgesia from primary TKA by race. We also found that – out of all the variables we included in our models – the hospital where a patient received care was most likely to predict whether they received a block, irrespective of race. These findings imply that – rather than race alone – TKA care may be influenced by systemic, geographically-driven and socioeconomic factors that affect healthcare access and resources based on where patients live.

References: 1. JAMA. 308;1227-36 2012.

2. 2022 QCDR Measure Specifications. https://www.aqihq.org/files/MIPS/2022/2022_QCDR_Measure_Book.pdf. Accessed August 24 2022.

3. Reg Anesth Pain Med. 46;971-985 2021.

4. Anesth Analg. 102;248-57 2006.

5. Anesth Analg. 134;1175-1184 2022.

6. JAMA Surg. 156;274-281 2021.

7. Curr Rev Musculoskelet Med. 14;434-440 2021.

8. J Rheumatol. 43;765-70 2016.

9. J Arthroplasty. 28;732-5 2013.

10. Black Patients are More Likely Than White Patients to be in Hospitals with Worse Patient Safety Conditions. https://www.urban.org/research/publication/black-patients-are-more-likely-white-patients-be-hospitals-worse-patient-safety-conditions. Accessed April 7 2022.

11. Med Care. 55;e170-e176 2017.

Figure 1: Unadjusted and Adjusted Probabilities of Block Administration for Total Knee Arthroplasty by Race

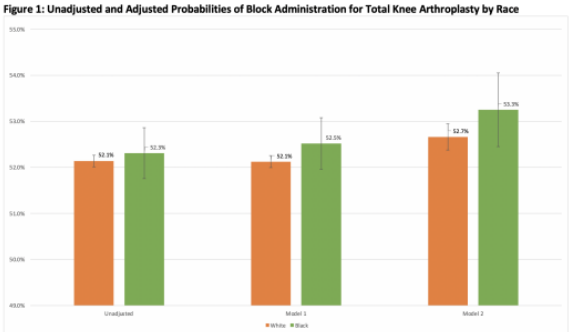

Figure 1 shows unadjusted and adjusted predicted probabilities of block administration for patients identified as White and Black. We found no statistically significant differences in administration of regional nerve blocks for postoperative analgesia from primary TKA by race in unadjusted and adjusted analyses. Adjusted estimates were calculated using multivariable logistic regression accounting for age, sex, Elixhauser comorbidities, and year (Model 1, 52.5% Black vs. 52.1% White, p=0.216) and further adjusting for hospital fixed effects (Model 2, 53.5% Black vs 52.7% White, p=0.174). Odds ratios were converted to predicted probabilities for ease of interpretation. A likelihood ratio test comparing Model 2 to Model 1 rejected the null hypothesis that these two models were the same ($p < 0.001$). The partial eta-squared of hospital fixed effects in Model 2 was 0.42 relative to an R-squared of 0.42, implying that hospital fixed effects accounted for the vast majority of variation in block administration out of all variables included in the model.

Figure 2: Hospital-Level Unadjusted Probabilities of Nerve Block Administration for Total Knee Arthroplasty, by Percent of Patient Population Identified as White

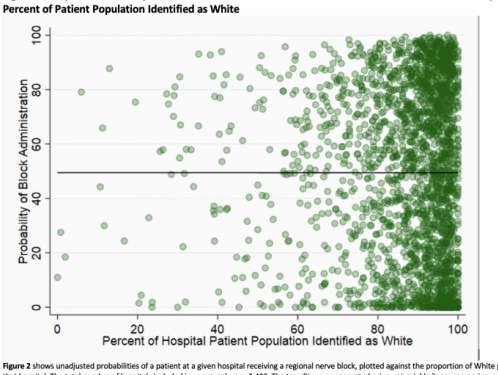

Figure 2 shows unadjusted probabilities of a patient at a given hospital receiving a regional nerve block, plotted against the proportion of White patients treated at that hospital. The total number of hospitals included in our sample was 2,402. The trendline was generated using univariable linear regression, weighted by the number of cases performed at a given hospital, and calculated with robust standard errors. It represents the change in likelihood of block utilization as the proportion of White patients changed: in other words, for every 10% increase in the proportion of White patients treated at a given hospital, there was a non-significant 2.6% increase in the likelihood of block utilization (β=0.026, 95% CI -0.102 to 0.153, p=0.692). This figure therefore illustrates the significant variability in block utilization by hospital that is likely unrelated to race.

Regional Anesthesia 5- From epidural to block: Continuous adductor canal block optimizes patient discharge disposition, reduces hospital length of stay, and reduces opioid consumption following total knee arthroplasty compared to epidural anesthesia

Isaac Freedman[1], Michael Mercier[1], Anoop Galivanche[1], Mani Sandhu[1], Mark Hocevar[2], Harold Moore[3], Jonathan Grauer[4], Lee Rubin[4], Jinlei Li[5]

Massachusetts General Hospital, Harvard Medical School[1] Warren Alpert Medical School of Brown University[2] University of Texas Southwestern Medical Center[3] Yale School of Medicine[4] Yale[5]

Introduction: To compare the efficacy of a postoperative continuous adductor canal block (cACB) with and without a steroid adjuvant to that of epidural analgesia (EA).

Methods: All patients who underwent inpatient, primary total TKA at a single institution between July 2011 and November 2017 were included for retrospective cohort analysis. TKA patients were stratified into one of three analgesia approaches based on the time period of their date of surgery: EA, cACB without steroid adjuvant, and cACB with steroid adjuvant. Hospital length of stay (LOS), discharge disposition, incidence of postoperative adverse events, and total milligram morphine equivalents (MME) requirements were compared between analgesia approaches. Recursive feature elimination (RFE)-optimized multivariate logistic regression was performed to assess the independent effect of analgesia approach on prolonged LOS greater than 3 days (pLOS), non-home discharge, and total and daily MME requirements (tMME and dMME) following TKA.

Results: Of 4,345 patients undergoing TKA, 1,556 (35.83%) received EA, 2,087 (48.03%) received cACB without steroids, and 702 (16.13%) cACB with steroids. On univariate analysis, cACB patients experienced lower rates of pLOS (without steroids: 8.53%; with steroids: 8.40%; EA: 12.66%; p<0.001), higher rates of discharge to home than EA patients (without steroids: 64.40%; with steroids: 75.07%; EA: 46.14%; p<0.001), and lower tMME and dMME (without steroids: 318.8 tMME and 89.3 dMME; with steroids: 323.8 tMME and 103.0 dMME; EA: 625.0 tMME and 163.3 dMME; p<0.001). On multivariate analysis, cACB groups were at a significantly lower odds of experiencing a pLOS compared to EA patients without steroids (OR=0.64; 95% CI 0.49–0.84; p<0.001; with steroids: OR=0.54; 95% CI 0.38-0.76; p<0.001). cACB groups had significantly lower odds of a non-home discharge when compared to EA patients (without steroids OR=0.42; 95% CI 0.36-0.48; with steroids: OR 0.22; 95% CI 0.18-0.27). On multivariate analysis, cACB groups required significantly less tMME compared to the EA group (without steroids β=-290 MME; 95% CI: -313 to -268 MME; with steroids: β=-261 MME; 95% CI: -289 to -233 MME) as well as significantly lower dMME (without steroids: β=-66 MME/day; 95% CI -72 to -60 MME/day; p<0.001; with steroids: β=-48 MME/day; 95% CI -55 to -40 MME/day; p<0.001).

Conclusions: The current study is the first to simultaneously evaluate the efficacy of EA, cACB without perineural steroids, and cACB with steroids as local anesthetic adjuvants. These findings suggest cACB is significantly associated with greater discharge to home rates, lower rates of pLOS, and lower tMME and dMME consumption.

References: Kim DH, …, Yadeau JT. Adductor canal block versus femoral nerve block for total knee arthroplasty: a prospective, randomized, controlled trial. Anesthesiology 2014;120:540-50.

Kayupov E, …, Della Valle CJ. Continuous Adductor Canal Blocks Provide Superior Ambulation and Pain Control Compared to Epidural Analgesia for Primary Knee Arthroplasty: A Randomized, Controlled Trial. J Arthroplasty 2018;33:1040-4 e1.

Willett A, Lew R, Wardhan R. Is continuous proximal adductor canal analgesia with a periarticular injection comparable to continuous epidural analgesia for postoperative pain after Total Knee Arthroplasty? A retrospective study. Rom J Anaesth Intensive Care 2019;26:9-15.

Table 1: Demographics of patients undergoing **primary total knee replacement** organized by nerve block type

Nerve Block Type	Epidural Analgesia	cACB without Steroids	cACB with Steroids	P-value
N = 4,345 (100%)	N = 1,556 (35.83%)	N = 2,087 (48.03%)	N = 702 (16.13%)	
Age: Mean [SD]	**67.0 [9.7]**	**67.9 [9.6]**	**67.4 [9.4]**	**0.015**
18 - 54	181 (11.62%)	176 (8.43%)	60 (8.55%)	
55 - 64	473 (30.37%)	615 (29.47%)	218 (31.05%)	
65 - 74	544 (34.96%)	819 (39.24%)	270 (38.46%)	
≥ 75	358 (22.99%)	477 (22.86%)	154 (21.94%)	
Sex				0.29
Male	572 (36.73%)	741 (35.51%)	272 (38.75%)	
Female	984 (63.26%)	1,346 (64.49%)	430 (61.25%)	
BMI: Mean [SD]	31.95 [6.58]	32.08 [6.46]	32.25 [6.59]	0.86
< 25	203 (13.13%)	257 (12.31%)	77 (10.97%)	
25 - 30	462 (30.31%)	608 (29.13%)	215 (30.63%)	
30 - 35	443 (27.77%)	600 (28.75%)	199 (28.35%)	
> 35	448 (28.18%)	622 (29.80%)	211 (30.06%)	
ASA				**0.001**
1	62 (3.98%)	80 (3.83%)	26 (3.70%)	
2	904 (58.10%)	1,197 (57.36%)	352 (50.14%)	
3	565 (36.31%)	790 (37.85%)	319 (45.44%)	
4+	25 (1.61%)	20 (0.96%)	5 (0.71%)	
Functional Status (prior to surgery):				**0.002**
Independent	1,554 (99.87%)	2,066 (98.99%)	693 (98.72%)	
Partially/Totally dependent	2 (.14%)	21 (1.00%)	9 (1.28%)	
Race				0.073
White	1,297 (83.35%)	1,741 (83.42%)	555 (79.06%)	
Black/African American	171 (10.99%)	249 (11.93%)	96 (13.68%)	
Asian	14 (0.89%)	13 (0.62%)	9 (1.28%)	
Not Reported	74 (4.76%)	84 (4.02%)	42 (5.98%)	

Bolding indicates statistical significance at p < 0.05
ASA = American Society of Anesthesiologists classification

Table 2: Postoperative analgesia and outcomes following **primary total knee replacement** organized by nerve block type

Nerve Block Type	Epidural Analgesia	cACB without Steroids	cACB with Steroids	P-value
N = 4,345 (100%)	N = 1,556 (35.83%)	N = 2,087 (48.03%)	N = 702 (16.13%)	
Postoperative MME (median [IQR])				
tMME (MME)	**625.0 [513.0, 759.0]**	**318.8 [110.6, 490.1]**	**323.8 [287.9, 535.2]**	**<0.001**
dMME (MME/d)	**163.3 [128.2, 192.8]**	**89.3 [37.7, 141.7]**	**103.0 [72.1, 162.7]**	**<0.001**
Discharge Disposition				**<0.001**
Home	718 (46.14%)	1,344 (64.40%)	527 (75.07%)	
Other	838 (53.86%)	743 (35.60%)	175 (24.93%)	
Mean Hospital Length of Stay (SD)	**3.14 (2.03)**	**2.69 (1.23)**	**2.54 (1.64)**	**<0.001**
Long hospital length of stay (> 3 days)	**197 (12.66%)**	**178 (8.53%)**	**59 (8.40%)**	**<0.001**
All Adverse Events	78 (5.01%)	107 (5.13%)	26 (3.70%)	0.31
Major Adverse Events	58 (3.72%)	71 (3.40%)	15 (2.13%)	0.17
Deep Infection	2 (0.13%)	2 (0.09%)	0 (.00%)	0.64
Sepsis/Septic shock	6 (0.39%)	8 (0.38%)	3 (.43%)	0.99
Ventilator >48 hrs	3 (0.19%)	0 (0.00%)	0 (.00%)	0.067
Unplanned Intubation	4 (0.26%)	2 (0.09%)	0 (.00%)	0.24
Acute Renal Failure	1 (0.06%)	0 (0.00%)	0 (.00%)	0.41
Venothrombolic Event	**53 (3.41%)**	**68 (3.26%)**	**11 (1.57%)**	**0.049**
Cardiac Arrest	0 (0.00%)	0 (0.00%)	1 (.14%)	0.074
Myocardial Infarction	1 (0.06%)	4 (0.19%)	1 (.14%)	0.59
Stroke	0 (0.00%)	2 (0.10%)	1 (.14%)	0.40
Minor Adverse Events	25 (1.61%)	45 (2.16%)	13 (1.85%)	0.52
Superficial Infection	6 (0.39%)	8 (0.38%)	5 (.71%)	0.48
Wound Disruption	1 (0.06%)	0 (0.00%)	1 (.14%)	0.29
Pneumonia	13 (0.84%)	15 (0.72%)	1 (.14%)	0.16
Urinary Tract Infection	7 (0.45%)	22 (1.05%)	5 (.75%)	0.12
Progressive Renal Insufficiency	0 (0.00%)	3 (0.14%)	0 (.00%)	0.20
Readmissions	77 (4.95%)	113 (5.41%)	41 (5.84%)	0.67

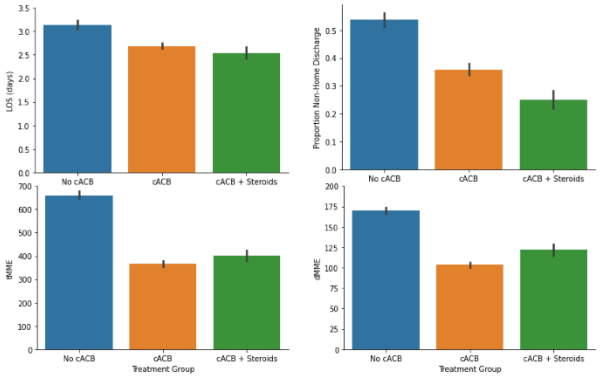

Table 3: Factors associated with **pLOS** following primary total knee arthroplasty

N = 4,345 (100%)	OR[1]	95% CI[1]	P-Value	Q-Value[2]
Analgesia Type				
Epidural*	1.00	–	–	–
CACB without steroids	0.64	**[0.49, 0.84]**	**<0.001**	**0.002**
CACB with steroids	0.54	**[0.38, 0.76]**	**<0.001**	**0.002**
Age				
18-54	1.00	–	–	–
55-64	0.73	[0.49, 1.09]	0.12	0.20
65-74	0.77	[0.53, 1.16]	0.20	0.30
≥75	0.89	[0.59, 1.36]	0.60	0.60
Sex (Female)	0.86	[0.68, 1.10]	0.20	0.30
Race				
White	1.00	–	–	–
Asian	**3.03**	**[1.10, 7.08]**	**0.017**	**0.032**
Black or African American	**2.03**	**[1.50, 2.72]**	**<0.001**	**<0.001**
Unknown/Not Reported	0.99	[0.54, 1.67]	>0.9	>0.9
ASA Class				
1	1.00	–	–	–
2	2.17	[0.96, 6.19]	0.10	0.20
3	**3.62**	**[1.61, 10.30]**	**0.006**	**0.012**
4+	**10.3**	**[3.53, 34.50]**	**<0.001**	**<0.001**
tMME (per 100mg)	**1.08**	**[1.05, 1.12]**	**<0.001**	**<0.001**

[1] OR = Odds Ratio, CI = Confidence Interval
[2] False discovery rate correction for multiple testing

Table 4: Impact of type of nerve block on **non-home discharge**.

N = 4,345 (100%)	OR[1]	95% CI[1]	P-Value	Q-Value[2]
Analgesia Type				
Epidural*	1.00	–	–	–
CACB without steroids	**0.42**	**[0.36, 0.48]**	**<0.001**	**<0.001**
CACB with steroids	**0.22**	**[0.18, 0.27]**	**<0.001**	**<0.001**
Age				
18-54	1.00	–	–	–
55-64	**1.37**	**[1.07, 1.75]**	**0.014**	**0.016**
65-74	**1.47**	**[1.15, 1.88]**	**0.002**	**0.003**
≥75	**2.62**	**[2.01, 3.42]**	**<0.001**	**<0.001**
Sex (Female)	**0.67**	**[0.58, 0.77]**	**<0.001**	**<0.001**
BMI	**1.16**	**[1.08, 1.25]**	**<0.001**	**<0.001**
Dependent Functional Status	**4.77**	**[2.06, 12.4]**	**<0.001**	**<0.001**
Race				
White	1.00	–	–	–
Asian	**2.57**	**[1.26, 5.30]**	**0.010**	**0.012**
Black or African American	**3.48**	**[2.82, 4.31]**	**<0.001**	**<0.001**
Unknown/Not Reported	**1.38**	**[1.01, 1.88]**	**0.043**	**0.046**
ASA Class				
1	1.00	–	–	–
2	1.46	[1.00, 2.17]	.058	0.058
3	**2.79**	**[1.89, 4.19]**	**<0.001**	**<0.001**
4+	**3.13**	**[1.56, 6.37]**	**0.001**	**0.002**

[1] OR = Odds Ratio, CI = Confidence Interval
[2] False discovery rate correction for multiple testing

Regional Anesthesia 6- Quality Improvement project to promote early use of preoperatively inserted epidural catheters

Richa Sharma[1], Roniel Weinberg[2]

New York Presbyterian Hospital, Weill Cornell Medicine[1] Weill Cornell Medicine[2]

Introduction: Presently at our institution patients who have epidural catheters placed preoperatively do not have an epidural infusion initiated until they arrive in the recovery room. Those whose epidural catheters are used intraoperatively, receive infusions prepared by intraoperative anesthesiology team which likely is not at par with that prepared in pharmacy in terms of sterility, standardization. This also places the burden on the OR anesthesia staff to obtain and prepare the drugs for infusion and manually bolus the epidural at certain intervals. The patients whose epidurals are not used or insufficiently used intraoperatively are denied multitude of proven benefits such as preemptive epidural analgesia(1), opioid sparing intraop course, decrease in endocrine(3) and metabolic(4) stress response perioperatively. They also experience pain in the recovery room while awaiting connection and start of epidural infusion.

We undertook this study to explore the causes of delay in use of epidural catheter and to institute measures to facilitate early use.

Methods: • The unique aspect of our QI project was that many anesthesia staff members had, at various times, invested efforts into finding the root cause and improving the process but never reached fruition. We got inputs from all of these leaders and consolidated the groundwork they had started to lay.
– We made a process map as it is at baseline and uncovered the root causes of the delay in use of epidural catheter
– We had enthusiastic support of our division's leadership and the QI committee leadership.
• We formed a multi-disciplinary including anesthesiologists (attendings and housestaff), pharmacists, nurses, electronic health record analysts and biomedical engineering.
– We knew that at baseline 0 patients were coming out with epidural infusion connected and running from the OR. A survey of more than 70 anesthesiology staff revealed that a major barrier to their use was unavailability of equipment and prepared infusion in the OR. Many of the staff were also unfamiliar with the equipment.
– Developed a comprehensive plan to make epidural infusions prepared by pharmacy stocked and available for OR teams, and for pumps to be available intraoperatively. We created job aids to help new users set up pumps. EPIC prompts were introduced to remind teams to administer and chart epidural medications.
– Outcome measures included number of patients arriving to PACU with epidural infusion running or ready to be connected, time to first epidural use since insertion, Patients' comfort in PACU. Process measures included delays due to delay in obtaining pumps/infusions and calls to the acute pain service.
– Counterbalances were taken into account to ensure no one team was burdened more than before the interventions. Nursing buy-in was ensured for sustainable availability of the pumps for every patient who had an epidural catheter and smooth transition into post-operative period and the responsibility of pump availability remained with their team. The calls to acute pain service for help with setting up intraoperative infusions were tracked.
– Ongoing evaluation and improvement will be undertaken.

Results: The results for this study are awaited and should be available after go-live in a month. They will be shared at the time of the conference.

Baseline data will include all the outcome measures from May 2021- November 2022. This will be compared against the same data from the prospective phase expected to start in January 2023.

Conclusions: We do not have the post-implementation data at present and baseline data including how long it takes for the epidural catheters to be first used at present are unavailable. We know that the infusions/ boluses that are administered through the catheters at present are not prepared by the pharmacy and therefore there is room for standardization and increased sterility of the solutions, and that no patients are coming out of the OR with a pump at their side connected or ready to be connected. All these numbers are expected to increase. Ultimately, the patient pain scores and opioid consumption in the PACU will be the most telling finding. We are currently gathering the baseline data.

References: (1) Preemptive epidural analgesia and recovery from radical prostatectomy: a randomized controlled trial. JAMA. 1998;279(14):1076-1082

(2) The efficacy of preemptive analgesia for acute postoperative pain management: a meta-analysis. Anesth Analg. 2005;100(3):757-773

(3) The effect of thoracic peridural analgesia on the cortisol and glucose response in surgery of the abdominal aorta. Reg Anaesth. 1988;11(1):16-20

(4) Thoracic peridural anesthesia for intra- and postoperative analgesia in lung resections. A comparison of stress reactions and postoperative lung function. Reg Anaesth. 1984;7(4):115-124

(4) Combined general/epidural anesthesia (ropivacaine 0.375%) versus general anesthesia for upper abdominal surgery. Anesth Analg. 2008;106(5):. doi:10.1213/ane.0b013e31816d1976

AUA 2023 Annual Meeting Scientific Abstracts

Background

- Patients with epidurals are arriving to PACU without PCEA ready immediately. This can lead to delays in treatment of pain.
- Unavailability of pumps in the OR denies patients the chance to benefit from intraoperative epidural use.
- Scope
  - Setting: 3N Pre-Op, G3 ORs, 3C/N PACU
  - Patients: Same-day admit
  - Stakeholders: Nursing, anesthesia teams, central supply, pharmacy, Epic IT personnel
- Process
  - Start: Patient arrives to pre-op / block space
  - End: PCEA pump connected

Problem Statement

- What - Delay to PCEA connection
- Who - Patients with epidurals in-place undergoing surgery
- When - Daily
- How - Approx 3x/day
- Where – Main hospital campus perioperative area.
- Why - medication safety, pain control, patient satisfaction, increased opioid use

SMART Goal

- 85% of patients arrive to PACU with epidural PCEA pump and tubing by January 31, 2023 5pm
- 70% of patients arrive to PACU with epidural PCEA connected by January 31, 2023 5pm.
- 60% of patients arrive to PACU with epidural PCEA running by January 31, 2023 5pm

Pearls from Literature Review:

- **Focused studies on intraoperative epidural analgesia – different regimens, use versus no use and controlled for post-op epidural infusion use are lacking.**
- **Studies that look at intra-op/postop epidural use vs. no use have established following benefits:**
  - **Pre-emptive epidural analgesia significantly decreases postoperative pain during hospitalization and long after discharge and is associated with increased activity levels after discharge.**
  - **Effect size was most pronounced for preemptive administration of epidural analgesia compared to NMDA antagonists and opioids.**
  - **Decreased metabolic and immune stress response**
- **Newer studies have shown decreased PACU LOS with intra-op epidural analgesia and correlate to the proportion of surgery that epidural catheter was used.**

Data- baseline observations and process map:

- **Data on outcome and process measures awaited from the CPO team.**
- **0% Patients currently arrive to the PACU with pumps at bedside currently.**

Key Measures

- Outcome Measures
  - % of patients arriving to PACU with PCEA (a) running, (b) connected, (c) ready to connect
  - Time between "anesthesia stop" and nursing documentation of epidural infusion
  - Patient pain scores and opioid requirement in PACU
  - Time between epidural catheter insertion and documentation of drug route as epidural?
- Process Measures
  - Obtaining PCEA pumps in a timely manner
  - Obtaining epidural bags in a timely manner
  - APS calls to help set up pumps

Respiration

Respiration 1- Disparities in lung-protective ventilation using low driving pressures among female and male patients undergoing surgery: a matter of compliance

Eva-Lotte Seibold[1], Ricardo Munoz[2], Simone Redaelli[1], Aiman Suleiman[1], Dario von Wedel[1], Guanqing Chen[1], Daniel Talmor[3], Elias Baedorf Kassis[1], Maximilian Schaefer[4]

Beth Israel Deaconess Medical Center, Harvard Medical School[1] BIDMC[2] Beth Israel Deaconess Medical Center[3] Beth Israel Deaconess Medical Center & Hospital[4]

Introduction: Lung-protective intraoperative ventilation can protect patients from ventilator-induced lung injury and subsequently postoperative pulmonary complications, which have been linked to substantial morbidity and a 20-fold increase in mortality [1]. Previous studies reported that female patients are at greater risk of receiving non-protective intraoperative mechanical ventilation [2,3]. However, protective mechanical ventilation was defined as the use of low tidal volumes, and more recent studies have shown that not the tidal volume, but the resulting driving pressure is the key driver of ventilator induced lung injury [4]. We hypothesized that compared to men, female patients are at greater risk of receiving intraoperative mechanical ventilation with high driving pressures due to lower respiratory system compliance [5].

Methods: In this retrospective study, we included adult patients who underwent general anesthesia between January 2011 and June 2022. We excluded patients with American Society of Anesthesiologists (ASA) class > IV, undergoing cardiac surgery, microlaryngoscopy surgery or who were already intubated prior to the procedure. The primary exposure was the patient sex, as defined in the Casemix billing system. The primary outcome was high driving pressure ventilation, defined as median intraoperative driving pressure >15 cmH2O. We applied multivariable logistic regression analyses, adjusted for a priori defined confounders that accounted for patient demographics (age, height, BMI), comorbidities (ASA, Elixhauser Comorbidity Score, obstructive sleep apnea, restrictive and obstructive pulmonary disease, chronic heart failure) and intraoperative factors. Further, we tested whether any association between sex and high driving pressure was mediated by patients' baseline dynamic respiratory system compliance.

Results: 150,729 cases were included in this study (**Figure 1**). 78,510 (52.1%) of which received intraoperative mechanical ventilation with high driving pressures. The median (IQR) driving pressure in female patients (83,704; 55.5%) was 15.7 cmH2O (12.2-20.0) and in male patients 15.0 cmH2O (12.0-19.0), as described in **Table 1.** Female patients had a lower baseline dynamic respiratory system compliance when compared to men (median (IQR) 33.5 mL/cmH2O vs. 38.1 mL/cmH2O, respectively, **Figure 2**). While ideal body weight-adjusted tidal volumes were similar between male and female patients (**Table 1**), female patients were at a slightly increased risk of receiving high-driving pressure ventilation, even when adjusting for potential confounding factors (adjOR 1.09; 95%CI 1.05-1.12; p<0.001). Mediation analysis revealed that this effect was completely mediated by lower baseline dynamic respiratory system compliance (**Figure 3**).

Conclusions: Female patients are at greater risk of receiving non-protective ventilation with high driving pressures. Our findings suggest that while physicians deliver similar weight-adjusted tidal volumes to male and female patients, they do not account for a lower respiratory system compliance in female patients.

References:

[1] Postoperative pulmonary complications. Br J Anaesth. 2017;118(3):317-334.

[2] Sex difference and intra-operative tidal volume: Insights from the LAS VEGAS study. Eur J Anaesthesiol. 2021;38(10):1034-1041.

[3] Short women with severe sepsis-related acute lung injury receive lung protective ventilation less frequently: an observational cohort study. Crit Care. 2011;15(6):R262.

[4] Association between intraoperative tidal volume and postoperative respiratory complications is dependent on respiratory elastance: a retrospective, multicentre cohort study. Br J Anaesth. 2022;129(2):263-272.

[5] Sex Differences in Thoracic Dimensions and Configuration. Am J Respir Crit Care Med. 2003;168(3):305-312.

Characteristics	Female (n=83,704)	Male (n=67,025)
Age, years	55.0 (42.0 - 67.0)	58.0 (45.0 - 68.0)
Body mass index, kg/m2	27.3 (23.4 - 32.5)	27.4 (24.4 - 31.4)
Height, m	1.6 (1.6 - 1.7)	1.8 (1.7 - 1.8)
ASA Physical Status		
1	8,808 (10.5%)	6,834 (10.2%)
2	42,397 (50.7%)	28,804 (43.0%)
3	29,701 (35.5%)	27,856 (41.6%)
4	2,798 (3.3%)	3,531 (5.3%)
Type of surgery		
Colorectal	2,473 (3.0%)	2,297 (3.4%)
Oral/maxillofacial surgery	229 (0.3%)	341 (0.5%)
Ear, nose, throat	2,756 (3.3%)	3,059 (4.6%)
Eye	175 (0.2%)	149 (0.2%)
General Surgery	13,596 (16.2%)	11,054 (16.5%)
Gastrointestinal	224 (0.3%)	252 (0.4%)
Neurosurgery	4,867 (5.8%)	4,733 (7.1%)
Orthopedic Surgery	18,088 (21.6%)	17,697 (26.4%)
Plastic Surgery	7,726 (9.2%)	3,519 (5.3%)
Podiatry	288 (0.3%)	300 (0.4%)
Surgical oncology	4,170 (5.0%)	1,708 (2.5%)
Thoracic Surgery	4,278 (5.1%)	4,332 (6.5%)
Transplant	1,256 (1.5%)	1,604 (2.4%)
Trauma / Surgical Critical Care	934 (1.1%)	1,350 (2.0%)
Urology	3,997 (4.8%)	8,470 (12.6%)
Vascular Surgery	2,858 (3.4%)	3,711 (5.5%)
Comorbidities		
Elixhauser Comorbidity Score	12.0 (4.0 - 23.0)	12.0 (4.0 - 23.0)
History of CHF	6,508 (7.8%)	6,527 (9.7%)
History of obstructive sleep apnea	6,812 (8.1%)	7,306 (10.9%)
History of obstructive pulmonary disease	23,361 (27.9%)	16,250 (24.2%)
History of restrictive pulmonary disease	3,351 (4.0%)	3,195 (4.8%)
Surgical factors		
Duration of surgery, min	134.0 (90.0 - 200.0)	133.0 (89.0 - 201.0)
Emergency surgery	6,962 (8.3%)	6,724 (10.0%)
Attending as primary provider	15,533 (18.6%)	11,020 (16.4%)
Total vasopressor dose (Norepinephrine equivalents), mg	0.0 (0.0 - 0.1)	0.0 (0.0 - 0.2)
Packed red blood cells, units	0.0 (0.0 - 0.0)	0.0 (0.0 - 0.0)
Crystalloids and colloids, ml	1000.0 (700.0 - 1500.0)	1000.0 (700.0 - 1500.0)
Total short-acting opioid dose (oral morphine equivalents), mg	25.0 (12.5 - 50.0)	25.0 (25.0 - 50.0)
Total long-acting opioid dose (oral morphine equivalents), mg	6.8 (0.0 - 17.0)	6.8 (0.0 - 17.0)
NMBA, ED95	2.0 (0.0 - 3.1)	1.9 (0.0 - 3.1)
Respiratory parameters		
PIP, cmH2O	19.8 (16.0 - 24.3)	19.3 (15.7 - 23.3)
PEEP, cmH2O	5.0 (2.0 - 5.1)	5.0 (2.0 - 5.1)
Tidal Volume, Median (mL)	500.0 (423.8 - 560.0)	560.0 (481.8 - 619.5)
Standardized Tidal Volume (mL/kg)	8.4 (7.2 - 9.6)	8.3 (7.1 - 9.3)
Baseline dynamic respiratory system compliance, mL/cmH2O	33.5 (26.9 - 40.9)	38.1 (30.8 - 46.2)
Driving pressure, cmH_2O	15.7 (12.2 - 20.0)	15.0 (12.0 - 19.0)
Airway device		
Endotracheal tube	69,546 (83.1%)	54,413 (81.2%)
Laryngeal mask airway	13,860 (16.6%)	12,292 (18.3%)
Combined	298 (0.4%)	320 (0.5%)

Table 1. Patient characteristics and distribution of variables. *Data are expressed as frequency (prevalence in %) or median (interquartile range). DP: driving pressure; ASA: American Society of Anaesthesiologists; CHF: congestive heart failure; ED95: dose of neuromuscular blocking agents (NMBA): median effective dose required to achieve a 95% reduction in maximal twitch response from baseline; NMBA: neuromuscular blocking agents; PIP: peak inspiratory pressure; PEEP: positive end-expiratory pressure*

Figure 1 Study flow diagram

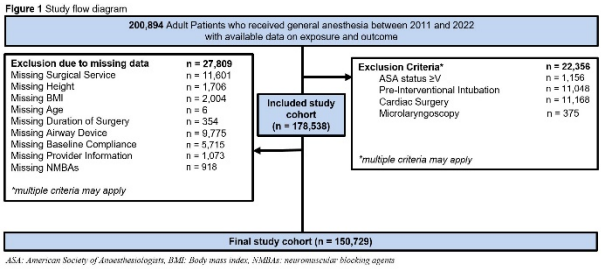

ASA: American Society of Anaesthesiologists; BMI: Body mass index; NMBAs: neuromuscular blocking agents

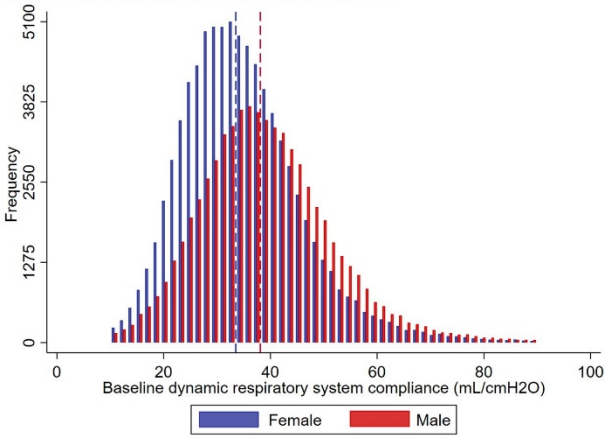

Figure 2. Distribution of patients' baseline dynamic respiratory system compliance by sex (female, in blue; male, in red)

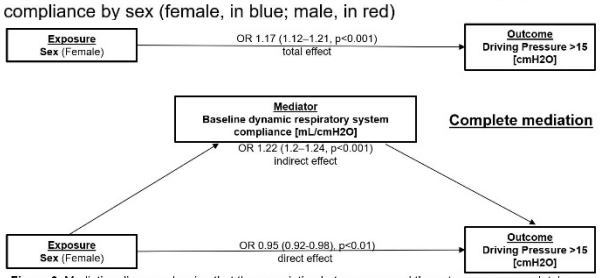

Figure 3. Mediation diagram showing that the association between sex and the outcome was completely mediated by baseline dynamic respiratory system compliance of the patient.

Respiration 2- Ginger metabolites and metabolite-inspired synthetic derivatives modulate cytoskeletal regulatory proteins controlling airway smooth muscle tone

Elvedin Lukovic[1], Yingdong Zhu[1], Shengmin Sang[1], Charles Emala[1]

Columbia University Medical Center, Depa[1]

Introduction: Asthma includes pathological alterations in airway smooth muscle (ASM). Due to poor symptom management in many asthmatics with available therapies, alternatives are imperative. Our lab demonstrated that 6-shogaol (6S), a bioactive constituent of ginger, relaxes *ex vivo* ASM by inhibiting phospholipase C (PLC). PLC generates inositol triphosphate (IP3) and diacylglycerol (DAG), both of which facilitate ASM contraction – IP3 by increasing intracellular calcium, and DAG by indirectly modulating cytoskeletal regulatory proteins including CPI-17 and MLC_{20}. Previously we showed that 6S affects both the IP3 and DAG arms of the pathway. However, 6S is metabolized rapidly and extensively. Recently we determined that metabolites and metabolite-inspired synthetic derivatives also acutely relax ASM by inhibiting the IP3-mediated calcium increases. Here we hypothesize that these metabolites and derivatives also inhibit the DAG arm of the PLC pathway, thereby affecting cytoskeletal regulatory proteins and relaxing ASM.

Methods: Human ASM cells were transduced with a viral vector encoding a DAG-specific fluorescent protein (Montana Molecular), then pretreated with 6S, metabolites, or synthetic derivatives, and challenged with the Gq-coupled ligand bradykinin (10 µM) to measure DAG synthesis. To examine the effect of these compounds on cytoskeletal proteins, ASM cells were pretreated with the derivatives (100 µM), then stimulated with the Gq-coupled ligand acetylcholine (Ach, 100 µM), lysed, and the levels of phosphorylated CPI-17 and MLC_{20} (normalized to GAPDH levels) were determined by immunoblotting. Statistical analysis included one-way ANOVA and was performed using GraphPad Prism.

Results: Treatment with 6S, 6S metabolites (M6, M9), and synthetic derivatives (M14-4, 404-1, 435-1, 441-2, 445-1) significantly decreased bradykinin-induced DAG levels ($p < 0.001$ to 0.01 compared to bradykinin, $n = 3$). Moreover, those compounds also modulate the phosphorylation of the downstream proteins CPI17 and MLC_{20}, which are important regulatory proteins in ASM contraction. 6S and its main metabolite M6 significantly decrease Ach-induced phosphorylation of CPI-17 ($p < 0.01$ compared to Ach, $n = 5$), and MLC_{20} ($p < 0.05$ compared to Ach, $n = 5$) by inhibiting the DAG arm of the PLC pathway.

Conclusions: 6S, a major bioactive compound in ginger, and its metabolites inhibit PLC and prevent Gq-coupled ASM contraction by preventing IP3-mediated calcium increases, and by regulating the activity of cytoskeletal regulatory proteins in the DAG arm of the PLC pathway. Moreover, novel synthetic compounds inspired by these metabolites retain the ability to modulate these pathways and may be promising new drugs for asthma.

Respiration 3- Cannabis use and postoperative respiratory complications: A hospital registry study

Sarah Ashrafian[1], Ricardo Munoz[2], Elena Ahrens[1], Luca Wachtendorf[3], Denys Shay[1], Aiman Suleiman[4], Simone Redaelli[4], Dario von Wedel[4], Laetitia Chiarella[5], Guanqing Chen[5], Kevin Hill[1], Maximilian Schaefer[6]

Beth Israel Deaconess Medical Center[1] BIDMC[2] Montefiore Medical Center[3] Beth Israel Deaconess Medical Center, Harvard Medical school[4] Director, Center for Anesthesia Research Excellence (CARE).[5] Beth Israel Deaconess Medical Center & Hospital[6]

Introduction: The use of cannabis is subject to a growing trend of legalization and decriminalization, leading to increased consumption in the overall population of the United States [1,2]. Some studies suggest that the chronic use of cannabis induces structural changes in the lung parenchyma and airways similar to those resulting from tobacco smoke [3]. By contrast, other studies showed that cannabis can act as an anti-inflammatory agent and bronchodilator. It is unknown whether these effects impact patients' risk of perioperative respiratory complications [1,4–6]. We hypothesized that patients who consume cannabis are at increased risk of respiratory complications after surgery.

Methods: Adult patients who underwent non-cardiac procedures under general anesthesia between 2008 and 2020 at a tertiary academic hospital in Massachusetts, USA, were included in this study. The primary exposure was ongoing use of cannabis, and patients were categorized into four groups - recreational cannabis users (identified from structured nursing or physician interviews), patients with a prescription for medical cannabinoids, patients diagnosed with a cannabis use disorder (identified through International Classification of Diseases (9th/10th Revision, Clinical Modification [ICD-9/10-CM]) diagnostic codes), and patients who were identified as non-users. The primary outcome was the occurrence of postoperative respiratory complications, defined as non-invasive ventilation or reintubation within seven days after the index procedure. Multivariable logistic regression analyses, adjusted for patient demographics and characteristics, including comorbidities, pre-procedural drug prescriptions as well as anesthesia-related and procedural factors was applied. We also adjusted for multiple socioeconomic factors, considering that patients who consumed cannabis and patients who did not are represented through strongly differing patient populations.

Results: 146,664 patients were included in this analysis (**Figure 1**). 13,368 (9.1%) were identified as cannabis users (**Table 1**), of whom 9,647 (72.2%) used cannabis for recreational purposes, 1,821 (13.6%) had a prescription for medical cannabinoids, and 1,900 (14.2%) had a diagnosed cannabis use disorder. 1,353 (0.9%) patients developed postoperative respiratory complications within seven days after surgery. In adjusted analyses, there was no association between recreational cannabis consumption (adjusted odds ratio [ORadj] 0.97; 95%CI 0.75–1.25; p=0.81), medical cannabinoid use (ORadj 0.93; 95%CI 0.63–1.37; p=0.71) or diagnosed cannabis use disorder (ORadj 0.80; 95%CI 0.51–1.25; p=0.32) with postoperative respiratory complications, respectively. Similarly, we did not observe an association between recreational cannabis use (ORadj 1.06; 95%CI 0.95–1.18; p=0.32), use of medical cannabinoids (ORadj 0.80; 95%CI 0.60–1.05; p=0.11) or a cannabis use disorder (ORadj 1.05; 95%CI 0.83–1.32; p=0.68) and post-extubation oxygen desaturation.

Conclusions: Neither cannabis consumption as "simple" recreational use, abuse or use for medical purposes is associated with postoperative respiratory complications. These data do not support that patients who consume cannabis are a population at increased risk of adverse respiratory events after surgery.

References: [1] Socioeconomic factors, psychiatric disorders and substance abuse associated with cannabinoid use in surgical patients, et al.Anesth. Analg. 2022;

[2] CDC. Available from: https://www.cdc.gov/marijuana/data-statistics.htm [accessed 2022 Dec 7]

[3] Legalizing Cannabis: A physician's primer on the pulmonary effects of marijuana, Curr Respir Care Rep 2014; 3(4):200–5.

[4] Pulmonary effects of inhaled cannabis smoke, Am J Drug Alcohol Abuse 2019; 45(6):596–609.

[5] Cannabidiol, a non-psychotropic plant-derived cannabinoid, decreases inflammation in a murine model of acute lung injury: role for the adenosine A(2A) receptor, Eur J Pharmacol 2012; 678(1–3):78–85.

[6] Cannabis-based medicines and the perioperative physician, Perioper Med Lond Engl 2019; 8:19.

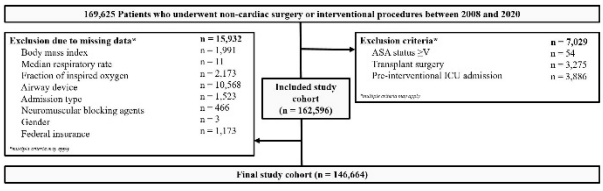

Figure 1. Study flow diagram. *Abbreviations: ASA: American Society of Anesthesiologists; ICU: Intensive care unit.*

	No cannabis consumption n=133,296	Cannabis consumption n=13,368	Standardized difference
Demographics			
Age (years)	55 ± 16	48 ± 16	0.451
Sex, female	53,376 (40.0%)	7,656 (57.3%)	-0.350
BMI (kg/m2)	27.4 (23.9 - 32.0)	26.7 (23.5 - 31.4)	0.081
Federal insurance	39,239 (29.4%)	3,942 (29.5%)	-0.001
Comorbidities			
ASA physical status			-0.040
1	15,978 (12.0%)	1,605 (12.0%)	
2	68,353 (51.3%)	6,470 (48.4%)	
3	45,890 (34.4%)	4,987 (37.3%)	
4	3,075 (2.3%)	306 (2.3%)	
Charlson comorbidity index	0 (0 - 2)	0 (0 - 2)	-0.136
Chronic heart failure	5,026 (3.8%)	451 (3.4%)	0.021
Anemia within 1 year prior	17,206 (12.9%)	2,042 (15.3%)	-0.068
Obstructive pulmonary disease	33,021 (24.8%)	3,929 (29.4%)	-0.104
Restrictive pulmonary disease	6,016 (4.5%)	631 (4.7%)	-0.010
Home oxygen dependency	1,083 (0.8%)	88 (0.7%)	0.018
Obstructive sleep apnoea	10,060 (7.5%)	1,134 (8.5%)	-0.034
History of drug use without cannabis	6,553 (4.9%)	2,153 (16.1%)	-0.371
Smoking	16,900 (12.7%)	3,691 (27.6%)	-0.379
Drug prescriptions			
Preoperative opioid prescription	24,071 (18.1%)	3,632 (27.2%)	-0.219
Ventilatory parameters			
Respiratory rate, median (IQR) (bpm)	11.8 (10.0 - 12.5)	12.0 (10.0 - 13.0)	-0.113
Tidal volume, median (IQR) (ml)	525.0 (430.5 - 599.5)	530.0 (442.1 - 600.0)	-0.059
Respiratory system compliance, median (IQR) (ml/cmH2O)	32.4 (25.7 - 40.0)	33.9 (26.9 - 41.7)	-0.117
Fraction of inspired oxygen (%)	56.0 (49.5 - 63.0)	56.0 (50.0 - 63.3)	-0.027
Positive end-expiratory pressure, median (IQR) (cmH2O)	3.5 (2.0 - 5.1)	4.1 (2.0 - 5.1)	-0.088
Airway device			0.007
Endotracheal tube	104,249 (78.2%)	10,499 (78.5%)	
Laryngeal mask	28,452 (21.3%)	2,804 (21.0%)	
Both	595 (0.4%)	65 (0.5%)	
Procedure characteristics			
Duration of surgery, median (IQR) (min)	129 (86 - 193)	130 (85 - 198)	-0.023
Admission type			-0.031
Ambulatory	63,300 (47.5%)	6,371 (47.7%)	
Same day admission	57,255 (43.0%)	5,424 (40.6%)	
Inpatient	12,741 (9.6%)	1,573 (11.8%)	
Surgical service			-0.005
Colorectal surgery	3,587 (2.7%)	403 (3.0%)	
Dental, oral surgery	167 (0.1%)	37 (0.3%)	
Ear, nose, throat surgery	5,675 (4.3%)	599 (4.5%)	
Ophthalmologic surgery	364 (0.3%)	22 (0.2%)	
General surgery	21,954 (16.5%)	2,055 (15.4%)	
Gastrointestinal surgery	415 (0.3%)	62 (0.5%)	
Gynecological surgery	17,607 (13.2%)	1,329 (9.9%)	
Neurological surgery	6,628 (5.0%)	947 (7.1%)	
Orthopedic surgery	32,712 (24.5%)	3,430 (25.7%)	
Plastic surgery	10,745 (8.1%)	1,222 (9.1%)	
Podiatric surgery	679 (0.5%)	62 (0.5%)	
Oncological surgery	5,473 (4.1%)	391 (2.9%)	
Thoracic surgery	7,129 (5.3%)	810 (6.1%)	
Trauma / Surgical critical care	2,647 (2.0%)	346 (2.6%)	
Urologic surgery	11,507 (8.6%)	1,141 (8.5%)	
Vascular surgery	6,007 (4.5%)	512 (3.8%)	
Crystalloid and colloid infusion, median (IQR) (ml)	1,000 (700- 1500)	1,000 (700 - 1500)	0.024
Units of packed red blood cells	0.0 (0.0 - 0.0)	0.0 (0.0 - 0.0)	0.020
Opioid dose, median (IQR) (mg oral morphine equivalents)	37.5 (25.0 - 62.5)	38.6 (25.0 - 64.1)	-0.006
Non-depolarizing NMBA, median (IQR) (ED95)	1.7 (0.0 - 2.8)	1.8 (0.0 - 3.0)	-0.078
Neostigmine use	63,177 (47.4%)	5,765 (43.1%)	0.079
Vasopressor dose, median (IQR) (mg norepinephrine equivalents)	0.0 (0.0 - 0.1)	0.0 (0.0 - 0.1)	0.007
Time of MAP <65 mmHg (min)	7.0 (2.0 - 16.0)	5.0 (1.0 - 14.0)	0.051
Age-adjusted mean alveolar concentration of inhalation anesthetics, median (IQR)	1.0 (0.9 - 1.1)	1.0 (0.9 - 1.1)	0.046
Sugammadex use	13,389 (10.0%)	2,050 (15.3%)	-0.140

Table 1. Patient characteristics by cannabis consumption.
Data are expressed as frequency (prevalence in %), or median (interquartile range [IQR, 25th-75th percentile]). Comorbidities were defined using International Classification of Diseases (9th/10th Revision, Clinical Modification [ICD-9/10-CM]) diagnostic codes.
ASA: American Society of Anesthesiologists; BMI: Body mass index; bpm: breaths per minute; ED95: Median effective dose required to achieve a 95% reduction in maximal twitch response from baseline; IQR: Interquartile range; MAP: Median arterial blood pressure; NMBA: Neuromuscular blocking agents.

Respiration 4- Diazepam Relaxes Murine Peripheral Airways and Modulates Mitochondrial Calcium Flux

Gene Yocum[1], Jose Perez-Zoghbi[1], Charles Emala[1]

Columbia University[1]

Introduction: Benzodiazepines directly relax airway smooth muscle (ASM)[1], but the mechanism remains unclear. Mitochondria affect ASM contraction in multiple ways, including ATP synthesis and cytosolic Ca^{2+} concentration ($[Ca^{2+}]_C$) modulation[2]. Interestingly, several benzodiazepines inhibit the mitochondrial Na^+-Ca^{2+} exchanger (NCLX), the primary route of mitochondrial Ca^{2+} efflux, in isolated mitochondria[3,4]. We aimed to determine the mechanism of diazepam-mediated airway relaxation using murine precision-cut lung slice (PCLS) experiments.

Methods: All studies were IACUC-approved. Viable mouse PCLSs were used to determine the effect of diazepam, and other experimental compounds, on peripheral airway area (C57BL/6 mice) and ASM cell $[Ca^{2+}]_C$ dynamics (GCaMP6f mice), *ex vivo*, using phase-contrast and confocal microscopy, respectively. Primary human ASM cell mitochondrial Ca^{2+} concentration ($[Ca^{2+}]_M$), mitochondrial membrane potential ($\Delta\psi_M$) and cellular adenosine triphosphate ([ATP]) and cyclic adenosine monophosphate ([cAMP]) concentrations were assessed *in vitro*.

Results: Diazepam rapidly relaxed methacholine (MCh)-constricted mouse peripheral airways in PCLSs in a dose-dependent manner. Flumazenil did not alter this relaxation. Furthermore, diazepam inhibited MCh-induced airway constriction in the absence of external Ca^{2+}, suggesting its mechanism of action is not wholly dependent upon modulation of external Ca^{2+} influx. Diazepam also limited constriction elicited by photo-uncaged inositol triphosphate (IP_3), but not that elicited by caffeine. This indicates that diazepam inhibits IP_3 receptor (IP_3R) function but not ryanodine receptor function. Consistent with this, diazepam rapidly suppressed MCh-induced $[Ca^{2+}]_C$ oscillations in PCLS ASM cells, a process mediated by the IP_3R, the SR/ER Ca^{2+} ATPase, store-operated Ca^{2+} entry (SOCE) and mitochondria. In separate *in vitro* experiments, diazepam led to a sustained elevation in human ASM cell $[Ca^{2+}]_M$ following exposure to MCh. CGP-37157, a classic inhibitor of NCLX, had a similar effect on $[Ca^{2+}]_M$. CGP-37157 also inhibited MCh-induced ASM $[Ca^{2+}]_C$ oscillations and airway constriction in PCLSs. Neither diazepam nor CGP-37157 altered $\Delta\psi_M$ or [cAMP] and both acutely increased [ATP] in ASM cells, *in vitro*.

Conclusions: Diazepam inhibits MCh-induced constriction and ASM $[Ca^{2+}]_C$ oscillations in mouse peripheral airways in a manner consistent with IP_3R inhibition. These effects were independent of the $GABA_A$ receptor and cAMP. Furthermore, diazepam increased $[Ca^{2+}]_M$ in ASM after MCh exposure, consistent with NCLX inhibition. Mitochondrial buffering of $[Ca^{2+}]_C$ in the IP_3R-mitochondria high $[Ca^{2+}]$ microdomain is thought to be necessary for normal IP_3R function[5-7]. By limiting mitochondrial Ca^{2+} efflux (resulting in a sustained elevation in $[Ca^{2+}]_M$), we propose that diazepam is restricting the ability of mitochondria to modulate $[Ca^{2+}]$ in this microdomain, thereby inhibiting IP_3R function, $[Ca^{2+}]_C$ oscillations and ultimately airway constriction. Additionally, diazepam-mediated modulation of mitochondrial Ca^{2+} flux may also alter SOCE, a key Ca^{2+} influx pathway in ASM cells that is necessary to maintain Ca^{2+} oscillations and airway constriction[8]. These possibilities are the focus of further study. The findings presented here support the role of mitochondria in modulating ASM $[Ca^{2+}]_C$ dynamics and airway constriction *ex vivo* and potentially represent a novel, "off target' effect of diazepam.

References: 1. Am J Respir Cell Mol Biol, 2022. 67(4): p. 482-490.

2. Arch Biochem Biophys, 2019. 663: p. 109-119.

3. Physiol Rev, 2014. 94(2): p. 519-608.

4. Trends Pharmacol Sci, 1993. 14(11): p. 408-13.

5. Curr Top Membr, 2010. 66: p. 235-72.

6. J Biol Chem, 2010. 285(3): p. 2040-50.

7. Cell Communication and Signaling, 2011.9(1):p. 19.

8. Adv Exp Med Biol, 2017. 993: p. 257-275.

Respiration 5- Quantitative assessment of postoperative hypoventilation after kidney transplantation surgery

Ana Fernandez-Bustamante[1], Matthew Fioravanti[1], Jacqueline Carrico[2], Erin Stewart[1]

University of Colorado School of Medicine[1] University of Colorado School of Medicine[2]

Introduction: Hypoventilation is a key contributor to atelectasis, hypoxemia, pneumonia, and other postoperative pulmonary complications. Postoperative hypoventilation is prevalent and multifactorial but largely unmonitored and poorly studied. An ongoing single-center clinical trial is enrolling patients receiving general anesthesia for kidney transplantation surgery and recording continuous quantitative monitoring of their minute ventilation (MV) for up to three days after surgery. We aimed to characterize the prevalence, severity, and duration of postoperative hypoventilation in study participants, and to evaluate the contribution of MV components, tidal volume and respiratory rate, to the detection of hypoventilation. We hypothesize that hypoventilation is prevalent after discharge from the post-anesthesia care unit (PACU).

Methods: We studied patients enrolled in an ongoing IRB-approved randomized clinical trial focused on neuromuscular blockade reversal and postoperative pulmonary function for patients undergoing kidney transplantation surgery. Patients after surgery are monitored continuously with a respiratory volume monitor that provides measurements of minute volume ventilation using noninvasive electrical bioimpedance technology (ExSpiron® monitor, Respiratory Motion, Inc.). Monitoring is continued until postoperative day 3 or earlier if the patient is fully ambulatory. Continuous recordings of MV and its components, tidal volume and respiratory rate, are extracted and analyzed for each individual. Hypoventilation events are identified, defined as any minute-long episode of MV<40% of expected value (expMV) for the patient's age, gender, height and weight or body surface area[1]. We will characterize the prevalence of hypoventilation events for each POD and patient during the PACU stay and after discharge from PACU (primary outcome). We will also summarize hypoventilation events severity (lowest expMV) and duration (e.g., minutes of longest event per day, accumulated minutes per day), MV components (tidal volume and respiratory rate), hospital resource utilization and pre-specified postoperative pulmonary complications[2] within the first 2 postoperative weeks. Primary and secondary outcomes will be compared from patients with any hypoventilation event after PACU discharge *versus* patients with no hypoventilation events observed.

Results: We studied 37 patients: 24 (64.9%) males, mean (SD) age 47.7 (13.4) years. At least one hypoventilation event was detected in the PACU in 20/37 (54.1%) patients and in 30/36 (83.3%) patients after PACU discharge (no monitoring available from one patient). Table 1 presents the summarized characteristics of hypoventilation events after discharge from PACU. Table 2 presents oxygen therapy duration and other hospital resource utilization in patients with any *versus* no hypoventilation events. At least one PPC was observed in 15/36 (41.7%) patients, primarily respiratory insufficiency (n=14), pneumonia (n=1), radiological atelectasis (n=1), and pleural effusion (n=1).

Conclusions: Postoperative hypoventilation is prevalent after discharge from PACU following kidney transplantation surgery. A better understanding of the impact of hypoventilation frequency, severity, and duration on the development of postoperative pulmonary complications is needed to improve outcomes.

References: 1. Galvagno, S.M., Jr., et al., *Evaluation of respiratory volume monitoring (RVM) to detect respiratory compromise in advance of pulse oximetry and help minimize false desaturation alarms.* J Trauma Acute Care Surg, 2016. **81**(5 Suppl 2 Proceedings of the 2015 Military Health System Research Symposium): p. S162-S170.

2. Fernandez-Bustamante, A., et al., *Postoperative Pulmonary Complications, Early Mortality, and Hospital Stay Following Noncardiothoracic Surgery: A Multicenter Study by the Perioperative Research Network Investigators.* JAMA Surg, 2017. **152**(2): p. 157-166.

Table 1. Summarized hypoventilation events detected after discharge from PACU.

	POD0	POD1	POD2	POD3
Patients with any hypoventilation event, number	24	26	8	1
Patients monitored, number	36	35	17	2
Hypoventilation event daily count, Mean(SD)	9.1 (15.4)	15.2 (21.0)	3.0 (6.6)	*
Longest event duration (minutes), Mean(SD)	6.1 (11.0)	11.0 (26.1)	14.5 (47.7)	*
Accumulated hypoventilation duration (minutes), Mean(SD)	24.2 (46.8)	46.4 (115.2)	5.8 (13.2)	*

(* Insufficient data to summarize)

Table 2. Hospital resource utilization.

	Patients with any hypoventilation event after PACU	Patients with no hypoventilation event after PACU
Patients requiring non-invasive ventilation, number	2	0
Hospital length of stay (days), Mean(SD)	3.4 (0.8)	3.3 (1.7)
Patients requiring Intensive Care Unit admission, number	2	1

Respiration 6- The causes of hypoxemia and their relative contribution in COVID-19 respiratory failure: a combined Multiple Inert Gas Elimination Technique and Dual-Energy Computed Tomography study

Mattia Busana[1], Anna Rau[1], Lorenz Biggemann[1], Luciano Gattinoni[1], Onnen Moerer[1], Leif Saager[1]

University Medical Center Goettingen[1]

Introduction: Hypoxemia that often follows a COVID-19 infection is the most frequent cause of therapy escalation and mortality. Since the beginning of the pandemic, a substantial scientific effort has been devoted to understanding the specific physiological aspects underlying this condition (1). Some peculiar aspects of the disease were progressively discovered, mainly the angiocentric nature of the pulmonary involvement with frequent microthrombosis and neoangiogenesis (2). While many speculations have been made over the genesis of hypoxemia, an in-vivo assessment of its causes and their relative contribution is still missing.

Methods: With approval from our local IRB and written informed consent by legal representatives, we studied 10 critically ill, PCR positive COVID-19 patients, intubated because of ARDS<7 days. Exclusion criteria were pregnancy, hepatic cirrhosis, Extracorporeal Membrane Oxygenation and known or newly discovered Patent Foramen Ovale (PFO). The recruitment of patients ran from November 2021 to March 2022. First, we performed the Multiple Inert Gas Elimination Technique (MIGET) (3). Briefly, we infused 6 inert gases (SF6, ethane, cyclopropane, isoflurane, ether, and acetone) while respiratory mechanics and hemodynamics were recorded. A time-aligned sample of arterial blood and mixed expired air through a heated mixing box were collected and analyzed with gas chromatography. The gas chromatography signals, together with the physiological variables were used as inputs into the MIGET software to calculate the distribution of ventilation and perfusion. Second, patients underwent a Dual-Energy Computed Tomography (DECT) (4). A virtual unenhanced and perfusion maps were extracted from the raw DICOM file through a three-material decomposition. The virtual unenhanced map was quantitatively analyzed to determine the amount of hyper-, well-, poorly- and non-inflated tissue. The Hounsfield Units of the perfusion map are automatically converted in grams/ml given the known density of the contrast agent. The overall sum of all lung regional perfusions corresponds to the whole cardiac output. We analyzed the distribution of the perfusion in relation to the aeration of the underlying lung tissue. The normal distribution of the variables was assessed with the Shapiro-Wilk test. Data are presented as mean ± standard deviation or median [interquartile range] as appropriate. Relationship between variables was assessed with linear regression. Two-tailed p values < 0.05 were considered statistically significant. The data analysis was performed in R for Statistical Computing 4.0

Results: Our study-population (n=10, 51±15 years) had a PaO_2/FiO_2 of 172±86 mmHg and a mortality of 50%. Patients were transferred to our center for an ECMO request. MIGET and DECT were performed 4 [2 - 6] days after intubation, but before ECMO. MIGET showed a true shunt of 25±16% and a deadspace of 53±12%. Ventilation and perfusion were highly mismatched, with a LogSD, Q of 0.86±0.33 (normal ~0.3). Unexpectedly, we also found evidence of diffusion limitation and/or post pulmonary shunting. At the DECT, the lungs were edematous (1427 ± 357 g, excess tissue mass 541.1 ± 248.4 g) and 100% of the patients had perfusion defects. Five patients had overt pulmonary embolism. In the non-aerated regions the fraction of lung tissue was in excess compared to the blood volume, while the latter tended to increase in better aerated lung regions. Shunt was directly proportional to the blood volume distributed in the consolidated tissue ($R^2 = 0.70$, $p = 0.003$). V_A/Q_T mismatch was correlated with the fraction of blood volume distributed to the poorly aerated tissue ($R^2 = 0.54$, $p = 0.016$). The overperfusion of the well-aerated tissue was a powerful sign of disease severity, being larger in patients with pulmonary embolism and being well related to the PaO_2/FiO_2 ($R^2 = 0.66$, $p = 0.002$), excess tissue mass ($R^2 = 0.84$, $p < 0.001$) and $EtCO_2/PaCO_2$ ($R^2 = 0.63$, $p = 0.004$)

Conclusions: These data support the hypothesis of a highly multifactorial genesis of the hypoxemia in severe COVID-19: shunt, V_A/Q_T mismatch and diffusion limitation/post-pulmonary shunting (which has never been described in ARDS from different causes) are combined in a rather unique way. The findings of MIGET and DECT combined strengthen the hypotesis that the microvascular alterations typical of COVID-19 force the augmentation of blood flow through certain lung regions, decreasing the V_A/Q_T ratio and possibly causing diffusion limitation.

References: 1) COVID-19 Does Not Lead to a 'Typical' Acute Respiratory Distress Syndrome. Am J Respir Crit Care Med 201, 1299–1300 (2020).

2) Pulmonary Vascular Endothelialitis, Thrombosis, and Angiogenesis in Covid-19. N Engl J Med 383, 120–128 (2020).

3) Continuous distributions of ventilation-perfusion ratios in normal subjects breathing air and 100 per cent O2. J Clin Invest 54, 54–68 (1974).

4) Pulmonary perfused blood volume with dual-energy CT as surrogate for pulmonary perfusion assessed with dynamic multidetector CT. Radiology 267, 747–56 (2013).

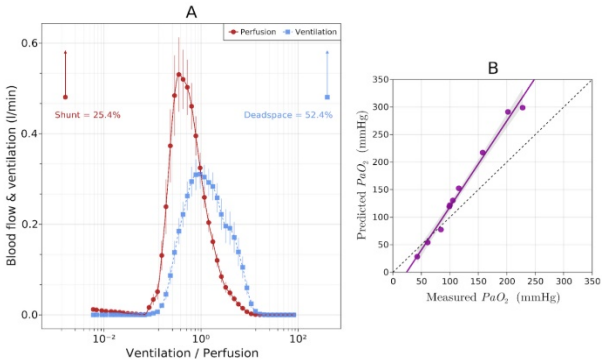

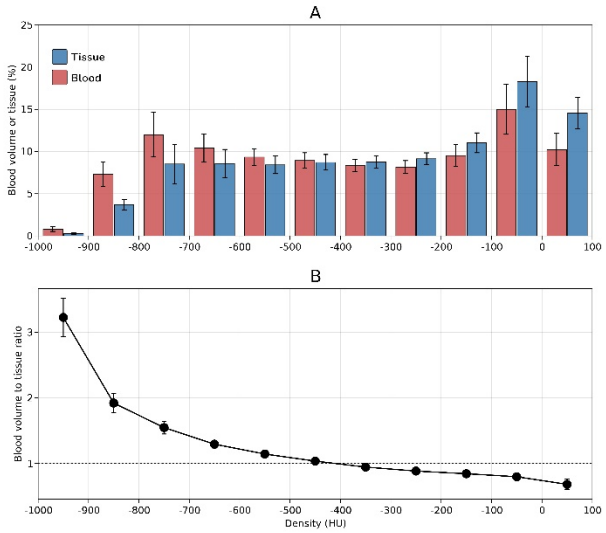

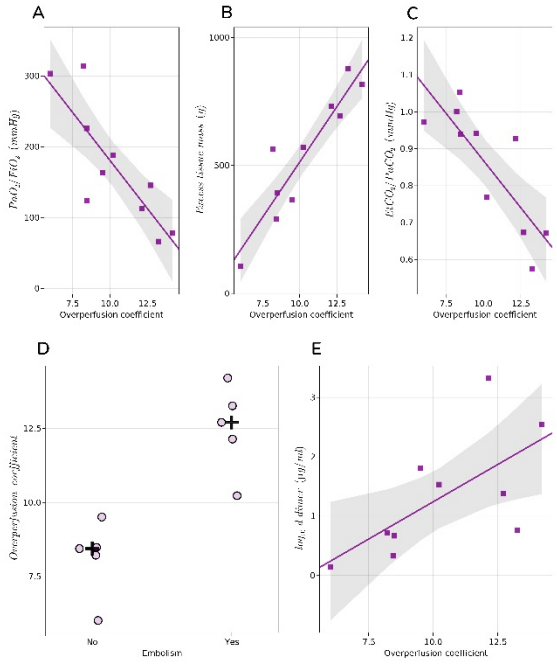

Anthropometrics	Population (n = 10)
Age (years)	51 ± 15
Female (n - %)	5 - 50%
BMI (kg*m-)	30 ± 7
Days from symptoms	12 [10 - 15]
Days from intubation	4 [2 - 6]
ICU length of stay	16 [10 - 28]
ECMO following study (n - %)	3 - 30%
ICU mortality (n - %)	5 - 50.0%
Hemodynamics	
Heart rate (bpm)	75 ± 15
Mean Arterial Pressure (mmHg)	84 ± 12
Cardiac Index (l*min-*m-)	3.13 ± 0.63
Systemic Vascular Resistance Index (dyn*s*cm-*m)	1989 ± 401
Stroke Volume Variation (%)	13 ± 7
Extravascular Lung Water Index (ml/kg)	14.7 [12.3 – 19.0]
Global End-Diastolic Volume (ml)	1213 ± 367
Gas exchange	
Tidal volume (ml/kg)	6.8 ± 2.0
Respiratory rate (bpm)	20.2 ± 7.9
Positive End-Expiratory Pressure (mmHg)	10 [9 - 11]
PaO_2/FiO_2 (mmHg)	172 ± 86
Alveolo-arterial PO_2 difference (mmHg)	289 ± 156
Qs/Qt (%)	34 ± 15
$EtCO_2$ (mmHg)	41 ± 9
Ventilatory ratio	1.48 ± 0.43
Vd/Vt (%)	47 ± 14

Ventilation - Perfusion	Population (n = 10)
Q_{mean}	0.65 ± 0.27
VA_{mean}	1.32 ± 0.77
LogSD, Q	0.86 ± 0.33
LogSD, VA	0.69 ± 0.25
Q_{zone}	0.48 [0.13 - 2.72]
VA_{zone}	0.19 [0.09 - 0.46]
Residual Sum of Squares	4.7 [3.5 - 6.9]
Perfusion distribution	
V_A/Q: 0.001 - 0.01 (%)	0 [0 - 2]
V_A/Q: 0.01 - 0.1 (%)	0 [0 - 1]
V_A/Q: 0.1 - 1 (%)	56 ± 22
V_A/Q: 1 -10 (%)	17 ± 12
V_A/Q: 10 - 100 (%)	0 [0 - 0]
Shunt (%)	25 ± 16
Ventilation distribution	
V_A/Q: 0.001 - 0.01 (%)	0 [0 - 0]
V_A/Q: 0.01 - 0.1 (%)	0 ± 0
V_A/Q: 0.1 - 1 (%)	22 ± 1
V_A/Q: 1 -10 (%)	25 ± 17
V_A/Q: 10 - 100 (%)	0 [0 - 0]
Deadspace (%)	53 ± 12

Sleep Medicine

Sleep Medicine 1- Sleep behavior traits and associations with opioid-related adverse events: a prospective cohort study

Rudy Chen[1], Ma Cherrysse Ulsa[1], Peng Li[1], Chenlu Gao[2], Xi Zheng[2], Jiawei Xu[2], Yong Luo[2], Shiqian Shen[1], Jacqueline Lane[3], Frank Scheer[2], Kun Hu[2], Lei Gao[1]

Massachusetts General Hospital[1] Brigham and Women's Hospital/ Harvard Medical School[2] Brigham and Women's Hospital[3]

Introduction: Opioid-related adverse events (OAEs) can result in serious potential consequences, including disability, relapse, overdose, poisoning, and death. In 2021 alone, overdose deaths involving opioids increased to over 80,000 in the USA.[1] Opioid use and misuse are often associated with disrupted sleep,[2–4] but the long-term relationship between poor sleep and subsequent OAE risk remains unknown. Our purpose was to investigate whether sleep behavior traits are associated with a higher risk of developing OAEs in a large population cohort.

Methods: We conducted a prospective cohort study of 444,039 participants (mean age±SD 57±8 years, range 37-74 years) from the UK general population who enrolled in the UK Biobank. Participants completed surveys (2006-2010) about their sleep behavior traits (sleep duration, daytime sleepiness, insomnia-like complaints, napping, and chronotype). The frequency of these self-reported sleep behavior traits determined an aggregate poor sleep behavior burden score (0-9). Diagnoses of incident OAEs were made using the first documentation of relevant International Classification of Disease (ICD) codes from electronic medical records during a median follow-up period of 12 years. We used Cox proportional hazards models to assess the association between sleep behavior traits and risk for OAEs.

Results: Participants were included if they were members of the UK general population and provided informed consent for enrollment in the UK Biobank. Participants were excluded if they reported baseline opioid use, developed OAEs before or within one year of the study baseline, withdrew, or lacked sleep assessment and other covariate data. A total of 1,400 participants developed OAEs. Short and long sleep duration, frequent daytime sleepiness, insomnia symptoms, and napping, but not chronotype, were associated with increased OAE risk in the adjusted model. Compared to the minimal poor sleep behavior burden group (scores of 0-1), moderate (scores of 4-5) and severe (scores of 6-9) poor sleep behavior burden groups had hazard ratios of 1.47 (95% confidence interval 1.27-1.71, p<0.001) and 2.19 (1.82-2.64, p<0.001) for developing OAEs, respectively. In participants with moderate or severe poor sleep behavior burden, subgroup analysis revealed that age <65 years was associated with an even higher OAE risk compared to those 65 years or older.

Conclusions: Certain sleep behavior traits and overall poor sleep behavior burden are associated with increased risk for OAEs. Further investigation is required to detail the relationship between poor sleep and OAEs.

References: 1. U.S. Overdose Deaths In 2021 Increased Half as Much as in 2020 – But Are Still Up 15%. Published online May 11, 2022. https://www.cdc.gov/nchs/pressroom/nchs_press_releases/2022/202205.htm

2. Correlates of sleep quality and excessive daytime sleepiness in people with opioid use disorder receiving methadone treatment. *Sleep Breath*. 2020;24(4):1729-1737.

3. Worsening sleep quality across the lifespan and persistent sleep disturbances in persons with opioid use disorder. *J Clin Sleep Med*. 2022;18(2):587-595.

4. Effects of Chronic Opioid Use on Sleep and Wake. *Sleep Med Clin*. 2018;13(2):271-281.

	Developed opioid-related adverse events (n=1,400)	Did not develop opioid-related adverse events (n=442,639)	
	Mean (SD, range), or %	Mean (SD, range), or %	*p*-value
Demographics			
Age (years)	58.9 (8.3, 40.0-70.5)	57.1 (8.1, 37.4-73.7)	<.001
Female	54.1%	54.4%	.81
College attendance	21.3%	32.4%	<.001
Ethnic background (European)	95.7%	94.1%	.01
Lifestyle/socioeconomic status			
BMI (kg/m²)	28.4 (5.6, 15.3-64.8)	27.4 (4.8, 12.1-74.6)	<.001
Physical Activity (MET-mins)	2143 (513, 0-19,278)	2076 (461, 0-19,278)	<.001
Townsend deprivation index	-0.76 (3.4, -6.3-0.9)	-1.30 (3.1, -6.3-11.0)	<.001
Morbidity/frailty			
Morbidity burden			<.001
None (0)	38.5%	45.7%	
Low to moderate (1-2)	49.6%	45.7%	
High (3+)	11.9%	8.5%	
CVD risk score	0.98 (1.0, 0-5)	0.63 (0.9, 0-5)	<.001
Fell in the last year	28.4%	19.8%	<.001
Had major operation	74.8%	65.0%	<.001
Bony fractures in the past 5 years	13.8%	9.5%	<.001
Psychiatric illness/non-opioid substance use			
Psychiatric illness burden			<.001
None (0)	81.0%	89.8%	
At least one (1+)	19.0%	10.2%	
Smoking (current or former)	66.7%	59.8%	<.001
Alcohol (≥4 drinks/week)	45.6%	47.0%	.30
Hypnotic/sedative use	3.4%	1.6%	<.001
Systemic inflammation			
CRP level (mg/L)	4.1 (6.7, 0.1-77.4)	2.6 (4.3, 0.1-80.0)	<.001
Sleep measures			
Sleep disorders	1.9%	0.8%	<.001
Sleep duration (hours/day)			<.001
Short (<6)	10.2%	5.5%	
Normal (6-9)	86.2%	92.6%	
Long (>9)	3.6%	1.8%	
Excessive daytime sleepiness			<.001
Never/rarely	70.0%	75.9%	
Sometimes	25.1%	21.2%	
Often/all the time	5.0%	2.8%	
Insomnia-like complaints			<.001
Never/rarely	16.4%	24.1%	
Sometimes	42.4%	47.9%	
Usually	41.2%	28.2%	
Napping			<.001
Never/rarely	48.1%	56.2%	

Sometimes	43.8%	38.5%	
Usually	8.2%	5.4%	
Chronotype			.04
Early/intermediate	91.8%	92.0%	
Late	8.2%	8.0%	
Poor Sleep Behavior Burden			<.001
Minimal (0-1)	19.3%	28.3%	
Mild (2-3)	46.9%	49.5%	
Moderate (4-5)	24.9%	18.2%	
Severe (6+)	9.0%	4.0%	

Table 1. Demographics, lifestyle/socioeconomic status, morbidity/frailty, psychiatric illness/non-opioid substance use, systemic inflammation, and baseline sleep measures. UK Biobank participant characteristics at baseline expressed as mean (SD, range) for continuous variables or percentage (%) for presence of categorical variables. Participants compared based on opioid-related adverse events (Developed/Did Not Develop). Categorical data presented as percentage of participants present. *P*-values from one-way ANOVA tests or Wilcoxon rank-sum tests for continuous measures and Pearson's chi-squared tests for categorical data. Physical activity: summed metabolic equivalent (MET) minutes per week for all activities. *SD* standard deviation.

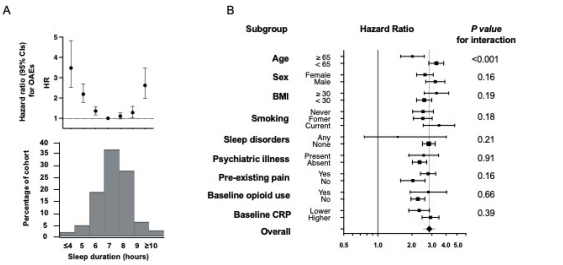

Figure 3. Subgroup analysis of OAE risk. **(A)** OAE risk by hourly sleep duration (adjusted for age, sex, education, and ethnicity). **(B)** Subgroup plot of hazard ratios with 95% confidence intervals for moderate/severe poor sleep behavior burden (vs. minimal) and associated OAE risk based on subgroups of age, sex, BMI, smoking status, sleep disorders, pre-existing pain, psychiatric illness, baseline opioid use, and baseline CRP level. For each subgroup, the square is proportional to the number of participants. Overall cohort hazard ratios comparing moderate/severe vs. minimal poor sleep behavior burden are shown by a diamond (left and right lines represent the 95% CI) and the dashed vertical line. *OAE* opioid-related adverse events. *CRP* C-reactive protein. *BMI* body mass index. *CI* confidence interval.

	Core model		Adjusted model	
	HR (95% CI)	*p*-value	HR (95% CI)	*p*-value
Sleep duration				
<6 hours/night	2.15 (1.81-2.54)	<0.0001*	1.62 (1.36-1.94)	<0.0001*
>9 hours/night	2.32 (1.77-3.04)	<0.0001*	1.54 (1.16-2.04)	0.003*
Excessive daytime sleepiness				
Sometimes	1.25 (1.11-1.41)	<.001*	1.08 (0.96-1.22)	0.22
Often/all the time	1.99 (1.57-2.52)	<0.0001*	1.32 (1.03-1.70)	0.03
Insomnia-like complaints				
Sometimes	1.27 (1.10-1.47)	0.001*	1.15 (0.99-1.33)	0.07
Usually	2.16 (1.87-2.51)	<0.0001*	1.68 (1.44-1.96)	<0.0001*
Napping				
Sometimes	1.28 (1.15-1.42)	<0.0001*	1.08 (0.96-1.20)	0.19
Usually	1.75 (1.44-2.12)	<0.0001*	1.26 (1.03-1.54)	0.02
Chronotype				
Late	1.21 (1.01-1.46)	0.04	0.97 (0.71-1.17)	0.72
Poor sleep behavior burden				
Mild	1.34 (1.17-1.54)	<0.0001*	1.18 (1.03-1.35)	0.01
Moderate	1.98 (1.70-2.32)	<0.0001*	1.47 (1.27-1.71)	<0.0001*
Severe	3.64 (2.97-4.49)	<0.0001*	2.19 (1.82-2.64)	<0.0001*

Table 2. Sleep behavior traits and poor sleep behavior burden score with associated risk for opioid-related adverse events. Cox proportional hazards models. Results presented as HR (95% CI), *p* value. The core model is controlled for demographics (age, sex, college education, and ethnicity) and the adjusted model is controlled for all covariates, including the above demographics, BMI, physical activity, material deprivation, morbidity burden, cardiovascular risk, falls in the last year, major operation(s), bony fracture(s) in the past 5 years, baseline CRP level, psychiatric illness, non-opioid substance use, and baseline pain. *Indicates statistical significance after Bonferroni adjustment for multiplicity. Abbreviations: *HR* hazard ratio, *CI* confidence interval.

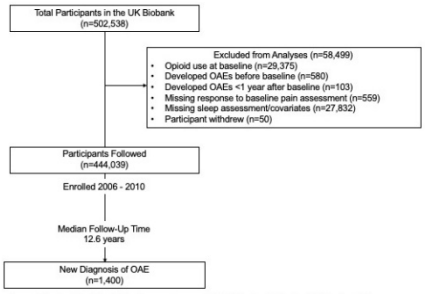

Figure 1. Flowchart of participant selection. How participants with opioid-related adverse events were selected in the study. From the UK Biobank. *OAE* opioid-related adverse event.

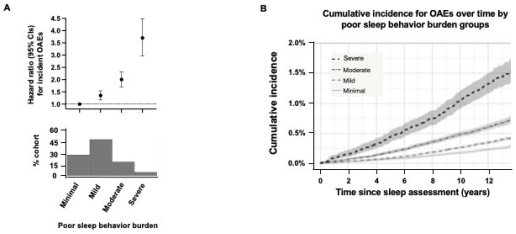

Figure 2. Poor sleep behavior burden groups and their associated risk for incident OAEs. Groupings were based on the poor sleep behavior burden score (Minimal = 0-1, Mild = 2-3, Moderate = 4-5, and Severe ≥ 6). **(A)** Hazard ratios (±95% CI) for OAEs using Cox proportional hazards regression models adjusted for age, sex, education and ethnicity; percentage of cohort by group in panel below **(B)** Unadjusted cumulative incidence plot showing percentage of cohort with a first diagnosis of OAE by group over time. *OAE* opioid-related adverse event. *CI* confidence interval.

Technology, Computing and Simulation, Equipment Monitoring

Technology, Computing and Simulation, Equipment Monitoring 1- Effect of Machine Learning Decision Support on Discrimination of Intraoperative Anesthesiology Clinician Prediction of Postoperative Complications: The ORACLE (Outcome Risk Assessment with Computer Learning Enhancement) Trial

Bradley Fritz[1], Christopher King[1], Yixin Chen[1], Alexander Kronzer[1], Joanna Abraham[1], Arbi Ben Abdallah[1], Thomas Kannampallil[1], Thaddeus Budelier[1], Arianna Montes de Oca[1], Bethany Pennington[1], Troy Wildes[2], Michael Avidan[1]

Washington University in St Louis[1] University of Nebraska Medical Center[2]

Introduction: Early recognition of patient risk for postoperative complications affords opportunities for the implementation of mitigation strategies that can improve patient outcomes. Machine learning (ML) algorithms may be able to enhance risk recognition by quickly processing large quantities of patient data [1-4]. The goal of this randomized clinical trial (RCT) was to determine whether anesthesiology clinicians working in an intraoperative telemedicine setting can predict postoperative death within 30 days and postoperative acute kidney injury (AKI) within 7 days more accurately with access to ML predictive algorithms than without ML.

Methods: This RCT was nested within the ongoing TECTONICS trial [5], which is evaluating the impact of intraoperative anesthesiology telemedicine support on clinical outcomes. Over a 12-month period, 5114 surgical patients receiving intraoperative telemedicine support at a single academic medical center were randomized to have ML decision support available when the clinicians reviewed a patient's electronic health record (EHR) or to have no ML support. ML decision support was provided in the form of numeric risk scores from random forest and XGBoost models trained on approximately 110,000 patients from the same institution, with a secure website interface (Figure 1).

After reviewing the patient's EHR with or without ML, each clinician (attending anesthesiologist, resident anesthesiologist, certified registered nurse anesthetist, or student nurse anesthetist) predicted on a 5-point scale (very low risk, low risk, average risk, high risk, very high risk) the likelihood of the patient to experience postoperative death within 30 days and postoperative AKI within 7 days using KDIGO creatinine criteria [6]. Patients with end stage renal disease or preoperative AKI were excluded from the AKI analyses. Within each group, clinician predictions were used to construct a logistic regression model for each complication. The primary outcome was the area under the receiver operating characteristic curve (AUC), which was compared between groups using DeLong's test [7].

Results: Among 4494 patients with data for both predicted and observed mortality, 99 patients (2.2%) died within 30 days (Table 1). The ML model demonstrated good discriminative performance both using its raw continuous predictions and when the continuous predictions were collapsed onto the same 5-point scale used by the clinicians (Figure 1). Clinicians with ML predicted mortality with AUC 0.793 (95% CI 0.736-0.850), compared to AUC 0.778 (95% CI 0.715-0.840) for clinicians without ML. This difference was not statistically significant ($p = 0.72$).

Among 4085 patients with data for both predicted and observed AKI, 451 patients (11%) experienced AKI (Table 2). The ML model demonstrated good discriminative performance both using its raw continuous predictions and when the continuous predictions were collapsed onto the same 5-point scale used by the clinicians (Figure 2). Clinicians with ML predicted AKI with AUC 0.732 (95% CI 0.701-0.764), compared to AUC 0.687 (95% CI 0.650-0.723) for clinicians without ML. This difference was not statistically significant ($p = 0.06$).

Conclusions: Anesthesiology clinicians predicted mortality and AKI with good discrimination both with and without ML support. For mortality, the observed difference in discrimination was neither statistically nor clinically significant. For AKI, the observed difference in discrimination was clinically significant but did not reach statistical significance, so a clinically meaningful difference cannot be ruled out. Clinician AUC values were lower than hypothesized (perhaps partly related to use of a 5-point scale rather than a continuous scale), which may have reduced statistical power. Future work using this cohort will examine whether clinicians made decisions faster with ML decision support than without, as well as whether clinicians' self-reported agreement or disagreement with the ML prediction impacted prediction discrimination.

References: 1. *J Anaesthesiol Clin Pharmacol.* 2013;29:151-159.

2. *Anesthesiology.* 2002;97:1281-1294.

3. *Anaesth Intensive Care.* 2000;28:178-183.

4. *JAMA Network Open.* 2021;4:e212240-e212240.

5. *F1000Research.* 2019;8:2032.

6. *Critical Care.* 2013;17:204.

7. *Biometrics.* 1988;44:837-845.

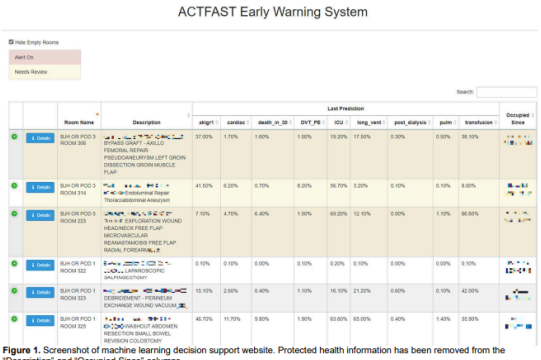

Figure 1. Screenshot of machine learning decision support website. Protected health information has been removed from the "Description" and "Occupied Since" columns.

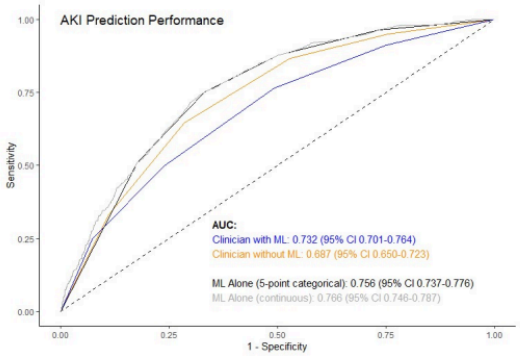

Figure 3. Receiver operating characteristic curves for prediction of postoperative acute kidney injury (AKI) within 7 days.

Table 1. Predicted and Observed Mortality

Prediction	Clinician With ML		Clinician Without ML	
	N	Observed Mortality	N	Observed Mortality
Very Low Risk	818	2 (0.2%)	776	3 (0.4%)
Low Risk	385	4 (1.0%)	506	6 (1.2%)
Average Risk	559	9 (1.6%)	618	16 (2.6%)
High Risk	318	21 (6.6%)	286	10 (3.5%)
Very High Risk	142	11 (7.7%)	86	17 (19.8%)
Total	***2222***	***47 (2.1%)***	***2272***	***52 (2.3%)***

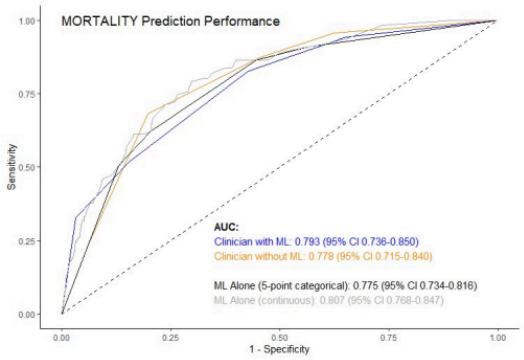

Figure 2. Receiver operating characteristic curves for prediction of postoperative 30-day mortality.

Table 2. Predicted and Observed AKI

Prediction	Clinician With ML		Clinician Without ML	
	N	Observed AKI	N	Observed AKI
Very Low Risk	454	12 (2.6%)	478	19 (4.0%)
Low Risk	425	19 (4.5%)	505	32 (6.3%)
Average Risk	491	52 (10.6%)	524	58 (11.1%)
High Risk	387	73 (18.9%)	358	54 (15.1%)
Very High Risk	277	78 (28.2%)	186	54 (29.0%)
Total	***2034***	***234 (11.5%)***	***2051***	***217 (10.6%)***

Technology, Computing and Simulation, Equipment Monitoring 2- Establishment and Evaluation of a Semi-Automated Data Extraction Methodology

Katherine McPherson[1], Arshia Harandi[1], Rodrigo Gutierrez[2], Jerry Chao[3]

Albert Einstein College of Medicine[1] Massachusetts General Hospital[2] Montefiore-Einstein[3]

Introduction: Gathering continuous clinical data is typically achieved with technically complicated server pulls (via SQL, etc.) or tedious manual data entry from patients' chart records.[1] However, inexperience with coding can deter clinicians from pursuing server pulls and manual data entry can be prone to errors or require time-intensive resources. In this abstract, we suggest a semi-automated data extraction methodology that does not require any coding skills or additional software other than Microsoft Excel. We hypothesize that data collected via this semi-automated methodology will have high concordance with manually extracted data.

Methods: *Manual Data Entry Method*: Data were manually extracted from the EMR anesthesia monitoring records of 30 patients by using the "ctrl-F" function to find "Sevoflurane Expired" and manually inputting time points and sevoflurane values into Microsoft Excel.
Semi-Automated Data Entry Method: All anesthesia monitoring data were extracted from the EMR to plain text file, using "copy-paste". These data were imported into Excel utilizing the "Legacy" (import from text) function with no delimiter screening. Raw data were filtered utilizing the "Begins With" function to select for "Sevoflurane Expired." Filtered data were separated using "space" and ")" as delimiters to isolate time points and sevoflurane expired. Isolated time and sevoflurane data were copy-pasted into an Excel file.
Data Analysis: Concordance between the two data extraction methodologies was determined via one-to-one comparison of each datapoint to look for discrepancies. Pearson's Correlation and Cohen's Kappa were calculated.

Results: Expired sevoflurane data were extracted for 30 patients undergoing elective surgery. There were a total of 2,210 unique data points assessing a total of 36.8 hours of anesthesia monitoring. Direct comparison of data points resulted in 1 (0.04%) discrepancy found between the manually entered data and the semi-automated data entry methodology. Post-hoc review of this datum reveals that it was missing from the manual data entry. Overall, these methods had a correlation coefficient of 1.00 (p<.001) and a cohen's Kappa of 1.00 (p<.001).

Conclusions: This study presents the reliability and accuracy of a semi-automated data extraction methodology with no need for experience with coding, server data pulling, or additional software. This methodology would enhance the speed of data extraction and reduce the potential for human error in EMR-based research projects. Increased access to clinical data extraction methods can help improve the ease and efficacy of research in non-academic hospitals and rural institutions, which typically have fewer research personnel. This could in turn increase the representation of under-studied populations in research.

References:

1. Cai, Tianrun et al. "EXTraction of EMR numerical data: an efficient and generalizable tool to EXTEND clinical research." BMC medical informatics and decision making vol. 19,1 226. 15 Nov. 2019, doi:10.1186/s12911-019-0970-1

Technology, Computing and Simulation, Equipment Monitoring 3- Interpretable machine learning identifies personalized risk factors for increased postoperative acute kidney injury risk

Minjae Kim[1], Shihui Zhu[2]

Columbia University Medical Center[1] Columbia University[2]

Introduction: Risk stratification for postoperative acute kidney injury after intraabdominal general surgery is enhanced by the addition of intraoperative management data to preoperative risk factors (1). However, as the models incorporate many different variables, it is difficult to determine the specific variables that "explain" the rationale for an individual patient's risk status.

Methods: With IRB approval, an institutional retrospective cohort of intraabdominal general surgery patients in the 2005-2015 American College of Surgeons National Surgical Quality Improvement Program was identified. Intraoperative data was obtained from the EHR (CompuRecord, Philips Medical). AKI was defined as an increase in serum creatinine ≥0.3 mg/dl within 48 hours of surgery or >50% within 7 days of surgery. The balanced random forest (RF) machine learning (ML) algorithm was used to fit a model for predicting postoperative AKI. A balanced RF model is selected here due to the imbalanced distribution of the negative (No AKI) and positive cases (AKI) in the data. Instead of randomly selecting bootstrap samples from the training set at each step, balanced RF applies random under-sampling of the majority class (No AKI) in each bootstrap sample to keep the sample balanced. Variables include preoperative data such as surgical procedure category, demographics, comorbidities and laboratory values, and intraoperative management data including medications, fluid management, and blood pressure. The dataset was divided into training and testing cohorts in a 4:1 ratio. Repeated 5-fold cross validation was used on the training dataset to fit parameters optimizing the F1-score (i.e., optimizing the precision and recall score). The area under the receiver operator characteristic (AUROC) is also used as a reference. The model was then applied to the test dataset. In addition, the area under the precision-recall curve (AUPRC) was determined to assess model performance. Model interpretation was performed using SHAP (SHapley Additive exPlanations), a method based on game theory to determine the marginal contribution of an individual variable on model prediction (2).

Results: The dataset consisted of 3845 observations and 68 variables. After converting categorical variables with dummy coding, a total of 86 variables were utilized in the models. Training and testing datasets consisted of 3076 and 769 observations, respectively, with AKI rates of 7.4% and 7.0%, respectively. The AUROC and AUPRC of the balanced RF model were 0.76 [95% CI 0.69-0.83] and 0.18 [0.11-0.27], respectively. The variables with the greatest mean SHAP values were preoperative hematocrit (prhct), standard deviation of systolic blood pressure (sd_sbp), estimated glomerular filtration rate (e_gfr), age, and preoperative albumin (pralbum) (Fig 1A). SHAP summary plots denote the variation in SHAP values for each variable (Fig 1B). Individual SHAP force plots highlight variables contributing to increased or decreased AKI risk for individual patients. Fig 2A highlights an individual with a high predicted AKI risk (68%) who developed AKI, with contributing variables such as intraoperative hypertension, blood pressure variance, and blood loss. Fig 2B highlights another individual with high predicted AKI risk (68%) who also developed AKI. Contributing variables included age, phenylephrine dose, intraoperative hypertension, and blood loss.

Conclusions: Balanced RF was used to fit a model predicting postoperative AKI after intraabdominal surgery with good performance characteristics as measured by AUROC and AUPRC. SHAP analysis of this model identified variables with the greatest effects on model prediction, both in aggregate and on an individual level. Thus, this model can be potentially applied at the end of surgery to predict subsequent AKI risk and to understand the factors that contributed to AKI risk in each patient. Further studies will be necessary to identify the ways in which this information can be used to optimize the postoperative management of high risk patients as well as to alter intraoperative management to reduce the risk of ultimately developing postoperative AKI.

References: 1. Anesth Analg. 2021;132:430-41.

2. Advances in Neural Information Processing Systems. 2017. 4765-74.

Figure 1

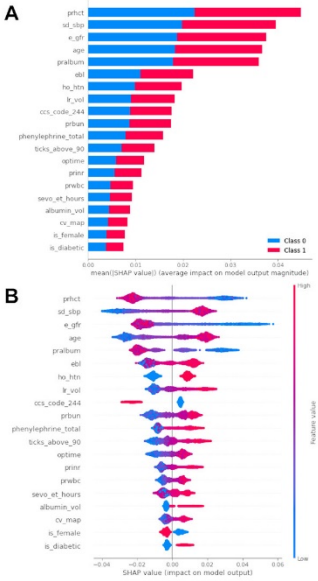

Figure 1. (A) Mean absolute SHAP (SHapley Additive exPlanations) values for variables in a balanced random forest model to predict postoperative acute kidney injury after intraabdominal surgery. (B) SHAP summary plots.

Figure 2

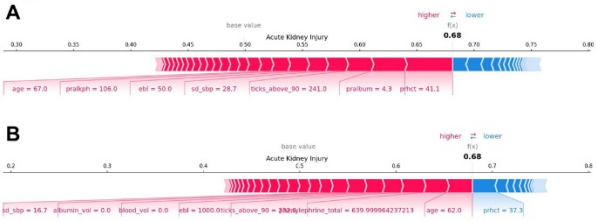

Figure 2. SHAP (SHapley Additive exPlanations) Force Plots indicating variables contributing to increased (red) or decreased (blue) postoperative acute kidney injury risk for individual patients and the magnitude of the SHAP value. All patients presented developed postoperative AKI. (A) Patient with predicted AKI risk of 68%. Contributors to AKI risk include intraoperative hypertension (ticks_above_90), intraoperative systolic blood pressure variance (sd_sbp), and estimated blood loss (ebl). (B) Patient with predicted AKI risk of 68%. Contributors to AKI risk include age, phenylephrine dose, intraoperative hypertension, and estimated blood loss.

Technology, Computing and Simulation, Equipment Monitoring 4- Comparison of two techniques of delivering the Valsalva Maneuver in patients under general anesthesia: A randomized controlled study

Shagun Shah[1], Rajiv Chawla[1]

Rajiv Gandhi Cancer Institute and Research Centre[1]

Introduction: Valsalva maneuver (VM; forced expiration against a closed glottis) can be active (in awake patients), accidental (straining/lifting weight), or passive (intraoperatively by positive pressure technique in manual mode). Rise in intrathoracic pressure, mean arterial pressure (MAP), and bradycardia occur during phase-I of VM followed by a rise in intracranial pressure in phase-II with accompanying fall in MAP and tachycardia.[1] Surgeons often request VM intraoperatively (thyroidectomy, head-neck surgery, craniotomy) to unmask covert venous bleeders and detect CSF leaks.[2,3,4] Observing the airway pressure values on the monitor during traditional VM administration by the intermittent positive pressure technique[1,4] revealed delivery of a highly variable airway pressure which seldom reached the set 40 cmH2O mark with this subjective technique.
We aimed to compare an anesthesia machine-generated objective technique for delivering VM under pressure-controlled (PC) mode and the traditional subjective technique of delivering VM in manual mode.

Methods: This prospective, interventional, two-arm, single-centric randomized controlled study was conducted at a tertiary care oncology setup. Written informed consent from all patients, and scientific and ethics committee approvals were obtained. The study included 60 adult ASA I-II patients randomly allocated into two groups: manual VM group (Group-M; n=30) and controlled ventilation VM group (Group-C; n=30) by computer-generated block-randomization, with group allocation concealed in sealed opaque envelopes. VM was performed after endotracheal intubation and arterial line placement but before surgical incision. Fresh gas flow was fixed at 2l/min in both groups. In Group M, the ventilator was put on manual/spontaneous mode and the APL-valve was partially closed to 40cmH_2O. The reservoir bag was manually compressed and maintained for 20 sec. Group-C patients were placed on PC-mode with 40cmH_2O pressure setting, PEEP 35cmH_2O, and R/R 3 breaths/min (inherent safety feature of our workstation) to deliver 20sec of 35-40 cmH_2O airway pressure (40 cmH_2O during inspiration; 35 cmH_2O during expiration). MAP, heart rate (HR), and internal jugular vein diameter (IJVD) were measured at 7 time points (T_0= baseline, T_1= initiation of VM, T_2= 20 secs after VM initiation, T_3 = VM release, T_4 = 1min, T_5= 2min and T_6 = 5 min post-VM). VM was repeated after tumor resection for unmasking covert bleeders and surgeon satisfaction was noted in both groups.
Our primary outcome measures were MAP, HR and IJVD measured at pre-determined time points. Our secondary outcome measure was surgeon satisfaction.
Categorical variables were expressed as numbers and percentages. Independent sample t-test for intergroup and paired sample t-test for intragroup comparison of normally distributed, quantitative variables were performed. Results were expressed as mean ± standard deviation, dotted box-whisker plots, trendlines, and correlograms. $P < 0.05$ was considered statistically significant.

Results: All patients of either sex, aged 18-60 years, weighing 45-80kg undergoing head-neck surgery requiring an arterial line were included (Table 1). Patients with aortic stenosis, hypertrophic obstructive cardiomyopathy, recent myocardial infarction, glaucoma, retinopathy, etc were excluded.
In both groups, the intragroup analysis revealed no statistically significant change, in baseline HR versus HR at all other time points. Intragroup analysis of MAP in both the groups showed a rise in MAP compared to baseline at T_1, a fall in MAP at T_2 and T_3, rise at T_4 followed by a fall at T_5 and T_6 (Table 2). The difference in mean HR at T_0, T_1, T_2, T_3, T_4, T_5, and T_6 was statistically insignificant between the two groups. MAP at T_0 and T_1, in both groups, was comparable. After 20 secs of VM, there was a statistically significant greater fall in MAP in Group-C as compared to Group-M (p=0.018). At T_3, the mean MAP was significantly lower in Group C versus Group M (p= 0.021). At T_4, T_5 and T_6, mean MAP was comparable between the two groups (Table 3).
VM performed in the PC mode produced greater IJV dilatation (p= 0.004; p= 0.044; Table-1; Figure-1). The correlogram depicts the Pearsons coefficient for correlation between changes in HR, MAP, and IJV diameter (Table 4).
Conclusions: Performing VM in PC mode is a better technique based on hemodynamics, IJVD, unmasking of bleeders, and surgeon satisfaction. It could potentially become the new standard of administering intraoperative VM.

References: 1. Intraoperative Valsalva maneuver: a narrative review. Can J Anaesth;65(5):578-85. 2018.

2. Effect of intraoperative Valsalva maneuver application on bleeding point detection and postoperative drainage after thyroidectomy surgeries. Int Surg; 100: 994-8. 2015.

3. Valsalva maneuver: its implications in clinical neurosurgery. Neurol India; 64: 1276-80. 2016.

4. A comparison of the efficacy of three different peak airway pressures on intraoperative bleeding point detection in patients undergoing thyroidectomy: a randomized, controlled, clinical trial. BMC surgery; 20(1)1-7. 2020.

Variable	N	Mean	SD	95% CI	P-value
mAge (years)	30	55.8	10.79	51.77 to 59.83	0.255
cAge (years)	30	52.8	9.13	49.42 to 56.24	
mWeight (kg)	30	69.09	12.05	64.59 to 73.59	0.914
cWeight (kg)	30	69.45	13.54	64.40 to 74.51	
mHeight (cm)	30	165.23	6.28	162.89 to 167.58	0.6827
cHeight (cm)	30	166.03	9.07	162.65 to 169.42	
mIJVa (cm)	30	0.23	0.15	0.17 to 0.28	0.004
cIJVa (cm)	30	0.36	0.2	0.28 to 0.44	
mIJVb (cm)	30	0.19	0.15	0.13 to 0.24	0.044
cIJVb (cm)	30	0.26	0.13	0.21 to 0.31	
mSex (Male: Female)		27:3	cSex (Male: Female)		24:6
mSurgeon Satisfaction (yes:no)		20:10	cSurgeon Satisfaction		29:1

Table1: Demographic and other variables

Pair		n	Variable 1		Variable 2		Paired differences			
			Mean	SD	Mean	SD	Mean	SD	95% CI	P
mHR0	mHR1	30	68.2	10.52	66.2	10.46	-1.97	5.67	-4.09 to 0.15	0.068
mHR0	mHR2	30	68.2	10.52	65.9	11.79	-2.27	7.33	-5.01 to 0.47	0.101
mHR0	mHR3	30	68.2	10.52	66.1	11.55	-2.07	6.94	-4.66 to 0.53	0.114
mHR0	mHR4	30	68.2	10.52	66.8	9.96	-1.40	6.93	-3.99 to 1.19	0.278
mHR0	mHR5	30	68.2	10.52	65.0	14.84	-3.20	15.02	-8.81 to 2.41	0.253
mHR0	mHR6	30	68.2	10.52	67.0	9.34	-1.35	7.09	-4.04 to 1.35	0.316
cHR0	cHR1	30	69.5	10.78	69.3	10.92	-0.13	2.42	-1.04 to 0.77	0.765
cHR0	cHR2	30	69.5	10.78	67.6	12.89	-1.83	5.84	-4.02 to 0.35	0.096
cHR0	cHR3	30	69.5	10.78	69.4	11.08	-0.03	5.41	-2.05 to 1.99	0.973
cHR0	cHR4	30	69.5	10.78	69.1	10.12	-0.33	3.92	-1.80 to 1.13	0.645
cHR0	cHR5	30	69.5	10.78	68.6	10.56	-0.83	3.83	-2.26 to 0.60	0.242
cHR0	cHR6	30	69.5	10.78	68.10	11.08	-1.37	5.03	-3.25 to 0.51	0.148
mMAP0	mMAP1	30	84.9	13.25	83.7	10.94	-1.2	9.18	-4.63 to 2.23	0.480
mMAP0	mMAP2	30	84.9	13.25	73.2	11.14	-11.7	9.58	-15.24 to -8.09	<0.001
mMAP0	mMAP3	30	84.9	13.25	73.7	13.93	-11.2	10.32	-15.02 to -7.32	<0.001
mMAP0	mMAP4	30	84.9	13.25	82.2	11.82	-2.7	9.80	-6.36 to 0.96	0.142
mMAP0	mMAP5	30	84.9	13.25	82.5	11.18	-2.3	9.55	-5.90 to 1.23	0.191
mMAP0	mMAP6	30	84.9	13.25	83.1	11.99	-1.8	9.60	-5.38 to 1.78	0.313
cMAP0	cMAP1	30	82.9	13.47	87.0	13.93	4.1	3.54	2.81 to 5.46	<0.001
cMAP0	cMAP2	30	82.9	13.47	64.9	14.94	-18.0	13.17	-22.88 to -13.05	<0.001
cMAP0	cMAP3	30	82.9	13.47	64.6	15.70	-18.3	13.77	-23.41 to -13.12	<0.001
cMAP0	cMAP4	30	82.9	13.47	83.6	13.36	0.7	8.65	-2.50 to 3.97	0.646
cMAP0	cMAP5	30	82.9	13.47	82.5	13.20	-0.4	8.11	-3.40 to 2.66	0.806
cMAP0	cMAP6	30	82.9	13.47	79.9	12.64	-2.9	9.72	-6.56 to 0.70	0.109

Table-2: Intragroup analysis of hemodynamic variables at various time points using the paired t-test (cHR = Heart rate in Group C; cMAP= Mean arterial pressure in Group C; mHR= Heart rate in Group M; mMAP= Mean arterial pressure in Group M).

Variable	Group-M			Group-C					
	n	Mean	SD	n	Mean	SD	Difference	95% CI	P
HR-0	30	68.20	10.52	30	69.47	10.78	1.27	-4.24 to 6.77	0.647
HR-1	30	66.23	10.46	30	69.33	10.92	3.10	-2.42 to 8.63	0.266
HR-2	30	65.93	11.79	30	67.63	12.89	1.70	-4.69 to 8.09	0.596
HR-3	30	66.13	11.55	30	69.43	11.08	3.30	-2.55 to 9.15	0.263
HR-4	30	66.80	9.96	30	69.13	10.12	2.33	-2.86 to 7.52	0.372
HR-5	30	65.00	14.84	30	68.63	10.56	3.63	-3.02 to 10.29	0.279
HR-6	29	66.97	9.34	30	68.10	11.08	1.14	-4.22 to 6.49	0.673
MAP-0	30	84.87	13.25	30	82.87	13.47	-2.00	-8.90 to 4.90	0.564
MAP-1	30	83.67	10.94	30	87.00	13.93	3.33	-3.14 to 9.81	0.307
MAP-2	30	73.20	11.14	30	64.90	14.94	-8.30	-15.11 to -1.49	0.018
MAP-3	30	73.70	13.93	30	64.60	15.70	-9.10	-16.77 to -1.43	0.021
MAP-4	30	82.17	11.82	30	83.60	13.36	1.43	-5.09 to 7.95	0.662
MAP-5	30	82.53	11.18	30	82.50	13.20	-0.03	-6.36 to 6.29	0.992
MAP-6	30	83.07	11.99	30	79.93	12.64	-3.13	-9.50 to 3.23	0.329

Table-3: Intergroup analysis of hemodynamic variables at various time points (HR= Heart rate; MAP= Mean arterial pressure)

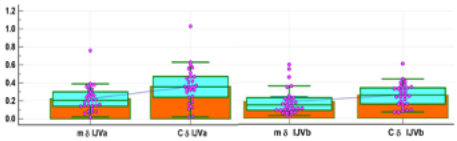

Figure-1: Dotted box-whisker plots comparing the dilatation of internal jugular vein (IJV) as a result of Valsalva Maneuver (VM) in both groups (mδIJVa = Change in mediolateral IJV diameter after 20 seconds of VM in Group M; CδIJVa = Change in mediolateral IJV diameter after 20 seconds of VM in Group C; mδIJVb = Change in anteroposterior IJV diameter after 20 seconds of VM in Group M; CδIJVb = Change in anteroposterior IJV diameter after 20 seconds of VM in Group C)

	CδIJVb	CδIJVa	mδIJVb	mδHR	mδIJVa	CδHR	CδMAP	mδMAP
CδIJVb		0.76	0.11	-0.03	0.12	0.23	-0.28	-0.19
CδIJVa	0.76		-0.08	-0.14	0.10	0.29	-0.45	-0.16
mδIJVb	0.11	-0.08		-0.10	0.51	-0.03	0.02	-0.38
mδHR	-0.03	-0.14	-0.10		-0.21	-0.23	-0.12	0.40
mδIJVa	0.12	0.10	0.51	-0.21		-0.03	-0.02	-0.49
CδHR	0.23	0.29	-0.03	-0.23	-0.03		-0.03	-0.29
CδMAP	-0.28	-0.45	0.02	-0.12	-0.02	-0.03		0.03
mδMAP	-0.19	-0.16	-0.38	0.40	-0.49	-0.29	0.03	

Table-4: Correlogram depicting the Pearsons correlation coefficient for changes in hemodynamic parameters and internal jugular vein diameter from baseline after 20 seconds of Valsalva maneuvre (mδIJVa = Change in mediolateral IJV diameter after 20 seconds of Valsalva maneuver in Group M; CδIJVa = Change in mediolateral IJV diameter after 20 seconds of Valsalva maneuver in Group C; mδIJVb = Change in anteroposterior IJV diameter after 20 seconds of Valsalva maneuver in Group M; CδIJVb = Change in anteroposterior IJV diameter after 20 seconds of Valsalva maneuver in Group C; mδHR= Change in heart rate in Group-M; CδHR= Change in heart rate in Group-C; ; mδMAP= Change in mean arterial pressure in Group-M; CδMAP= Change in mean arterial pressure in Group-C)

Technology, Computing and Simulation, Equipment Monitoring 5- CRISPR Mediated Chemotherapy with Destruction of Recurrent Therapy-Resistant Glioblastoma Multiforme

Alexander Perez[1]

University of California, San Francisco (UCSF)[1]

Introduction: Glioblastoma (GBM) is a common and lethal primary brain cancer. Despite treatment, growth of recurrent tumor occurs frequently and often leads to therapy resistance and patient demise. At recurrence, a third to a quarter of all gliomas have hypermutated genomes following chemotherapy, with mutational burdens orders of magnitude greater than in normal tissue. Such tumors result in poor survival, making novel therapies an urgent need. CRISPR systems have revolutionized medicine by enabling genome engineering through RNA-guided introduction of DNA double-strand breaks. We leverage hypermutation to exploit two avenues of cancer vulnerabilities. First, we quantified mutational progression in a patient's GBM by whole-genome sequencing and uncovered targetable repeat elements. We show that CRISPR-mediated genome destruction (sgCIDE) by targeting highly repetitive loci enables rapid elimination of GBM cells, an approach we term "Genome Shredding". We investigate repetitive targets across vertebrates to define minimal thresholds for efficient cell ablation and identified the non-coding genome as key source of effective and conserved targets for Genome Shredding. Secondly, we identify unique sequences in a patient's recurrent GBM that carry a chemotherapy mutational signature, demonstrating a path for the destruction of cancer through genome-specific CRISPR targeting

Methods: Competitive proliferation assay
To assay the effect of Genome Shredding on cell viability and depletion, U-251, LN-229, T98G, LN-18, SF11411, GL261, and DF-1 cells with or without Cas9 expression were transduced at ~50-70% efficiency with lentiviral vectors to deliver mNeonGreen tagged sgRNAs. The percentage of mNeonGreen+ cells was quantified by flow cytometry at 1-, 2-, 3-, 5-, and 7-days post-transduction.

Comet assay
To detect DNA double-strand breaks (DSBs), a neutral comet assay was conducted following the manufacturer's protocol of the Comet Assay kit . In short, Cas9-expressing U-251 and LN-229 cells were transduced with lentiviral vectors expressing sgNTs or sgCIDEs (with 5mg/mL of polybrene). Cells were collected 24 hours post-transduction at a concentration of 1x10^5/mL, embedded in molten LMAgarose at a ratio of 1:10 (v/v), and transferred onto a CometSlide. Slides were immersed in Lysis solution at 4°C overnight. The next day, slides were washed in 1X TBE buffer, and gel electrophoresis using TBE buffer was performed (22 volts, 20 minutes). Slides were then fixed in 70% ethanol for 5 minutes, dried at 37°C for 15 minutes, and stained with SYBR safe for 30 minutes. Images were taken using fluorescence microscopy.

Quantification of sgCIDE Targets
Reference genomes for the hg38, mm10, and gal6 assemblies of the human, mouse, and chicken genomes were downloaded from the UCSC genome browser. FASTA files were extracted and the GuideScan was utilized to determine the identity, coordinate, and target occurrence of gRNAs in the Cas9 CRISPR system. Circos plots were generated using the Circa software.

Results: Genome Shredding enables rapid cell elimination
Administration of sgCIDEs into live GBM cells revealed drastic growth inhibition and cell death starting as early as day two. Rare tumor escape was shown to be due to Cas9 enzyme failing to enter cell. These experiments show that targeting of highly repetitive sequences leads to rapid elimination of GBM cells (Fig 1).

Chemotherapy Signature
In the recurrent GBM, we discovered 129 unique essential gene loci. Variant analysis shows majority of unique targetable essential gene mutations in the recurrent GBM were C>T conversions. Together, this demonstrates that TMZ-signature mutations in recurrent GBM can result in unique, cancer-specific sequences that are targetable by CRISPR (Fig 2).

Conclusions: We demonstrate CRISPR system's ability to be used as a novel cancer chemotherapy that is effective at stages where a cancer is recurrent, metastatic, or chemo-resistant. We provide an innovative paradigm leveraging the non-coding genome and therapy-induced mutational signatures for robust GBM cell depletion and treatment of recurrent GBM, and other tumors with hypermutated genomes. This novel and innovative approach to cancer therapy signals a pathway in which anesthesiologists can become CRISPR oncologists as this therapy will require careful, close, intensive monitoring, as CRISPR based medicine is administered systemically. The design, administration, and management of CRISPR based chemotherapy is ripe for the field of anesthesiology.

Figure 1

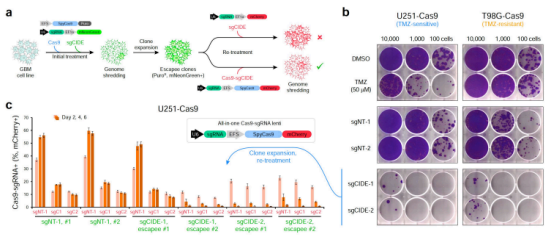

Figure 1: a.) schematic demonstrating administration of sgCIDE to GBM cells with retreatment of rare tumor escapees. Retreatment with same sgCIDE but new Cas9 gave resolute GBM destruction. b.) Agar plate showing effects of sgCIDEs as compared to positive control (TMZ) and negative controls (sgNT). c.) Demonstration of robust destruction of GBM cells following administration of sgCIDE with new Cas9 enzyme

Figure 2

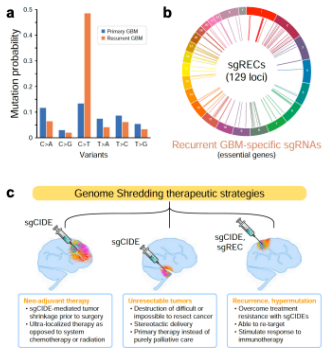

Figure 2: a.) Variants of primary GBM and Recurrent GBM. Recurrent GBM shows TMZ mutational signature b.) Guide RNAs specific to recurrent tumor that arise secondary to TMZ treatment c.) Schematic demonstrating how sgCIDEs and tumor specific gRNAs can be utilized in treatment of GBM.

Technology, Computing and Simulation, Equipment Monitoring 6- Effects of intraoperative postural changes on internal carotid artery blood flow in gynecological laparoscopic surgeries

Chaoxuan Dong[1], Xi Tan[2], Wenyi Sun[2], Hao Zhou[2], Li Zhang[3]

The First Affiliated Hospital of Jinan U[1] The First Affiliated Hospital of Jinan University[2] The International School of Jinan University[3]

Introduction: The combined effects of anesthesia, pneumoperitoneum, and posture will change patients' cerebrovascular physiology during laparoscopic surgery(1). The mechanical compression caused by pneumoperitoneum may lead to a significant decrease in cerebral blood flow. In addition, carbon dioxide retention can lead to cerebral vasodilation and a secondary increase in intracranial pressure(2). The Trendelenburg position of gynecological laparoscopic may further increase intracranial pressure and intraperitoneal pressure, raising the risk of potential brain damage(3). As the main blood supply to the brain, the blood flow on the internal carotid artery (ICA) can indirectly reflect the changes in cerebral blood flow (CBF)(4). Monitoring the changes on ICA blood flow by Doppler ultrasonic provides a method for indirectly reflecting the changes in CBF during gynecological laparoscopic(5). In this study, we evaluated the ICA blood flow measured by Doppler ultrasound, to explore the effects of postural changes on ICA blood flow in patients with laparoscopic gynecological surgery.

Methods: We performed a single center, prospective, observational study, patients who underwent gynecological laparoscopic surgery were prospectively recruited. ICA blood flow as the primary outcome was measured at the following seven time points: awake(T1), after anesthesia induction (T2), after induction of pneumoperitoneum (T3), immediately after the Trendelenburg position (T4), 10min (T5), and 20 min (T6) after the Trendelenburg position, at the end of surgery in the supine position after insufflation of the pneumoperitoneum (T7). Hemodynamic and cerebrovascular variables were measured at each time point. Descriptive statistics are reported as mean±standard error. One-way repeated-measures analysis of variance with Bonferroni *post hoc* tests was utilized to assess changes in ICA blood flow and other variables at each time point.

Results: A total of 59 patients were evaluated. The correction results of Greenhouse & Geisser showed that the changes on ICA blood flow at different time points were statistically significant ($F(4.149, 240.616)=30.339$, $P< .001$, partial $\eta^2=0.34$). The ICA blood flows were significantly lower at T3, T4 than at T2 (524.2 ± 22.4 [T3] vs. 638.0 ± 31.7 [T2]; $P=0.005$; 557.0 ±31.6 [T4] vs. 638.0 ± 31.7 [T2]; $P=0.037$). The ICA blood flow showed a significant difference between T4 and T7 (557.0 ±31.6 vs. 447.8 ± 20.7 ml/min; $P< 0.001$). There was no significant difference between T3 and T4.($P>0.05$) (Figure 1)

Conclusions: Intraoperative postural changes will influence the internal carotid artery blood flow, pneumoperitoneum and Trendelenburg position leads to the decrease of internal carotid artery blood flow, suggesting that anesthetist should guard against insufficient cerebral perfusion caused by postural changes during gynecological laparoscopic surgery, especially in patients with the risk of postoperative cerebrovascular accident.

References:

1. Ann Transl Med., 9(14), 1177, 2021
2. BMC Anesthesiol., 19(1), 202, 2019
3. J Anesth., 33(2), 336-40, 2019
4. Neurosurgery, 17(4), 663-78, 1985
5. J Med Ultrason, 49(4), 581-92, 2022

Figure 1

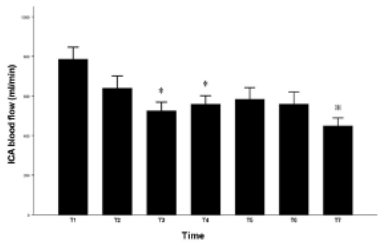

Figure 1. Comparisons of the ICA blood flow at seven different time points

T1, enter operation room; T2, after anesthesia induction, with the patient in the supine; T3, after induction of pneumoperitoneum; T4, right after the Trendelenburg position; T5, 10min late after the Trendelenburg position; T6, 20min late after the Trendelenburg position; T7, right after insufflation of the pneumoperitoneum in the supine at the end of surgery. The ICA blood flow at T3 were significantly less than that at T2 (*P<0.001). Also, The ICA blood flow at T4 is lower than that at T2 (*P<0.001). A significant reduction of the ICA blood flow was found between T4 and T7 (※ P<0.001). Data were shown in Mean±SEM. ICA, internal carotid artery.

Technology, Computing and Simulation, Equipment Monitoring 7- Intraoperative Methadone Use and Postoperative Opioid Requirements: A Retrospective Study in Cardiac Surgery Patients

John-Paul Tsai[1], Elijah Christensen[2], Nathan Clendenen[2]

University of Colorado School of Medicine[1] University of Colorado - Anschutz[2]

Introduction: Most individuals experience a peak in postoperative pain in the first one or two days after cardiac surgery, followed by a decrease in their pain intensity over the subsequent months[1-3]. While many experience resolution of their postsurgical pain, others continue to report pain months to years out from the surgery[4,5]. Methadone has been discussed in Anesthesia literature regarding pain control for decades, yet the drug remains sparingly used for pain control. The primary aim of this study is to investigate the impact single-dose intraoperative methadone has on post-operative opioid requirements as measured in oral morphine milligram equivalents (MME) for the patient's hospital stay. The primary hypothesis is that individuals will require less MME when administered a single dose of intraoperative methadone.

Methods: This retrospective cohort study was conducted using data collected at University of Colorado Hospital from 2011-2022. The in-house database is maintained and managed by members of the lab. A total of 4,226 individuals undergoing cardiac bypass surgery were selected for the study. This represents all the cardiac bypass encounters stored in the database. The primary outcome of the study is the amount of MME required for the encounter, normalized to the patient's hospital length of stay in days. Additional outcomes included death during the encounter. Total opioid administration was calculated for each individual after their procedure stop time. The total opioids administered were converted to MMEs using conversion ratios accepted in literature and an in-house script, which is available upon request[6]. Average MME per day was calculated for both individuals exposed to single-dose intraoperative methadone and for those not exposed to methadone. Sub-group analysis for sex was also conducted. A two-tailed t-test with alpha = 0.05 was calculated to determine if the difference in means was statistically significant.

Results: Out of the 4,226 individuals presenting for cardiac bypass surgery, 2,981 were males, 1239 were females, and 6 individuals were missing sex data. Out of all the individuals, 46 received a single dose of intraoperative methadone and 4,180 did not. Doses of methadone administered ranged from 5mg-30mg. The mean MMEs normalized to the patient's hospital length of stay for total individuals exposed to a single dose of methadone was 13.9, while the mean day-adjusted MME for total individuals not exposed was 13.6 (t-statistic = 0.034 and p = 0.97). Neither group had a death during the encounter. A total of 31 males and 12 females received methadone and a total of 2,950 males and 1227 females did not receive methadone. Mean day-adjusted MME for males who received methadone was 13.8 versus 12.6 for males who did not receive methadone (t-statistic = 0.128, p=0.89). Mean MME for females who received methadone was 16.8 versus 15.9 for females who did not receive methadone (t-statistic 0.049 p=0.96).

Conclusions: Single dose intraoperative methadone is not associated with increased encounter mortality. Individuals exposed to methadone still required additional opioid doses in the PACU and required more opioids than those not exposed to methadone after adjusting for length in hospital stay. This finding did not change after investigating methadone exposure and opioid requirements in males versus females. Exposure to methadone may increase the total amount of opioids required during the encounter, contrary to the study hypothesis. Methadone appears to be a relatively safe adjunct medication in the intraoperative period for postoperative pain control, but may not be effective in reducing post-operative opioid requirements.

References: 1. Assessment and pathophysiology of pain in cardiac surgery. *J Pain Res*. 11, 1599-1611, 2018.

2. Pain Location, Distribution, and Intensity After Cardiac Surgery. *Chest*. 118(2), 391-396, 2000.

3. Day-to-day experience in resolution of pain after surgery. *Pain*. 158(11), 2147-2154, 2017.

4. A Prospective Study of Chronic Pain after Thoracic Surgery. *Anesthesiology*. 126(5), 938-951, 2017.

5. Acute Pain after Thoracic Surgery Predicts Long-Term Post-Thoracotomy Pain. *Clin J Pain*. 12(1), 50-55, 1996.

6. Comparing opioids: A guide to estimating oral morphine equivalents (OME) in research. NDARC Technical Report No.329, 1-10.

	N (%)
Total Individuals	4226
Male Sex (%)	2981 (70%)
Methadone (%)	46 (1%)
No Methadone (%)	4180 (99%)

Table 1: Basic characteristics of individuals in the study, including intraoperative methadone exposure.

	Received Methadone	Did not receive Methadone	P-value
MMEs per day	13.89	13.63	0.97
Death During Encounter	0	0	

Table 2: Individual's opioid administration represented as oral morphine milligram equivalents (MME) adjusted for length of hospital stay in days.

Technology, Computing and Simulation, Equipment Monitoring 8- Novel Method to assess Swimming Induced Pulmonary Edema Severity Using Non-invasive Gas Exchange Monitor

Yousef Ahmed[1], Peter Lindholm[2], Gil Boswell[3], Charles Volk[3]

Duke University Hospital[1] Dept Emergency Medicine[2] US Navy[3]

Introduction: U.S. Naval Special Warfare (NSW) Candidates undergo the world's most physically demanding military training, exposing them to rare physiological stressors. Swimming induced pulmonary edema (SIPE) is seen in this population with an incidence up to 5%. Patients experience symptoms of dyspnea, cough, hemoptysis; all of which can result in termination of their training, with possible risk to life. The purpose of this study is to develop a proof of concept to allow for faster, non-invasive diagnosis of SIPE while validating a novel gas exchange measuring tool. The MediPines Gas Exchange Monitor AGM-100 is cleared by the FDA for non-invasive, point-of-care testing of numerous real-time and calculated clinical parameters, including: P_aO_2, P_aO_2/P_AO_2 gradient, P_aO_2/F_iO_2, RQ, oxygen saturation, heart rate, respiratory rate, P_iO_2, end-tidal oxygen, end-tidal carbon dioxide, and other less frequently used values.

Methods: This study is an observational, prospective review of all NSW candidates that participated in training from February 2020 to July 2020 at the Naval Amphibious Base in Coronado, California. Study informed consent was performed and IRB approval was obtained. We evaluated NSW candidates, males aged 18-30, who are healthy and do not have a previous history of cardio-pulmonary abnormalities. The data analysis focused on the PO_2 difference between end-tidal gas and the calculated serum value derived from a proprietary Medipines algorithm. We expected the PO_2 difference to be small in normal subjects who have normal lungs and therefore a very small ventilation-perfusion gradient. Ten asymptomatic candidates were tested with the AGM-100 device as part of a health screening assessment to obtain a baseline measurement. Afterwards, point-of-care testing was performed with vital signs measurements when patients demonstrated pulmonary complaints, specifically in those who were suspected of SIPE.

Results: The principal finding is that the Medipines AGM-100 works in field settings and values derived from this device, namely O_2 deficit, seem to correlate well with SIPE severity. Use of the AGM-100 device during assessment for SIPE allowed for an objective measurement of severity. The benefit of the AGM-100 device was that it allows for rapid and non-invasive assessment of gas exchange deficit and derives an objective severity measurement for SIPE, which is currently lacking. In the study period, 22 NSW Candidates demonstrated symptoms consistent with SIPE. Of those, 3 were excluded due to incomplete AGM-100 measurements and chest X-ray data. Immediately following exposure to ocean temperature water, Navy Corpsmen collected the AGM-100 data in field environments. Seventeen patients were diagnosed with SIPE with O_2 deficits ranging from 0-39. Of these, six were unable to continue training due to symptoms. Those with the greatest O_2 deficits correlated with more severe disease and increased likelihood for removal from training.

Conclusions: This study demonstrated a proof of concept for the use of the Medipines non-invasive gas exchange monitor AGM-100 in field settings for the assessment of severity of SIPE in NSW candidates. Larger O_2 deficits correlated to increased severity of SIPE and subsequent removal from training. This pilot study is useful because no current non-invasive technologies allow for stratification of SIPE severity and prediction of training status outcomes. Additional, higher powered studies are needed to validate this device even further. We anticipate benefit of using the AGM-100 device in other field environments such as combat field hospitals to assist in rapid diagnosis of non-cardiogenic pulmonary edema.

Technology, Computing and Simulation, Equipment Monitoring 9- Rule-based natural language processing approach to detect delirium on a pre-trained deep learning model framework

Ricardo Munoz[1], Yining Hua[1], Eva-Lotte Seibold[2], Elena Ahrens[3], Simone Redaelli[2], Aiman Suleiman[2], Dario von Wedel[2], Sarah Ashrafian[3], Guanqing Chen[3], Maximilian Schaefer[4], Haobo Ma[4]

BIDMC[1] Beth Israel Deaconess Medical Center, Harvard Medical School[2] Beth Israel Deaconess Medical Center[3] Beth Israel Deaconess Medical Center & Hospital[4]

Introduction: Delirium is an often-underdiagnosed neuropsychiatric syndrome associated with prolonged hospitalisation, increased in-hospital mortality and higher economic burden [1-2]. In retrospective cohort studies, delirium is commonly identified through International Classification of Diseases (9th/10th Revision, Clinical Modification [ICD-9/10-CM]) diagnostic codes. However, this approach is limited by identification of only a fraction of patients who develop delirium [3-4]. Manual chart review provides more accurate classification but is often impossible in large outcome research [3-4]. Natural language processing (NLP) showed promising results in automated identification of delirium cases using unstructured clinical notes [3-4]. In this study, we built a rule-based NLP classification algorithm based on the confusion assessment method (CAM) framework and assessed its performance on discharge summaries.

Methods: We included 81,108 adult patient cases with available discharge summaries who underwent anesthesia care between 2005 and 2020 as inpatient or same day admissions (Figure 1) at a tertiary academic teaching hospital in Massachusetts. In the rule building phase, we randomly selected 400 discharge summaries from patients with positive ICD-9/10-CM diagnostic code for delirium and tuned the rules (Table 1) through an iterative process. In the algorithm testing phase, physicians reviewed a separate random sample of 300 discharge summaries and annotated them as delirium positive or delirium negative. The algorithm was written in Python (version 3.11.0) the NLP package Spacy-Stanza, a well-tested NLP toolkit [5-7]. Negex algorithm was used to identify the negation of delirium and other symptoms, such as “Patient did not present delirium.” [8]. We applied the algorithm to classify the case and compared the automated classification with the physicians' annotation. The rates of true positive, false positive, true negative, false negative, and recall, precision, F1 score (2*precision*recall/(precision+recall)) were used to assess the performance of the algorithm.

Results: In the test dataset, delirium ICD-9/10-CM was coded for 5 (1.6%) out of 300 patients, while the incidence based on the NLP algorithm was 32 (10.6%) patients. Clinician chart review annotated 30 (10%) out of 300 cases positive for delirium. When compared to chart review as gold standard, ICD-9/10-CM diagnostic codes detected 4 true positive documents and had a F1 score of 0.23. The NLP classification was able to detect 25 true positive cases with a F1 score of 0.81. False negative identifications were only slightly increased by the NLP algorithm, compared to ICD-9/10 CM diagnostic codes (0.3% versus 2.3%, Table 2). Table 2 shows true positives and negatives as well as false positive and negative rates based on ICD-9/-10 diagnoses, as well as single components of the NLP algorithm.

Conclusions: Natural language processing of discharge notes provides a significant improvement in detection rates of postoperative delirium over ICD-9/10-CM, even when analysing in a limited scope of document type.

References: [1] Nat Rev Neurol. 2009 Apr;5(4):210-20.

[2] Psychogeriatrics. 2018 Jul;18(4):268-275.

[3] JMIR Form Res. 2022 Jun 24;6(6):e33834.

[4] J Gerontol A Biol Sci Med Sci. 2022 Mar 3;77(3):524-530.

[5](Online only); spaCy: Industrial-strength Natural Language Processing in Python. https://doi.org/10.5281/zenodo.1212303

[6](Online only); Stanza: A Python Natural Language Processing Toolkit for Many Human Languages. https://doi.org/10.48550/arXiv.2003.07082

[7]J Am Med Inform Assoc. 2021 Aug 13;28(9):1892-1899

[8] J Biomed Inform. 2001 Oct;34(5):301-10.

Figure 1. Study flow

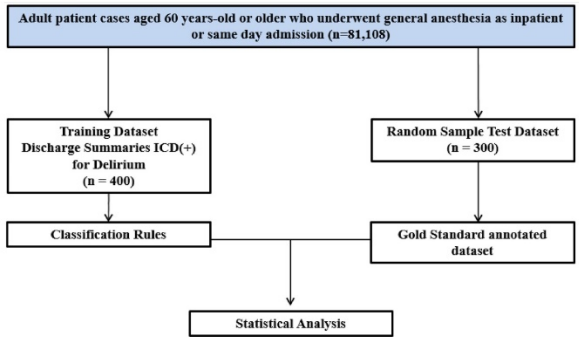

Table 1. Rule definition for annotation and classification

Rule	Description
Definitive Delirium	1. Explicit diagnosis of delirium and/or encephalopathy. 2. Symptoms comprising CAM A + B + (C | D)

CAM: Confusion Assessment Method (A:Acute onset and fluctuating course, B: Inattention, C: disorganised thinking, D: Altered level of consciousness)

Table 2. Rule based classification performance per components

	Delirium ICD-9/10-CM	Delirium keyword	Encephalopathy keyword	Both keywords	Gold Standard
True positives	4 (1.3%)	21 (7%)	9 (3%)	25 (8.5%)	30 (10%)
True negatives	269 (89.7%)	265 (88.3%)	268 (89.3%)	263 (87.7%)	270 (90%)
False negatives	26 (8.7%)	19 (6.3%)	21 (7%)	5 (1.6%)	*n/a*
False positives	1 (0.3%)	5 (1.6%)	2 (0.7%)	7 (2.3%)	*n/a*
Recall	0.13	0.66	0.3	0.83	*n/a*
F_1 Score	0.23	0.74	0.43	0.81	*n/a*

A total of 30 positive cases were annotated in the 300 discharge summaries dataset.

Trauma

Trauma 1- Characterization of A Ferret Model Of Under-Vehicle Blast-Induced Traumatic Brain Injury

Gary Fiskum[1], Julie Proctor[1], Molly Goodfellow[1], Boris Piskoun[1], Amanda Hrdlick[1], Su Xu[1], Ulrich Leiste[1], William Fourney[1], Rao Gullapalli[1]

University of Maryland School of Medicine[1]

Introduction: Under-vehicle blast (UVB)-induced TBI, generated from improvised explosive devices (IEDs), is a unique etiological mechanism of TBI affecting warfighters present in vehicles targeted by blasts. The hyperacceleration load caused by an IED-generated UVB can directly result in a TBI independent of an impact event, however, a secondary head impact injury in the cabin can also occur. Rodent models of TBI recapitulate the cellular pathophysiology and neurobehavioral deficits seen in humans [3], however, successfully translating these findings to improved patient outcomes is challenging. One explanation could be the neuroanatomical differences between humans and rodents, with the latter lacking the gyri and sulci present in the former. To address this modeling difference, a ferret TBI model was developed to evaluate the effects of UVB-alone, CCI-alone, and combined blast + CCI (BCCI) [1,2].

Methods: The protocol was reviewed and approved by the University of Maryland, Baltimore Institutional Animal Care and Use Committee (0620009) and the U.S. Air Force Surgeon General's Office of Research Oversight and Compliance as protocol number FWR-2020-0015A. Animal activities were conducted in compliance with all federal regulations governing the protection of animals and research. Adult male ferrets were either exposed to UVB-alone (n=13) or CCI-alone (n=8). Once the blast level (G force) and CCI depth were finalized, a third set of ferrets were exposed to that combination of BCCI (n=8) or sham injury (n=5). Underbody blast acceleration was induced in sedated animals via detonation of pentaerythritol tetranitrate under a blast plate resulting in acceleration of 2000 – 2500 G. Mild traumatic brain injury was induced under 2-2.5% isoflurane anesthesia via CCI (4 – 6 mm depth, 6 m/s). A subset of ferrets in blast-alone and BCCI groups (n=5 each group) received an MRI scan one week prior to and 7 days after injury. Six days after injury, mood (play behavior observation), motor dysfunction (ladder walk, open field), and memory (novel object recognition and location) were assessed in BCCI (n=6) and sham (n=5) animals. All ferrets were euthanized by terminal perfusion with paraformaldehyde on day 7 and brains histologically analyzed for blood-brain barrier (BBB) disruption (immunoglobulin G, IgG) and diffuse axonal injury (beta-amyloid precursor protein, βAPP).

Results: Results indicate that a single UVB is sufficient to induce acute BBB disruption. CCI-alone leads to both BBB disruption and diffuse axonal injury near the site of cortical impact but this is not further exacerbated by combination with UVB. BCCI does, however, result in several alterations in key cortical metabolites indicative of increased neuronal injury, oxidative stress, and glial activation as well as impaired neurotransmission and energy generation. Additionally, we found evidence that BCCI in ferrets increases depressive-like behavior and hyperactivity, as well as impairs spatial memory.

Conclusions: Taken together, we provide a military, combat-relevant model of under-vehicle bTBI in a gyrencephalic animal, the ferret. The results presented here will be used to address questions on the effects of aeromedical evacuation (hypobaria) on secondary injury development to determine protocols for safe transport following TBI.

The views expressed are those of the authors and do not reflect the official guidance or position of the United States Government, the Department of Defense or of the United States Air Force. Supported by US Air Force FA8650-20-2-6H20.

References: 1. J Neurotrauma. 2022 Oct;39(19-20):1442-1452.

2. J. Neurosci. Methods. 2017, 285: 82–96.

3. Experimental Neurology 2017, 289: 9-20.

Trauma 2- Chronic Behavioral Changes in A Ferret Model of Combined Under-Vehicle Blast and Controlled Cortical Impact-Induced Traumatic Brain Injury

Gary Fiskum[1], Molly Goodfellow[1], Boris Piskoun[1], Amanda Hrdlick[1], Julie Proctor[1], Parisa Rangghran[1], Ulrich Leiste[1], William Fourney[1]

University of Maryland School of Medicine[1]

Introduction: Under-vehicle blast (UVB) causes a unique traumatic brain injury (TBI) in warfighters targeted by improvised explosive devices. UVB hyper-acceleration can produce a TBI independent of impact, however, an impact injury can also occur. Previous studies in rats have shown that aeromedical evacuation-relevant hypobaria exposure within 72 hours of TBI exacerbates neurologic injury [1]. While rat studies investigating TBI are useful, translating findings to improved patient outcomes is challenging, perhaps due to differences in cerebral architecture between rodents and humans. Thus, a model of UVB + impact TBI was developed in ferrets, who possess human-like gyrencephalic brains.

Methods: The protocol was reviewed and approved by the University of Maryland, Baltimore Institutional Animal Care and Use Committee (0620009) and the U.S. Air Force Surgeon General's Office of Research Oversight and Compliance as protocol number FWR-2020-0015A. Animal activities were conducted in compliance with all federal regulations governing the protection of animals in research. In this study, adult male ferrets were sedated, secured to a metal plate "vehicle," exposed to UVB via detonation of pentaerythritol tetranitrate, and then anesthetized and given a controlled cortical impact (BCCI). Twenty-four hours post-injury, animals underwent a 6-hour simulated aeromedical evacuation by exposing them to ambient pressures equivalent to those at 8000 ft (hypobaria; HB; 574 mmHg) or remained at sea level (normobaria; NB; 760 mmHg). Mood (play behavior) and motor function (ladder walk) were assessed monthly in BCCI and age-matched naïve animals. Additional tests examining mood and motor function (open field), as well as memory (novel object recognition and object location) were employed only once at six months post-injury. One/Two-way and repeated measures analysis of variance (ANOVA) and one-sample t-tests were used to analyze the data.

Results: Decreased time spent in the center zone of the open field apparatus suggests increased anxiety-like behavior in BCCI ferrets at 6 months post-injury, particularly in those exposed to hypobaria. Perirhinal cortex-dependent and, perhaps, hippocampus-dependent learning and memory may be impaired 6 months following BCCI+HB but not BCCI+NB. No significant differences were noted in play behavior though it is likely that repeated exposures of ferrets to assays of mood may decrease the sensitivity of the tests. Impairments in gross motor function/learning may persist for at least six months, however, injured animals do show improvement over time.

Conclusions: The preliminary results of this study indicate that ferrets have great potential as a gyrencephalic model for brain injury, allowing for the collection of rich neurobehavioral data [2,3]. Experimentation for this project is ongoing and will, eventually, compare neurobehavioral outcomes from animals exposed to 0-5 simulated flights. Results will inform the creation of guidelines for the safe transport of TBI patients. The views expressed are those of the authors and do not reflect the official guidance or position of the United States Government, the Department of Defense or of the United States Air Force. Supported by US Air Force FA8650-20-2-6H20.

References:

1. *Shock. 2021, 56*(5): 793-802.
2. *J Neurotrauma. 2022, 39*(19-20): 1442-1452.
3. *J. Neurosci. Methods. 2017,* 285: 82–96.

Trauma 3- Enolase-2 in circulating extracellular vesicles as a biomarker to predict the severity of traumatic brain injury in male mice

Balaji Krishnamachary[1], Liwen Wi[1], Yun Li[2], Zhoufan Lei[2], Hui Li[2], Junfang Wu[3]

University of Maryland[1] University of Maryland, School of Medicine[2] University of Maryland School of Medicine[3]

Introduction: Traumatic brain injury (TBI) is a major cause of mortality and disability worldwide. TBI biomarkers secreted from neurons and glial cells after insults have been extensively studied for injury evaluation, management, and prognosis. Despite the advances in TBI biomarker research, the lack of reliable biomarkers that fully corresponded with the pathogenesis and progression of TBI on the molecular level reflect significant unmet healthcare challenges.Extracellular vesicles (EVs) are lipid bound vesicles secreted by all types of brain cells into body biofluids. Emerging data indicate that EVs are responsible for intercellular communication through specific markers on their surface including DNA, RNA, lipids, protein, and metabolites. Thus alterations of EVs cargo may reflect the state of glial cells and neurons during TBI. Yet, the identification of these markers in the circulating EVs and their role in potentiating secondary injury has been understudied. The present study examined the proteome of plasma EVs in mice using a controlled cortical impact (CCI) model of TBI.

Methods: All animal experiments and surgical procedures were performed according to the protocol approved by the Institutional Animal Care and Use Committee (IACUC) from the University of Maryland School of Medicine. Young adult male C57BL/6J mice subjected to CCI surgery were categorized into mild, moderate, and severe injury groups based on the deformation depth of 1.0, 1.5, and 2 mm. After 24h, blood was collected and the EVs were isolated from the platelet-free plasma samples (PFP). First, the larger EVs were isolated from PFP followed by the isolation of smaller EVs by ultracentrifugation method. Smaller EVs were used for all the experiments. The isolated EVs were characterized for Nanoparticle Tracking Analysis (NTA) by ViewSizer and EV markers by western blot analysis. EV proteomics was analyzed using the Olink mouse exploratory panel. Partial Least Squares Discriminant Analysis (PLS-DA) was generated using R and the individual plots of the differentially expressed proteins (DEP) were generated using Graph pad prism. Furthermore, the astrocyte, microglia, and neuron-derived EVs were captured using specific biotinylated antibodies linked to streptavidin magnetic beads using the CSFLOW-BASICA-1 kit. The flow cytometry and western blot analysis were used to confirm the captured EVs.

Results: NTA showed that there was no significant difference in particle number or the average particle size between the four groups **(Fig. 1A-B)**. Western blot analysis confirmed the presence of EV markers CD63, CD81, CD9, Flotillin-1, and TSG101 in all the groups. From the PLS-DA plot, the sham and severe groups showed distinct profiles from each other, suggesting the level of differences in their protein cargo **(Fig. 1C)**. The heatmap of differences in the protein cargo shown in **Figure 1D**, highlighted the alteration between the sham and severe group EV samples. Some of the DEP between the four groups were Eno2, Matn2, Pdgfb, and Tgfb1 **(Fig. 1E)**. Remarkably the level of Eno2 (Enolase-2) was significantly higher in the severe and moderate groups compared to all the other groups suggesting as this can be used as a biomarker in EVs to predict the disease severity. To determine which cell type secrets more Enolase-2, the captured population of the astrocyte (GLAST), microglia (CD11b), and neuron-derived EVs (L1CAM) were stained using the Exo-FITC and the flow cytometry confirmed the staining of EVs on the beads **(Fig. 1F)**. Moreover, the EVs were eluted from the beads using the elution buffer. Western blot analysis showed a higher expression of Enolase-2 in astrocyte-derived EVs along with the presence of EV markers CD9 and CD63 **(Fig. 1G)**, indicating that astrocyte-derived EVs carry elevated levels of Enolase-2 into circulation.

Conclusions: Taken together, this study demonstrates the increased levels of Enolase-2 in the circulating EVs in an injury-severity dependent manner, and TBI-induced elevation of Enolase-2 was derived from the astrocyte-specific population. Thus, plasma EVs-carried Enolase-2 may act as a potential biomarker involved in pathology and recovery processes during head trauma.

References: 1. Essentials of Neuroanesthesia. 2017 587-591.

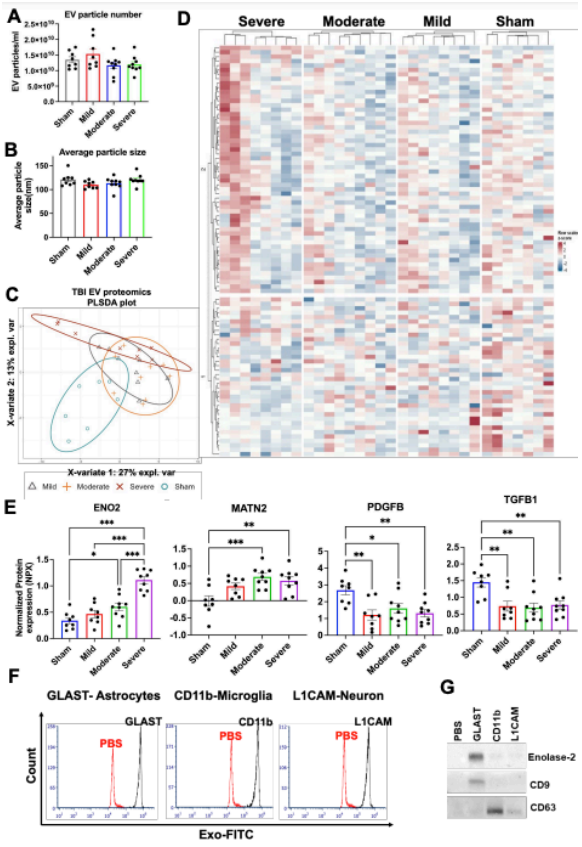

Figure legend:

Extracellular vesicles (EVs) can be used to predict the severity of traumatic brain injury in mice. A. NTA particle number and **B.** Average particle size for smaller EVs isolated by UC at 110,000g. There was no significant change in particle number and size at 1d post-injury. Proximity Extension Analysis (PEA) data of circulating Small EVs from experimentally induced TBI mice **(C-E)**. EVs isolated from EDTA plasma from Sham (n = 7), mild injury (n = 8), moderate injury (n = 8), and Severe (n = 8) groups were used for the comparison of mouse exploratory panel protein cargo in EVs by employing Olink's multiplex PEA platform. **C**. Partial least squares-discriminate analysis (PLS-DA) score plot and **D.** heat map of different proteins from severe, moderate, mild, and sham groups. **E.** Alterations in the selected proteins in EVs indicate to predict the TBI severity. Plots with Mean±SEM indicate normalized protein expression (NPX) expressed in a log2 scale. * P < 0.05, ** P < 0.01, *** P < 0.001. **F.** Flow cytometry of captured EVs stained with Exo-FITC. The panel shows the degree of separation between negative control PBS and Exo-FITC stained EVs in GLAST, CD11b, and L1CAM captured EVs. **G.** Western blot showing the presence of Enolase-2 and EV markers in the captured population.

Trauma 4- Idebenone Post-treatment Mitigates Mouse Traumatic Brain Injury-induced Acute Changes to Ephrin a Signaling Pathway Genes

Brian Polster[1], Brian Polster[1], Nagendra Yadava[1], Boris Piskoun[1], Hyehyun Hwang[2], Marta Lipinski[2], Chinmoy Sarkar[2]

University of Maryland School of Medicine[1] Staff[2]

Introduction: Traumatic Brain Injury (TBI) leads to progressive neurodegeneration associated with long-term cognitive deficits. The extent of persistent pro-inflammatory microglial activation following mouse TBI correlates with the severity of neurological impairments, suggesting that unresolved neuroinflammation is pathogenic[1]. The synthetic Coenzyme Q10 analogue idebenone can suppress pro-inflammatory changes to microglia *in vitro*[2]. This study employed a neuropathology gene expression panel to test the predictions that 1) idebenone post-treatment decreases the expression of microglia signature genes in peri-lesional brain cortex following mouse experimental TBI and 2) mitigates TBI pathology-associated perturbations in gene expression.

Methods: The study was approved by the University of Maryland Institutional Animal Care and Use Committee. Adult male C57BL6/J mice were subjected to moderate controlled cortical impact (CCI) TBI (6 m/s impact velocity, 2 mm deformation depth) or sham control (anesthesia only). Idebenone (100 mg/kg) or vehicle (corn oil) was given by intraperitoneal injection at one hour, and again at five hours, after CCI. Messenger RNA from peri-lesion brain cortex (n=3 per group) was extracted at 24 h post-injury for analysis by the NanoString nCounter® Neuropathology panel that consists of 770 neuropathology-associated or housekeeping genes. The following panel-provided housekeeping genes were used for normalization: *Fam104a, Supt7l, Csnk2a2, Ccdc127, Tada2b,* and *Mto1*. Gene set enrichment analysis for the sham *vs.* CCI comparison and the CCI+vehicle *vs.* CCI+ idebenone comparison were done on housekeeping gene-normalized NanoString mRNA data using ROSALIND® software. The p value for pathway analysis was adjusted using a false discovery rate of 0.05; an adjusted p value (adj p) of <0.05 was considered significant. A one-way ANOVA with Tukey's post hoc analysis was used to test for significant changes in individual gene transcripts across multiple groups at $p<0.05$. To evaluate the effect of idebenone on microglia, we developed a microglia gene signature within the Neuropathology gene expression panel by reanalyzing the raw data from a published data set (GEO; GSE160651)[3]. Genes that decreased by more than three-fold in mice pre-treated with the microglia-depleting drug PLX5622 relative to vehicle for both sham and 24-hour TBI groups were included in the microglia gene signature set.

Results: The expression of several activation-associated microglia genes significantly increased following CCI. Contrary to our expectations, several microglial signature genes that were upregulated by TBI, e.g., *Fcrls, Stab1,* and *Ccr5*, were further increased by idebenone post-treatment, whereas no microglia signature genes were decreased by idebenone. TBI decreased several genes encoding enzymes or receptors important for neurotransmission, e.g., that mediated by acetylcholine, dopamine, or gamma-aminobutyric acid (GABA). Idebenone failed to significantly prevent these changes, though strong trends were observed (n=3, p values between 0.05 and 0.1). Gene set enrichment analysis comparing the TBI and TBI plus idebenone groups revealed that "EPHA forward signaling" was the most significantly altered pathway by idebenone at 24 hours post-TBI (adj p=0.00024). The related "EphrinA-EPHA pathway" (adj p = 0.00027) and "Ephrin A reverse signaling" pathway (adj p=0.02558) were the next most changed. Idebenone significantly mitigated TBI-induced gene expression changes in both Ephrin A ligand-encoding genes (*Efna1* and *Efna5*) and Ephrin A receptor-encoding genes (*Epha5* and *Epha6*).

Conclusions: Idebenone post-treatment significantly ameliorated many gene expression changes to peri-lesion cortex caused by TBI at an acute (24 hour) post-injury timepoint, most notably in the Ephrin A signaling pathway. A subset of microglial signature genes elevated following TBI was increased even further by idebenone ($p<0.05$), which may reflect an increased number of phagocytic, debris-clearing microglia in the drug-treated animals. Overall, results from this pilot transcriptomics study suggest that idebenone may be neuroprotective and support a more extensive evaluation of idebenone for TBI treatment.

References: 1. *Exp. Neurol*. 275 Pt 3:316-327, 2016.

2. *Front Cell Neurosci*. 12:529, 2018.

3. *J Neurosci*. 41:1597-1616, 2021.

Trauma 5- Loss of the voltage-gated proton channel Hv1 aggravates chronic brain injury-induced peripheral inflammation leading to worsened outcomes in male mice

Zhuofan Lei[1], Rodney Ritzel[2], Yun Li[3], Junyun He[3], Kavitha Brunner[4], Hui Li[4], Junfang Wu[1]

University of Maryland School of Medicine[1] University of Texas Health Science Center[2] University of Maryland, School of Medicine[3] University of Maryland, Baltimore School of Medicine[4]

Introduction: Clinical and experimental studies indicate that traumatic brain injury (TBI) can have profound pathophysiological effects on peripheral organs. We have previously reported widespread dysfunction of innate and adaptive immune responses after experimental TBI [1], however, the long-term effects of TBI on peripheral tissues are largely unknown. Moreover, our understanding of the molecular mechanisms underlying systemic immune impairment after TBI remains poor. Hv1, a highly conserved voltage-gated proton channel, is exclusively expressed in microglia of the central nervous system. We and others have shown that microglial Hv1 is a key driver of tissue acidosis, oxidative stress, and neuroinflammation in models of acute CNS injury [2]. However, Hv1 is also widely expressed in peripheral immune cells. Ablation of Hv1 caused detrimental effects on neutrophil function and impaired mitochondrial respiration and glycolysis in peripheral tissues [3]. The present study examined the pathogenesis and long-term impact of TBI on the peripheral organs in the presence and absence of Hv1 in mice using a controlled cortical impact (CCI) model.

Methods: Young adult (3-month-old) male Hv1 knock out (Hv1KO) mice and their wildtype (WT) littermates were subjected to moderate CCI surgery. Functional recovery was evaluated at 17-months post-injury by open field, Y-maze, novel object recognition (NOR), novelty-suppressed feeding (NSF), and social interaction (SI) test. At 18 months after completion of all behavioral tests, the ipsilateral cerebral cortex and the liver, lung, spleen, bone marrow were dissected and processed for flow cytometry and transcriptomic analysis using NanoString Neuropathology or Myeloid Innate Immunity Panels.

Results: In Hv1 KO mice, TBI resulted in significant higher mortality beginning at 13-months post-injury compared to WT animals. At 17-months post-injury, no significant differences were detected in spontaneous locomotor activities tested in the open field among the groups. In a battery of neurobehavioral tests, Hv1 KO/TBI mice displayed significant cognitive deficits as demonstrated by reduced % spontaneous alternation in Y maze test, reduced time with novel object in NOR test, and poor performance in NSF and SI tests. NanoString Neuropathology analysis demonstrated that Hv1KO/TBI mice had a pronounced dysregulation in genes related to Oxidative Stress, Cytokines, and Activated microglia in the ipsilateral cortex. Myeloid Innate Immunity Panels analysis showed impaired immune function in the liver, lung, and spleen tissues in the absence of Hv1.

Conclusions: Taken together, our data indicate an important role for Hv1 in regulating peripheral immune function-mediated functional damage after chronic TBI.

References: J Neurotrauma. 2018 Jul 1;35(13):1419-1436.

Glia. 2021 Mar;69(3):746-764.

Front Cell Neurosci. 2021 Apr 9;15:662971.

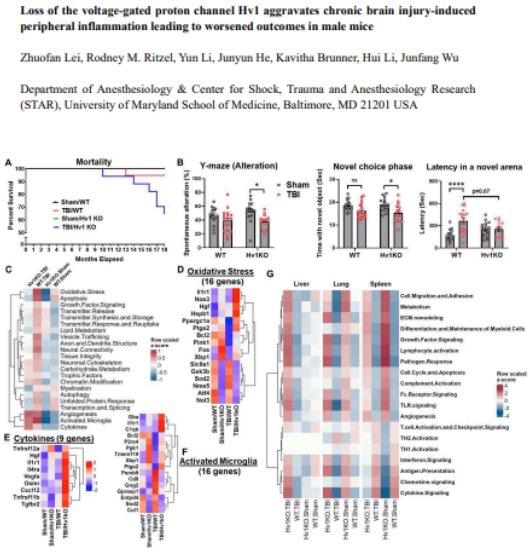

Figure Legend: Loss of the voltage-gated proton channel Hv1 aggravates chronic brain injury-induced peripheral inflammation leading to increased mortality and worsened outcomes in male mice. Young adult (3-month-old) male Hv1 knock out (Hv1KO) mice and their wildtype (WT) littermates were subjected to moderate CCI surgery. **A)** Percent survival. N=16 (WT/Sham), 20 (WT/TBI), 16 (Hv1 KO/Sham), and 17 (Hv1 KO/TBI, n=17. **B)** Behavioral tests. **C-F)** NanoString Neuropathology analysis in the cortex. **G)** NanoString Myeloid Innate Immunity Panels analysis in the liver, lung, and spleen tissues.

Trauma 6- Sexually dimorphic extracellular vesicle responses after chronic spinal cord injury are associated with neuroinflammation and neurodegeneration in the brain

Yun Li[1], Niaz Khan[2], Zhuofan Lei[2], Rodney Ritzel[3], Hui Li[3], Kavitha Brunner[4], Alan Faden[4], Junfang Wu[2]

University of Maryland, School of Medicine[1] University of Maryland School of Medicine[2] University of Texas Health Science Center[3] University of Maryland, Baltimore School of Medicine[4]

Introduction: Advancements in treatment and healthcare allow many patients suffering a spinal cord injury (SCI) to live for several decades after their traumatic event. Amongst the long-term consequences of SCI, cognitive decline has garnered high interest that is further complicated by the factor of biological sex [1]. Emerging data suggest that male and female utilize different pathological mechanisms after injury, which may in turn lead to differences in functional outcome [2]. Extracellular vesicles (EVs), containing microRNAs (miRs), proteins, and lipids from their originating cells, have emerged as potentially important regulators of secondary injury after SCI, not only locally but also systemically and in the brain. We have previously shown that SCI in young adult male mice leads to robust changes in plasma EV count and microRNA (miR) content [3]. Here, our goal was to investigate the impact of biological sex and aging on EVs and brain after SCI.

Methods: Young adult age-matched male and female C57BL/6 mice were subjected to moderate thoracic spinal cord contusion. At 19 months post-injury, total plasma EVs were isolated by ultracentrifugation. Particle count and size distribution were assessed by nanoparticle tracking analysis, while individual EV protein expression was quantified by Western blot. EVs microRNA (miR) cargo was examined using the Fireplex® assay. The transcriptional changes in the brain were assessed by a NanoString nCounter Neuropathology panel. Neuropathology in the brain regions was further examined by Western blot (WB) and flow cytometry (FC). A battery of behavioral tests was performed for assessment of locomotor and cognitive function as well as depression. All animal experiments and surgical procedures were performed according to protocol approved by the Institutional Animal Care and Use Committee (IACUC) from the University of Maryland School of Medicine.

Results: NanoString analysis demonstrated that males had greater transcriptional changes than females in the brain following chronic SCI. Furthermore, males had a pronounced reduction in genes related to vesicle trafficking, growth factor signaling and myelination in the cortex. In contrast, females showed an improved oxidative stress and unfolded protein response profile. Decreased expression of anti-inflammatory cytokines (Il6, Cxcr4, Tgfb1, Il10ra) in the hippocampus may be detrimental to neuronal survival and adult neurogenesis. Across both regions and sexes, gene expression related to homeostatic microglia were reduced (C1qa and Egr1). Examination of the injured spinal cord with FC showed higher lymphocyte counts in SCI/Female mice compared to their male counterparts, along with higher production of reactive oxygen species (ROS). In the brain, SCI/Female mice showed higher levels of TNF and MitoSpyRed positive microglia as well as ROS production. WB and NTA showed that EV markers, CD63 and CD81, are elevated in the plasma of male mice after SCI. Furthermore, particle concentration in the cortex also increased after injury, with SCI/Female mice showing significantly higher counts than SCI/Male. Cargo analysis of the plasma and tissue derived EVs showed dramatic changes of miR content driven by injury and sex differences. Alterations in EV miRs paralleled those reported with neurodegenerative disease, depression and inflammatory processes. SCI impaired locomotor and cognitive function and caused depression-like behavior in both sexes. However, neither behavior test showed sex differences.

Conclusions: Collectively, these studies are the first to describe changes in circulating EVs after chronic SCI and in aged animals and support a potential EV-mediated mechanism for SCI-induced brain changes.

References: 1. Li, Y., et al., *Dementia, Depression, and Associated Brain Inflammatory Mechanisms after Spinal Cord Injury.* Cells, 2020. **9**(6).

2. Li, Y., et al., *Sexual dimorphism in neurological function after SCI is associated with disrupted neuroinflammation in both injured spinal cord and brain.* Brain Behav Immun, 2022. **101**: p. 1-22.

3. Khan, N.Z., et al., *Spinal cord injury alters microRNA and CD81+ exosome levels in plasma extracellular nanoparticles with neuroinflammatory potential.* Brain Behav Immun, 2021. **92**: p. 165-183.

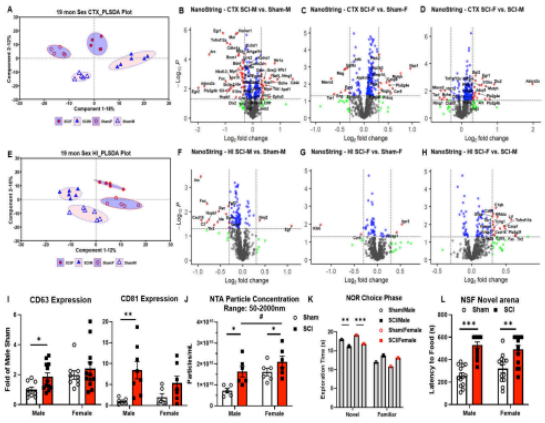

Figure 1. Sexually dimorphic EV responses after chronic spinal cord injury are associated with neuroinflammation and neurodegeneration in the brain. Young adult age-matched male and female C57BL/6 mice were subjected to moderate SCI for up to 19 months. (**A**) PLSDA plot for NanoString results of the cortex region. (**B-D**) Volcano plot for pairwise comparison of cortex DEG. (**E**) PLSDA plot for NanoString results of the hippocampus. n=5~6/group. (**F-H**) Volcano plot for pairwise comparison of hippocampus DEG. (**I**) WB analysis showed elevated expression of EV markers CD63 and CD81 in plasma extracted from mice. (**J**) NTA of cortex derived EVs shows significantly higher particle concentration in SCI groups. (**K**) NOR (novel object recognition) indicated deficits with hippocampus-dependent spatial memory after chronic SCI. (**L**) NSF (novelty suppressed feeding) showed depression-like behavior in SCI groups at 19m post-injury. n=13~14/group. *p<0.05, **p<0.01 vs Sham, # p<0.05 vs SCI/Male using Mann Whitney test (**I,J**). **p<0.01, ***p<0.001 vs Sham using 2-way ANOVA group analysis with Tukey's test for multiple comparisons (**K, L**).

A.

EV miRs: Sex Main Effect			
Probe	▲ OR ▼	Linear MFI Fold Change	adj. p-value
Hippocampus			
hsa-miR-34a-5p	▲	1.59	**
hsa-miR-124-3p	▲	1.46	*
hsa-miR-146a-5p	▼	0.63	*
hsa-miR-338-3p	▼	0.59	*
hsa-let-7f-5p	▼	0.49	*
hsa-miR-7-5p	▼	0.43	*
Spinal cord			
hsa-let-7i-5p	▼	0.69	*
hsa-miR-22-3p	▼	0.64	*
Plasma			
hsa-miR-497-5p	▲	1.63	*

B.

EV miRs: Injury Main Effect			
Probe	▲ OR ▼	Linear MFI Fold Change	adj. p-value
Hippocampus			
hsa-miR-370-3p	▲	1.89	*
hsa-miR-7b-5p	▲	1.55	*
hsa-miR-328-3p	▲	1.36	*
hsa-miR-24-3p	▲	1.30	*
hsa-miR-103a-3p	▼	0.74	*
hsa-miR-107	▼	0.73	*
hsa-miR-532-5p	▼	0.7	*
hsa-let-7i-5p	▼	0.69	*
hsa-miR-22-3p	▼	0.64	*
Cortex			
hsa-miR-323a-3p	▲	1.62	*
hsa-let-7d-5p	▲	1.21	*
hsa-miR-128-5p	▲	1.16	*
Spinal cord			
hsa-miR-497-5p	▲	1.63	*
hsa-let-7b-5p	▲	1.33	*
Plasma			
hsa-let-7d-5p	▲	1.08	*
hsa-miR-15a-5p	▼	0.82	*
hsa-miR-93-5p	▼	0.79	*
hsa-miR-16-5p	▼	0.76	*
hsa-miR-486-5p	▼	0.68	*
hsa-miR-451a	▼	0.65	*

Figure 2. EVs miRNA cargo is modified after chronic SCI. Table shows miRs with main sex effect (**A**) or main injury effect (**B**) by region. Linear fold change of the mean fluorescent intensity (MFI) data between relevant groups are shown as well as adjusted (adj.) p-value of significance.

Trauma 7- Traumatic brain injury-induced inflammatory changes in the olfactory bulb disrupt neuronal networks leading to olfactory dysfunction in male mice

Junfang Wu[1], Xiang Liu[1], Dylan Gilhooly[1], Junyun He[1], Yun Li[2], Zhuofan Lei[1], Rodney Ritzel[3], Hui Li[3], Long-Jun Wu[3], Shaolin Liu[4]

University of Maryland School of Medicine[1] University of Maryland, School of Medicine[2] University of Texas Health Science Center[3] Howard University[4]

Introduction: Approximately 20–68% of traumatic brain injury (TBI) patients exhibit trauma-associated olfactory deficits (OD) which can compromise not only the quality of life but also cognitive and neuropsychiatric functions. Although post-traumatic anosmia has been documented in the medical literature for more than a century, few studies to date have examined the impact of experimental TBI on OD. While increased glial reactivity has been observed in the post-TBI olfactory bulb (OB), a site remote to non-contusive brain injury, neither the underlying mechanisms nor treatment remains clear. The present study examined microglia/macrophage-mediated inflammation and neuronal dysfunction in the OB as well as the underlying mechanisms associated with OD in mice using a controlled cortical impact (CCI) model.

Methods: Young adult (10-12 weeks) male C57BL/6 mice were subjected to mild/moderate-level CCI. Flow cytometry, qPCR, and immunohistochemistry were used to examine inflammation in the OB after TBI. In vivo OB neuronal firing activities were recorded in the glomerular layer (GL) and the mitral cell layer (MCL) using the linear 16-channel probe. Transgenic mice with ablation of the voltage-gated proton channel Hv1 or NADPH oxidase (NOX2) as well as a specific NOX2 inhibitor [1-3] were used to determine the effects of Hv1 and NOX2 activity on TBI-mediated OD. Olfactory function was assessed for up to 6 months post-injury with behavioral tests, including buried food, two-bottle odor discrimination, and odor memory. All animal experiments and surgical procedures were performed according to protocols approved by the Institutional Animal Care and Use Committee (IACUC) from both the University of Maryland School of Medicine and Howard University College of Medicine.

Results: Cortical contusion TBI without direct damage of the OB caused a rapid inflammatory response in the OB as early as 24h post-injury, including elevated mRNA levels of proinflammatory cytokines, increased numbers of microglia and infiltrating myeloid cells, and increased IL1b and IL6 production in these cells. Microglial activation in the OB was sustained for up to 90 days after TBI. Moreover, we observed significant upregulation of Hv1 and NOX2 expression levels at 1 d and 3 days post-injury, which were predominantly localized in microglia/macrophages and accompanied by increased reactive oxygen species production. TBI induced early neuronal hyperexcitation and later hypo-neuronal activity in both GL and MCL and disrupted network function in the OB which were improved in the absence of Hv1. In a battery of olfactory behavioral tests, WT/TBI mice displayed significant OD. In contrast, neither Hv1 KO/TBI nor NOX2 KO/TBI mice showed robust olfactory dysfunction. Finally, seven days of intranasal delivery of a NOX2 inhibitor (NOX2ds-tat) ameliorated post-traumatic OD.

Conclusions: Our data indicate that Hv1/NOX2-mediated proinflammatory changes in the OB disrupts OB neuronal circuits leading to poorer olfactory function late after TBI. Conversely, blocking or inhibiting Hv1/NOX2 signaling improved outcomes. These findings highlight the importance of OB neuronal networks and its role in TBI-mediated OD. Thus, targeting Hv1/NOX2 may be a potential intervention for improving post-traumatic anosmia.

References: 1. Glia, 2021 Mar;69(3):746-764.

2. Brain, Behavior, and Immunity, 2019, 80, 73-80.

3. Front Cell Neurosci. 2021 Apr 9; 15: 662971.

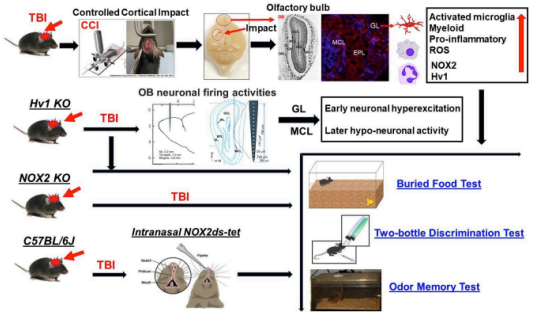

Graphical abstract. Hv1/NOX2-mediated proinflammatory changes in the olfactory bulb (OB) disrupt OB neuronal circuits leading to poorer olfactory function after traumatic brain injury (TBI). Mice were subjected to mild/moderate-level injury using a controlled cortical impact (CCI) model of TBI. We demonstrate that TBI induced microglia/macrophages-related neuroinflammation in the OB, accompanied by upregulation of Hv1/NOX2. OB neuronal firing activities indicate that TBI induced early neuronal hyperexcitation and later hypo-neuronal activity and disrupted network function in the OB which were improved in the Hv1 KO mice. Genetically or pharmacologically manipulating Hv1/NOX2 signaling can improve TBI-mediated olfactory dysfunction.

Trauma 8- Type I Interferon Responses Are Increased In Aged Mice Following Traumatic Brain Injury

James Barrett[1], Alan Faden[1], Bogdan Stoica[1]

University of Maryland[1]

Introduction: Aging is associated with increased inflammatory activity within the central nervous system (CNS), characterized by increased levels of pro-inflammatory cytokines and evidence of enhanced microglial activation. Experimental and clinical evidence has demonstrated that following TBI, age is associated with worsened neurological dysfunction and exacerbated neuroinflammatory responses. Recently, we have demonstrated that Type I Interferons (IFN-I) are involved in the development of neurological dysfunction, neuroinflammation, neurodegeneration after traumatic brain injury (TBI). Activation of cyclic GMP-AMP synthase (cGAS) and Stimulator of Interferon Genes (STING) pathway, key molecules involved in the induction of IFN-I responses, have been implicated in neuroinflammatory activity in a number of neurodegenerative disorders. We have demonstrated that TBI in aged animals induces a robust neuroinflammatory response that is associated with increased expression of DNA/RNA recognition pathways and IFN-related genes. In the present study, using the controlled cortical impact (CCI) model of TBI we set out to examine the effect of IFN-I inhibition on these age-related responses during the acute phase of injury.

Methods: Young (12 week old) and Aged (20 month old) C57BL/6 mice underwent controlled cortical impact (CCI, a well-established TBI model) or Sham surgery. received daily intraperitoneal injections of anti-IFNAR (MAR1-5A3) or appropriate Igg control at 1 hour, 24 hour and 48 hours. Animals were sacrificed at either 3 and 7days after injury; using magnetic bead isolation, CD11b+ cells were isolated from the hippocampus and cortex. CD11b+ cells were prepared for RNAseq analysis.

Results: RNAseq analysis revealed increased expression of proinflammatory mediators in microglia from young mice, the expression of which was amplified further in microglia from aged mice. Pathway analysis revealed that TBI in aged mice was associated with elevated expression of viral response genes, including many IFN-related genes (e.g. Irf7, Isg15, IFI204). Anti-IFNAR treatment significantly reduced the expression of these viral response genes in both young and aged animals. Significantly the age-related increase in several key pro-inflammatory pathways was significantly reduced in aged microglia.

Conclusions: This age-related enhancement of IFN-I signaling may prove to be a key pathophysiological mechanistic link inducing microglial dysfunction and neurodegeneration in the aged TBI brain.

Trauma 9- Hdac Inhibitor Romidepsin Reduces Neuroinflammation Following Tbi

James Barrett[1], Aidan Smith[1], Bogdan Stoica[1], Alan Faden[1]

University of Maryland[1]

Introduction: Traumatic brain injury (TBI) triggers delayed molecular and cellular responses, including neuroinflammation, that contribute to neuronal loss and neurological dysfunction. TBI-induced epigenetic changes may promote excessive inflammation and neurodegeneration. For example, activation of histone deacetylases (HDACs) may alter microglia transcriptomic signatures that promote pro-inflammatory, neurotoxic phenotypes. Conversely, HDAC inhibitor (HDACi)-induced changes in the chromatin at key promoter regions may favor gene expression that facilitates neurorestorative microglia phenotypes. Romidepsin (RMD) is a potent, class 1/2 HDACi that increases histone acetylation and improves cognitive outcome in experimental autism models. The current study evaluated effects of RMD on transcriptomic changes in microglia following experimental TBI.

Methods: 12 week old male C57Bl/6 mice mice underwent controlled cortical impact (CCI, a well-established TBI model) or Sham surgery. Mice received daily intraperitoneal injections of RMD or vehicle at 1 hour, 24 hour and 48 hours following TBI. Animals were sacrificed at either 3, 7 or 35 days after injury; using magnetic bead isolation, CD11b+ cells were isolated from the hippocampus and cortex. CD11b+ cells were prepared for RNAseq analysis.

Results: TBI resulted in significant upregulation in genes and pathways related to inflammation. While TBI-induced changes were observed at all timepoints examined, the peak of inflammation was observed at 3 days after injury. RMD attenuated TBI-induced expression of the pro-inflammatory genes, while also upregulating a number of pathways associated with repair and resolution of injury.

Conclusions: Our previous findings demonstrated that RMD improves cognitive function after TBI, the present data suggest that this may be as a result of modulating microglia responses following TBI. Thus, RMD may be a promising therapeutic intervention for brain injury.